

TECHNICAL SPECIFICATIONS

1.0 DEFINITIONS

The following terms are defined for uniform interpretation of the specifications.

1.1 Thermal Power

The rate that the thermal energy generated by the fuel is accumulated by the coolant as it passes through the reactor vessel.

1.2 Reactor Operating Modes

| <u>Mode</u> | <u>Reactivity $\Delta k/k\%$</u> | <u>Coolant Temperature (°F)</u> |
|---------------|---|---|
| Refueling | ≤ -5 | $T_{avg} \leq 140$ |
| Cold Shutdown | ≤ -1 | $T_{avg} \leq 200$ |
| Hot Shutdown | ≤ -1 | $T_{avg} \geq 540$ |
| Operating | ≥ 0 | $T_{avg} \sim 580$ |

1.3 Refueling

Any operation within the containment involving movement of fuel and/or control rods when the vessel head is unbolted.

1.4 Operable

Capable of performing all intended functions in the intended manner.

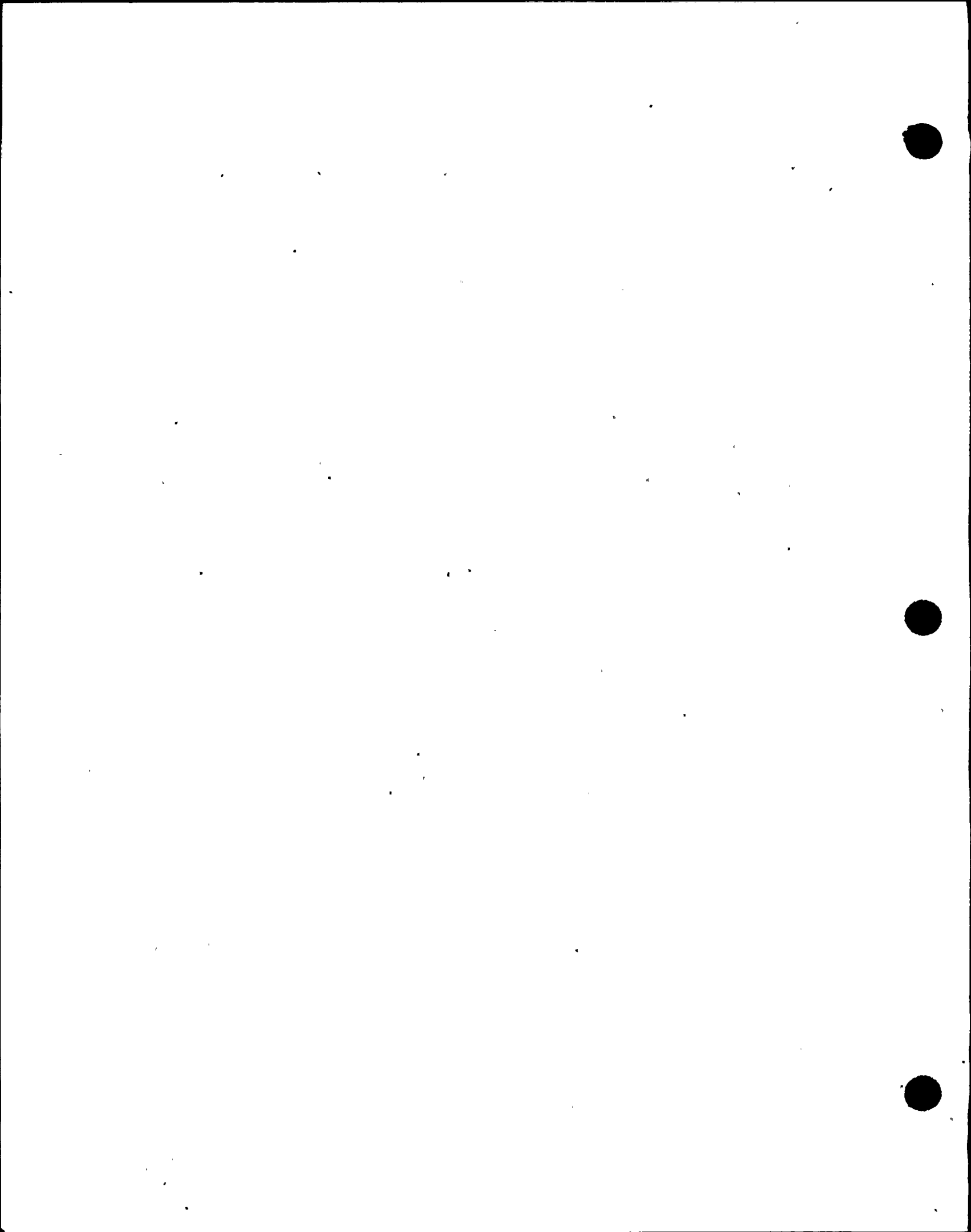
8401040350 831220
PDR ADCK 05000244
PDR



regime is termed departure from nucleate boiling (DNB) and at this point there is a sharp reduction of the heat transfer coefficient which would result in high clad temperatures and the possibility of clad failure. DNB is not, however, an observable parameter during reactor operation. Therefore, the observable parameters, thermal power, reactor coolant temperature and pressure have been related to DNB through the W-3 and/or WRB-1 DNB correlation. These DNB correlations have been developed to predict the DNB flux and the location of DNB for axially uniform and non-uniform heat flux distributions. The local DNB heat flux ratio, defined as the ratio of the heat flux that would cause DNB at a particular core location to the local heat flux, is indicative of the margin to DNB. A minimum value of the DNB ratio, MDNBR, is specified so that during steady state operation, normal operational transients and anticipated transients, there is a 95% probability at a 95% confidence level that DNB will not occur.⁽¹⁾ The curves of Figure 2.1-1 represent the loci of points of thermal power, coolant system pressure and average temperature for which this minimum DNB value is satisfied. The area of safe operation is below these lines.

Since it is possible to have somewhat greater enthalpy rise hot channel factors at part power than at full power due to the deeper control bank insertion which is permitted at part power, a conservative allowance has been made in obtaining the curves in Figure 2.1-1 for an increase in $F_{\Delta H}^N$ with decreasing power levels. Rod withdrawal block and load runback occurs before reactor trip set points are reached.

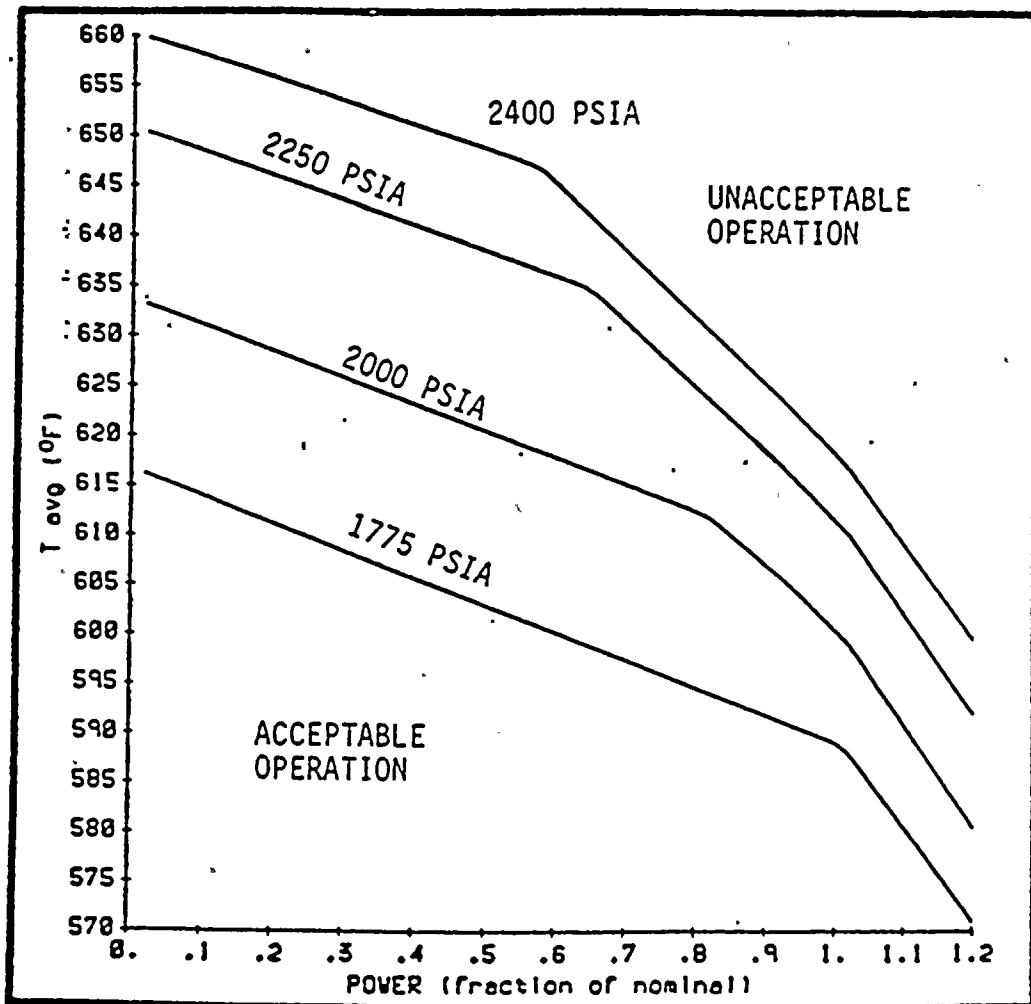
The Reactor Control and Protective System is designed to prevent any anticipated combination of transient conditions for reactor coolant system temperature, pressure and thermal power level that would result in there being less than a 95% probability at a 95% confidence level that DNB would not occur. (3)



- (1) FSAR, Section 3.2.2
- (2) FSAR, Section 3.2.1
- (3) FSAR, Section 14.1.1



FIGURE 2.1-1
 CORE DNB SAFETY LIMITS
 2 LOOP OPERATION



Amendment No. 10, 40
 Proposed

d. Overtemperature ΔT

$$\leq \Delta T_o [K_1 + K_2(P-P^1) - K_3(T-T^1) \left(\frac{1 + \tau_1 S}{1 + \tau_2 S} \right)] - f(\Delta I)$$

where

ΔT_o = indicated ΔT at rated power, °F

T = average temperature, °F

T^1 = 573.5°F

P = pressurizer pressure, psig

P^1 = 2235 psig

K_1 = 1.20

K_2 = .000900

K_3 = .0209

τ_1 = 25 sec

τ_2 = 5 sec

and $f(\Delta I)$ is a function of the indicated difference between top and bottom detectors of the power-range nuclear ion chambers; with gains to be selected based on measured instrument response during plant startup tests where q_t and q_b are the percent power in the top and bottom halves of the core respectively, and $q_t + q_b$ is the total core power in percent of rated power such that:

(i) for $q_t - q_b$ less than +21 percent, $f(\Delta I) = 0$



(ii) for each percent that the magnitude of $q_t - q_b$ is more positive than +21 percent, the ΔT trip set point shall be automatically reduced by an equivalent of 1.6 percent of rated power.

e. Overpower ΔT

$$\leq \Delta T_o [K_4 - K_5(T-T^1) - K_6 \frac{\tau_3 ST}{\tau_3 S + 1}] + f(\Delta I)$$

where

ΔT_o = indicated ΔT at rated power, °F

T = average temperature, °F

T^1 = indicated T avg at nominal conditions at rated power, °F

K_4 = 1.077

K_5 = .0.0 for $T < T^1$
 = 0.0011 for $T \geq T^1$

K_6 = 0.0262 for increasing T
 = 0.0 for decreasing T

τ_3 = 10 sec

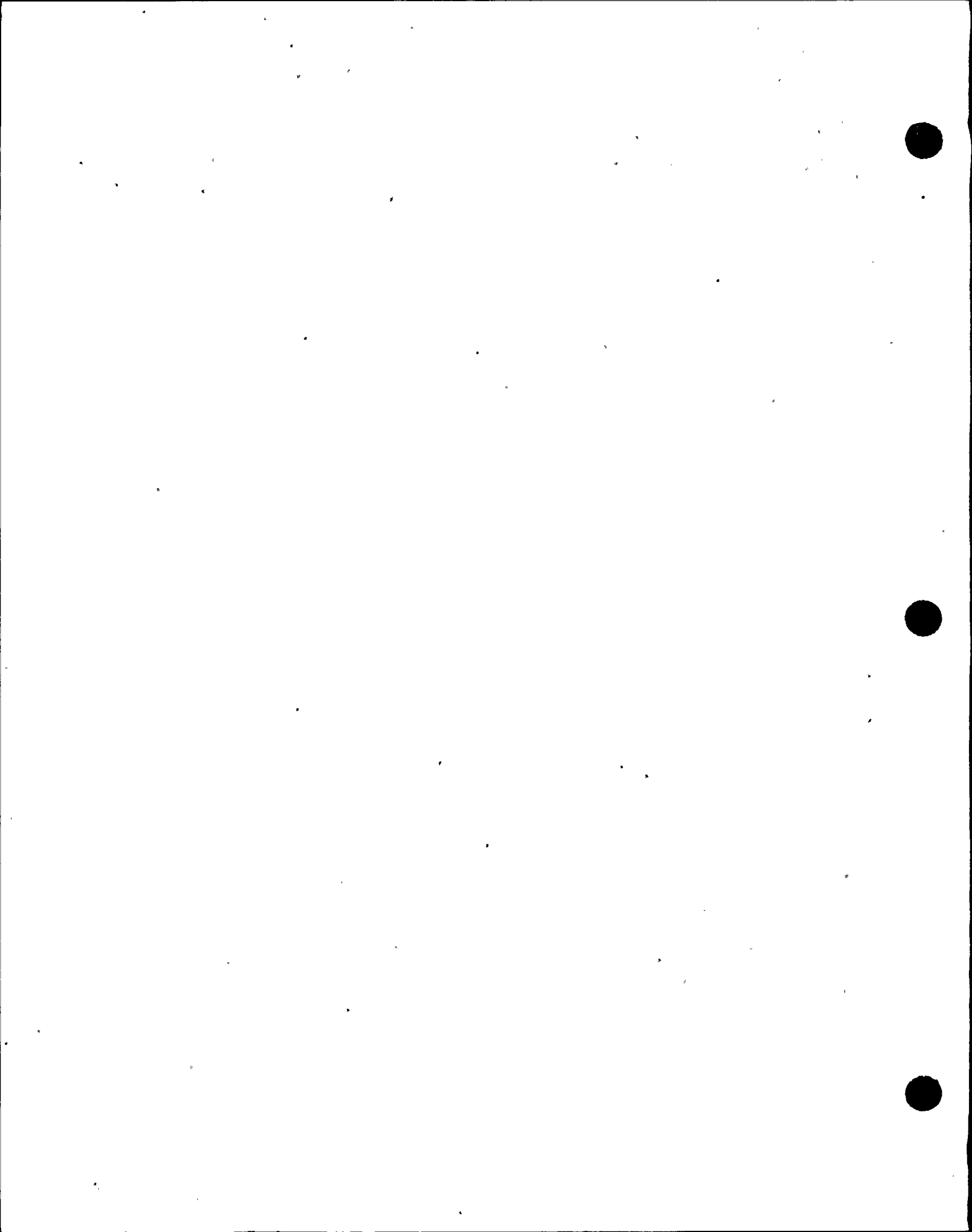
$f(\Delta I)$ = as defined in 2.3.1.2.d.

3.1.1.5 Pressurizer

Whenever the reactor is at hot shutdown or critical the pressurizer shall have at least 100 kw of heaters operable and a water level maintained between 12% and 87% of level span. If the pressurizer is inoperable due to heaters or water level, restore the pressurizer to operable status within 6 hrs. or have the RHR system in operation within an additional 6 hrs.

Bases

The plant is designed to operate with all reactor coolant loops in operation and maintain the DNBR above the limit value during all normal



3.1.3 Minimum Conditions for Criticality

3.1.3.1 Except during low power physics tests, the reactor shall not be made critical at a temperature below 500°F, and if the moderate temperature coefficient is more positive than

- a. 5 pcm/°F (below 70 percent of rated thermal power)
- b. 0 pcm/°F (at or above 70 percent of rated thermal power)

3.1.3.2 In no case shall the reactor be made critical above and to the left of the criticality limit line shown on Figure 3.1-1 of these specifications.

3.1.3.3 When the reactor coolant temperature is below the minimum temperature specified above, the reactor shall be subcritical by an amount equal to or greater than the potential reactivity insertion due to depressurization.

Basis

Previous safety analyses have assumed that for Design Basis Events (DBE) initiated from the hot zero power or higher power condition, the moderator temperature coefficient (MTC) was either zero or negative.⁽¹⁾⁽²⁾ Beginning in Cycle 14, the safety analyses have assumed that a maximum MTC of +5 pcm/°F can exist up to 70% power. Analyses have shown that the design criteria can be satisfied for the DBE's with this assumption.⁽³⁾ At greater than 70% power the MTC must be zero or negative.

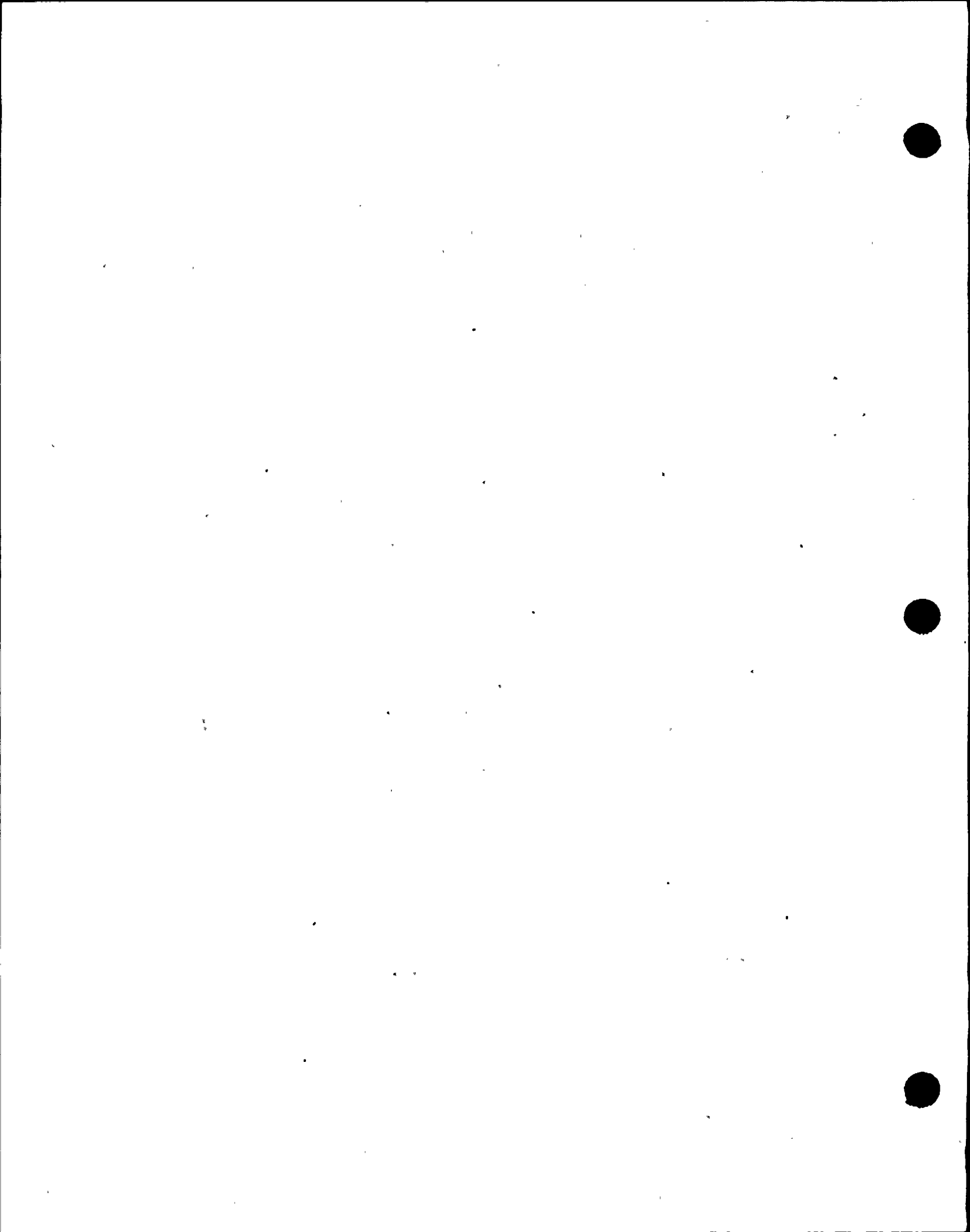
The limitations on MTC are waived for low power physics tests to permit measurement of the MTC and other physics design parameters of interest. During these tests special operating precautions will be taken.

The requirement that the reactor is not to be made critical above and to the left of the criticality limit provides increased assurance that the proper relationship between reactor coolant pressure and temperature will be maintained during system heatup and pressurization. Heatup to this temperature will be accomplished by operating the reactor coolant pumps.

If the specified shutdown margin is maintained, there is no possibility of an accidental criticality as a result of an increase in moderator temperature or a decrease of coolant pressure.

Reference

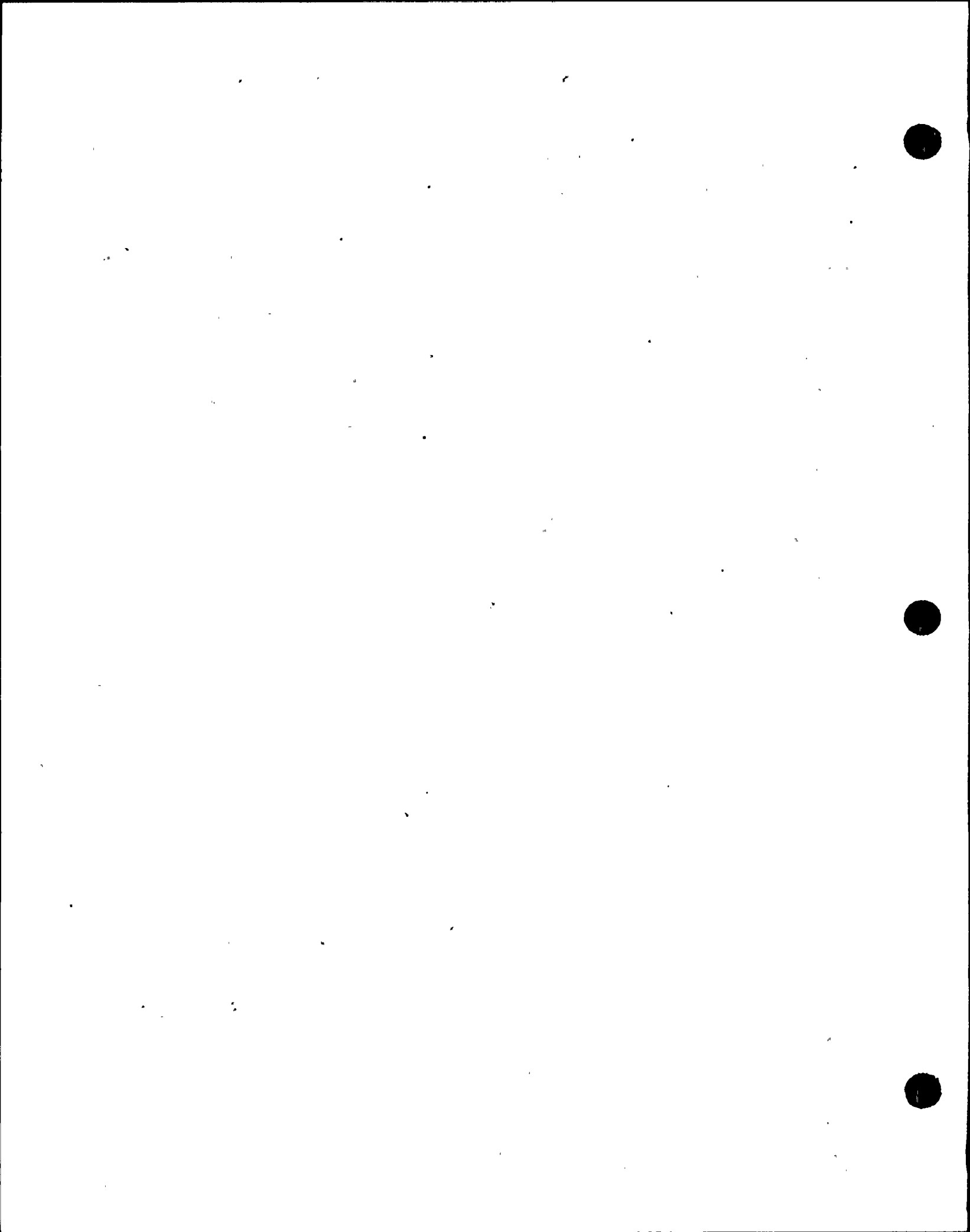
- (1) FSAR Table 3.2.1-1
- (2) FSAR Figure 3.2.1-8
- (3) Safety Evaluation for R. E. Ginna Transition to 14 x 14 Optimized Fuel Assemblies, Westinghouse Electric Corporation, November 1983.



to public health and safety. (1) Whenever changes are not being made in core geometry one flux monitor is sufficient. This permits maintenance of the instrumentation. Continuous monitoring of radiation levels and neutron flux provides immediate indication of an unsafe condition. The residual heat pump is used to maintain a uniform boron concentration.

The shutdown margin as indicated will keep the core subcritical, even if all control rods were withdrawn from the core. During refueling, the reactor refueling cavity is filled with approximately 230,000 gallons of borated water. The boron concentration of this water at 2000 ppm boron is sufficient to maintain the reactor subcritical by at least 5% $\Delta k/k$ in the cold condition with all rods inserted (best estimate of 10% subcritical), and will also maintain the core subcritical even if no control rods were inserted into the reactor. (2) Periodic checks of refueling water boron concentration insure the proper shutdown margin. Communication requirements allow the control room operator to inform the manipulator operator of any impending unsafe condition detected from the main control board indicators during fuel movement.

In addition to the above safeguards, interlocks are utilized during refueling to insure safe handling. An excess weight interlock is



provided on the lifting hoist to prevent movement of more than one fuel assembly at a time. The spent fuel transfer mechanism can accommodate only one fuel assembly at a time. In addition interlocks on the auxiliary building crane will prevent the trolley from being moved over storage racks containing spent fuel.

The operability requirements for residual heat removal loops will ensure adequate heat removal while in the refueling mode. The requirement for 23 feet of water above the reactor vessel flange while handling fuel and fuel components in containment is consistent with the assumptions of the fuel handling accident analysis.

References:

- (1) FSAR - Section 9.5.2
- (2) Reload Transition Safety Report, Cycle 14
- (3) FSAR - Section 9.3.1

average power tilt ratio shall be determined once a day by at least one of the following means:

- a. Movable detectors
- b. Core-exit thermocouples

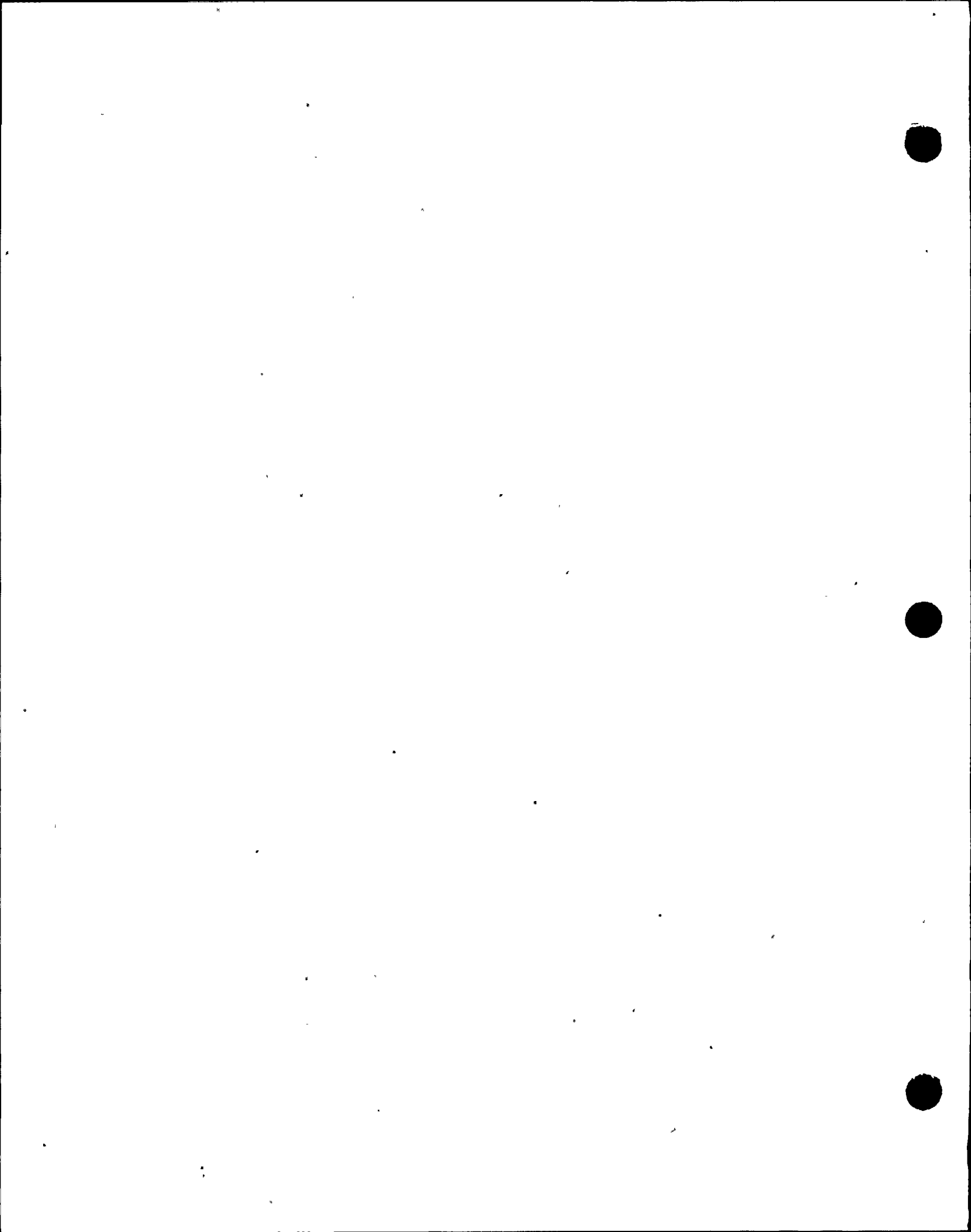
3.10.2.2 Power distribution limits are expressed as hot channel factors. At all times, except during low power physics tests the hot channel factors must meet the following limits:

$$\begin{aligned} F_Q(Z) &= (2.32/P)*K(Z) && \text{for } P \geq .5 \\ F_Q(Z) &= 4.64*K(Z) && \text{for } P \leq .5 \\ F_{\Delta H}^N &= 1.66 [1 + .3(1-P)] && \text{for } 0 \leq P \leq 1.00 \end{aligned}$$

where P is the fraction of rated power at which the core is operating, K(Z) is the function given by Figure 3.10-3, and Z is the height in the core. The measured F_Q^N shall be increased by three percent to yield F_Q . If the measured F_Q or $F_{\Delta H}^N$ exceeds the limiting value, with due allowance for measurement error, the maximum allowable reactor power level and the Nuclear Overpower Trip set point shall be reduced on percent for each percent which $F_{\Delta H}^N$ or F_Q exceeds the limiting value, whichever is more restrictive. If the hot channel factors cannot be reduced below the limiting values within one day, the Overpower ΔT trip setpoint and the Overtemperature ΔT trip setpoint shall be similarly reduced.

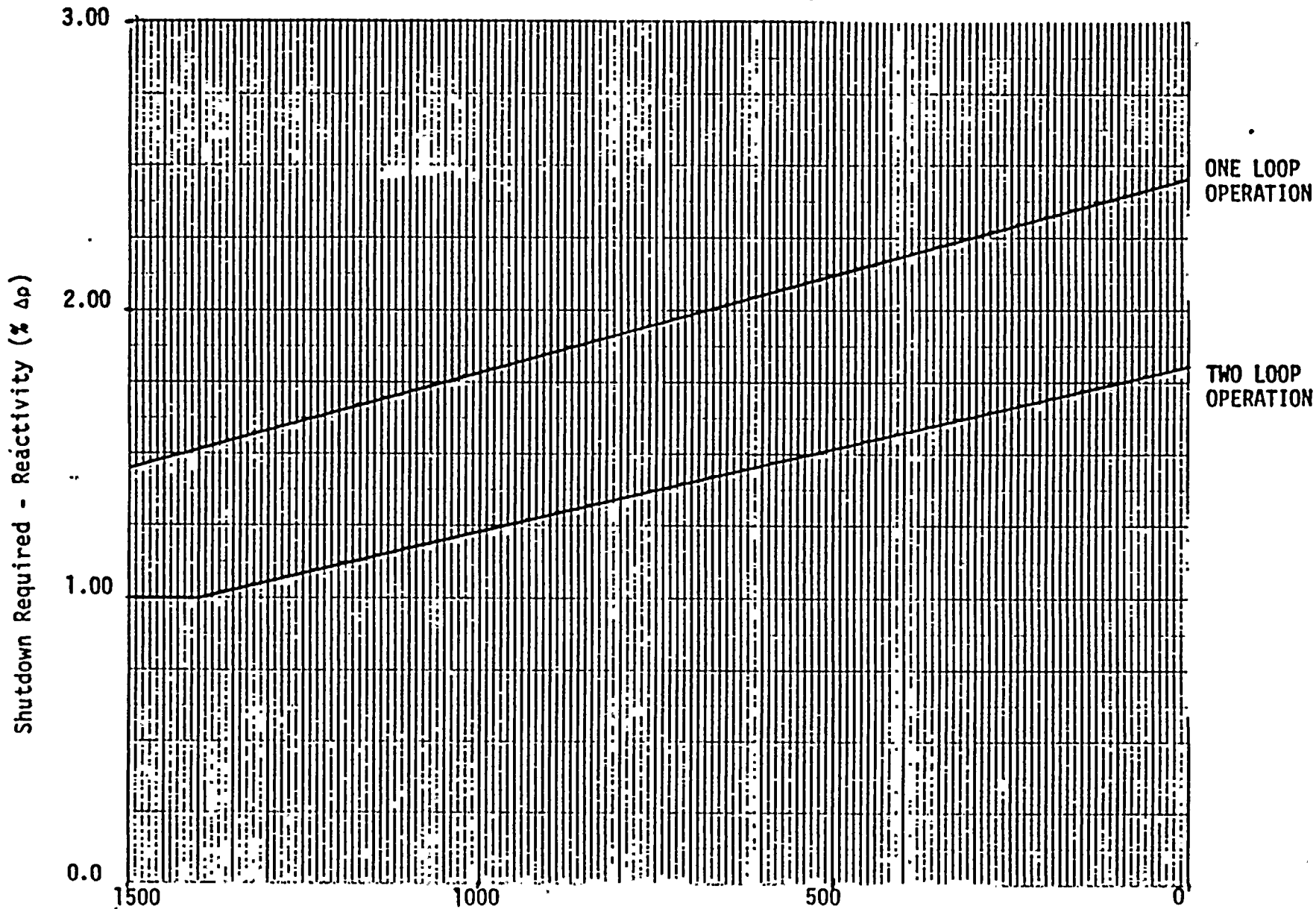
3.10.2.3 Except for physics tests, if the quadrant to average power tilt ratio, exceeds 1.02 but is less than 1.12, then within two hours:

- a. Correct the situation, or
- b. Determine by measurement the hot channel factors, and apply Specification 3.10.2.2, or
- c. Limit power to 75% of rated power.



- 3.10.2.4 If the quadrant to average power tilt ratio exceeds 1.02 but is less than 1.12 for a sustained period of more than 24 hours without known cause, or if such a tilt recurs intermittently without known cause, the reactor power level shall be restricted so as not to exceed 50% of rated power. If the cause of the tilt is determined, continued operation at a power level consistent with 3.10.2.2 above, shall be permitted.
- 3.10.2.5 Except for physics test, if the quadrant to average power tilt ratio is 1.12 or greater, the reactor shall be put in the hot shutdown condition utilizing normal operating procedures. Subsequent operation for the purpose of measuring and correcting the tilt is permitted provided the power level does not exceed 50% of rated power and the Nuclear Overpower Trip "set point is reduced by 50%".
- 3.10.2.6 Following any refueling and at least every effective full power month thereafter, flux maps, using the movable detector system, shall be made to confirm that the hot channel factor limits of Specification 3.10.2.2 are met.
- 3.10.2.7 The reference equilibrium indicated axial flux difference as a function of power level (called the target flux difference) shall be measured at least once per equivalent full power quarter. The target flux difference must be updated at least each equivalent full power month using a measured value or by linear interpolation using the most recent measured value and the predicted value at the end of the cycle life.
- 3.10.2.8 Except during physics tests, control rod exercises, excore detector calibration, and except as modified by 3.10.2.9 through 3.10.2.12, the indicated axial flux difference shall be maintained within $\pm 5\%$ of the target flux difference (defines the target band on axial flux difference). Axial flux difference for power distribution control is defined as the average value for the four excore detectors. If one excore detector is out of service, the remaining three shall be used to derive the average.

3.10-12



COOLANT BORON CONCENTRATION (PPM)

Amendment No. 10, 10
PROPOSED

REQUIRED SHUTDOWN MARGIN

FIGURE 3.10-2

1.5000

1.2500

1.0000

0.7500

0.5000

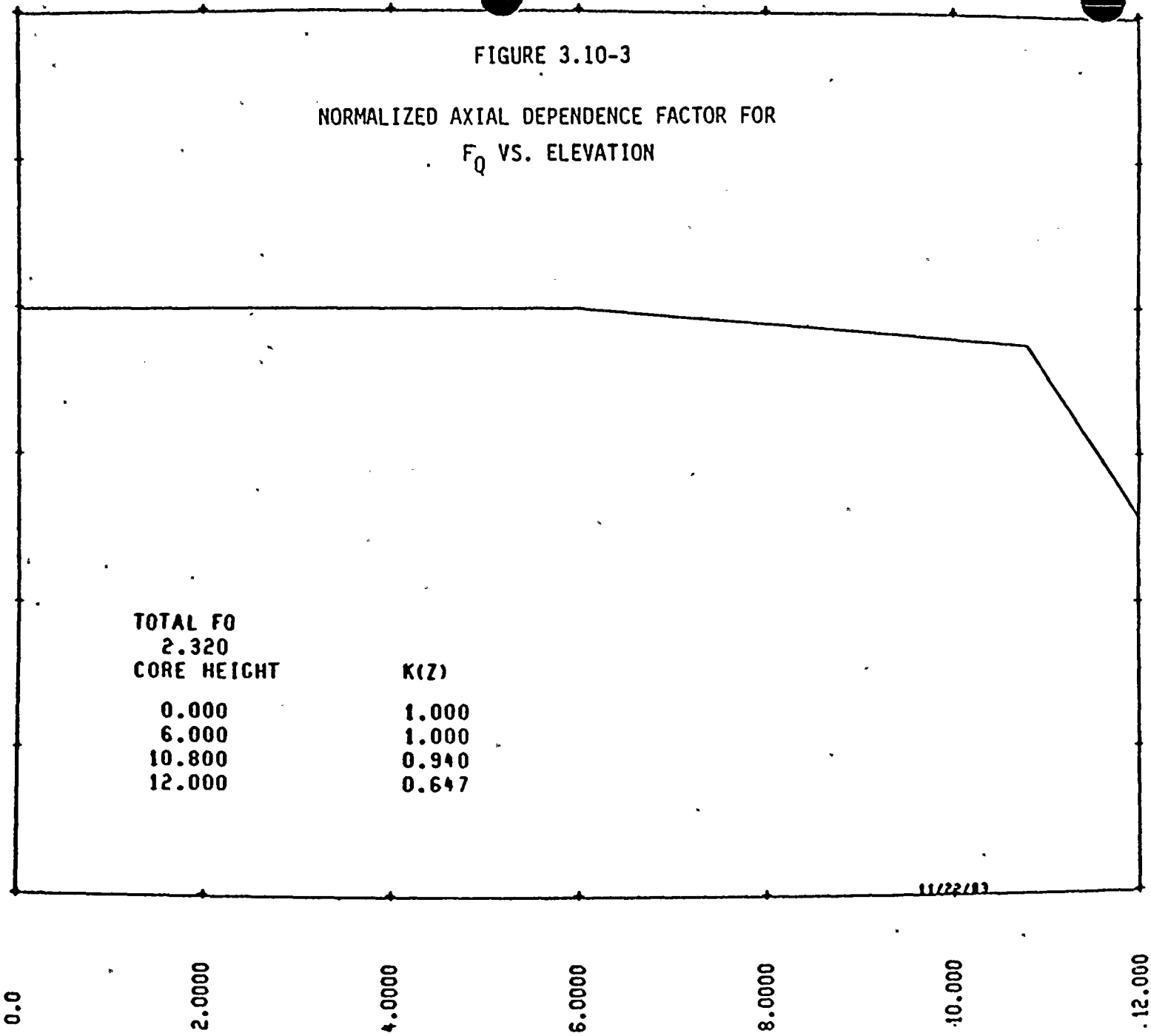
0.2500

0.0

3:11:01
E

FIGURE 3.10-3

NORMALIZED AXIAL DEPENDENCE FACTOR FOR
 F_Q VS. ELEVATION



TOTAL F_Q

2.320

CORE HEIGHT

$K(z)$

0.000

1.000

6.000

1.000

10.800

0.940

12.000

0.647

11/22/83

0.0

2.000

4.000

6.000

8.000

10.000

12.000

CORE HEIGHT (FT)

Amendment No. 18, 19
PROPOSED

Appendix B

Beginning with the reload for Cycle 14, scheduled for insertion in the spring of 1984, Rochester Gas & Electric will use the Westinghouse Optimized Fuel Assembly (OFA) 14 x 14 design with natural uranium axial blankets. In order to store and use fuel assemblies of this design several changes to Ginna Technical Specifications are required.

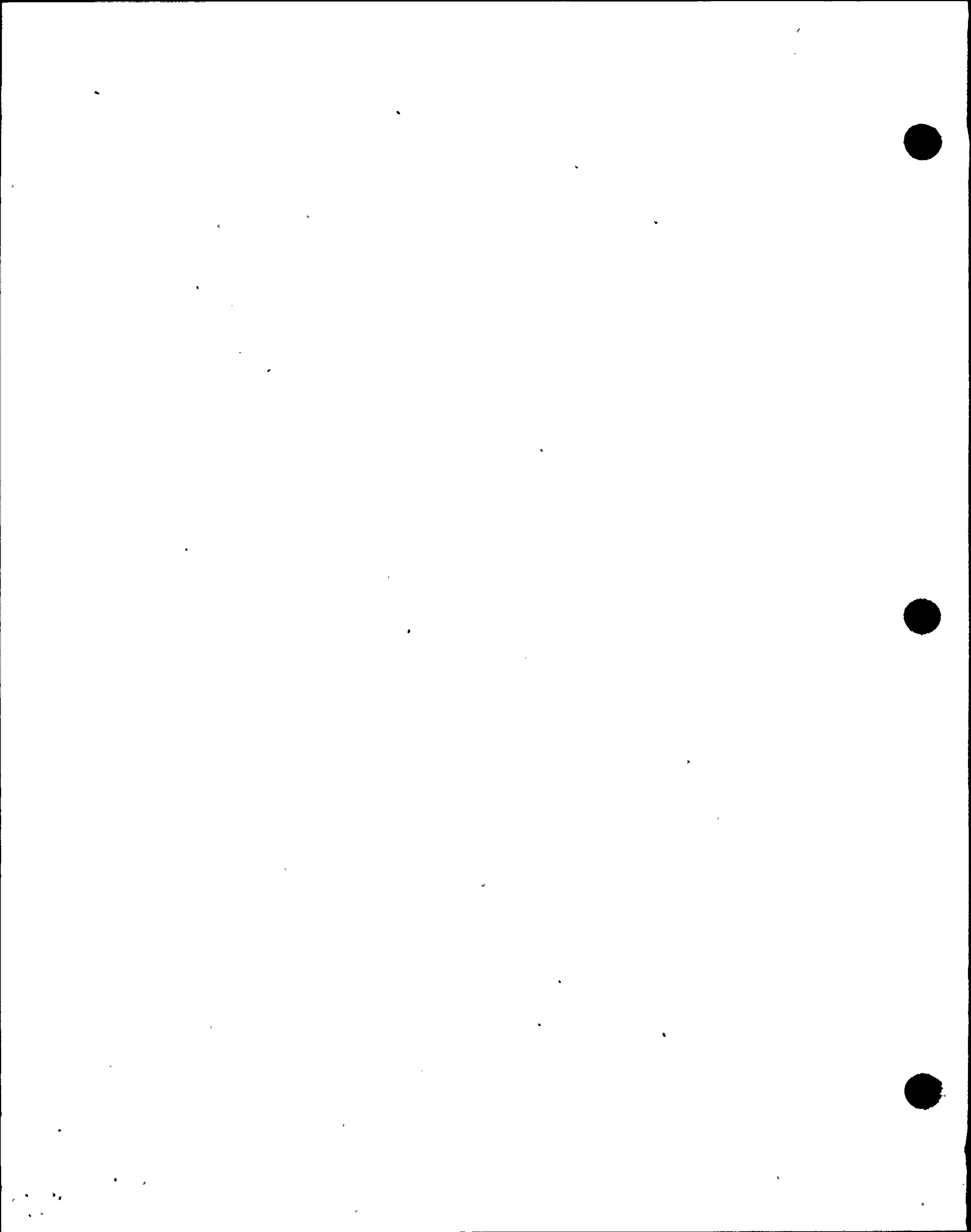
On February 23, 1982, RG&E requested a change to the Technical Specification to permit storage of the higher enrichment OFA fuel in the spent fuel pool. In response to questions from the NRC staff concerning this submittal RG&E provided a criticality analysis of the new fuel storage racks on September 12, 1983.

Attached are three reports comprising the safety analysis prepared by Westinghouse covering the transition from an all Exxon fueled core to a full core of the OFA design. This safety analysis is not cycle specific, but uses parameters which will bound those experienced during the transition period. The safety analysis is composed of a summary of the mechanical, thermal-hydraulic and accident analysis and detailed results of the non-LOCA and LOCA analysis. These analyses incorporate the proposed changes to the Technical Specifications and show that the applicable design criteria for the Exxon and OFA are satisfied..

In brief, the proposed changes to the Technical Specifications are the following:

1. Allowing a positive MTC (+5 pcm °F) up to 70% power.
2. A reduction in shutdown margin at EOC from 1900 pcm to 1800 pcm.
3. A change in the ΔH limits at less than 100% power.
4. A change in the core protection limits (OTAT and OPAT setpoint equations).
5. A deletion of the limits on Target Axial Offset.

The first four changes are incorporated into the accident analyses. The deletion of the limit on target axial offset (TAO) is not treated explicitly in the Westinghouse safety analysis. Worst case power distributions that bound any that would occur during operation are assumed by Westinghouse. For every reload Westinghouse must assure that the potential worst case power distribution does not exceed those assumed in the safety analysis. Therefore, the limitation on TAO is unnecessary. The deletion of the limitations is consistent with the provisions of the Standard Technical Specification.



Four mixed oxide assemblies (MOX) will remain in the core for Cycle 14⁽¹⁾. These assemblies are mechanically identical to the Westinghouse HIPAR design used as reload fuel to Ginna prior to Cycle 8. Exxon previously has performed a safety analysis⁽²⁾ and concluded on a best estimate basis that in a mixed core configuration the flow to each assembly was within one percent of the core average. Applying a DNBR penalty equivalent to a decrease in one percent of flow to the minimum DNBR for Exxon fuel calculated by Westinghouse indicates that sufficient margin to the design DNBR limit exists. Other analyses remain valid, as previously approved by the NRC.⁽¹⁾

- Reference 1. Letter, D. C. Ziemann, USNRC to L. D. White, RG&E
April 15, 1980.
2. R. E. Ginna Nuclear Plant Cycle 8 Safety Analysis
Report, Exxon Nuclear Company, December, 1977.

Attachment C

In accordance with 10CFR 50.91 these changes to the Technical Specifications have been evaluated against three criteria to determine if the operation of the facility in accordance with the proposed amendment would:

1. involve a significant increase in the probability or consequences of an accident previously evaluated; or
2. create the possibility of a new or different kind of accident from any accident previously evaluated; or
3. involve a significant reduction in a margin of safety.

As outlined below, Rochester Gas & Electric submits that the issues associated with this amendment request are outside the criteria of 10CFR 50.91, and therefore, a no significant hazards finding is warranted.

The proposed changes are required to allow the insertion of, and subsequent transition to, a full core of fuel assemblies of the Westinghouse Optimized Fuel Assembly Design (W-OFA). These changes have been incorporated into the assumptions and methodology used by Westinghouse to verify that a Design Basis Event does not cause the appropriate acceptance criteria to be violated. In all cases the assumptions, methods and results are consistent with Westinghouse standard reload safety evaluation techniques and other plant submittals to the NRC for insertion of W-OFA.

Therefore, a no significant hazards finding is warranted for the following reasons:

1. The insertion of W-OFA fuel assemblies will not cause an increase in the probability of any accident, and because the acceptance criteria are satisfied, the consequences of an accident are not increased.
2. The possibility of a new or different kind of accident is not created.
3. While it is not possible to simply compare the results to previous analyses because of the different analytical techniques used by vendors, and the constant evolution of their methods, the Westinghouse analysis has demonstrated that appropriate margin exists between results and the acceptance criteria.

Safety Evaluation
for
R. E. Ginna
Transition to Westinghouse 14x14
Optimized Fuel Assemblies

Edited by
J. C. Miller

Rochester Gas and Electric Corporation
Docket No. 50-244

Approved:



M. G. Ariotti, Manager
Fuel Licensing and Program Support

Westinghouse Electric Corporation
Nuclear Energy Systems
Nuclear Fuel Division
P. O. Box 3912
Pittsburgh, PA 15230



TABLE OF CONTENTS

| <u>Section</u> | Page |
|--|------|
| 1.0 INTRODUCTION | 1-1 |
| 2.0 SUMMARY AND CONCLUSIONS | 2-1 |
| 3.0 MECHANICAL EVALUATION | 3-1 |
| 4.0 NUCLEAR EVALUATION | 4-1 |
| 5.0 THERMAL AND HYDRAULIC EVALUATION | 5-1 |
| 6.0 ACCIDENT EVALUATION | 6-1 |
| 7.0 REFERENCES | 7-1 |
| ATTACHMENT A TECHNICAL SPECIFICATIONS | |
| ATTACHMENT B NON-LOCA ACCIDENT ANALYSIS FSAR CHAPTER 14 | |
| ATTACHMENT C LOCA ACCIDENT ANALYSIS FSAR SECTIONS 14.3.1/14.3.2 | |

LIST OF TABLES

| <u>Table No.</u> | | <u>Page</u> |
|------------------|--|-------------|
| 1 | FSAR Chapter 14 Accident Analysis Sensitivity to Proposed Changes | 6-6 |

LIST OF FIGURES

| <u>Figure No.</u> | | <u>Page</u> |
|-------------------|-----------------------|-------------|
| 1 | R. E. Ginna 14x14 OFA | 3-5 |

1.0. INTRODUCTION

R. E. Ginna is a Westinghouse designed PWR and is currently operating with an all Exxon Nuclear Company (ENC) 14x14 fueled core except for four Westinghouse Mixed Oxide (MOX) assemblies. R. E. Ginna was last supplied with Westinghouse fuel during the cycle 7 reload. Cycle 14 is the first cycle in a transition phase from ENC to Westinghouse 14x14 9 grid Optimized Fuel Assembly (OFA) fuel with core loadings ranging from approximately a 15% OFA and 85% ENC fueled core to eventually an all-OFA-fueled core. The OFA fuel is very similar to the Westinghouse 7 grid 14x14 low parasitic fuel which has had substantial operating performance in a number of nuclear plants.

This report summarizes the safety evaluation/analysis for the region-by-region reload transition from the present ENC-fueled core to an all-Westinghouse OFA-fueled core. This report examines the differences between the OFA and ENC fuel assembly designs and evaluates the effect of these differences on the cores during the transition to an all-OFA-fueled core. The evaluation considers the standard reload design methods described in Reference 1, and the transition effects described in Chapter 18 of Reference 2.

Reference 3 presents the operating experience through December 1981 of OFA demonstration assemblies. There are four 14x14 7 grid demonstration assemblies that have completed two cycles of operation (established burnup ~20,000 MWD/MTU). Post-test examination at the completion of the first cycle of irradiation indicated no abnormalities. However, one demonstration assembly at the end of the second cycle of irradiation was damaged and removed. It was concluded that the cause of the damage was an isolated event and not a generic OFA design problem (see Letter Report IT-83-222, "Failure Investigation of Point Beach Unit 2 OFA Rods," July 1983). The demonstration assemblies will have experienced approximately 35,000 MWD/MTU of burnup in 1984.

Sections 3.0 through 6.0 summarize the Mechanical, Nuclear, Thermal and Hydraulic, and Accident Evaluations, respectively.



2.0 SUMMARY AND CONCLUSIONS

Consistent with the Westinghouse standard reload methodology (Reference 1), parameters are chosen to maximize the applicability of the transition evaluations presented herein for future cycles. The objective of subsequent cycle specific Reload Safety Evaluation Reports (RSE's) will be to verify that applicable safety limits are satisfied based on the reference evaluation/analyses established by this report.

The transition design and safety evaluations presented herein consider the following nominal operating conditions: 1520 Mwt core power, 2250 psia system pressure, 573.5°F vessel average coolant temperature (HFP) at 2250 psia, and 174,000 gpm primary system thermal design flow.

The results of evaluation/analyses and tests described herein lead to the following conclusions:

1. The Westinghouse OFAs are mechanically and hydraulically compatible with the ENC fuel assemblies, control rods, and reactor internals interfaces. All design criteria for the Westinghouse OFA's are satisfied.
2. Generally changes in the nuclear characteristics because of the transition from ENC to OFA fuel will lie within the cycle-to-cycle variations observed for past fuel reload designs. The moderator temperature coefficient is the most significant exception to this. Since the H/U ratio is larger for OFA, the moderator temperature coefficient is more positive than observed in past Westinghouse fueled R. E. Ginna cores. This has been accounted for in the accident evaluations.

3. Demonstration experience with Westinghouse OFAs containing Zircaloy grids provides reason to expect satisfactory operation from OFA Zircaloy grids.
4. The proposed technical specifications changes (Attachment A) are applicable to cores containing any combination of OFA and ENC fuel and plant operating limitations will be satisfied with these proposed changes.
5. A reference is established upon which to base future cycle safety evaluations for Westinghouse OFA reload fuel.

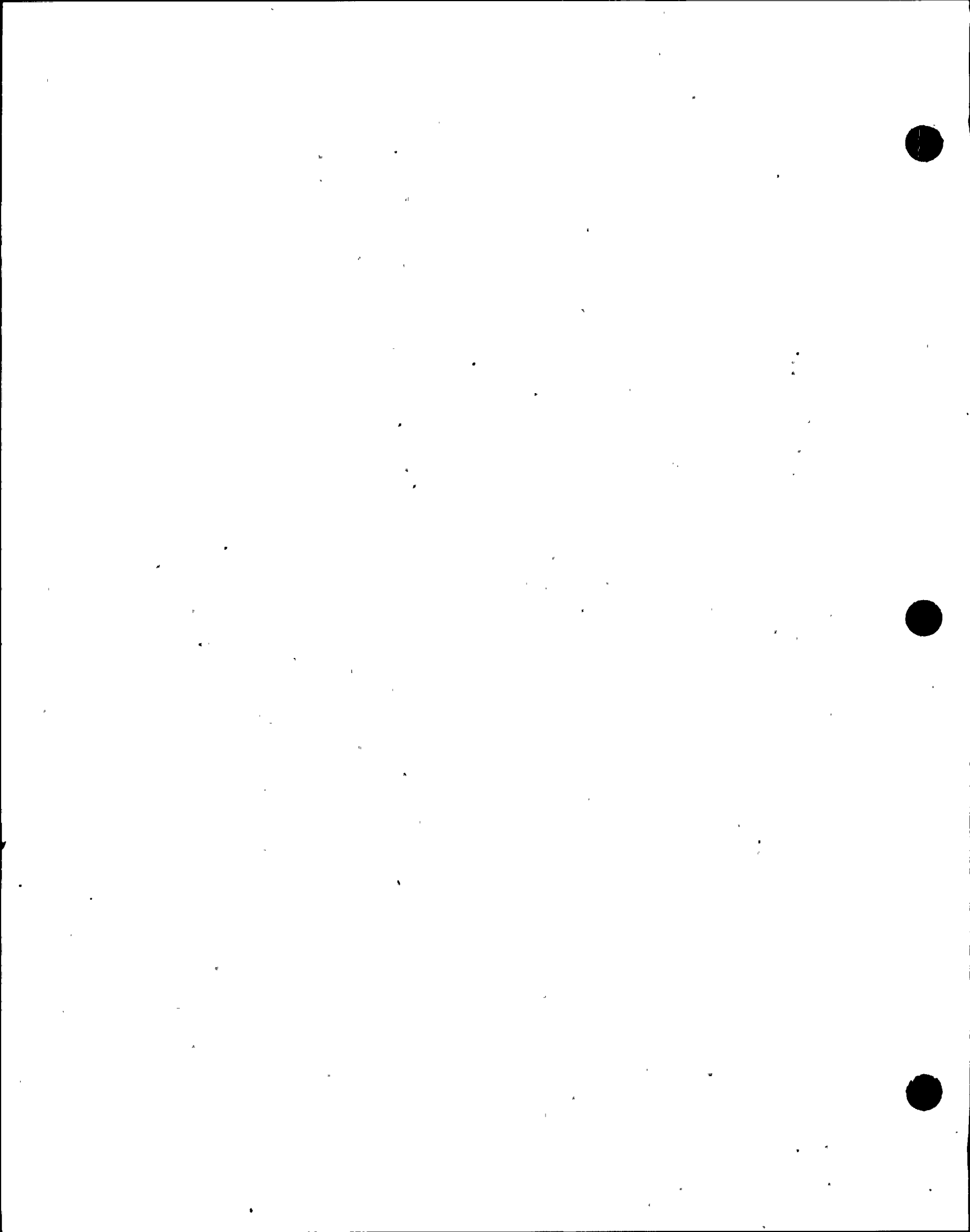
3.0 MECHANICAL EVALUATION

The mechanical design requirements and criteria approved by the NRC for the 17x17 OFA design are described in Reference 2. The 14x14 OFA design meets these same basic design requirements and criteria.

ENC, in establishing their assembly design, demonstrated their fuel's compatibility with the Westinghouse design which was the initial R. E. Ginna fuel. Westinghouse has demonstrated the compatibility of its OFA design with its initial 9 grid design and has performed the reviews described below thereby demonstrating compatibility of the Westinghouse OFA and ENC fuel assemblies.

The similarities between the OFA design and previous Westinghouse fuel include the number of fuel rods, grids, guide thimbles and instrumentation tube. The materials of the top and bottom nozzles, fuel rod, and top and bottom grids are the same in both the Westinghouse OFA and initial designs. The design changes between the two designs include a reduction in fuel rod, guide thimble, and instrumentation tube diameters, and change of material (SS to zirc) and seven intermediate grids made of Zircaloy with the thickness and height increased to retain the required grid strength. In addition to the reduction of the fuel rod diameter, 6.2 inches of natural uranium pellets replace the standard slightly enriched pellets at both ends of the fuel stack (axial blanket). Also changed is the bottom nozzle which includes a locking cup feature which facilitates reconstitutability of the fuel assembly. This is identical to the standard bottom nozzle except for the reconstitution feature. This design change of the bottom nozzle and grid modifications were evaluated and determined to have no impact on the safe operation of the plant and the performance of the fuel. These changes were made as allowed per the requirements of 10CFR50.59.

The fuel design bases and criteria for Westinghouse 14x14 OFA's are the same as those discussed in Sections 4.2 and 4.4.1.2 of Reference 2 for the Westinghouse 17x17 OFA design. Verification that these criteria are



met for Westinghouse fuel in the R. E. Ginna plant is performed using the design methodology and models discussed in Reference 1. An improved thermal safety model, Reference 4, is being used to generate fuel temperatures for safety analysis.

The top and bottom grids of the OFA are fabricated from Inconel and the seven intermediate grids are fabricated from Zircaloy. The elevation of the centerline of each of the OFA grids match that of the ENC grids in order to minimize crossflow during operation. Figure 1 shows the OFA. The Zircaloy grid height is 2.25 inches as compared to the Inconel grid which is 1.5 inches. These dimensional changes were made to compensate for differences in material strength properties. Each fuel rod is given support at six contact points within each grid cell by a combination of support dimples and springs.

The Westinghouse OFA thimble tubes are fabricated from Zircaloy. There are two sections with a large diameter and two with a smaller diameter. The larger diameter at the top permits rapid control rod insertion. Both of the reduced diameter sections produce a dashpot action near the end of the control rod travel to decelerate the control rod and reduce impact forces.

The instrumentation tube is also fabricated from Zircaloy. This tube is of constant diameter and is designed to accept the R. E. Ginna incore instrumentation. The OFA instrumentation tube has a 0.004 inch diametral increase when compared to the ENC assembly instrumentation tube. There is sufficient diametral clearance for the instrumentation thimble to traverse the OFA instrumentation tube.

The OFA top and bottom nozzles are fabricated from stainless steel. Both nozzles index the fuel assembly in the core and direct flow into and out of the assembly through perforated nozzle plates. The axial spacing between the top and bottom nozzle is established to accommodate the growth of the fuel rods due to irradiation effects on the Zircaloy fuel tube. The OFA bottom nozzle design has a reconstitution feature which facilitates easy removal of the nozzle from the fuel assembly.

Holddown of the OFA is provided by four sets of two leaf springs. The Inconel 718 spring design permits both a high spring rate and large travel, which is required to accommodate the difference in thermal expansion between the Zircaloy thimbles and the stainless steel reactor internals. This spring design also accommodates the growth of the Zircaloy thimbles during service and prevents fuel assembly liftoff during normal operation.

The fuel rod fretting evaluation performed on the Westinghouse 14x14 seven grid OFA design has shown that even with no grid spring force acting on the fuel rod by the five Zircaloy grids at end of life, the clad wear criterion is met. Since the R. E. Ginna OFA design contains nine grids including seven Zircaloy grids, considerable additional wear margin exists for the R. E. Ginna fuel design than for the seven-grid OFA design.

The rod bow behavior of the R. E. Ginna OFA is expected to be better than that of the 7 grid Westinghouse fuel assembly. The R. E. Ginna OFA will have reduced grid spring forces due to the Zircaloy grids shorter span lengths and a higher fuel tube thickness-to-diameter ratio than the 7 grid fuel assembly. These design changes should result in reduced rod bow.

The Zircalloy grid spring forces are lower during service than those typically used on Inconel grids. Therefore, lower friction forces are generated by the differential thermal expansion and irradiation growth of the fuel rods. This results in lower loads applied to the skeleton components than are present in the 7 grid Westinghouse assemblies. The skeleton components are conservatively designed to accept these loads with margin.



New thimble-plugging devices and secondary source assemblies were designed to be compatible with the OFA's only. These new core components were designed to accommodate the growth of the fuel assembly and the difference in thermal expansion between the Zircaloy thimbles of the fuel assembly and stainless steel reactor internals. The control rods used in the R. E. Ginna reactor core are compatible with the OFA. The current thimble plugging devices and secondary sources will continue to be used with previously supplied fuel.

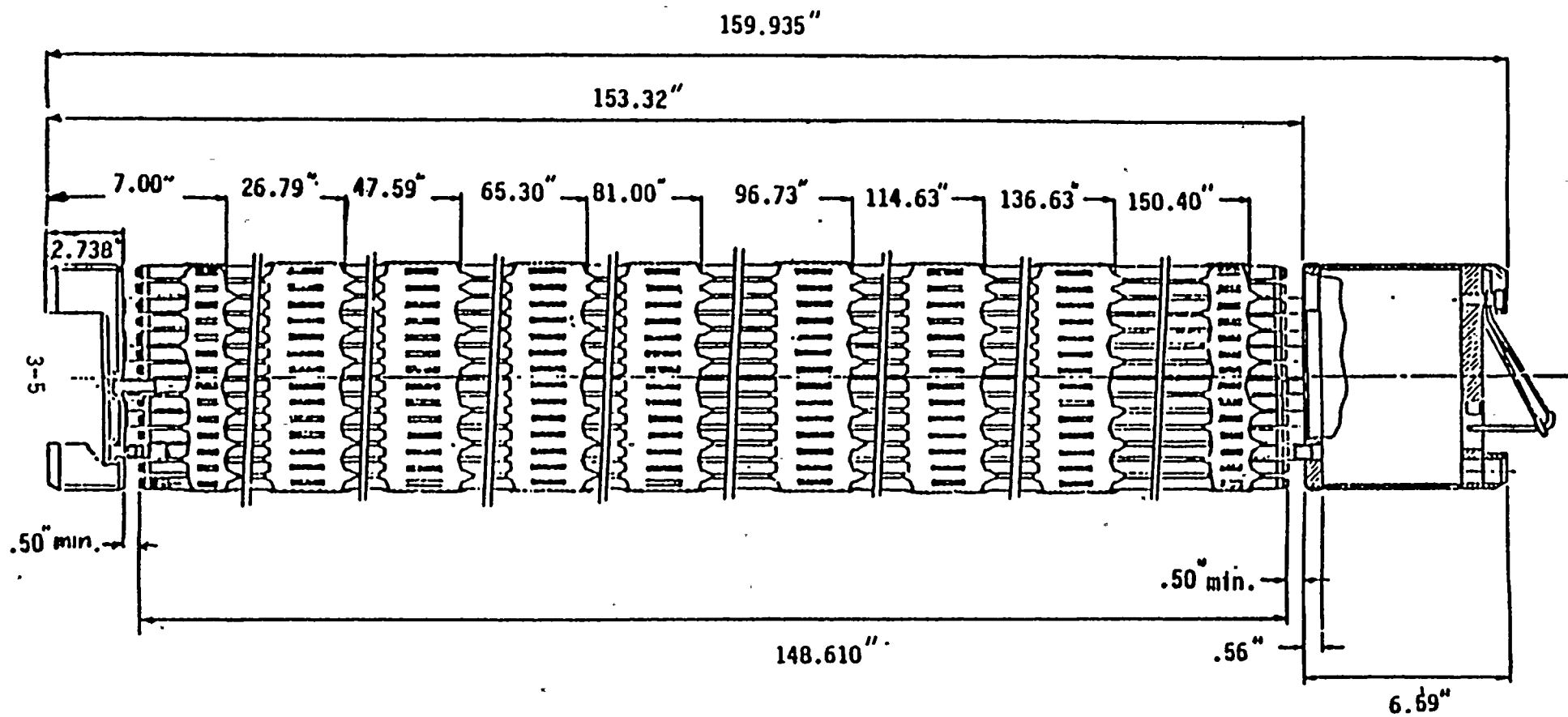


FIGURE 1

RGE 14x14 OPTIMIZED FUEL ASSEMBLY



4.0 NUCLEAR EVALUATION

The key safety parameters evaluated for the conceptual transition and full OFA designs show that the expected ranges of variation for many of the parameters will lie within the normal cycle-to-cycle variations observed for past ENC fuel reload designs. The parameters which fall outside of these ranges are those which are sensitive to fuel type, e.g., the moderator temperature coefficient. The accident evaluation, documented in Section 6.0, has considered ranges of parameters which are appropriate for the transition cycles and beyond.

The methods and core models used in the reload transition analysis are identical to those employed and described in References 1, 2, and 5. These are the same methods and models which have been used in other Westinghouse reload cycle designs. No changes to the nuclear design philosophy, methods, or models are necessary due to the transition to OFA fuel.

A number of changes to the R. E. Ginna Technical Specifications (Attachment A) will be proposed as part of the transition to OFA fuel. Some of these changes, whether directly related to OFA fuel or not, impact the core nuclear design. These changes include: (1) the positive moderator temperature coefficient (MTC) specification; and (2) the 0.3 multiplier in the $F_{\Delta H}$ limit function; (3) a reduction in the required shutdown margin (SDM) to 1.8% $\Delta\rho$.

Power distributions and peaking factors are primarily loading-pattern-dependent. The usual methods, such as enrichment variation can be employed in the transition and full OFA cores to ensure compliance with the peaking factor Technical Specifications.



5.0 THERMAL AND HYDRAULIC EVALUATION

HYDRAULIC COMPATIBILITY

The hydraulic characteristics of an ENC fuel assembly were evaluated by performing tests on a clean, unirradiated ENC fuel assembly at the R. E. Ginna site using the Westinghouse Fuel Assembly Compatibility Systems (FACTS) loop. A similar test was conducted on a clean unirradiated seven grid Westinghouse OFA in the same loop. Since the Westinghouse OFA design for R. E. Ginna is slightly different from the regular seven grid OFA tested (two extra mixing vane grids and a slightly shorter fuel rod length) the effect of these design differences on the hydraulic characteristics of the test assembly was addressed.

The results showed that the net mismatch in overall core loss coefficient was less than one percent. It was therefore concluded that the two assemblies are hydraulically compatible.

CALCULATIONAL METHODS

The calculational methods used in the analysis employ three changes from methods presently employed for the R. E. Ginna thermal-hydraulic analysis. These methods are: (1) the THINC IV computer code, (2) the WRB-1 DNB Correlation for the OFA, and (3) the Improved Thermal Design Procedure (ITDP).

The THINC IV program is used to perform thermal-hydraulic calculations. The THINC IV code calculates coolant density, mass velocity, enthalpy, void fractions, static pressure, and DNBR distributions along flow channels within a reactor core under all expected operating conditions. The THINC IV code is described in detail in References 8 and 9.

In this application, the WRB-1 DNB Correlation (Reference 6) is employed in the thermal-hydraulic design of the Westinghouse OFA. The WRB-1 Correlation (References 6 and 13) provides a significant improvement in Critical Heat Flux (CHF) predictions over previous DNB correlations.

The 17x17 OFA DNB tests showed that the WRB-1 Correlation correctly accounted for the geometry changes in going from the 17x17 0.374" rod OD design to the 17x17 0.360" rod OD design, and that the design limit of 1.17 was still applicable, Reference 13. The 14x14 OFA design involved very similar geometry changes from the 7 grid 14x14 STD fuel design, namely, the reduction of the rod OD from 0.422" to 0.400" and the incorporation of a grid design with an increased height and strap thickness due to the change from Inconel to Zircaloy. Confirmatory DNB tests performed on the 14x14 OFA typical cell geometry verified that the WRB-1 Correlation accurately predicted CHF values for this geometry type and that the design limit of 1.17 was still appropriate.

The W-3 DNBR Correlation (Reference 14 and 15) was used in the design of the ENC fuel assembly. A correlation limit DNBR of 1.30 is applicable.

The design method employed to meet the DNB design basis is the ITDP, Reference 7. Uncertainties in plant operating parameters, nuclear and thermal parameters, and fuel fabrication parameters are considered statistically such that there is at least a 95 percent probability that the minimum DNBR will be greater than or equal to DNBR for the peak power rod. Plant parameter uncertainties are used to determine the plant DNBR uncertainty. This DNBR uncertainty, combined with the DNBR limit, establishes a design DNBR value which must be met in plant safety analyses. Since the parameter uncertainties are considered in determining the design DNBR value, the plant safety analyses are performed using values of input parameters without uncertainties. In addition, the limit DNBR values are increased to values designated as the safety analysis limit DNBR's. The plant allowance available between the safety analysis limit DNBR values and the design limit DNBR values

is not required to meet the design basis. The allowance will be used for flexibility in the design and operation of this plant.

The DNBR margin is defined as

$$\text{Safety analysis DNBR value} = \frac{\text{Design DNBR value}}{1 - \text{Margin}}$$

The table below indicates the relationship between the correlation limit DNBR, design limit DNBR, and the safety analysis limit DNBR values used for this design.

| | <u>W</u> 14x14 OFA | | ENC 14x14 | |
|-----------------------|--------------------|---------|-----------|---------|
| | Typical | Thimble | Typical | Thimble |
| Correlation Limit | 1.17 | 1.17 | 1.30 | 1.30 |
| Design Limit | 1.34 | 1.33 | 1.58 | 1.50 |
| Safety Analysis Limit | 1.52 | 1.51 | 1.62 | 1.54 |

The margin between the design limit and the safety analysis limit DNBR is more than enough to offset the rod bow penalty and the transition core penalty.

ROD BOW

The OFA for R. E. Ginna has nine grids and an active fuel length of 141.4 inches. Based on the current NRC approved licensing basis, Reference 16, the fractional closure at any given burnup for the OFA for R. E. Ginna can be compared to that of the 7-grid assembly. The relevant parameters for making such a comparison are L^2/I (L = span length between grids, I = fuel rod moment of inertia) and the initial

rod-to-rod gap. The 1/I ratio is higher for the OFA, but the initial rod-to-rod gap is also larger, therefore, these efforts offset each other. The fractional closure at any burnup for the 9-grid Westinghouse OFA can be obtained by direct L^2 scaling from that of the 7-grid assembly.

The results indicated that a maximum rod bow penalty of 4.2% DNBR is applicable for the R. E. Ginna OFA. Sufficient margin between the safety analysis limit DNBR and the design limit DNBR has been maintained to accommodate this penalty as well as the transition core DNB penalty.

The ENC fuel assembly would be expected to have less gap closure than the Westinghouse OFA, due to the ENC fuel's thicker cladding as shown in Reference 17. Data obtained by other investigations, References 18 and 19, show that gap closures up to 55% have no measurable effect on DNB. Therefore, no resultant rod bow DNBR penalty is required for ENC fuel.

TRANSITION CORE DNB METHODOLOGY

The OFA has a larger hydraulic diameter and flow area compared to the ENC fuel assembly. Thus, if it is assumed that the same mass flow exists in an ENC assembly and an OFA and that there is no allowance for flow redistribution to occur, the ENC fuel assembly will have a higher velocity in the rod bundle. The higher velocity, together with the lower value of rod bundle hydraulic diameter, will cause the rod bundle pressure drop to be higher in the ENC fuel assembly. Thus, for the same value of mass flow rate into an adjacent set of ENC and OFA, the flow would have a tendency to redistribute from the ENC to the OFA in the rod bundle region.

In the gridded regions, however, the OFA has a higher value of mixing vane grid loss coefficient. This will induce localized flow redistribution from the OFA to the ENC at the axial zones near the mixing vane grid positions.



The net consequence of this flow redistribution on DNBR is primarily due to the effect this redistribution has on the hot channel mass velocity and the local quality. Depending on the axial location of the minimum DNBR, a DNB penalty can be postulated on either type of fuel assembly when compared to a full core of similar fuel.

A 2% transition core DNB penalty, on the Westinghouse OFA and a 1% DNB penalty on the ENC fuel were determined to be applicable by analyzing different assembly loading patterns at various core conditions in a manner consistent with previously approved analysis, Reference 20.

Thus the transition cores will be analyzed in the following manner: the ENC fuel in a transition core will be analyzed as a full core of ENC fuel applying a 1% DNB transition core penalty; and the OFA fuel in a transition core will be analyzed as full core of OFA fuel applying a 2% DNB transition core penalty.

The DNB margins previously described for the ENC and OFA fuel are more than enough to accommodate the transition core penalty and the rod bow penalty.



6.0 ACCIDENT EVALUATION

This section addresses the impact on accident analyses of the following proposed changes for R. E. Ginna.

- OFA
- Positive MTC
- $F_{\Delta H}$ Multiplier Change

A revised FSAR Chapter 14 given in Attachment B contains the descriptions, methodology, results and conclusion for each accident reanalyzed.

OFA

The principal mechanical design characteristic of the OFA design which could have an effect on accidents is the smaller fuel rod. This leads to a higher fuel rod temperature, surface heat flux, and a DNB penalty. The larger hydraulic diameter and lower coolant flow velocity cause a reduction in heat transfer after DNB. The smaller fuel rod also leads to a faster heatup rate for severe reactivity transients such as Rod Cluster Control Assembly (RCCA) ejection.

As a result of the smaller fuel rod, for the same power level, the OFA design will have a lower DNB ratio than the initial design.

The DNB penalty was offset for the OFA core through the use of the WRB-1 DNB Correlation, Reference 6, and the ITDP, Reference 7. Those transients impacted by the OFA design are shown in Table 1. A discussion of Loss-of-Coolant Accidents (LOCA) is addressed later in this section.

Positive MTC

The present R. E. Ginna Technical Specifications require the MTC to be zero or negative at all times while the reactor is critical. This

requirement is overly restrictive, since a small positive coefficient at reduced power levels could result in a significant increase in fuel cycle flexibility, but would have only a minor effect on the safety analysis of the accident events presented in the FSAR.

The proposed Technical Specification change, given in Attachment A, allows a +5 pcm/°F MTC below 70 percent of rated power, changing to a 0 pcm/°F MTC at 70 percent power and above. A power-level dependent MTC was chosen to minimize the effect of the specification on postulated accidents at high power levels. Moreover, as the power level is raised, the average core water temperature becomes higher as allowed by the programmed average temperature for the plant, tending to make the moderator coefficient more negative. Also, the boron concentration can be reduced as xenon builds into the core. Thus, there is less need to allow a positive coefficient as full power is approached. As fuel burnup is achieved, boron is further reduced and the MTC will become negative over the entire operating power range.

The impact of a positive MTC on the accident analyses presented in Chapter 14 of the R. E. Ginna FSAR, Reference 10, has been assessed. Those incidents which were found to be sensitive to minimum or near-zero moderator coefficients were reanalyzed. In general, these incidents are limited to transients which cause reactor coolant temperature to increase. With the exceptions below, the analyses presented herein were based on a +5 pcm/°F MTC, which was assumed to remain constant for variations in temperature.

The bank withdrawal from subcritical and control rod ejection analyses are based on a coefficient which is at least +5 pcm/°F at zero power nominal average temperature, and which becomes less positive for higher temperatures. This is necessary since the TWINKLE computer code, on which the analysis is based, is a diffusion-theory code rather than a point-kinetics approximation and the moderator temperature feedback cannot be artificially held constant with temperature. For all

accidents which are reanalyzed, the assumption of a positive MTC existing at full power is conservative, since as noted in Attachment A, the proposed Technical Specification requires that the coefficient be zero or negative at or above 70 percent power.

Accidents not reanalyzed included those resulting in excessive heat removal from the reactor coolant system for which a large negative MTC is conservative, and those for which heatup effects following reactor trip are investigated, which are not sensitive to the moderator coefficient.

F_{ΔH} Multiplier Change

A proposed change from K=0.2 to K=0.3 in the following equation for the Nuclear Hot Channel Factor (F_{ΔH}^N) was evaluated with regard to its effect on accident analyses:

$$F_{\Delta H}^N \leq 1.66 [1.0 + .3(1-P)]$$

where P is the fraction of full power and .3 is the power correction constant.

The effect on accident analyses is through the core safety limits at very high pressure and low power levels. Since the steam generator safety valves prevent the plant from reaching these limiting conditions, the protection setpoints are unaffected by this change. The change sometimes impacts the axial offset envelope such that the f(ΔI) changes. However, no credit for the f(ΔI) protection is assumed in the accident analyses. Therefore, the safety analyses are not impacted by the proposed F_{ΔH} multiplier change.



Non-LOCA

The impact of the proposed changes as identified earlier in this section has been assessed for the non-LOCA as provided in Chapter 14 of the R. E. Ginna FSAR given in Attachment B. The following accidents have been reanalyzed:

- Uncontrolled RCCA Bank Withdrawal From a Subcritical Condition
- Uncontrolled RCCA Bank Withdrawal at Power
- RCCA Drop
- Chemical and Volume Control System Malfunction
- Startup of an Inactive Reactor Coolant Loop
- Reduction in Feedwater Enthalpy Incident
- Excessive Load Increase Incident
- Loss of Reactor Coolant Flow/Locked Rotor
- Loss of External Electrical Load
- Loss of Normal Feedwater/Station Blackout
- Rupture of a Steam Pipe
- Rupture of a Control Rod Mechanism Housing-RCCA Ejection

For each of the accidents analyzed, it was found that the appropriate safety criteria are met.

Large Break LOCA

The large break LOCA analysis for R. E. Ginna, applicable to transition and full OFA core cycles, was reanalyzed due to the differences between ENC and Westinghouse OFA designs. This analysis is consistent with the methodology employed in WCAP-9500, Reference Core Report 17x17 Optimized Fuel Assembly. The currently approved 1981 large break Emergency Core Cooling System (ECCS) Evaluation Model, Reference 11, was utilized for a spectrum of cold leg breaks. The revised PAD Fuel Thermal Safety Model, Reference 4, generated the initial fuel rod conditions. The R. E. Ginna analysis was performed for an assumed steam generator tube plugging level of 12%.

A revised FSAR Chapter 14.3.2 given in Attachment C contains a full description of the methods and assumptions utilized for the Westinghouse OFA ECCS LOCA analysis, and the results of the analyses.

The large break OFA LOCA analysis for R. E. Ginna utilizing the currently approved 1981 evaluation model resulted in a PCT of 1833°F for the 0.4 C_D LOCA case at a total peaking factor of 2.32. Addition of the UPI penalty of 21°F results in a final PCT of 1854°F.

The small impact of crossflow for transition core cycles is conservatively evaluated as at most a 4°F effect on the Westinghouse fuel, which is easily accommodated in the margin to 10 CFR 50.46 limits.

Small Break LOCA

The small break LOCA analysis for R. E. Ginna applicable to transition and full OFA core cycles, was reanalyzed due to the differences between ENC and Westinghouse OFA designs. This is consistent with the methodology employed in WCAP-9500. The currently approved October 1975 small break ECCS evaluation model was utilized for a spectrum of cold-leg breaks, Reference 12. The revised PAD fuel thermal safety model generated the initial fuel rod conditions.

The revised FSAR Chapter 14.3.1, given in Attachment C, contains a full description of the analysis and assumption utilized for the Westinghouse OFA ECCS LOCA analysis.

The small break OFA LOCA analysis for R. E. Ginna utilizing the currently approved 1975 Small Break Evaluation model resulted in a PCT of 1092°F for the 6 inch diameter cold leg break. The analysis assumed the worst small break power shape consistent with a LOCA F_q envelope of 2.32 at core midplane elevation and 1.5 at the top of the core.

Analyses show that the high and low head portions of the ECCS, together with the accumulators, provide sufficient core flooding to keep the calculated PCT well below the required limits of 10 CFR 50.46. Adequate protection is therefore afforded by the ECCS in the event of a small break LOCA.

TABLE 1

FSAR CHAPTER 14 ACCIDENT ANALYSIS
SENSITIVITY TO PROPOSED CHANGES

| <u>Accidents</u> | <u>OFA</u> | <u>+MTC</u> |
|---|------------|-------------|
| 1. Uncontrolled Rod Withdrawal from a Subcritical Condition FSAR Section 14.1.1. | X | X |
| 2. Uncontrolled RCCA With- drawal at Power. FSAR Section 14.1.2. | X | X |
| 3. Rod Cluster Control Assembly (RCCA) Drop FSAR Section 14.1.4. | X | |
| 4. Chemical and Volume Control System Mal- function FSAR Section 14.1.5. | X | X |
| 5. Startup of an Inactive Reactor Coolant Loop FSAR Section 14.1.7. | | |
| 6. Reduction in Feedwater Enthalpy Incident FSAR Section 14.1.10. | X | |
| 7. Excessive Load Increase Incident FSAR Section 14.1.11. | X | X |

TABLE 1 (Con't)

FSAR CHAPTER 14 ACCIDENT ANALYSIS
 SENSITIVITY TO PROPOSED CHANGES
 (CONTINUED)

| <u>Accidents</u> | <u>OFA</u> | <u>+MTC</u> |
|---|------------|-------------|
| 8. Loss of Reactor Coolant Flow FSAR Section 14.1.6. | X | X |
| 9. Loss of External Electrical Load FSAR Section 14.1.8. | X | X |
| 10. Loss of Normal Feed- water FSAR Section 14.1.9. | | |
| 11. Loss of All AC Power to the Station Aux- iliaries FSAR Section 14.4.12. | | |
| 12. Rupture of a Steam Pipe FSAR Section 14.2.5. | X | |
| 13. Rupture of a Control Rod Mechanism Housing- RCCA Ejection FSAR Section 14.2.6. | X | X |
| 14. LOCA FSAR Section 14.3.1 | X | |

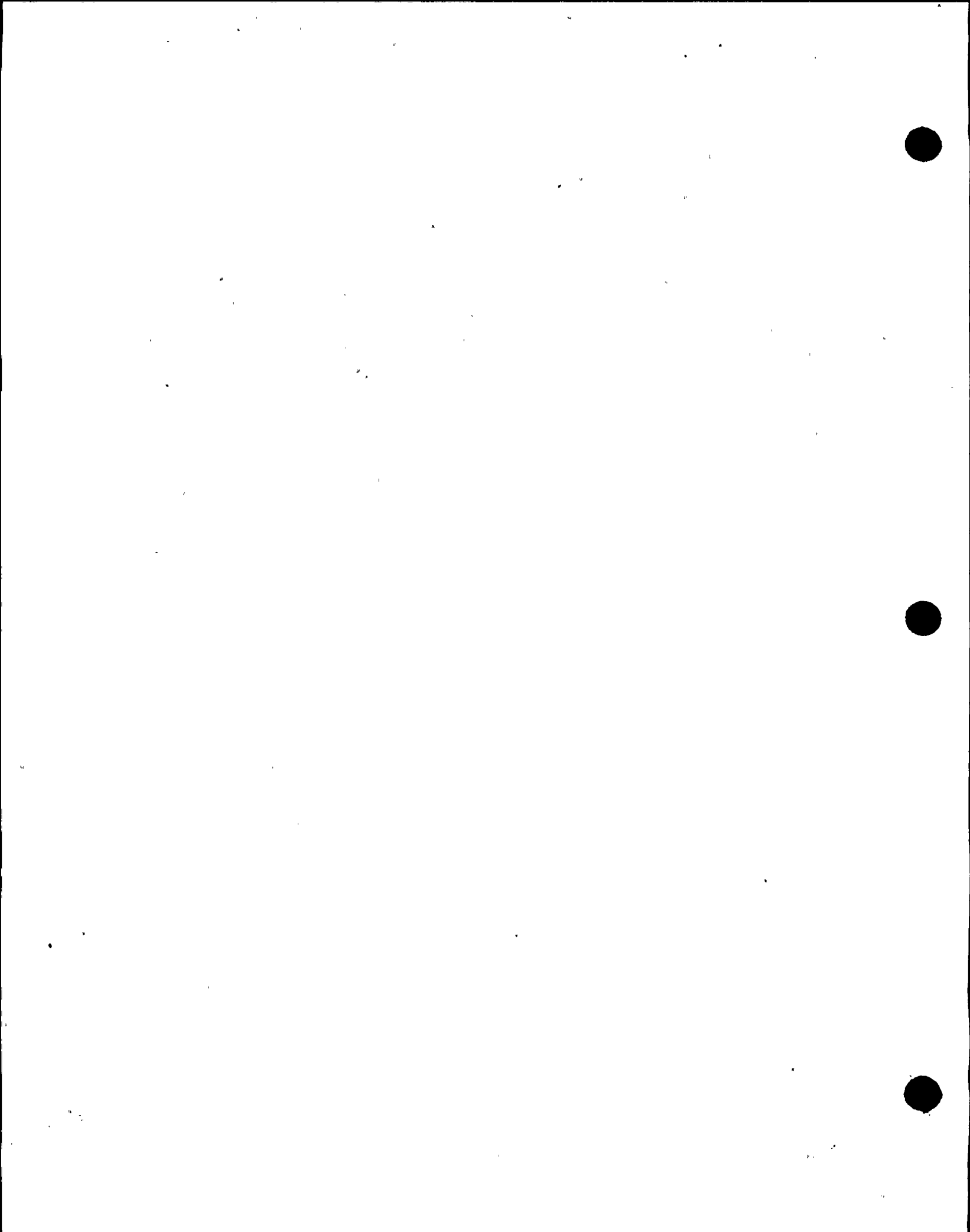


7.0 REFERENCES

1. Bordelon, F. M., et al., "Westinghouse Reload Safety Evaluation Methodology," WCAP-9272 (Proprietary) and WCAP-9273 (Non-Proprietary), March 1978.
2. Davidson, S. L.; Iorii, J. A., "Reference Core Report - 17x17 Optimized Fuel Assembly," WCAP-9500-A, May 1982.
3. Skaritka, J.; Iorii, J. A., "Operational Experience with Westinghouse Cores," WCAP-8183, Revision 12, August 1983.
4. Letter from E. P. Rahe (Westinghouse) to C. O. Thomas (NRC), NS-EPR-2673, "Westinghouse Revised PAD Code Thermal Safety Model," WCAP-8720, Addendum 2, October 27, 1982, (Proprietary).
5. Camden, T. M., et al., "PALADON-Westinghouse Nodal Computer Code," WCAP-9485A (Proprietary) and WCAP-9486A (Non-Proprietary), December 1979, and Supplement 1, September 1981.
6. Motley, F. E., et al., "New Westinghouse Correlation WRB-1 For Predicting Critical Heat Flux In Rod Bundles With Mixing Vane Grids," WCAP-8762, July 1976.
7. Chelemer, H., et al., "Improved Thermal Design Procedure," WCAP-8567, July 1975.
8. Chelemer, H., et al., "THINC IV - An Improved Program for Thermal-Hydraulic Analysis of Rod Bundle Cores," WCAP-7956, June 1973.
9. Hochreiter, L. E., et al., "Application of the THINC IV Program to PWR Design," WCAP-8054, September 1973.
10. Final Safety Analysis Report, R. E. Ginna Nuclear Power Plant, Docket No. 50-244.

7.0 REFERENCES (Continued)

11. Eicheldinger, C., "Westinghouse ECCS Evaluation Model, 1981 Version," WCAP-9200-P-A (Proprietary), WCAP-9221-A (Non-Proprietary) Revision 1, 1981.
12. Skwarek, R. J.; Johnson, W. J.; and Meyer, P. E., "Westinghouse Emergency Core Cooling System Small Break," October 1975 Model, WCAP-8970-P-A (Proprietary) and WCAP-8971-A (Non-Proprietary), January 1979.
13. Davidson, S. L.; Iorii, J. A. (Eds.), "Verification Testing and Analyses of the 17x17 Optimized Fuel Assembly," WCAP-9401-P-A and WCAP-9402, March 1979.
14. Tong, L. S., "Critical Heat Fluxes in Rod Bundles, Two Phase Flow and Heat Transfer in Rod Bundles," Annual ASME Winter Meeting, November 1969, p. 3146.
15. Tong, L. S., "Boiling Crisis and Criteria Heat Flux, ...," AEC Office of Information Services, TID-25887, 1972.
16. Letter from R. A. Clark (NRC) to W. G. Council Northeast Nuclear Engineering Company, Subject: Fuel Safety Evaluation of Millstone, Unit No. 2 BSR, NRC Docket No. 50-336.
17. Letter from G. F. Owsley (ENC) to T. A. Ippolito (NRC), XN-75-32, Supplement 1, "Computational Procedure for Evaluating Fuel Rod Bowing," July 17, 1979.
18. Markowski, et al., "Effect of Rod Bowing on CHF in PWR Fuel Assemblies," ASME paper 77-HT-91.



7.0 REFERENCES (Continued)

19. Letter from J. H. Taylor to S. A. Varga, "Status Report on R&D Programs described in Semi-Annual Topical Report BAW-10097A," Revision 2, November 13, 1978.

20. Letter from C. O. Thomas (NRC) to E. P. Rahe (Westinghouse), "Supplemental Acceptance Number 2 for Referencing of Licensing Topical Reports WCAP-9500 and WCAPs 9401/9402," January 24, 1983.

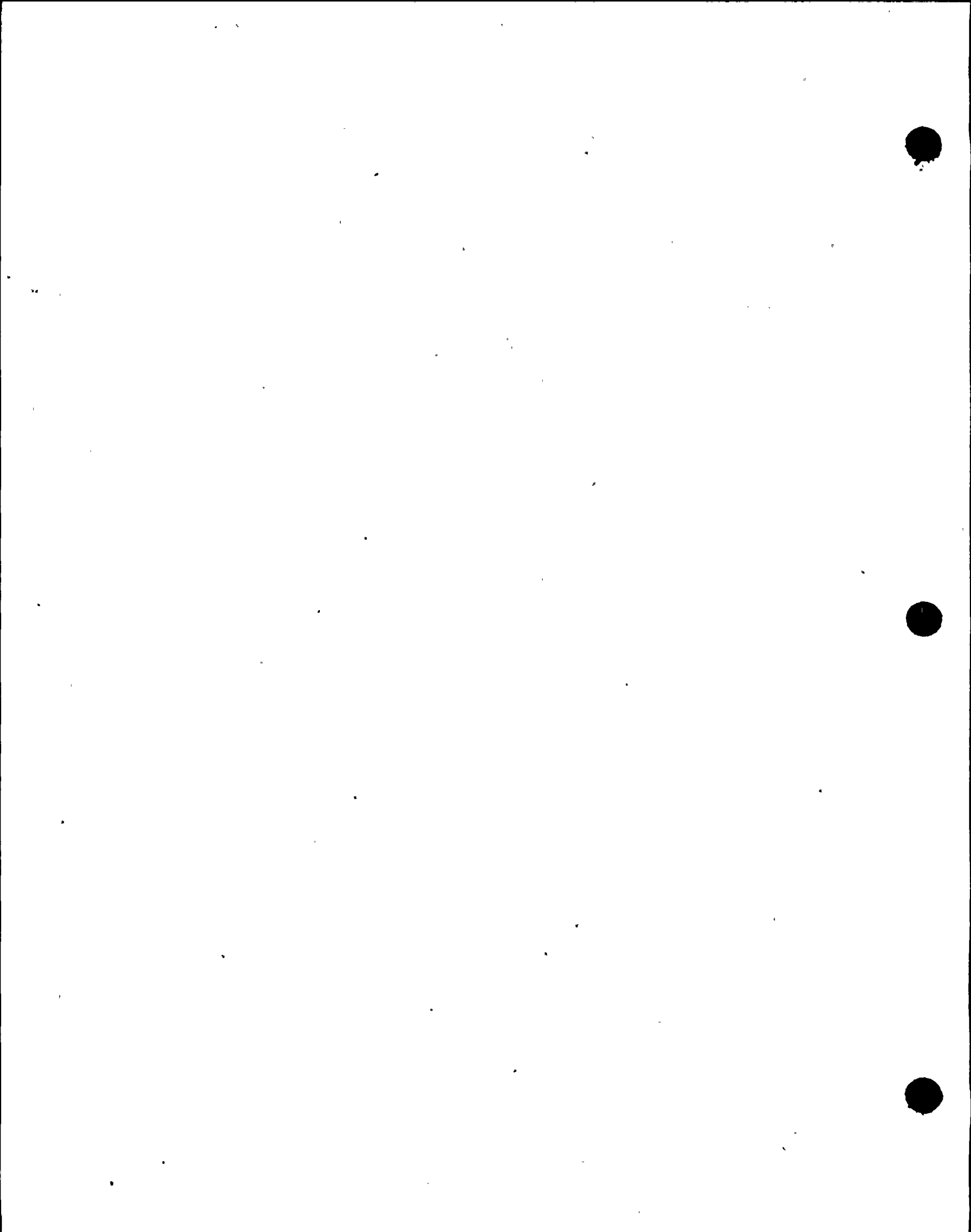
ATTACHMENT A

A list of the Technical Specification changes required by the use of the OFA design and a positive MTC is provided as Attachment A to the Application for Amendment to Operating License.



ATTACHMENT B

NON-LOCA ACCIDENT ANALYSIS RESULTS
FSAR CHAPTER 14



ATTACHMENT B
NON-LOCA SAFETY ANALYSIS

Presented in Attachment B are those non-LOCA accident analyses of the R. E. Ginna FSAR Chapter 14 impacted by the proposed changes as determined in Section 5. Provided below is a discussion of initial conditions, assumptions, and computer codes used to analyze the accidents presented. Further discussion is provided for each individual analysis. Section numbers in this appendix correspond to those used in the FSAR.



TABLE OF CONTENTS

| Section | Description | Page |
|---------|---|-----------|
| 14.0 | Accident Analysis | 14-1 |
| 14.1.1 | Uncontrolled RCCA Withdrawal From A Subcritical Condition | 14.1.1-1 |
| 14.1.2 | Uncontrolled RCCA Withdrawal At Power | 14.1.2-1 |
| 14.1.4 | Rod Cluster Control Assembly (RCCA) Drop | 14.1.4-1 |
| 14.1.5 | Chemical and Volume Control System Malfunction | 14.1.5-1 |
| 14.1.6 | Loss of Reactor Coolant Flow | 14.1.6-1 |
| 14.1.8 | Loss of External Electrical Load | 14.1.8-1 |
| 14.1.10 | Excessive Heat Removal Due To Feedwater Temperature Decrease | 14.1.10-1 |
| 14.1.11 | Excessive Load Increase Incident | 14.1.11-1 |
| 14.2.5 | Rupture of a Steam Pipe | 14.2.5-1 |
| 14.2.6 | Rupture of a Control Rod Mechanism Housing-RCCA Ejection | 14.2.6-1 |



LIST OF TABLES

| Table | Description | Page |
|----------|--|-----------|
| 14-1 | Summary of Initial Conditions and Computer Codes Used | 14-10 |
| 14-2 | Nominal Values of Pertinent Plant Parameters for Non-LOCA Accident Analysis | 14-12 |
| 14-3 | Trip Points and Time Delays to Trip Assumed in Accident Analysis | 14-13 |
| 14-4 | Determination of Maximum Overpower Trip Point - Power Range Neutron Flux Channel - Based on Nominal Setpoint Considering Inherent Instrument Errors | 14-15 |
| 14.1.1-1 | Time Sequence of Events for Uncontrolled RCCA Withdrawal From a Subcritical Condition | 14.1.1-8 |
| 14.1.2-1 | Time Sequence of Events for Uncontrolled RCCA Withdrawal at Power | 14.1.2-8 |
| 14.1.6-1 | Time Sequence of Events for Loss of Reactor Coolant Flow | 14.1.6-10 |
| 14.1.6-2 | Summary of Limiting Results for Locked Rotor Accident | 14.1.6-11 |
| 14.1.6-3 | Time Sequence of Events for Locked Rotor Incident | 14.1.6-12 |

LIST OF TABLES
(continued)

| Table | Description | Page |
|-----------|---|-----------|
| 14.1.8-1 | Time Sequence of Events for Loss of External Electrical Load | 14.1.8-6 |
| 14.1.11-1 | Time Sequence of Events for Excessive Load Increase Incident | 14.1.11-4 |
| 14.2.5-1 | Time Sequence of Events for Steamline Rupture | 14.2.5-9 |
| 14.2.6-1 | Parameters Used in the Analysis of the Rod Cluster Control Assembly Ejection Accident | 14.2.6-14 |
| 14.2.6-2 | Time Sequence of Events RCCA Ejection | 14.2.6-15 |

LIST OF FIGURES

| Figure | Description | Page |
|----------|--|-----------|
| 14-1 | Core Limits and Overpower - Overtemperature ΔT Setpoints | 14-17 |
| 14.2 | Reactivity Coefficients Used in Non-LOCA Safety Analysis | 14-18 |
| 14-3 | Reactivity Insertion SCRAM Curves | 14-19 |
| 14.1.1-1 | Uncontrolled RCCA Bank Withdrawal From Subcritical | 14.1.1-9 |
| 14.1.1-2 | Uncontrolled RCCA Bank Withdrawal From Subcritical | 14.1.1-10 |
| 14.1.2-1 | Uncontrolled RCCA Bank Withdrawal At Power, Maximum Feedback, 100% Power, 90 pcm/sec | 14.1.2-9 |
| 14.1.2-2 | Uncontrolled RCCA Bank Withdrawal at Power, Maximum Feedback, 100% Power, 90 pcm/sec | 14.1.2-10 |
| 14.1.2-3 | Uncontrolled RCCA Bank Withdrawal at Power, Maximum Feedback, 100% Power, 90 pcm/sec | 14.1.2-11 |
| 14.1.2-4 | Uncontrolled RCCA Bank Withdrawal at Power, Maximum Feedback, 100% Power, 7 pcm/sec | 14.1.2-12 |

LIST OF FIGURES
(continued)

| Figure | Description | Page |
|----------|---|-----------|
| 14.1.2-5 | Uncontrolled RCCA Bank Withdrawal at Power, Maximum Feedback, 100% Power, 7 pcm/sec | 14.1.2-13 |
| 14.1.2-6 | Uncontrolled RCCA Bank Withdrawal at Power, Maximum Feedback, 100% Power, 7 pcm/sec | 14.1.2-14 |
| 14.1.2-7 | Uncontrolled Bank Withdrawal From 100% Power | 14.1.2-15 |
| 14.1.2-8 | Uncontrolled Bank Withdrawal From 60% Power | 14.1.2-16 |
| 14.1.2-9 | Uncontrolled Bank Withdrawal From 10% Power | 14.1.2-17 |
| 14.1.4-1 | Dropped Rod - 100 pcm | 14.1.4-4 |
| 14.1.4-2 | Dropped Rod - 100 pcm | 14.1.4-5 |
| 14.1.4-3 | Dropped Rod - 100 pcm | 14.1.4-6 |
| 14.1.4-4 | Dropped Rod - 800 pcm | 14.1.4-7 |
| 14.1.4-5 | Dropped Rod - 800 pcm | 14.1.4-8 |
| 14.1.4-6 | Dropped Rod - 800 pcm | 14.1.4-9 |

LIST OF FIGURES
(continued)

| Figure | Description | Page |
|-----------|--|-----------|
| 14.1.6-1 | Full Loss of Flow | 14.1.6-13 |
| 14.1.6-2 | Full Loss of Flow | 14.1.6-14 |
| 14.1.6-3 | Full Loss of Flow | 14.1.6-15 |
| 14.1.6-4 | Partial Loss of Flow | 14.1.6-16 |
| 14.1.6-5 | Partial Loss of Flow | 14.1.6-17 |
| 14.1.6-6 | Partial Loss of Flow | 14.1.6-18 |
| 14.1.6-7 | Partial Loss of Flow | 14.1.6-19 |
| 14.1.6-8 | Locked Rotor | 14.1.6-20 |
| 14.1.6-9 | Locked Rotor | 14.1.6-21 |
| 14.1.6-10 | Locked Rotor | 14.1.6-22 |
| 14.1.8-1 | Loss of Load - Minimum Feedback With Automatic Pressure Control | 14.1.8-9 |
| 14.1.8-2 | Loss of Load - Minimum Feedback With Automatic Pressure Control | 14.1.8-10 |
| 14.1.8-3 | Loss of Load - Minimum Feedback With Automatic Pressure Control | 14.1.8-11 |

LIST OF FIGURES
(continued)

| Figure | Description | Page |
|-----------|--|-----------|
| 14.1.8-4 | Loss of Load - Maximum Feedback With Automatic Pressure Control | 14.1.8-12 |
| 14.1.8-5 | Loss of Load - Maximum Feedback With Automatic Pressure Control | 14.1.8-13 |
| 14.1.8-6 | Loss of Load - Maximum Feedback With Automatic Pressure Control | 14.1.8-14 |
| 14.1.8-7 | Loss of Load - Minimum Feedback Without Pressure Control | 14.1.8-15 |
| 14.1.8-8 | Loss of Load - Minimum Feedback Without Pressure Control | 14.1.8-16 |
| 14.1.8-9 | Loss of Load - Minimum Feedback Without Pressure Control | 14.1.8-17 |
| 14.1.8-10 | Loss of Load - Maximum Feedback Without Pressure Control | 14.1.8-18 |
| 14.1.8-11 | Loss of Load - Maximum Feedback Without Pressure Control | 14.1.8-19 |
| 14.1.8-12 | Loss of Load - Maximum Feedback Without Pressure Control | 14.1.8-20 |

LIST OF FIGURES
(continued)

| Figure | Description | Page |
|-----------|---|------------|
| 14.1.10-1 | Feedwater Enthalpy Decrease - Automatic Rod Control | 14.1.10-5 |
| 14.1.10-2 | Feedwater Enthalpy Decrease - Automatic Rod Control | 14.1.10-6 |
| 14.1.10-3 | Feedwater Enthalpy Decrease - Automatic Rod Control | 14.1.10-7 |
| 14.1.10-4 | Feedwater Enthalpy Decrease - Manual Rod Control | 14.1.10-8 |
| 14.1.10-5 | Feedwater Enthalpy Decrease - Manual Rod Control | 14.1.10-9 |
| 14.1.10-6 | Feedwater Enthalpy Decrease - Manual Rod Control | 14.1.10-10 |
| 14.1.11-1 | Excess Load Increase - Minimum Feedback Without Rod Control | 14.1.11-5 |
| 14.1.11-2 | Excess Load Increase - Minimum Feedback Without Rod Control | 14.1.11-6 |
| 14.1.11-3 | Excess Load Increase - Minimum Feedback Without Rod Control | 14.1.11-7 |

LIST OF FIGURES
(continued)

| Figure | Description | Page |
|------------|---|------------|
| 14.1.11-4 | Excess Load Increase - Maximum Feedback Without Rod Control | 14.1.11-8 |
| 14.1.11-5 | Excess Load Increase - Maximum Feedback Without Rod Control | 14.1.11-9 |
| 14.1.11-6 | Excess Load Increase - Maximum Feedback Without Rod Control | 14.1.11-10 |
| 14.1.11-7 | Excess Load Increase - Minimum Feedback With Automatic Rod Control | 14.1.11-11 |
| 14.1.11-8 | Excess Load Increase - Minimum Feedback With Automatic Rod Control | 14.1.11-12 |
| 14.1.11-9 | Excess Load Increase - Minimum Feedback With Automatic Rod Control | 14.1.11-13 |
| 14.1.11-10 | Excess Load Increase - Maximum Feedback With Automatic Rod Control | 14.1.11-14 |
| 14.1.11-11 | Excess Load Increase - Maximum Feedback With Automatic Rod Control | 14.1.11-15 |
| 14.1.11-12 | Excess Load Increase - Maximum Feedback With Automatic Rod Control | 14.1.11-16 |
| 14.2.5-1 | Steamline Rupture | 14.2.5-11 |

LIST OF FIGURES
(continued)

| Figure | Description | Page |
|-----------|---|-----------|
| 14.2.5-2 | Steamline Rupture | 14.2.5-12 |
| 14.2.5-3 | Steamline Rupture - 4.6 ft ² Break With Power 2 Loops in Service | 14.2.5-13 |
| 14.2.5-4 | Steamline Rupture - 4.6 ft ² Break With Power 2 Loops in Service | 14.2.5-14 |
| 14.2.5-5 | Steamline Rupture - 4.6 ft ² Break With Power | 14.2.5-15 |
| 14.2.5-6 | Steamline Rupture - 4.6 ft ² Break With Power | 14.2.5-16 |
| 14.2.5-7 | Steamline Rupture - 4.6 ft ² Break With Power | 14.2.5-17 |
| 14.2.5-8 | Steamline Rupture - 4.6 ft ² Break Without Power 2 Loops in Service | 14.2.5-18 |
| 14.2.5-9 | Steamline Rupture - 4.6 ft ² Break Without Power 2 Loops in Service | 14.2.5-19 |
| 14.2.5-10 | Steamline Rupture - 4.6 ft ² Break Without Power 2 Loops in Service | 14.2.5-20 |
| 14.2.5-11 | Steamline Rupture - 4.6 ft ² Break Without Power 2 Loops in Service | 14.2.5-21 |

x

LIST OF FIGURES
(continued)

| Figure | Description | Page |
|-----------|---|-----------|
| 14.2.5-12 | Steamline Rupture - 4.6 ft ² Break Without Power | 14.2.5-22 |
| 14.2.5-13 | Steamline Rupture - Failed Safety Valve | 14.2.5-23 |
| 14.2.5-14 | Steamline Rupture - Failed Safety Valve 2 Loops in Service | 14.2.5-24 |
| 14.2.5-15 | Steamline Rupture - Failed Safety Valve 2 Loops in Service | 14.2.5-25 |
| 14.2.5-16 | Steamline Rupture - Failed Safety Valve | 14.2.5-26 |
| 14.2.5-17 | Steamline Rupture - Failed Safety Valve | 14.2.5-27 |
| 14.2.5-18 | Steamline Rupture - 4.6 ft ² Break With Power One Loop in Service | 14.2.5-28 |
| 14.2.5-19 | Steamline Rupture - 4.6 ft ² Break With Power One Loop in Service | 14.2.5-29 |
| 14.2.5-20 | Steamline Rupture - 4.6 ft ² Break With Power One Loop in Service | 14.2.5-30 |
| 14.2.5-21 | Steamline Rupture - 4.6 ft ² Break With Power One Loop in Service | 14.2.5-31 |
| 14.2.5-22 | Steamline Rupture Break With Power One Loop in Service | 14.2.5-32 |

LIST OF FIGURES
(continued)

| Figure | Description | Page |
|-----------|--|-----------|
| 14.2.5-23 | Steamline Rupture Failed Safety Valve One Loop in Service | 14.2.5-33 |
| 14.2.5-24 | Steamline Rupture Failed Safety Valve One Loop in Service | 14.2.5-34 |
| 14.2.5-25 | Steamline Rupture Failed Safety Valve One Loop in Service | 14.2.5-35 |
| 14.2.5-26 | Steamline Rupture Failed Safety Valve One Loop in Service | 14.2.5-36 |
| 14.2.6-1 | RCCA Ejection - Beginning of Life, Full Power | 14.2.6-16 |
| 14.2.6-2 | RCCA Ejection - Beginning of Life, Zero Power | 14.2.6-17 |





Power Distribution

The transient response of the reactor system is dependent on the initial power distribution. The nuclear design of the reactor core minimizes adverse power distribution through the placement of control rods and operating instructions. The constant axial offset control (CAOC) strategy is used for R. E. Ginna. Power distribution may be characterized by the radial factor ($F_{\Delta H}$) and the total peaking factor (F_Q). The peaking factor limits are given in the Technical Specifications and in Section 5.0 of this report.

For transients which may be DNB-limited, the radial peaking factor is of importance. The radial peaking factor increases with decreasing power level due to rod insertion. This increase in $F_{\Delta H}$ is included in the core limits illustrated in Figure 14-1. All transients that may be DNB limited are assumed to begin with a $F_{\Delta H}$ consistent with the initial power level defined in the Technical Specifications.

The axial power shape used in the DNB calculations are discussed in Section 4. The radial and axial power distributions described above are input to the THINC Code as described in Section 4.

For transients which may be overpower limited, the total peaking factor (F_Q) is of importance. All transients that may be overpower limited are assumed to begin with plant conditions including power distributions which are consistent with reactor operation as defined in the Technical Specifications.

For overpower, transients which are slow with respect to the fuel rod thermal time constant, for example, the Chemical and Volume Control System malfunction that results in a decrease in the boron concentration in the reactor coolant incident which lasts many minutes, and the excessive increase in secondary steam flow incident which may reach equilibrium without causing a reactor trip, the fuel rod thermal evaluations are performed as discussed in Section 4. For overpower transients

which are fast with respect to the fuel rod thermal time constant, for example, the uncontrolled rod cluster control assembly bank withdrawal from subcritical and rod cluster control assembly ejection incidents which result in a large power rise over a few seconds, a detailed fuel heat transfer calculation must be performed. Although the fuel rod thermal time constant is a function of system conditions, fuel burnup and rod power, a typical value at beginning-of-life for high power rods is approximately five seconds.

Reactivity Coefficients Assumed in the Accident Analyses

The transient response of the reactor system is dependent on reactivity feedback effects, in particular the moderator temperature coefficient and the Doppler power coefficient. These reactivity coefficients and their values are discussed in detail in Section 3.0 of the main text.

In the analysis of certain events, conservatism requires the use of large reactivity coefficient values, whereas in the analysis of other events, conservatism requires the use of small reactivity coefficient values. Some analyses such as loss of coolant from cracks or ruptures in the Reactor Coolant System do not depend on reactivity feedback effects. The justification for use of conservatively large versus small reactivity coefficient values is treated on an event-by-event basis. In some cases conservative combinations of parameters are used to bound the effects of core life, although these combinations may not represent possible realistic situations. The limiting values of the moderator density and Doppler power coefficients used in the safety analyses are shown in Figure 14-2.

Rod Clusters Control Assembly Insertion Characteristics

The negative reactivity insertion following a reactor trip is a function of the position versus time of the rod cluster control assemblies and the variation in rod worth as a function of rod position. With respect to accident analyses, the critical parameter is the time of insertion up to the dashpot entry.

The rod cluster control assembly position versus time assumed in accident analyses is shown in Figure 14-3. The rod cluster control assembly insertion time to dashpot entry is normalized to 1.8 seconds.

RC
New
Sketches

Figure 14-3 also shows the fraction of total negative reactivity insertion versus normalized rod position. This curve is used to compute the negative reactivity insertion versus time following a reactor trip. A total negative reactivity insertion following a trip of 4 percent Δk is assumed in the transient analyses except where specifically noted otherwise. This assumption is conservative with respect to the calculated trip reactivity worth available.

Trip Points and Time Delays to Trip Assumed to Accident Analyses

A reactor trip signal acts to open two trip breakers connected in series feeding power to the control rod drive mechanisms. The loss of power to the mechanism coils causes the mechanisms to release the rod cluster control assemblies which then fall by gravity into the core. There are various instrumentation delays associated with each trip function, including delays in signal actuation, in opening the trip breakers, and in the release of the rods by the mechanisms. The total delay to trip is defined as the time delay from the time that trip conditions are reached to the time the rods are free and begin to fall. Limiting trip setpoints assumed in accident analyses and the time delay assumed for each trip function are given in Table 14-3.

Reference is made in that table to Overtemperature and Overpower ΔT trip shown in Figure 14-1. This figure presents the allowable Reactor Coolant Loop Average Temperature and ΔT for the design flow and power distribution, as described in Section 4, as a function of primary coolant pressure. The boundaries of operation defined by the overpower ΔT trip and the overtemperature ΔT trip are represented as "Protection Lines" on this diagram. The protection lines are drawn to



include all adverse instrumentation and setpoint errors so that under nominal conditions trip would occur well within the area bounded by these lines. The utility of this diagram is that the limit imposed by any given DNBR can be represented as a line. The DNB lines represent the locus of conditions for which the DNBR equals the limit value. The limit values for Westinghouse fuel are 1.52 (typical cell) and 1.51 (thimble cell). For EXXON fuel, the values are 1.62 (typical cell) and 1.54 (thimble cell). All points below and to the left of a DNB line for a given pressure have a DNBR greater than the limit value. The diagram shows that DNB is prevented for all cases, if the area enclosed with the maximum protection lines is not traversed by the applicable DNBR line at any point.

N° of RCP

The area of permissible operation (power, pressure, and temperature) is bounded by the combination of reactor trips: high neutron flux (fixed setpoint); high pressure (fixed setpoint); low pressure (fixed setpoint); overpower and overtemperature ΔT (variable setpoints).

The limit value, which was used as the DNBR limit for all accidents analyzed with the Improved Thermal Design Procedure (see Table 14-1), is conservative compared to the actual design DNBR value required to meet the DNB design basis as discussed in Section 4.

RCP

The difference between the limiting trip point assumed for the analysis and the normal trip point represents an allowance for instrumentation channel error and setpoint error. Nominal trip setpoints are specified in the plant Technical Specifications.

Instrumentation Drift and Calorimetric Errors - Power Range Neutron Flux

The instrumentation drift and calorimetric errors used in establishing the power range high neutron flux setpoint are presented in Table 14-4. The calorimetric error is the error assumed in the determination of core thermal power as obtained from secondary plant measurements. The total ion chamber current (sum of the top and bottom sections) is calibrated (set equal) to this measured power on a periodic basis.

The secondary power is obtained from measurement of feedwater flow, feedwater inlet temperature to the steam generators and steam pressure. High-accuracy instrumentation is provided for these measurements with accuracy tolerances much tighter than those which would be required to control feedwater flow.

Computer Codes Utilized

Summaries of some of the principal computer codes used in transient analyses are given below. The codes used in the analyses of each transient have been listed in Table 14-1.

FACTRAN

FACTRAN calculates the transient temperature distribution in a cross section of metal clad UO_2 fuel rod and the transient heat flux at the surface of the clad using as input the nuclear power and time-dependent coolant parameters (pressure, flow, temperature, and density). The code uses a fuel model which exhibits the following features simultaneously:

1. A sufficiently large number of radial space increments to handle fast transients such as rod ejection accidents.
2. Material properties which are functions of temperature and a sophisticated fuel-to-clad gap heat transfer calculation.
3. The necessary calculations to handle post-DNB transients: film boiling heat transfer correlations, Zircaloy-water reaction, and partial melting of the materials.

FACTRAN is further discussed in Reference 2.

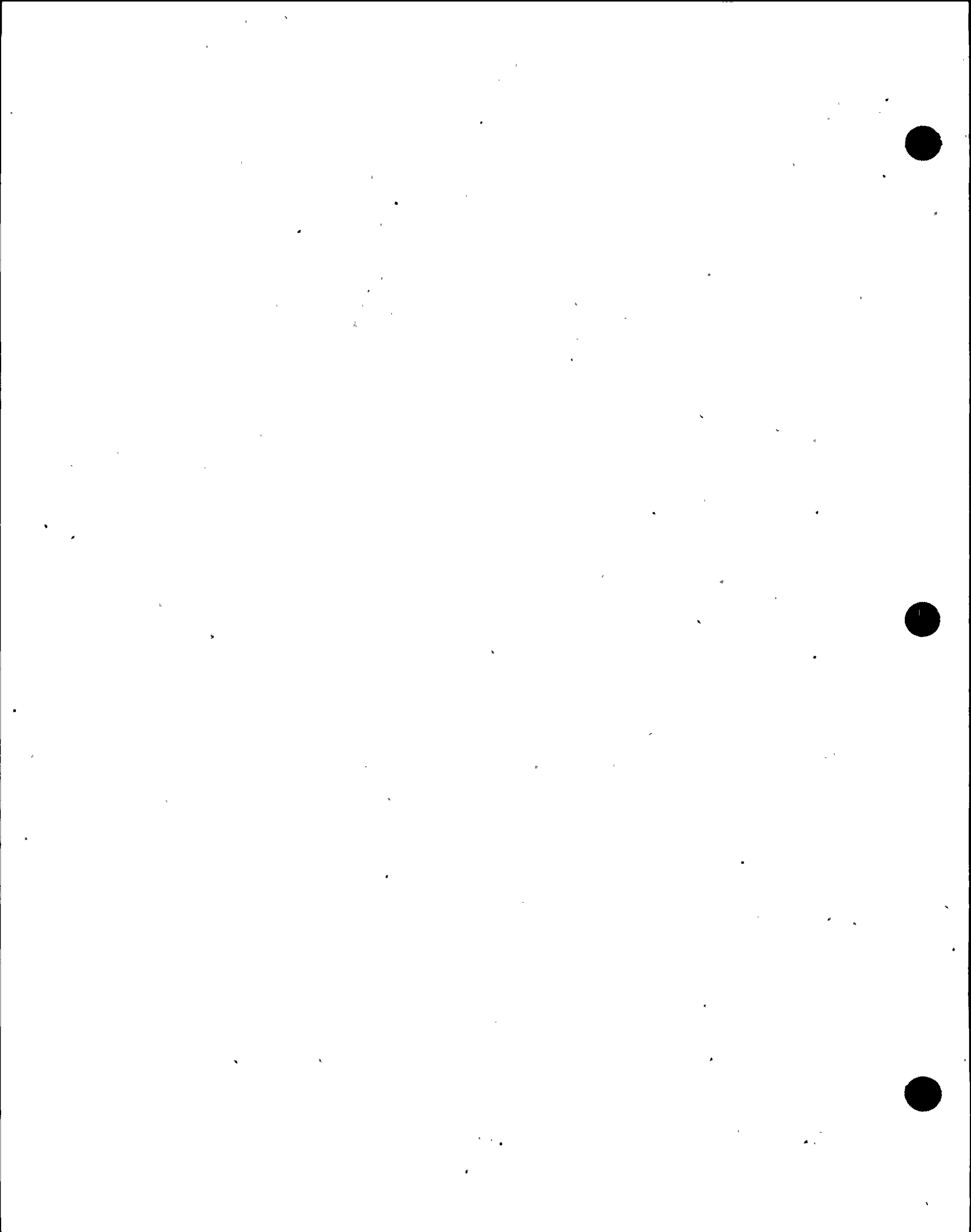
LOFTRAN

The LOFTRAN program is used for studies of transient response of a PWR system to specified perturbations in process parameters. LOFTRAN simulates a multiloop system by a model containing reactor vessel, hot- and cold-leg piping, steam generator (tube and shell sides) and the pressurizer. The pressurizer heaters, spray, relief, and safety valves are also considered in the program. Point model neutron kinetics, and reactivity effects of the moderator, fuel, boron, and rods are included. The secondary side of the steam generator utilizes a homogeneous, saturated mixture for the thermal transients and a water-level correlation for indication and control. The Reactor Protection System is simulated to include reactor trips on high neutron flux, Overtemperature ΔT , Overpower ΔT , high and low pressure, low flow, and high pressurizer level. Control systems are also simulated including rod control, steam dump, feedwater control, and pressurizer pressure control. The Emergency Core Cooling System, including the accumulators and upper-head injection, is also modeled.

LOFTRAN is a versatile program which is suited to both accident evaluation and control studies as well as parameter sizing.

LOFTRAN also has the capability of calculating the transient value of DNBR based on the input from the core limits illustrated in Figure 14-1. The core limits represent the minimum value of DNBR as calculated for typical or thimble cell.

LOFTRAN is further discussed in Reference 3.



TWINKLE

The TWINKLE program is a multi-dimensional spatial neutron kinetics code. The code uses an implicit finite-difference method to solve the two-group transient neutron diffusion equations in one, two, and three dimensions. The code uses six delayed neutron groups and contains a detailed multi-region fuel-clad-coolant heat transfer model for calculating pointwise Doppler and moderator feedback effects. The code handles up to 2000 spatial points, and performs its own steady state initialization. Aside from basic cross-section data and thermal-hydraulic parameters, the code accepts as input basic driving functions such as inlet temperature, pressure, flow, boron concentration, control rod motion, and others. Various edits are provided, e.g., channelwise power, axial offset, enthalpy, volumetric surge, pointwise power, and fuel temperatures.

The TWINKLE Code is used to predict the kinetic behavior of a reactor for transients which cause a major perturbation in the spatial neutron flux distribution.

TWINKLE is further discussed in Reference 4.

THINC

The THINC Code is described in References 18 and 19, (main text).

References

1. Chelemer, H., et al., "Improved Thermal Design Procedure," WCAP-8567-P (Proprietary), July, 1975, and WCAP-8568 (Non-Proprietary), July 1975.
2. Hargrove, H. G., "FACTRAN - A Fortran-IV Code for Thermal Transients in a UO_2 Fuel Rod," WCAP-7908, June 1972.

3. Burnett, T. W. T., et al., "LOFTRAN Code Description," WCAP-7907, June 1972.
4. Risher, D. H., Jr.; Barry, R. F., "TWINKLE - A Multi-Dimensional Neutron Kinetics Computer Code," WCAP-7979-P-A (Proprietary), and WCAP-8028-A (Non-Proprietary), January 1975.



TABLE 14-1

SUMMARY OF INITIAL CONDITIONS AND COMPUTER CODES USED

| Accidents | Computer Codes Utilized | DNB* Correlation | Improved Thermal Design Procedure | Initial NSSS Thermal Power Output (MWT) | Reactor Vessel Coolant Flow (GPM) | Vessel Average Temp. (°F) | Pressurizer Pressure (psia) |
|---|-----------------------------|------------------|-----------------------------------|---|-----------------------------------|---------------------------|-----------------------------|
| Uncontrolled RCCA Withdrawal from a Subcritical Condition | TWINKLE FACTRAN THINC | WRB-1 W-3 | Yes | 0 | 82432** | 547 | 2250 |
| Uncontrolled RCCA Withdrawal at Power | LOFTRAN | WRB-1 W-3 | Yes | 1520 912 152 | 179200 | 573.5 562.9 549.7 | 2250 |
| Rod Cluster Control Assembly (RCCA) Drop | LOFTRAN THINC | WRB-1 W-3 | Yes | 1520 | 179200 | 573.5 | 2250 |
| Chemical and Volume Control System Malfunction | NA | NA | NA | 0 and 1520 | NA | NA | NA |
| Reduction in Feedwater Enthalpy | LOFTRAN | WRB-1 W-3 | Yes | 0 and 1520 | 179200 | 547 573.5 | 2250 |
| Excessive Load Increase | LOFTRAN | WRB-1 W-3 | Yes | 1520 | 179200 | 573.5 | 2250 |
| Loss of Load Turbine Trip | LOFTRAN | WRB-1 W-3 | Yes | 1520 | 179200 | 573.5 | 2250 |
| Steamline Break | LOFTRAN THINC | W-3 | No | 0 | 174000 80040** | 547 | 2250 |

* Where two correlations are listed, WRB-1 applies to Westinghouse fuel
W-3 applies to EXXON fuel

**One pump in operation. Accounts for reverse flow through other loop.

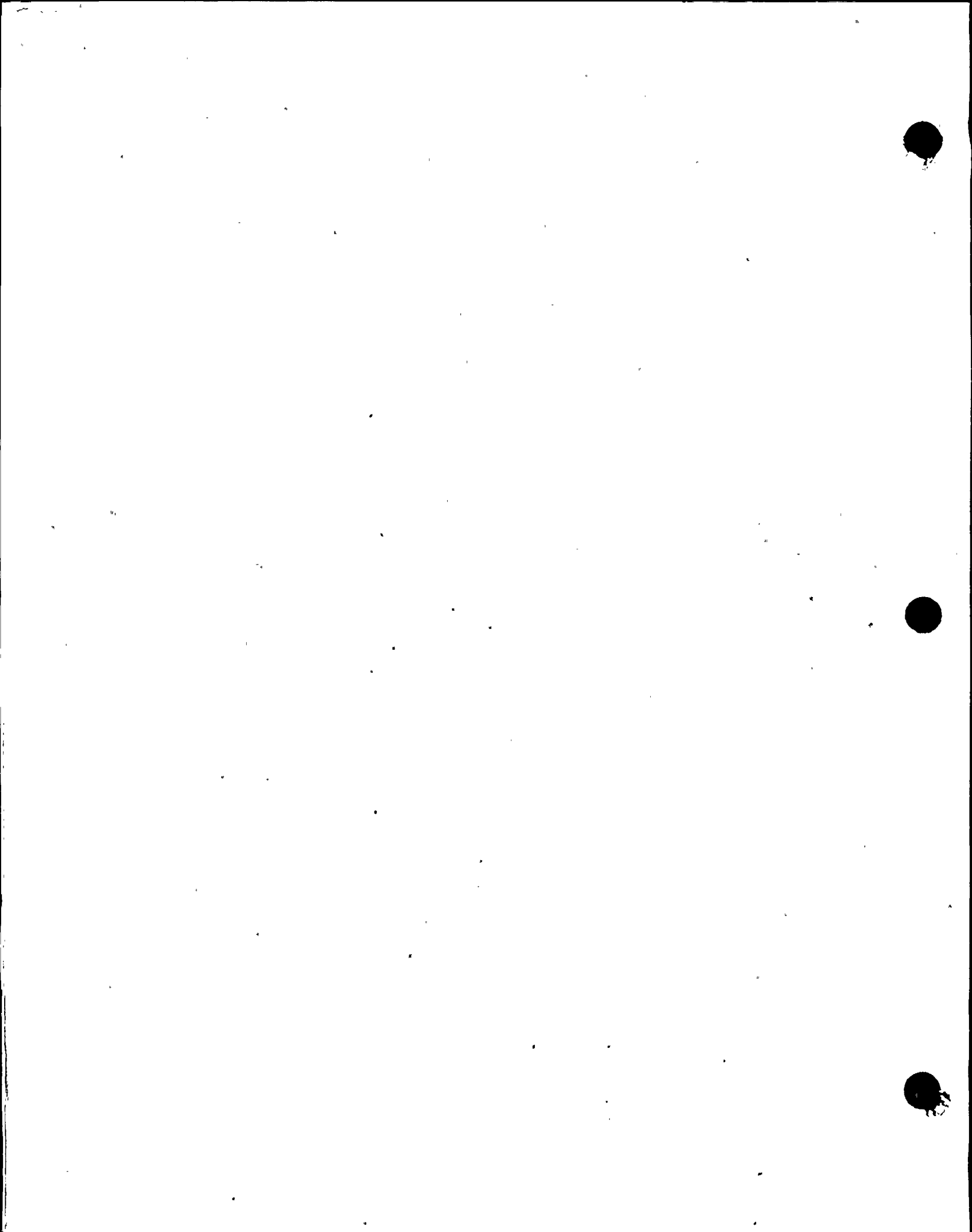


TABLE 14-1 (Continued)

SUMMARY OF INITIAL CONDITIONS AND COMPUTER CODES USED

| Accidents | Computer Codes Utilized | DNB Correlation | Improved Thermal Design Procedure | Initial NSSS Thermal Power Output (MWT) | Reactor Vessel Coolant Flow (GPM) | Vessel Average Temp. (°F) | Pressurizer Pressure (psia) |
|--------------|-----------------------------|-----------------|-----------------------------------|---|-----------------------------------|---------------------------|-----------------------------|
| Loss of Flow | LOFTRAN FACTRAN THINC | WRB-1 W-3 | Yes | 1520 | 179200 | 573.5 | 2250 |
| Locked Rotor | LOFTRAN FACTRAN | N/A | No | 1550 | 174000 | 577.5 | 2280 |
| Rod Ejection | TWINKLE FACTRAN | N/A | No | 1550 and 0 | 174000 80040** | 547 and 573.5 | N/A |

**One pump in operation. Accounts for reverse flow through other loop.



TABLE 14-2

NOMINAL VALUES OF
PERTINENT PLANT PARAMETERS
FOR NON-LOCA ACCIDENTS ANALYSIS*

| <u>Parameter</u> | <u>With ITDP</u> | <u>Without ITDP</u> |
|--|------------------|---------------------|
| Thermal Output of NSSS (MWt) | 1520 | 1520 |
| Core Inlet Temperature (°F) | 543.7 | 543.7 |
| Vessel Average Temperature (°F) | 573.5 | 573.5 |
| Reactor Coolant System Pressure (psia) | 2250 | 2250 |
| Reactor Coolant Flow Per Loop (gpm) | 89600 | 87000 |
| Total Reactor Coolant Flow (10 ⁶ LBM/hr) | 67.9 | 65.9 |
| Steam Flow from NSSS (10 ⁶ LBM/hr) | 6.58 | 6.58 |
| Steam Pressure at Steam Generator Outlet (psia) | 746.5 | 746.5 |
| Assumed Feedwater Temperature at Steam Generator Inlet (°F) | 432.3 | 432.3 |
| Average Core Heat Flux (BTU/hr-ft ²) | 189440 | 189440 |

*RC
All Pumps*

* The non-LOCA analyses assume a steam generator tube plugging level of 10%.

TABLE 14-3

TRIP POINTS AND TIME DELAYS TO TRIP
ASSUMED IN ACCIDENT ANALYSES

| <u>Trip Function</u> | <u>Limiting Trip Point Assumed In Analysis</u> | <u>Time Delays (Seconds)</u> |
|---|--|------------------------------|
| Power range high neutron flux, high setting | 118% | 0.5 |
| Power range high neutron flux, low setting | 35% | 0.5 |
| Overtemperature ΔT | Variable see Figure 14-1 | 6.0 ^a |
| Overpower ΔT | Variable see Figure 14-1 | 2.0 ^a |
| High pressurizer pressure | 2425 psia | 2.0 |
| Low pressurizer pressure | 1775 psia | 2.0 |

^aTotal time delay (including RTD time response, and trip circuit, channel electronics delay) from the time the temperature difference in the coolant loops exceeds the trip setpoint until the rods are free to fall.

TABLE 14-3 (Continued)

TRIP POINTS AND TIME DELAYS TO TRIP
ASSUMED IN ACCIDENT ANALYSES

| <u>Trip Function</u> | <u>Limiting Trip Point Assumed In Analysis</u> | <u>Time Delays (Seconds)</u> |
|--|--|------------------------------|
| Low reactor coolant flow (From loop flow detectors) | 87% loop flow | 1.0 |
| Undervoltage trip | Not applicable | 1.5 |
| Turbine trip | Not applicable | 2.0 |
| Low-low steam generator level | 0% of narrow range level span | 2.0 |

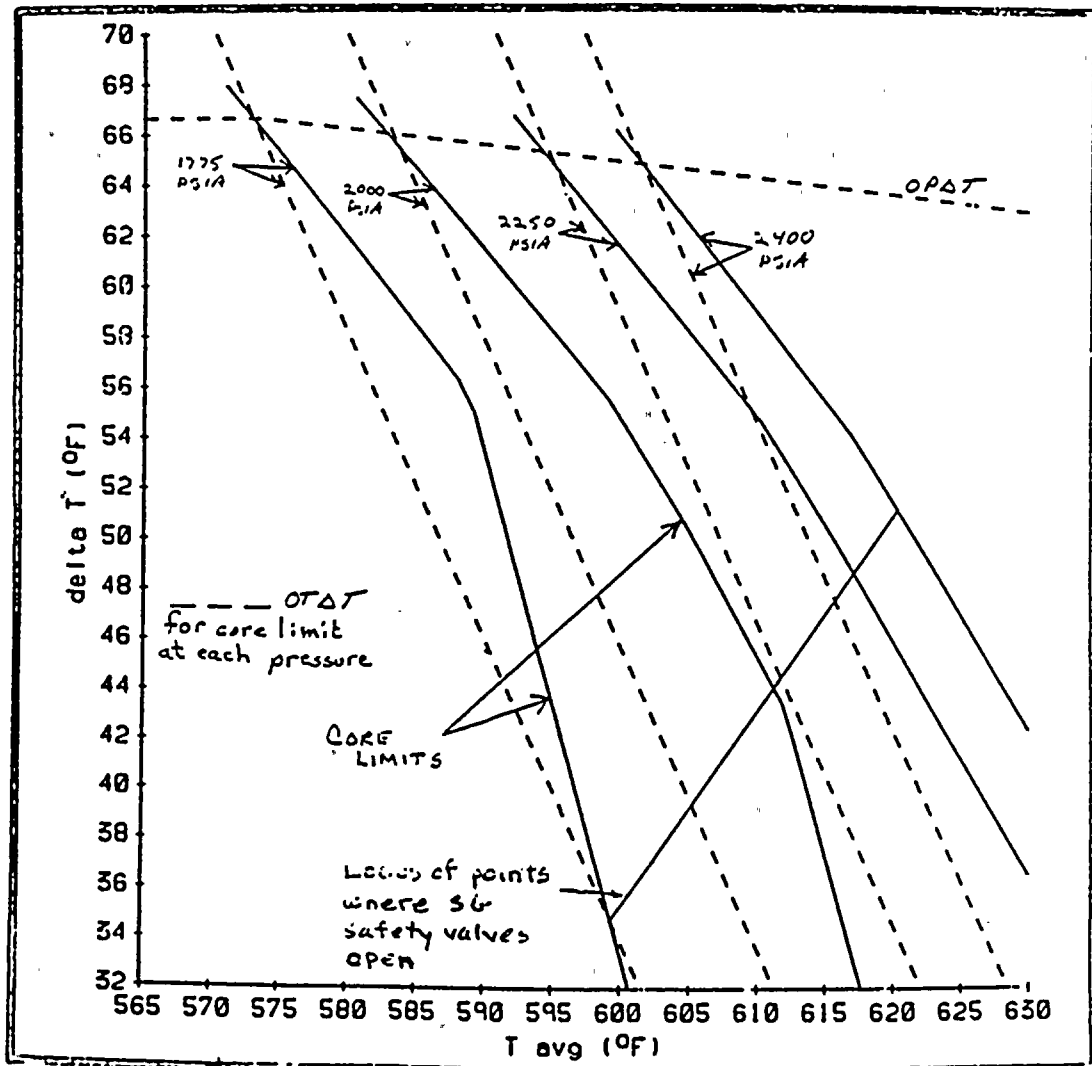
TABLE 14-4
 DETERMINATION OF MAXIMUM OVERPOWER TRIP POINT - POWER RANGE
 NEUTRON FLUX CHANNEL - BASED ON NOMINAL SETPOINT CONSIDERING
 INHERENT INSTRUMENT ERRORS

| <u>Variable</u> | <u>Accuracy of Measurement of Variable (% error)</u> | <u>Effect On Thermal Power Determination (% error)</u> | |
|---|--|--|-----------|
| | | (Estimated) | (Assumed) |
| Calorimetric Errors in the Measurement of Secondary System Thermal Power: | | | |
| Feedwater temperature | ± 0.5 | | |
| Feedwater pressure (small correction on enthalpy) | ± 0.5 | 0.3 | |
| Steam pressure (small correction on enthalpy) | ± 2 | | |
| Feedwater flow | ± 1.25 | 1.25 | |
| Assumed Calorimetric Error (% of rated power) | | | ±2(a) |
| Axial power distribution effects on total ion chamber current | | | |
| Estimated Error (% of rated power) | | 3 | |
| Assumed Error (% of rated Power) | | | ± 5(b) |

TABLE 14-4 (Continued)
 DETERMINATION OF MAXIMUM OVERPOWER TRIP POINT - POWER RANGE
 NEUTRON FLUX CHANNEL - BASED ON NOMINAL SETPOINT CONSIDERING
 INHERENT INSTRUMENT ERRORS

| <u>Variable</u> | <u>Accuracy of Measurement of Variable (% error)</u> | <u>Effect On Thermal Power Determination (% error)</u> |
|---|--|--|
| | | (Estimated) (Assumed) |
| Instrumentation channel drift and setpoint reproducibility | | |
| Estimated Error (% of rated power) | | 1 |
| Assumed Error (% of rated power) | | ±2(c) |
| Total assumed error in setpoint (a) + (b) + (c) | | ±9 |
| | | <u>Percent of Rated Power</u> |
| Nominal Setpoint | | 109 |
| Maximum overpower trip point assuming all individual errors are simultaneously in the most adverse direction | | 118 |

Figure 14-1
 Ginna Core Limits and
 Overpower - Overtemperature ΔT Setpoints



RCP

Figure 14-2

Reactivity Coefficients Used
in Non-Loca Safety Analysis

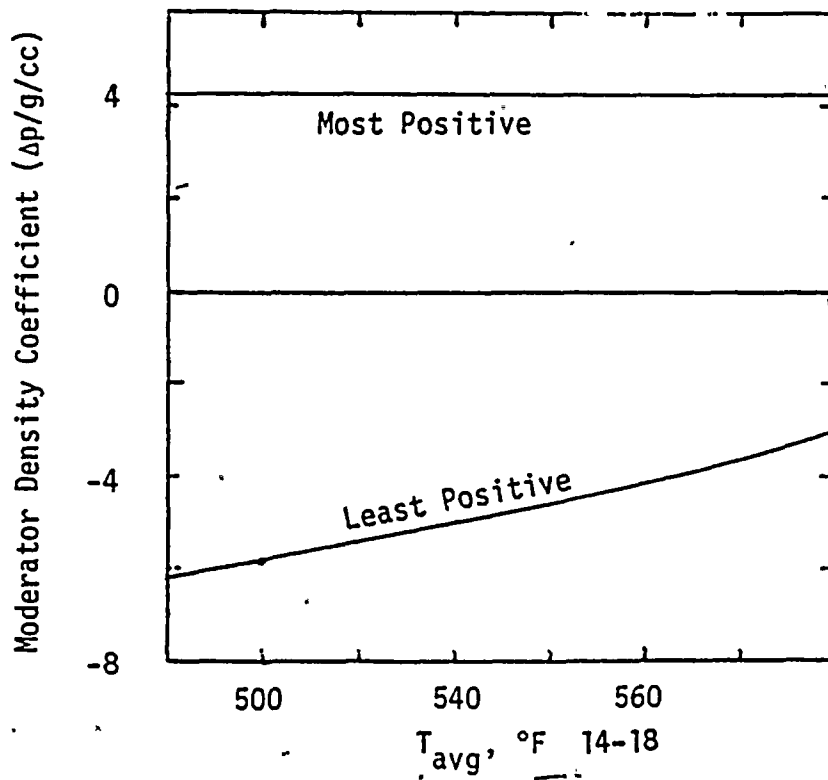
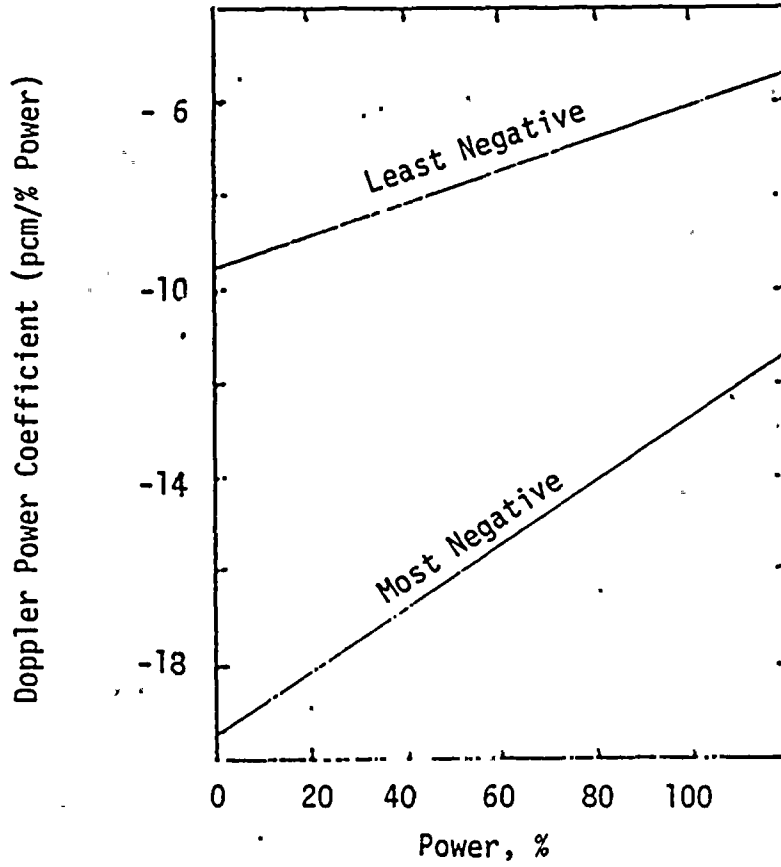
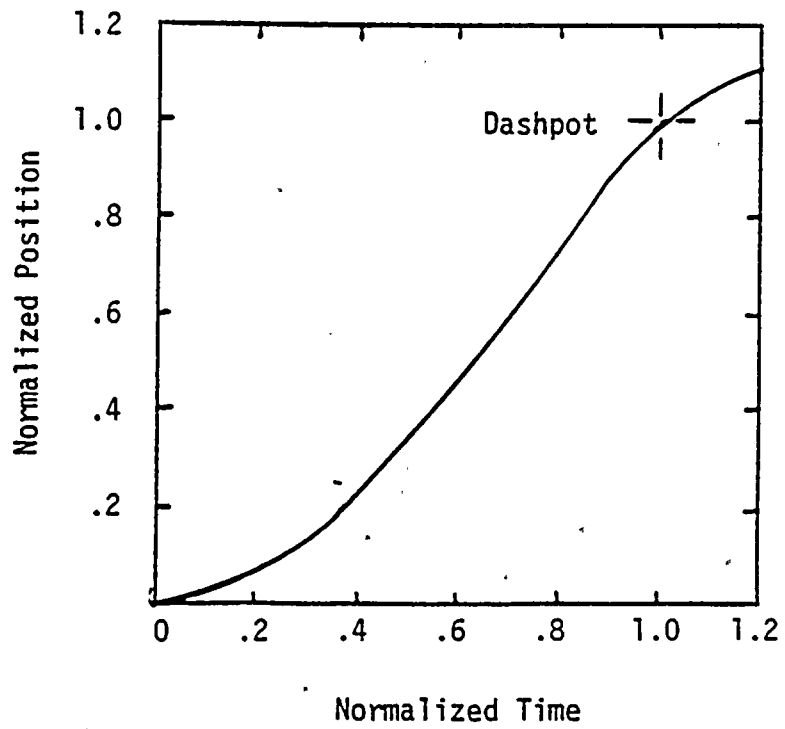
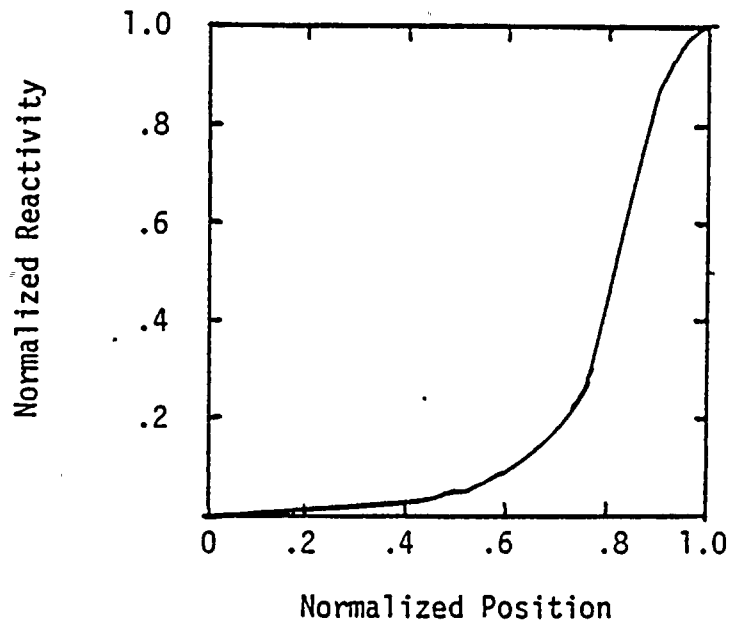


Figure 14-3

Reactivity Insertion Scram Curves



14.1.1 Uncontrolled RCCA Withdrawal from a Subcritical Condition

A RCCA withdrawal incident is defined as an uncontrolled addition of reactivity to the reactor core by withdrawal of rod cluster control assemblies resulting in a power excursion. While the probability of a transient of this type is extremely low, such a transient could be caused by a malfunction of either the reactor control or control rod drive systems. This could occur with the reactor either subcritical or at power. The "at power" case is discussed in Section 14.1.2.

Reactivity is added at a prescribed and controlled rate in bringing the reactor from a shutdown condition to a lower power level during startup by RCCA withdrawal. Although the initial startup procedure uses the method of boron dilution, the normal startup is with RCCA withdrawal. RCCA motion can cause much faster changes in reactivity than can be made by changing boron concentration.

The rod cluster drive mechanisms are wired into preselected groups, and these group configurations are not altered during core life. The rods are therefore physically prevented from withdrawing in other than their respective groups. Power supplied to the rod groups is controlled such that no more than two groups can be withdrawn at any time. The rod drive mechanism is of the magnetic latch type and the coil actuation is sequenced to provide variable speed rod travel. The maximum reactivity insertion rate is analyzed in the detailed plant analysis assuming the simultaneous withdrawal of the combination of the two rod groups with the maximum combined worth at maximum speed.

The neutron flux response to a continuous reactivity insertion is characterized by a very fast rise, terminated by the reactivity feedback effect of the negative Doppler coefficient. This self-limitation of the power excursion is of primary importance, since it limits the power to a tolerable level during the delay time for protective action. If a continuous rod cluster control assembly withdrawal accident occurs, the transient is terminated by the following automatic features of the reactor protection system:

1. Source range level trip - actuated when either of two independent source range channels indicates a flux level above a preselected, manually adjustable value. This trip function may be manually bypassed when either of the intermediate range flux channels indicate a flux level above the source range cutoff power level. It is automatically reinstated when both intermediate range channels indicate a flux level below the source range cutoff power level.
2. Intermediate range rod stop - actuated when either of two independent intermediate range channels indicates a flux level above a preselected, manually adjustable value. This rod stop may be manually bypassed when two out of the four power range channels indicate a power level above approximately 10% power. It is automatically reinstated when three of the four power range channels are below this value.
3. Intermediate range flux level trip - actuated when either of two independent intermediate range channels indicates a flux level above a preselected, manually adjustable value. This trip function may be manually bypassed when two of the four power range channels are reading above approximately 10% power and is automatically reinstated when three of the four channels indicate a power level below this value.

4. Power range flux level trip (low setting) - actuated when two out of the four power range channels indicate a power level above approximately 25%. This trip function may be manually bypassed when two of the four power range channels indicate a power level above approximately 10% power and is automatically reinstated when three of the four channels indicate a power level below this value.
5. Power range flux level trip (high setting) - actuated when two out of the four power range channels indicate a power level above a preset set point. This trip function is always active.

Method of Analysis

A rod cluster control assembly withdrawal accident is analyzed by three digital computer codes. The analysis is performed in three stages: first, an average core nuclear power transient calculation; then an average core heat transfer calculation; and finally the DNBR calculation. The average nuclear calculation is performed using a spatial neutron kinetics code, TWINKLE, average power generation with time including the various total core feedback effects, i.e., Doppler and moderator reactivity. The FACTRAN code is then used to calculate the thermal heat flux transient, based on the nuclear power transient calculated by TWINKLE. FACTRAN also calculates the fuel and clad temperatures. The average heat flux is next used in THINC, References 18 and 19, for transient DNBR calculation. ✓

This accident is analyzed using the Improved Thermal Design Procedure as described in Reference 6. Plant characteristics and initial conditions are discussed in Section 4.

In order to give conservative results for a startup accident, the following additional assumptions are made concerning the initial reactor conditions:

1. Since the magnitude of the nuclear power peak reached during the initial part of the transient, for any given rate of reactivity insertion, is strongly dependent on the Doppler coefficient, conservatively low values (low absolute magnitude) as a function of temperature are used.
2. The contribution of the moderator reactivity coefficient is negligible during the initial part of the transient because the heat transfer time between the fuel and the moderator is much longer than the nuclear flux response time. However, after the initial nuclear flux peak, the succeeding rate of power increase is affected by the moderator reactivity coefficient. Accordingly, a conservative value of $+5.0$ pcm/ $^{\circ}$ F at zero power is used, because this yields the maximum peak heat flux.
3. The reactor is assumed to be just critical at hot zero power (no-load average temperature). This assumption is more conservative than that of a lower initial system temperature. The higher initial system temperature yields a larger fuel water heat transfer coefficient, larger specific heats, and a less negative (smaller absolute magnitude) Doppler coefficient -- all of which tend to reduce the Doppler feedback effect, thereby increasing the neutron flux peak. The initial effective multiplication factor is assumed to be 1.0, since this results in maximum neutron flux peaking and, thus, the most severe nuclear power transient.

4. Reactor trip is assumed to be initiated by the power range flux level trip (low setting). The most adverse combination of instrument and setpoint errors, as well as delays for trip signal actuation and rod cluster control assembly release, is taken into account. A 10 percent increase is assumed for the power range flux trip setpoint, raising it from the nominal value of 25 percent to 35 percent. Previous results, however, show that rise in the neutron flux is so rapid that the effect of errors in the trip setpoint on the actual time at which the rods are released is negligible. In addition, the reactor trip insertion characteristic is based on the assumption that the highest worth rod cluster control assembly is stuck in its fully withdrawn position.
5. The maximum positive reactivity insertion rate assumed (97.5 pcm/sec) is greater than that for the simultaneous withdrawal of the combination of the two control banks having the greatest combined worth at maximum speed (45 inches/minute).
6. The most limiting axial and radial power shapes, associated with having the two highest combined worth sequential banks in their highest worth position, are assumed for DNB analysis.
7. The initial power level was assumed to be below the power level expected for any shutdown condition (10^{-9} of nominal power). The combination of highest reactivity insertion rate and lowest initial power produces the highest peak heat flux.
8. One reactor coolant pump is assumed to be in operation. This lowest initial flow minimizes the resulting DNBR.

Results

The calculated sequence of events is shown in Table 14.1.1-1. Figures 14.1.1-1 and 14.1.1-2 show the transient behavior for the indicated reactivity insertion rate with the accident terminated by reactor trip at 35 percent nominal power. This insertion rate is greater than that for the two highest worth control banks, both assumed to be in their highest incremental worth region. Figure 14.1.1-1 shows the neutron flux transient.

The energy release and the fuel temperature increases are relatively small. The thermal flux response, of interest for departure from nucleate boiling considerations, is shown in Figure 14.1.1-1. The beneficial effect on the inherent thermal lag in the fuel is evidenced by a peak heat flux less than the full-power nominal value. There is a large margin-to-departure from nucleate boiling during the transient, since the rod surface heat flux remains below the design value, and there is a high degree of subcooling at all times in the core. Figure 14.1.1-2 shows the response of the hot spot average fuel and cladding temperature. The average fuel temperature increases to a value lower than the nominal full-power value.

The minimum DNBR at all times remains above the limit value. The calculated sequence of events for this accident is shown in Table 14.1.1-1. With the reactor tripped, the plant returns to a stable condition. The plant may subsequently be cooled down further by following normal plant shutdown procedures.

Conclusion

If a rod cluster control assembly withdrawal accident from the subcritical condition occurs, the core and the reactor coolant system are not adversely affected, since the departure from nucleate boiling ratio remains above the limit value.

TABLE 14.1.1-1

TIME SEQUENCE OF EVENTS FOR
UNCONTROLLED RCCA WITHDRAWAL FROM
A SUBCRITICAL CONDITION

| <u>Event</u> | <u>Time of Each Event (Seconds)</u> |
|---|---|
| Initiation of uncontrolled rod withdrawal, 97.5 pcm/second reactivity insertion rate, from 10^{-9} of nominal power | 0 |
| Power range high neutron flux low setpoint reached | 8.09 |
| Peak nuclear power occurs | 8.21 |
| Rods begin to fall into core | 8.59 |
| Peak heat flux occurs | 10.14 |
| Minimum DNBR occurs | 10.25 |
| Peak clad temperature occurs | 10.53 [?] |
| Peak average fuel temperature occurs | 10.63 |

Figure 14.1.1-1

GINNA UNCONTROLLED RCCA BANK WITHDRAWAL FROM SUBCRITICAL

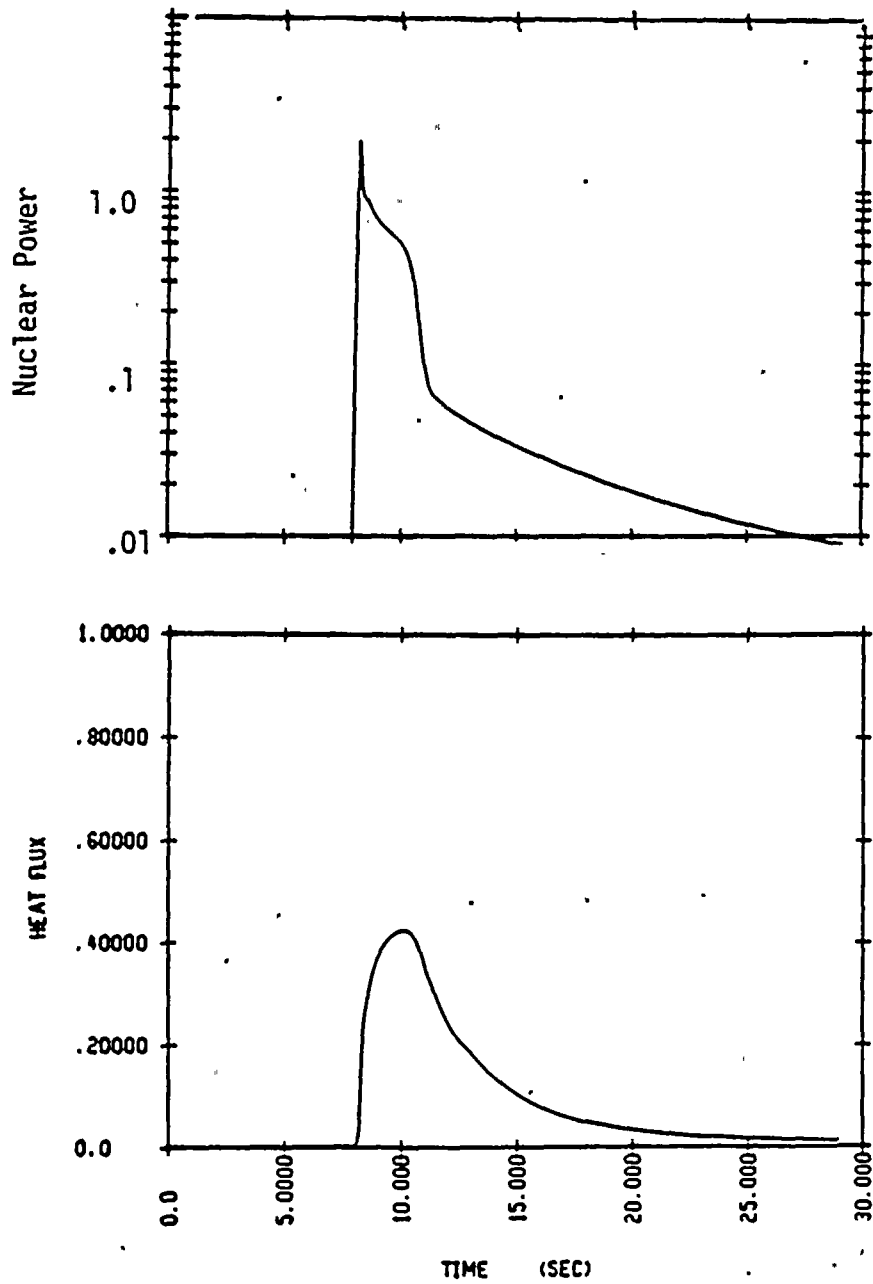
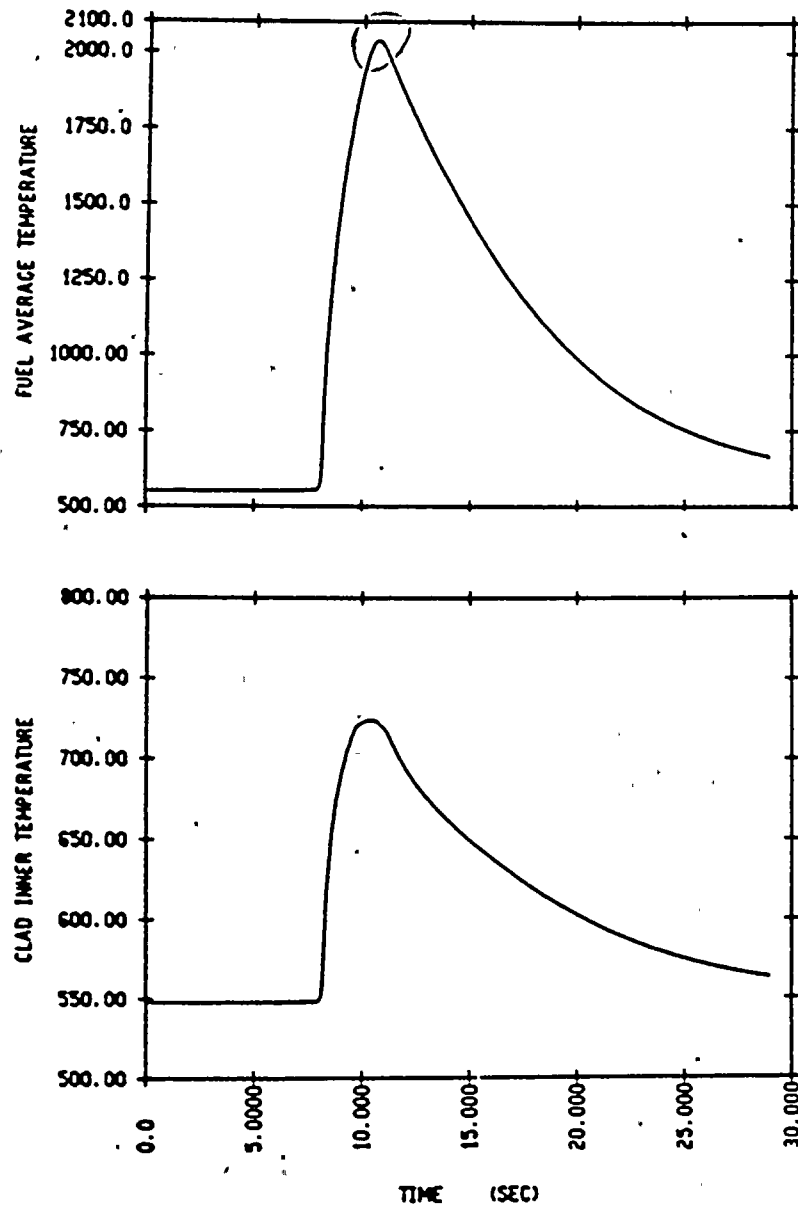


Figure 14.1.1-2

GINNA Uncontrolled RCCA Bank Withdrawal from Subcritical



14.1.2 Uncontrolled RCCA Withdrawal at Power

An uncontrolled RCCA withdrawal at power results in an increase in core heat flux. Since the heat extraction from the steam generator remains constant, there is a net increase in reactor coolant temperature. Unless terminated by manual or automatic action, this power mismatch and resultant coolant temperature rise would eventually result in DNB. Therefore, to prevent the possibility of damage to the cladding, the Reactor Protection System is designed to terminate any such transient with an adequate margin to DNB.

The automatic features of the Reactor Protection System which prevent core damage in a rod withdrawal accident at power include the following:

1. Nuclear power range instrumentation actuates a reactor trip if two out of the four channels exceed an overpower setpoint. *which*
2. Reactor trip is actuated if any two out of four ΔT channels exceed an overtemperature ΔT setpoint. This setpoint is automatically varied with axial power imbalance, coolant temperature and pressure to protect against DNB.
3. Reactor trip is actuated if any two out of four ΔT channels exceed an overpower ΔT setpoint. This setpoint is automatically varied with axial power imbalance and coolant temperature to ensure that the allowable heat generation rate (kw/ft) is not exceeded.
4. A high pressure reactor trip, actuated from any two out of three pressure channels, is set at a fixed point. This set pressure will be less than the set pressure for the pressurizer safety valves.

5. A high pressurizer water level reactor trip, actuated from any two out of three level channels, is actuated at a fixed setpoint. This affords additional protection for RCCA withdrawal accidents.

The manner in which the combination of overpower and overtemperature ΔT trips provides protection over the full range of reactor coolant system conditions is illustrated in Figure 14-1. Figure 14-1 presents allowable reactor loop average temperature and ΔT for the design power distribution and flow as a function of primary coolant pressure. The boundaries of operation defined by the overpower ΔT trip and the overtemperature ΔT trip are represented as "protection lines" on this diagram. These protection lines are drawn to include all adverse instrumentation and setpoint errors, so that under nominal conditions trip would occur well within the area bounded by these lines. A maximum steady-state operating condition for the reactor is also shown on the Figure.

The utility of the diagram just described is in the fact that the operating limit imposed by any given DNB ratio can be represented as a line on this coordinate system. The DNB lines represent the locus of conditions for which the DNBR equals the limit value. All points below and to the left of this line have a DNB ratio greater than this value. The diagram shows that DNB is prevented for all cases if the area enclosed within the maximum protection lines is not traversed by the applicable DNB ratio line at any point.

The region of permissible operation (power, pressure and temperature) is completely bounded by the combination of reactor trips: nuclear overpower (fixed setpoint); high pressure (fixed setpoint); low pressure



(fixed setpoint); overpower and overtemperature ΔT (variable set-points). These trips are designed to prevent overpower and a DNB ratio of less than the limit value.

*No. of Rec.
Pumps*

Method of Analysis

Uncontrolled rod cluster control assembly bank withdrawal is analyzed by the LOFTRAN code. This code simulates the neutron kinetics, reactor coolant system, pressurizer, pressurizer relief and safety valves, pressurizer spray, steam generator, and steam generator safety valves. The code computes pertinent plant variables, including temperatures, pressures, and power level. The core limits, as illustrated in Figure 14-1, are used as input to LOFTRAN to determine the minimum departure from nucleate boiling ratio during the transient. This accident is analyzed with the Improved Thermal Design Procedure as described in Reference 6. Plant characteristics and initial conditions are discussed in Section 14.

In order to obtain conservative values of departure from nucleate boiling ratio, the following assumptions are made:

1. Initial Conditions - Initial reactor power, reactor coolant average temperatures, and reactor coolant pressure are assumed to be at their nominal values. Uncertainties in initial conditions are included in the limit DNBR as described in Reference 6.
2. Reactivity Coefficients - Two cases are analyzed.
 - a. Minimum Reactivity Feedback - A positive (5 pcm/°F) moderator coefficient of reactivity is assumed, corresponding to the beginning-of-core-life. A variable Doppler power coefficient with core power is used in the analysis. A conservatively small (in absolute magnitude) value is assumed.

- b. Maximum Reactivity Feedback - A conservatively large positive moderator density coefficient and a large (in absolute magnitude) negative Doppler power coefficient are assumed.
3. The rod cluster control assembly trip insertion characteristic is based on the assumption that the highest worth assembly is stuck in its fully withdrawn position.
4. The reactor trip on high neutron flux is assumed to be actuated at a conservative value of 118% of nominal full power. The overtemperature ΔT trip includes all adverse instrumentation and setpoint errors; the delays for trip actuation are assumed to be the maximum values. No credit was taken for the other expected trip functions.
5. The maximum positive reactivity insertion rate is greater than that for the simultaneous withdrawal of the combination of the two control banks having the maximum combined worth at maximum speed.

The effect of rod cluster control assembly movement on the axial core power distribution is accounted for by causing a decrease in overtemperature and overpower ΔT trip setpoints proportional to a decrease in margin to DNB.

Results

Figures 14.1.2-1 through 14.1.2-3 show the plant response (including neutron flux, pressure, average coolant temperature, and departure from nucleate boiling ratio) to a rapid rod cluster control assembly withdrawal incident starting from full power. Reactor trip on high neutron flux occurs shortly after the start of the accident. Since this is rapid with respect to the thermal time constants of the plant, small changes in T_{avg} and pressure result, and a large margin to DNB is maintained.

The plant response for a slow control rod assembly withdrawal from full power is shown in Figures 14.1.2-4 through 14.1.2-6. Reactor trip on overtemperature ΔT occurs after a longer period, and the rise in temperature and pressure is consequently larger than for rapid rod cluster control assembly withdrawal. Again, the minimum DNBR is greater than the limit value.

Figure 14.1.2-7 shows the minimum departure from nucleate boiling ratio as a function of reactivity insertion rate from initial full-power operation for the minimum and maximum reactivity feedback cases. It can be seen that two reactor trip channels provide protection over the whole range of reactivity insertion rates. These are the high neutron flux and overtemperature ΔT trip channels. The minimum DNBR is never less than the limit value.

Figures 14.1.2-8 and 14.1.2-9 show the minimum departure from nucleate boiling ratio as a function of reactivity insertion rate for rod cluster control assembly withdrawal incidents starting at 60% and 10% power respectively. The results are similar to the 100% power case, except that as the initial power is decreased, the range over which the overtemperature ΔT trip is effective is increased. In neither case does the departure from nucleate boiling ratio fall below the DNBR limit value.

In the referenced figures, the shape of the curves of minimum departure from nucleate boiling ratio versus reactivity insertion rate is due both to reactor core and coolant system transient response and to protection system action in initiating a reactor trip.

Referring to Figure 14.1.2-9, for example, it is noted that:

1. For high reactivity insertion rates (i.e., between $\sim 1 \times 10^{-3} \Delta k/\text{second}$ and $\sim 3.0 \times 10^{-5} \Delta k/\text{second}$), reactor trip is initiated by the high neutron flux trip for the minimum reactivity feedback cases. The neutron flux level in the core rises rapidly for these insertion rates, while core heat flux and coolant system temperature lag behind due to the thermal capacity of the fuel and coolant system fluid. Thus, the reactor is tripped prior to significant increase in heat flux or water temperature with resultant high minimum departure from nucleate boiling ratios during the transient. Within this range, as the reactivity insertion rate decreases, core heat flux and coolant temperatures can remain more nearly in equilibrium with the neutron flux; minimum DNBR during the transient thus decreases with decreasing insertion rate.
2. With further decrease in reactivity insertion rate, the over-temperature ΔT and high neutron flux trips become equally effective in terminating the transient (e.g., at $\sim 3.0 \times 10^{-5} \Delta k/\text{second}$ reactivity insertion rate).

The overtemperature ΔT reactor trip circuit initiates a reactor trip when measured coolant loop ΔT exceeds a setpoint based on measured reactor coolant system average temperature and pressure. It is important in this context to note, however, that the average temperature contribution to the circuit is lead-lag compensated in order to decrease the effect of the thermal capacity of the reactor coolant system in response to power increases.

For reactivity insertion rates between $\sim 3.0 \times 10^{-5} \Delta k/\text{second}$ and $\sim 6.0 \times 10^{-6} \Delta k/\text{second}$, the effectiveness of the over-temperature ΔT trip increases (in terms of increased minimum departure from nucleate boiling ratio) due to the fact that,

with lower insertion rates, the power increase rate is slower, the rate of rise of average coolant temperature is slower, and the lead-lag compensation provided can increasingly account for the coolant system thermal capacity lag.

3. For maximum reactivity feedback cases reactivity insertion rates less than $\sim 5.0 \times 10^{-4} \Delta k/\text{second}$, the rise in reactor coolant temperature is sufficiently high so that the steam generator safety valve setpoint is reached prior to trip. Opening these valves, which act as an additional heat load on the reactor coolant system, sharply decreases the rate of rise of reactor coolant system average temperature. This decrease in rate of rise of the average coolant system temperature during the transient is accentuated by the lead-lag compensation, causing the overtemperature ΔT trip setpoint to be reached later with resulting lower minimum departure from nucleate boiling ratios.

Figures 14.1.2-7, 14.1.2-8, and 14.1.2-9 illustrate minimum departure from nucleate boiling ratio calculated for minimum and maximum reactivity feedback. The calculated sequence of events for this accident is shown in Table 14.1.2-1.

Conclusions

In the unlikely event of a control rod withdrawal incident, from full-power operation or lower power levels, the core and reactor coolant system are not adversely affected since the minimum value of DNB ratio reached is in excess of the DNB limit value for all rod reactivity rates. Protection is provided by nuclear flux overpower and overtemperature ΔT . Additional protection would be provided by the high pressurizer level, overpower ΔT , and the high pressure reactor trip. The preceding sections have described the effectiveness of these protection channels.

4 of 21 (P)

TABLE 14.1.2-1

TIME SEQUENCE OF EVENTS FOR
UNCONTROLLED RCCA WITHDRAWAL AT POWER

| <u>Event</u> | <u>Time of Each Event (Seconds)</u> |
|---|---|
| <u>Case A:</u> | |
| Initiation of uncontrolled rod cluster control assembly withdrawal at full power and maximum reactivity insertion rate (90 pcm/sec) | 0 |
| Power range high neutron flux high trip point reached | 3.21 |
| Rods begin to fall into core | 3.71 |
| Minimum departure from nucleate boiling ratio occurs | 4.00 |
| <u>Case B:</u> | |
| Initiation of uncontrolled rod cluster control assembly withdrawal at full power and at a small reactivity insertion rate (7 pcm/sec) | 0 |
| Overtemperature ΔT reactor trip signal initiated | 264.7 |
| Rods begin to fall into core | 266.7 |
| Minimum departure from nucleate boiling ratio occurs | 267.0 |

Figure 14.1.2-1

GINNA UNCONTROLLED RCCA BANK WITHDRAWAL AT POWER
MAXIMUM FEEDBACK
100% POWER, 90 pcm/SEC

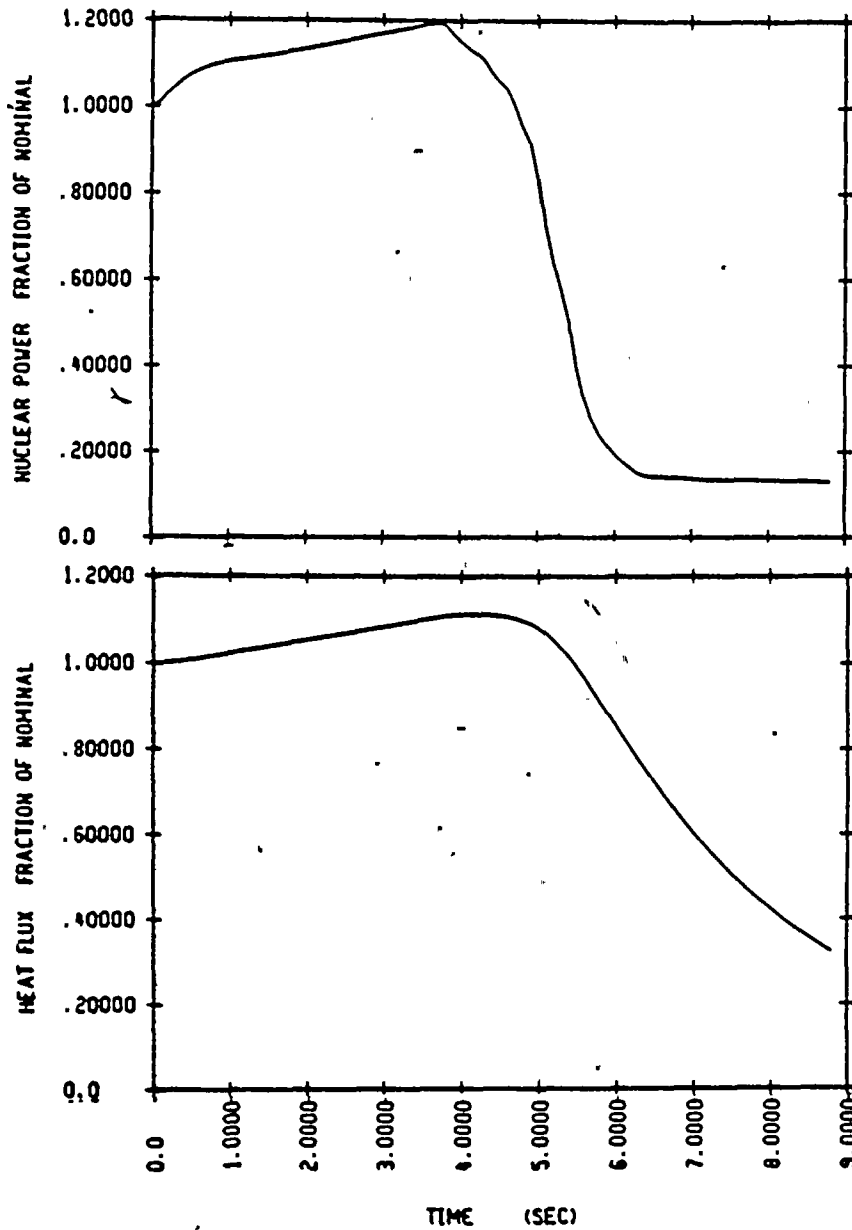


Figure 14.1.2-2
 Ginna Uncontrolled RCCA Bank Withdrawal at Power
 100% Power, 90 pcm/sec
 MAXIMUM FEEDBACK

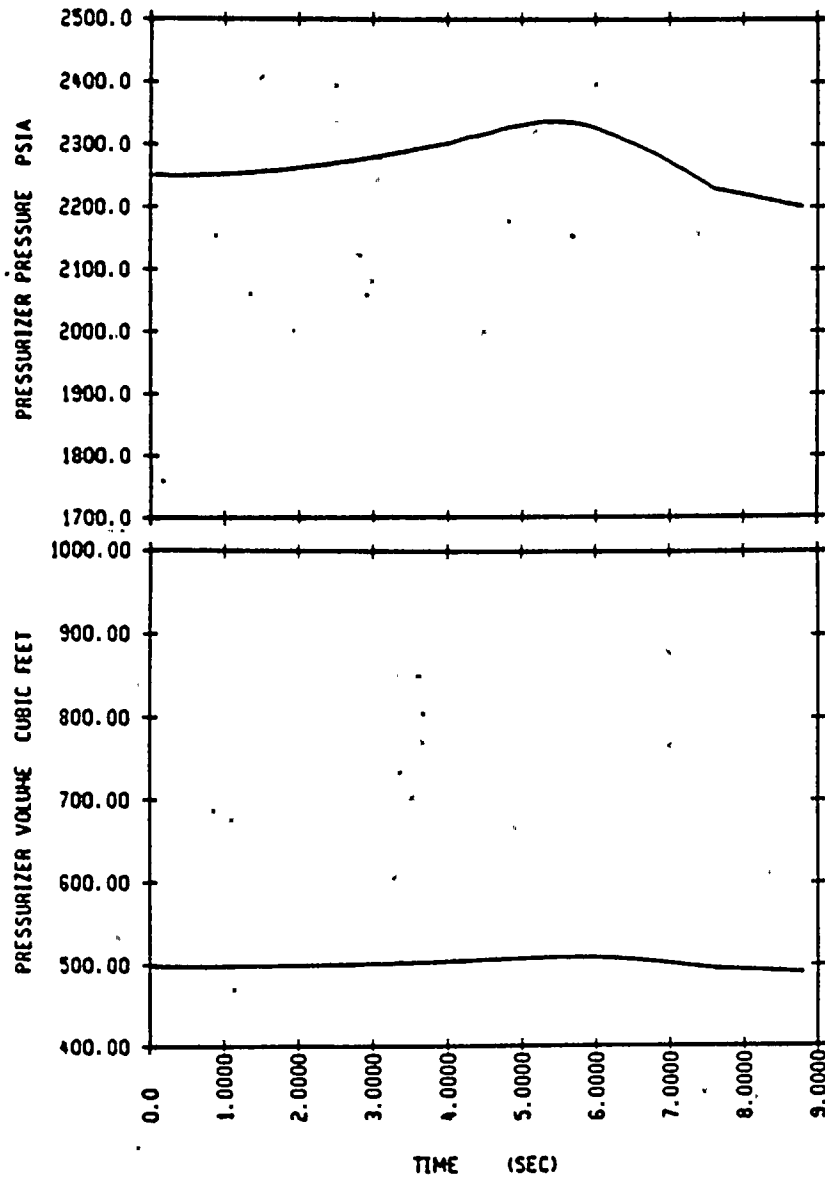


Figure 14.1.2-3

Ginna Uncontrolled RCCA Bank Withdrawal at Power
MAXIMUM FEEDBACK
100% Power, 90 pcm/sec

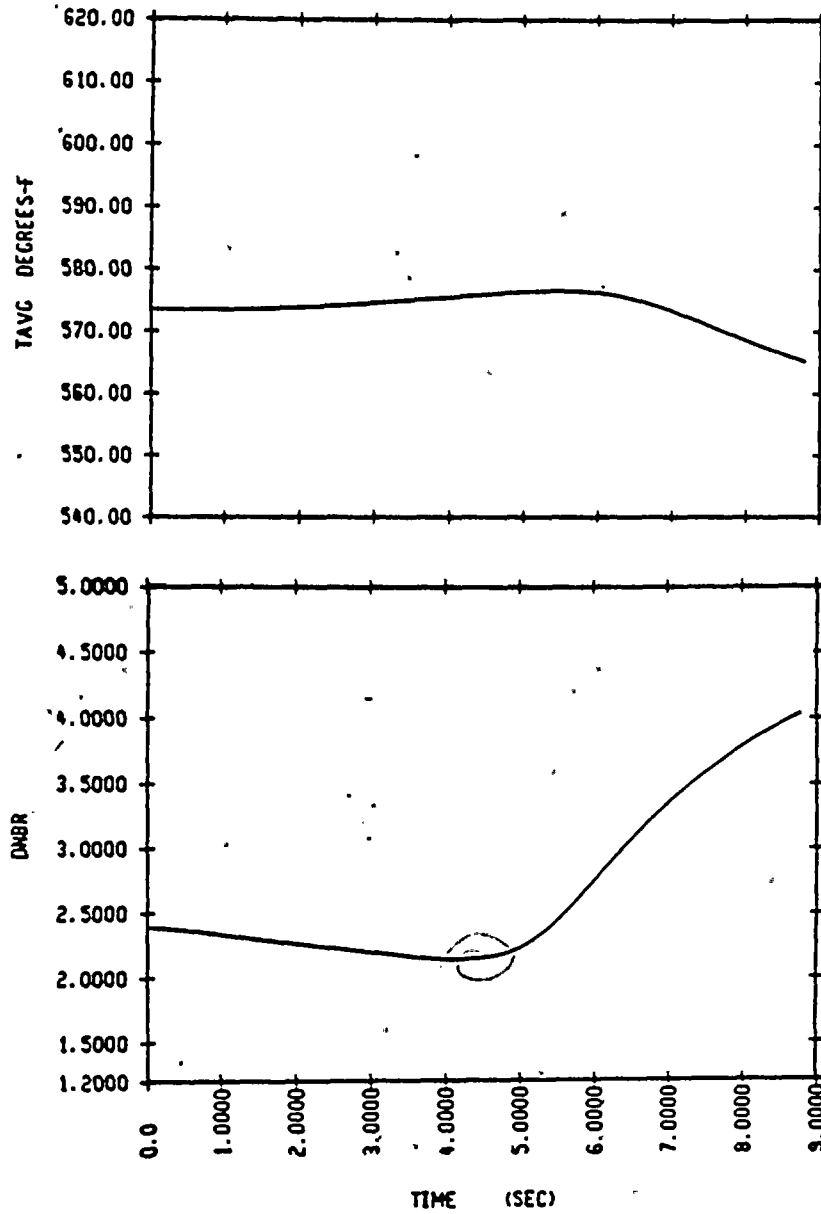


Figure 14.1.2-4

GINNA UNCONTROLLED RCCA BANK WITHDRAWAL AT POWER

100% POWER, 7 pcm/SEC
MAXIMUM FEEDBACK

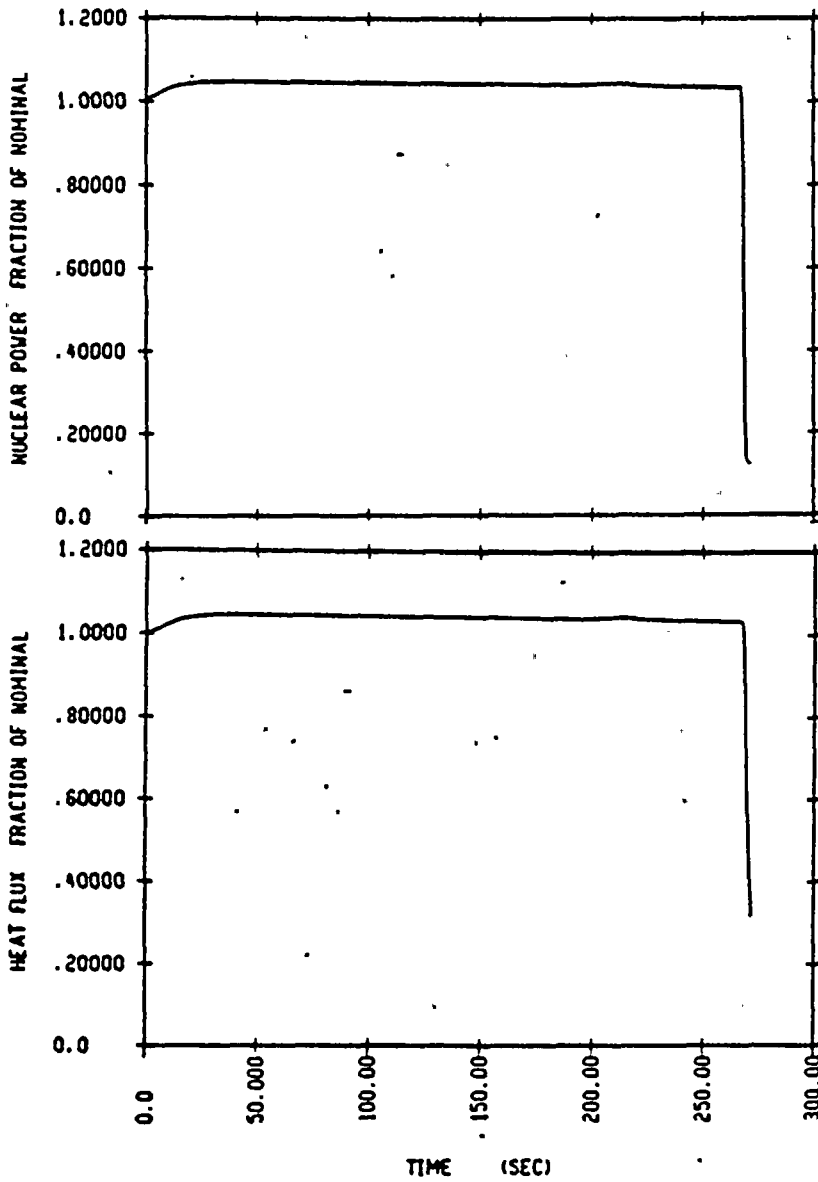




Figure 14.1.2-5

Ginna Uncontrolled RCCA Bank Withdrawal at Power

100% Power, 7 pcm/sec

MAXIMUM FEEDBACK

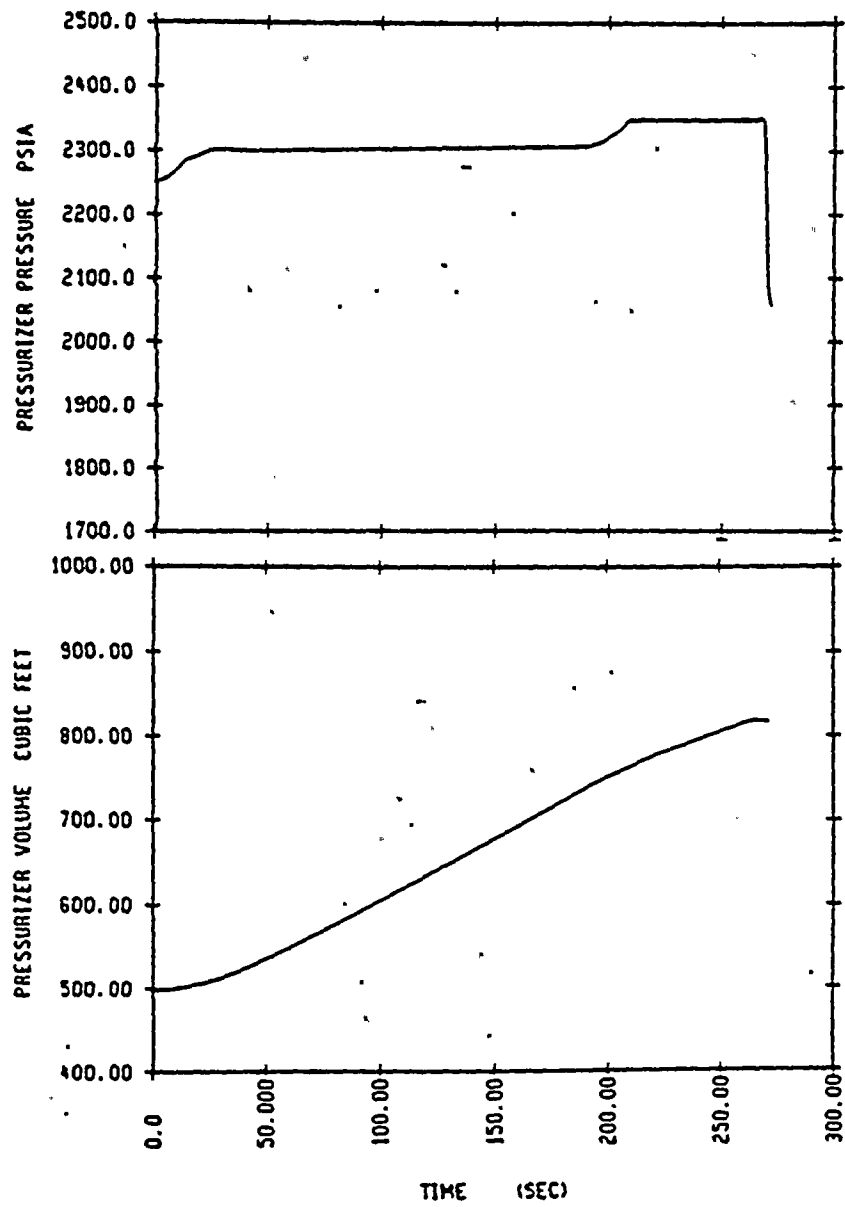


Figure 14.1.2-6

· Ginna Uncontrolled RCCA Bank Withdrawal at Power

100% Power, 7 pcm/sec

MAXIMUM FEEDBACK

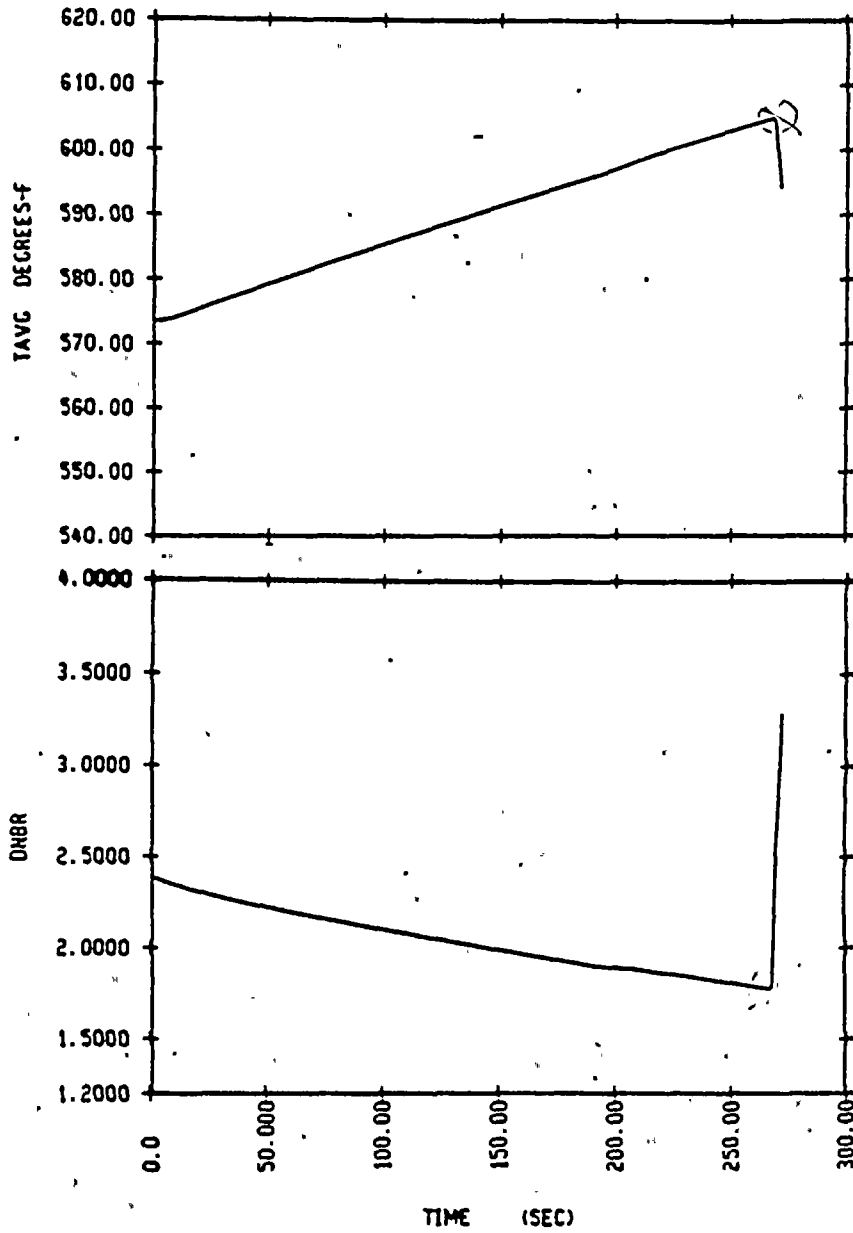
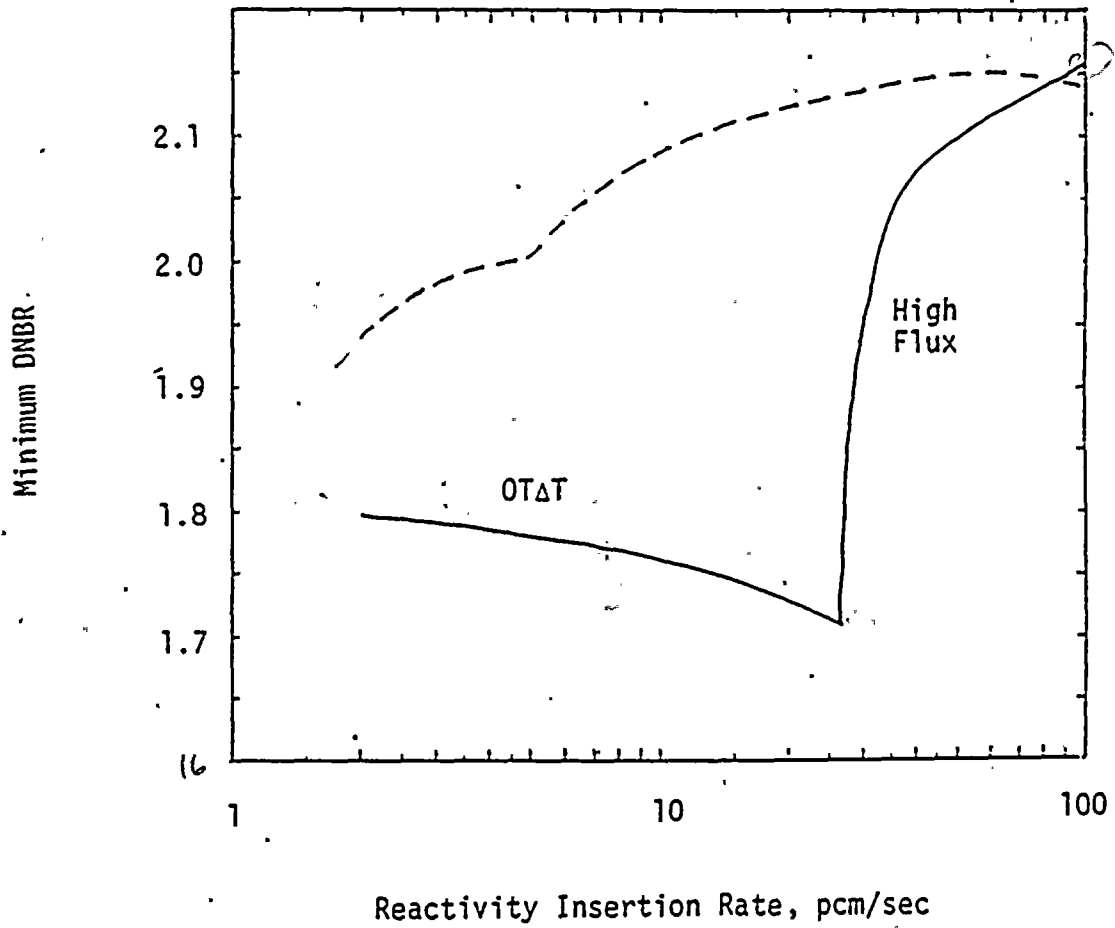


Figure 14.1.2- 7
Ginna Uncontrolled Bank Withdrawal
from 100% Power

— Maximum Feedback
- - - Minimum Feedback



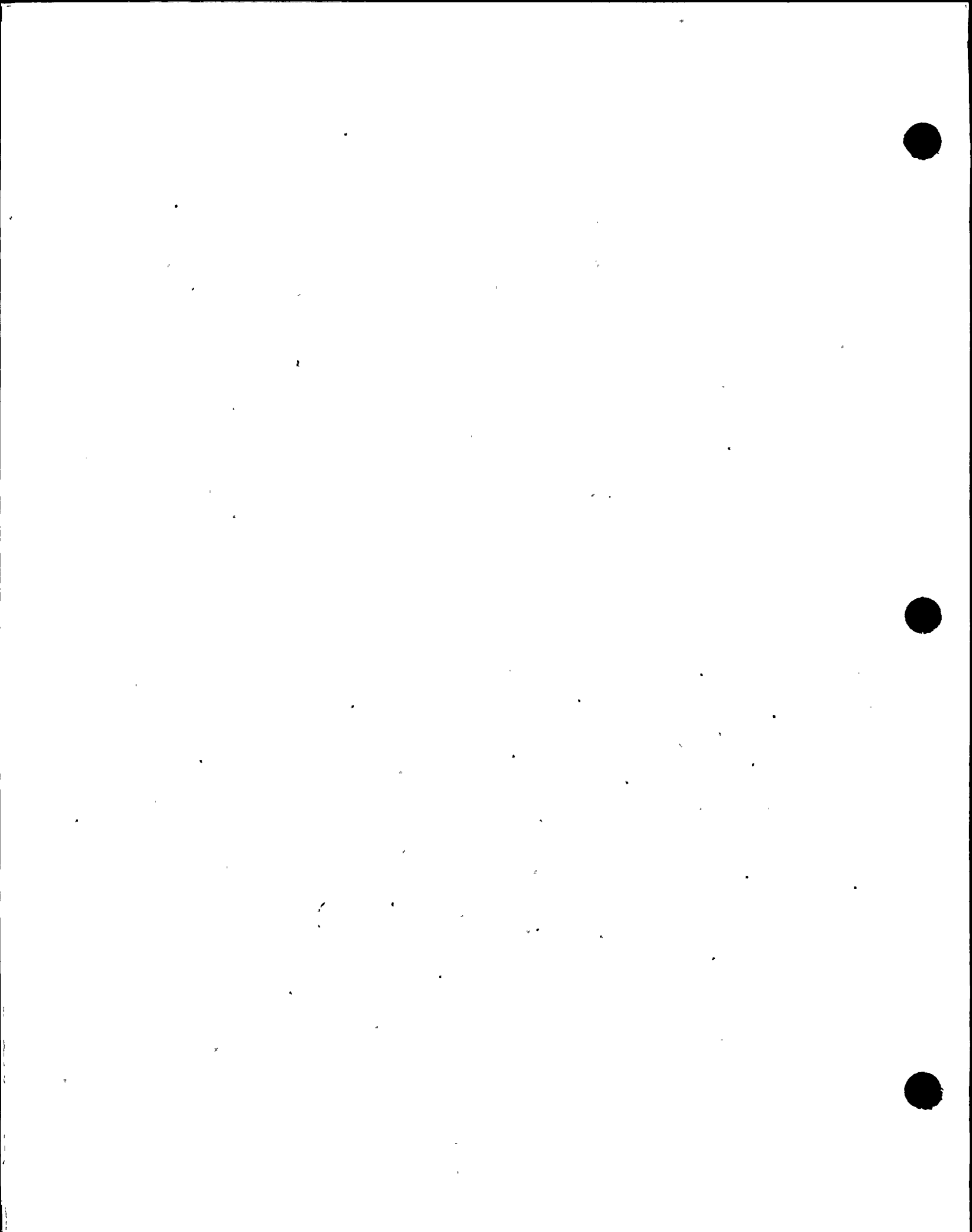


Figure 14.1.2-8

Ginna Uncontrolled Bank Withdrawal
from 60% Power

—— Maximum Feedback
- - - Minimum Feedback

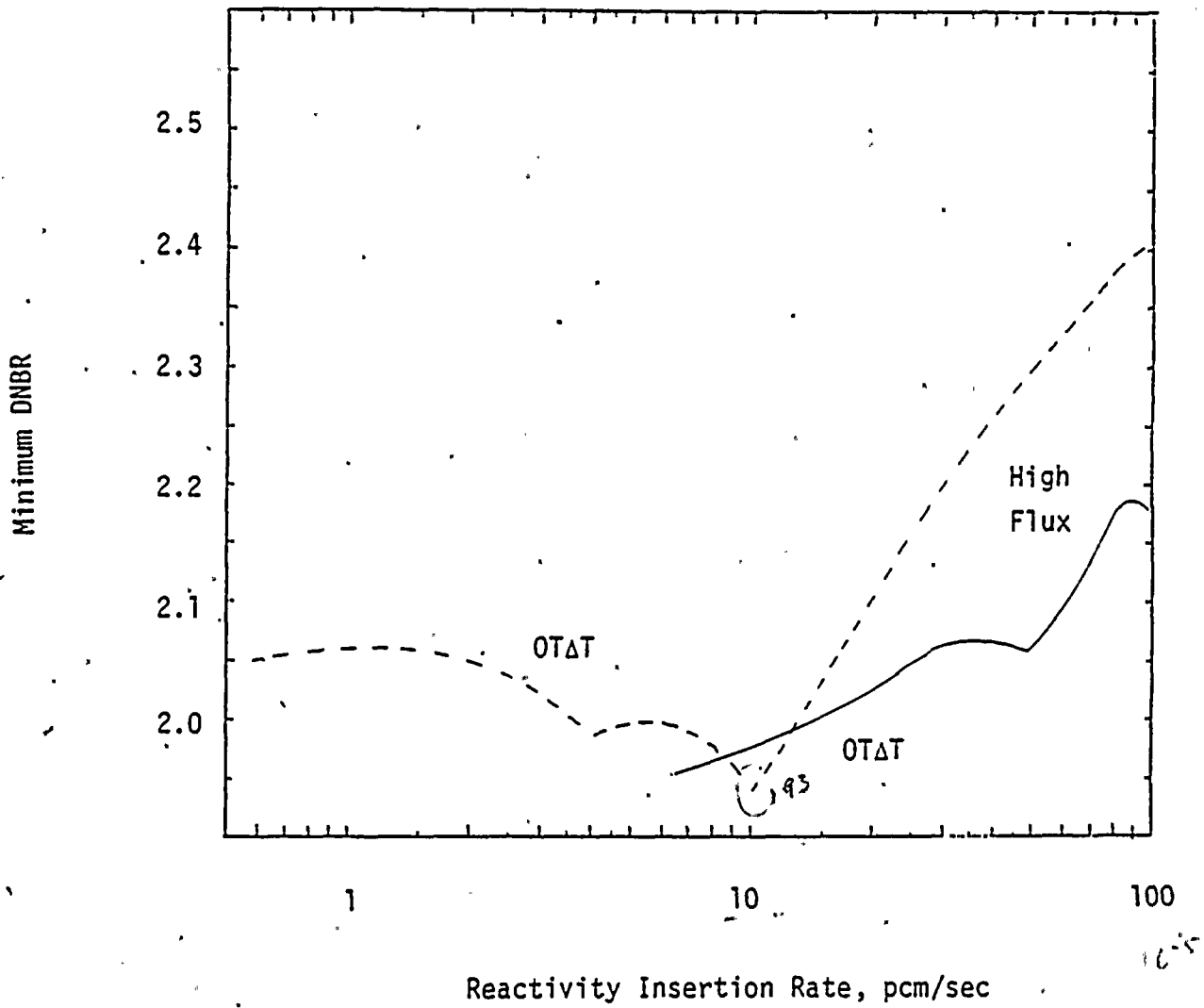
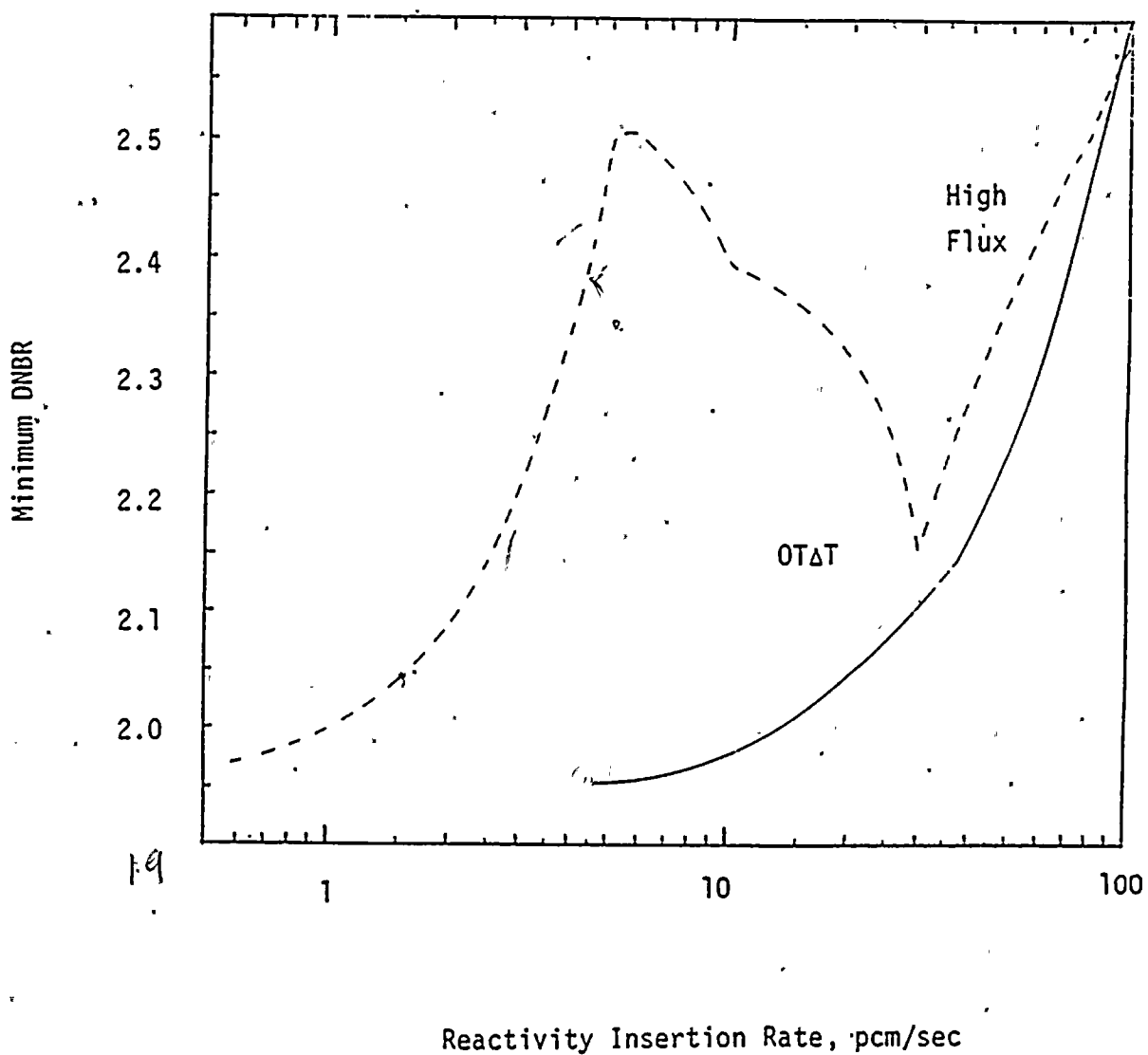


Figure 14.1.2-9

Ginna Uncontrolled Bank Withdrawal
from 10% Power

— Maximum Feedback
- - - Minimum Feedback



1



14.1.4 Rod Cluster Control Assembly (RCCA) Drop

Dropping of a full-length RCCA occurs when the drive mechanism is deenergized. This would cause a power reduction and an increase in the hot channel factor. If no protective action occurred, the Reactor Control System would restore the power to the level which existed before the incident. This would lead to a reduced safety margin or possibly DNB, depending upon the magnitude of the resultant hot channel factor.

If an RCCA drops into the core during power operation, it would be detected either by a rod bottom signal, by an out-of-core chamber, or by both. The rod bottom signal device provides an indication signal for each RCCA. The other independent indication of a dropped RCCA is obtained by using the out-of-core power range channel signals. This rod drop detection circuit is actuated upon sensing a rapid decrease in local flux and is designed such that normal load variations do not cause it to be actuated.

A rod drop signal from any rod position indication channel, or from one or more of the four power range channels, initiates the following protective action: reduction of the turbine load by a preset adjustable amount and blocking of further automatic rod withdrawal. The turbine runback is achieved by acting upon the turbine load limit and on the turbine load reference. The rod withdrawal block is redundantly achieved.

Method Analysis

The transient following a dropped RCCA accident is determined by a detailed digital simulation of the plant. The dropped rod causes a step decrease in reactivity and the core power generation is determined using the LOFTRAN code. The overall response is calculated by simulating the turbine load runback and preventing rod withdrawal. The analysis is presented for the case in which the load cutback very closely matches the power decrease from the negative reactivity for a dropped rod

(800 pcm) and also for the case in which the load cutback is greater than that required to match the worth of the dropped rod (100 pcm). In both cases the load is assumed to be cut back from 100 to 84% of full load at a conservatively slow rate of approximately 1% per second.

The most negative values of moderator and Doppler temperature coefficients of reactivity are used in this analysis resulting in the highest heat flux during the transient. These are a moderator density coefficient of reactivity of $.43 \Delta\rho/\text{gm/cc}$ and a Doppler temperature coefficient of reactivity of $-2.9 \times 10^{-5} \Delta k/^\circ\text{F}$.

This accident is analyzed with the Improved Thermal Design Procedure as described in WCAP-8567 (Reference 6). Plant characteristics and initial conditions are discussed in Section 14.

Results

Figures 14.1.4-1 through 14.1.4-3 illustrate the transient response following a dropped rod of worth 100 pcm. The coolant temperature decreases initially due to the fact that more energy is taken out from the secondary than produced in the primary, then increases under the influence of the negative reactivity effect of the moderator and Doppler temperature coefficients. The peak heat flux following the initial response to the dropped rod is 97% of nominal.

Figures 14.1.4-4 and 14.1.4-6 illustrate the transient response following a dropped rod of worth 800 pcm. Again the reactor coolant average temperature decreases initially, and then increases because of the negative reactivity feedback. For this case, the peak heat flux following the initial response to the dropped rod is 84% of nominal. At the same time the core average temperature drops 11.8°F and the pressure drops 130 psia.

An analysis has been made for the dropped rods at the conditions of peak heat flux following the initial response to the dropped rod. This analysis incorporates the increase in radial hot channel factor caused by the dropped rods. It was found that the DNBR does not fall below the limit value.

An analysis has been also made of the amount of a statically misaligned RCCA for the maximum full power operating conditions (100% power; core water inlet temperature of 543.7°F; primary pressure of 2250 psia). The effect of the static misaligned rod incident was represented by an increase in the radial heat flux hot channel factor. It was found that the increased $F_{\Delta H}$ could be accommodated without the DNBR falling below the limit value.

Conclusions

Protection for a dropped RCCA is provided by automatic turbine runback and blocking of automatic rod withdrawal. As the analyses show, the protection system, in conjunction with the turbine runback, protects the core from DNB. Additionally, for a static misalignment at maximum full-power conditions, DNB will not occur.

Figure 14.1.4-1.
Ginna Dropped Rod - 100 pcm

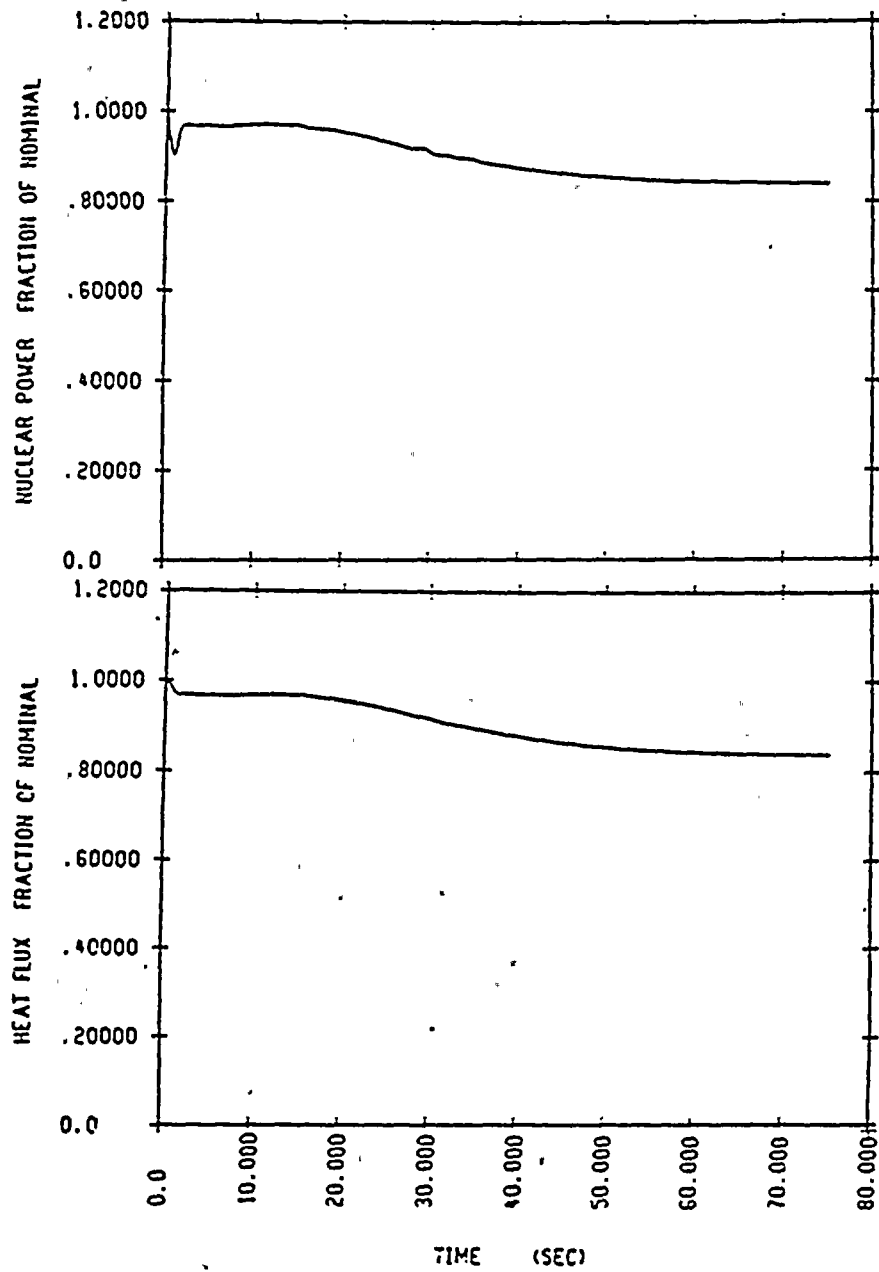


Figure 14.1.4-2.

Ginna Dropped Rod - 100 pcm

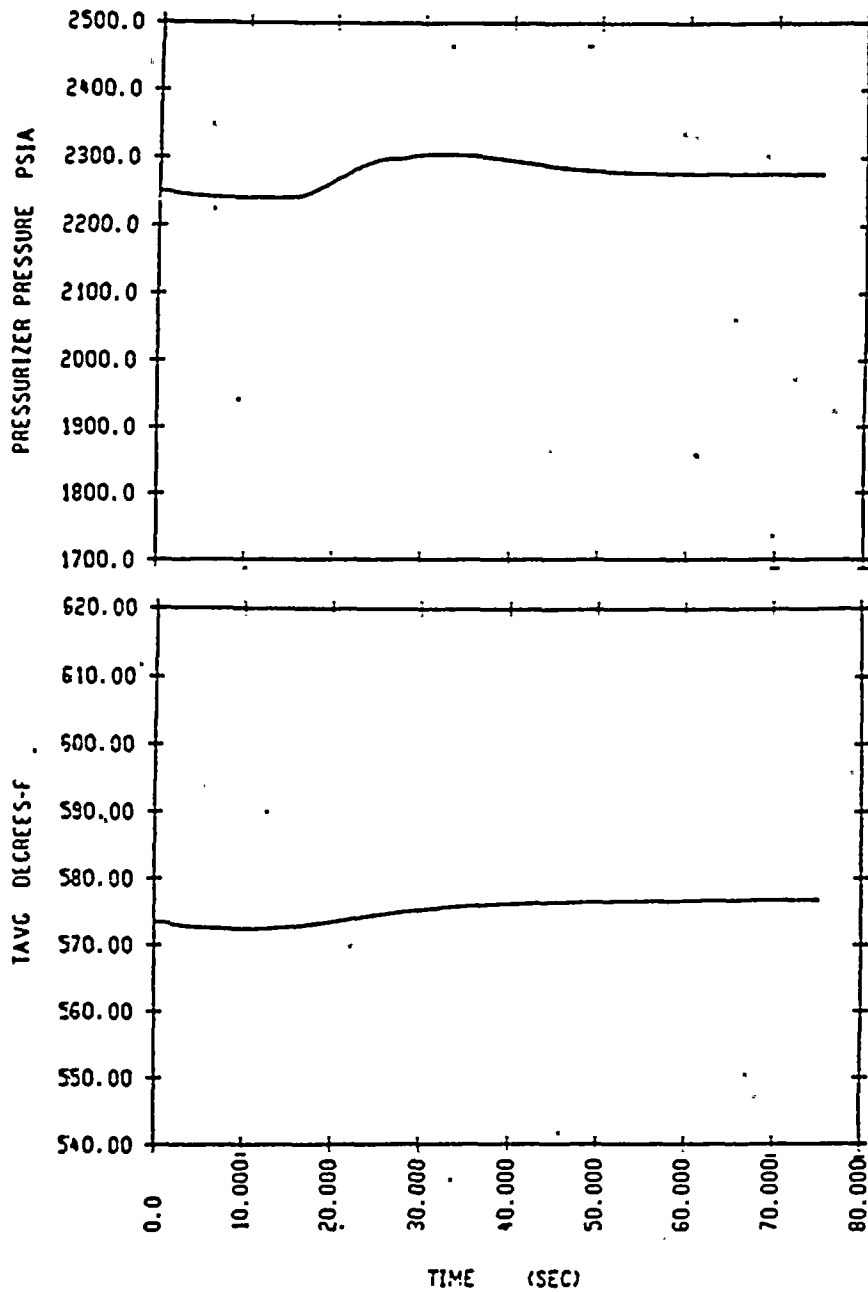


Figure 14.1.4-3
Ginna Dropped Rod - 100 pcm

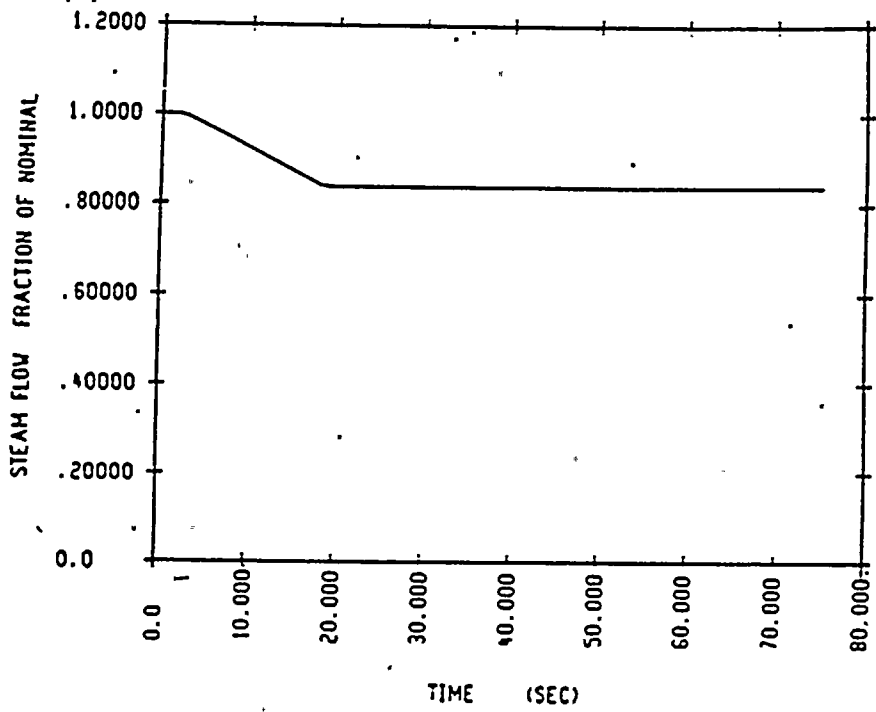


Figure 14.1.4-4
Ginna Dropped Rod - 800 pcm

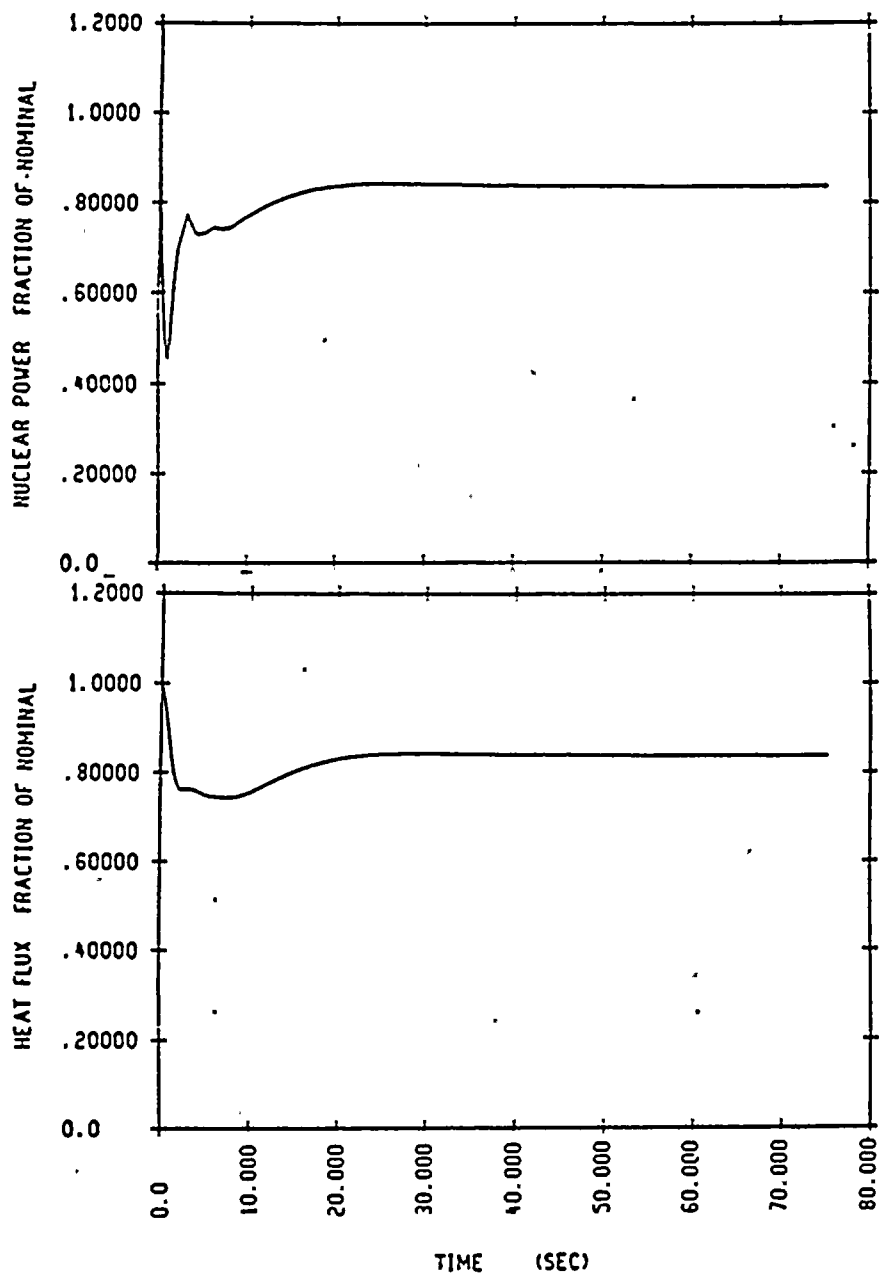
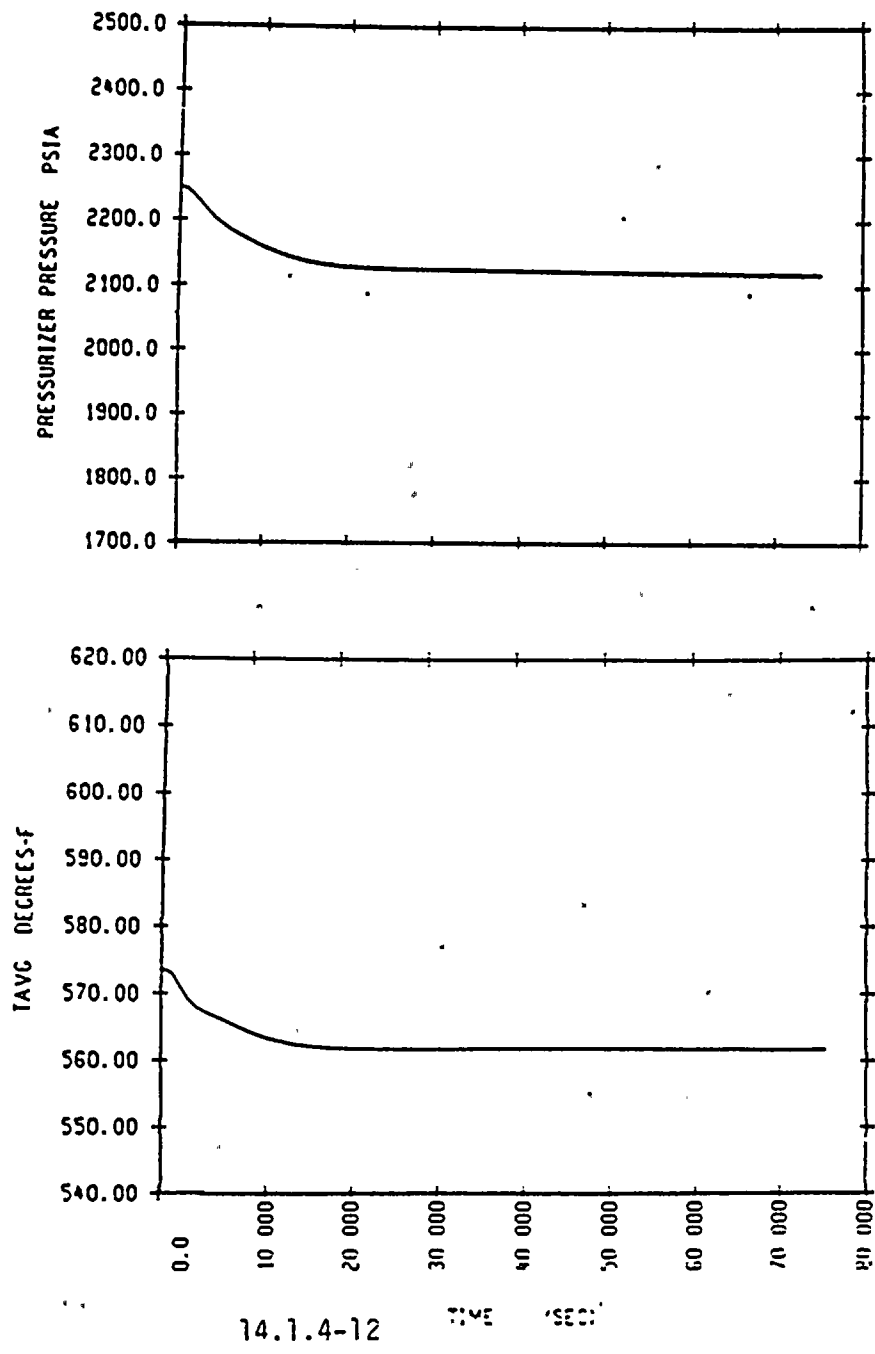


Figure 14.1.4-5
Ginna Dropped Rod - 800 pcm

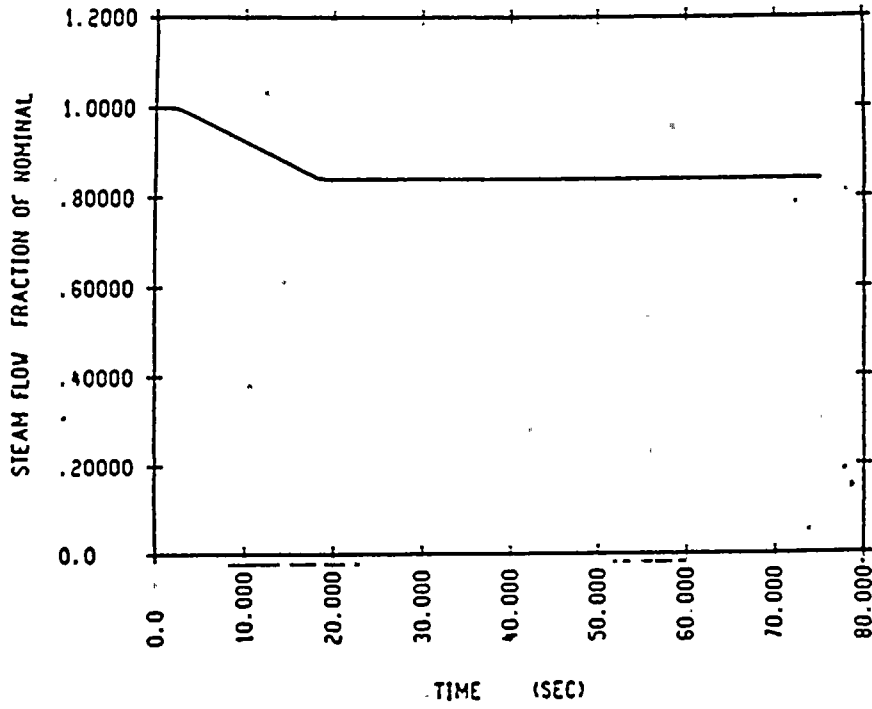


14.1.4-12

TIME (SECS)

Figure 14.1.4-6

Ginna Dropped Rod -.800 pcm



14.1.5 Chemical and Volume Control System Malfunction

Reactivity can be added to the core with the Chemical and Volume Control System by feeding reactor makeup water into the Reactor Coolant System via the reactor makeup control system. The normal dilution procedures call for a limit on the rate and magnitude for any individual dilution, under strict administrative controls. Boron dilution is a manual operation. A boric acid blend system is provided to permit the operator to match the concentration of reactor coolant makeup water to that existing in the coolant at the time. The Chemical and Volume Control System is designed to limit, even under various postulated failure modes, the potential rate of dilution to a value which, after indication through alarms and instrumentation, provides the operator sufficient time to correct the situation in a safe and orderly manner.

There is only a single common source of reactor makeup water to the Reactor Coolant System from the reactor makeup water storage tank, and inadvertent dilution can be readily terminated by isolating this single source. The operation of the reactor makeup water pumps which take suction from this tank provides the only supply of makeup water to the Reactor Coolant System. In order for makeup water to be added to the Reactor Coolant System the charging pumps must be running in addition to the reactor makeup water pumps.

The rate of addition of unborated water makeup to the Reactor Coolant System is limited to the capacity of the makeup water pumps. This limiting addition rate is 120 gpm for two reactor makeup water pumps. For totally unborated water to be delivered at this rate to the Reactor Coolant System at pressure, two charging pumps must be operated at full speed. Normally, two charging pumps are operating at half speed, while the third pump is idle.

The boric acid from the boric acid tank is blended with the reactor makeup water in the blender and the composition is determined by the present flow rates of boric acid and reactor makeup water on the Reactor



Makeup Control. Two separate operations are required. First, the operator must switch from the automatic makeup mode to the dilute mode. Second, the start button must be depressed. Omitting either step would prevent dilution. This makes the possibility of inadvertent dilution very small.

Information on the status of the reactor coolant makeup is continuously available to the operator. Lights are provided on the control board to indicate the operating condition of pumps in the Chemical and Volume Control System. Alarms are actuated to warn the operator if boric acid or demineralized water flow rates deviate from preset values as a result of system malfunction.

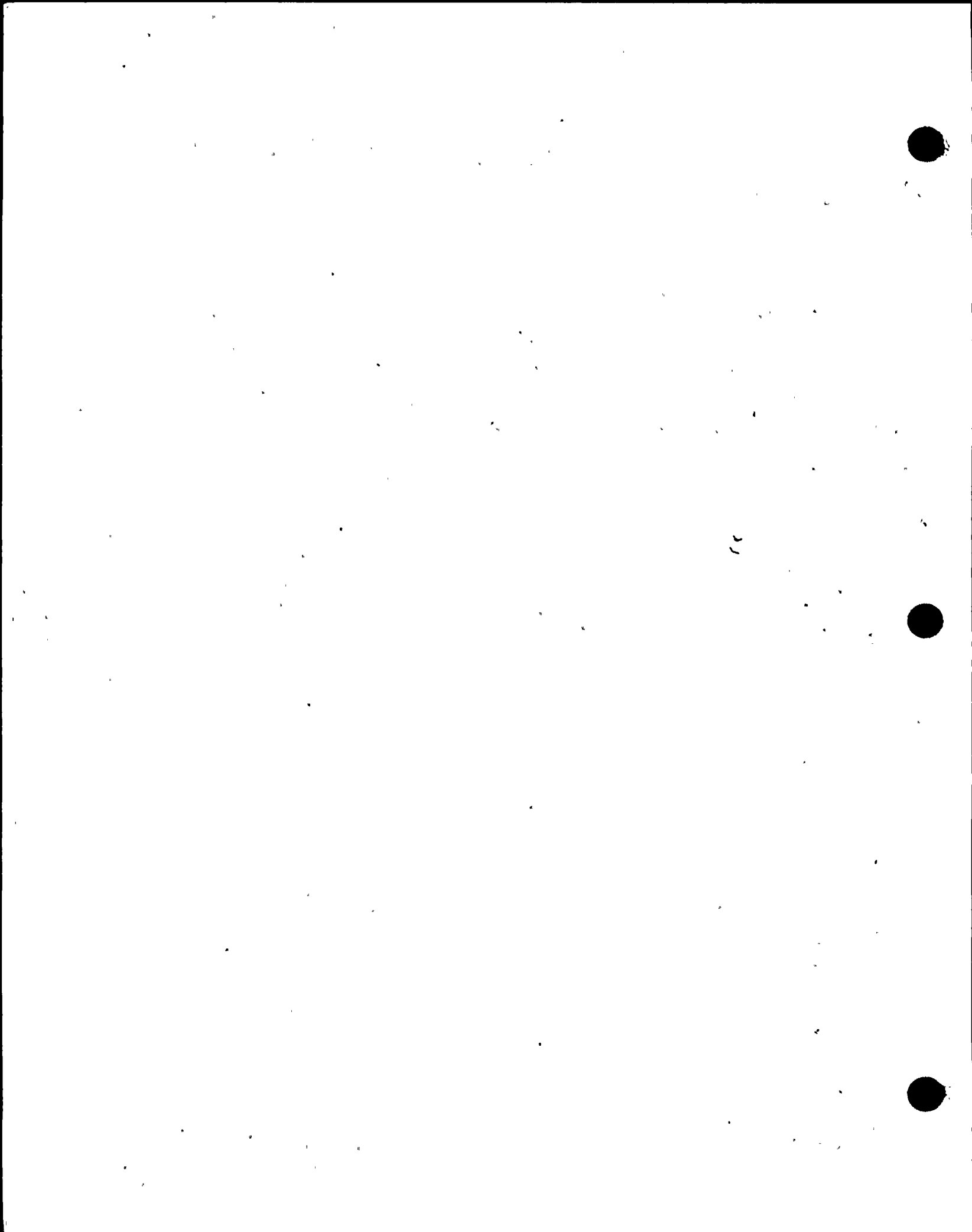
To cover all phases of plant operation, boron dilution during refueling, startup, and power operation are considered in this analysis.

Method of Analysis and Results

Dilution During Refueling

During refueling the following conditions exist:

- a) One residual heat removal pump is running to ensure continuous mixing in the reactor vessel,
- b) The valve in the seal water header to the reactor coolant pumps is closed,
- c) The valves on the suction side of the charging pumps are adjusted for addition of concentrated boric acid solution.
- d) The boron concentration of the refueling water is a minimum of 2000 ppm, corresponding to a shutdown of 5 percent Δk with all control rods in; periodic sampling ensures that this concentration is maintained, and



- e) Neutron sources are installed in the core and BF_3 detectors connected to instrumentation giving audible count rates to provide direct monitoring of the core.

A minimum water volume in the Reactor Coolant System of 2724 ft³ is considered. This corresponds to the volume necessary to fill the reactor vessel to the midplane of the nozzles to ensure mixing via the residual heat removal loop. The maximum dilution flow of 120 gpm and uniform mixing are also considered. Administrative procedures limit the charging flow to one pump available (two pumps locked out). The maximum dilution flow assumes the single failure, such that two pumps are delivering maximum flow.

The operator has prompt and definite indication of any boron dilution from the audible count rate instrumentation. High count rate is alarmed in the reactor containment and the main control room. The count rate increase is proportional to the inverse multiplication factor. At 1420 ppm, for example, a typical core is 4 percent shutdown and the count rate is increased by a factor of 3.3 over the count rate at 2000 ppm.

The boron concentration must be reduced from 2000 ppm to approximately 1500 ppm before the reactor will go critical. This would take at least 48.8 minutes. This is ample time for the operator to recognize the audible high count rate signal and isolate the reactor makeup water source by closing valves and stopping the reactor makeup water pumps.

Dilution During Startup

Prior to refueling, the Reactor Coolant System is filled with borated water from the refueling water storage tank. Core monitoring is by external BF_3 detectors. Mixing of reactor coolant is accomplished by operation of the reactor coolant pumps. Again, the maximum dilution flow (120 gpm) is considered. The volume of reactor coolant is



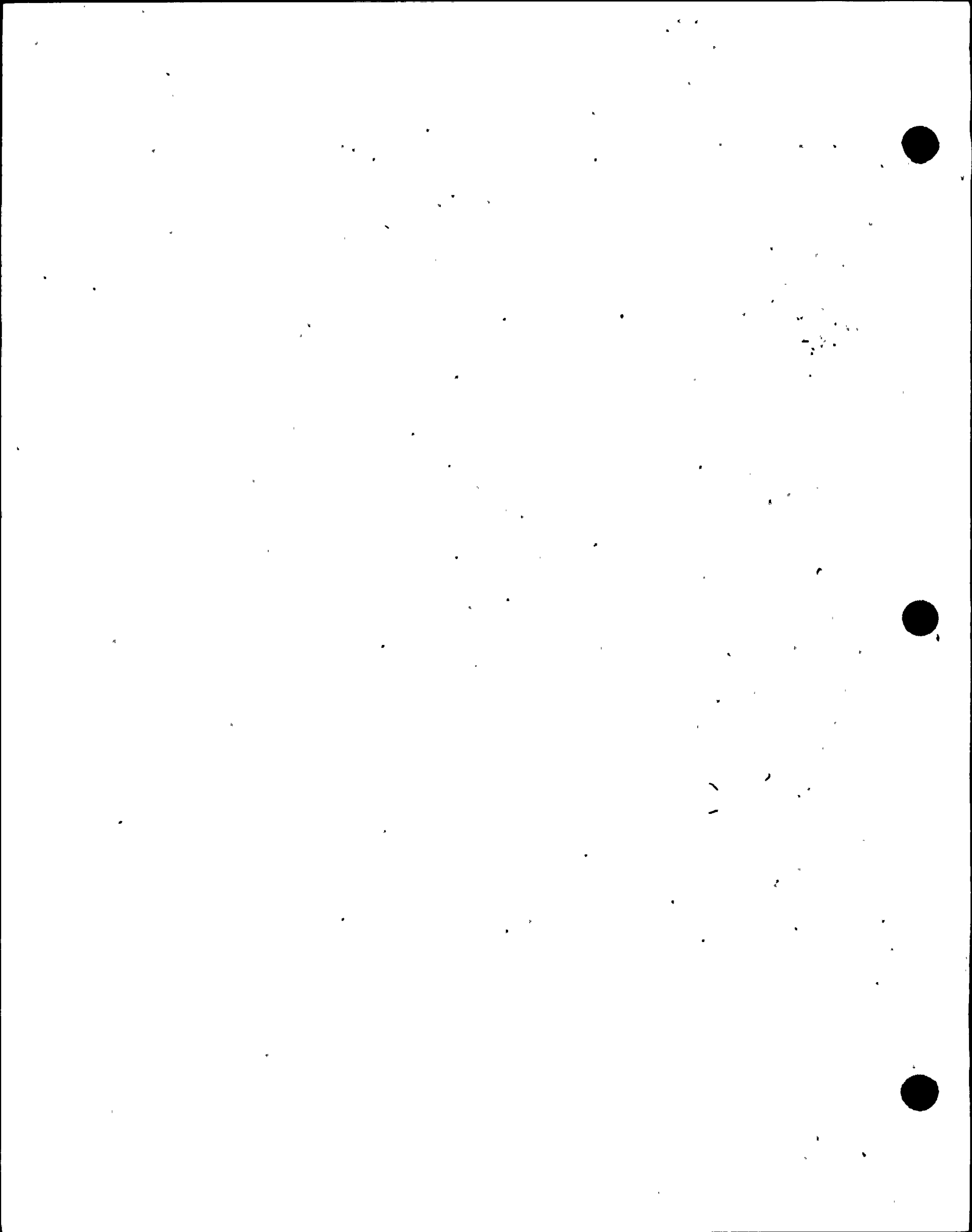
approximately 4755 ft³ which is the volume of the Reactor Coolant System excluding the pressurizer. This volume accounts for 10 percent steam generator tube plugging. High source level and all reactor trip alarms are effective.

The minimum time required to reduce the reactor coolant boron concentration to 1500 ppm, where the reactor could go critical with all rods at the insertion limits, is about 64.1 minutes. Once again, this should be more than adequate time for operator action to the high count rate signal, and termination of dilution flow.

In any case, if continued dilution occurs, the reactivity insertion rate and consequences thereof are considerably less severe than those associated with the uncontrolled rod withdrawal analyzed in Section 14.1.1, Uncontrolled RCCA Withdrawal from a Subcritical Condition.

Dilution at Power

For dilution at power, it is necessary that the time to lose shutdown margin be sufficient to allow identification of the problem and termination of the dilution. As in the dilution during startup case, the RCS volume reduction due to steam generator tube plugging is considered. The effective reactivity addition rate is a function of the reactor coolant temperature and boron concentration. The reactivity insertion rate calculated is based on a conservatively high value for the expected boron concentration at power (1500 ppm) as well as a conservatively high charging flow rate capacity (127 gpm). The reactor is assumed to have all rods out in either automatic or manual control. With the reactor in manual control and no operator action to terminate the transient, the power and temperature rise will cause the reactor to reach the reactor protection (i.e., OTAT, high nuclear flux) trip setpoint, resulting in a reactor trip. After reactor trip there is at least 53.5 minutes for operator action prior to return to



criticality. The boron dilution transient in this case is essentially the equivalent to an uncontrolled rod withdrawal at power. The maximum reactivity insertion rate for a boron dilution transient is conservatively estimated to be 1.6 pcm/sec and is within the range of insertion rates analyzed for uncontrolled rod withdrawal at power. Prior to reaching the reactor protection trip, the operator will have received an alarm on Overtemperature ΔT and turbine runback.

With the reactor in automatic control, a boron dilution will result in a power and temperature increase such that the rod controller will attempt to compensate by slow insertion of the control rods. This action by the controller will result in rod insertion limit and axial flux alarms. The minimum time to lose the shutdown margin at beginning of life would be greater than 54.4 minutes. The time would be significantly longer at end of life due to the low initial boron concentration.

Conclusions

Because of the procedures involved in the dilution process, an erroneous dilution is considered incredible. Nevertheless, if an unintentional dilution of boron in the reactor coolant does occur, numerous alarms and indications are available to alert the operator to the condition. The maximum reactivity addition due to the dilution is slow enough to allow the operator to determine the cause of the addition and take corrective action before excessive shutdown margin is lost.

14.1.6 Loss of Reactor Coolant Flow

Flow Coastdown Accidents

A loss-of-coolant flow incident can result from a mechanical or electrical failure in one or more reactor coolant pumps, or from a fault in the power supply to these pumps. If the reactor is at power at the time of the incident, the immediate effect of loss-of-coolant flow is a rapid increase in coolant temperature. This increase could result in departure from nucleate boiling (DNB) with subsequent fuel damage if the reactor is not tripped promptly. The following trip circuits provide the necessary protection against a loss of coolant flow incident and are actuated by:

1. Low voltage on pump power supply bus
2. Pump circuit breaker opening (low frequency on pump power supply bus opens pump circuit breaker)
3. Low reactor coolant flow

These trip circuits and their redundancy are further described in Section 7.2 of the FSAR, Reactor Control and Protection System.

Simultaneous loss of electrical power to all reactor coolant pumps at full power is the most severe credible loss-of-coolant flow condition. For this condition reactor trip together with flow sustained by the inertia of the coolant and rotating pump parts will be sufficient to prevent fuel failure and reactor coolant system overpressure and to prevent the DNB ratio from going below the limit value.

Method of Analysis

The following loss-of-flow cases are analyzed:

1. Loss of two pumps from a reactor coolant system, heat output of 1520 MWt with two loops operating.

Covered in NRSIS

2. Loss of one pump from a reactor coolant system, heat output of 1520 MWt with two loops operating.

The first case represents the worst credible coolant flow loss. The second case is less severe. Loss of one pump above a preset power level causes a reactor trip by a low flow signal. The power level above which this trip occurs is assumed to be set at 49% of full load.

The normal power supplies for the pumps are the two buses connected to the generator, each of which supplies power to one of the two pumps. When a generator trip occurs, the pumps are automatically transferred to a bus supplied from external power lines. Therefore, the simultaneous loss of power to all reactor coolant pumps is a highly unlikely event.

Following any turbine trip, where there are no electrical faults which require tripping the generator from the network, the generator remains connected to the network for a least one minute. Since both pumps are not on the same bus, a single bus fault would not result in the loss of all pumps.

This transient is analyzed by three digital computer codes. First, the LOFTRAN code is used to calculate the loop and core flow during the transient, the time of the reactor trip based on the calculated flow, the nuclear power transient, and the primary system pressure and temperature transients. The FACTRAN code is then used to calculate the heat flux transient based on the nuclear power and flow from LOFTRAN.

Finally, the THINC code is used to calculate the DNBR during the transient based on the heat flux from FACTRAN and flow from LOFTRAN. The DNBR transients presented represent the minimum of the typical or thimble cell.

This accident is analyzed with the Improved Thermal Design Procedure as described in WCAP-8567 (Reference 6). Plant characteristics and initial conditions are discussed in Section 14.

Initial Operating Conditions

Initial reactor power, pressure, and RCS temperature are assumed to be at their nominal values. Uncertainties in initial conditions are included in the limit DNBR as described in WCAP-8567.

Reactivity Coefficients

A conservatively large absolute value of the Doppler-only power coefficient is used. This serves to maximize power level while it is decreasing after reactor trip. The total integrated Doppler reactivity (power defect) between 0% and 100% power is assumed to be $0.016\Delta k$, consistent with Figure 14-2.

The most positive value of the moderator temperature coefficient (+5 pcm/°F) is assumed, since this results in the maximum core power during the initial part of the transient, when the minimum departure from nucleate boiling ratio is reached.

Flow Cooldown

The flow cooldown analysis is based on a momentum balance around each reactor coolant loop and across the reactor core. This momentum balance



is combined with the continuity equation, a pump momentum balance and the pump characteristics and is based on high estimates of system pressure losses.

No single activate failure in the plant systems and equipment which are necessary to mitigate the effects of the accident will adversely affect the consequences of the accident during the transient mostly as a result of the change of fuel gap conductance. A conservatively evaluated overall heat transfer was used in the analysis.

Results

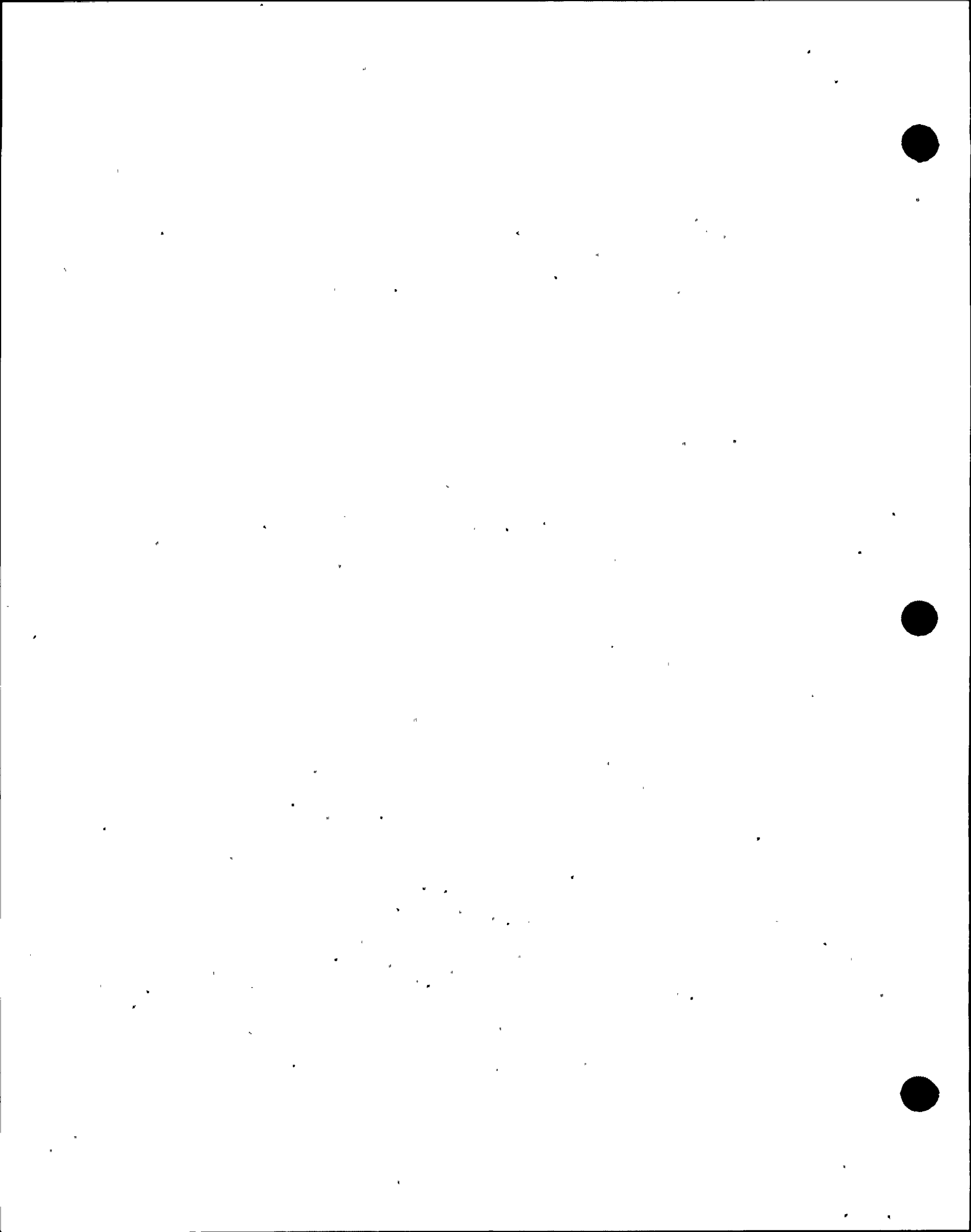
Reactor coolant flow coastdown curves are shown in Figure 14.1.6-1.

Figures 14.1.6-1 and 14.1.6-3 show the nuclear flux, the average channel heat flux, and the hot channel heat flux response for the two-pump loss. Figure 14.1.6-2 shows the DNB ratio as a function of time for this case. The minimum WRB-1 DNB ratio is reached 3.0 seconds after initiation of the incident.

Figures 14.1.6-4 through 14.1.6-6 show the transient for loss of one pump with both loops operating and Figure 14.1.6-7 shows the DNB ratio as a function of time for this case. The minimum DNB ratio occurs 3.5 seconds after initiation of the transient.

Conclusions

Since DNB does not occur in any loss-of-coolant flow incident, there is no cladding damage and no release of fission products into the reactor coolant. Therefore, once the fault is corrected, the plant can be returned to service in the normal manner. The absence of fuel failures would, of course, be verified by analysis of reactor coolant samples.



Locked Rotor Accident

A hypothetical transient analysis is performed for the postulated instantaneous seizure of a reactor coolant pump rotor. Flow through the reactor coolant system is rapidly reduced, leading to a reactor trip on a low-flow signal. Following the trip, heat stored in the fuel rods continues to pass into the core coolant, causing the coolant to heat up and expand. At the same time, heat transfer to the shell side of the steam generator is reduced, first because the reduced flow results in a decreased tube side film coefficient and then because the reactor coolant in the tubes cools down while the shell side temperature increases (turbine steam flow is reduced to zero upon plant trip). The rapid expansion of the coolant in the reactor core, combined with the reduced heat transfer in the steam generator, causes an insurge into the pressurizer and a pressure increase throughout the reactor coolant system. The insurge into the pressurizer compresses the steam volume, actuates the automatic spray system, opens the power-operated relief valves, and opens the pressurizer safety valves, in that sequence. The two power-operated relief valves are designed for reliable operation and would be expected to function properly during the accident. However, for conservatism, their pressure-reducing effect, as well as the pressure-reducing effect of the spray, is not included in the analysis.

Method of Analysis

Two digital computer codes are used to analyze this transient. The LOFTRAN code is used to calculate the resulting loop core and flow transients following the pump seizure, the time of reactor trip based on loop flow transients, and the nuclear power following reactor trip, and to determine peak pressure. The thermal behavior of the fuel located at the core hot spot is investigated using the FACTRAN code, which uses the core flow and nuclear power calculated by LOFTRAN. The FACTRAN code includes a film boiling heat transfer coefficient.



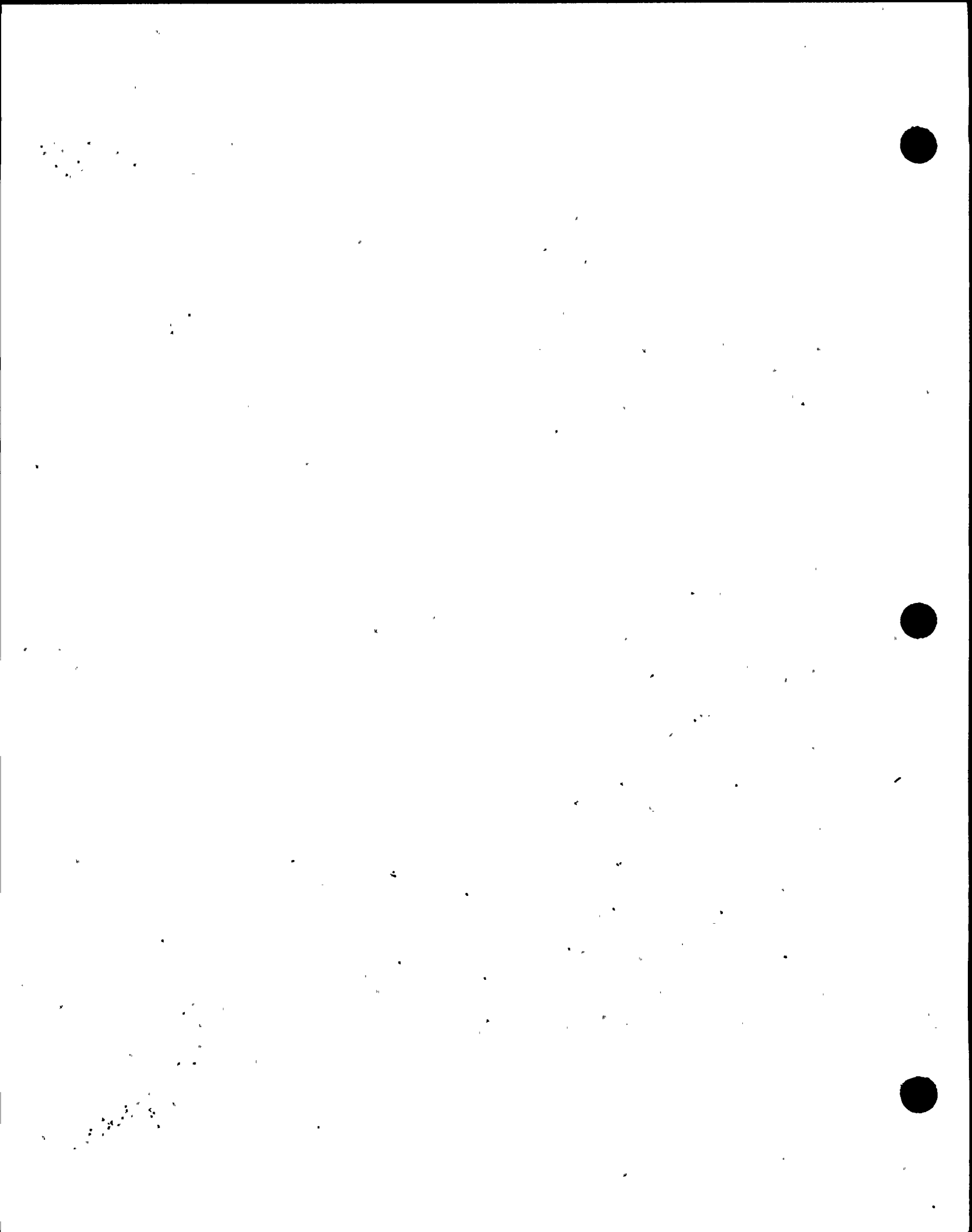
One case is analyzed with both loops operating and one locked rotor. At the beginning of the postulated locked rotor accident (i.e., at the time the shaft in one of the reactor coolant pumps is assumed to seize), the plant is assumed to be in operation under the most adverse steady-state operating conditions with respect to the pressure, i.e., maximum steady-state power level, maximum steady-state pressure (2280 psia), and maximum steady-state coolant average temperature.

The locked rotor event is not analyzed with a consequential loss of offsite power. At the R. E. Ginna plant, the generator breakers will not open until one minute after the loss of offsite power. Thus, power will be maintained to the intact reactor coolant pump throughout the limiting portion of the transient. This is within the first 10 seconds when the peak clad temperature occurs.

For the peak pressure evaluation, the initial pressure is conservatively estimated as 30 psi above nominal pressure (2250 psia) to allow for errors in the pressurizer pressure measurement and control channels. This is done to obtain the highest possible rise in the coolant pressure during the transient. To obtain the maximum pressure in the primary side, conservatively high loop pressure drops are added to the calculated pressurizer pressure. The pressure response shown in Figure 14.1.6-9 is the response at the point in the reactor coolant system having the maximum pressure.

Evaluation of the Pressure Transient - After pump seizure, the neutron flux is rapidly reduced by control rod insertion effect. Rod motion is assumed to begin one second after the flow in the affected loop reaches 87% of nominal flow. No credit is taken for the pressure-reducing effect of the pressurizer relief valves, pressurizer spray, steam dump, or controlled feedwater flow after plant trip.

Although these operations are expected to occur and would result in a lower peak pressure, an additional degree of conservatism is provided by ignoring their effect.



The pressurizer safety valves are full open at 2575 psia, and their total capacity for steam relief is 20 ft³/s.

Evaluation of Departure from Nucleate Boiling in the Core During the Accident - For this accident, departure from the nucleate boiling is assumed to occur in the core, and therefore, an evaluation of the consequence with respect to fuel rod thermal transients is performed. Results obtained from analysis of this hot spot condition represent the upper limit with respect to clad temperature and zirconium-water reaction. In the evaluation, the rod power at the hot spot is assumed to be three times the average rod power ($F_Q=3$) at the initial core power level.

Film Boiling Coefficient - The film boiling coefficient is calculated in the FACTRAN code using the Bishop-Sandberg-Tong film boiling correlation. The fluid properties are evaluated at film temperature, which is the average between the wall and bulk temperatures. The program calculates the film coefficient at every time step, based on the actual heat transfer conditions at the time. The neutron flux, system pressure, bulk density, and mass flow rate as a function of time are used as program input.

For this analysis, the initial values of the pressure and the bulk density are used throughout the transient, since they are the most conservative with respect to clad temperature response. For conservatism, departure from nucleate boiling was assumed to start at the beginning of the accident.

Fuel Clad Gap Coefficient - The magnitude and the time dependence of the heat transfer coefficient between fuel and clad (gap coefficient) have a pronounced influence on the thermal results. The larger the value of the gap coefficient, the more heat is transferred between the pellet and the clad. Based on investigations of the effect of the gap coefficient on the maximum clad temperature during the transient, the gap coefficient is assumed to increase from a steady-state value consistent with an initial fuel temperature to 10,000 Btu per hour-square

feet-°F at the initiation of the transient. Thus, the large amount of energy stored in the fuel because of the small initial value is released to the clad at the initiation of the transient.

Zirconium-Steam Reaction - The zirconium-steam reaction can become significant above a clad temperature of 1,800°F. The Baker-Just parabolic rate equation shown below is used to define the rate of the zirconium-steam reaction:

$$\frac{d(w)^2}{dt} = 33.3 \times 10^6 \exp \frac{(45,000)}{1.986T}$$

where:

w = amount reacted (mg/cm²)

t = time (seconds)

T = temperature (°F).

The reaction heat is 1,510 cal/gm.

Results

Figure 14.1.6-18 and Figure 14.1.6-9 show the nuclear power, core flow, and loop flow transients and Figure 14.1.6-18 shows the pressurizer pressure transients. The heat flux and clad temperature transients are given in Figure 14.1.6-10. The results of these calculations are summarized in Table 14.1.6-2. The sequence of events is shown in Tables 14.1.6-1 and 14.1.6-3.

Conclusions

Since the peak reactor coolant system pressure (2836 psia) reached during any of the transients is less than 120% of design pressure the integrity of the primary coolant system is not endangered. This value can be considered an upper limit, since the assumptions used in the analysis are conservative.

Since the peak clad surface temperature (2176°F) calculated for the hot spot during the more severe transient remains considerably less than 2,700°F and the amount of zirconium-water reaction is small, the core remains in place and intact with no consequential loss of core cooling capability.

TABLE 14.1.6-1

TIME SEQUENCE OF EVENTS
FOR LOSS OF REACTOR COOLANT FLOW

| <u>Case</u> | <u>Event</u> | <u>Time of Each Event (Seconds)</u> |
|---|---|---|
| a. Partial loss of reactor coolant flow (two loops operating, one pump coasting down) | Coastdown begins | 0 |
| | Low flow reactor trip | 1.27 |
| | Rods begin to drop | 2.27 |
| | Minimum DNBR occurs | 3.5 |
| b. Complete loss of forced reactor coolant flow | Both operating pumps lose power and begin coasting down | 0 |
| | Reactor coolant pump undervoltage trip point reached | 0 |
| | Rods begin to drop | 1.5 |
| | Minimum DNBR occurs | 3.0 |



TABLE 14.1.6-2

SUMMARY OF LIMITING RESULTS FOR
LOCKED ROTOR ACCIDENT

| | |
|--|-------|
| Maximum Reactor Coolant System Pressure (psia) | 2836 |
| Maximum Cladding Temperature (°F) Core Hot Spot | 2176 |
| Zr-H ₂ O Reaction at Core Hot Spot (% by weight) | .9935 |



TABLE 14.1.6-3

TIME SEQUENCE OF EVENTS FOR
LOCKED ROTOR INCIDENT

| <u>Event</u> | <u>Time of Each Event (Seconds)</u> |
|---------------------------------|---|
| Rotor on one pump locks | 0 |
| Low flow trip point reached | .09 |
| Rods begin to drop | 1.09 |
| Maximum RCS pressure occurs | 3.20 |
| Maximum clad temperature occurs | 3.41 |

Figure 14.1.6-1

jinna Full Loss of Flow

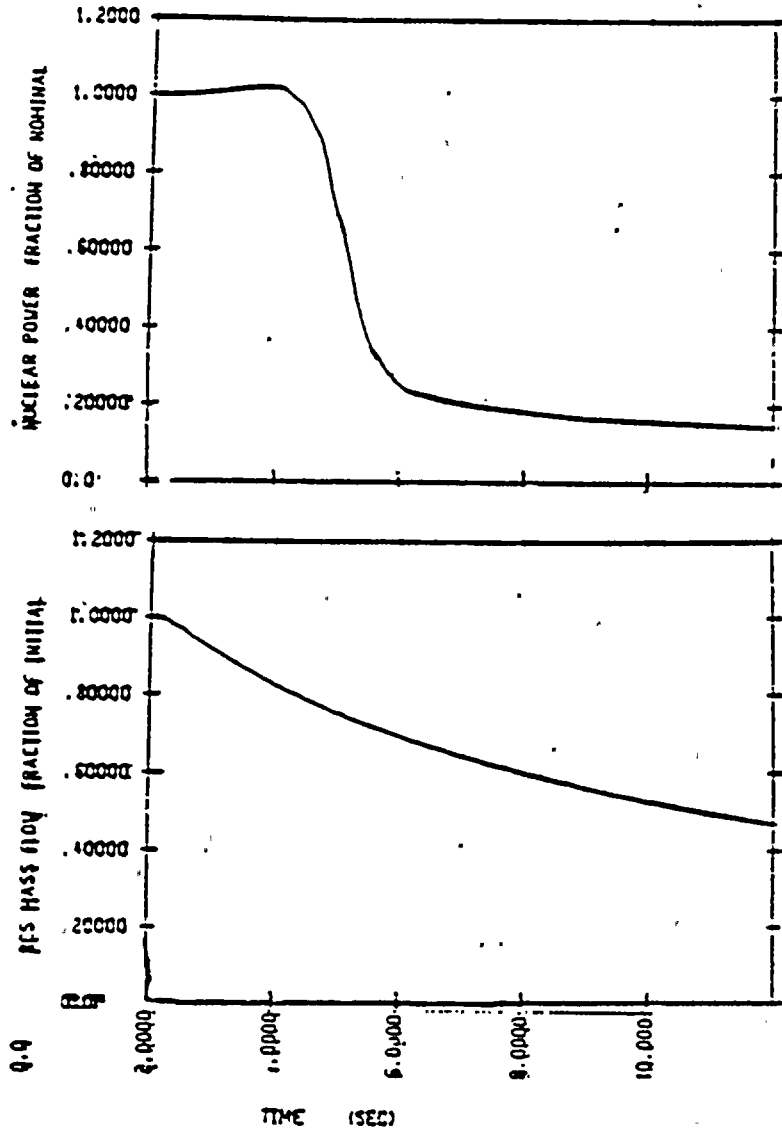
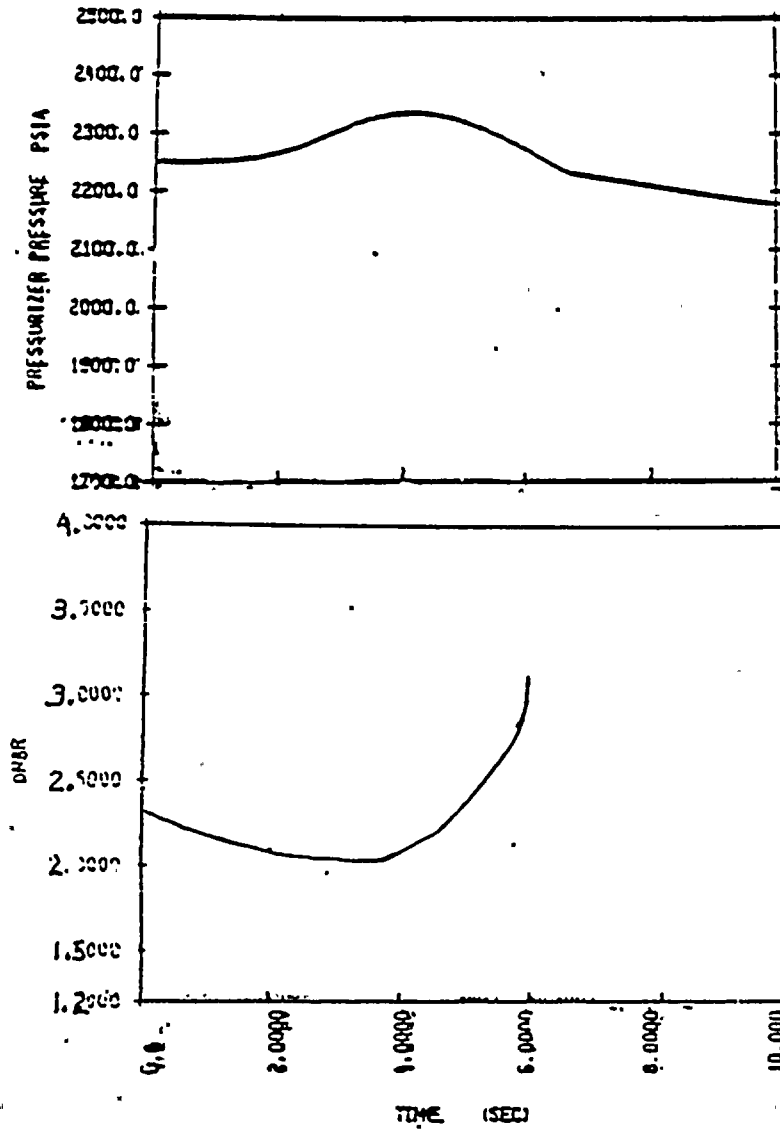


Figure 14.1.6-2

Ginna Full Loss of Flow



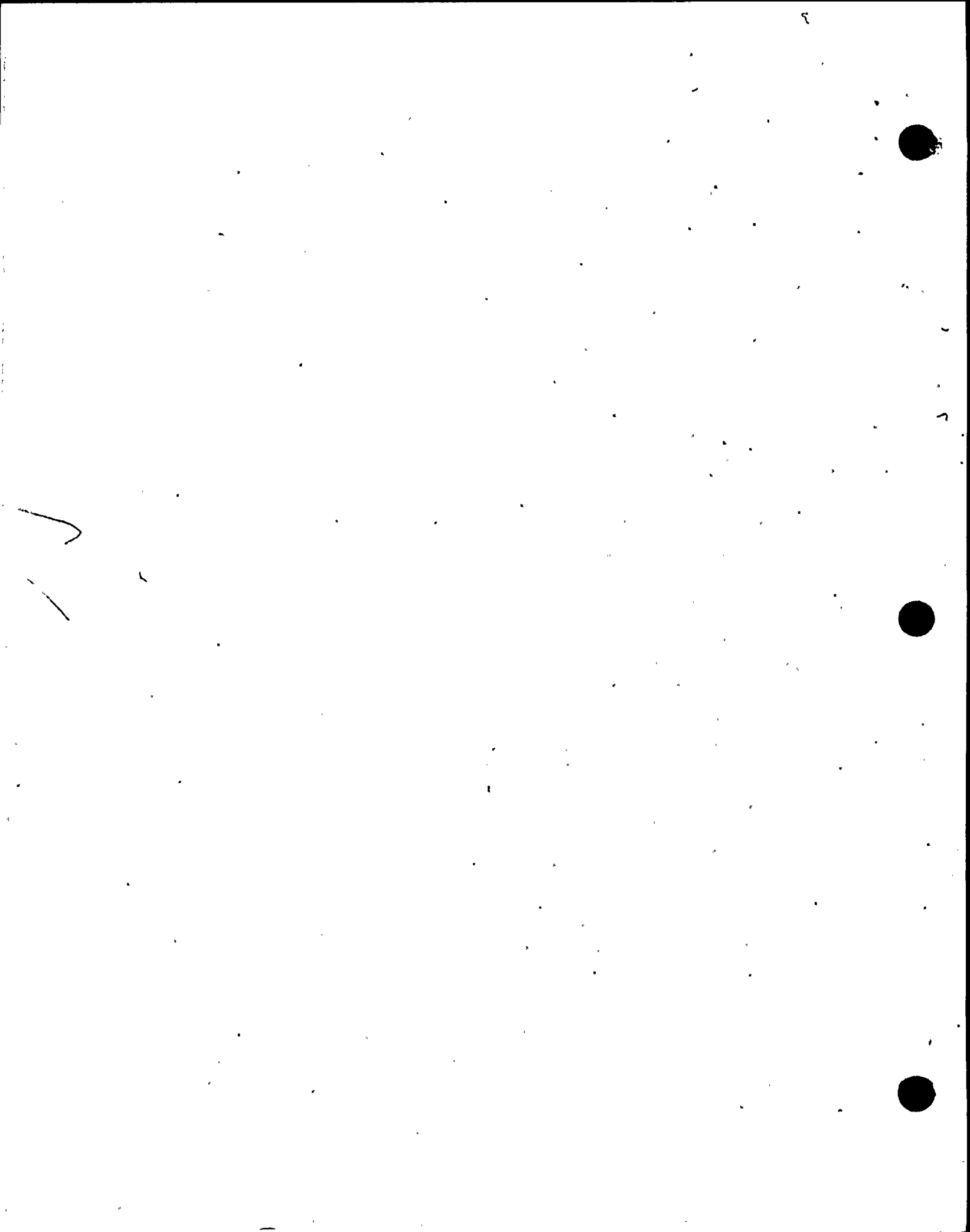


Figure 14.1.6-3

Ginna Full Loss of Flow

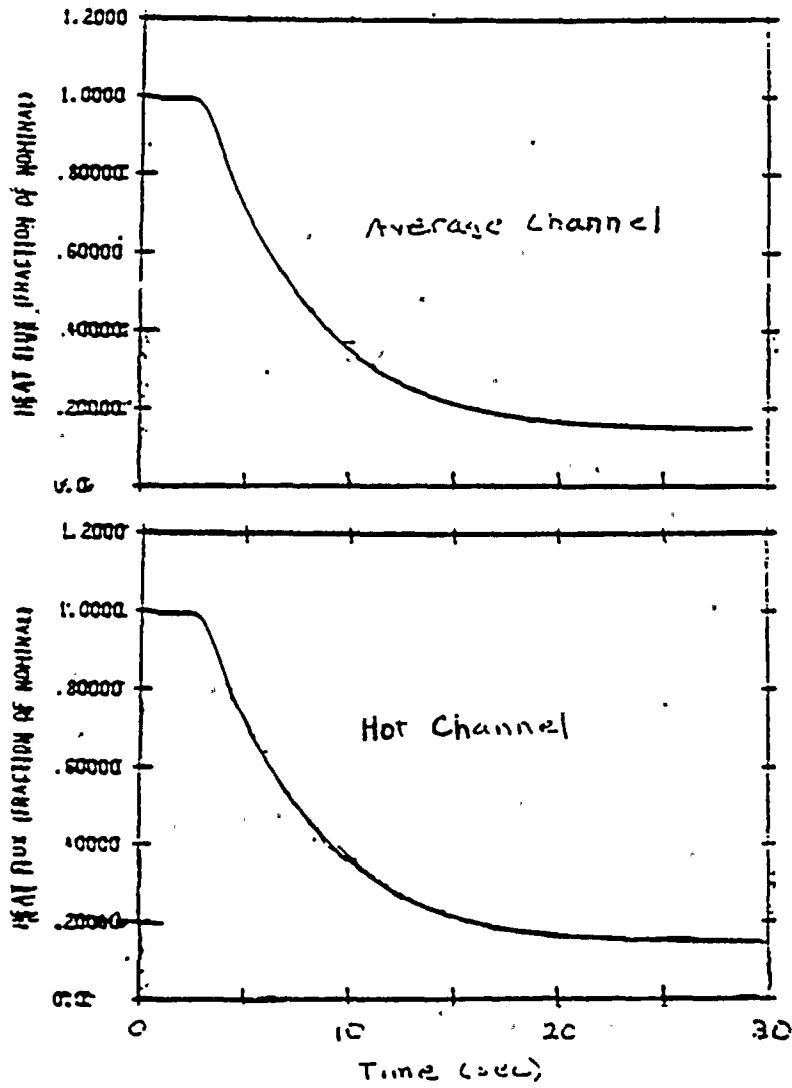




Figure 14.1.6-4

Ginna Partial Loss of Flow

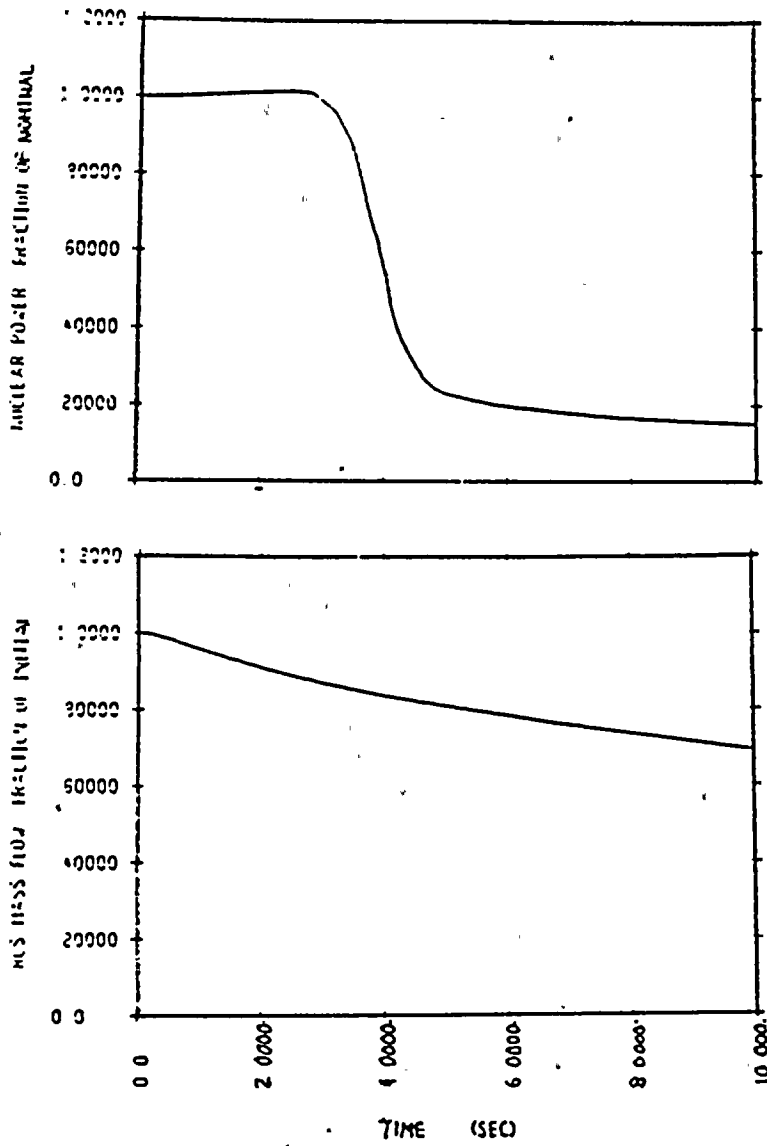
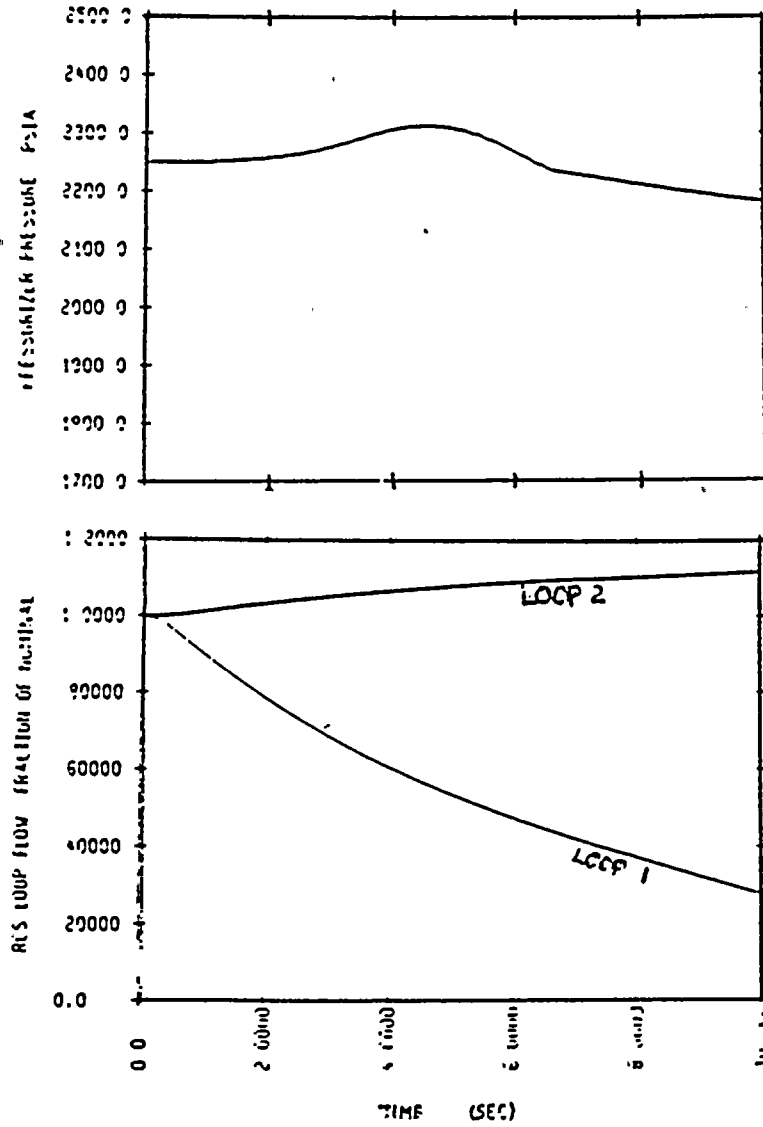


Figure 14.1.6-5

Ginna Partial Loss of Flow



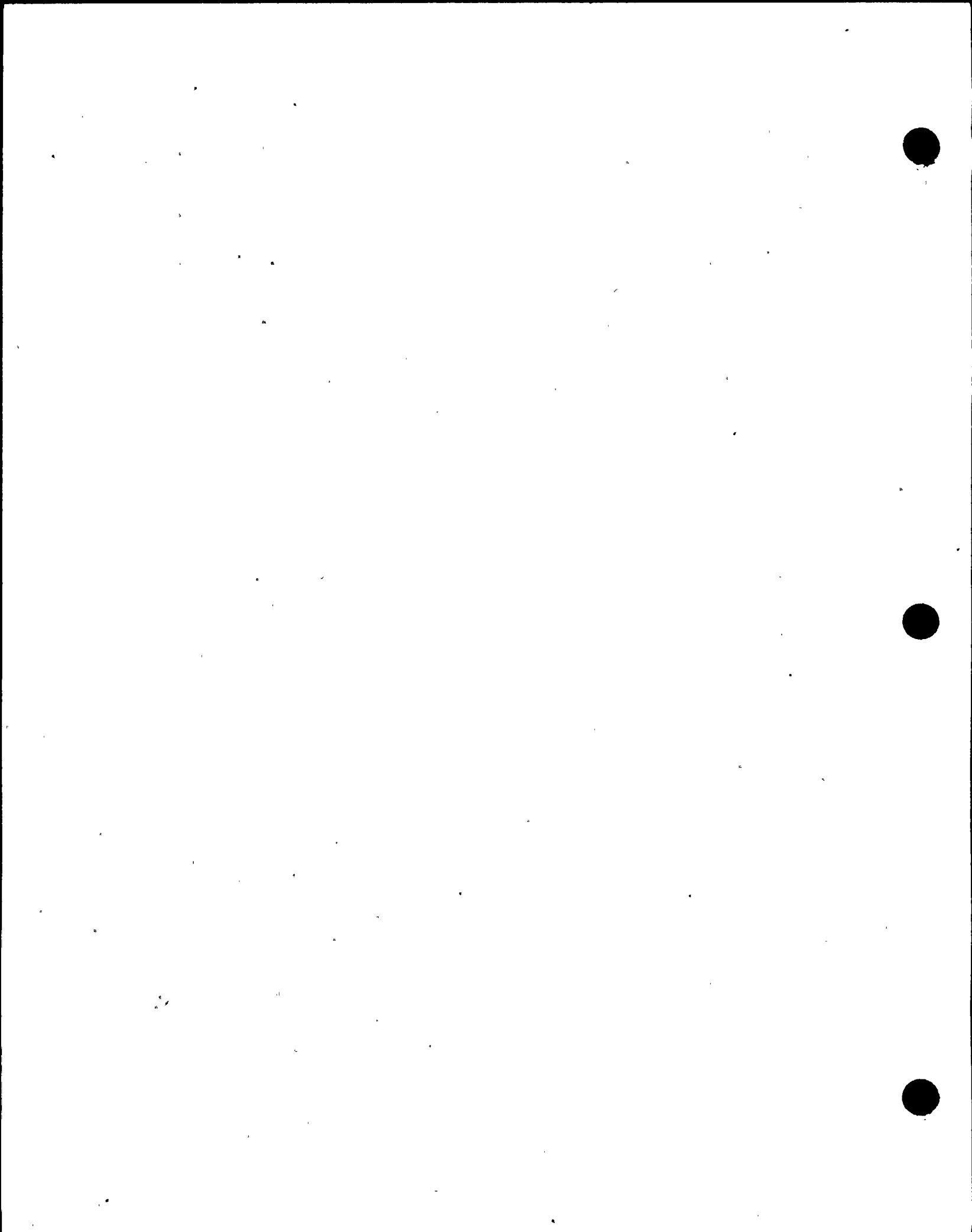


Figure 14.1.6-6

Ginna Partial Loss of Flow

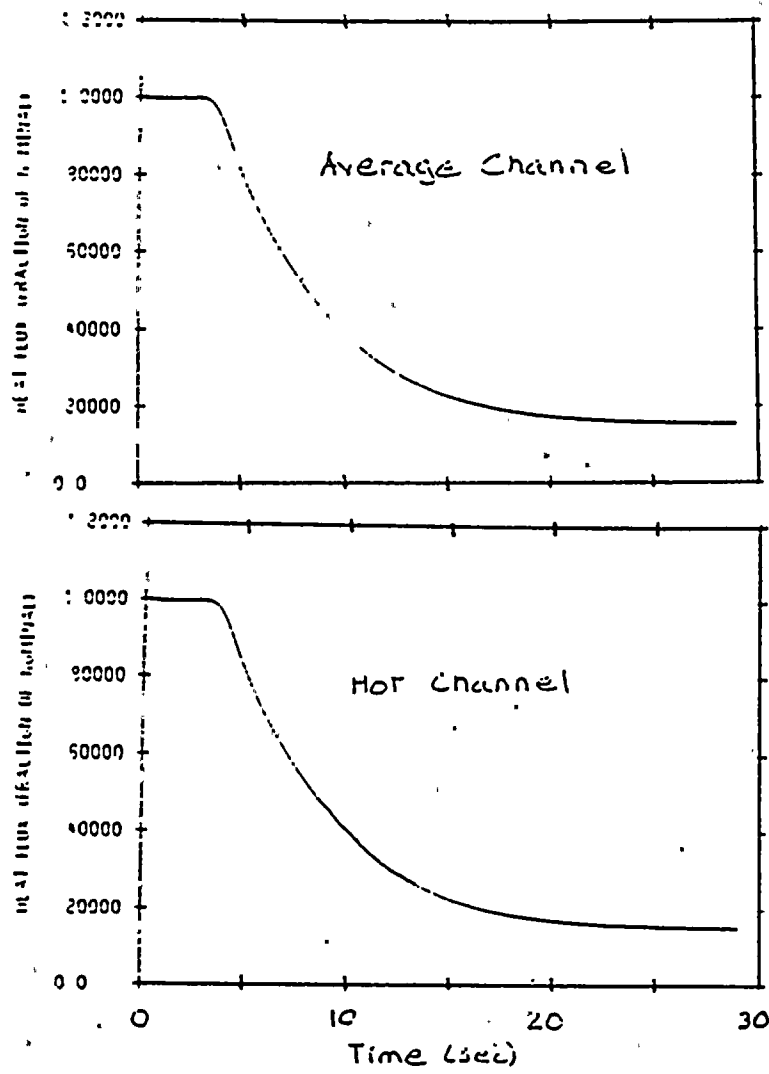




Figure 14.1.6-7

GINNA Partial Loss of Flow

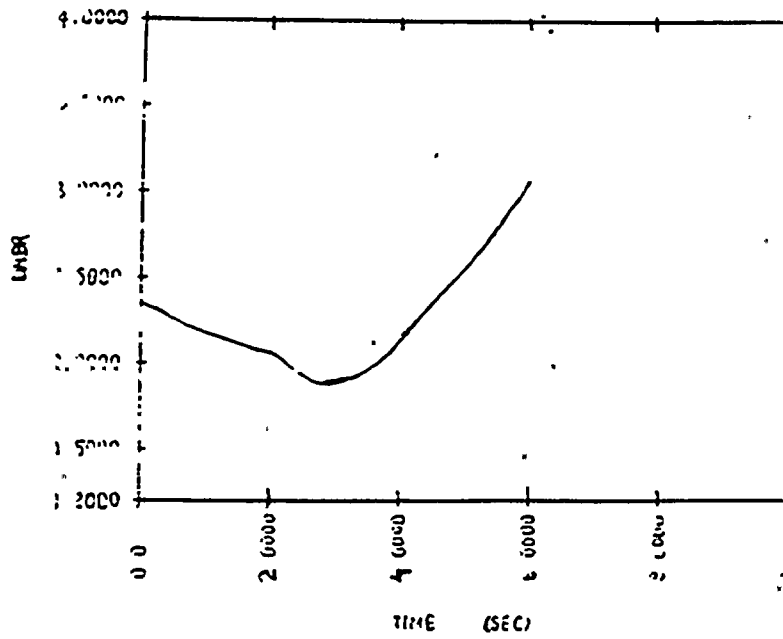




Figure 14.1.6-8

GINNA Locked Rotor

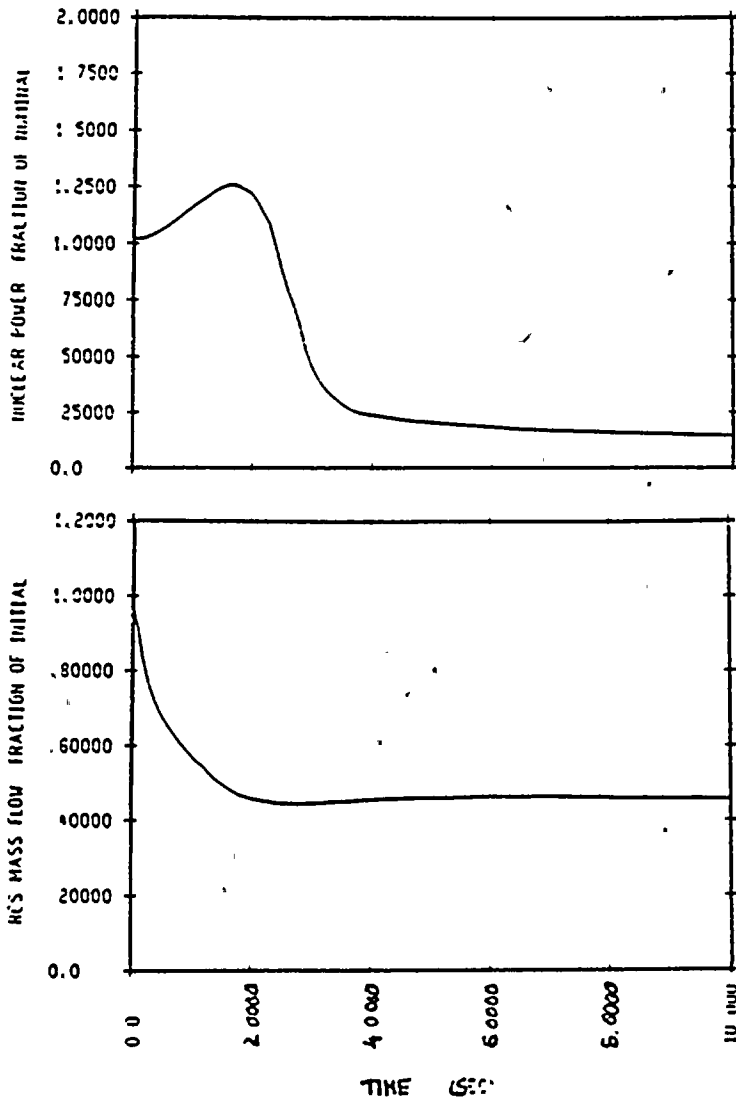


Figure 14.1.6-9

GINNA Locked Rotor

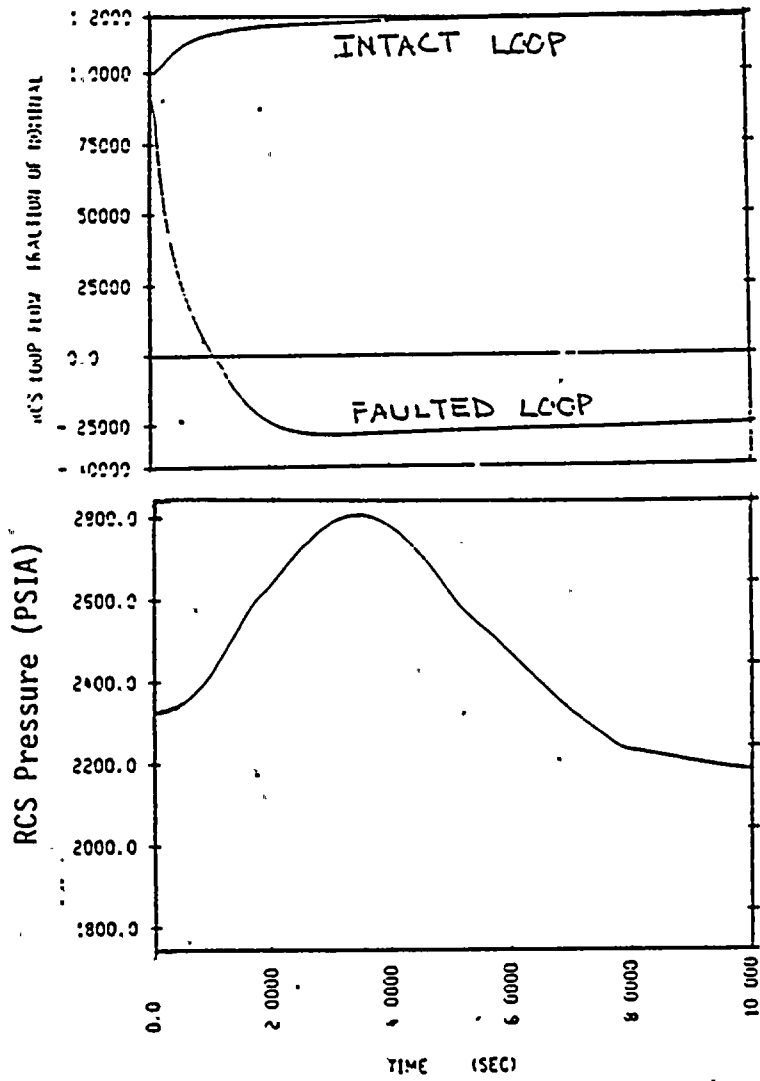
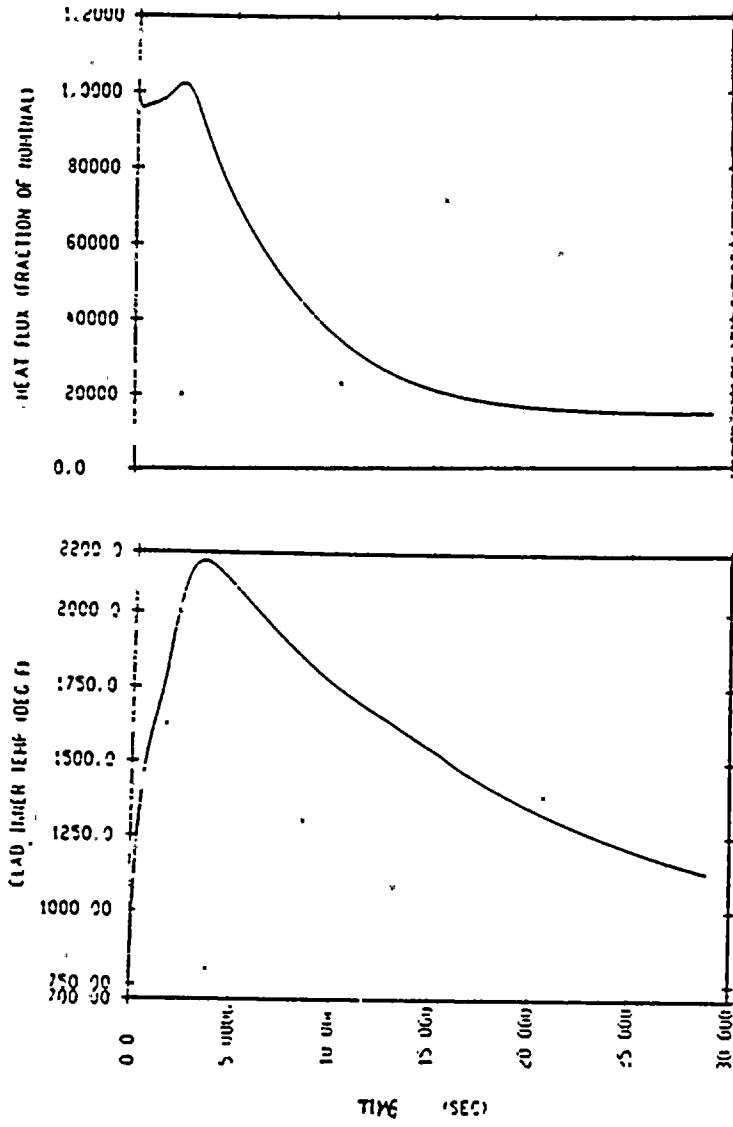




Figure 14.1.6-10

Ginna Locked Rotor



14.1.8 Loss of External Electrical Load

The plant is designed to accept a 50% loss of electrical load while operating at full power or a complete loss of load while operating below 50% power without actuating a reactor trip. The automatic steam bypass system with 40% steam dump capacity to the condenser is able to accommodate this load rejection by reducing the transient imposed upon the reactor coolant system. The reactor power is reduced to the new equilibrium power level at a rate consistent with the capability of the rod control system. Should the reactor suffer a complete loss of load from full power, the reactor protection system would automatically actuate a reactor trip.

The most likely source of a complete loss of load on the nuclear steam supply system is a trip of the turbine-generator. In this case, there is a direct reactor trip signal derived from either the turbine autostop oil pressure or a closure of the turbine stop valves, provided the reactor is operating above 50% power. Reactor temperature and pressure do not increase significantly if the steam bypass system and pressurizer pressure control system are functioning properly. However, the plant behavior is evaluated for a complete loss of load from full power without a direct reactor trip, primarily to show the adequacy of the pressure relieving devices and also to show that no core damage occurs. The reactor coolant system and steam system pressure relieving capacities are designed to ensure the safety of the plant without requiring the automatic rod control, pressurizer pressure control, and/or steam bypass control systems.

Method of Analysis

The total loss of load transients are analyzed by employing the detailed digital computer program LOFTRAN. The program simulates the neutron



kinetics, reactor coolant system, pressurizer, pressurizer relief and safety valves, pressurizer spray, steam generator, and steam generator safety valves.

The program computes pertinent plant variables, including temperatures, pressures, and power level.

In this analysis, the behavior of the unit is evaluated for a complete loss of steam load from 100% of full power without direct reactor trip, primarily to show the adequacy of the pressure-relieving devices and also to demonstrate core protection margins.

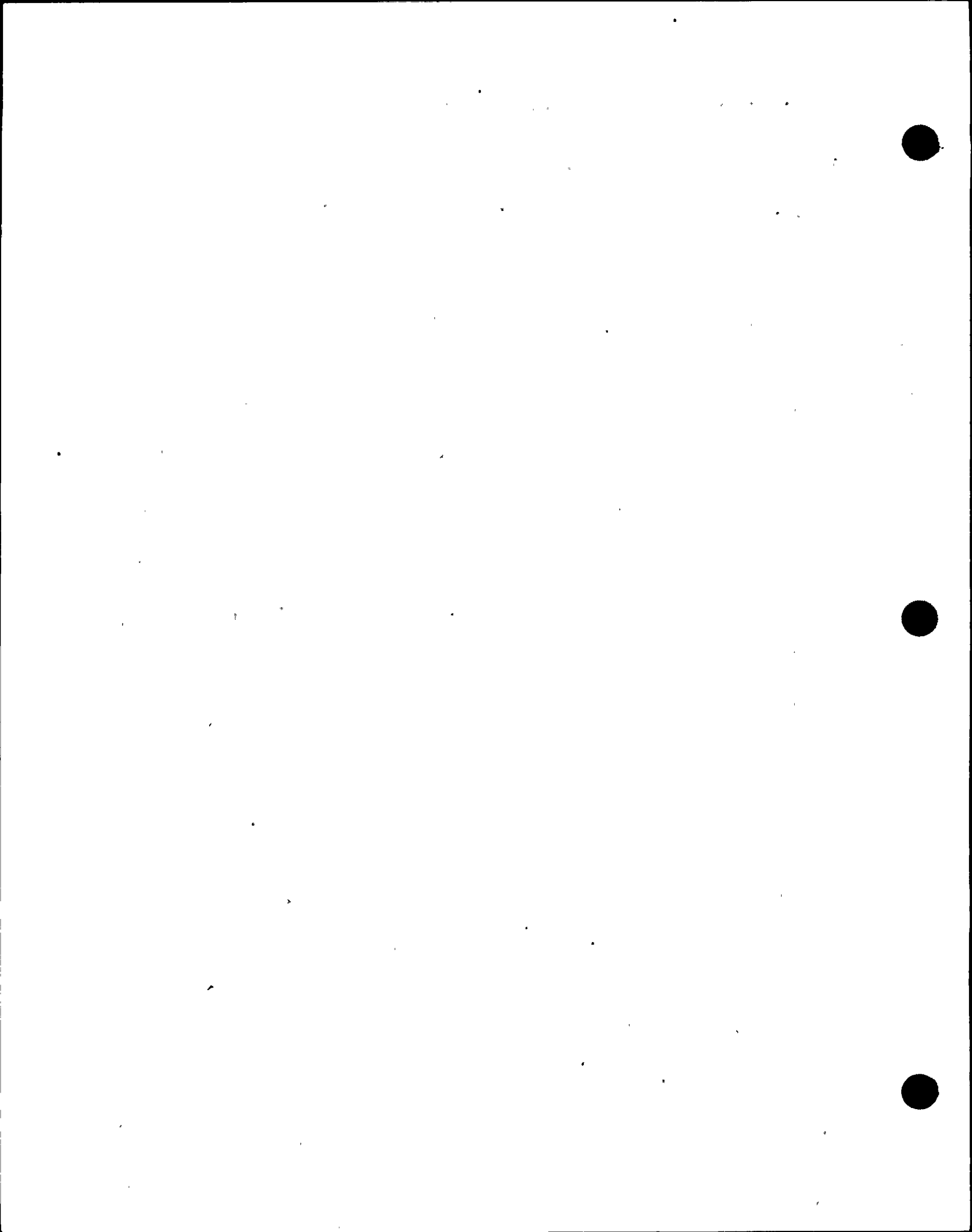
This accident is analyzed with the Improved Thermal Design Procedures in WCAP-8567, Reference 6 (main text). Plant characteristics and initial conditions are discussed in Section 14.1.

Initial Operating Conditions - The initial reactor power and reactor coolant system temperatures are assumed at their nominal values. Uncertainties in initial conditions are included in the limit DNBR as described in WCAP-8567.

Moderator and Doppler Coefficients of Reactivity - The loss-of-load accident is analyzed with both maximum and minimum reactivity feedback. The maximum feedback cases assume a large negative moderator temperature coefficient and the most negative Doppler power coefficient. The minimum feedback cases assume positive moderator temperature coefficient (+5 pcm/°F) and the least negative Doppler coefficient.

Reactor Control - From the standpoint of the maximum pressures attained, it is conservative to assume that the reactor is in manual control.

Steam Release - No credit is taken for the operation of the steam dump system or steam generator power-operated relief valves. The steam



generator pressure rises to the safety valve setpoint, where steam release through safety valves limits secondary steam pressure at the setpoint value.

Pressurizer Spray and Power-Operated Relief Valves - Two cases, for both maximum and minimum feedback, are analyzed.

- a. Full credit is taken for the effect of pressurizer spray and power-operated relief valves in reducing or limiting the coolant pressure.
- b. No credit is taken for the effect of pressurizer spray and power-operated relief valves in reducing or limiting the coolant pressure. Safety valves are operable.

Feedwater Flow - Main feedwater flow to the steam generators is assumed to be lost at the time of loss of external electrical load.

Reactor trip is actuated by the first reactor protection system trip setpoint reached, with no credit taken for the direct reactor trip on turbine trip.

Results

The transient responses for a total loss of load from full-power operation are shown for four cases -- two cases for minimum reactivity feedback and two cases for maximum reactivity feedback illustrated in Figures 14.1.8-1 through 14.1.8-12.

Figures 14.1.8-1 through 14.1.8-3 show the transient responses for the total loss-of-steam load with minimum reactivity feedback, assuming full credit for the pressurizer spray and pressurizer power-operated relief valves. No credit is taken for the steam dump.



The reactor is tripped by the high pressurizer pressure signal. The minimum departure from nucleate boiling ratio is well above the limit value. The pressurizer safety valves are not actuated.

Figures 14.1.8-4 through 14.1.8-6 show the response for the total loss-of-steam load with a large negative moderator temperature coefficient. As temperature increases nuclear power decreases due to negative reactivity feedback. Power then stabilizes at a lower power level until the low steam generator level trip setpoint is reached. The DNBR increases throughout the transient and never drops below its initial value. Pressurizer relief valves and steam generator safety valves prevent overpressurization in primary and secondary systems, respectively. The pressurizer safety valves are not actuated for this case. Following the low steam generator water level reactor trip, auxiliary feedwater would be used to remove decay heat with the results less severe than those presented in Section 14.1.9 of the FSAR, Loss of Normal Feedwater Flow.

The total loss of load accident was also studied assuming the plant to be initially operating at 100% of full power, with no credit taken for the pressurizer spray, pressurizer power-operated relief valves, or steam dump. The reactor is tripped on the high pressurizer pressure signal. Figures 14.1.8-7 through 14.1.8-9 show the minimum feedback transients. The neutron flux increases slightly until the reactor is tripped. The departure from nucleate boiling ratio increases throughout the transient. In this case, the pressurizer safety valve is actuated.

Figures 14.1.8-10 through 14.1.8-12 show the transients with maximum feedback and all other assumptions being the same as those in Figures 14.1.8-7 through 14.1.8-9. Again, the departure from nucleate boiling ratio increases throughout the transient, and the pressurizer safety valves are actuated.

The calculated sequence of events for these four cases is shown in Table 14.1.8-1.

Conclusions

Results of the analyses show that the plant design is such that a total loss of external electrical load without a direct or immediate reactor trip presents no hazard to the integrity of the reactor coolant system or the main steam system. Pressure-relieving devices incorporated in the two systems are adequate to limit the maximum pressures within the design limits.

The integrity of the core is maintained by operation of the reactor protection system; i.e., the departure from nucleate boiling ratio is maintained above the limit value.

TABLE 14.1.8-1

TIME SEQUENCE OF EVENTS FOR
LOSS OF EXTERNAL ELECTRICAL LOAD

| <u>Case</u> | <u>Event</u> | <u>Time of Each Event (Seconds)</u> |
|--|--|---|
| a. With pressurizer control (minimum feedback) | Loss of electrical load | 0 |
| | High pressurizer pressure reactor trip point reached | 12.6 |
| | Rod begins to drop | 14.6 |
| | Peak pressurizer pressure occurs | 16.0 |
| | Minimum departure from nucleate boiling ratio occurs | 16.0 |
| b. With pressurizer control (maximum feedback) | Loss of electrical load | 0 |
| | Peak pressurizer pressure occurs | 13.0 |

TABLE 14.1.8-1
(continued)

| <u>Case</u> | <u>Event</u> | <u>Time of Each Event (Seconds)</u> |
|---|---|---|
| | Low steam generator level reactor trip point | 81.3 |
| | Rods begin to drop | 83.3 |
| | Minimum departure from nucleate boiling ratio occurs | * |
| c. Without pressurizer control (minimum feedback) | Loss of electrical load | 0 |
| | High pressurizer pressure reactor trip point reached | 5.4 |
| | Rods begin to drop | 7.4 |
| | Peak pressure occurs | 9.0 |
| | Initiation of release from S/G safety valves | 13.0 |
| | Minimum departure from nucleate boiling ratio occurs | * |

* DNBR does not decrease below its initial value.

TABLE 14.1.8-1
(continued)

| <u>Case</u> | <u>Event</u> | <u>Time of Each Event (Seconds)</u> |
|---|---|---|
| d. Without pressurizer control (maximum feedback) | Loss of electrical load | 0 |
| | High pressurizer pressure reactor trip point reached | 5.3 |
| | Rods begin to drop | 7.3 |
| | Peak pressure occurs | 8.0 |
| | Initiation of release from S/G safety valves | 13.0 |
| | Minimum departure from nucleate boiling ratio occurs | * |

* DNBR does not decrease below its initial value.



Figure 14.1.8-1
Ginna Loss of Load

Minimum Feedback with Automatic Pressure Control

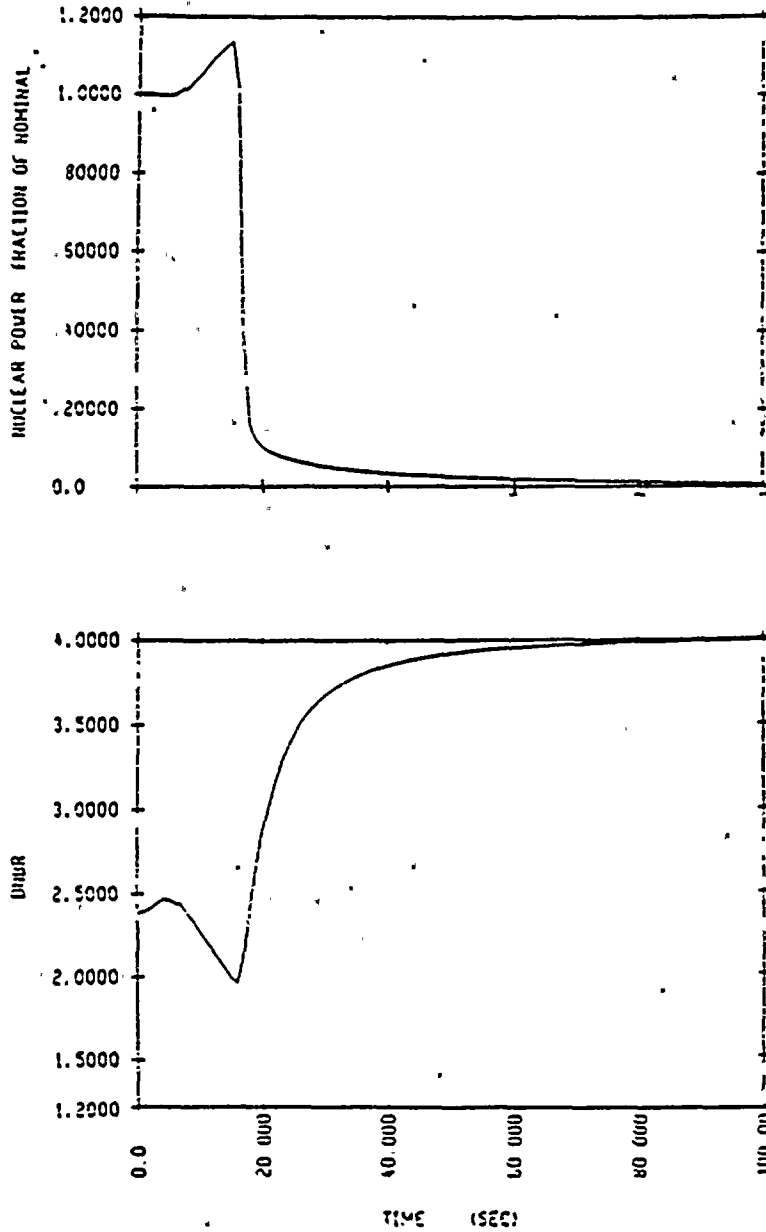


Figure 14.1.8-2

Ginna Loss of Load

Minimum Feedback with Automatic Pressure Control

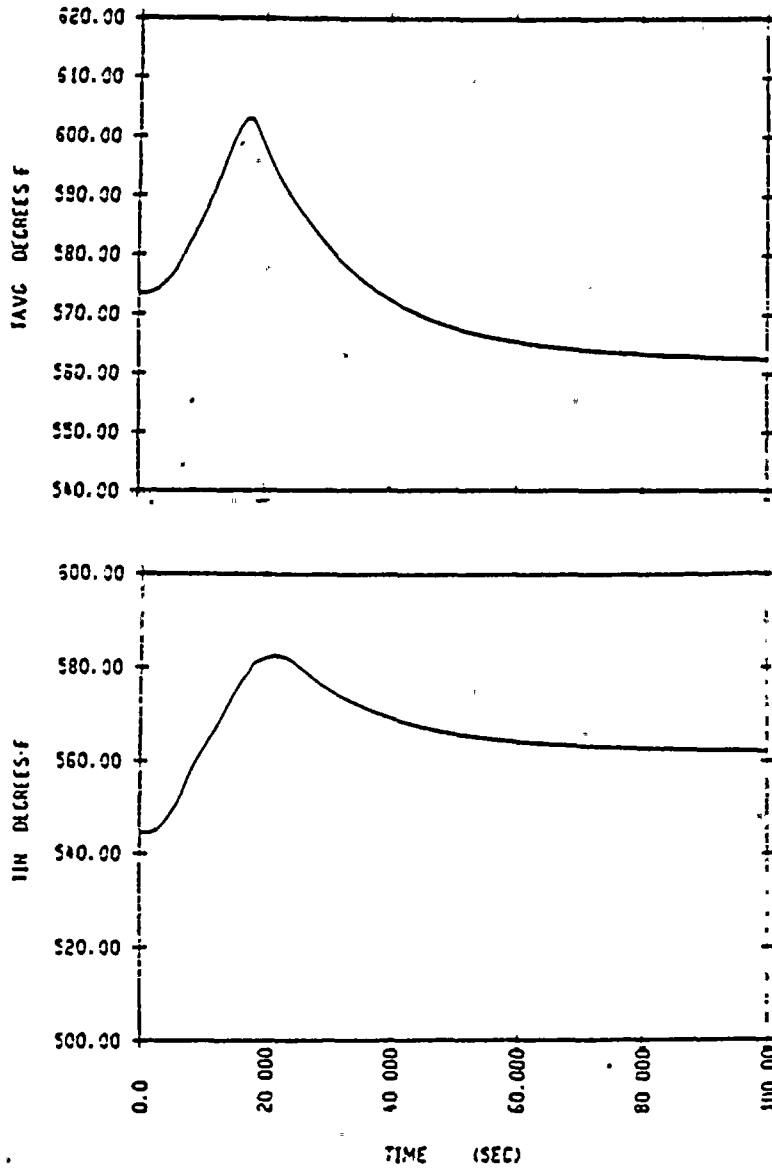


Figure 14.1.8-3

Ginna Loss of Load

Minimum Feedback with Automatic Pressure Control

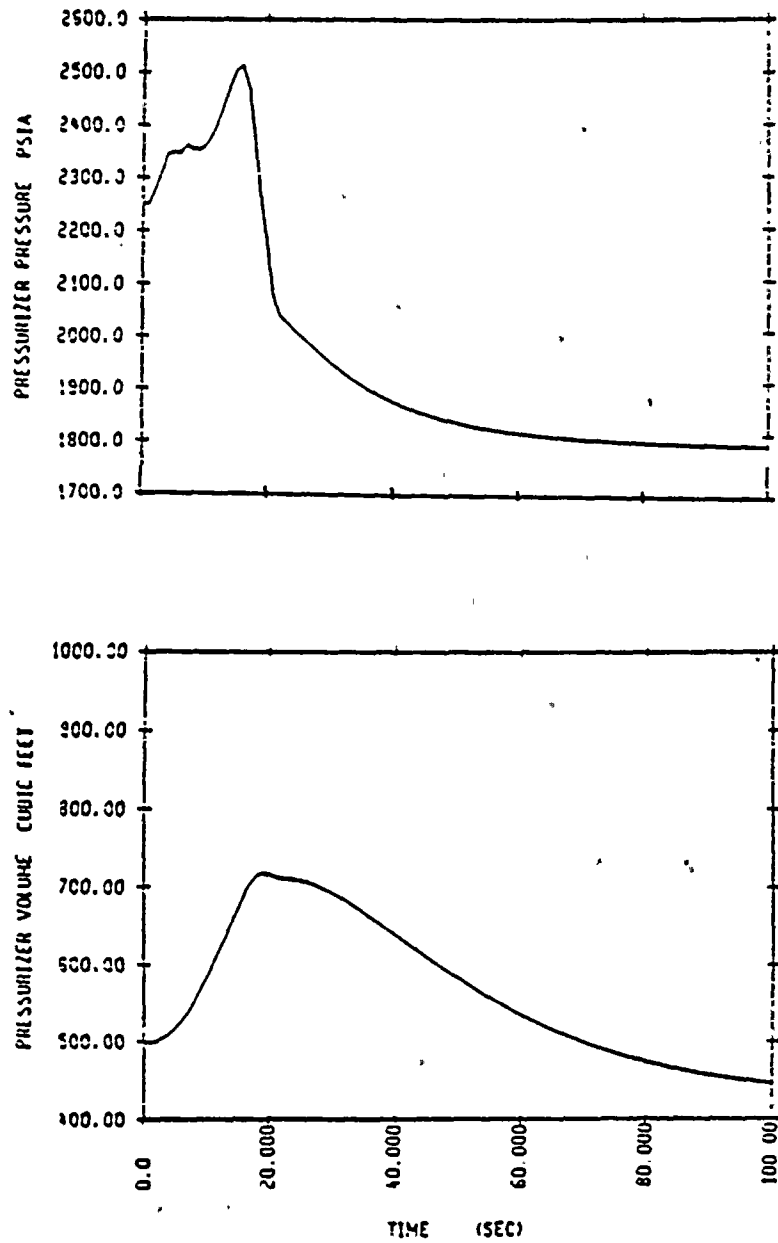


Figure 14.1.8-4

Ginna Loss of Load

Maximum Feedback with Automatic Pressure Control

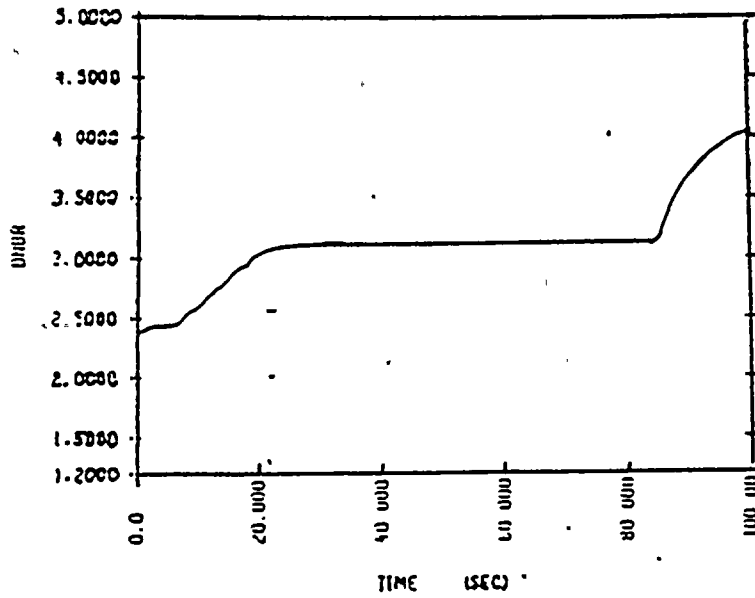
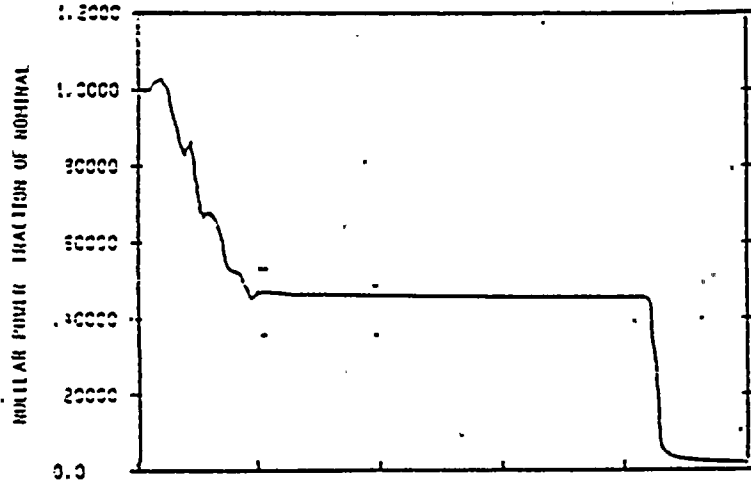




Figure 14.1.8-5

Ginna Loss of Load

Maximum Feedback with Automatic Pressure Control

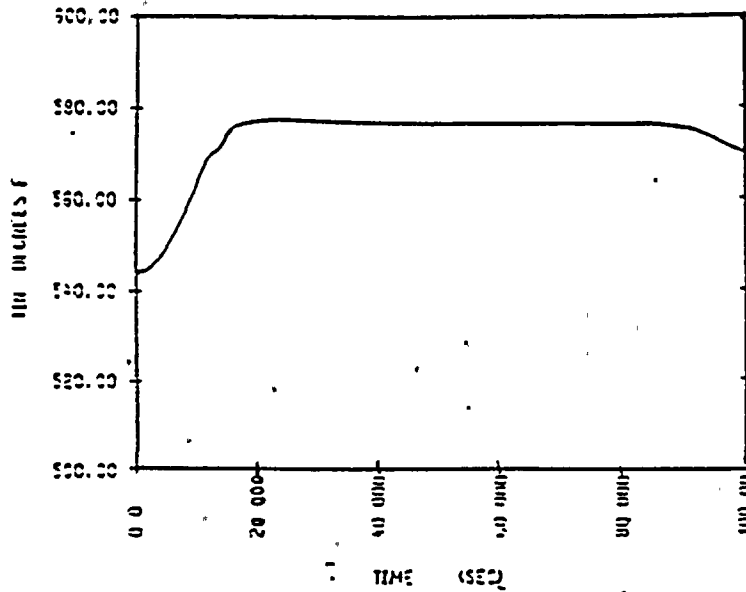
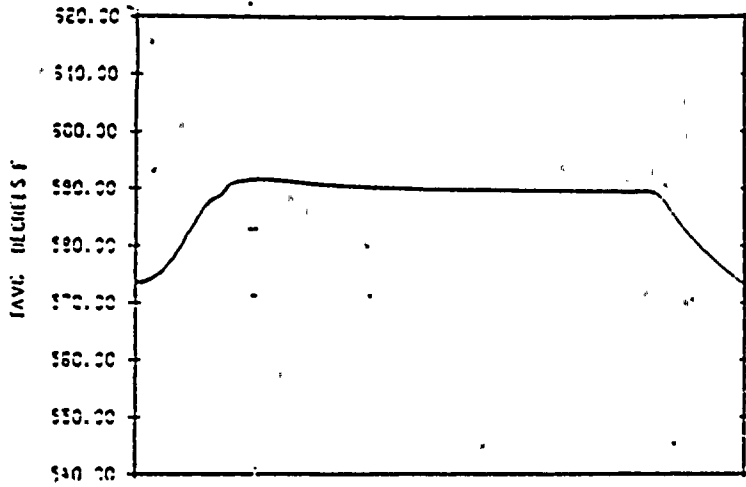




Figure 14.1.8-6 .

Ginna Loss of Load

Maximum Feedback with Automatic Pressure Control

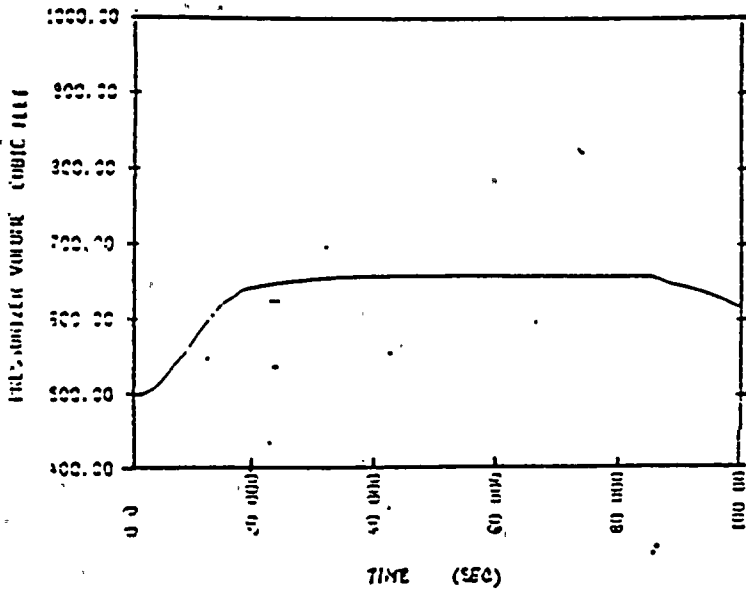
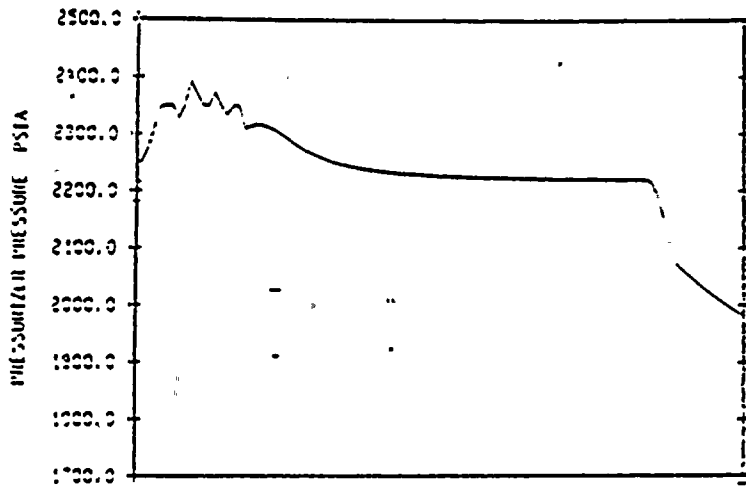




Figure 14.1.8-7

Ginna Loss of Load

Minimum Feedback Without Pressure Control

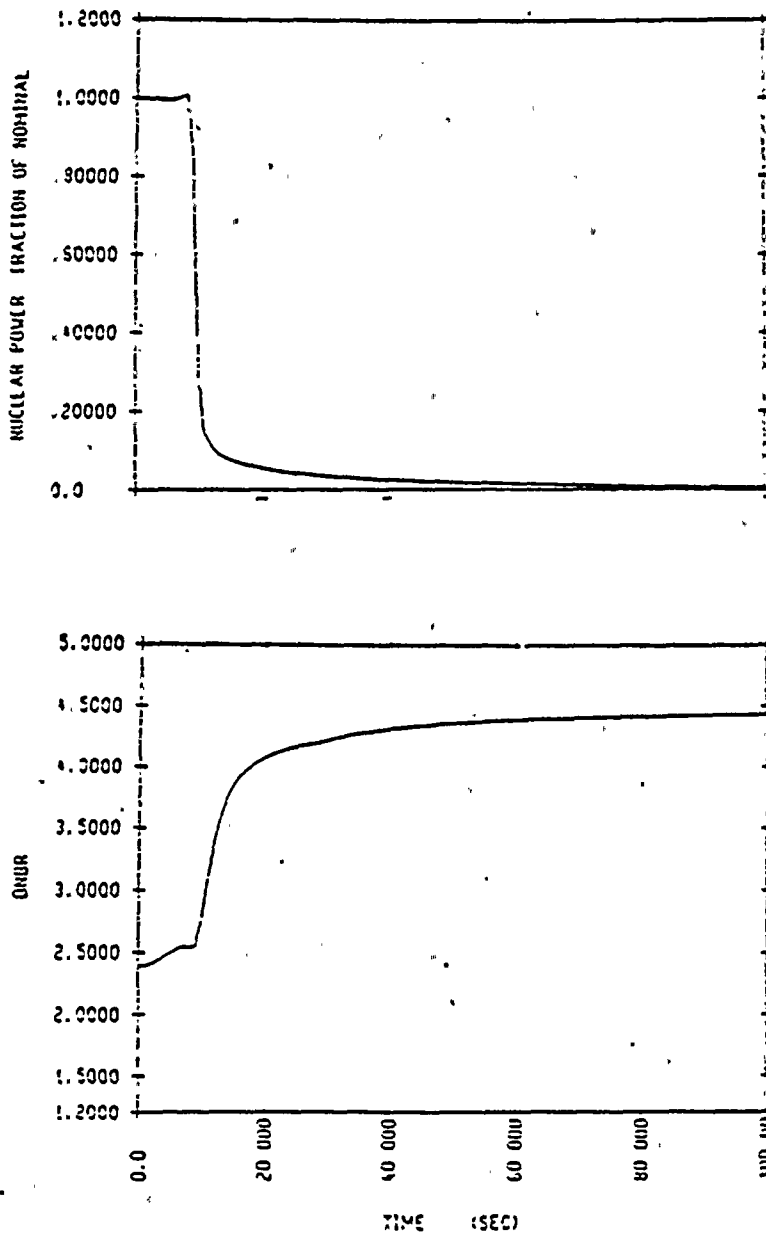




Figure 14.1.8-8

Ginna Loss of Load

Minimum Feedback Without Pressure Control

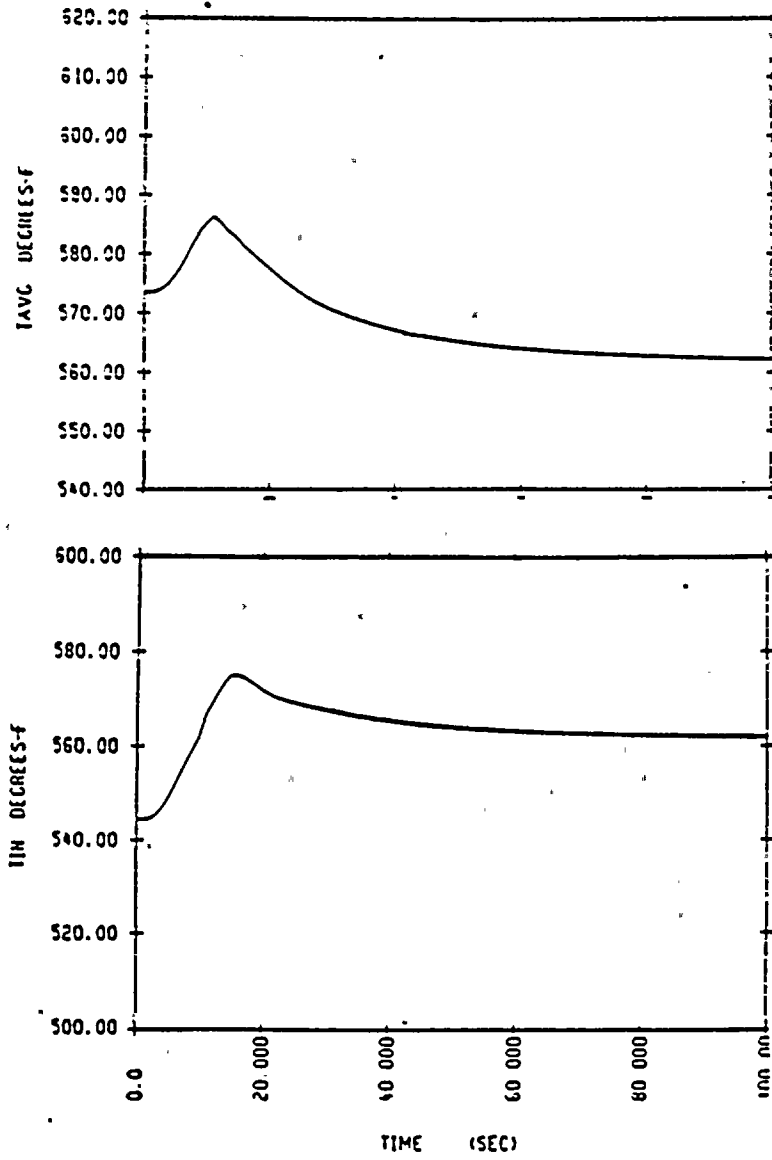


Figure 14.1.8-9

Ginna Loss of Load

Minimum Feedback Without Pressure Control

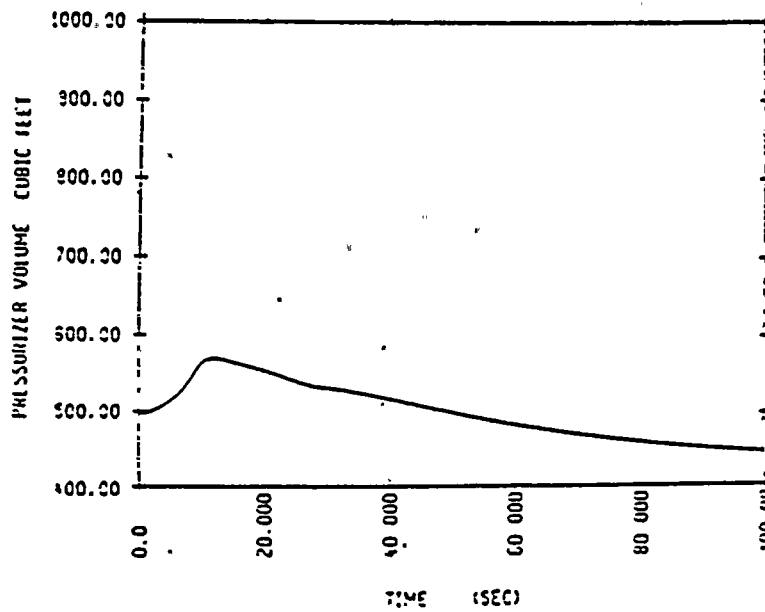
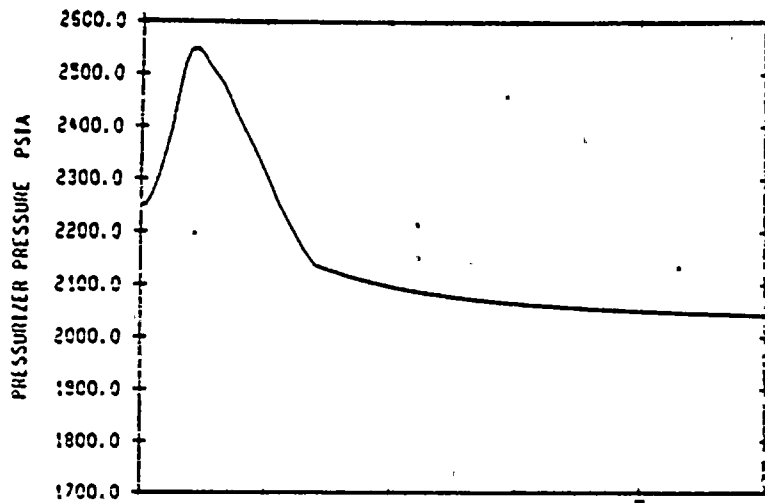
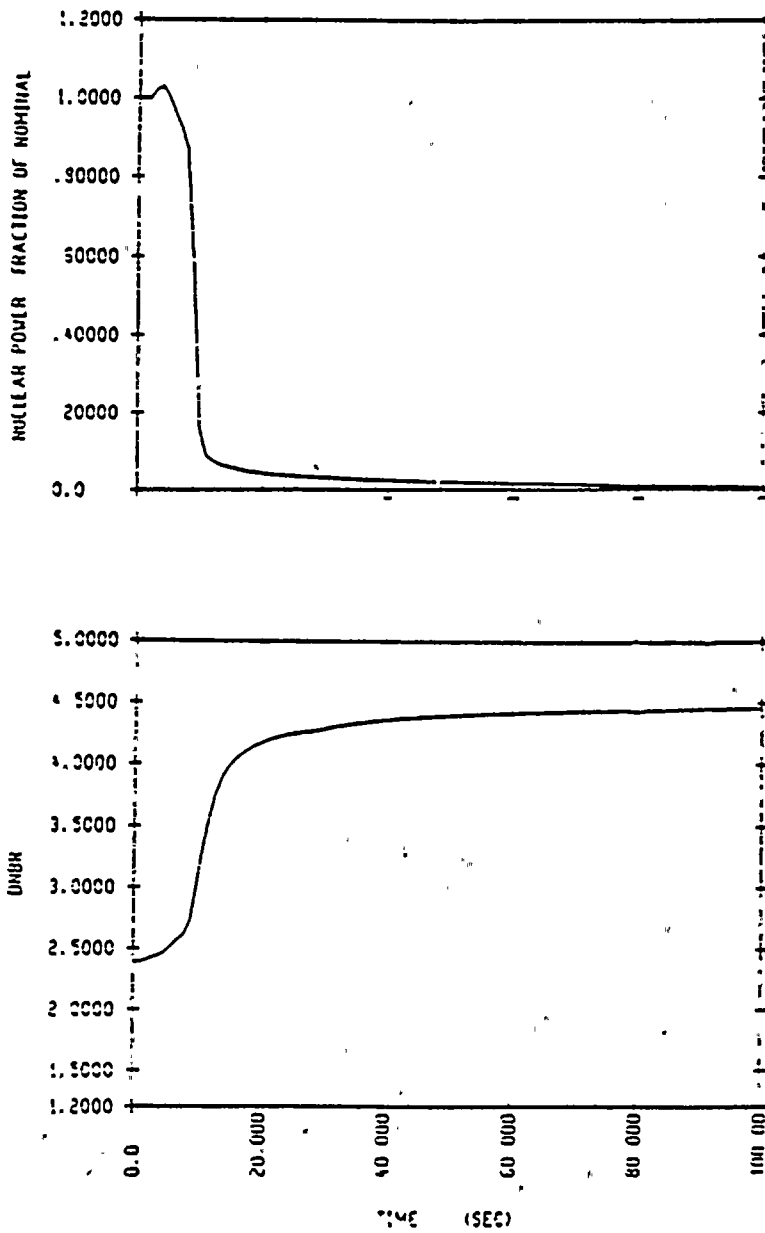




Figure 14.1.8-10

Ginna Loss of Load
Maximum Feedback Without Pressure Control



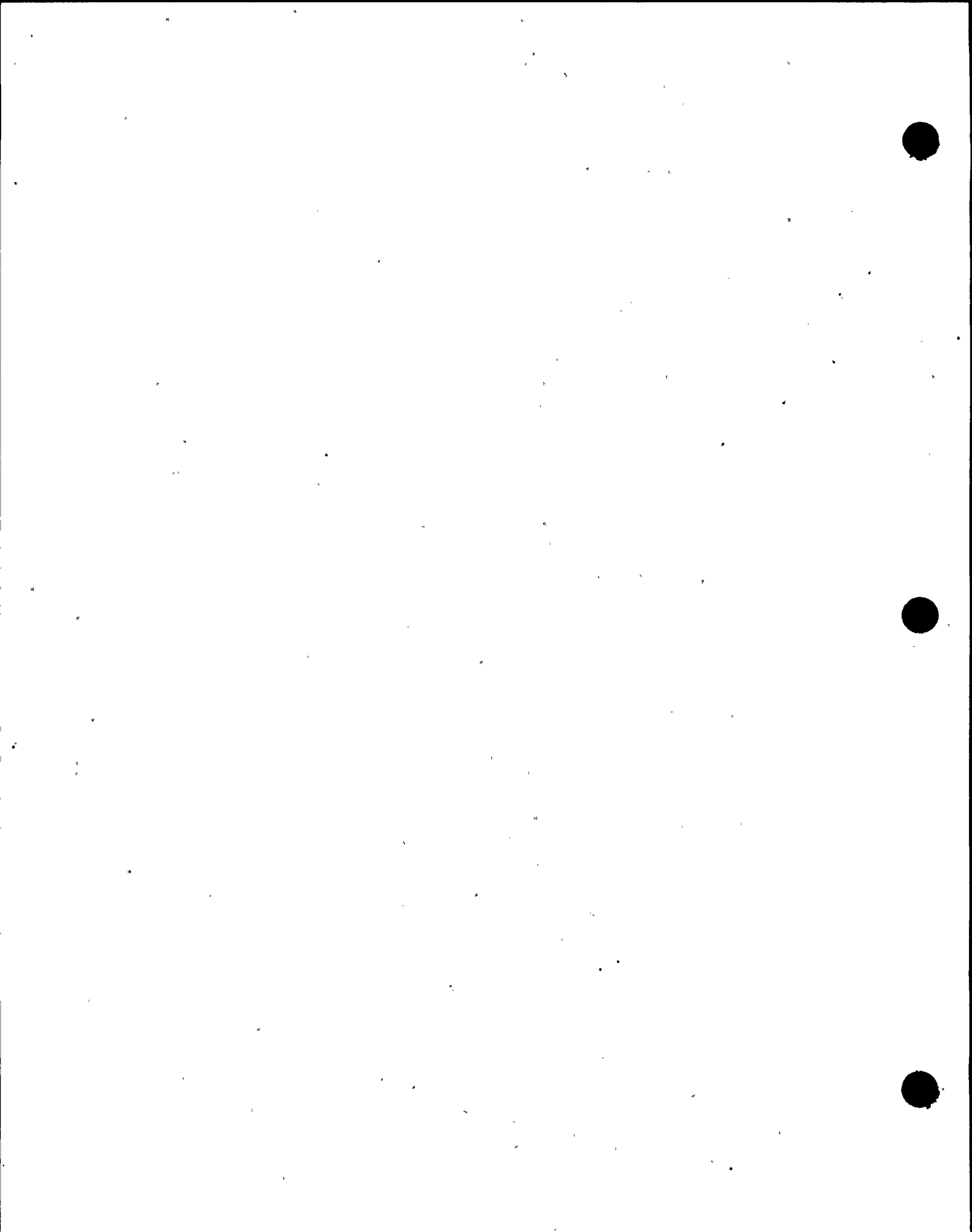


Figure 14.1:8-11

Ginna Loss of Load

Maximum Feedback Without Pressure Control

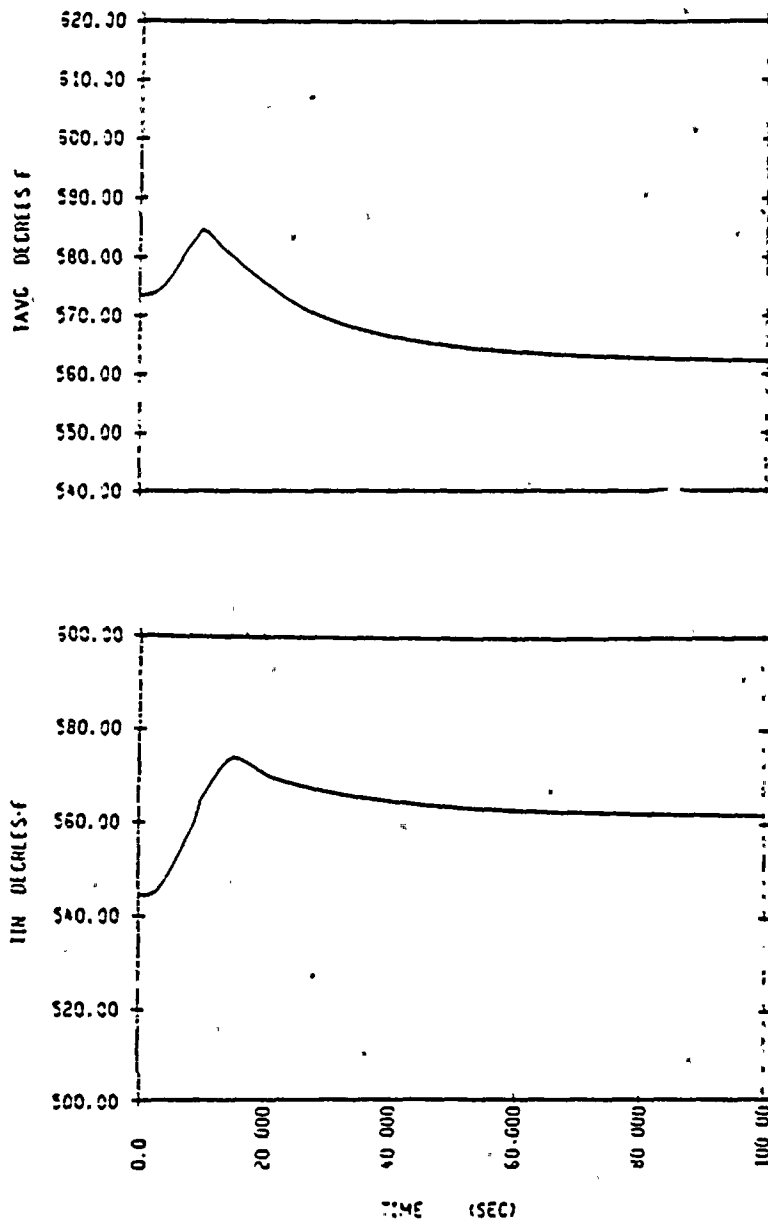
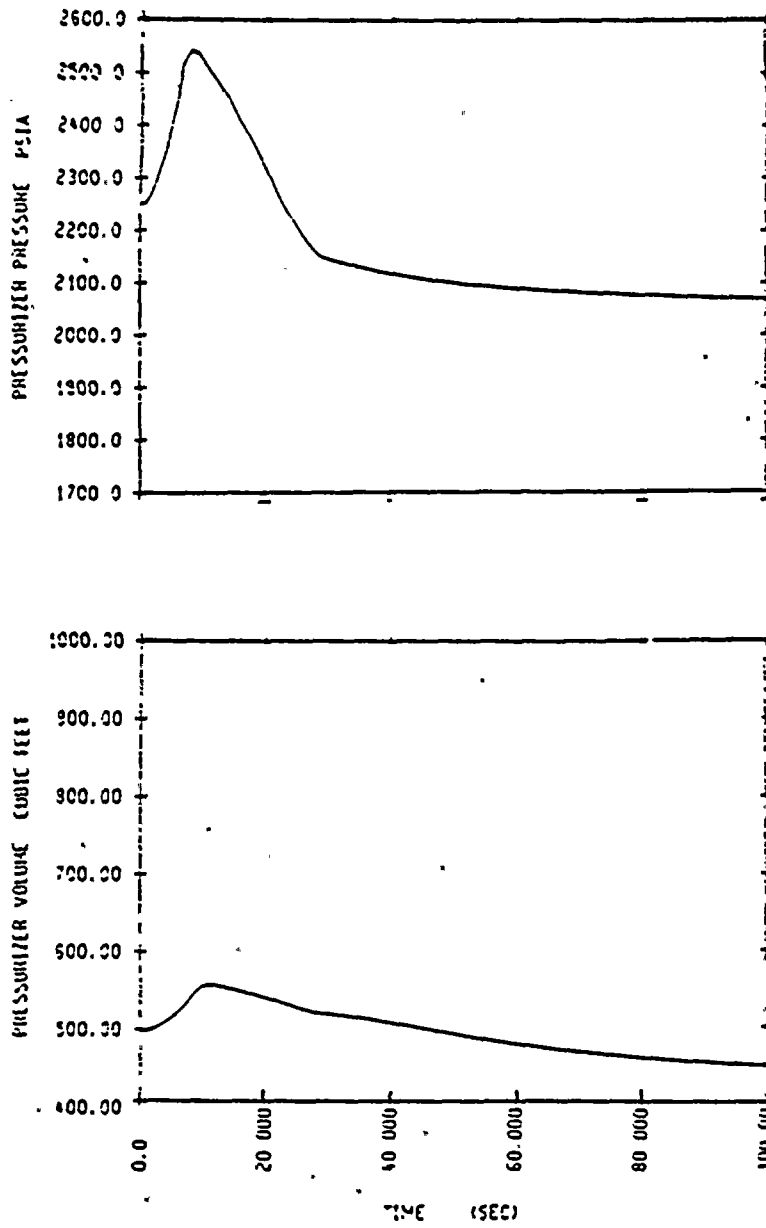
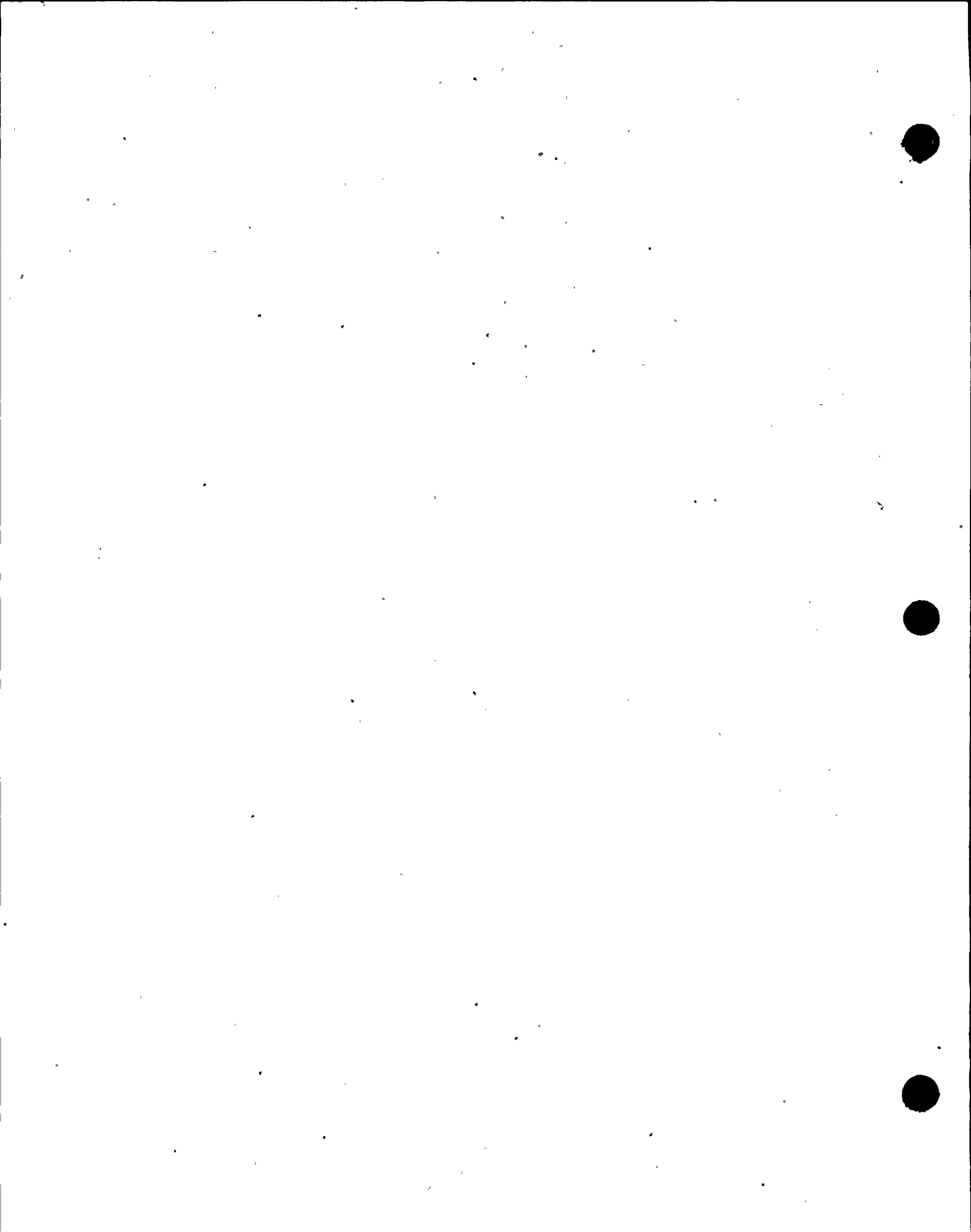


Figure 14.1.8-12

GINNA Loss of Load

Maximum Feedback Without Pressure Control





14.1.10 Excessive Heat Removal Due to Feedwater Temperature Decrease

The reduction in feedwater enthalpy is another means of increasing core power above full power. Such increases are attenuated by the thermal capacity in the secondary plant and in the Reactor Coolant System. The overpower-temperature protection (nuclear overpower and ΔT trips) prevents any power increase which could lead to a DNBR less than limit value.

An extreme example of excess heat removal by the feedwater system is the transient associated with the accidental opening of the feedwater bypass valve which diverts flow around the low pressure feedwater heaters. The function of this valve is to maintain net positive suction head on the main feedwater pump in the event that the heater drain pump flow is lost, e.g., during a large load decrease.

In the event of an accidental opening there is a sudden reduction in inlet feedwater temperature, to the steam generators. The increased subcooling will create a greater load demand on the primary system which can lead to a reactor trip. The three-element feedwater control system operates to regulate the feedwater flow and maintain a water level approximately constant in the steam generator. Action of the three-way boiler control under emergency condition has no bearing on safety since emergency feedwater is injected downstream of the control valves. However, the feedwater control valves are used for feedwater line isolation. Any safety injection signal will redundantly isolate the feedwater lines by a) venting the supply air to all feedwater control valves, causing valves to close; and by b) tripping off the main feedwater pumps, including closure of the feedwater discharge valves.

The wet effect on the RCS due to a reduction in feedwater enthalpy is similar to the effect of increasing secondary steam flow, i.e., the reactor will reach a new equilibrium condition at a power level corresponding to the new steam generator ΔT .

Method of Analysis

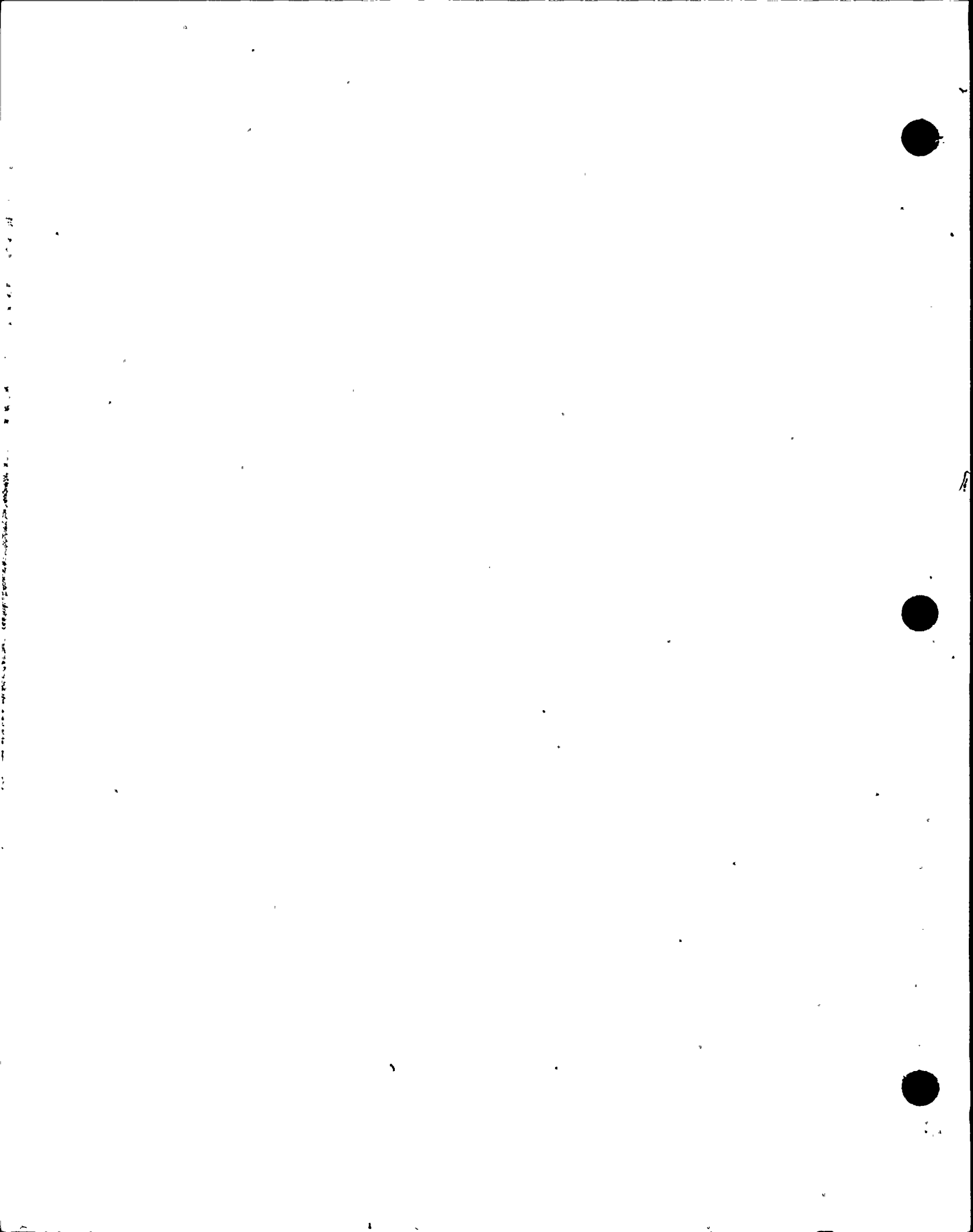
This accident is analyzed using the LOFTRAN code. The code simulates the neutron kinetics, reactor coolant system, pressurizer, pressurizer relief and safety valves, pressurizer spray, steam generator, steam generator safety valves, and feedwater system. The code computes pertinent plant variables, including temperatures, pressures, and power level.

This transient is analyzed by reducing the feedwater enthalpy by the amount corresponding to the loss of one feedwater heater. Two cases have been analyzed to demonstrate the plant behavior in the event of a sudden feedwater temperature reduction resulting from accidental opening of the bypass valve.

1. Reactor control in manual with maximum moderator reactivity feedback.
2. Reactor control in automatic with maximum moderator reactivity feedback.

The reactivity insertion rate at no load following an excessive feedwater accident has also been calculated with the following assumptions:

1. A step increase in feedwater flow to one steam generator from 0 to the nominal full load value for one steam generator.
2. The most negative reactivity moderator coefficient at end of life.



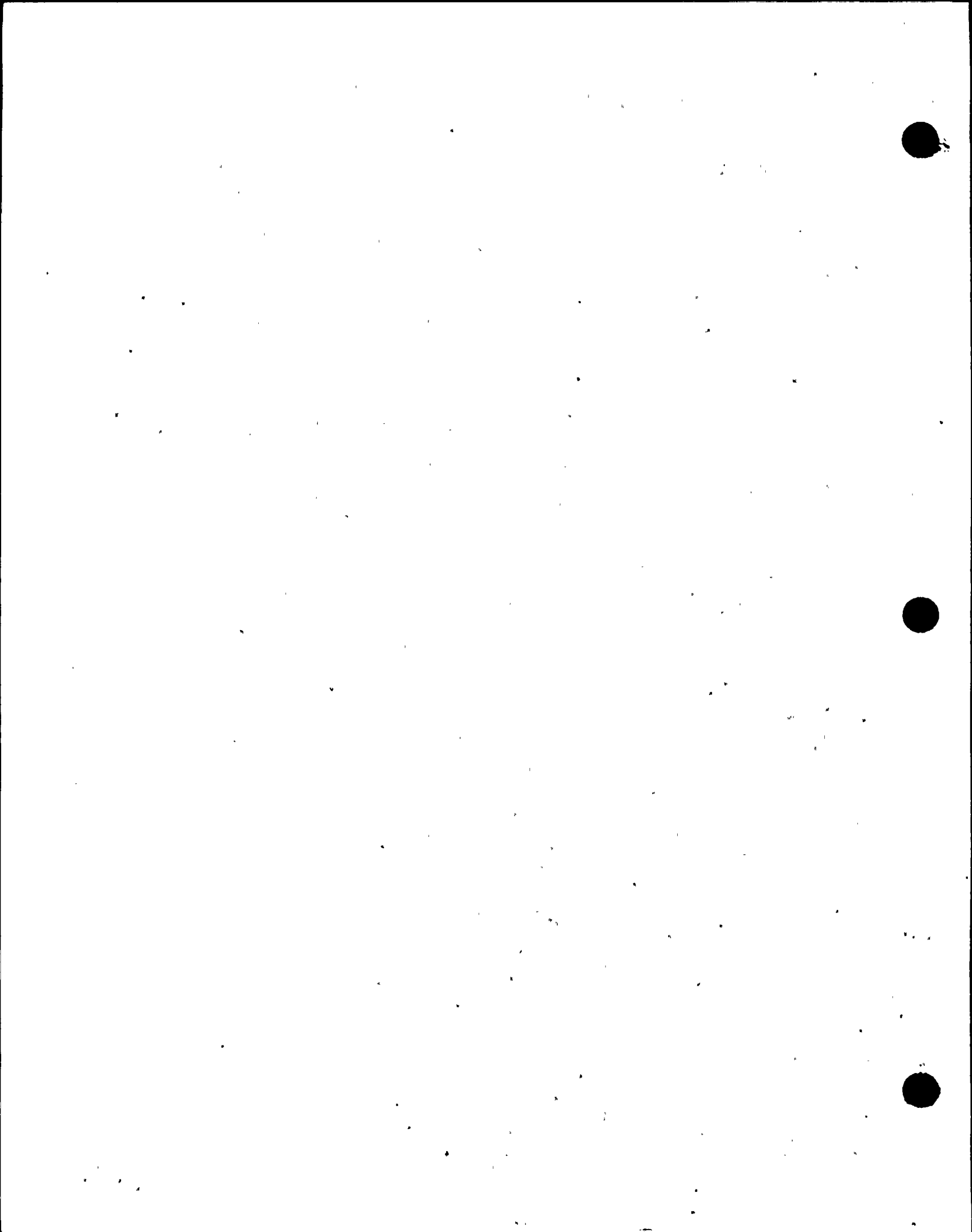
3. A constant feedwater temperature of 70°F.
4. Neglect of the heat capacity of the reactor coolant system and steam generator shell thick metal.
5. Neglect of the energy stored in the fluid of the unaffected second steam generator..

Continuous addition of cold feedwater after a reactor trip is prevented since the reduction of reactor coolant system temperature, pressure, and pressurizer level will lead to the actuation of safety injection on low pressurizer pressure. The safety injection signal will trip the ^{main} feedwater pumps and close the feedwater pump discharge valves as well as close the main feedwater control valves.

This accident is analyzed with the Improved Thermal Design Procedure as described in Reference 12. Plant characteristics and initial conditions are discussed in Section 14.1. Initial reactor power, pressure, and RCS temperatures are assumed to be at their nominal values. Uncertainties in initial conditions are included in the limit DNBR as described in Reference 6.

Results

Figures 14.1.10-1 through 14.4.10-3 illustrate the transient with the reactor in the automatic control mode. Due to the action of the control rods and moderator feedback, the nuclear power increases while temperature and pressure decrease until a steady-state condition is reached. A reduction in departure from nucleate boiling ratio is experienced, but the departure from nucleate boiling ratio remains above the limit value.



Figures 14.1.10-4 through 14.1.10-6 illustrate the transient when the reactor is assumed to be in the manual control mode. Again, the core power increases due to the decrease in coolant average temperature. The departure from nucleate boiling ratio decreases but remains above the limit value.

The feedwater enthalpy decrease incident is similar to an excessive load increase and is an overpower transient for which the fuel temperatures rise. When a reactor trip does not occur, the plant reaches a new equilibrium condition at a higher power level corresponding to the increase in steam flow.

At zero power, for the excessive feedwater flow to one steam generator, the maximum reactivity insertion rate was calculated to be 4.5×10^{-4} $\Delta k/\text{second}$. This is less than the maximum reactivity insertion rate analyzed in Section 14.1.1, Uncontrolled RCCA Withdrawal from a Subcritical Condition. It should be noted that if the accident occurs with the plant just critical at no load, the reactor will be tripped by the power range flux level trip (low setting) set at approximately 25%. As shown in Section 14.1.1, the DNB remains above the limit value. *with Trip*

Conclusions

It has been demonstrated that, for a feedwater enthalpy decrease at full power, minimum DNBR does not fall below the limit value. At zero power, the results are less limiting than those presented in Section 14.1.1. *with one Trip Run*



Figure 14.1.10-1

Ginna Feedwater Enthalpy Decrease

Automatic Rod Control

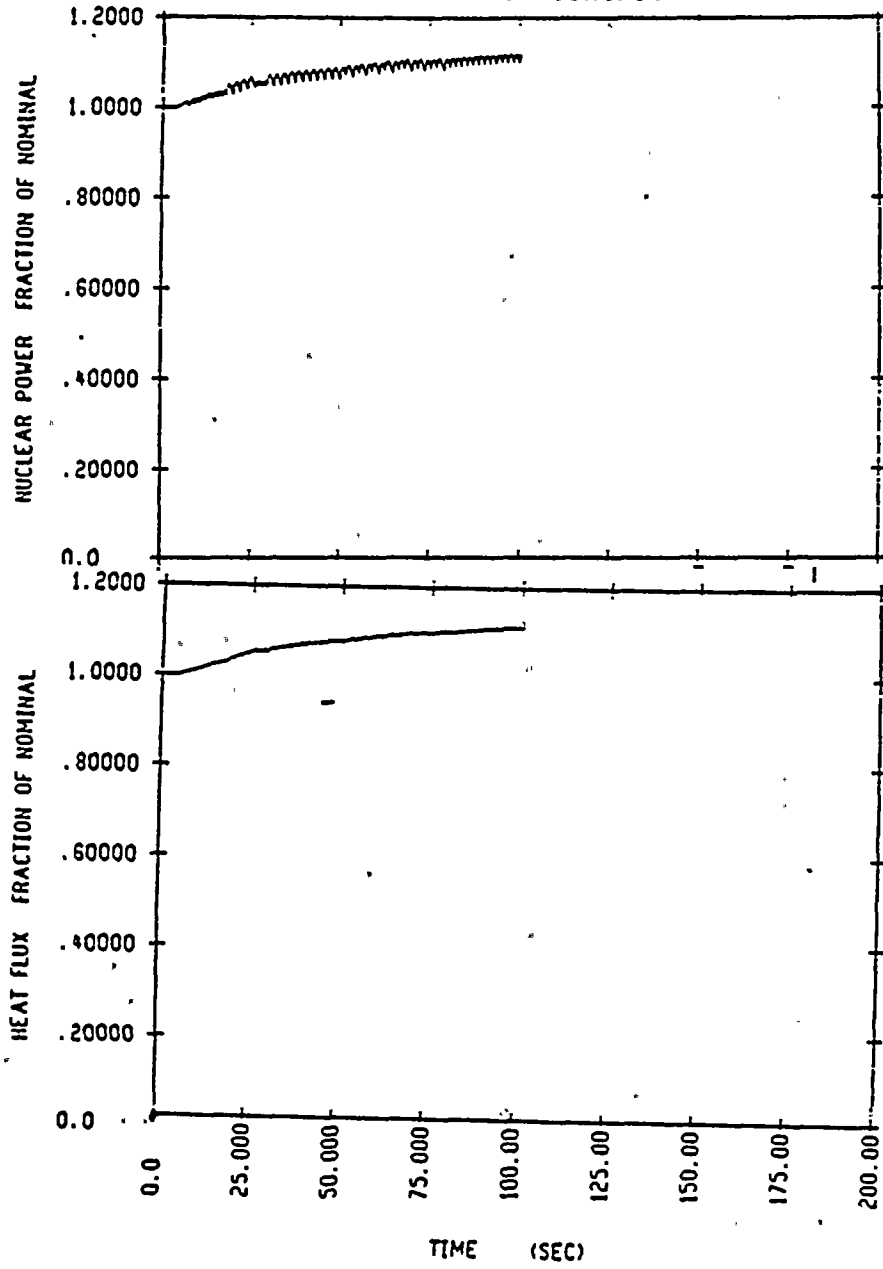


Figure 14.1.10-2
Ginna Feedwater Enthalpy Decrease
Automatic Rod Control

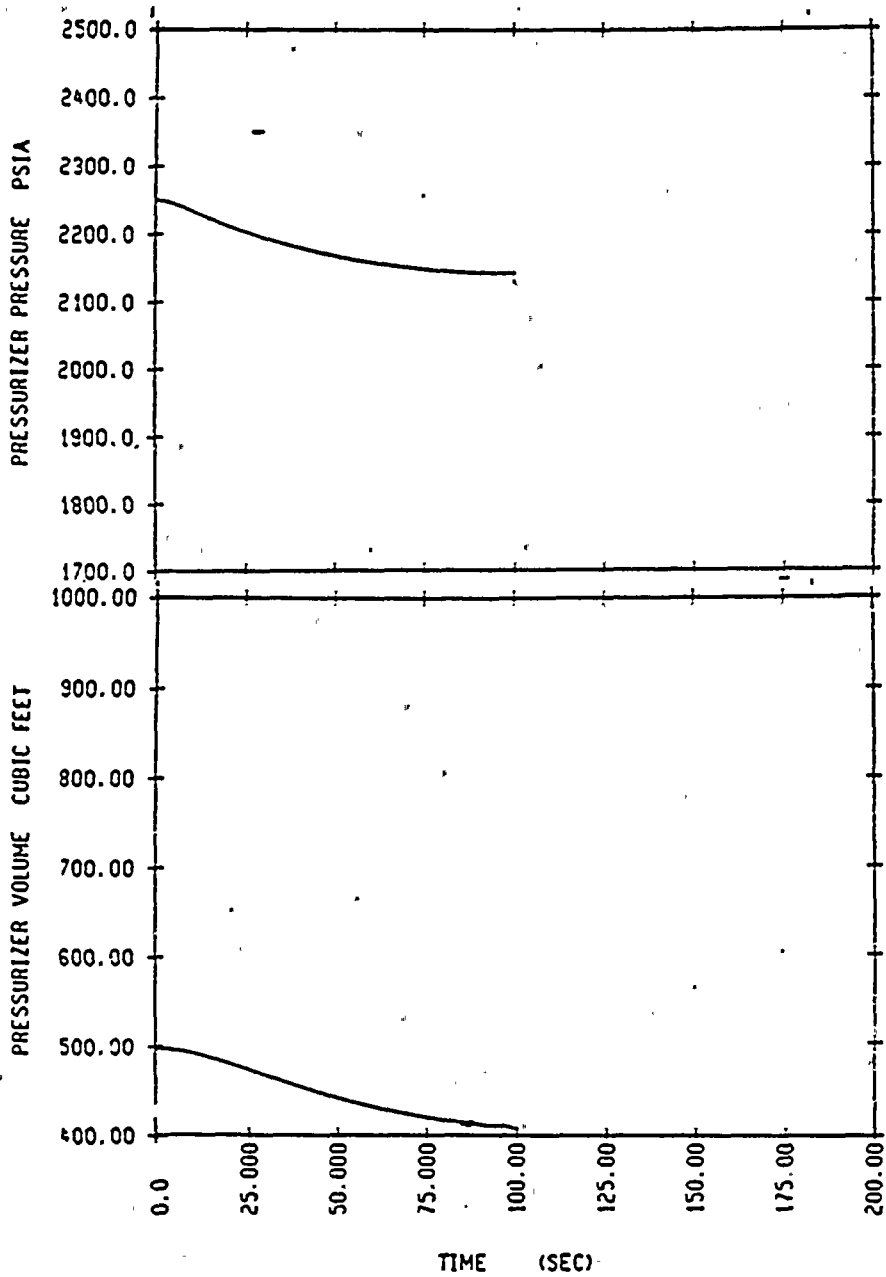


Figure 14.1.10-3

Ginna Feedwater Enthalpy Decrease
Automatic Rod Control

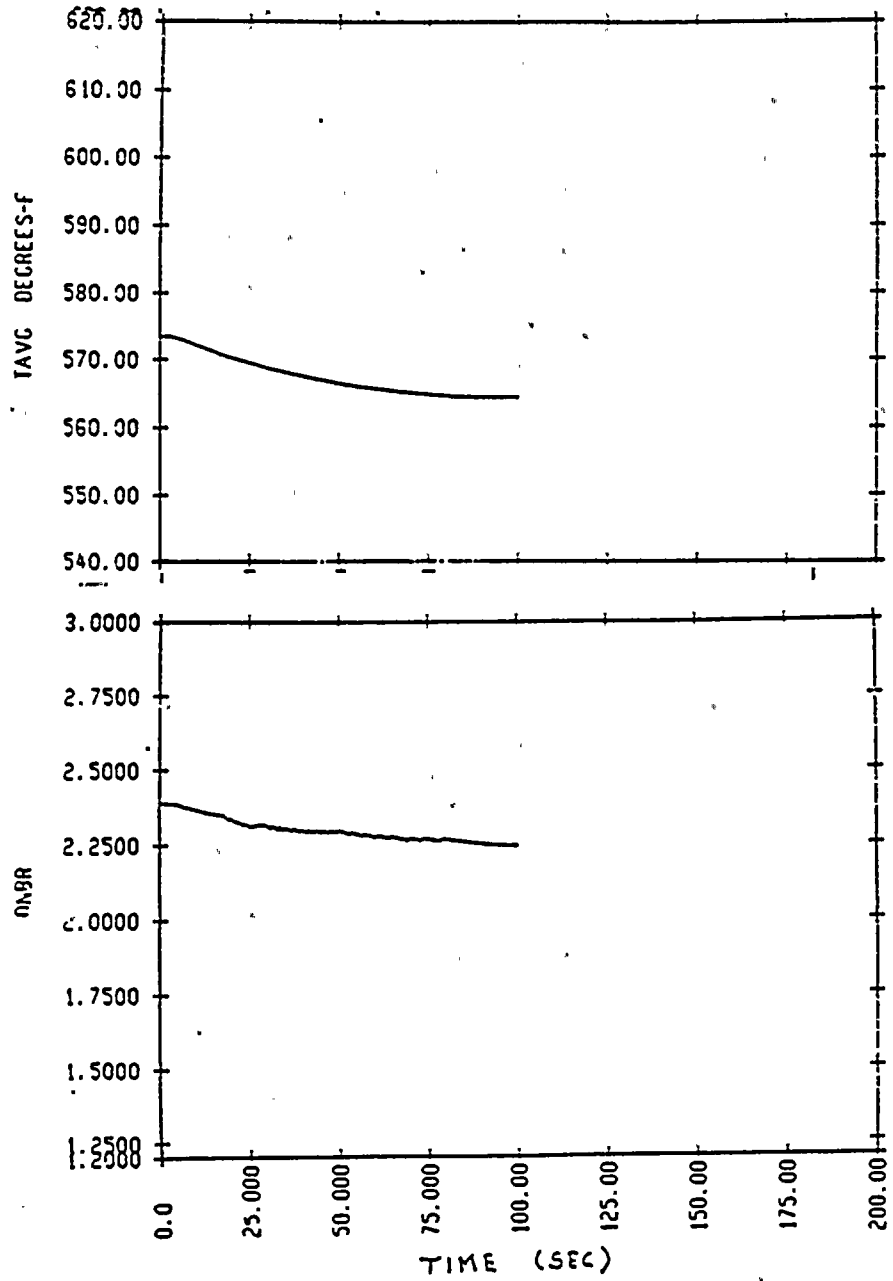




Figure 14.1.10-4

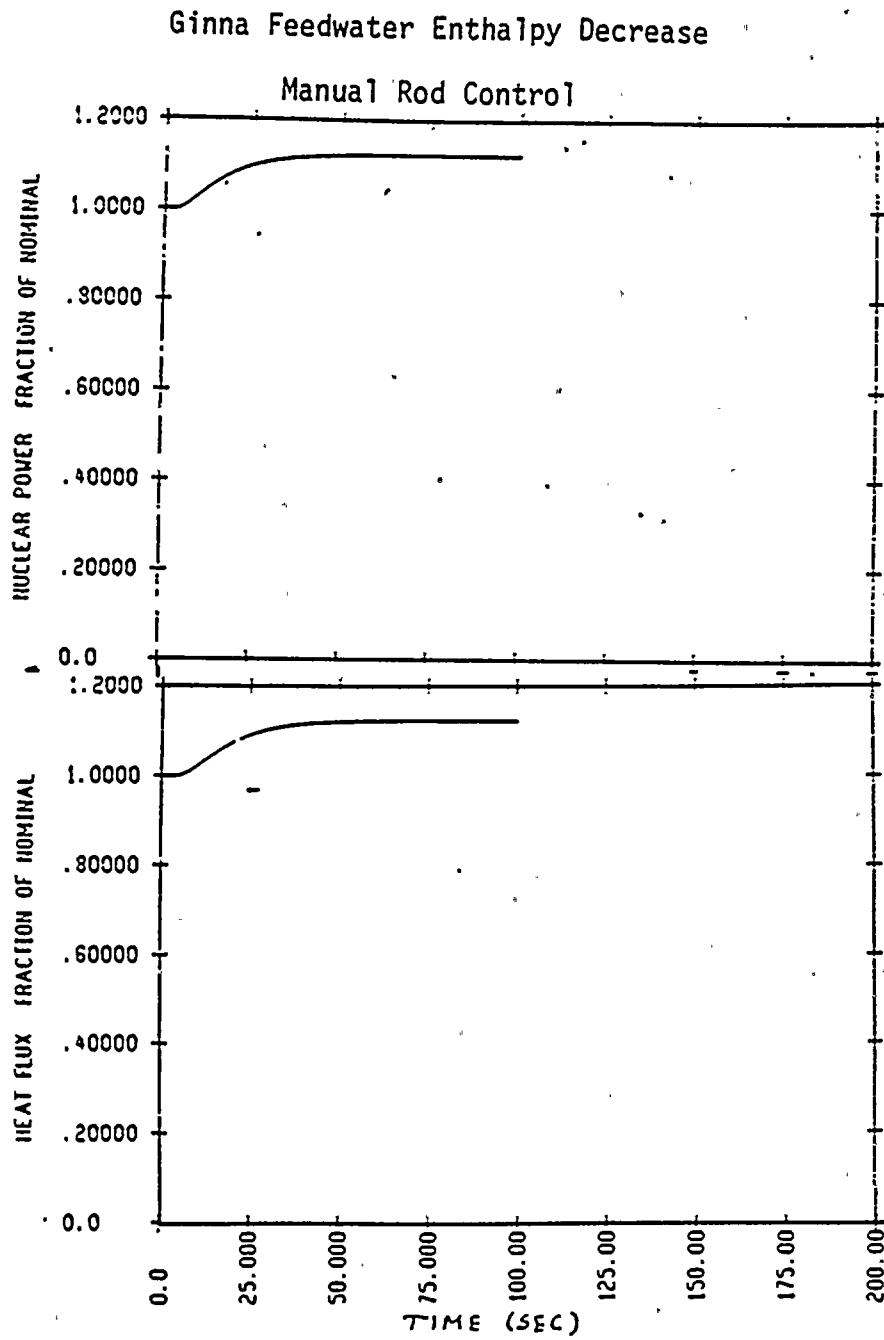




Figure 14.1.10-5

Ginna Feedwater Enthalpy Decrease
Manual Rod Control

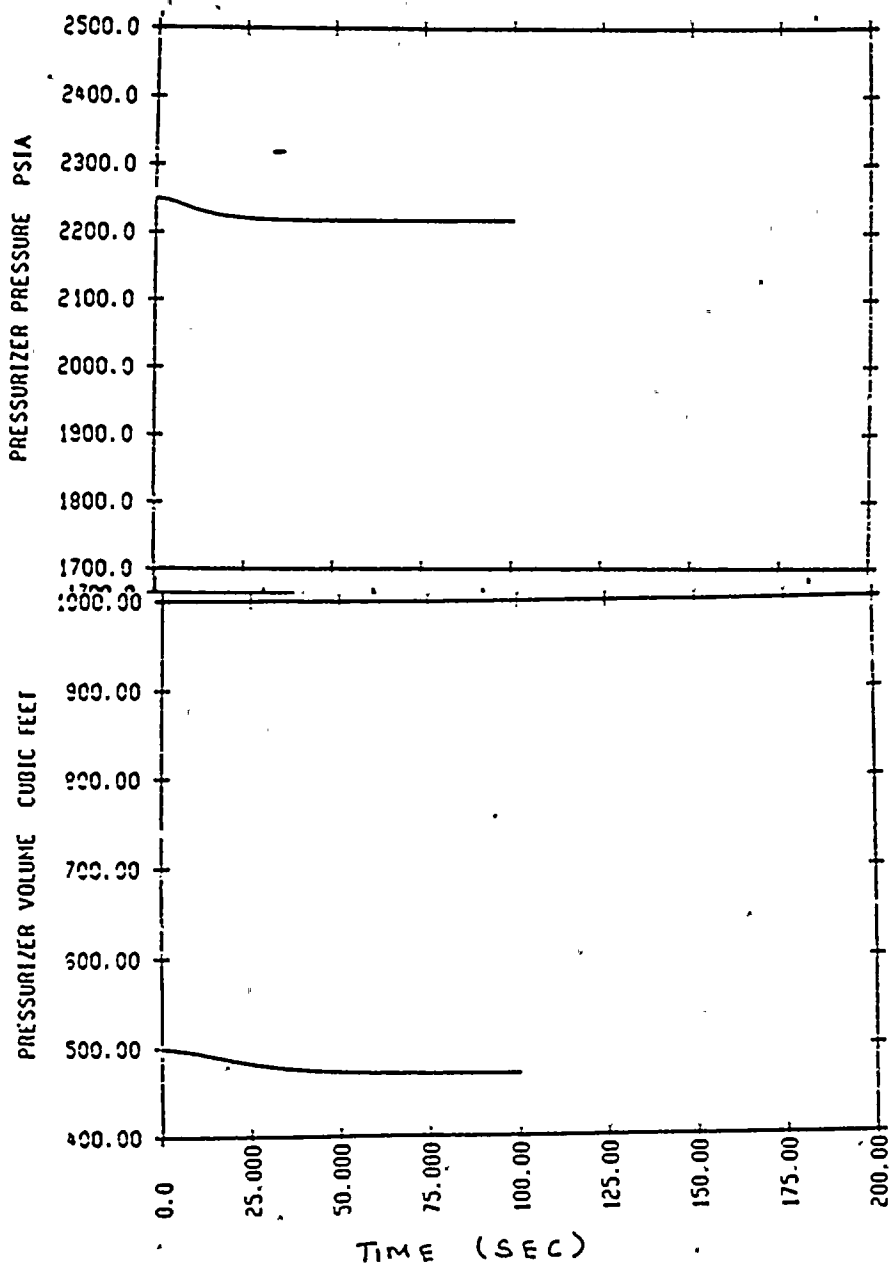
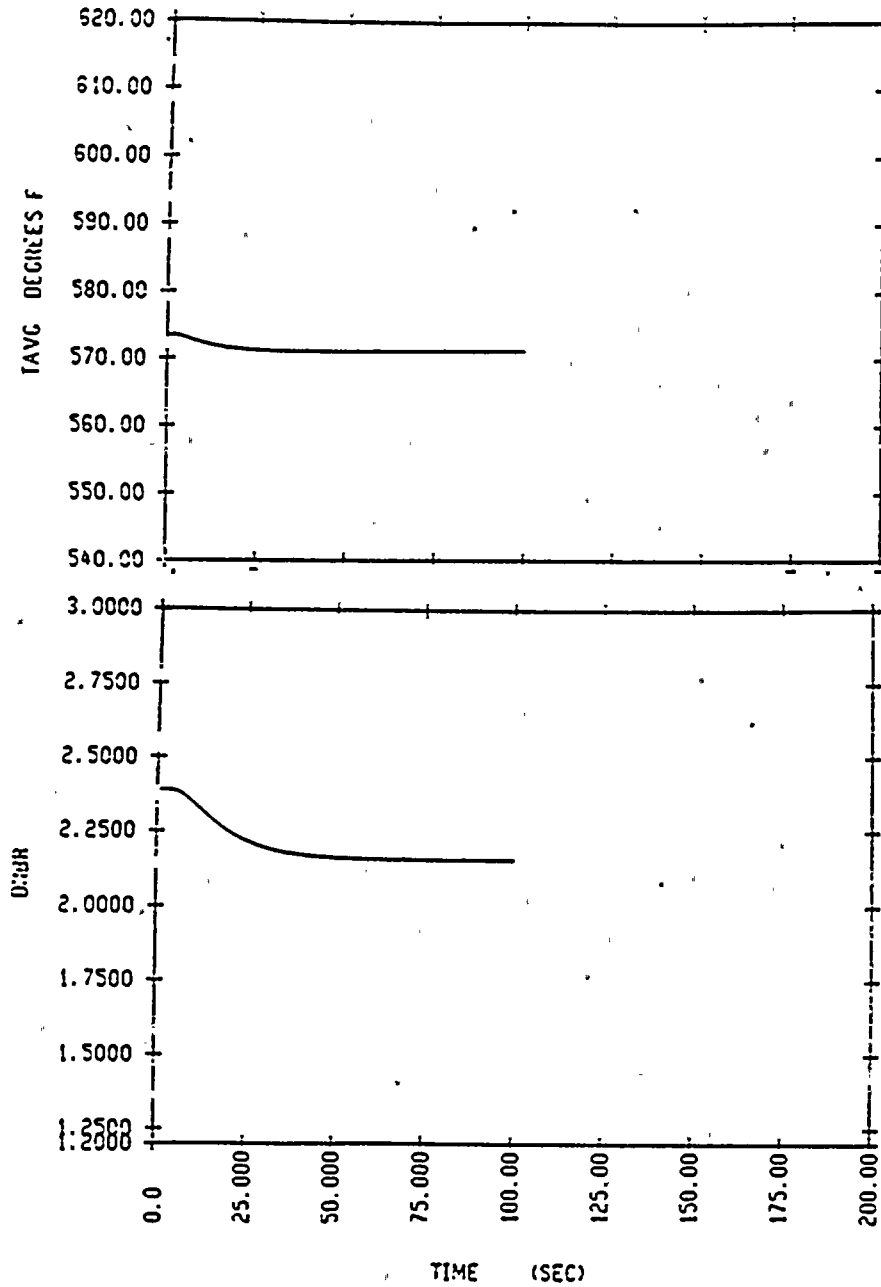




Figure 14.1.10-6

Ginna Feedwater Enthalpy Decrease
Manual Rod Control



14.1.11 Excessive Load Increase Incident

An excessive load increase incident is defined as a rapid increase in steam generator steam flow that causes a power mismatch between the reactor core power and the steam generator load demand. The reactor control system is designed to accommodate a 10% step load increase and/or a 5% per minute ramp load increase (without a reactor trip) in the range of 15% to 100% full power. Any loading rate in excess of these values may cause a reactor trip actuated by the reactor protection system. If the load increase exceeds the capability of the reactor control system, the transient is terminated in time to prevent DNBR less than the limiting value by a combination of the nuclear overpower trip and the overpower-temperature ΔT trips. An excessive load increase incident could result from either an administrative violation, such as steam bypass control or turbine speed control.

For excessive loading by the operator or by system demand, the turbine load limiter keeps maximum turbine load below 100% rated load.

During power operation, steam bypass to the condenser is controlled by reactor coolant condition signals, i.e., abnormally high reactor coolant temperature indicates a need for steam bypass. A single controller malfunction does not cause steam bypass; an interlock is provided which blocks the control signal to the valves unless a large turbine load decrease or a turbine trip has occurred.

Method of Analysis

This accident is analyzed using the LOFTRAN code. The code simulates the neutron kinetics, reactor coolant system, pressurizer, pressurizer relief and safety valves, pressurizer spray, steam generator, steam



generator safety valves, and feedwater system. The code computes pertinent plant variables, including temperatures, pressures, and power level.

Four cases are analyzed to demonstrate the plant behavior following a 10% step-load increase from rated load. These cases are as follows:

1. Reactor control in manual with minimum moderator reactivity feedback.
2. Reactor control in manual with maximum moderator reactivity feedback.
3. Reactor control in automatic with minimum moderator reactivity feedback.
4. Reactor control in automatic with maximum moderator reactivity feedback.

For the minimum moderator feedback cases, the core has a 5.0 pcm/°F moderator temperature coefficient of reactivity and, therefore, the least inherent transient capability. For the maximum moderator feedback cases, the moderator temperature coefficient of reactivity has its most negative value. This results in the largest amount of reactivity feedback due to changes in coolant temperature.

A conservative limit on the turbine valve opening is assumed, and all cases are studied without credit being taken for pressurizer heaters. This accident is analyzed with the Improved Thermal Design Procedure as described in Reference 12. Plant characteristics and initial conditions are as discussed in Section 14.1. Initial reactor power, pressure, and

RCS temperatures are assumed to be at their nominal values. Uncertainties in initial conditions are included in the limit DNBR as described in Reference 6.

Results

Figures 14.1.11-1 through 14.1.11-6 illustrate the transient with the reactor in the manual control mode. For the minimum feedback case, the positive MTC causes the nuclear power to decrease with temperature and pressure until a reactor trip on low pressurizer pressure occurs. This results in a departure from nucleate boiling ratio that increases above its initial value. For the maximum feedback, manually controlled case, there is an increase in reactor power due to the moderator feedback. A reduction in departure from nucleate boiling ratio is experienced, but the departure from nucleate boiling ratio remains above the limit value.

Figures 14.1.11-7 through 14.1.11-12 illustrate the transient when the reactor is assumed to be in the automatic control mode. Both the minimum and maximum feedback cases show that core power increases, thereby reducing the rate of decrease in coolant average temperature and pressurizer pressure. For both the minimum and maximum feedback cases, the minimum departure from nucleate boiling ratio remains above the limit value. The calculated sequence of events is shown in Table 14.1.11-1.

The excessive load increase incident is an overpower transient for which the fuel temperatures rise. When a reactor trip does not occur, the plant reaches a new equilibrium condition at a higher power level corresponding to the increase in steam flow.

Conclusion

It has been demonstrated that, for an excessive load increase, the minimum departure from nucleate boiling ratio during the transient will not be below the limit value.

TABLE 14.1.11-1

TIME SEQUENCE OF EVENTS FOR
EXCESSIVE LOAD INCREASE INCIDENT

| <u>Case</u> | <u>Event</u> | <u>Time of Each Event (Seconds)</u> |
|---|---|---|
| a. Manual reactor control (minimum feedback) | 10% step load increase | 0 |
| | Lower pressurizer pressure trip reached | 213.9 |
| | Rods begin to fall into core | 215.9 |
| b. Manual reactor control (maximum feedback) | 10% step load increase | 0 |
| | Equilibrium conditions reached (approximate times only) | 50.0 |
| c. Automatic reactor control (minimum feedback) | 10% step load increase | 0 |
| | Equilibrium conditions reached (approximate times only) | 35.0 |
| d. Automatic reactor control (maximum feedback) | 10% step load increase | 0 |
| | Equilibrium conditions reached (approximate times only) | 60.0 |

Figure 14.1.11-1
Ginna Excess Load Increase
Minimum Feedback without Rod Control

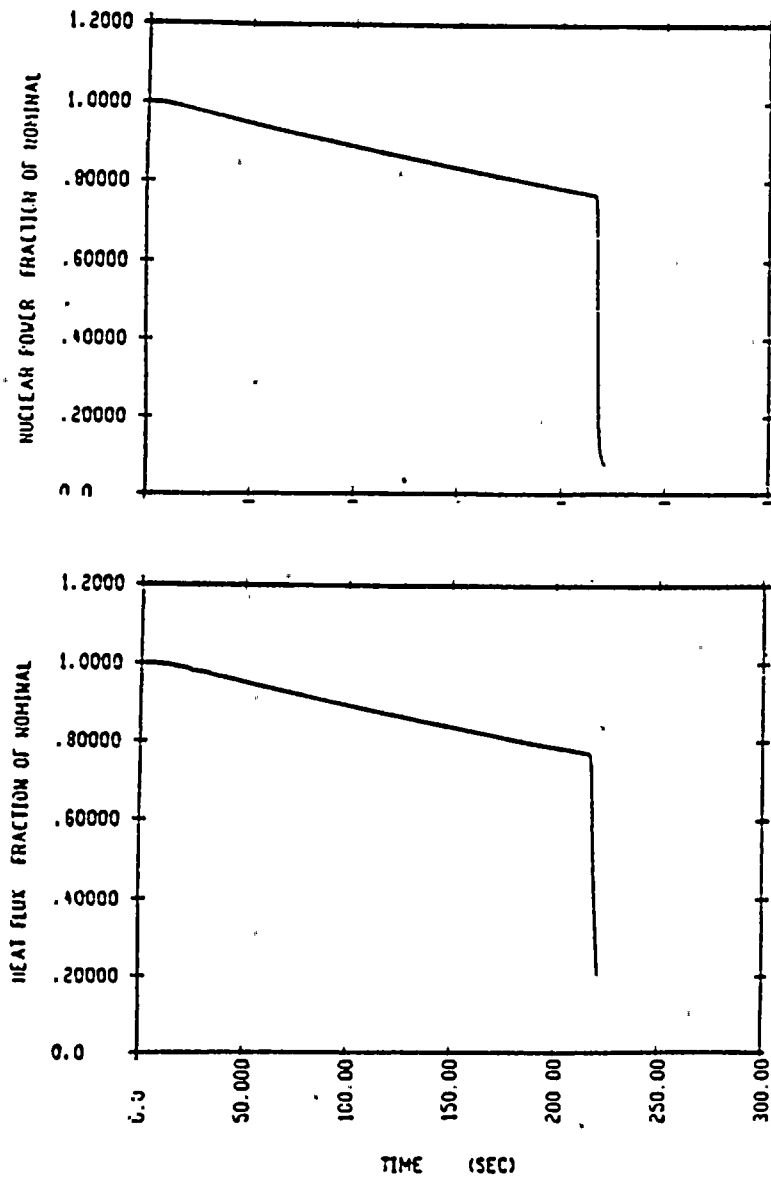
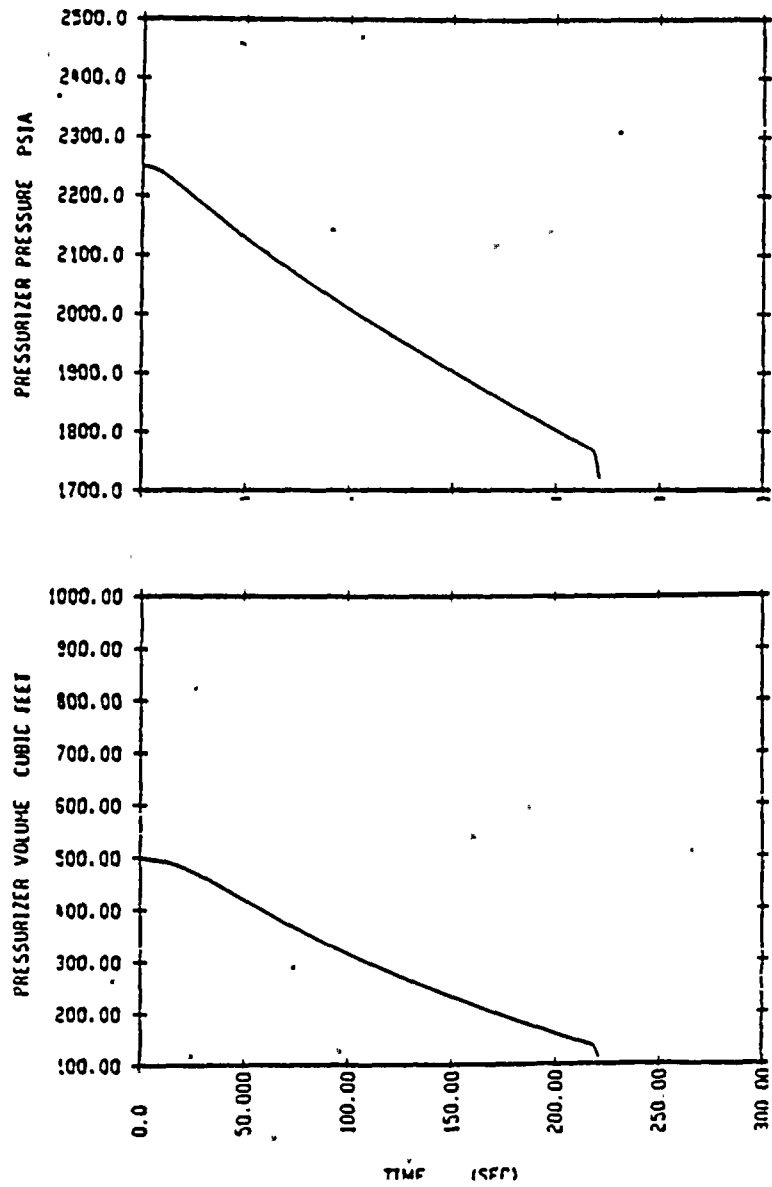


Figure 14.1.11-2

Ginna Excess Load Increase

Minimum Feedback without Rod Control



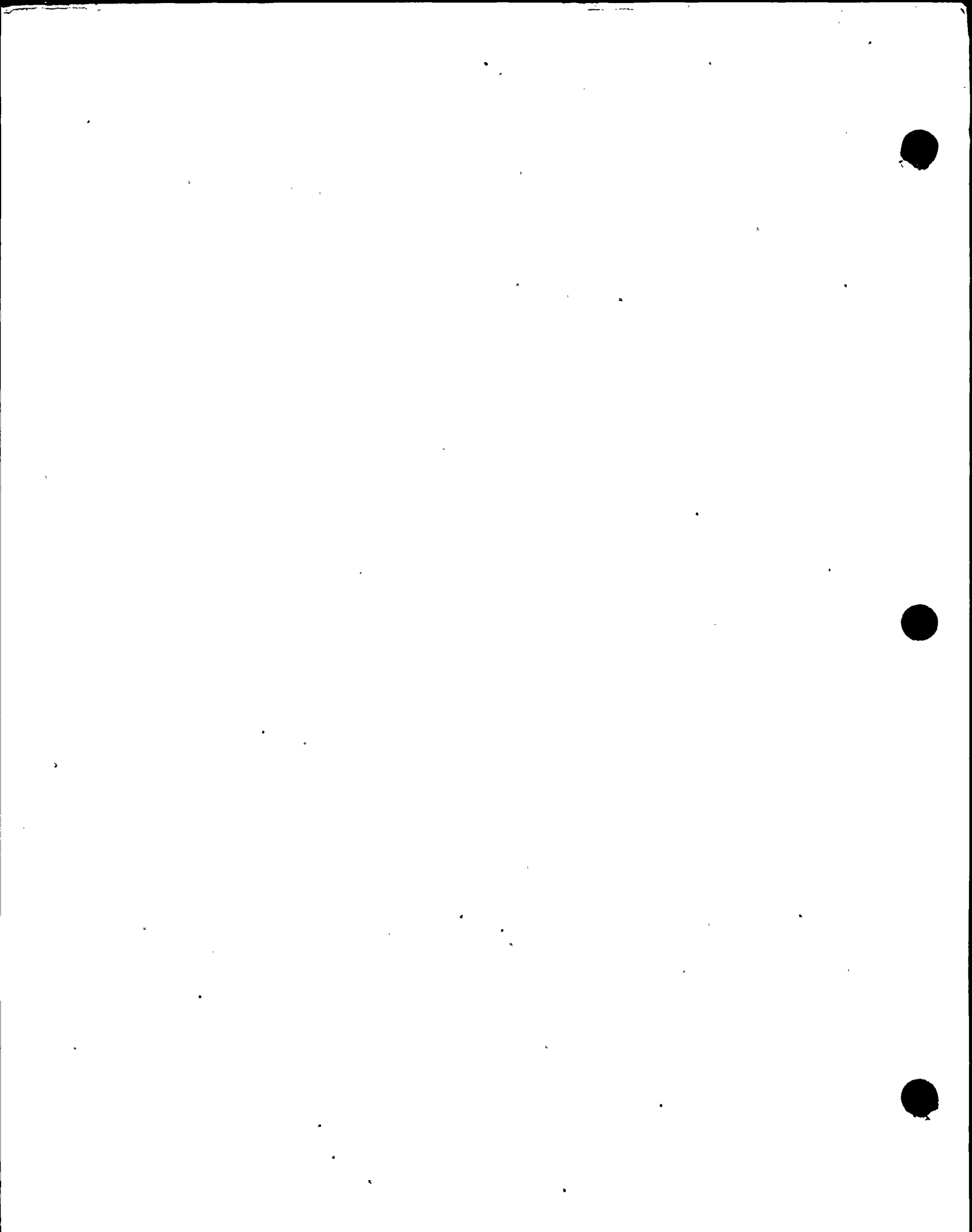


Figure 14.1.11-3

• Ginna Excess Load Increase
Minimum Feedback without Rod Control

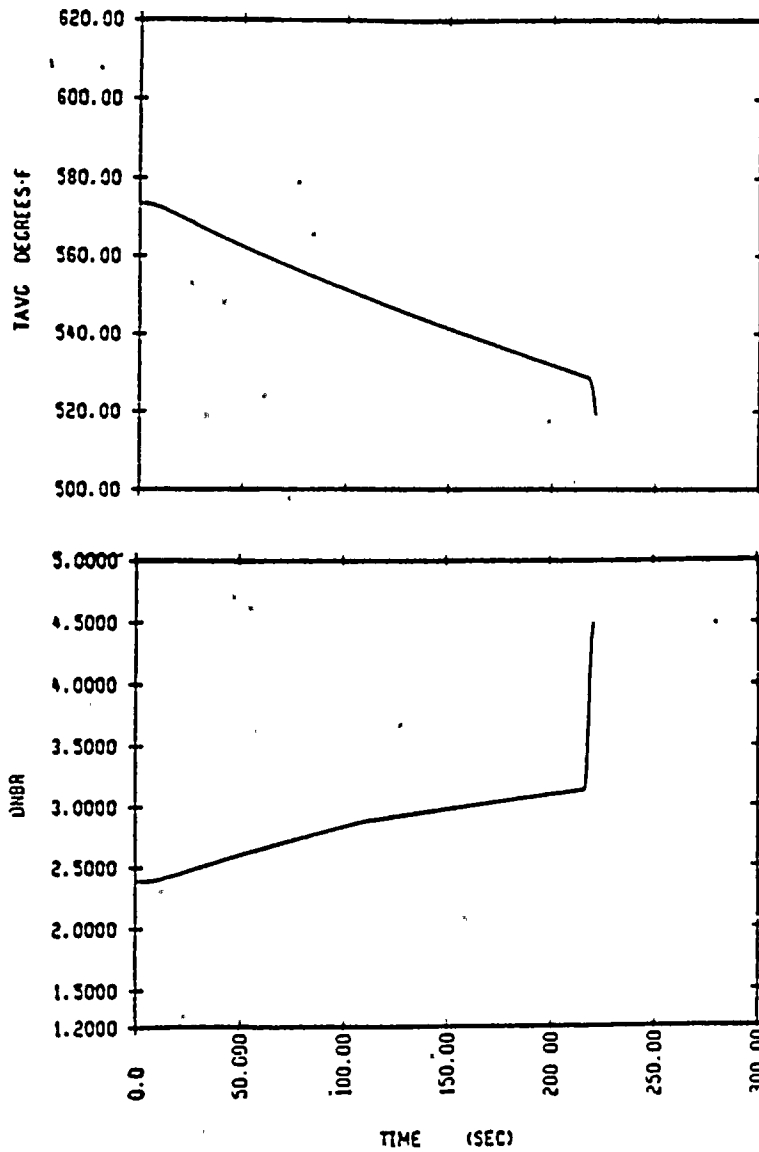




Figure 14.1.11-4

GINNA Excess Load Increase

Maximum Feedback without Rod Control

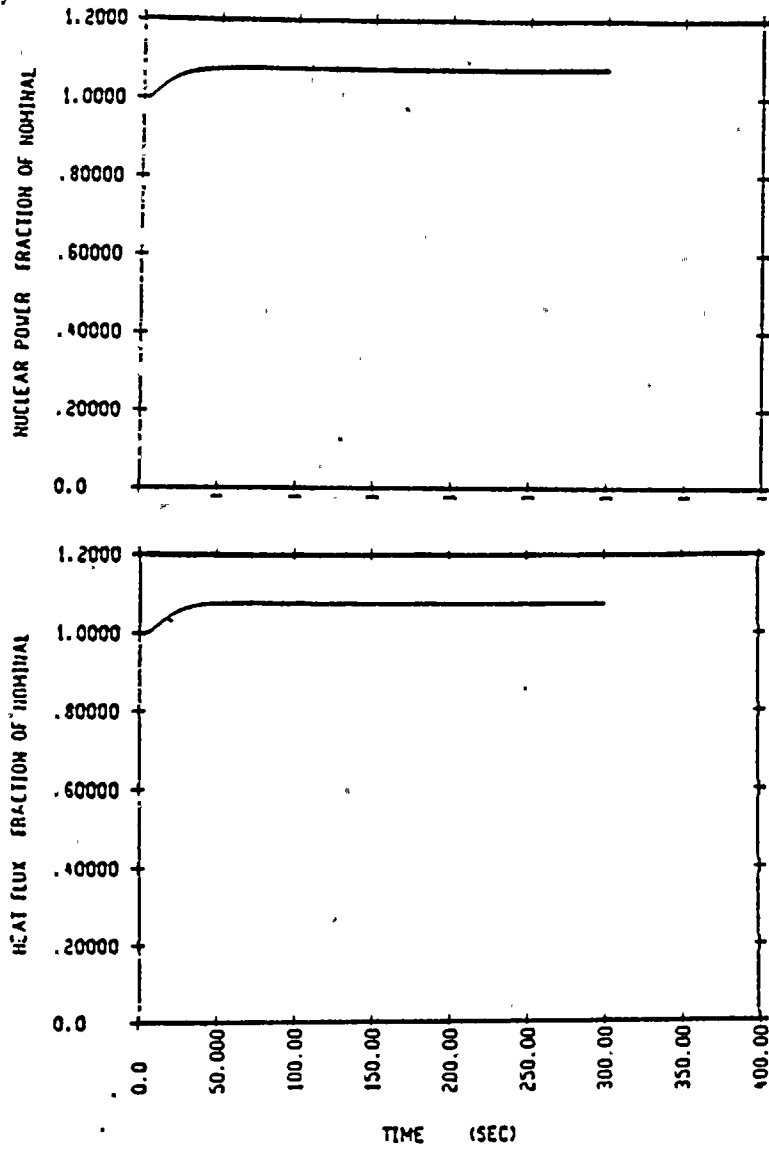


Figure 14.1.11-5

Ginna Excess Load Increase
Maximum Feedback Without Rod Control

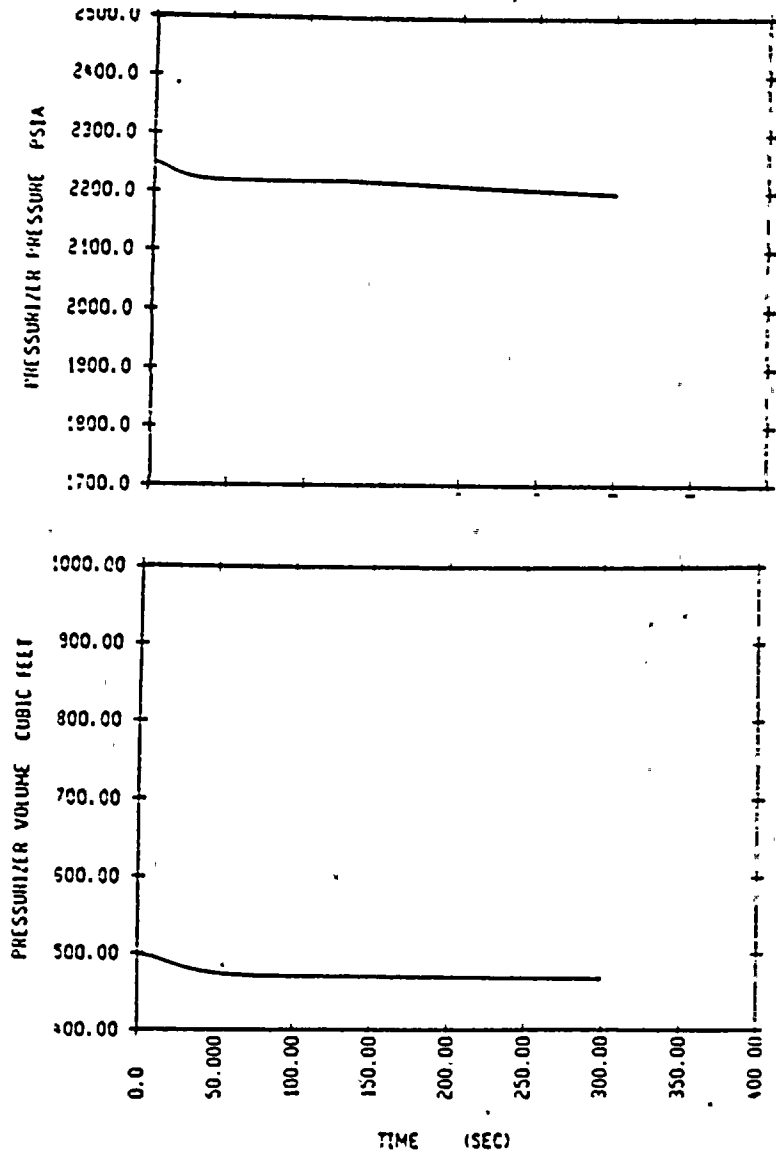


Figure 14.1.11-6

GINNA Excess Load Increase

Maximum Feedback without Rod Control

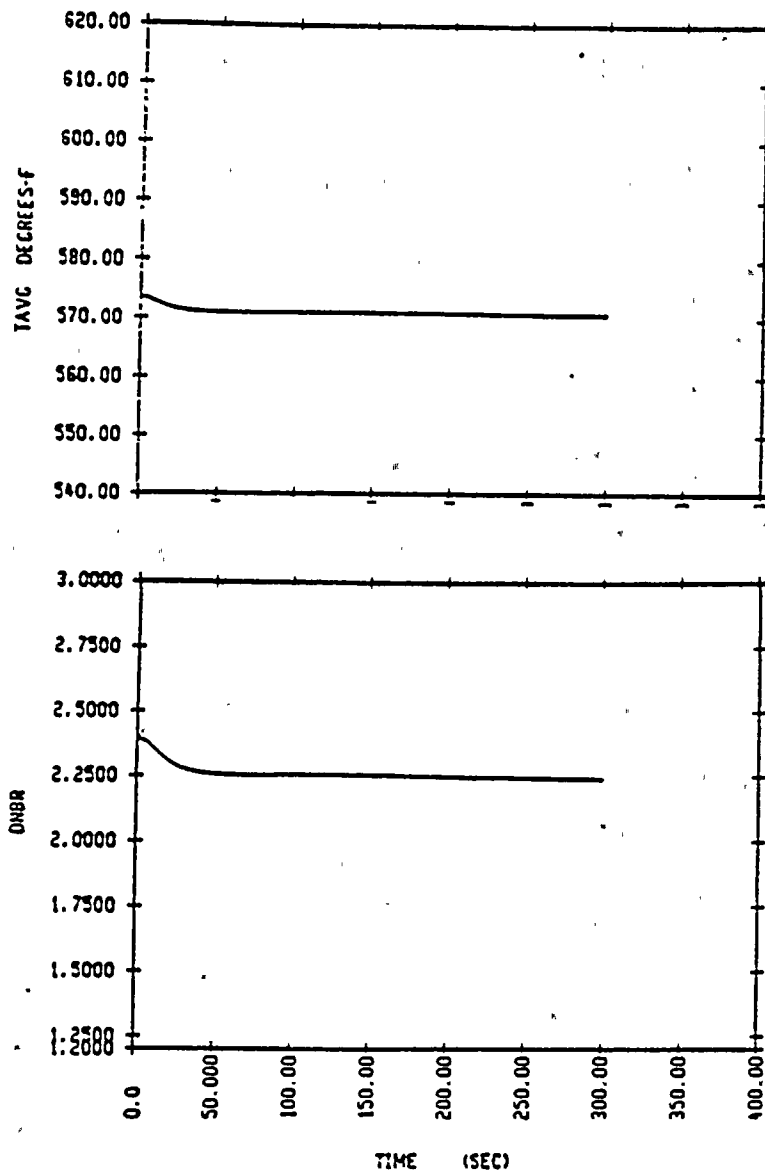


Figure 14.1.11-7

Ginna Excess Load Increase
Minimum Feedback with Automatic Rod Control

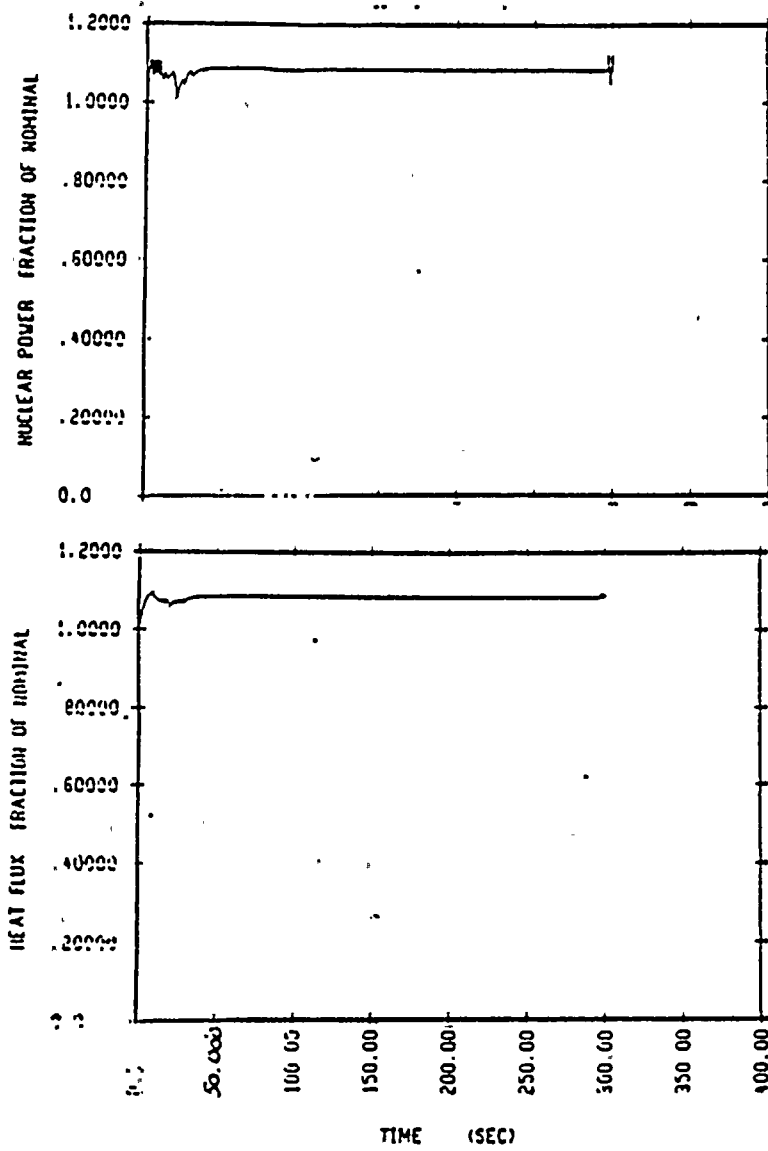


Figure 14.1.11-8

GINNA Excess Load Increase

Minimum Feedback with Automatic Rod Control

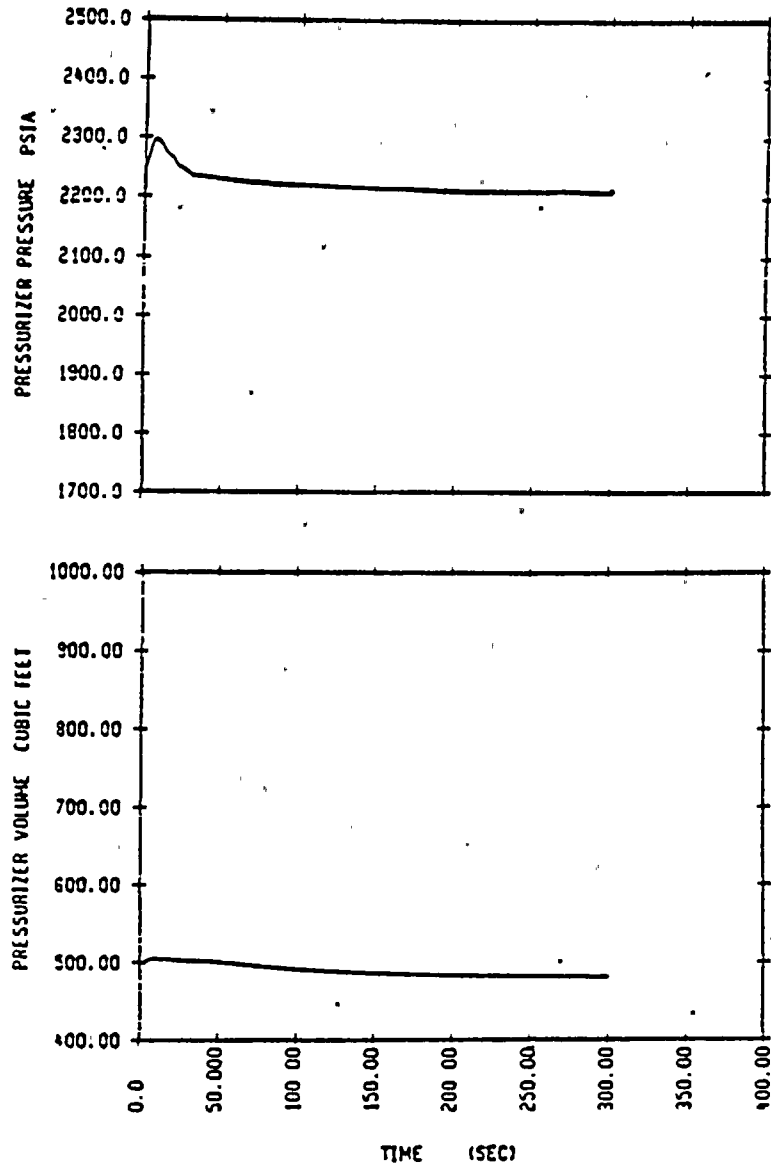


Figure 14.1.11-9
Ginna Excess Load Increase
Minimum Feedback with Automatic Rod Control

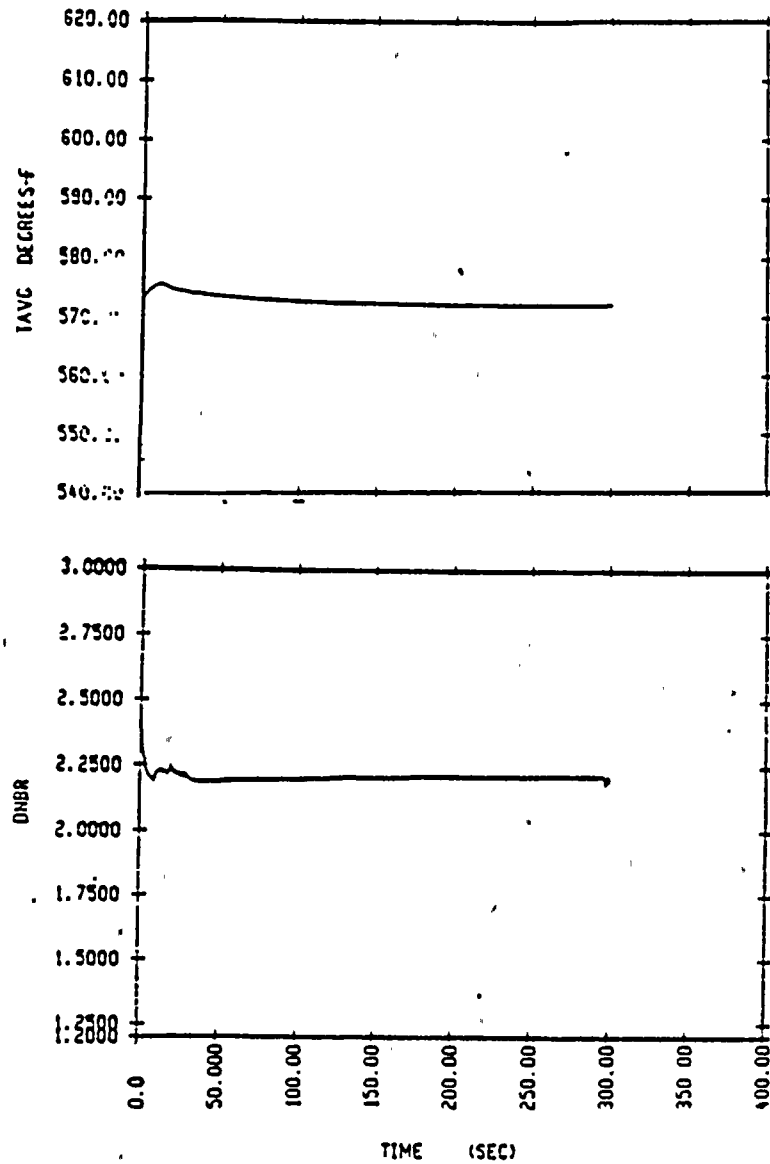




Figure 14.1.11-10

Ginna Excess Load Increase

Maximum Feedback with Automatic Rod Control

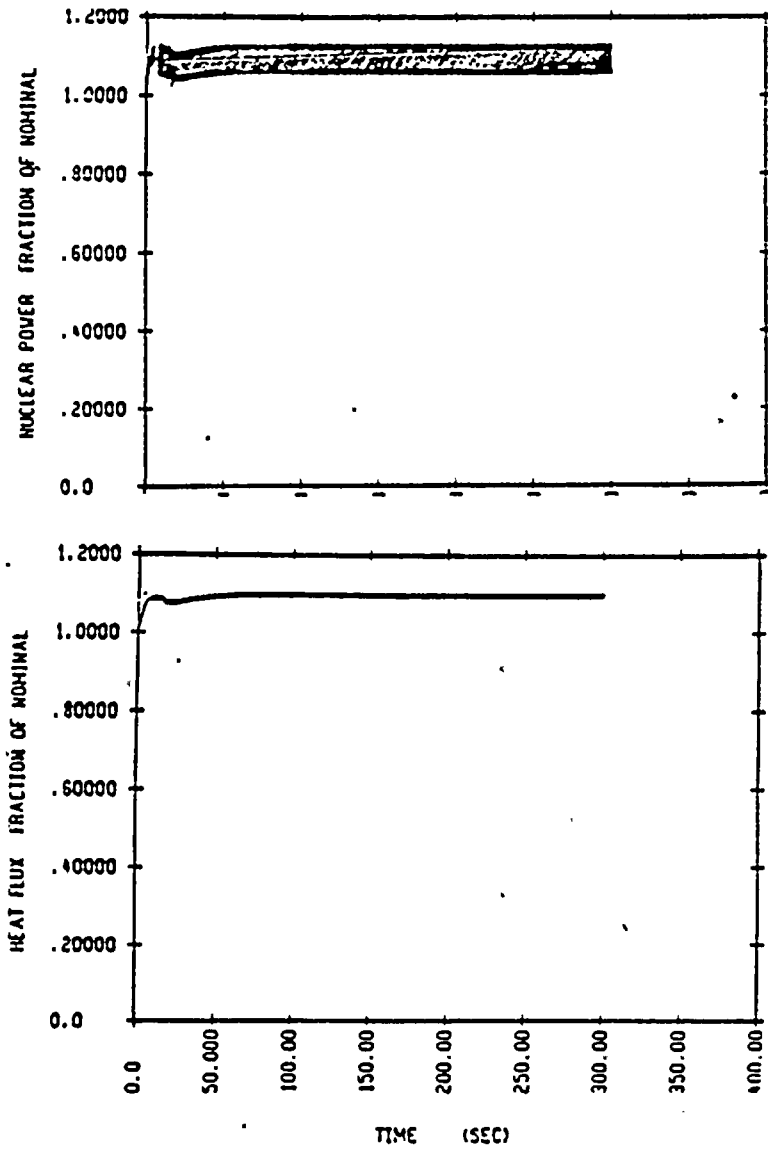


Figure 14.1.11-11

Ginna Excess Load Increase

Maximum Feedback with Automatic Rod Control

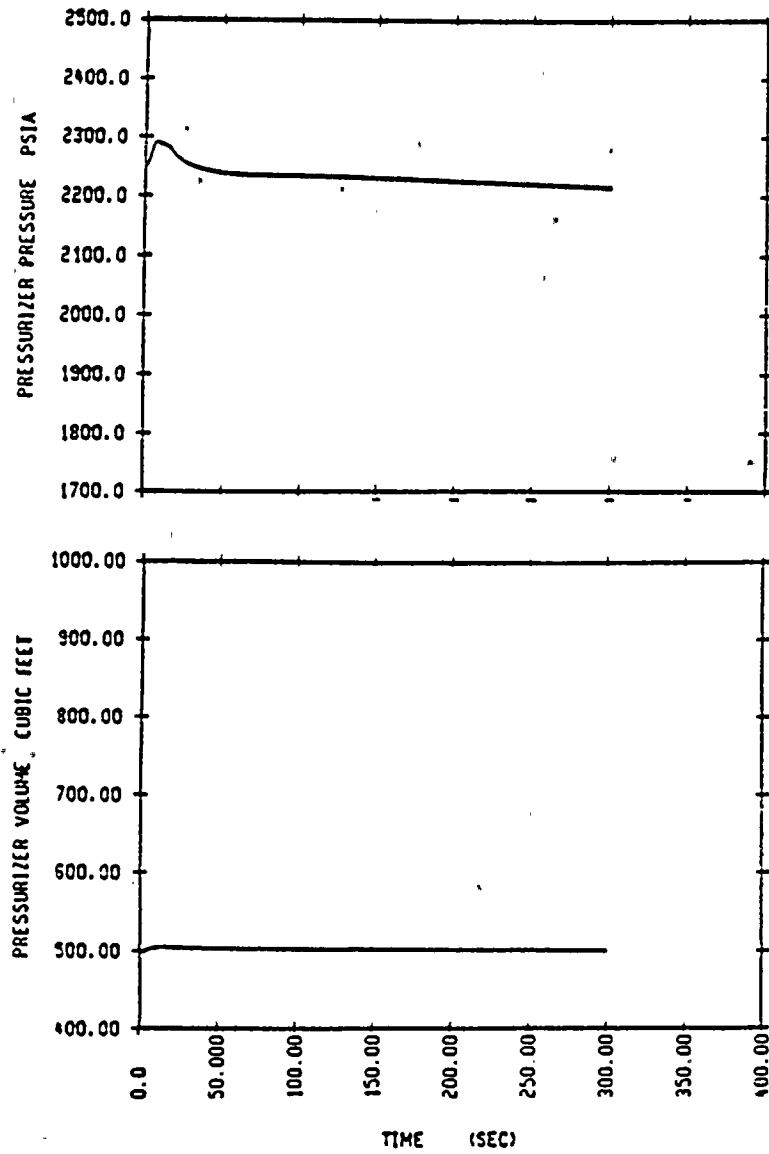
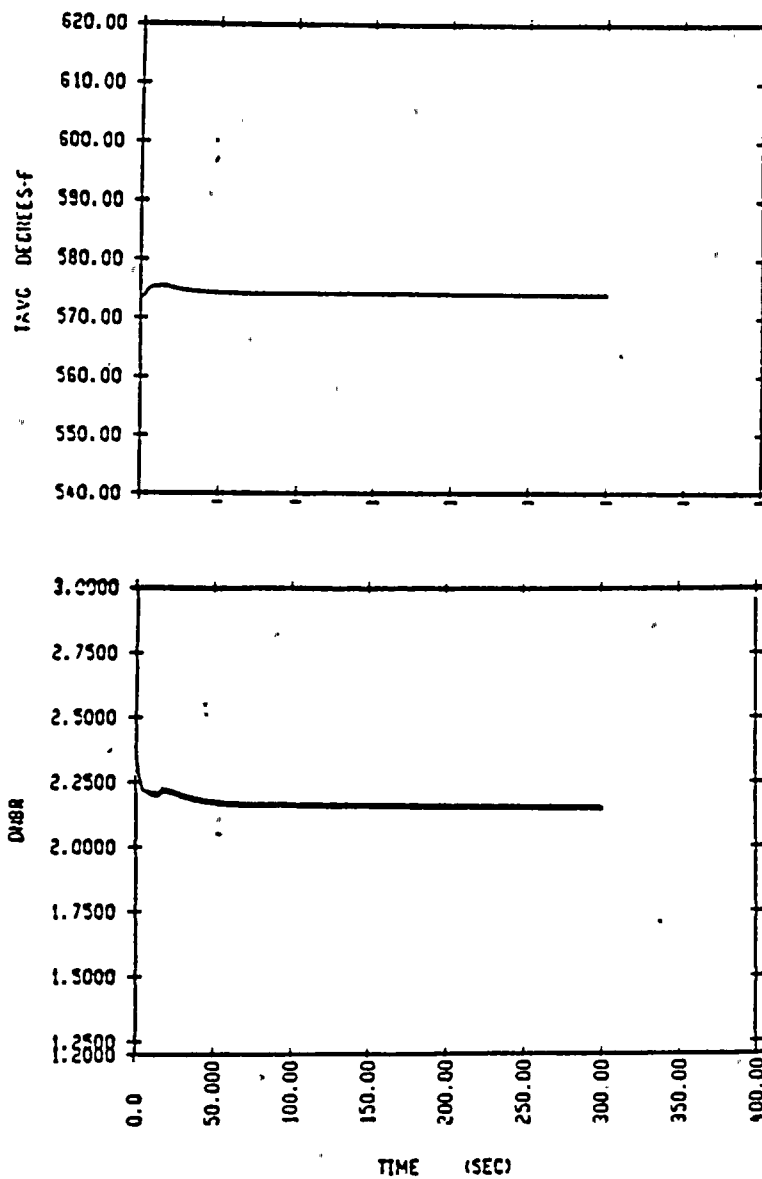


Figure 14.1.11-12

Ginna Excess Load Increase

Maximum Feedback with Automatic Rod Control



14.2.5 Rupture of a Steam Pipe

A rupture of a steam pipe is assumed to include any accident which results in an uncontrolled steam release from a steam generator. The release can occur due to a break in a pipe line or due to a valve malfunction. The steam release results in an initial increase in steam flow which decreases during the accident as the steam pressure falls. The energy removal from the Reactor Coolant System causes a reduction of coolant temperature and pressure. With a negative moderator temperature coefficient, the cooldown results in a reduction of core shutdown margin. If the most reactive control rod is assumed to be stuck in its fully withdrawn position, there is a possibility that the core will become critical and return to power even with the remaining control rods inserted. A return to power following a steam pipe rupture is a potential problem only because of the high hot channel factors which may exist when the most reactive rod is assumed stuck in its fully withdrawn position. Assuming the most pessimistic combination of circumstances which could lead to power generation following a steam line break, the core is ultimately shutdown by the boric acid in the Safety Injection System.

The analysis of a steam pipe rupture is performed to demonstrate that with a stuck rod and minimally engineered safety features, the core remains in place and essentially intact so as not to impair effective cooling of the core.

Although DNB and possible clad perforation (no clad melting or zirconium-water reaction) following a steam pipe rupture are not necessarily unacceptable, the following analysis, in fact, shows that no DNB occurs for any rupture, assuming that the most reactive rod is stuck in its fully withdrawn position.

The following systems provide the necessary protection against a steam pipe rupture:

1. Safety Injection System actuation on:
 - a. Two out of three pressurizer low pressure signals.
 - b. Two out of three low pressure signals in any steam line.
 - c. Two out of three high containment pressure signals.
2. The overpower trips (neutron flux and ΔT) and the reactor trip occurring upon actuation of the Safety Injection System.
3. Redundant isolation of the main feedwater lines. Sustained high feedwater flow would cause additional cooldown; thus, in addition to the normal control action which will close the main feedwater valves, any safety injection signal will rapidly close all feedwater control valves, trip the main feedwater pumps, and close the feedwater pump discharge valves.
4. Trip of the fast acting steam line isolation valves (designed to close in less than five seconds with no flow) on:
 - a. One out of the two steam flow signals in that steam line in coincidence with any safety injection signal. (Dual setpoints are provided, with the lower setpoint used in coincidence with two out of four indications of low reactor coolant average temperature.)

- b. Two out of three high containment pressure signals.

Each steam line has a fast closing isolation valve and a check valve. These four valves prevent blowdown of more than one steam generator for any break location even if one valve fails to close. For example, for a break upstream of the isolation valve in one line, closure of either the check valve in that line or the isolation valve in the other line will prevent blowdown of the other steam generator.

Steam flow is measured by monitoring dynamic head in nozzles inside the steam pipes. The nozzles (16-in. ID versus a pipe diameter of 28-in. ID) are located inside the containment near the steam generator and also serve to limit the maximum steam flow for any break further downstream. In particular, the nozzles limit the flow for all breaks outside the containment.

Method of Analysis

The analysis of the steam pipe rupture has been performed to determine:

1. The core heat flux and reactor coolant system temperature and pressure resulting from the cooldown following the steam line break. The LOFTRAN code has been used.
2. The thermal and hydraulic behavior of the core following a steam line break. A detailed thermal and hydraulic digital-computer code, THINC has been used to determine if DNB occurs for the core conditions computed in (1) above.

The following assumptions were made:

1. A 0.018 shutdown reactivity from the rods at no load conditions with 2 loops in operation. This is the end-of-life design value including design margins with the most reactive rod stuck in its fully withdrawn position. Operation of rod cluster control assembly banks during core burnup is restricted in such a way that addition of positive reactivity in a secondary system steam release accident will not lead to a more adverse condition than the case analyzed. A 0.0245 shutdown reactivity is assumed for cases where one loop is in service.
2. The negative moderator temperature coefficient corresponding to the end of life core with all but the most reactive rod inserted. The variation of the coefficient with temperature and pressure has been included. The k versus temperature at 1000 psia corresponding to the negative moderator temperature coefficient used is shown in Figure 14.2.5-1. In computing the power generation following a steam line break, the local reactivity feedback from the high neutron flux in the region of the core near the stuck control rod has been included in the overall reactive balance. The local reactivity feedback is composed of Doppler reactivity from the high fuel temperatures near the stuck control rod and moderator feedback from the high water enthalpy near the stuck rod. For the cases analyzed where steam generation occurs in the high flux regions of the core, the effect of void formation on the reactivity has been included. The effect of power generation in the core on overall reactivity is presented in Figure 14.2.5-2. The curve assumes end of life core conditions with all rods in except the most reactive rod which is assumed stuck in its fully withdrawn position.
3. Minimum safety injection capability corresponding to two out of three safety injection pumps in operation. Two thousand (2000) ppm boron is assumed in the safety injection system. The time delays required to sweep the low concentration boric acid from the safety

injection piping prior to the delivery of the boron have been included in the analysis. Twenty thousand (20,000) ppm boron is assumed in the cases with one loop in service.

4. Power peaking factors corresponding to one stuck RCCA and nonuniform core inlet coolant temperatures are determined at end of core life. The coldest core inlet temperatures are assumed to occur in the sector with the stuck rod. The power peaking factors account for the effect of the local void in the region of the stuck control rod assembly during return to power phase following the steamline break. This void in conjunction with the large negative moderator coefficient partially offsets the effect of the stuck assembly. The power peaking factors depend upon the core power, temperature, pressure, and flow, and, thus, are different for each case studied.
5. Three combinations of break sizes and initial plant conditions have been considered in determining the core power and reactor coolant system transient.
 - a. Complete severance of a pipe inside the containment at the outlet of the steam generator at initial no-load conditions with outside power available and two loops in service. The equivalent break area is 4.6 ft².
 - b. Case (a) above with loss of outside power simultaneous with the steam break.
 - c. A break equivalent to steam release through one steam generator safety valve with outside power available and two loops in service.
 - d. Case (a) above with only one loop in service.
 - e. Case (c) above with only one loop in service.

The severance of a pipe downstream of the steam flow measuring nozzle is not analyzed. The equivalent break area (1.4 ft^2) is less than that of case (a) and would result in a less severe cooldown. Thus, this break is bounded by cases (a) and (b).

The cases above assume initial hot shutdown conditions with the rods inserted (except for one stuck rod) at time zero. Should the reactor be just critical or operating at power at the time of a steam line break the reactor will be tripped by the normal overpower protection system when the power level reaches a trip point.

Following a trip at power the reactor coolant system contains more stored energy than at no-load, the average coolant temperature is higher than at no-load and there is appreciable energy stored in the fuel. Thus, the additional stored energy is removed via the cooldown caused by the steam line break before the no load conditions of reactor coolant system temperature and shutdown margin assumed in the analyses are reached. After the additional stored energy has been removed, the cooldown and reactivity insertions proceed in the same manner as in the analyses which assume no-load conditions at time zero.

Results

The results presented are a conservative indication of the events which would occur assuming a steam line rupture. The worst case assumes that all of the following occur simultaneously.

1. Minimum shutdown reactivity margin equal to 1.80% (2 loops in service). Minimum shutdown reactivity margin equal to 2.45% (1 loop in service).
2. The most negative moderator temperature coefficient for the rodged core at end of life.
3. The rod having the most reactivity stuck in its fully withdrawn position.



4. One safety injection pump fails to function as designed.

Core Power and Reactor Coolant System Transient

Figures 14.2.5-3 through 14.2.5-7 show the reactor coolant system transient and core heat flux following a steam pipe rupture (complete severance of a pipe) at the exit of a steam generator at initial no-load conditions with two loops in operation. The break assumed is the largest break which can occur anywhere either upstream or downstream of the isolation valves. Offsite power is assumed available such that full reactor coolant flow exists. The transient shown assumes the rods inserted at time 0 (with one rod stuck in its fully withdrawn position) and steam release from both steam generators. Should the core be critical at near zero power when the rupture occurs, the initiation of safety injection by low steam line pressure will trip the reactor. Steam release from at least one steam generator will be prevented by either the check valve or by automatic trip of the fast acting isolation valve in the steam line by the high steam flow signal in coincidence with the safety injection signal. Even with the failure of one valve, release is limited to no more than seven seconds for one steam generator while the second generator blows down. (The steam line isolation valves are designed to be fully closed in less than five seconds with no flow through them. With the high flow existing during a steam line rupture, the valves will close considerably faster.)

The core becomes critical with the rods inserted (with the design shutdown assuming one stuck rod) at 14.5 seconds. Boron solution at 2,000 ppm enters the reactor coolant system from the safety injection system (initiated automatically by the low steam line pressure) at 41.0 seconds which includes the delay required to clear the safety injection system lines of low concentration boric acid. No credit has been taken for the 2,000 ppm boron which enters the reactor coolant system prior the 2,000 ppm boric acid. The peak core heat flux is 31% of 1520 Mwt.



Figures 14.2.5-8 through 14.2.5-12 show the responses for case a assuming a loss of outside power at time 0 which then results in a reactor coolant system flow coastdown. The safety injection system delay time includes the time required to start a safety injection pump on the diesel. Only one diesel is assumed to start. Credit is taken for only the safety injection flow entering the cold-leg lines, since the flow to the hot leg flow paths are valved shut. The peak power is 20% of nominal.

Figures 14.2.5-13 through 14.2.5-17 show the responses for a failed steam generator safety valve with two loops in operation. Criticality occurs at 220 seconds. Boron enters the core due to a low pressurizer pressure safety injection signal at 200 seconds.

Figures 14.2.5-18 through 14.2.5-22 show the transient for a double ended rupture assuming one loop in service. The loop having the affected steam generator is assumed to be in operation. The sequence of events is similar to the case with both loops in operation. The core becomes critical at 22.0 seconds. Boron solution at 20,000 ppm enters the core at 37.0 seconds. The peak core heat flux is 27% of 1520 MWth.

The transient for a failed safety valve with one loop in service is presented in Figures 14.2.5-23 through 14.2.5-26. Boron solution at 20,000 ppm enters the core at 160 seconds. Criticality does not occur.

The sequence of events for each case is presented in Table 14.2.5-1.

Conclusion

A DNB analysis was performed for each case. It was found that all cases have a minimum DNBR greater than the limit value.

The analysis has shown that the criteria stated in Section 14.2.5 are satisfied. Although DNB and possible cladding perforation following a steam pipe rupture are not necessarily unacceptable and not precluded by the criteria, the above analysis, in fact, shows that the DNB design basis is met as stated in Section 4.

TABLE 14.2.5-1

TIME SEQUENCE OF EVENTS FOR STEAMLINE RUPTURE

| <u>Case</u> | <u>Event</u> | <u>Time of Event (Seconds)</u> |
|-------------|---|------------------------------------|
| a. | Steamline ruptures | 0 |
| | Pressurizer empties | 8.5 |
| | Criticality attained | 14.5 |
| | Boron enters core | 41.0 |
| b. | Steamline rupture; offsite power lost | 0 |
| | Pressurizer empties | 9.5 |
| | Criticality attained | 19.0 |
| | Boron enters core | 53.0 |
| c. | Safety valve fails open | 0 |
| | Pressurizer empties | 97 |
| | Low pressurizer pressure SI setpoint reached | 100 |
| | Boron enters core | 200 |
| | Criticality occurs | 220 |

TABLE 14.2.5-1 (Continued)

TIME SEQUENCE OF EVENTS FOR STEAMLINE RUPTURE

| <u>Case</u> | <u>Event</u> | <u>Time of Event (Seconds)</u> |
|-------------|---|------------------------------------|
| d. | Steamline ruptures | 0 |
| | Pressurizer empties | 9.0 |
| | Criticality attained | 22.0 |
| | Boron enters core | 37.0 |
| e. | Safety valve fails open | 0.0 |
| | Pressurizer empties | 93.0 |
| | Low pressurizer pressure SI setpoint reached | 99.0 |
| | Boron enters core | 160 |

FIGURE 14.2.5-1
GINNA STEAMLINER RUPTURE

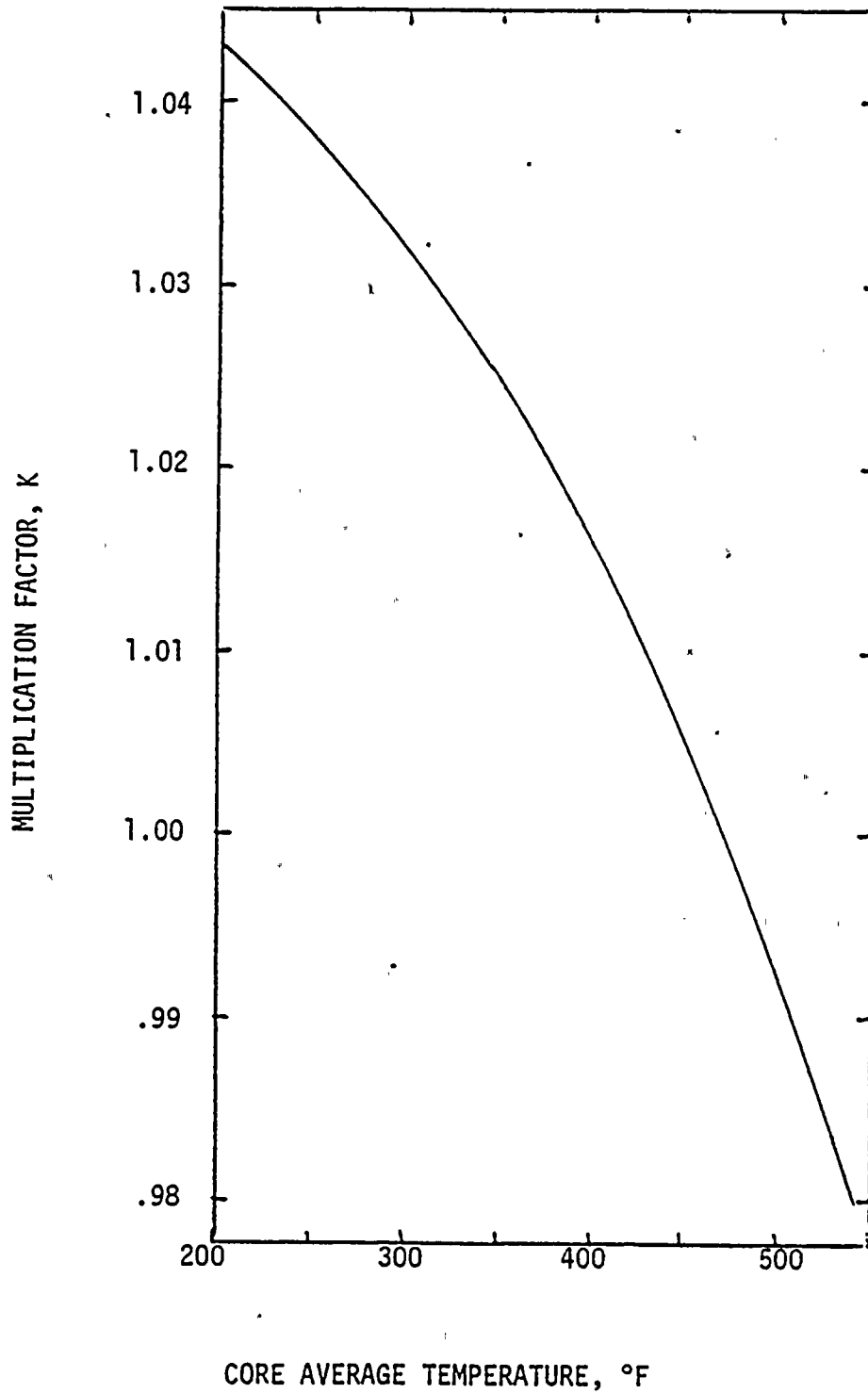


Figure 14.2.5-2
GINNA STEAMLINER RUPTURE

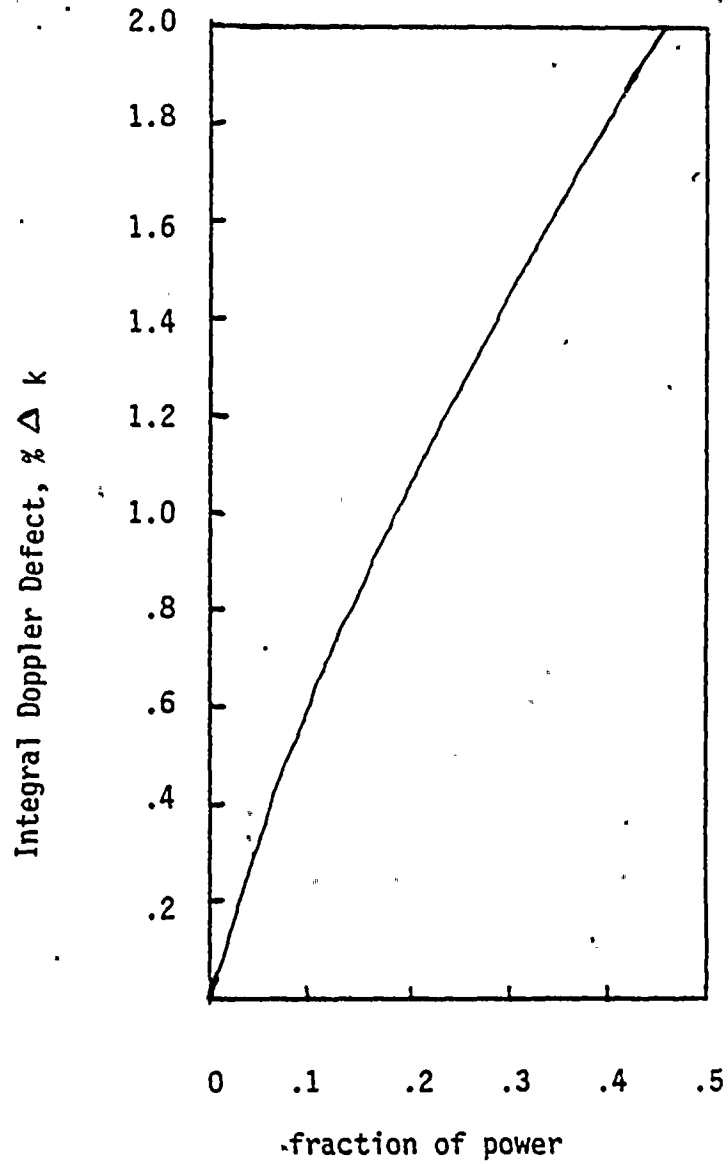


FIGURE 14.2.5-3

GINNA STEAMLINER RUPTURE
4.6 ft² Break with Power 2 Loops in Service

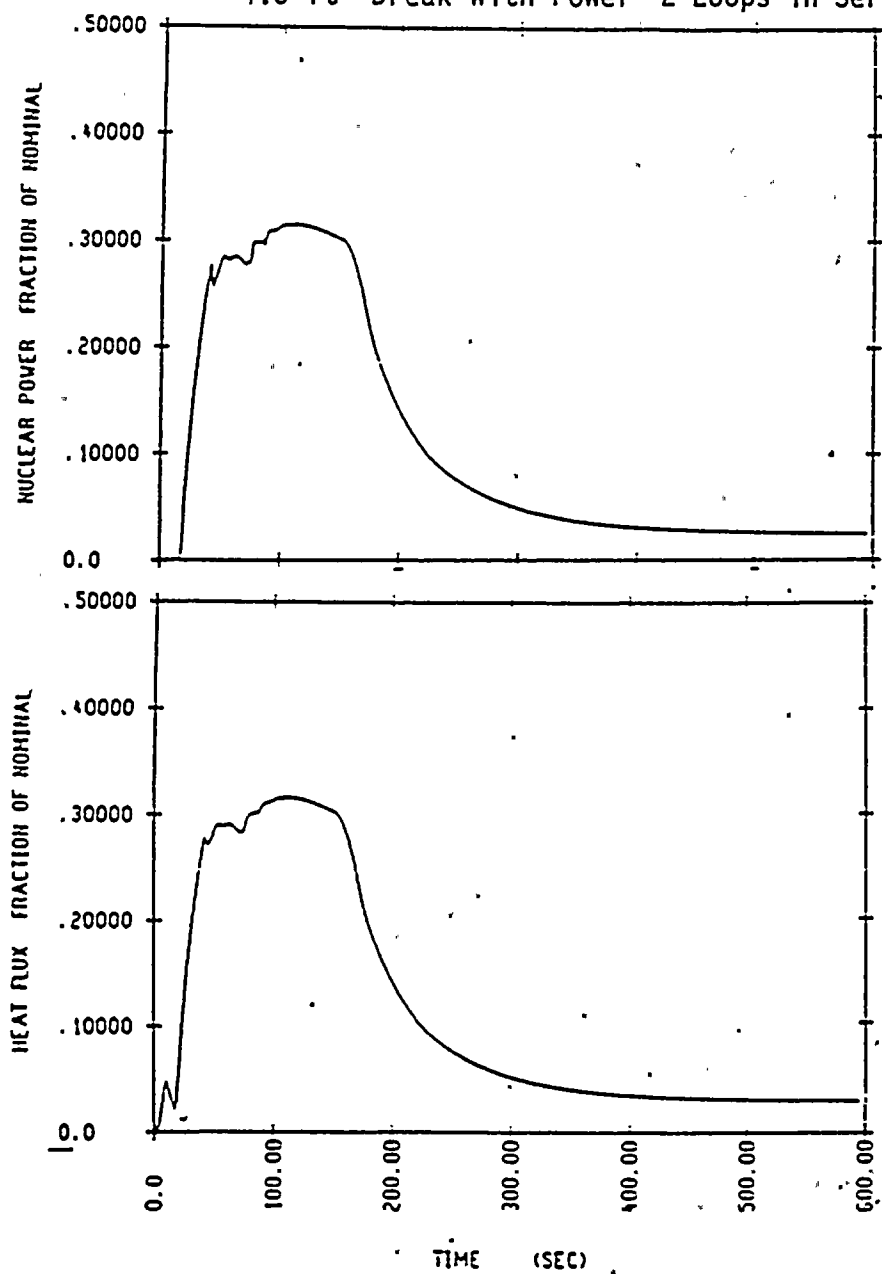


FIGURE 14.2.5-4

GINNA STEAMLINER RUPTURE
4.6 ft² Break with Power
2 Loops in Service

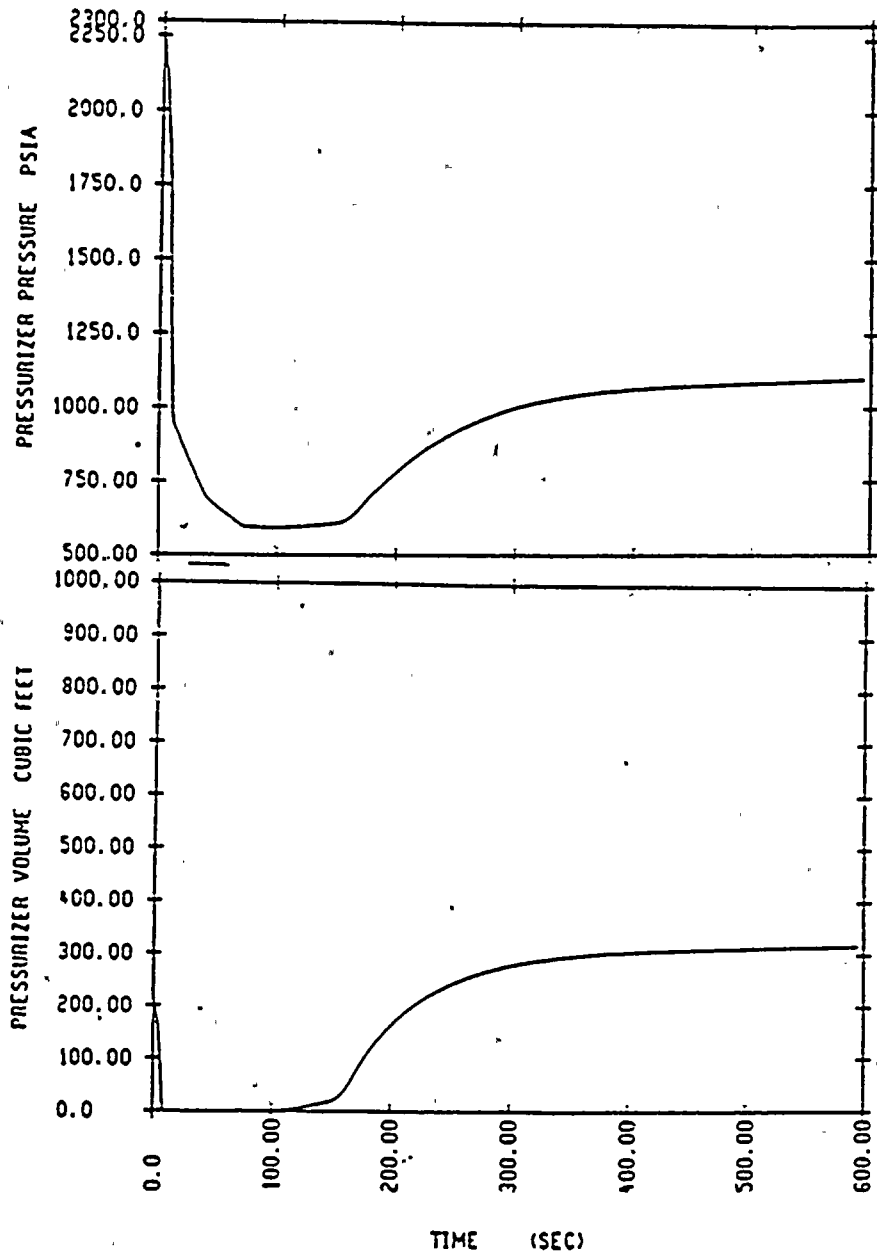


FIGURE 14.2.5-5

GINNA STEAMLINE RUPTURE
4.6 ft² Break with Power

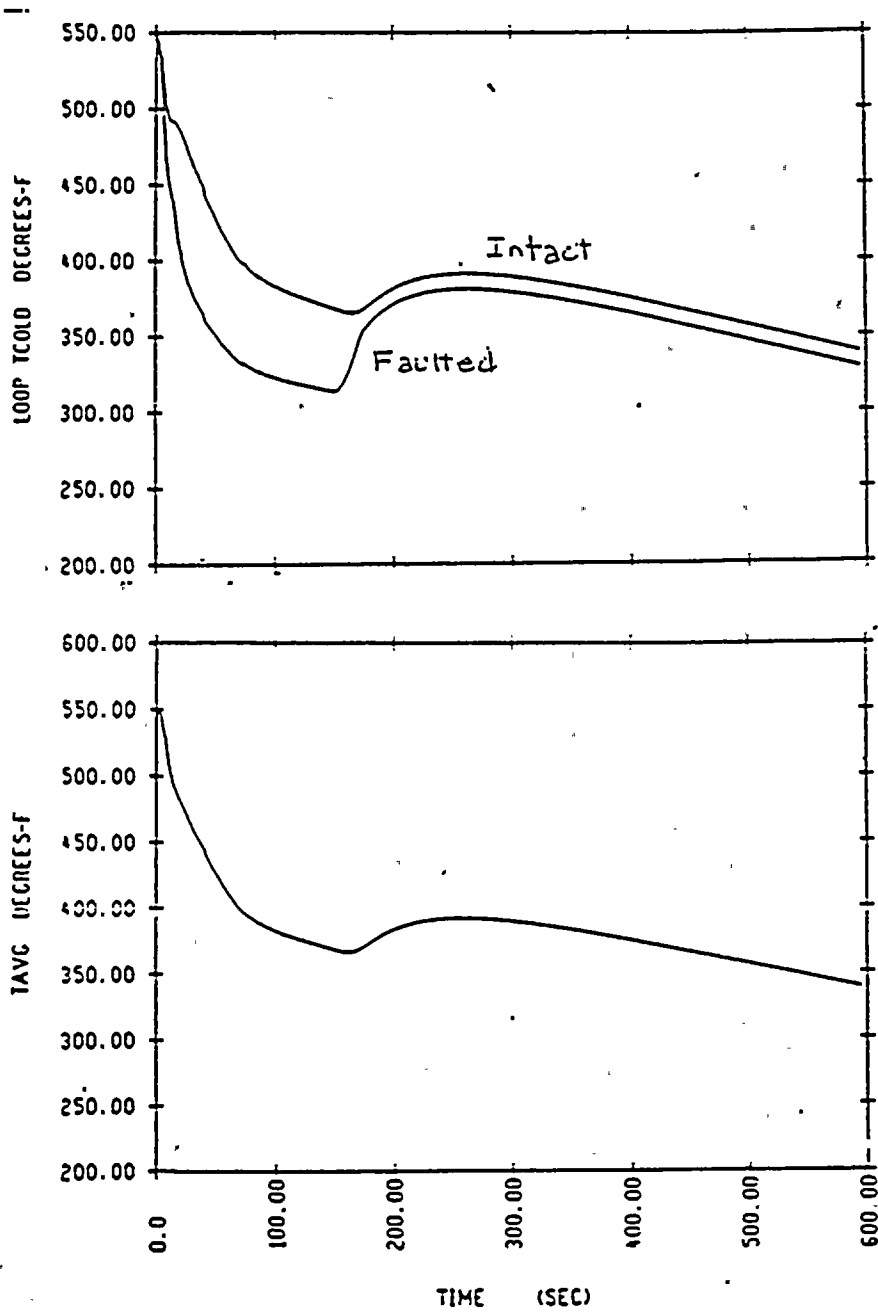


FIGURE 14.2.5-6

GINNA STEAMLINE RUPTURE
4.6 ft² Break with Power

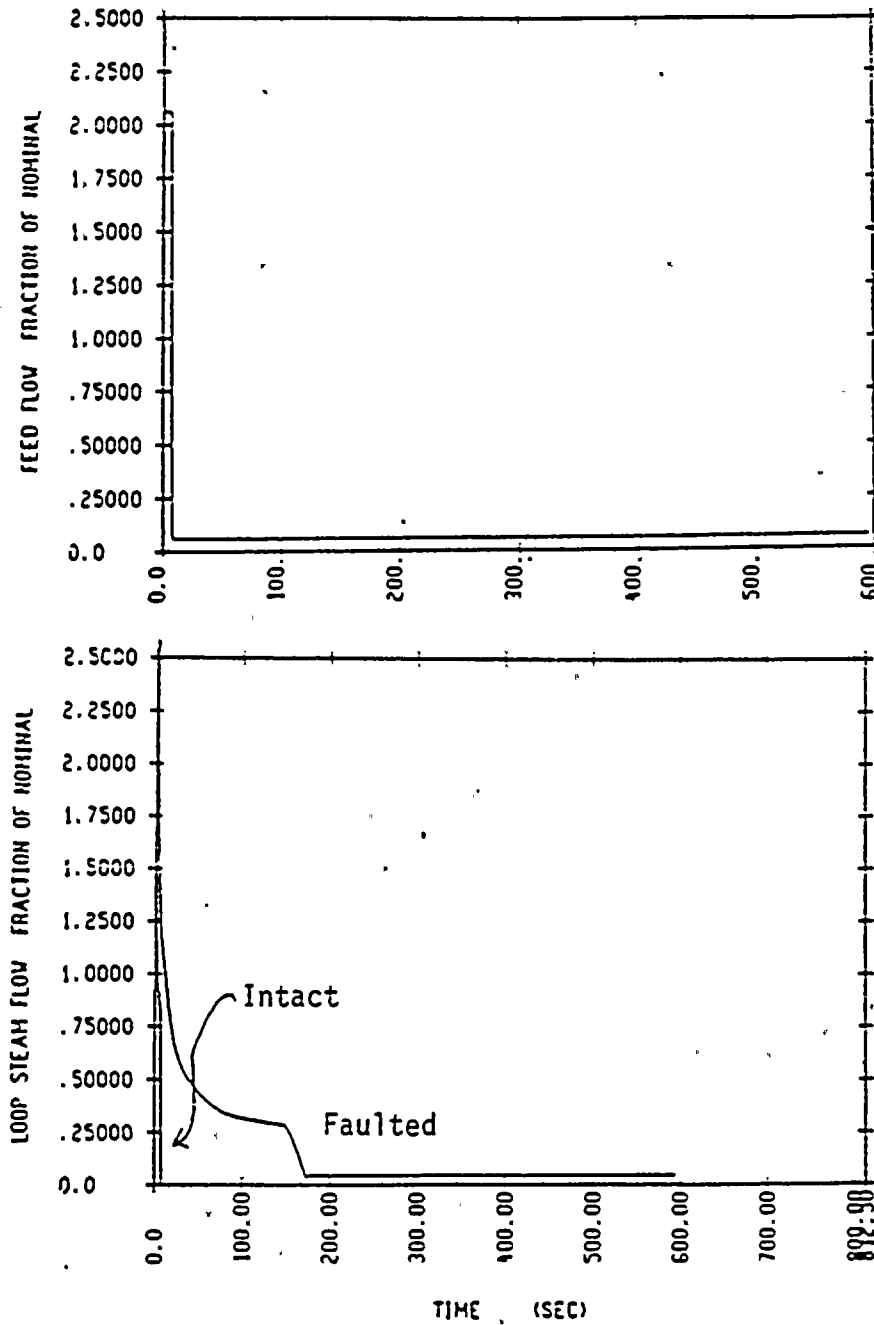


FIGURE 14.2.5-7

GINNA STEAMLINE RUPTURE
4.6 ft² Break with Power

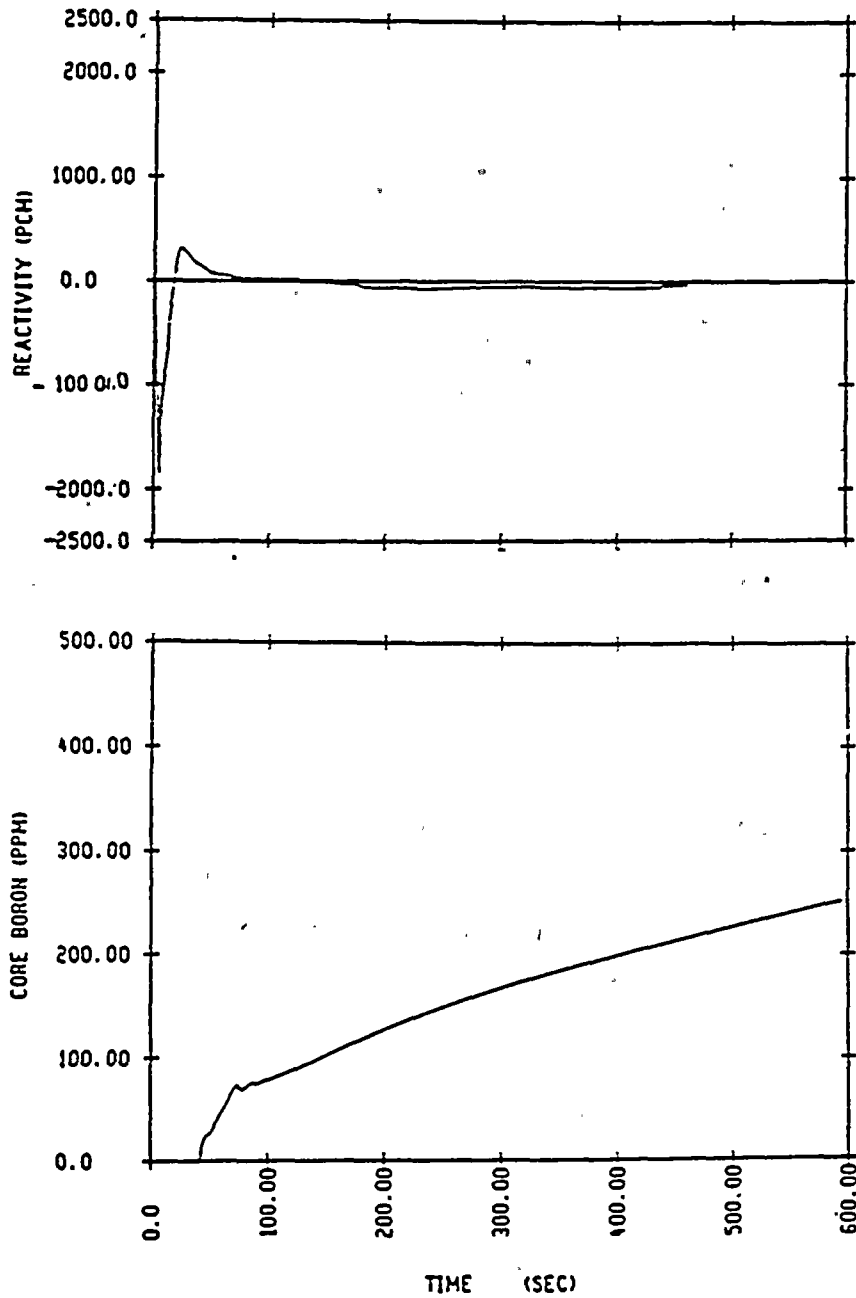


FIGURE 14.2.5-8

GINNA STEAMLINE RUPTURE

4.6 ft² Break w/o Power - 2 Loops in Service

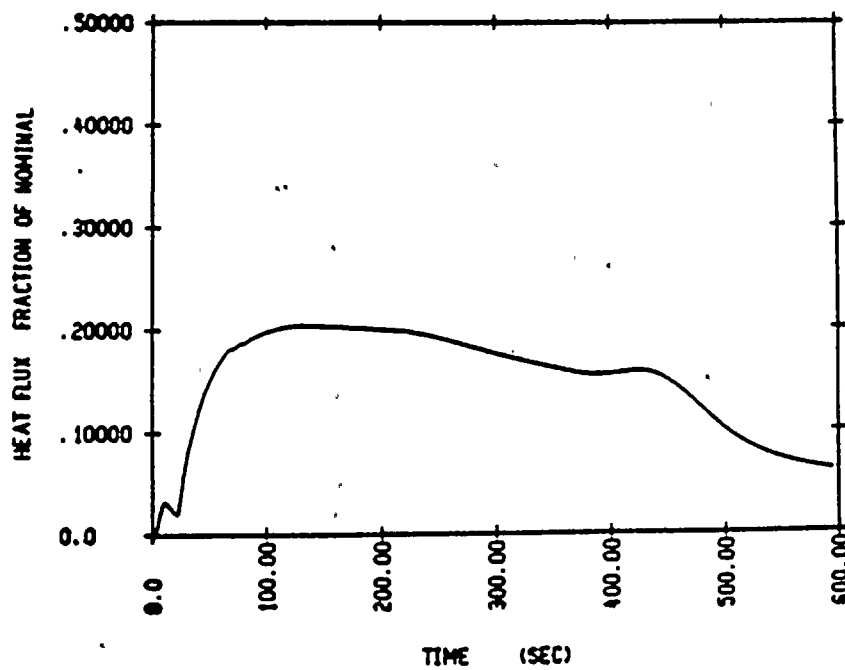
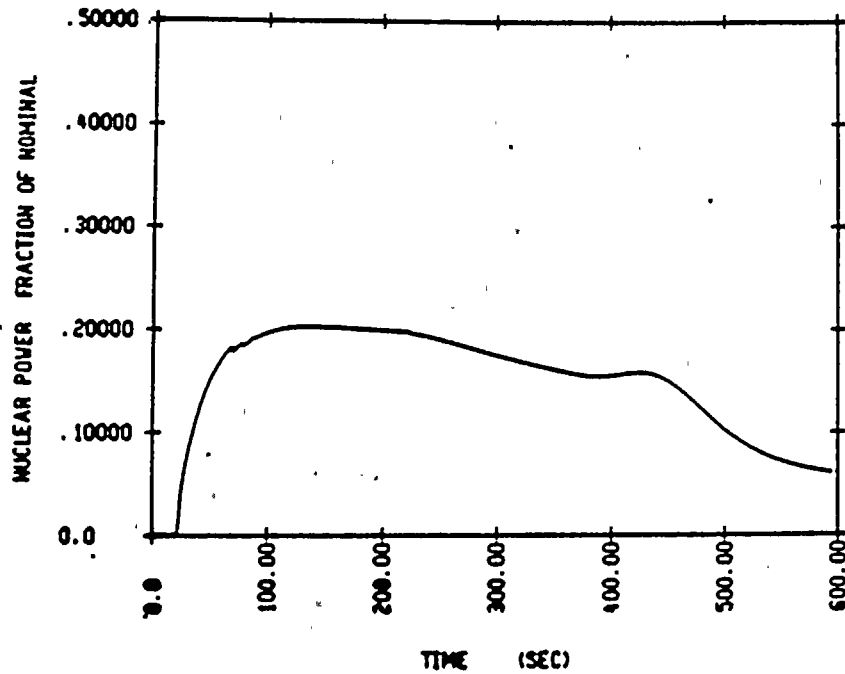


FIGURE 14.2.5-9

GINNA STEAMLINER RUPTURE

4.6 ft² w/o Power - 2 Loops in Service

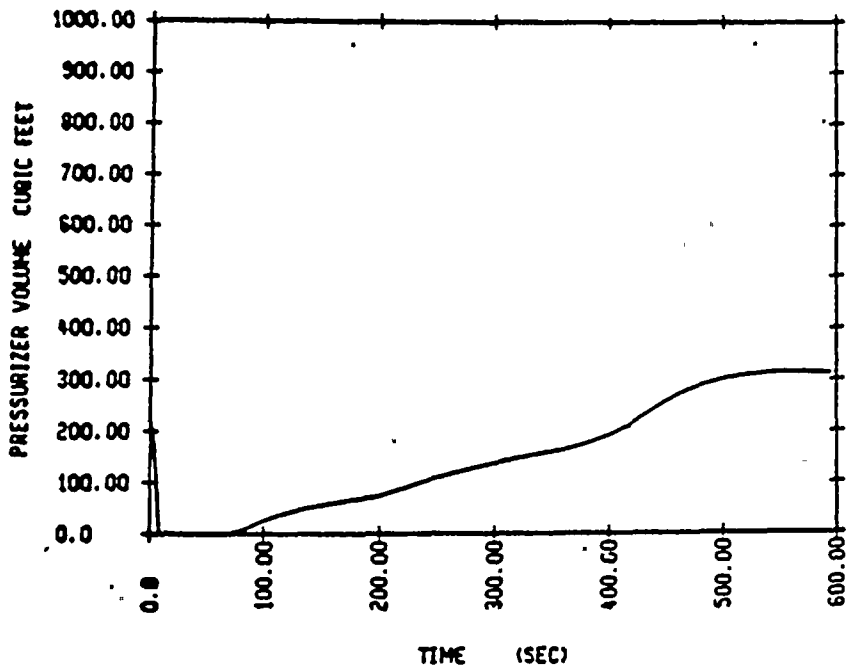
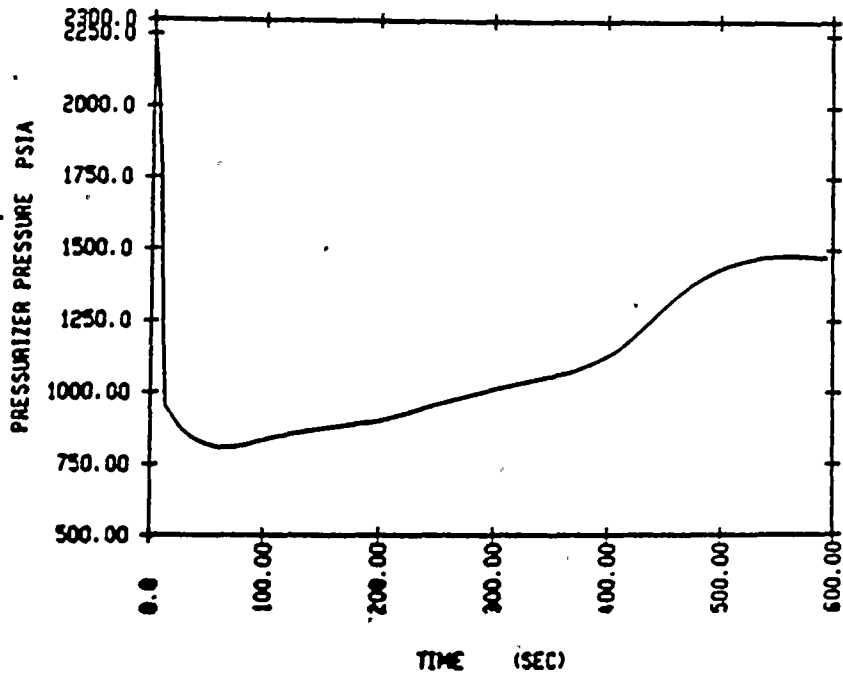


FIGURE 14.2.5-10

GINNA STEAMLINE RUPTURE

4.6 ft² w/o Power - 2 Loops in Service

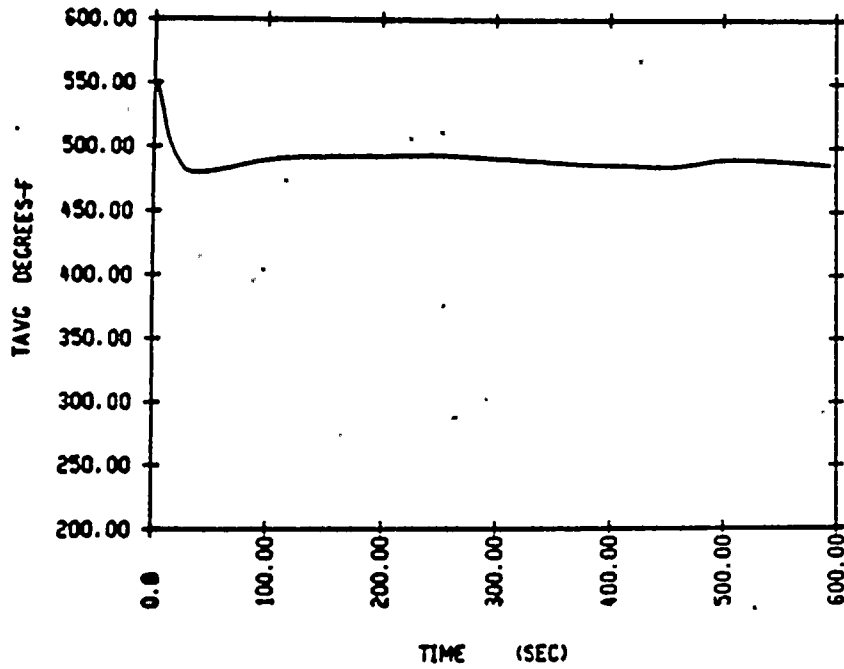
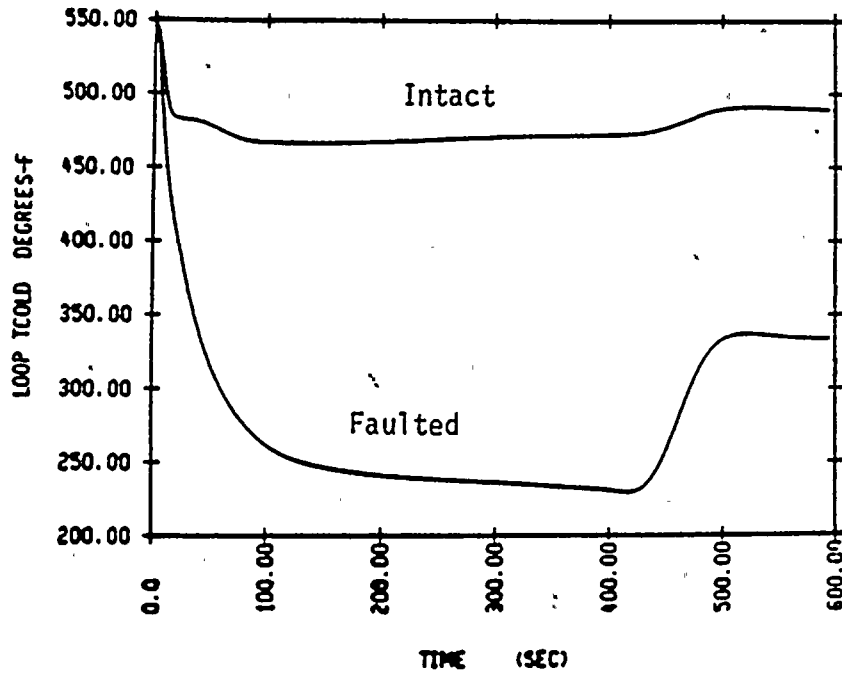


FIGURE 14.5.2-11

GINNA STEAMLINE RUPTURE

4.6 ft² w/o Power - 2 Loops in Service

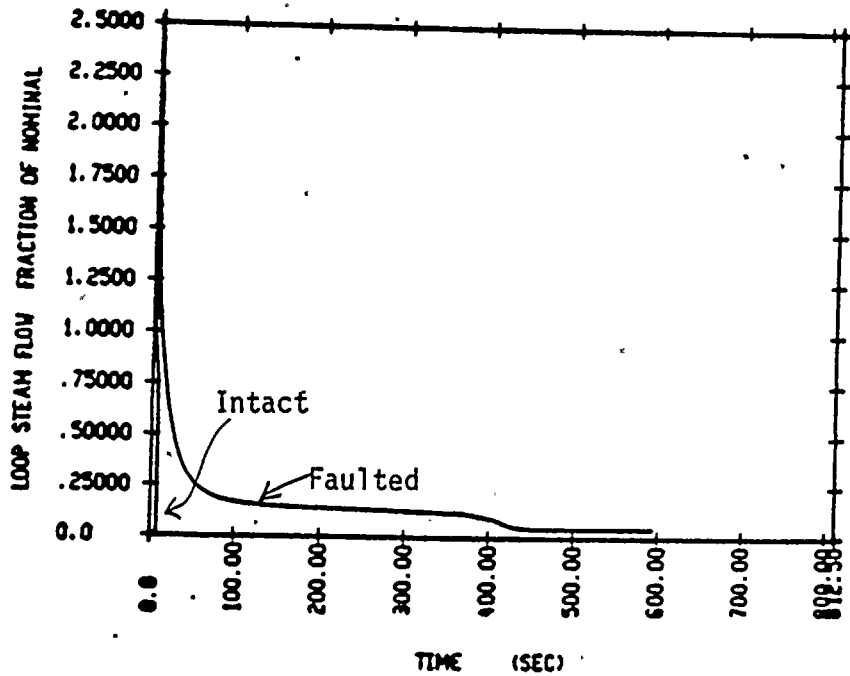
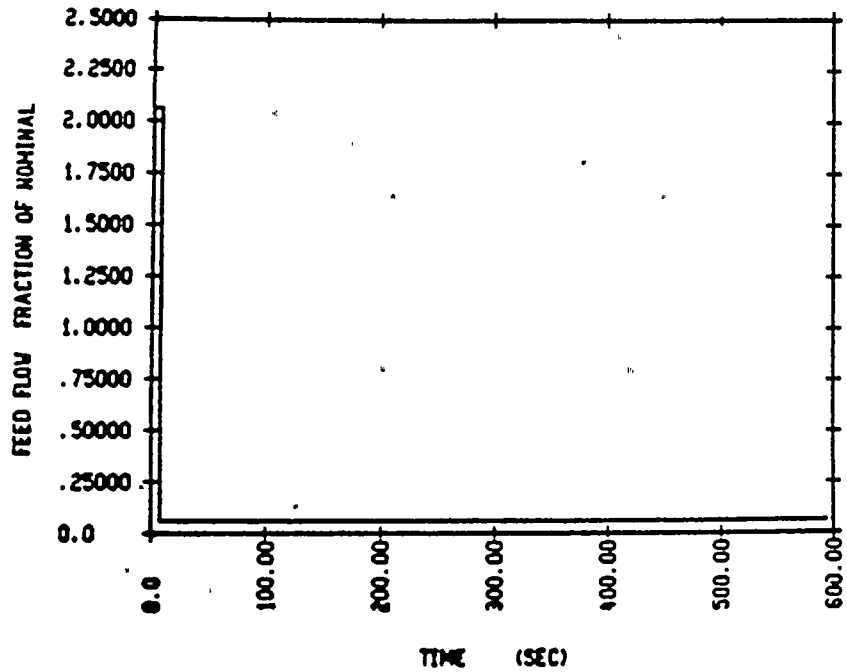


FIGURE 14.2.5-12

GINNA STEAMLINE RUPTURE
4.6 ft² Break w/out Power

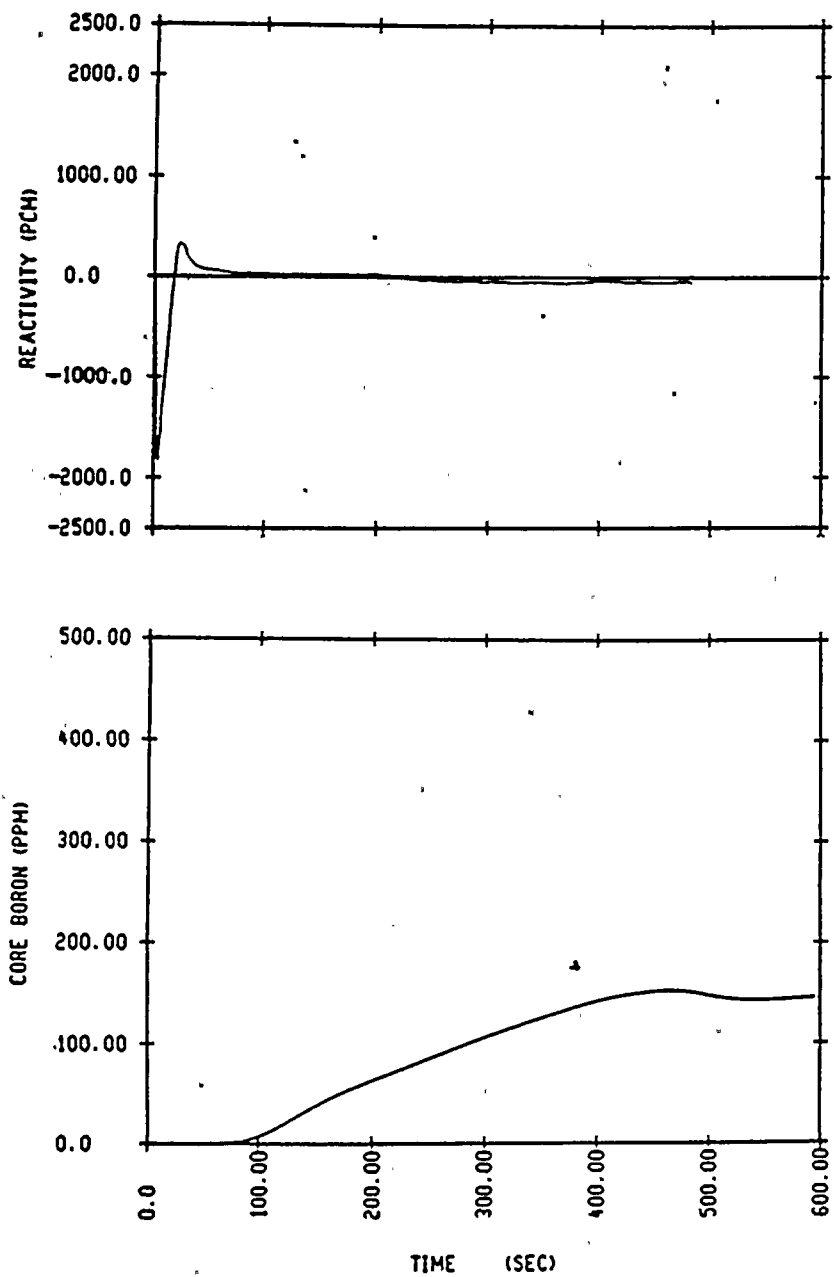


FIGURE 14.2.5-13

GINNA STEAMLINE RUPTURE -
FAILED SAFETY VALVE

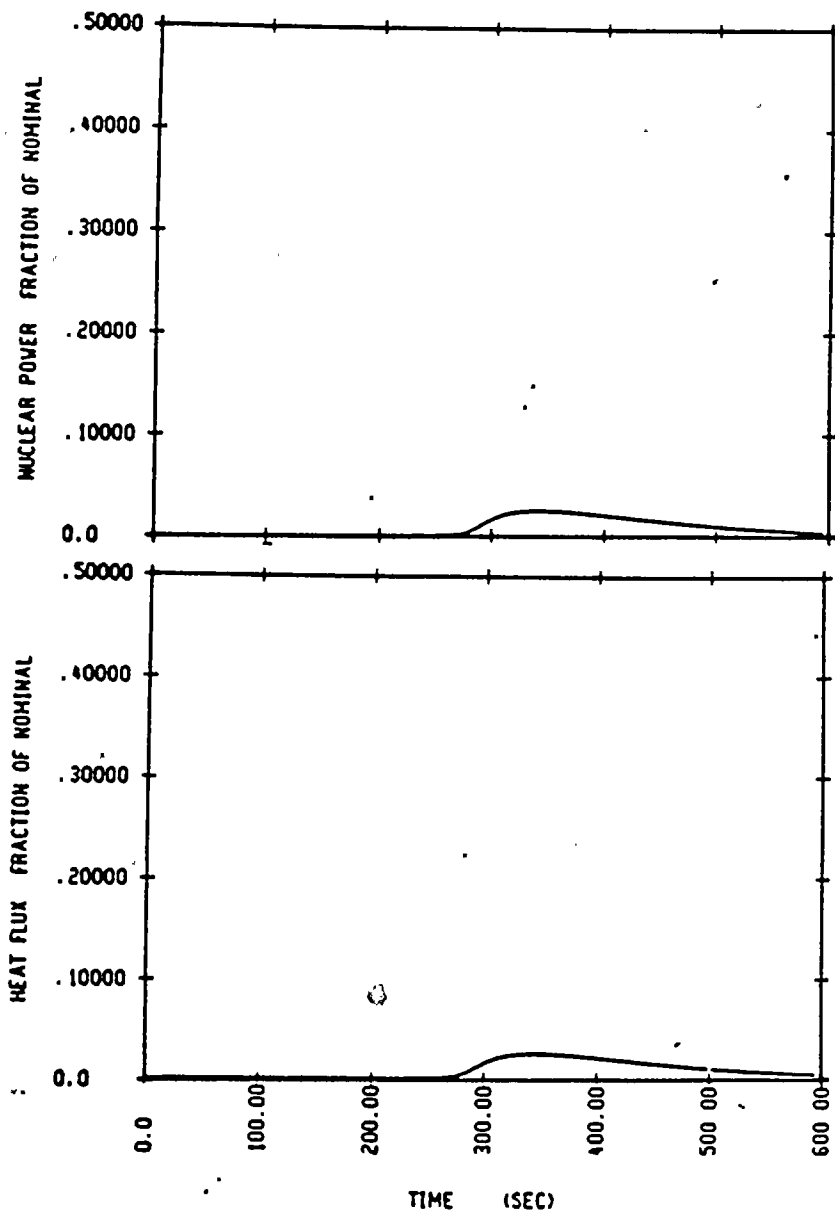


FIGURE 14.2.5-14

GINNA STEAMLINE RUPTURE -
FAILED SAFETY VALVE
2 Loops in Service

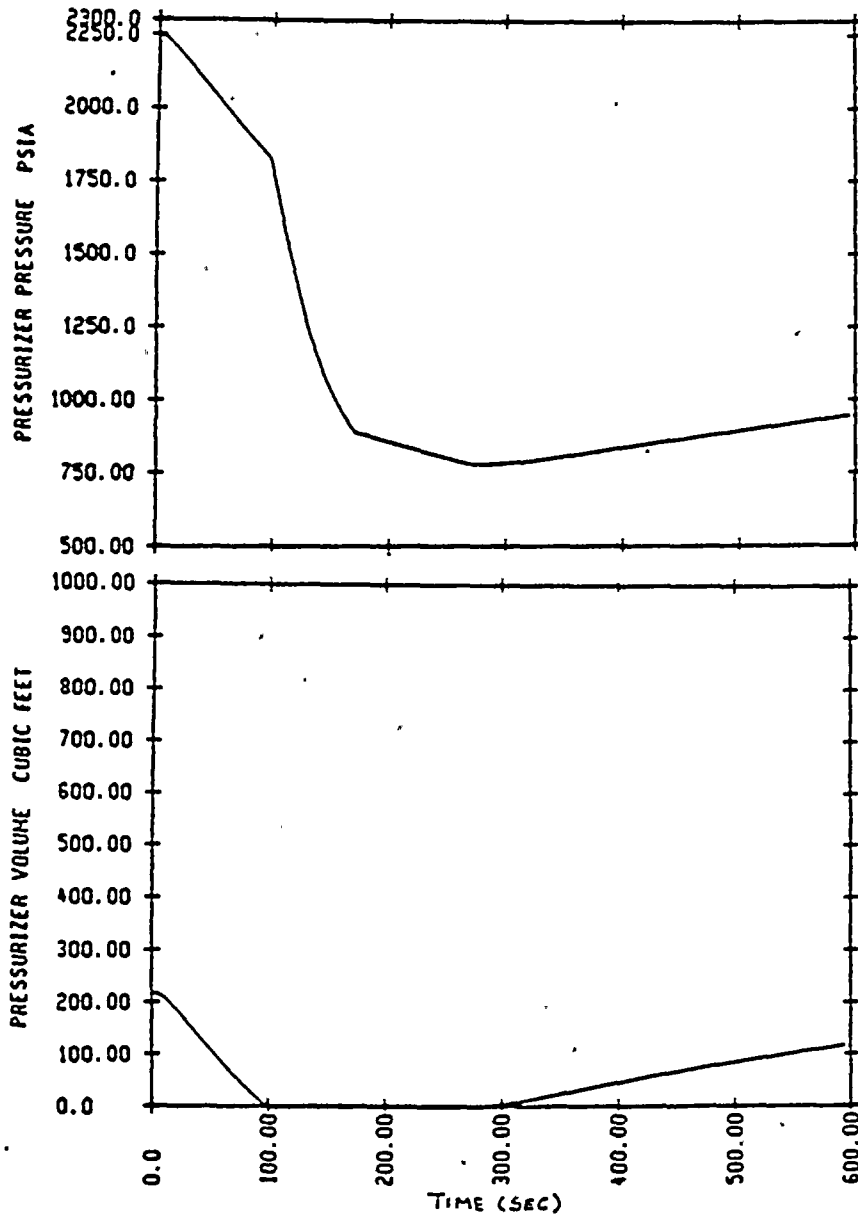


FIGURE 14.2.5-15

GINNA STEAMLINER RUPTURE -
FAILED SAFETY VALVE
2 Loops in Service

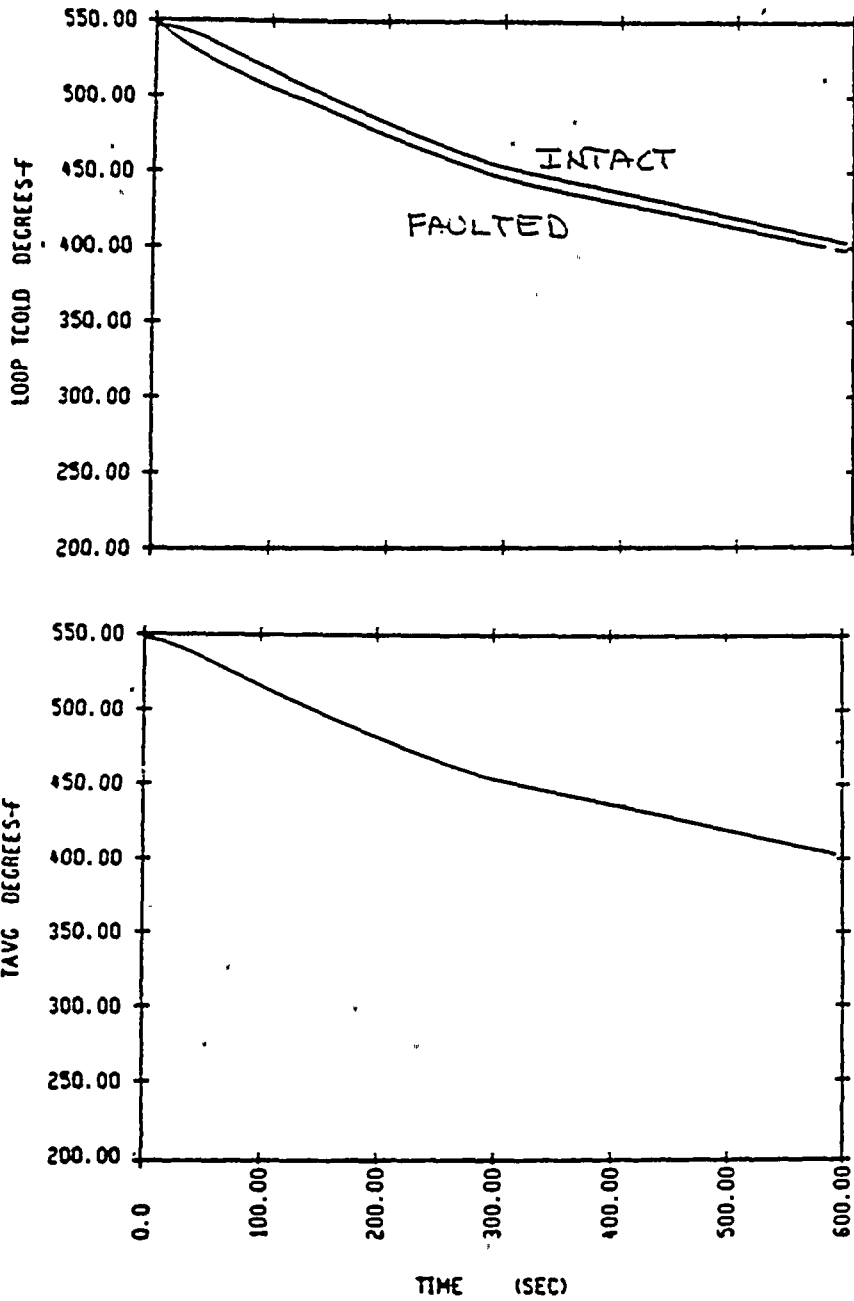


FIGURE 14.2.5-16

GINNA STEAMLINER RUPTURE -
FAILED SAFETY VALVE

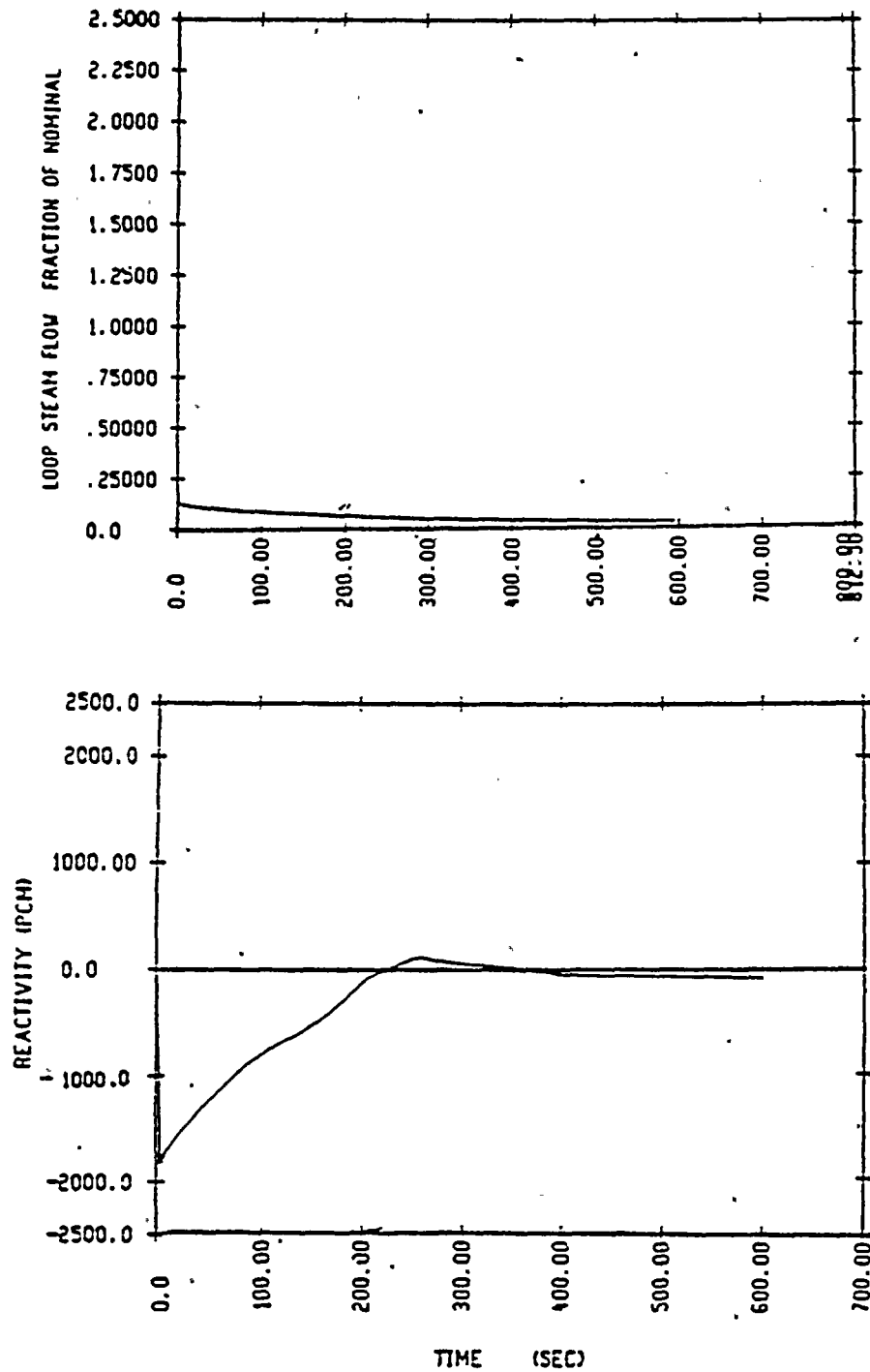


FIGURE 14.2.5- T7

GINNA STEAMLINE RUPTURE -
FAILED SAFETY VALVE

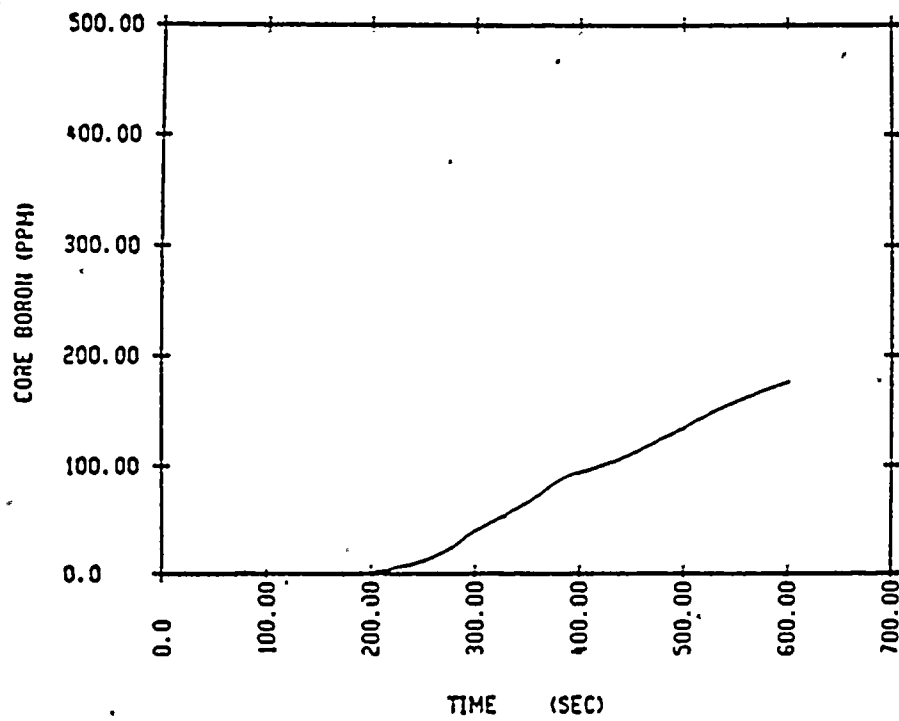


Figure 14.2.5 - 18
Ginna Steamline Rupture
4.6 ft² Break with Power - One Loop in Service

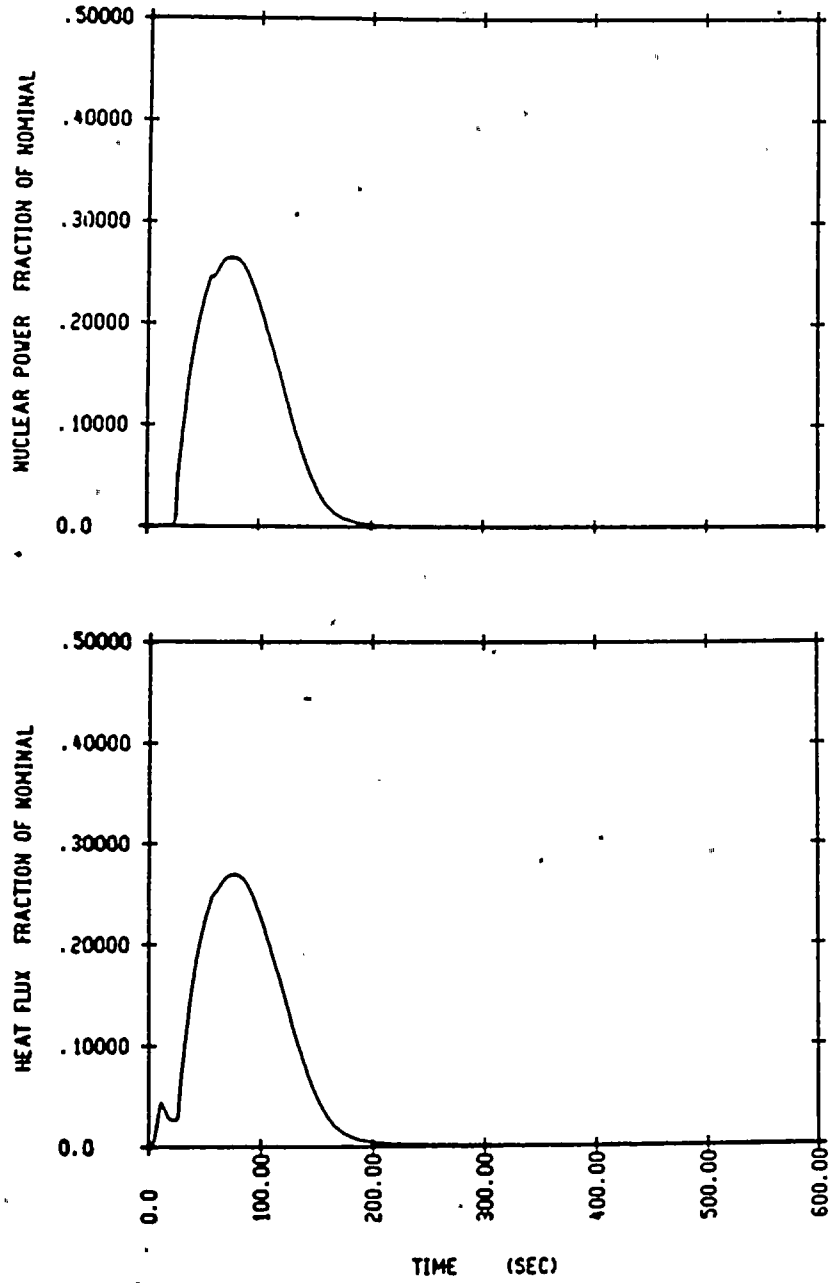




Figure 14.2.5 - 19
Ginna Steamline Rupture
4.6 ft² Break with Power - One Loop in Service

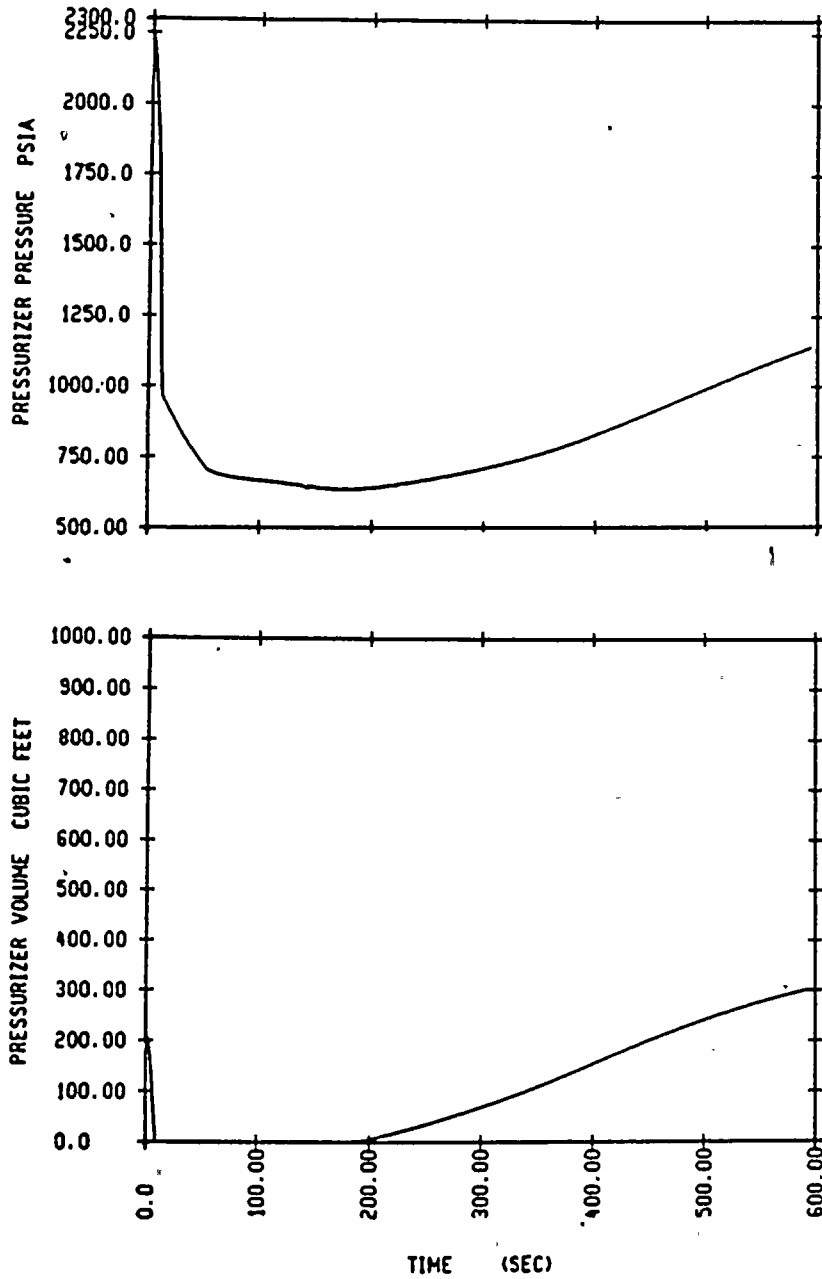


Figure 14.2.5 - 20
Ginna Steamline Rupture
4.6 ft² Break with Power - One Loop in Service

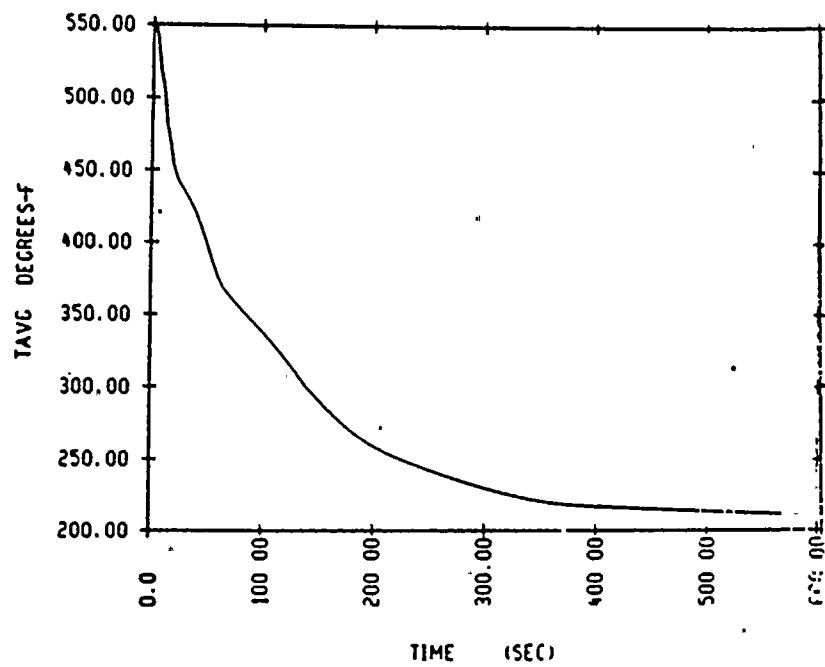
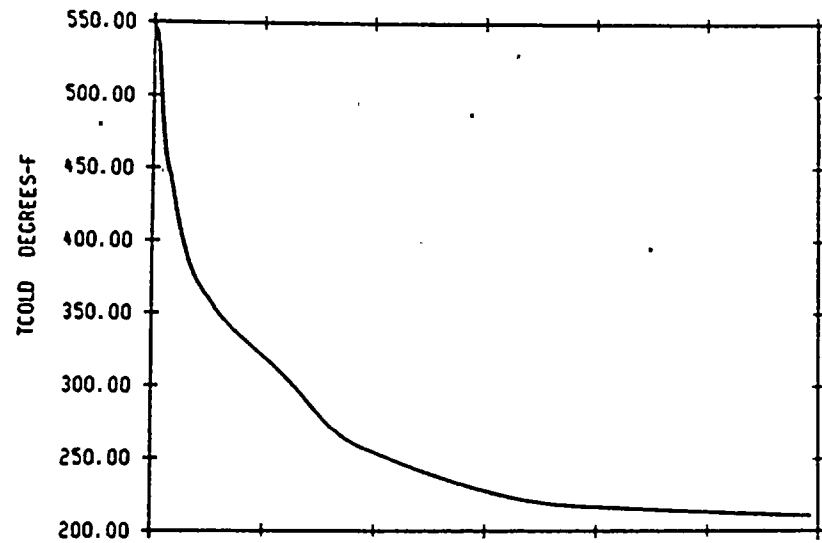


Figure 14.2.5 - 21
Ginna Steamline Rupture
4.6 ft² Break with Power - One Loop in Service

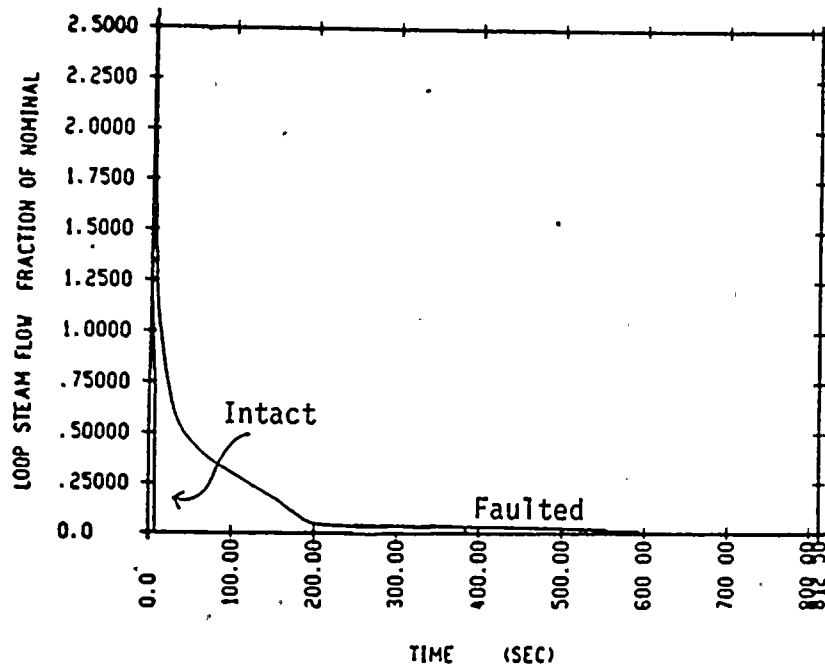
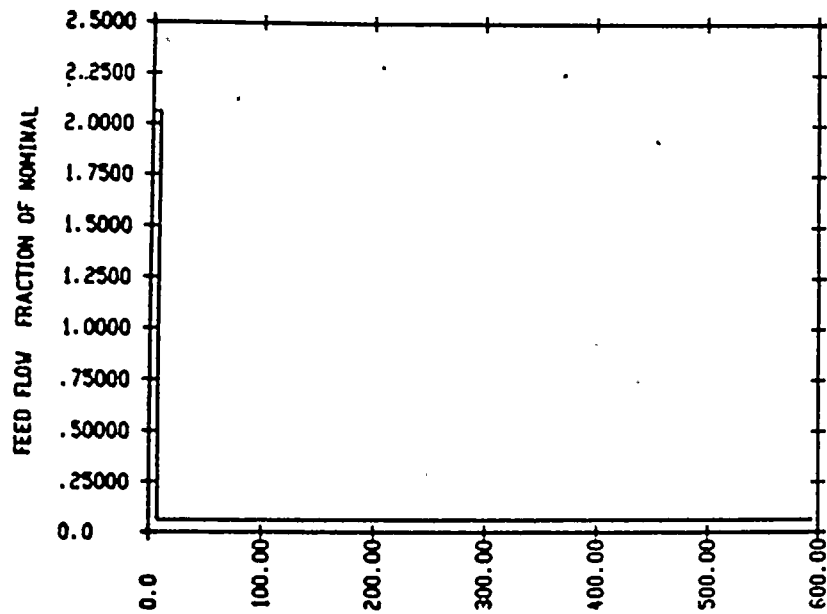


FIGURE 14.2.5-22
GINNA STEAMLINER RUPTURE
4.6 ft² Break with Power

One Loop in Service

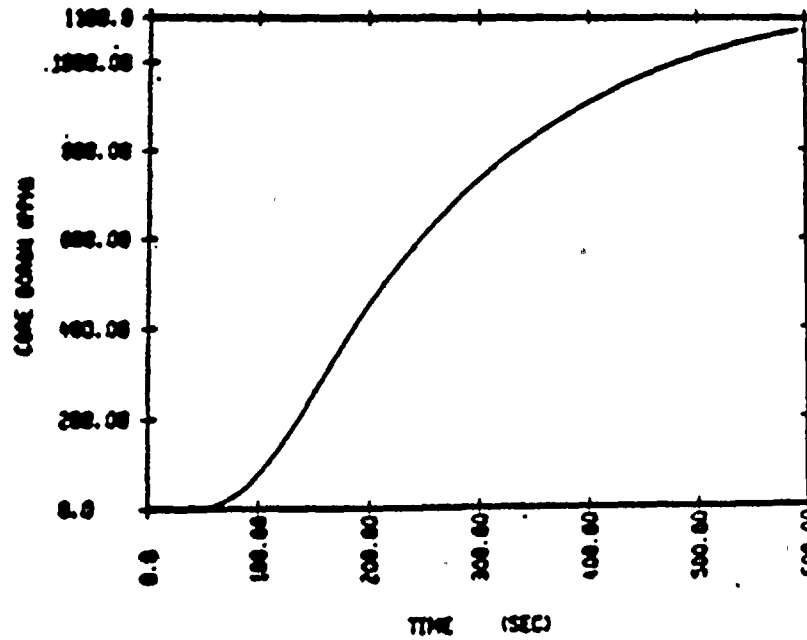
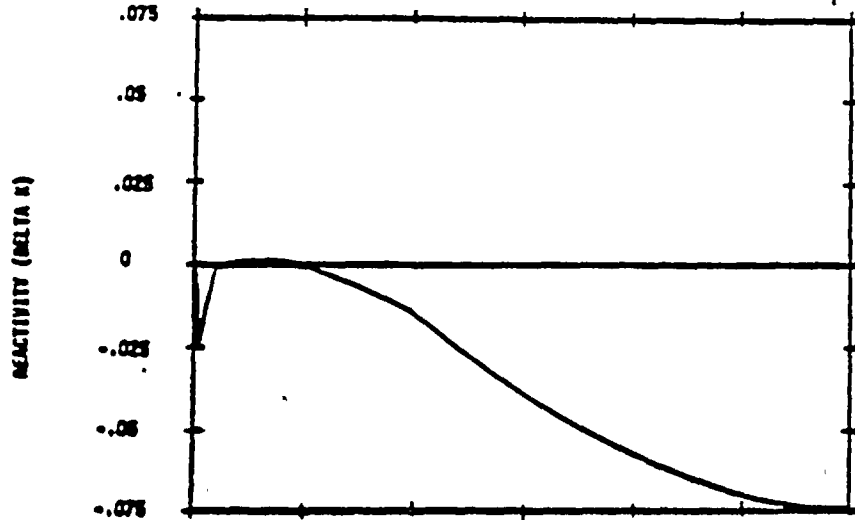


Figure 14.2.5 - 23
Ginna Steamline Rupture
Failed Safety Valve - One Loop in Service

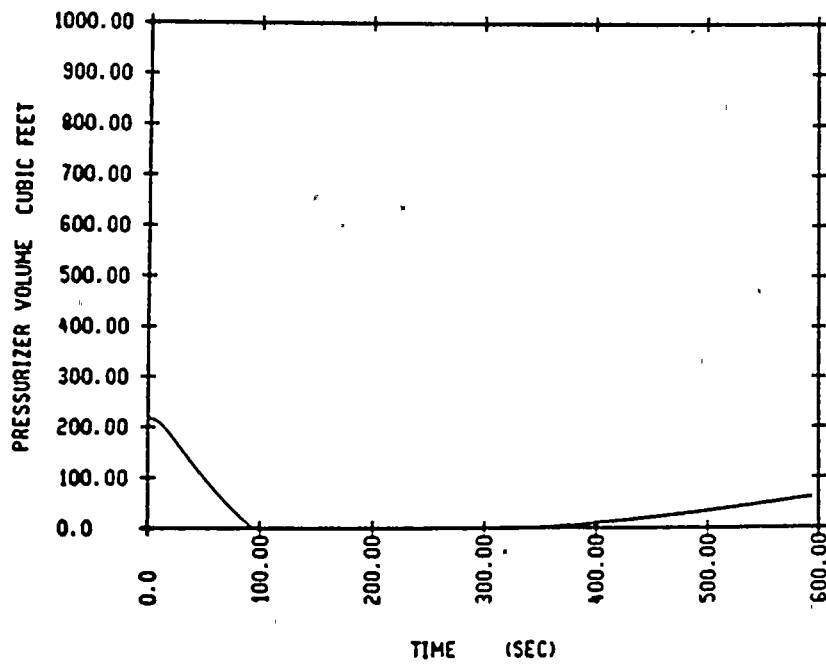
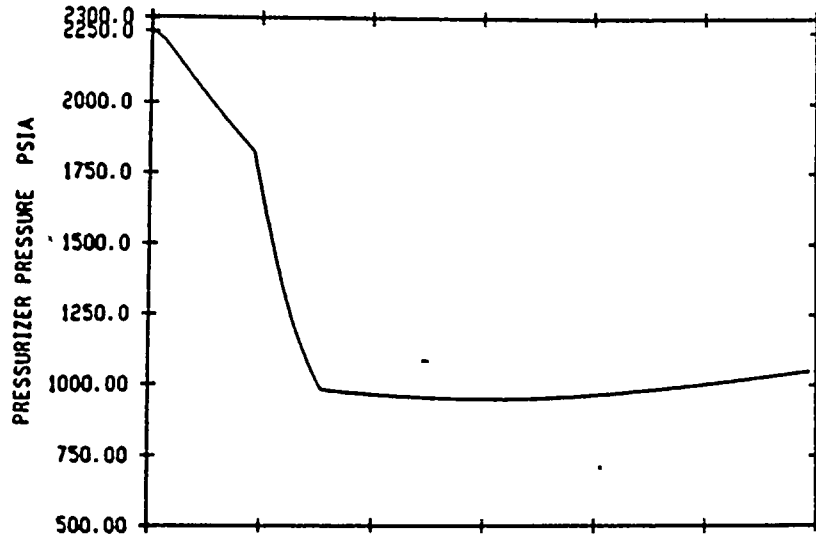


Figure 14.2.5 - 24
Ginna Steamline Rupture
Failed Safety Valve - One Loop in Service

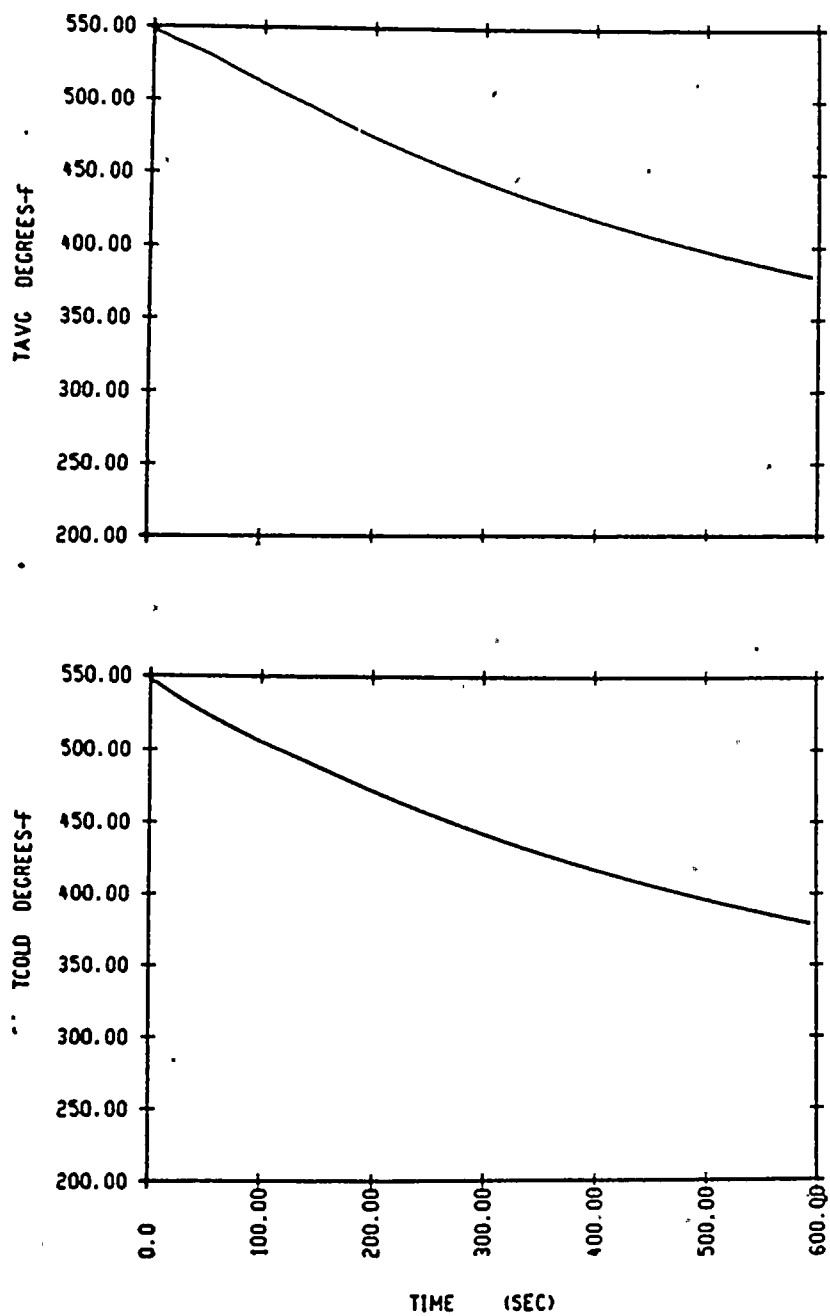




FIGURE 14.2.5- 25

GINNA STEAMLINER RUPTURE

Failed Safety Valve - One Loop in Service

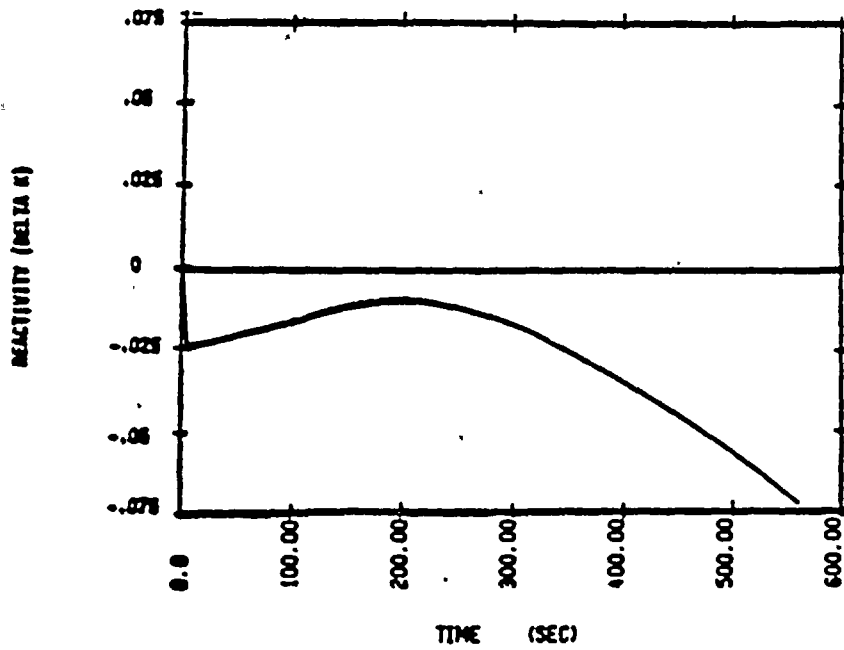
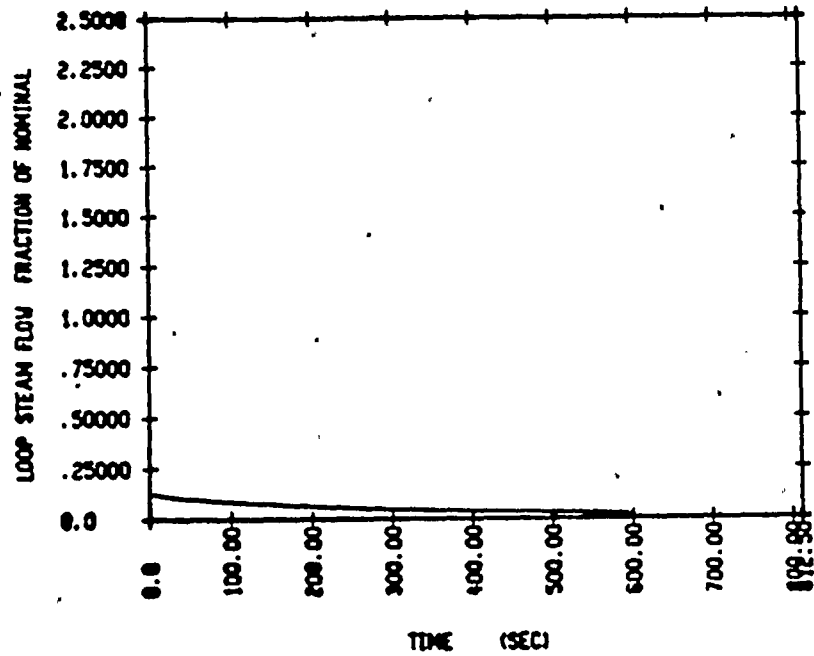
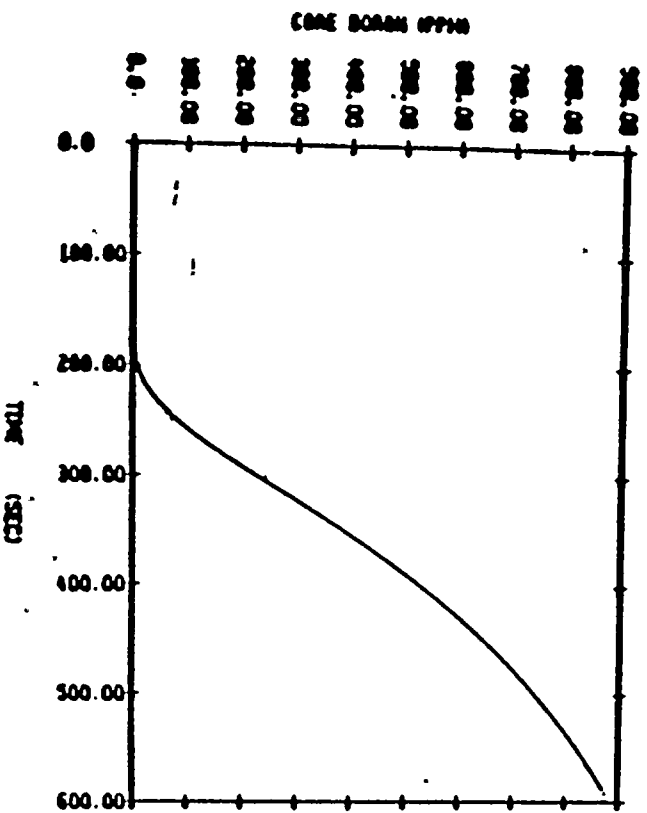


FIGURE 14.2.5 - 26
GINNA STEAMLINER RUPTURE
Failed Safety Valve - One Loop in Service



14.2.6 Rupture of a Control Rod Mechanism Housing-RCCA Ejection

In order for this accident to occur, a rupture of the control rod mechanism housing must be postulated creating a full system pressure differential acting on the drive shaft. The resultant core thermal power excursion is limited by the Doppler reactivity effects of the increased fuel temperature and terminated by reactor trip actuated by high nuclear power signals.

A failure of a control rod mechanism housing sufficient to allow a control rod to be rapidly ejected from the core is not considered credible for the following reasons:

1. Each control rod drive mechanism housing is completely assembled and shop-tested at 4100 psi.
2. The mechanism housing are individually hydrotested to 3105 psig as they are installed on the reactor vessel head to the head adapters, and checked during the hydrotest of the completed reactor coolant system.
3. Stress levels in the mechanism are not affected by system transients at power, or by the thermal movement of the coolant loops. Moments induced by the design earthquake can be accepted within the allowable primary working stress range specified by the ASME Code, Section III, for Class A components.
4. The latch mechanism housing and rod travel housing are each a single length of forged type-304 stainless steel. This material exhibits excellent notch toughness at all temperatures that will be encountered. The joints between the latch mechanism housing and head adapter, and between the latch mechanism housing and rod travel housing, are threaded joints reinforced by canopy type rod welds.

Nuclear Design

Even if a rupture of a RCCA drive mechanism housing is postulated, the operation of a plant utilizing chemical shim is such that the severity of an ejected RCCA is inherently limited. In general, the reactor is operated with the RCCA's inserted only far enough to permit load follow. Reactivity changes caused by core depletion and xenon transients are compensated by boron changes. Further, the location and grouping of control RCCA banks are selected during the nuclear design to lessen the severity of a RCCA ejection accident. Therefore, should a RCCA be ejected from its normal position during full power operation, only a minor reactivity excursion, at worst, could be expected to occur.

However, it may be occasionally desirable to operate with larger than normal insertions. For this reason, a rod insertion limit is defined as a function of power level. Operation with the RCCA's above this limit guarantees adequate shutdown capability and acceptable power distribution. The position of all RCCA's is continuously indicated in the control room. An alarm will occur if a bank of RCCA's approaches its insertion limit or if one RCCA deviates from its bank. Operating instructions require boration at low level alarm and emergency boration at the low-low alarm.

Reactor Protection

The reactor protection in the event of a rod ejection accident has been described in Reference 4. The protection for this accident is provided by high neutron flux trip (high and low setting). These protection functions are described in detail in Section 7.2 of the FSAR.



Effects on Adjacent Housings

Disregarding the remote possibility of the occurrence of a RCCA mechanism housing failure, investigations have shown that failure of a housing due to either longitudinal or circumferential cracking would not cause damage to adjacent housings. However, even if damage is postulated, it would not be expected to lead to a more severe transient, since RCCA's are inserted in the core in symmetric patterns, and control rods immediately adjacent to the worst ejected rods are not in the core when the reactor is critical. Damage to an adjacent housing could, at worst, cause that RCCA not to fall on receiving a trip signal; however, this is already taken into account in the analysis by assuming a stuck rod is adjacent to the ejected rod.

Limiting Criteria

This event is classified as an ANS Condition IV incident. Due to the extremely low probability of a RCCA ejection accident, some fuel damage could be considered an acceptable consequence.

Comprehensive studies, both of the threshold of fuel failure and of the threshold or significant conversion of the fuel thermal energy to mechanical energy, have been carried out as part of the SPERT project by the Idaho Nuclear Corporation. Extensive tests of UO_2 zirconium clad fuel rods representative of those in pressurized water reactor type cores have demonstrated failure thresholds in the range of 240 to 257 cal/gm. However, other rods of a slightly different design have exhibited failures as low as 225 cal/gm. These results differ significantly from the TREAT results, which indicated a failure threshold of 280 cal/gm. Limited results have indicated that this threshold decreases by about 10% with fuel burnup. The clad failure mechanism appears to be melting for zero burnup rods and brittle



fracture for irradiated rods. Also important is the conversion ratio of thermal to mechanical energy. This ratio becomes marginally detectable above 300 cal/gm for unirradiated rods and 200 cal/gm for irradiated rods; catastrophic failure (large fuel dispersal, large pressure rise) even for irradiated rods did not occur below 300 cal/gm.

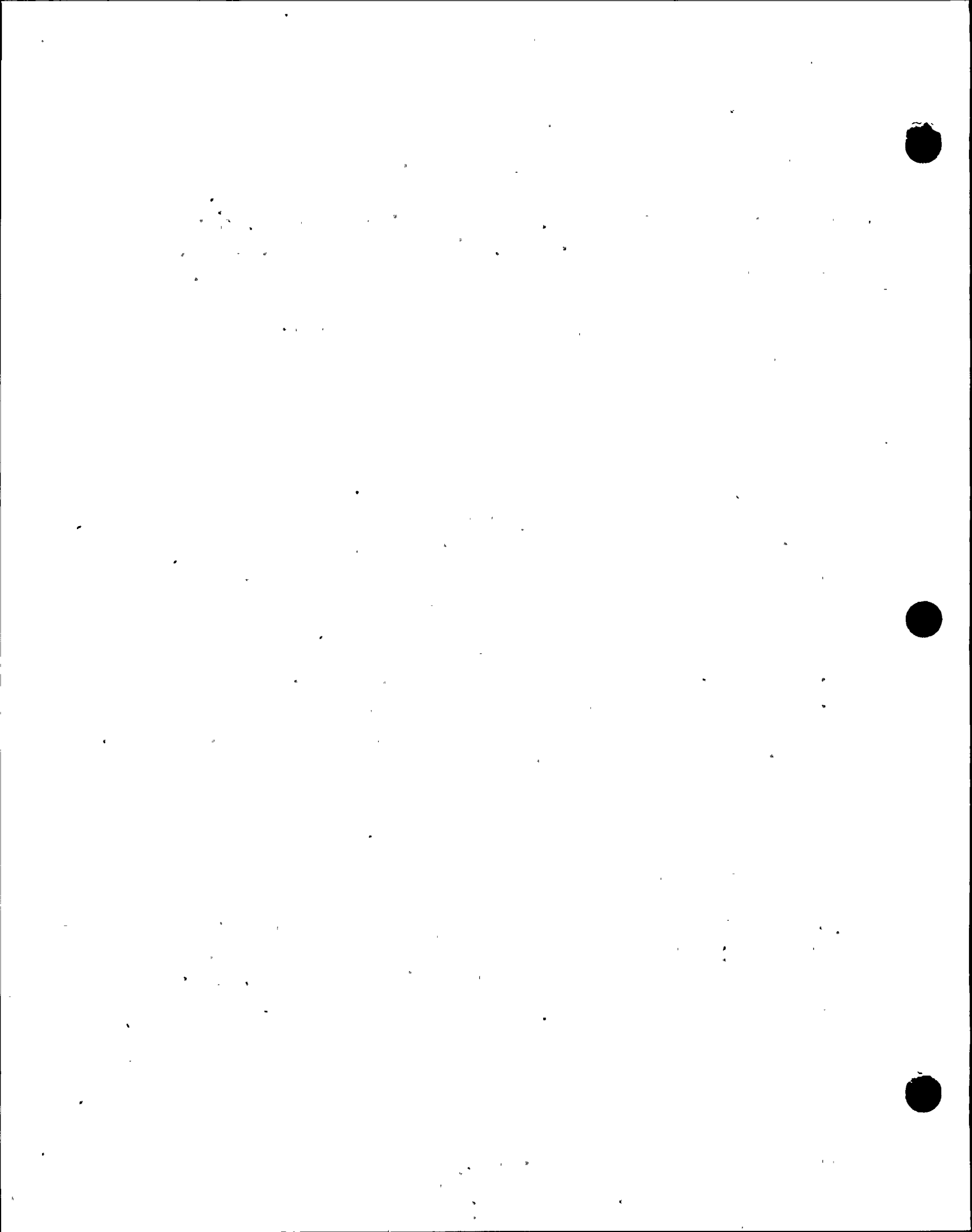
In view of the above experimental results, criteria are applied to ensure that there is little or no possibility of fuel dispersal in the coolant, gross lattice distortion, or severe shock waves. These criteria are:

- a. Average fuel pellet enthalpy at the hot spot below 200 cal/gm.
- b. Average clad temperature at the hot spot below the temperature at which clad embrittlement may be expected (2700°F).
- c. Peak reactor coolant pressure less than that which could cause stresses to exceed the faulted condition stress limits.
- d. Fuel melting will be limited to less than ten percent of the fuel volume at the hot spot even if the average fuel pellet enthalpy is below the limits of criterion (a) above.

Analysis of Effects and Consequences

Method of Analysis

The calculation of the RCCA ejection transient is performed in two stages, first an average core channel calculation and then a hot region calculation. The average core calculation is performed using spatial neutron kinetics methods to determine the average power generation with time including the various total core feedback effects, i.e., Doppler



reactivity and moderator reactivity. Enthalpy and temperature transients in the hot spot are then determined by multiplying the average core energy generation by the hot channel factor and performing a fuel rod transient heat transfer calculation. The power distribution calculated without feedback is pessimistically assumed to persist throughout the transient.

A detailed discussion of the method of analysis can be found in Reference 4.

Average Core Analysis

The spatial kinetics computer code, TWINKLE (Reference 4), is used for the average core transient analysis. This code solves the two group neutron diffusion theory kinetic equation in one, two or three spatial dimensions (rectangular coordinates) for six delayed neutron groups and up to 2000 spatial points. The computer code includes a detailed multiregion, transient fuel-clad-coolant heat transfer model for calculation of pointwise Doppler and moderator feedback effects. In this analysis, the code is used as a one dimensional axial kinetics code, since it allows a more realistic representation of the spatial effects of axial moderator feedback and RCCA movement. However, since the radial dimension is missing, it is still necessary to employ very conservative methods (described in the following) of calculating the ejected rod worth and hot channel factor. Further description of TWINKLE appears in Section 14.

Hot Spot Analysis

In the hot spot analysis, the initial heat flux is equal to the nominal times the design hot channel factor. During the transient, the heat flux hot channel factor is linearly increased to the transient value in 0.1 second, the time for full ejection of the rod. Therefore, the

assumption is made that the hot spots before and after ejection are coincident. This is very conservative, since the peak after ejection will occur in or adjacent to the assembly with the ejected rod, and prior to ejection the power in this region will necessarily be depressed.

The hot spot analysis is performed using the detailed fuel-and cladding transient heat transfer computer code, FACTRAN (Reference 2). This computer code calculates the transient temperature distribution in a cross section of a metal clad UO_2 fuel rod, and the heat flux at the surface of the rod, using as input the nuclear power versus time and the local coolant conditions. The zirconium-water reaction is explicitly represented, and all material properties are represented as functions of temperature. A conservative pellet radial power distribution is used within the fuel rod.

FACTRAN uses the Dittus-Boelter or Jens-Lottes correlation to determine the film heat transfer before DNB, and the Bishop-Sandburg-Tong correlation to determine the film boiling coefficient after DNB. The BST correlation is conservatively used assuming zero bulk fluid quality. The DNB ratio is not calculated, instead the code is forced into DNB by specifying a conservative DNB heat flux. The gap heat transfer coefficient can be calculated by the code; however, it is adjusted in order to force the full power steady-state temperature distribution to agree with the fuel heat transfer design codes. Further description of FACTRAN appears in Section 14.

System Overpressure Analysis

Because safety limits for fuel damage specified earlier are not exceeded, there is little likelihood of fuel dispersal into the coolant. The pressure surge may therefore be calculated on the basis of conventional heat transfer from the fuel and prompt heat generation in the coolant.

The pressure surge is calculated by first performing the fuel heat transfer calculation to determine the average and hot spot heat flux versus time. Using these heat flux data, a THINC (Section 4) calculation is conducted to determine the volume surge. Finally, the volume surge is simulated in a plant transient computer code. This code calculates the pressure transient taking into account fluid transport in the reactor coolant system and heat transfer to the steam generators. No credit is taken for the possible pressure reduction caused by the assumed failure of the control rod pressure housing.

Calculation of Basic Parameters

Input parameters for the analysis are conservatively selected on the basis of values calculated for this type of core. The more important parameters are discussed below. Table 14.2.6-1 presents the parameters used in this analysis.

Ejected Rod Worths and Hot Channel Factors

The values for ejected rod worths and hot channel factors are calculated using either three-dimensional static methods or by a synthesis method employing one-dimensional and two-dimensional calculations. Standard nuclear design codes are used in the analysis. No credit is taken for the flux flattening effects of reactivity feedback. The calculation is performed for the maximum allowed bank insertion at a given power level, as determined by the rod insertion limits. Adverse xenon distributions are considered in the calculation.

Appropriate margins are added to the ejected rod worth and hot channel factors to account for any calculational uncertainties, including an allowance for nuclear power peaking due to densification.

Reactivity Feedback Weighting Factors

The largest temperature rises, and hence the largest reactivity feedbacks, occur in channels where the power is higher than average. Since the weight of a region is dependent on flux, these regions have high weights. This means that the reactivity feedback is larger than that indicated by a simple channel analysis. Physics calculations have been carried out for temperature changes with a flat temperature distribution, and with a large number of axial and radial temperature distributions. Reactivity changes were compared and effective weighting factors determined. These weighting factors take the form of multipliers which when applied to single channel feedbacks correct them to effective whole core feedbacks for the appropriate flux shape. In this analysis, since a one-dimensional (axial) spatial kinetics method is employed, axial weighting is not necessary if the initial condition is made to match the ejected rod configuration. In addition, no weighting is applied to the moderator feedback. A conservative radial weighting factor is applied to the transient fuel temperature to obtain an effective fuel temperature as a function of time accounting for the missing spatial dimension. These weighting factors have also been shown to be conservative compared to three-dimensional analysis (Reference 4).

Moderator and Doppler Coefficient

The critical boron concentrations at the beginning of life and end of life are adjusted in the nuclear code in order to obtain moderator density coefficient curves which are conservative compared to actual design conditions for the plant. As discussed above, no weighting factor is applied to these results.



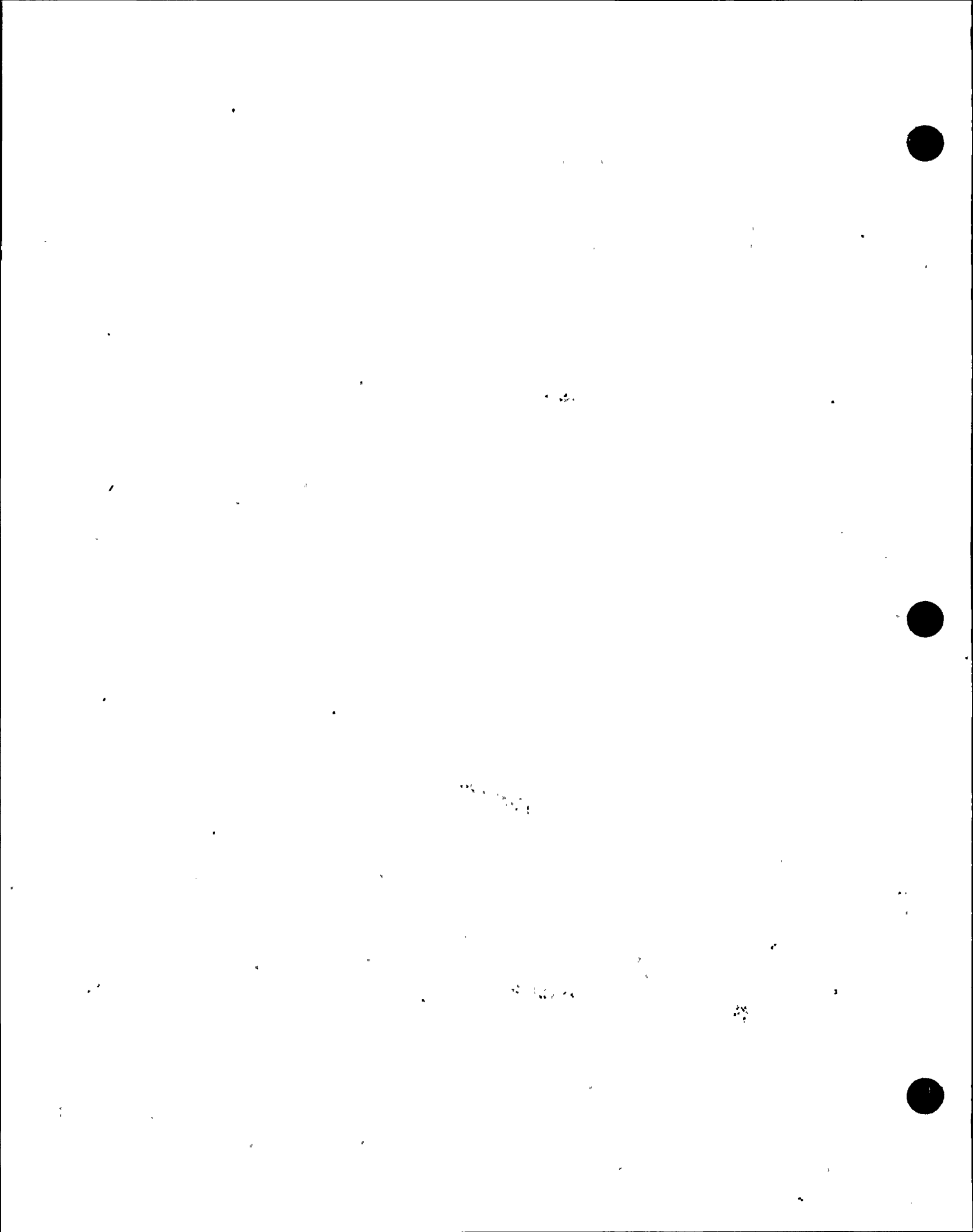
The Doppler reactivity defect is determined as function of power level using a one-dimensional steady-state computer code with a Doppler weighting factor of 1.0. The Doppler defect used is given in Section 3.0. The Doppler weighting factor will increase under accident conditions, as discussed above.

Delayed Neutron Fraction, β

Calculations of the effective delayed neutron fraction (β_{eff}) typically yield values no less than 0.70% at beginning of life and 0.50% at end of life for the first cycle. The accident is sensitive to β if the ejected rod worth is equal to or greater than β as in zero power transients. In order to allow for future cycles, pessimistic estimates of β of 0.49% at beginning of cycle and 0.43% at end of cycle were used in the analysis.

Trip Reactivity Insertion

The trip reactivity insertion assumed is given in Table 14.2.6-1 and includes the effect of one stuck RCCA. The shutdown reactivity was simulated by dropping a rod of the required worth into the core. The start of rod motion occurred 0.5 seconds after the high neutron flux trip point was reached. This delay is assumed to consist of 0.2 second for the instrument channel to produce a signal, 0.15 second for the trip breaker to open and 0.15 second for the coil to release the rods. A curve of trip rod insertion versus time was used which assumed that insertion to the dashpot does not occur until 1.8 seconds after the start of fall. The choice of such a conservative insertion rate means



that there is over one second after the trip point is reached before significant shutdown reactivity is inserted into the core. This is a particularly important conservatism for hot full-power accidents:

Reactor Protection

Reactor protection for a rod ejection is provided by high neutron flux trip (high and low setting). These protection functions are part of the reactor trip system. No single failure of the reactor trip system will negate the protection functions required for the rod ejection accident, or adversely affect the consequences of the accident.

Results

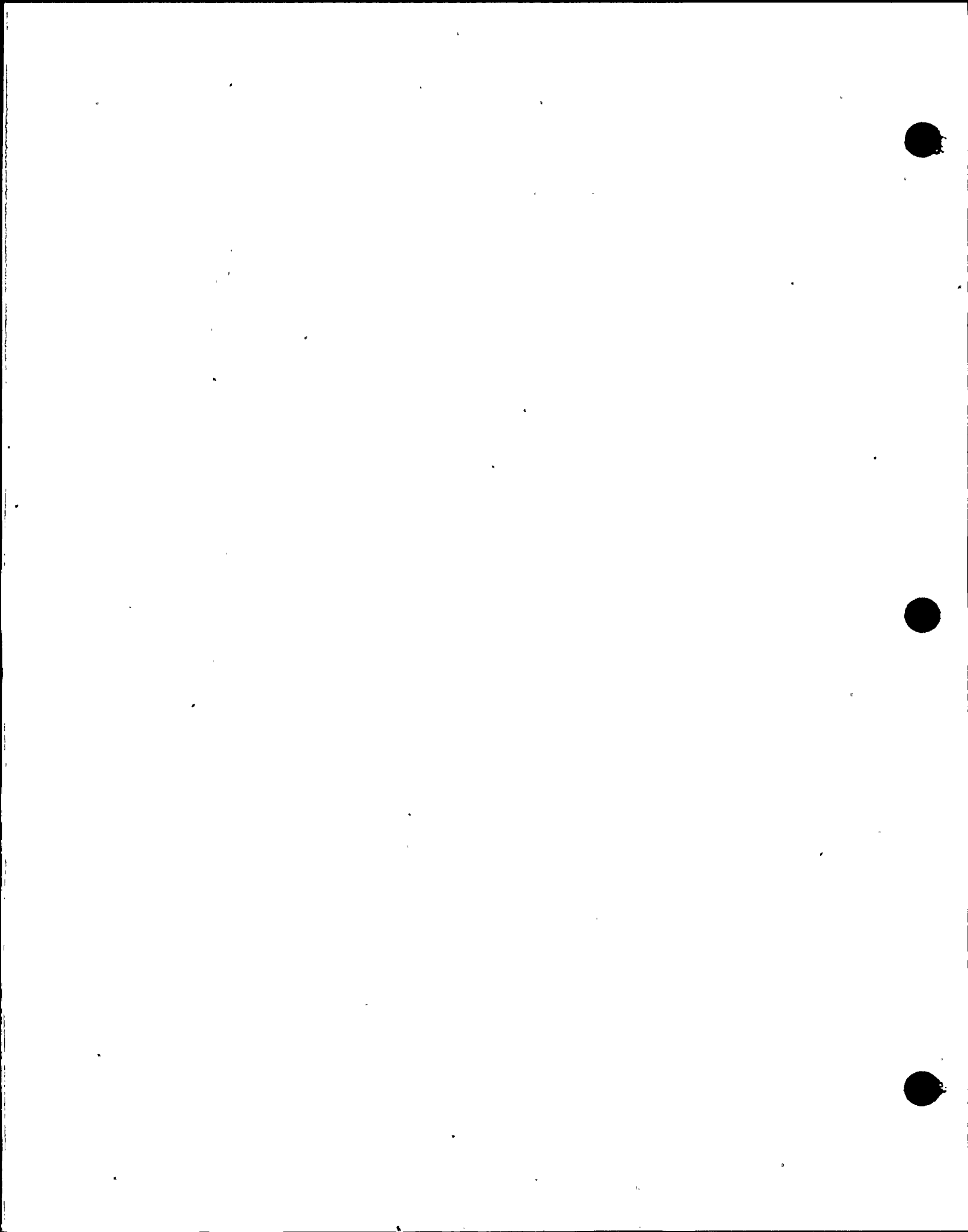
Cases are presented for both beginning and end of life at zero and full power.

1. Beginning of Cycle, Full Power

Control bank D was assumed to be inserted to its insertion limit. The worst ejected rod worth and hot channel factor were conservatively calculated to be $.40\% \Delta k$ and 5.61 respectively. The peak hot spot clad average temperature was 2543°F . The peak hot spot fuel center temperature reached melting, was conservatively assumed at 4990°F . However, melting was restricted to less than 10% of the pellet.

2. Beginning of Cycle, Zero Power

For this condition, control bank D was assumed to be fully inserted and banks B and C were at their insertion limits. The worst ejected rod is located in control bank D and has a worth of $.78\% \Delta k$ and a hot channel factor of 7.80. The peak hot spot clad temperature reached 2639°F , the fuel center temperature was 3861°F .



3. End of Cycle, Full Power

Control bank D was assumed to be inserted to its insertion limit. The ejected rod worth and hot channel factors were conservatively calculated to be $.42\% \Delta k$ and 5.69 respectively. This resulted in a peak clad average temperature of 2246°F . The peak hot spot fuel temperature reached melting conservatively assumed at 4800°F . However, melting was restricted to less than 10% of the pellet.

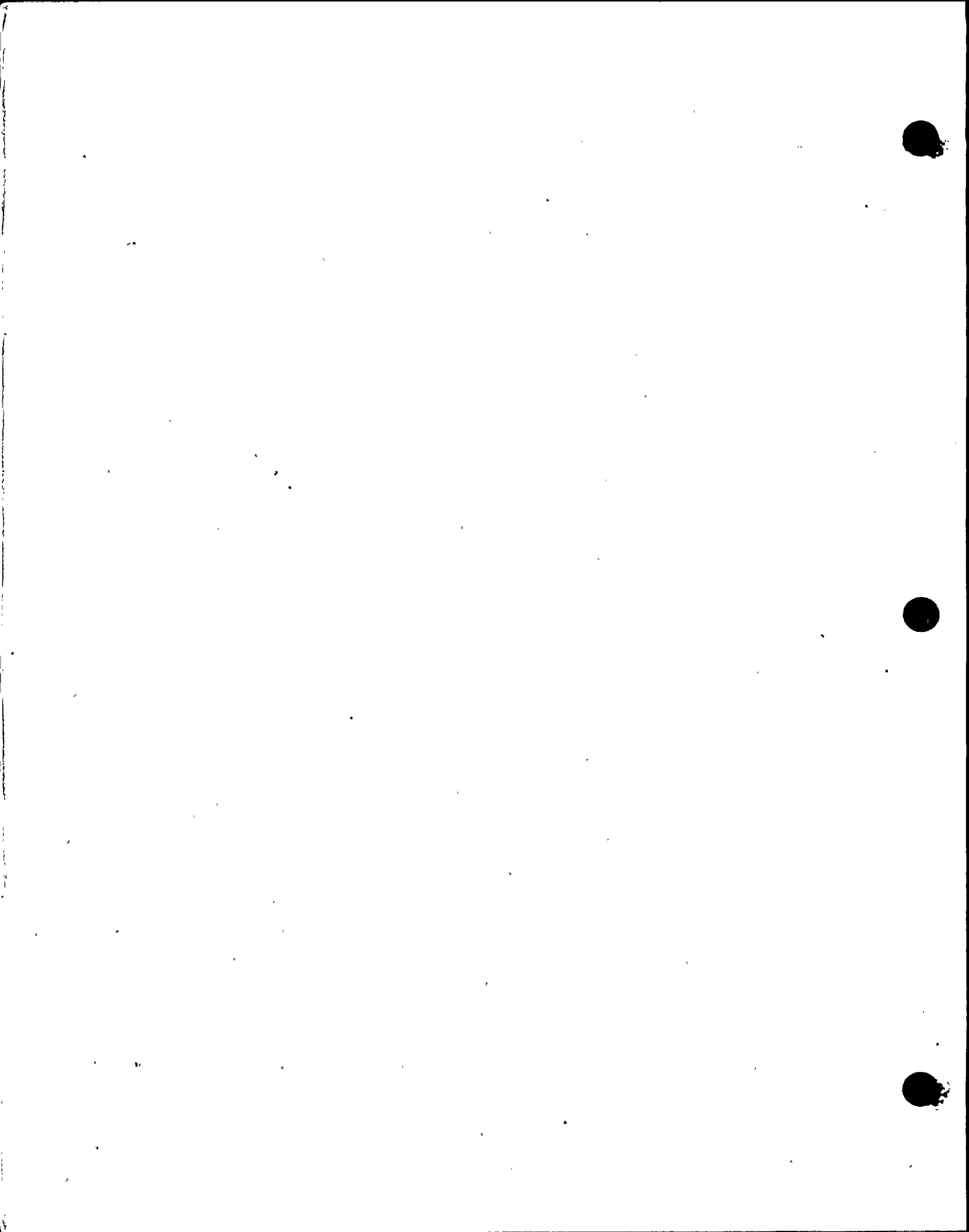
4. End of Cycle, Zero Power

The ejected rod worth and hot channel factor for this case were obtained assuming control bank D to be fully inserted and banks C and B at their insertion limits. The results were $.95\% \Delta k$ and 9.4°F respectively. The peak clad average and fuel center temperatures were 2421 and 3449°F . The Doppler weighting factor for this case is significantly higher than for the other cases due to the very large transient hot channel factor.

A summary of the cases presented above is given in Table 14.2.6-1. The nuclear power and hot spot fuel and clad temperature transients for the worst cases are presented in Figures 14.2.6-1 through 14.2.6-2 (beginning-of-life full power and beginning-of-life zero power). The sequence of events for these two cases is presented in Table 14.2.6-2.

For all cases, reactor trip occurs very early in the transient, after which the nuclear power excursion is terminated. As discussed previously, the reactor will remain subcritical following reactor trip.

The ejection of an RCCA constitutes a break in the Reactor Coolant System, located in the reactor pressure vessel head. The effects and consequences of loss-of-coolant accidents are discussed in Section 14.3. Following the RCCA ejection, the operator would follow the same



emergency instructions as for any other loss of coolant accident to recover from the event.

Fission Product Release.

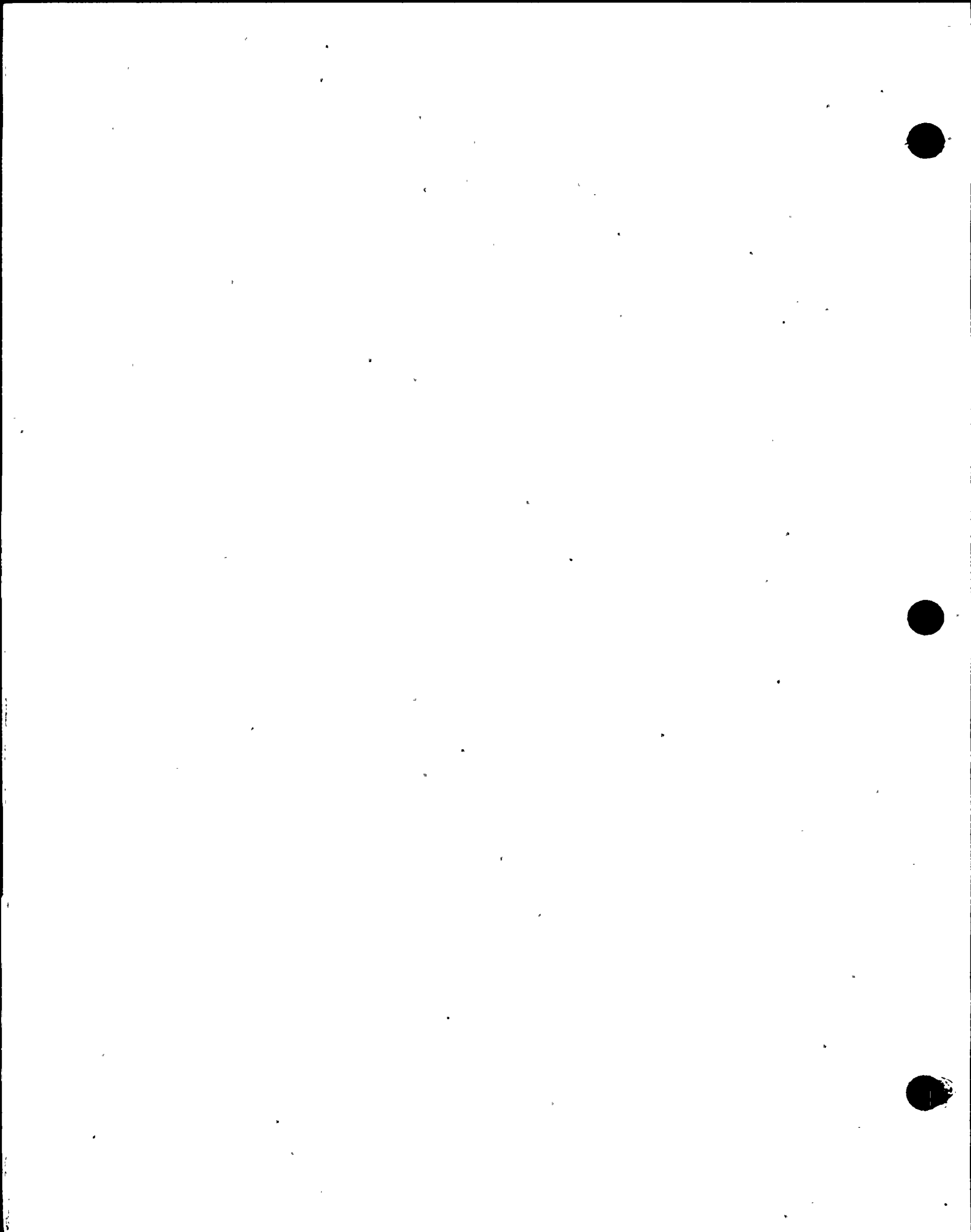
It is assumed that fission products are released from the gaps of all rods entering DNB. In all cases considered, less than 10% of the rods entered DNB based on a detailed three-dimensional THINC analysis.

Pressure Surge

A detailed calculation of the pressure surge for an ejection worth of one dollar at beginning of life, hot full power, indicates that the peak pressure does not exceed that which would cause stress to exceed the faulted condition stress limits. Since the severity of the present analysis does not exceed the "worst case" analysis, the accident for this plant will not result in an excessive pressure rise or further damage to the reactor coolant system.

Lattice Deformations

A large temperature gradient will exist in the region of the hot spot. Since the fuel rods are free to move in the vertical direction, differential expansion between separate rods cannot produce distortion. However, the temperature gradients across individual rods may produce a differential expansion tending to bow the midpoint of the rods toward the hotter side of the rod. Calculations have indicated that this bowing would result in a negative reactivity effect at the hot spot since Westinghouse cores are under-moderated, and bowing will tend to increase the under-moderation at the hot spot. Since the 14 x 14 fuel design is also under-moderated, the same effect would be observed. In practice, no significant bowing is anticipated, since the structural rigidity of the core is more than sufficient to withstand the forces produced. Boiling in the hot spot region would produce a net flow away from that region. However, the heat from the fuel is released to the



water relatively slowly, and it is considered inconceivable that cross flow will be sufficient to produce significant lattice forces. Even if massive and rapid boiling, sufficient to distort the lattice, is hypothetically postulated, the large void fraction in the hot spot region would produce a reduction in the total core moderator to fuel ratio and a large reduction in this ratio at the hot spot. The net effect would therefore be a negative feedback. It can be concluded that no conceivable mechanism exists for a net positive feedback resulting from lattice deformation. In fact, a small negative feedback may result. The effect is conservatively ignored in the analysis.

Conclusions

Conservative analyses indicate that the described fuel and cladding limits are not exceeded. It is concluded that there is no danger of sudden fuel dispersal into the coolant. Since the peak pressure does not exceed that which would cause stresses to exceed the faulted condition stress limits, it is concluded that there is no danger of further consequential damage to the reactor coolant system. The analyses have demonstrated that the fission product release, as a result of a number of fuel rods entering DNB, is limited to less than 10% of the fuel rods in the core.

TABLE 14.2.6-1

PARAMETERS USED IN THE ANALYSIS OF THE ROD CLUSTER CONTROL
ASSEMBLY EJECTION ACCIDENT

| Parameters | Time in Life | | | |
|--|--------------|-----------|------|------|
| | Beginning | Beginning | End | End |
| Power level, percent | 102 | 0 | 102 | 0 |
| Ejected rod worth, percent Δk | .40 | .78 | .42 | .95 |
| Delayed neutron fraction, percent | .49 | .49 | .43 | .43 |
| Feedback reactivity weighting | 1.3 | 1.417 | 1.3 | 1.74 |
| Trip reactivity, percent Δk | 4.0 | 2.0 | 4.0 | 2.0 |
| F_q before rod ejection | 2.5 | -- | 2.5 | -- |
| F_q after rod ejection | 5.61 | 7.80 | 5.69 | 9.40 |
| Number of operational pumps | 2 | 1 | 2 | 1 |
| Maximum fuel pellet average temperature, °F | 4190 | 3422 | 3726 | 3099 |
| Maximum fuel center temperature, °F | 4971 | 3861 | 4838 | 3449 |
| Maximum clad average temperature, °F | 2543 | 2639 | 2246 | 2421 |
| Maximum fuel stored energy, cal/g | 184 | 145 | 160 | 129 |
| Maximum fuel melt, percent | <10 | 0.0 | <10 | 0.0 |

TABLE 14.2.6-2

TIME SEQUENCE OF EVENTS RCCA EJECTION

| <u>Case</u> | <u>Event</u> | <u>Time of Each Event (Seconds)</u> |
|----------------------------------|--|---|
| a. Beginning-of-Life, Full Power | Initiation of rod ejection | 0.0 |
| | Power range high neutron flux setpoint reached | 0.03 |
| | Peak nuclear power occurs | 0.13 |
| | Rods begin to fall into core | 0.53 |
| | Peak fuel average temperature occurs | 1.87 |
| | Peak clad temperature occurs | 2.00 |
| | Peak heat flux occurs | 2.00 |
| b. Beginning-of-Life, Zero Power | Initiation of rod ejection | 0.0 |
| | Power range high neutron flux low setpoint reached | 0.24 |
| | Peak nuclear power occurs | 0.29/ |
| | Rods begin to fall into core | 0.74 |
| | Peak clad temperature occurs | 2.14 |
| | Peak head flux occurs | 2.14/ |
| | Peak fuel average temperature occurs | 2.27 |

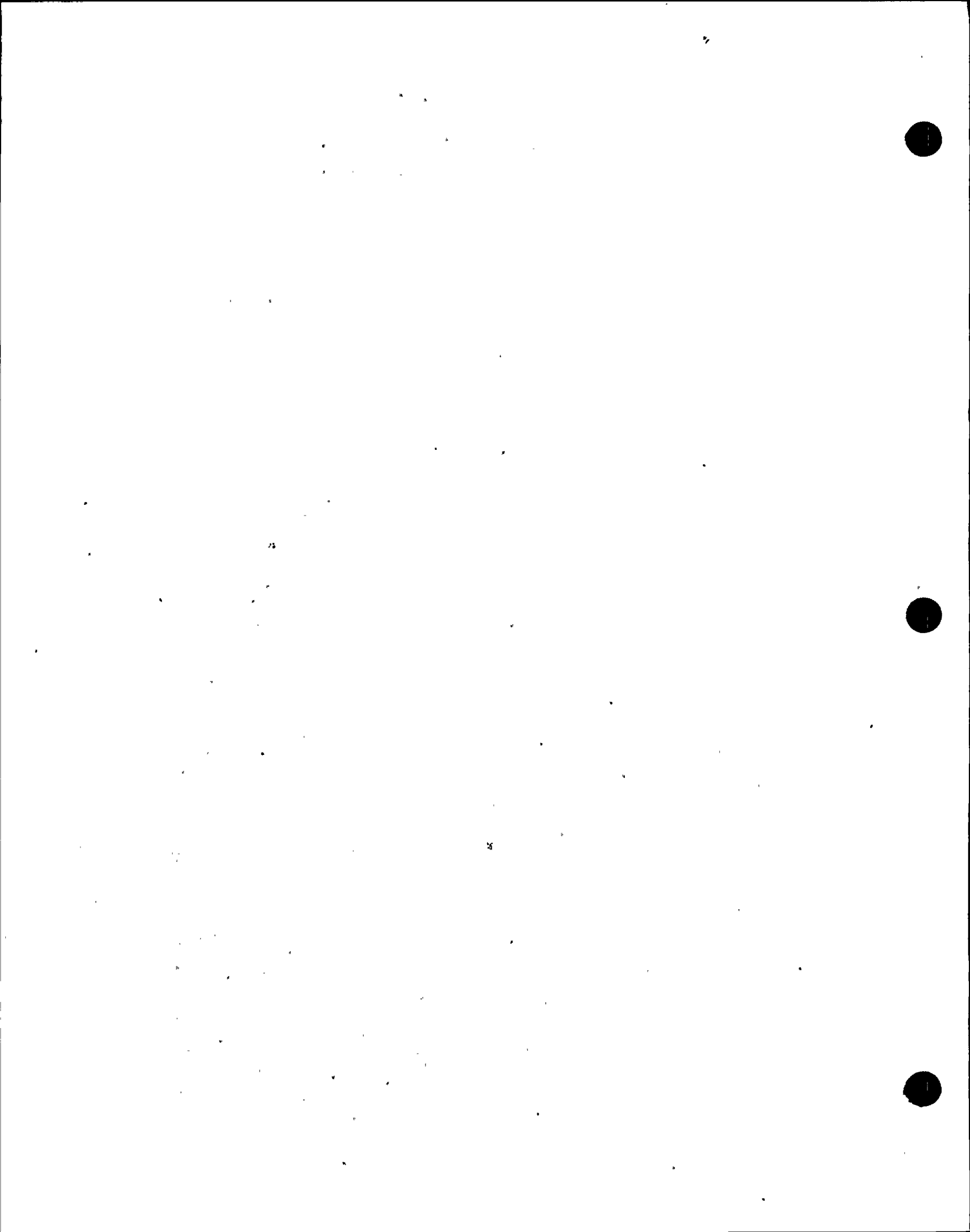


Figure 14.2.6-1
Ginna RCCA Ejection
Beginning of Life, Full Power

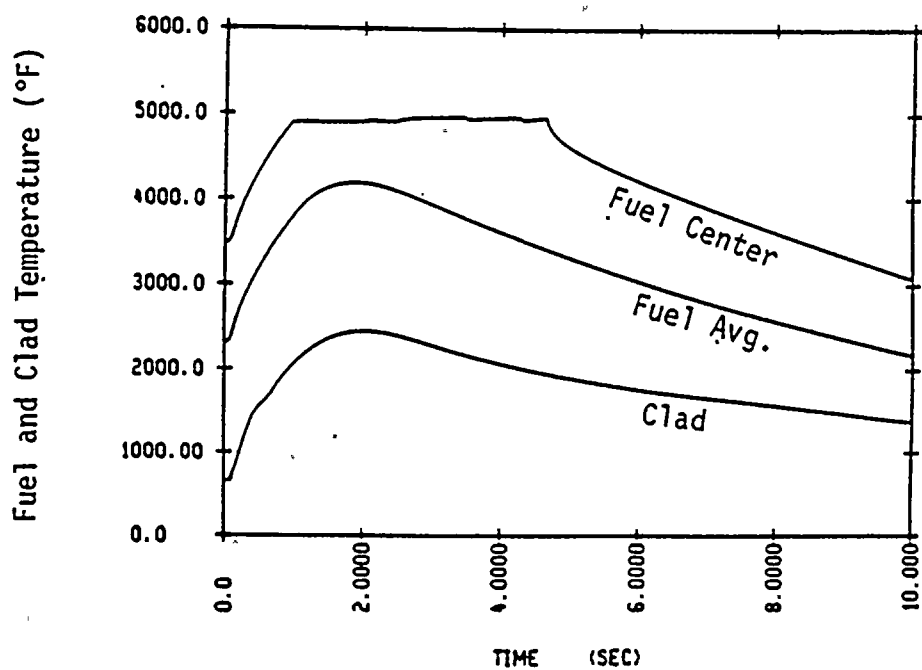
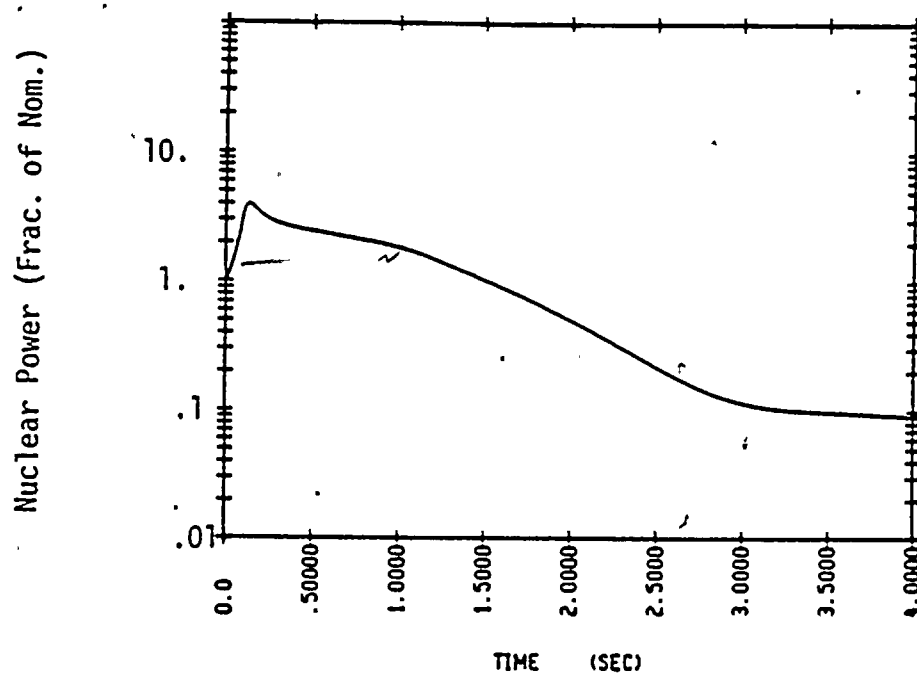
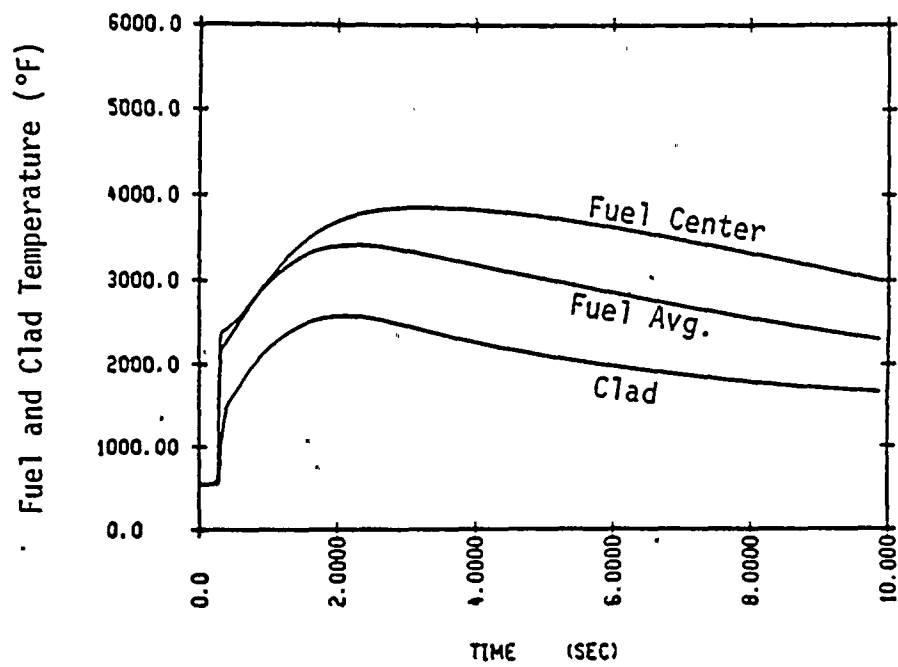
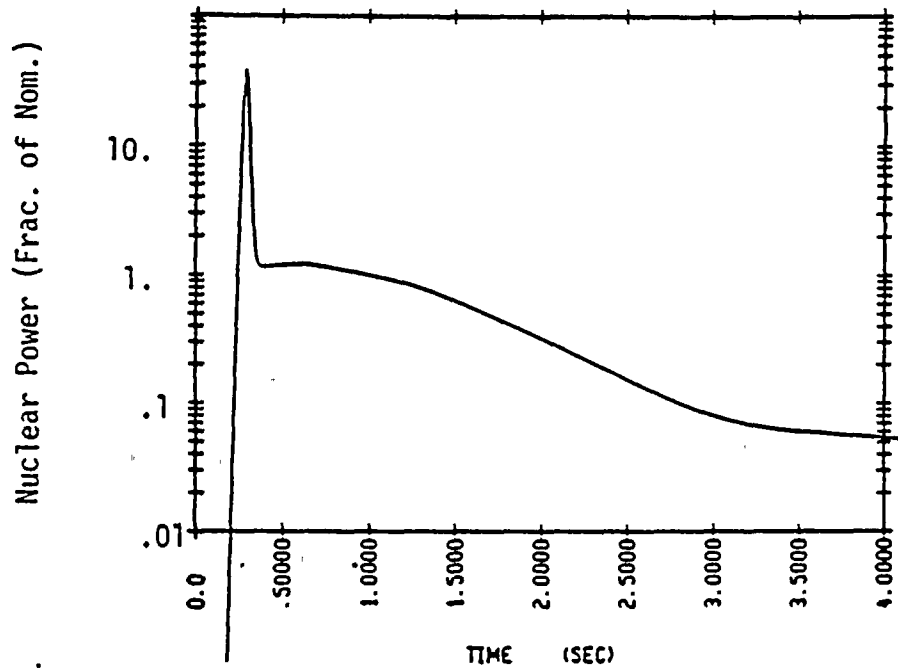


Figure 14.2.6-2
Ginna RCCA Ejection
Beginning of Life, Zero Power



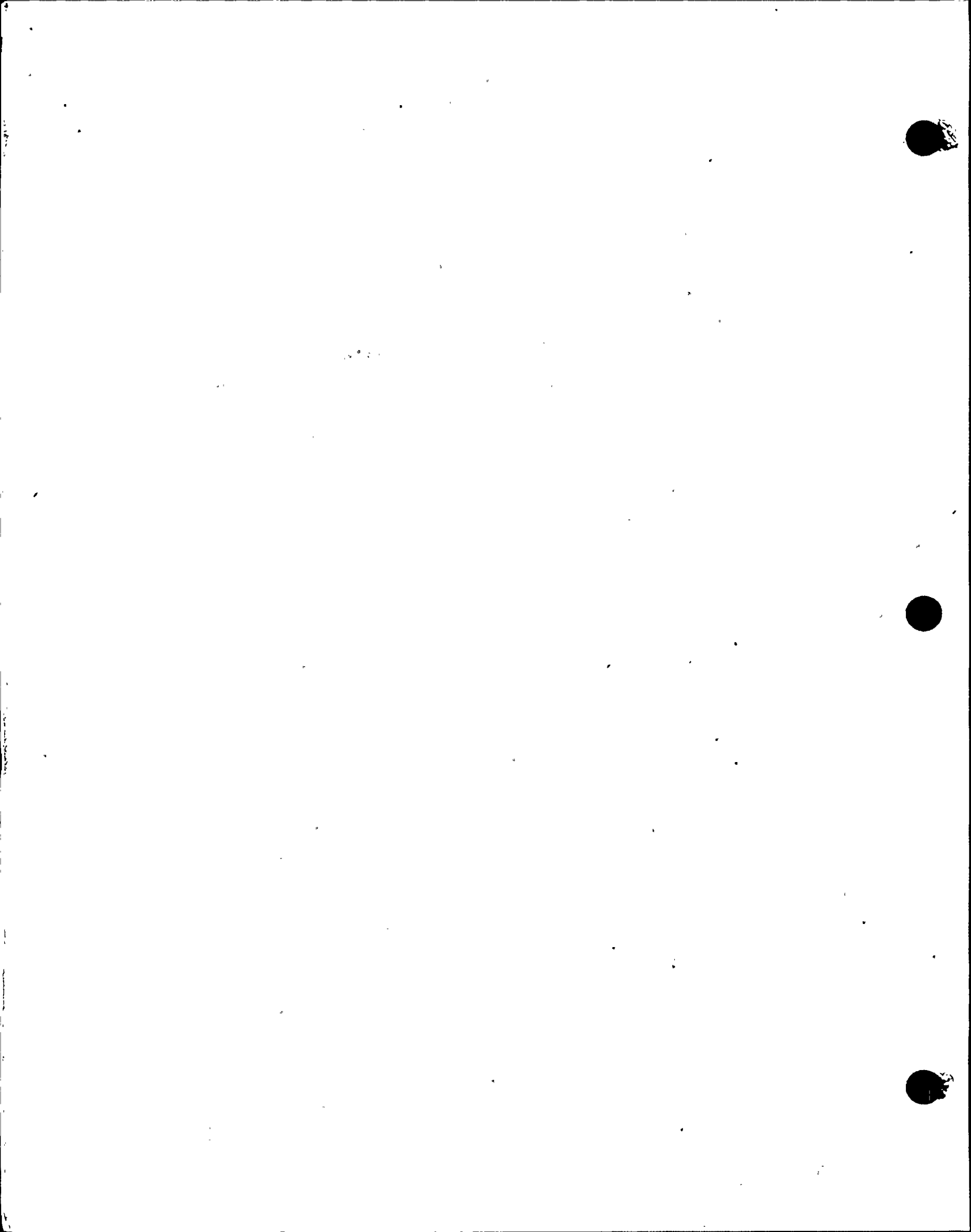


ATTACHMENT C
LOCA ACCIDENT ANALYSIS REVISED
FSAR SECTIONS 14.3.1/14.3.2



TABLE OF CONTENTS

| Section | Description | Page |
|---------|--|----------|
| 14.3 | Primary System Pipe Ruptures | 14.3.1-1 |
| 14.3.1 | Loss of Reactor Coolant From Small Ruptured Pipes or From Cracks in Large Pipes Which Actuates Emergency Core Cooling System | 14.3.1-1 |
| 14.3.1 | References | 14.3.1-7 |
| 14.3.2 | Major Reactor Coolant System Pipe Ruptures (Loss of Coolant Accident) | 14.3.2-1 |
| 14.3.2 | References | 14.3.2-7 |

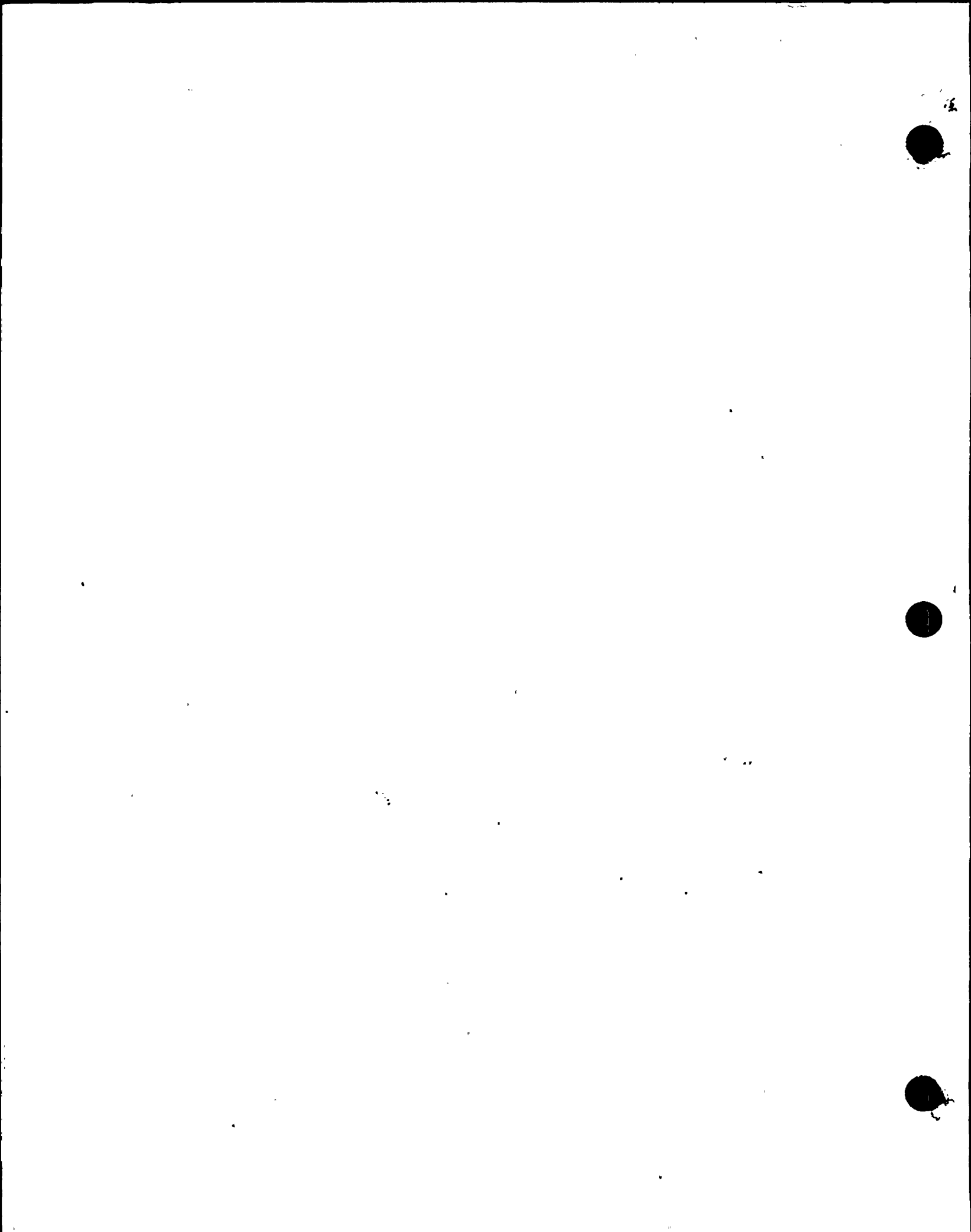


LIST OF TABLES

| Table | Description | Page |
|----------|--|-----------|
| 14.3.1-1 | Small Break - Time Sequence of Events | 14.3.1-8 |
| 14.3.1-2 | Small Break - Analysis Input and Results | 14.3.1-9 |
| 14.3.2-1 | Large Break - Time Sequence of Events | 14.3.2-10 |
| 14.3.2-2 | Large Break - Analysis Input and Results | 14.3.2-11 |
| 14.3.2-3 | Large Break - Containment Data | 14.3.2-12 |
| 14.3.2-4 | Reflood Mass and Energy Release | 14.3.2-15 |
| 14.3.2-5 | Broken Loop Accumulator Mass and Energy Release | 14.3.2-16 |

LIST OF FIGURES

| Figure | Description | Page |
|------------|--|-----------|
| 14.3.1-1a | High Head Safety Injection Flow Rate | 14.3.1-10 |
| 14.3.1-1b | Low Head Safety Injection Flow Rate | 14.3.1-11 |
| 14.3.1-2 | Hot Rod Axial Power Shape | 14.3.1-12 |
| 14.3.1-3 | Depressurization Transient (6-Inch) | 14.3.1-13 |
| 14.3.1-4 | Core Mixture Height (6-Inch) | 14.3.1-14 |
| 14.3.1-5 | Peak Clad Temperature Transient (6-Inch) | 14.3.1-15 |
| 14.3.1-6 | Steam Flow Rate | 14.3.1-16 |
| 14.3.1-7 | Rod Film Coefficients | 14.3.1-17 |
| 14.3.1-8 | Hot Spot Fluid Temperature | 14.3.1-18 |
| 14.3.1-9a | Depressurization Transient (4-Inch) | 14.3.1-19 |
| 14.3.1-9b | Depressurization Transient (8-Inch) | 14.3.1-20 |
| 14.3.1-10a | Core Mixture Height (4-Inch) | 14.3.1-21 |
| 14.3.1-10b | Core Mixture Height (8-Inch) | 14.3.1-22 |
| 14.3.1-11a | Clad Temperature Transient (4-Inch) | 14.3.1-23 |
| 14.3.1-11b | Clad Temperature Transient (8-Inch) | 14.3.1-24 |
| 14.3.2-1a | Fluid Quality - DECLG (CD = 0.8) | 14.3.2-17 |



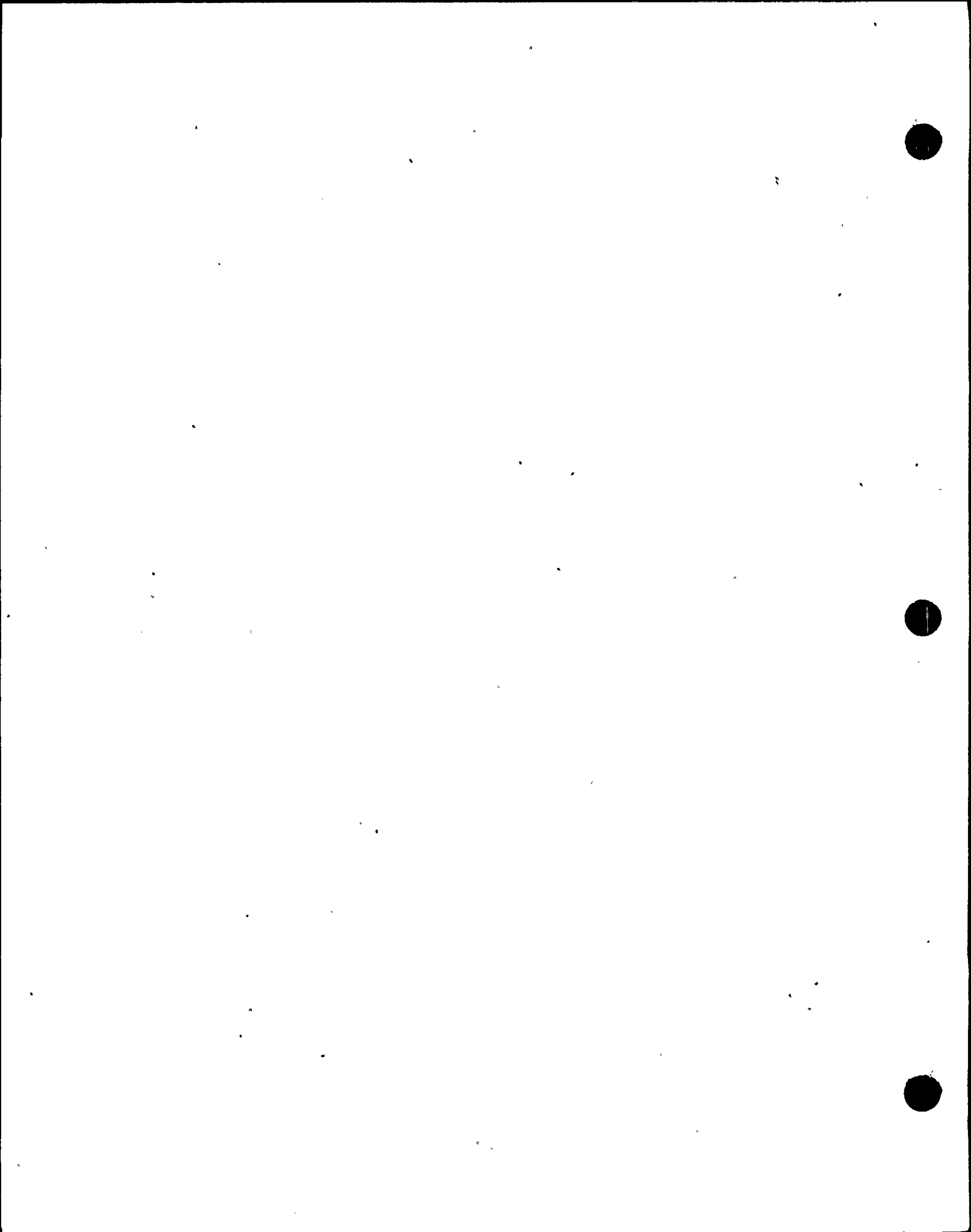
LIST OF FIGURES
(continued)

| Figure | Description | Page |
|------------|--|-----------|
| 14.3.2-18 | Fluid Quality - DECLG (CD = 0.6) | 14.3.2-18 |
| 14.3.2-19 | Fluid Quality - DECLG (CD = 0.4) | 14.3.2-19 |
| 14.3.2-20 | Mass Velocity - DECLG (CD = 0.8) | 14.3.2-20 |
| 14.3.2-21 | Mass Velocity - DECLG (CD = 0.6) | 14.3.2-21 |
| 14.3.2-22 | Mass Velocity - DECLG (CD = 0.4) | 14.3.2-22 |
| 14.3.2-23a | Heat Transfer Coefficient - DECLG (CD = 0.8) | 14.3.2-23 |
| 14.3.2-23b | Heat Transfer Coefficient - DECLG (CD = 0.6) | 14.3.2-24 |
| 14.3.2-23c | Heat Transfer Coefficient - DECLG (CD = 0.4) | 14.3.2-25 |
| 14.3.2-26 | Core Pressure - DECLG (CD = 0.8) | 14.3.2-26 |
| 14.3.2-27 | Core Pressure - DECLG (CD = 0.6) | 14.3.2-27 |
| 14.3.2-28 | Core Pressure - DECLG (CD = 0.4) | 14.3.2-28 |
| 14.3.2-29a | Break Flow Rate - DECLG (CD = 0.8) | 14.3.2-29 |
| 14.3.2-29b | Break Flow Rate - DECLG (CD = 0.6) | 14.3.2-30 |
| 14.3.2-29c | Break Flow Rate - DECLG (CD = 0.4) | 14.3.2-31 |
| 14.3.2-32a | Core Pressure Drop - DECLG (CD = 0.8) | 14.3.2-32 |

A
185

LIST OF FIGURES
(continued)

| Figure | Description | Page |
|-----------|--|-----------|
| 14.3.2-1b | Fluid Quality - DECLG (CD = 0.6) | 14.3.2-18 |
| 14.3.2-1c | Fluid Quality - DECLG (CD = 0.4) | 14.3.2-19 |
| 14.3.2-2a | Mass Velocity - DECLG (CD = 0.8) | 14.3.2-20 |
| 14.3.2-2b | Mass Velocity - DECLG (CD = 0.6) | 14.3.2-21 |
| 14.3.2-2c | Mass Velocity - DECLG (CD = 0.4) | 14.3.2-22 |
| 14.3.2-3a | Heat Transfer Coefficient - DECLG (CD = 0.8) | 14.3.2-23 |
| 14.3.2-3b | Heat Transfer Coefficient - DECLG (CD = 0.6) | 14.3.2-24 |
| 14.3.2-3c | Heat Transfer Coefficient - DECLG (CD = 0.4) | 14.3.2-25 |
| 14.3.2-4a | Core Pressure - DECLG (CD = 0.8) | 14.3.2-26 |
| 14.3.2-4b | Core Pressure - DECLG (CD = 0.6) | 14.3.2-27 |
| 14.3.2-4c | Core Pressure - DECLG (CD = 0.4) | 14.3.2-28 |
| 14.3.2-5a | Break Flow Rate - DECLG (CD = 0.8) | 14.3.2-29 |
| 14.3.2-5b | Break Flow Rate - DECLG (CD = 0.6) | 14.3.2-30 |
| 14.3.2-5c | Break Flow Rate - DECLG (CD = 0.4) | 14.3.2-31 |
| 14.3.2-6a | Core Pressure Drop - DECLG (CD = 0.8) | 14.3.2-32 |



LIST OF FIGURES
(continued)

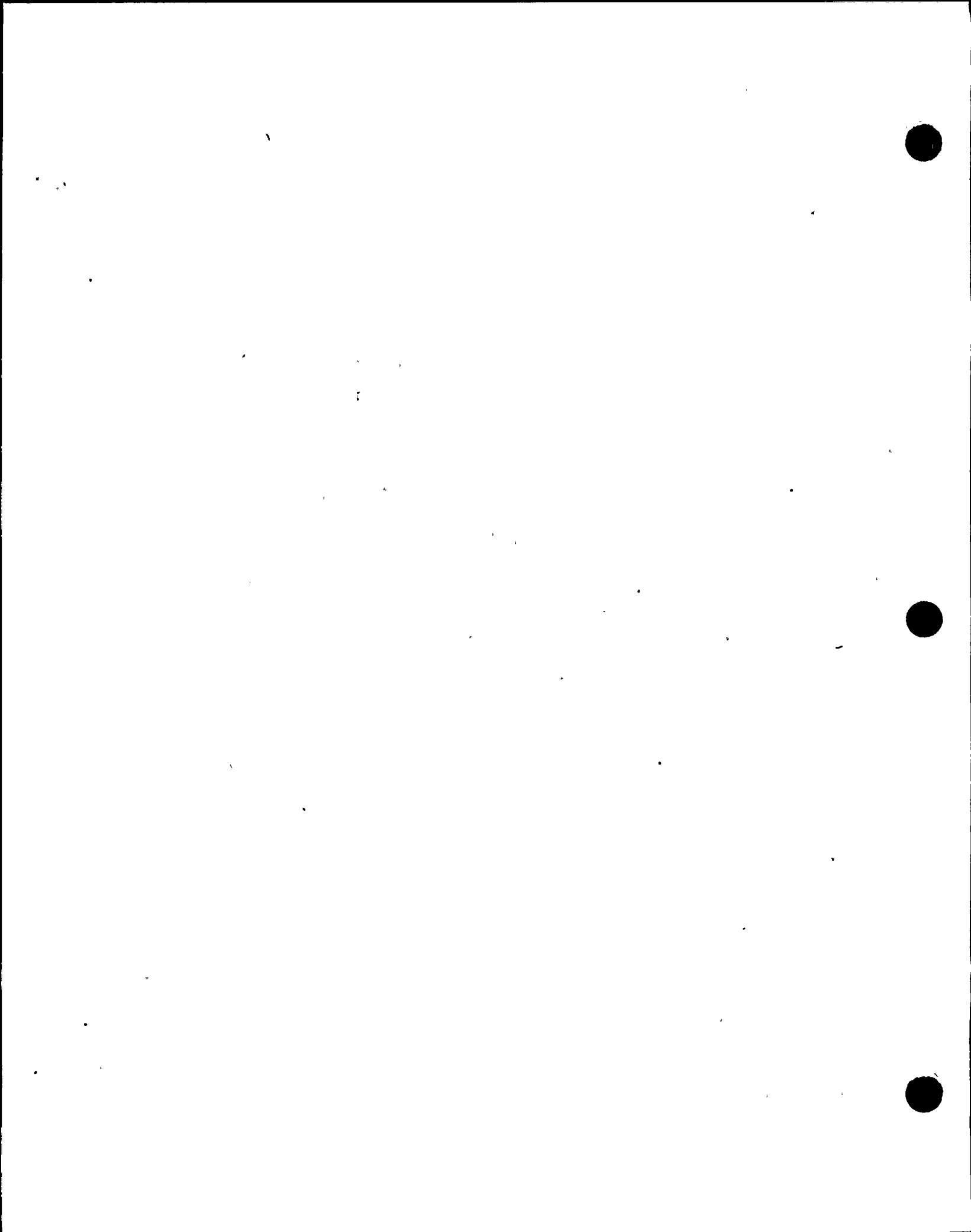
| Figure | Description | Page |
|------------|---|-----------|
| 14.3.2-6b | Core Pressure Drop - DECLG (CD = 0.6) | 14.3.2-33 |
| 14.3.2-6c | Core Pressure Drop - DECLG (CD = 0.4) | 14.3.2-34 |
| 14.3.2-7a | Peak Clad Temperature - DECLG (CD = 0.8) | 14.3.2-35 |
| 14.3.2-7b | Peak Clad Temperature - DECLG (CD = 0.6) | 14.3.2-36 |
| 14.3.2-7c | Peak Clad Temperature - DECLG (CD = 0.4) | 14.3.2-37 |
| 14.3.2-8a | Fluid Temperature - DECLG (CD = 0.8) | 14.3.2-38 |
| 14.3.2-8b | Fluid Temperature - DECLG (CD = 0.6) | 14.3.2-39 |
| 14.3.2-8c | Fluid Temperature - DECLG (CD = 0.4) | 14.3.2-40 |
| 14.3.2-9a | Core Flow (Top and Bottom) - DECLG (CD = 0.8) | 14.3.2-41 |
| 14.3.2-9b | Core Flow (Top and Bottom) - DECLG (CD = 0.6) | 14.3.2-42 |
| 14.3.2-9c | Core Flow (Top and Bottom) - DECLG (CD = 0.4) | 14.3.2-43 |
| 14.3.2-10a | Reflood Transient - Core Inlet Velocity - DECLG (CD = 0.8) | 14.3.2-44 |
| 14.3.2-10b | Reflood Transient - Core Inlet Velocity - DECLG (CD = 0.6) | 14.3.2-45 |

LIST OF FIGURES
(continued)

| Figure | Description | Page |
|------------|---|-----------|
| 14.3.2-10c | Reflood Transient - Core Inlet Velocity - DECLG (CD = 0.4) | 14.3.2-46 |
| 14.3.2-11a | Reflood Transient - Core and Downcomer Water Levels - DECLG (CD = 0.8) | 14.3.2-47 |
| 14.3.2-11b | Reflood Transient - Core and Downcomer Water Levels - DECLG (CD = 0.6) | 14.3.2-48 |
| 14.3.2-11c | Reflood Transient - Core and Downcomer Water Levels - DECLG (CD = 0.4) | 14.3.2-49 |
| 14.3.2-12a | Accumulator Flow (Blowdown) - DECLG (CD = 0.8) | 14.3.2-50 |
| 14.3.2-12b | Accumulator Flow (Blowdown) - DECLG (CD = 0.6) | 14.3.2-51 |
| 14.3.2-12c | Accumulator Flow (Blowdown) - DECLG (CD = 0.4) | 14.3.2-52 |
| 14.3.2-13a | Pumped ECCS Flow (Reflood) - (CD = 0.8) | 14.3.2-53 |
| 14.3.2-13b | Pumped ECCS Flow (Reflood) - (CD = 0.6) | 14.3.2-54 |
| 14.3.2-13c | Pumped ECCS Flow (Reflood) - (CD = 0.4) | 14.3.2-55 |
| 14.3.2-14a | Containment Pressure - DECLG (CD = 0.8) | 14.3.2-56 |
| 14.3.2-14b | Containment Pressure - DECLG (CD = 0.6) | 14.3.2-57 |

LIST OF FIGURES
(continued)

| Figure | Description | Page |
|------------|---|-----------|
| 14.3.2-14c | Containment Pressure - DECLG (CD = 0.4) | 14.3.2-58 |
| 14.3.2-15 | Core Power Transient - DECLG (CD = 0.4) | 14.3.2-59 |
| 14.3.2-16 | Break Energy Released to Containment - DECLG (CD = 0.4) | 14.3.2-60 |
| 14.3.2-17 | Containment Wall Condensing Heat Transfer Coefficient - DECLG (CD = 0.4) | 14.3.2-61 |



14.3 PRIMARY SYSTEM PIPE RUPTURES

14.3.1 Loss Of Reactor Coolant From Small Ruptured Pipes Or From Cracks in Large Pipes Which Actuates Emergency Core Cooling System

Identification of Causes and Accident Description

A loss of coolant accident is defined as a rupture of the reactor coolant system piping or of any line connected to the system up to the first closed valve. Ruptures of small cross section will cause loss of the coolant at a rate which can be accommodated by the charging pumps which would maintain an operational water level in the pressurizer permitting the operator to execute an orderly shutdown. A moderate quantity of coolant containing such radioactive impurities as would normally be present in the coolant, would be released to the containment.

The maximum break size for which the normal makeup system can maintain the pressurizer level is obtained by comparing the calculated flow from the reactor coolant system through the postulated break against the charging pump makeup flow at normal reactor coolant system pressure i.e., 2250 psia. A makeup flow rate from one charging pump is typically adequate to sustain pressurizer pressure at 2250 psia for a break through a 3/8 in. diameter hole. This break results in a loss of approximately 17.5 lb/sec.

Should a larger break occur, depressurization of the reactor coolant system causes fluid to flow to the reactor coolant system from the pressurizer resulting in a pressure and level decrease in the pressurizer. Reactor trip occurs when the pressurizer low pressure trip setpoint is reached. The consequences of the accident are limited in two ways:

1. Reactor trip and borated water injection complement void formation in causing rapid reduction of nuclear power to a residual level corresponding to the delayed fission and fission product decay.

2. Injection of borated water ensures sufficient flooding of the core to prevent excessive clad temperatures.

Before the break occurs, the plant is in an equilibrium condition, i.e., the heat generated in the core is being removed via the secondary system. During blowdown, heat from decay, hot internals and the vessel continues to be transferred to the reactor coolant system. The heat transfer between the reactor coolant system and the secondary system may be in either direction depending on the relative temperatures. In the case of continued heat addition to the secondary, system pressure increases and steam dump may occur. Makeup to the secondary side is automatically provided by the auxiliary feedwater pumps. The safety injection signal stops normal feedwater flow by closing the main feedwater line isolation valves and initiates emergency feedwater flow by starting auxiliary feedwater pumps. The secondary flow aids in the reduction of reactor coolant system pressure. When the RCS depressurizes to 715 psia, the accumulators begin to inject water into the reactor coolant loops. The reactor coolant pumps are assumed to be tripped at the initiation of the accident and effects of pump coastdown are included in the blowdown analyses.

Analysis of Effects and Consequences

Method of Analysis

For small breaks less than 1.0 ft² the WFLASH digital computer code References 1, 2 and 3, is employed to calculate the transient depressurization of the reactor coolant system as well as to describe the mass and enthalpy of flow through the break. The analysis was performed for an assumed steam generator tube plugging level of 12% and a reactor coolant system loop flowrate of 84,000 gpm.

Small Break LOCA Analysis Using WFLASH

The WFLASH program used in the analysis of the small break loss of coolant accident is an extension of the FLASH-4 code, Reference 3,



developed at the Westinghouse Bettis Atomic Power Laboratory. The WFLASH program permits a detailed spatial representation of the reactor coolant system.

The reactor coolant system is nodalized into volumes interconnected by flowpaths. Both the broken loop and the intact loop are modeled explicitly for two loop plants. The transient behavior of the system is determined from the governing conservation equations of mass, energy, and momentum applied throughout the system. A detailed description of WFLASH is given in Reference 1 and 2.

The use of WFLASH in the analysis involves, among other things, the representation of the reactor core as a heated control volume with the associated bubble rise model to permit a transient mixture height calculation. The multi-node capability of the program enables an explicit and detailed spatial representation of various system components. In particular, it enables a proper calculation of the behavior of the loop seal during a loss-of-coolant transient.

Safety injection flow rate to the reactor coolant system as a function of the system pressure is used as part of the input. The Safety Injection (SI) system was assumed to be delivering to the RCS, 25 seconds after the generation of a safety injection signal.

For these analyses, the SI delivery considers pumped injection flow which is depicted in Figures 14.3.1-1a and 14.3.1-1b as a function of RCS pressure. Figure 14.3.1-1a represents injection flow from one HHSI pump based on performance curves degraded 5% from the design head. Figure 14.3.1-1b represents injection flow from one LHSI pump. The 25 second delay includes time required for diesel startup and loading of the safety injection pumps onto the emergency buses. Also minimum Safeguards Emergency Core Cooling System capability and operability has been assumed in these analyses.

Peak clad temperature analyses are performed with the LOCTA IV code, References 2 and 4. Input for the code is obtained from the WFLASH code which determines the RCS pressure, fuel rod power history, steam flow past the uncovered part of the core and mixture height history.

Figure 14.3.1-2 presents the axial power shape utilized to perform the small break analysis presented here. This power shape was chosen because it provides an appropriate distribution of power versus core height and also linear power is maximized in the upper regions of the reactor core (10 ft. to 12 ft.). This power shape is skewed to the top of the core with the peak linear power occurring at the 10 ft. core elevation. The linear power for this power shape above 10 ft. essentially matches the shape of the generic operation F_Q envelope for normal plant operation and hence linear power is maximized for the 10 ft. core elevation and above. This is limiting for small break analysis because of the uncover process for small break. As the core uncovers, the cladding in the upper elevation of the core heats up and is sensitive to the linear power at that elevation.

The cladding temperatures in the lower elevations of the core, below the two phase mixture height, remains low. The peak clad temperature occurs above 10 ft.

Results of Small Break Analysis

This section presents results of the limiting break size in terms of highest peak clad temperature. The worst break size (small break) is a 6 in. diameter break. The depressurization transient for this break is shown in Figure 14.3.1-3. The extent to which the core is uncovered is shown in Figure 14.3.1-4.

During the earlier part of the small break transient, the effect of the break flow is not strong enough to overcome the flow maintained by the reactor coolant pumps through the core as they are coasting down



following reactor trip. Therefore, upward flow through the core is maintained. The resultant heat transfer cools the fuel rod and clad to very near the coolant temperatures as long as the core remains covered by a two phase mixture.

The maximum hot spot clad temperature calculated during the transient is 1092 °F including the effects of fuel densification as described in Reference 5. The peak clad temperature transient is shown in Figure 14.3.1-5 for the worst break size, i.e., the break with the highest peak clad temperature. The steam flow rate for the worst break is shown on Figure 14.3.1-6. When the mixture level drops below the top of the core, the steam flow computed in WFLASH provides cooling to the upper portion of the core. The rod film coefficients for this phase of the transient are given in Figure 14.3.1-7. The hot spot fluid temperature for the worst break is shown in Figure 14.3.1-8.

The reactor scram time is equal to the reactor trip signal time plus 4.4 seconds for signal transmission and rod insertion. During this period, the reactor is conservatively assumed to operate at rated power.

Additional Break Sizes

Additional break sizes were analyzed. Figures 14.3.1-9a and 14.3.1-9b present the RCS pressure transient for the 4 and 8 in. breaks respectively and Figures 14.3.1-10a and 14.3.1-10b present the volume history (mixture height) plots for these breaks. The peak clad temperatures for these cases are less than the peak clad temperature of the 6 in. break. The peak clad temperatures for these cases are given in Figures 14.3.1-11a and 14.3.1-11b.

Conclusions

Analyses presented in this section show that the high head and low head portions of the emergency core cooling system, together with

accumulators, provide sufficient core flooding to keep the calculated peak clad temperatures below required limits of 10 CFR 50.46. Hence, adequate protection is afforded by the emergency core cooling system in the event of a small break loss of coolant accident. Table 14.3.1-1 presents the results of these analyses.

REFERENCES - Section 14.3.1

1. Esposito, V.J., Kesavan, D., Maul, B.A., "WFLASH-A FORTRAN IV Computer Program for Simulation of Transients in a Multi-Loop PWR", WCAP-8261, Rev. 1, July, 1974.
2. Skwarek, R.J., Johnson, W.J., and Meyer, P.E., "Westinghouse Emergency Core Cooling System Small Break October 1975 Model," WCAP-8970-P-A (Proprietary) and WCAP-8971-A (Non-Proprietary) January 1979.
3. Porsching, T.A., Murphy, J.H., Redfield, J.A., and Davis, V.C., "FLASH-4: A Fully Implicit FORTRAN-IV Program for the Digital Simulation of Transients in a Reactor Plant", WAPD-TM-84; Bettis Atomic Power Laboratory, March, 1969.
4. Bordelon, F.M., et al., "LOCTA-IV Program: Loss-of-Coolant Transient Analysis", WCAP-8301 (Proprietary Version), WCAP-8305 (Non-Proprietary Version), June 1974.
5. Hellman, J.M., "Fuel Densification Experimental Results and Model for Reactor Application", WCAP-8219, October, 1973.

TABLE 14.3.1-1

SMALL BREAKTIME SEQUENCE OF EVENTS

| <u>Event</u> | <u>4 in.</u> | <u>6 in.</u> | <u>8 in.</u> |
|-------------------------------------|--------------|--------------|--------------|
| Start | 0.0 | 0.0 | 0.0 |
| Reactor Trip Signal (Sec.) | 12.5 | 10.0 | 9.5 |
| Top of Core Uncovered (Sec.) | 165. | 74. | 69. |
| Accumulator Injection Begins (Sec.) | 323. | 138. | 75. |
| PCT Occurs (Sec.) | 333.7 | 121.4 | 92.0 |
| Top of Core Covered (Sec.) | 374. | 168. | 101. |

TABLE 14.3.1-2

SMALL BREAK ANALYSIS INPUT AND RESULTS

| <u>Results</u> | <u>4 in.</u> | <u>6 in.</u> | <u>8 in.</u> |
|--|--------------|--------------|--------------|
| Peak Clad Temp. °F | 976 | 1092 | 758 |
| Peak Clad Location Ft. | 11.75 | 10.75 | 10.75 |
| Local Zr/H ₂ O Rxn (max)% | 0.0678 | 0.0689 | 0.0675 |
| Local Zr/H ₂ O Location Ft. | 11.75 | 10.75 | 10.75 |
| Total Zr/H ₂ O Rxn % | <0.3 | <0.3 | <0.3 |
| Hot Rod Burst Time sec | no burst | no burst | no burst |
| Hot Rod Burst Location Ft. | no burst | no burst | no burst |

Calculation

| | |
|---|---------------------|
| Core Power MWt 102% of | 1520 |
| Peak Linear Power kw/ft 102% of | See Figure 14.3.1-2 |
| Peaking Factor (At License Rating) | See Figure 14.3.1-2 |
| Accumulator Water Volume Ft. ³ | 1100 |



FIGURE 14.3.1-1a
HIGH HEAD SAFETY INJECTION FLOW RATE
One Pump in Operation

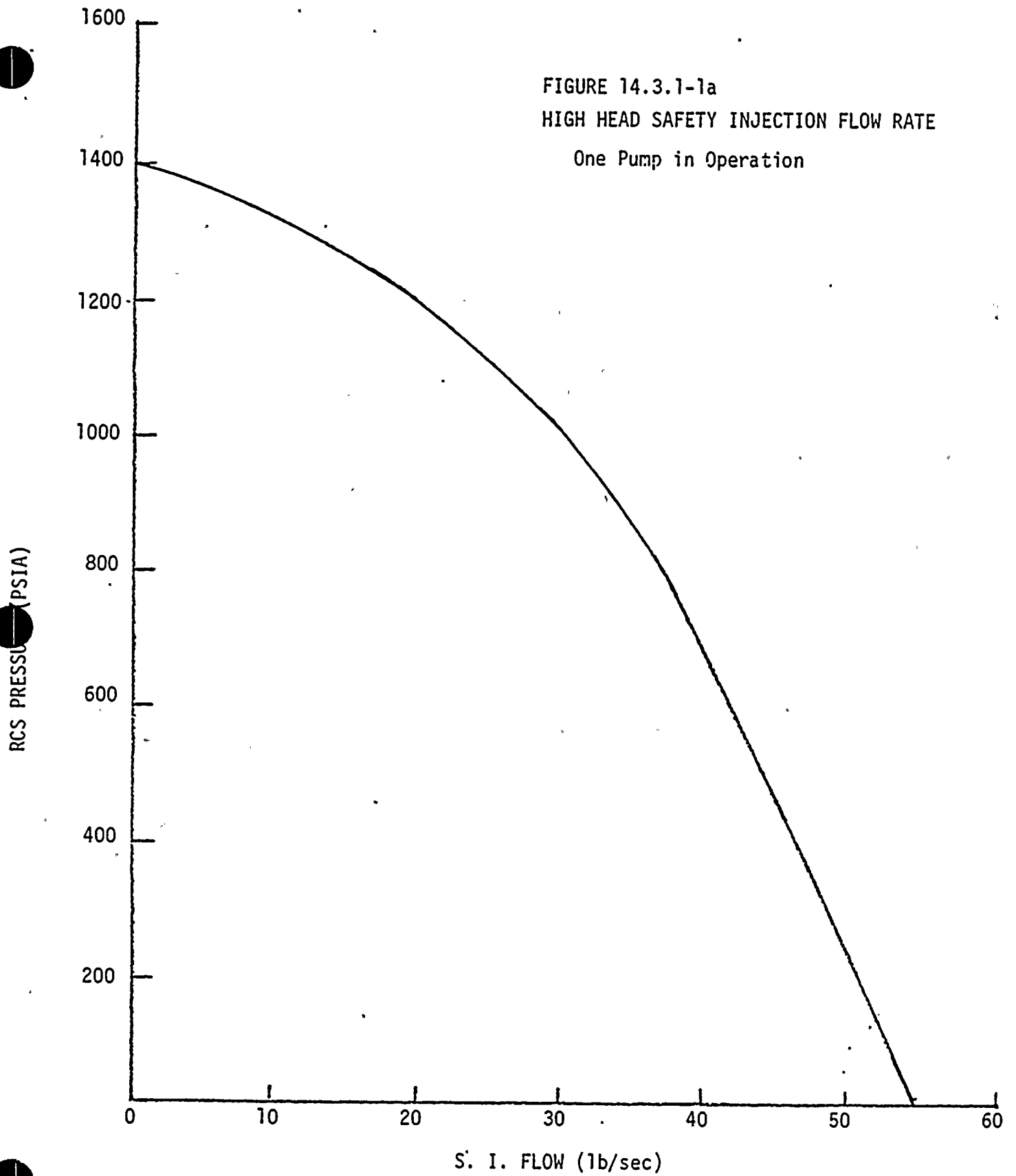


FIGURE 14.3.1-1b
LOW HEAD SAFETY INJECTION FLOW RATE
One Pump in Operation

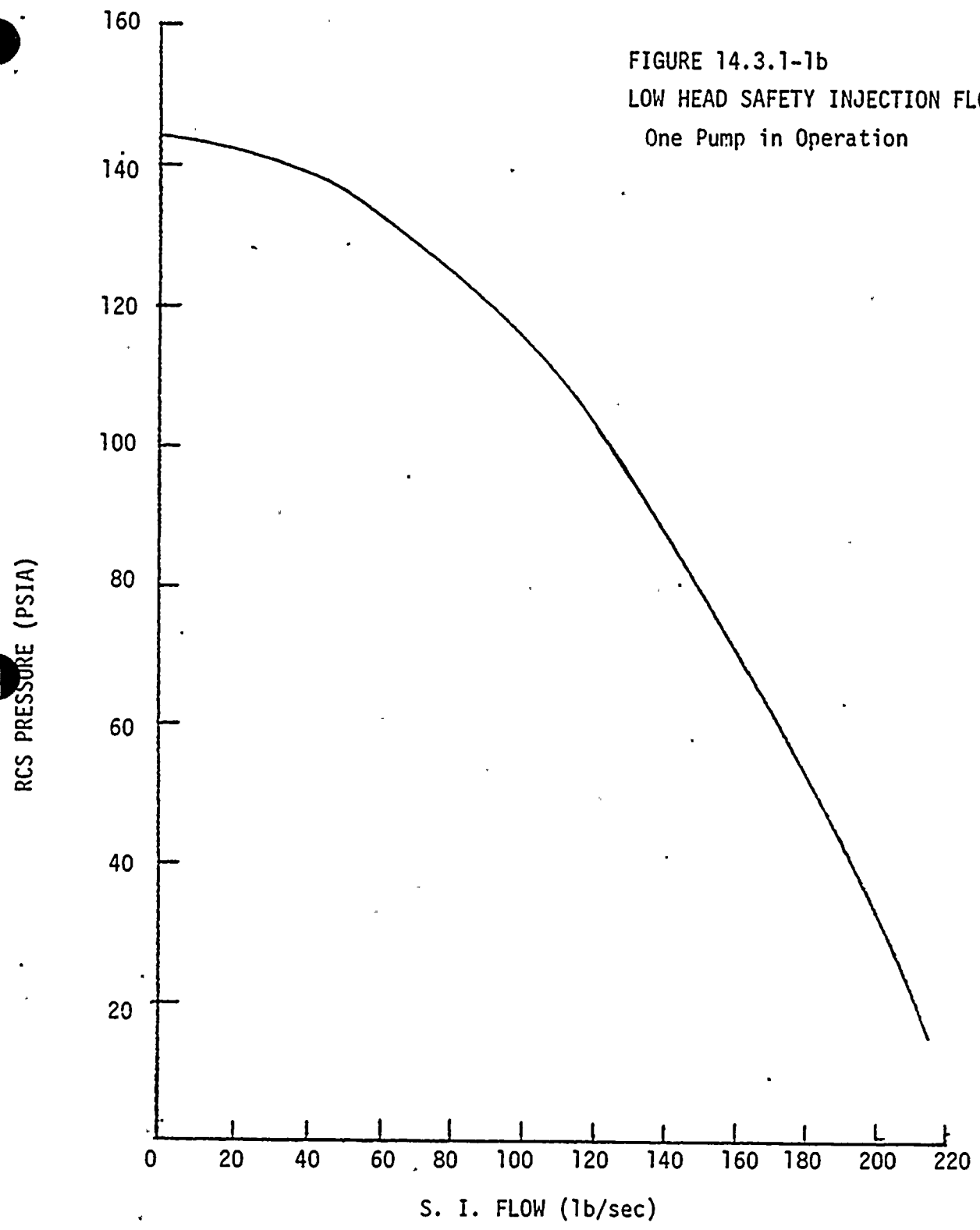


FIGURE 14.3.1-2
HOT ROD AXIAL POWER SHAPE

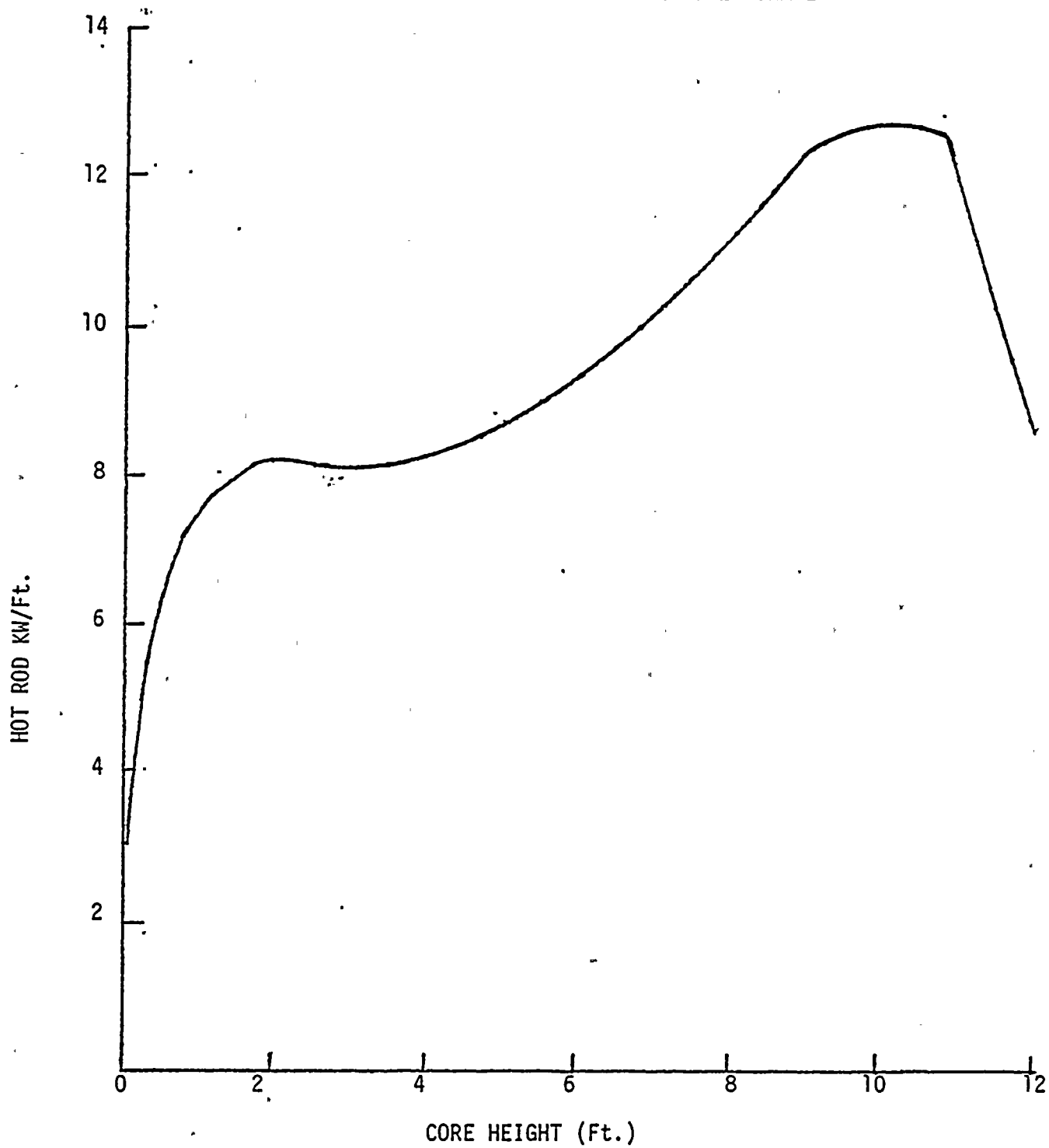


FIGURE 14.3.1-3

DEPRESSURIZATION TRANSIENT (6 INCH)

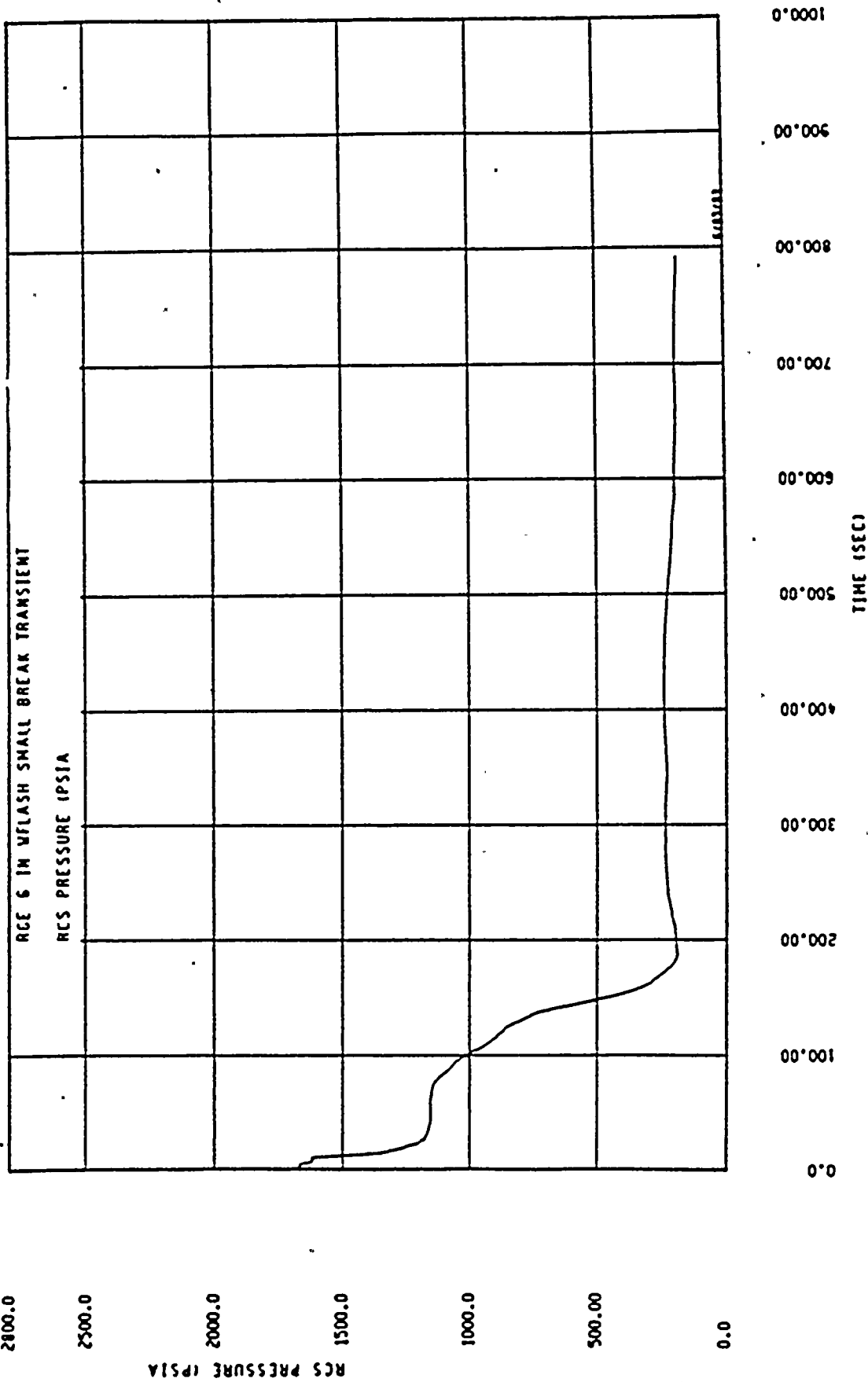
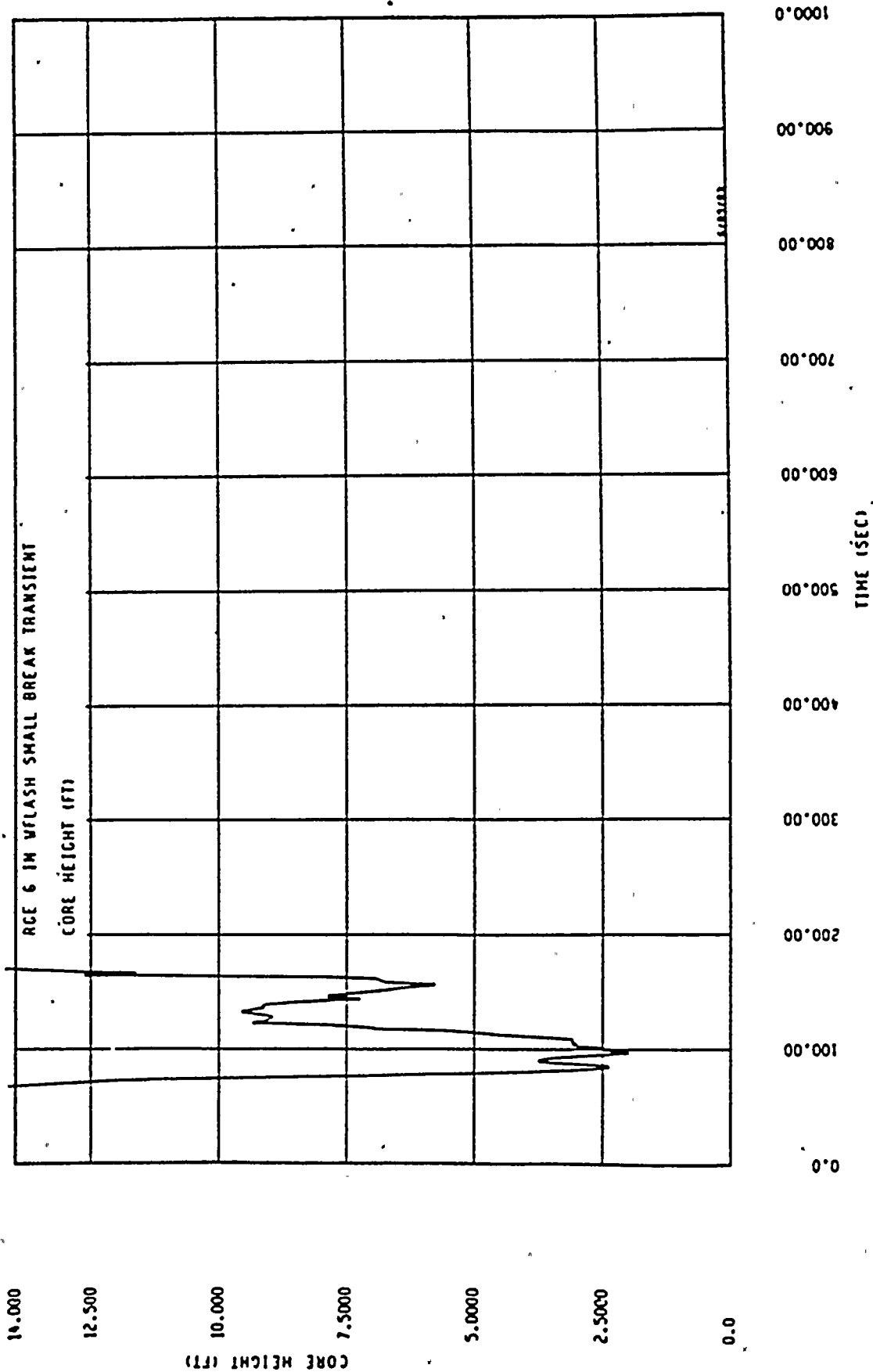




FIGURE 14.3.1-4
CORE MIXTURE HEIGHT (6 INCH)



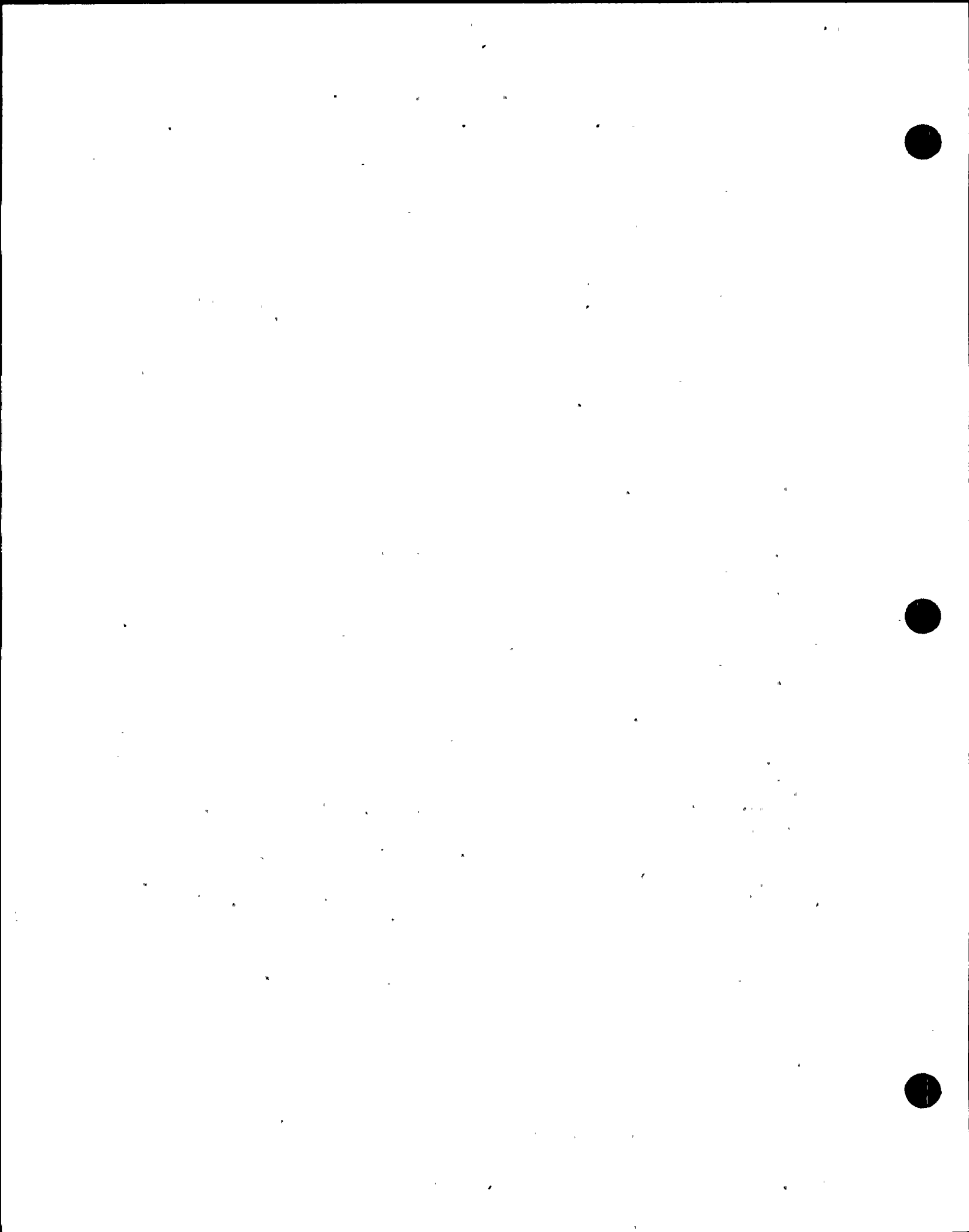


FIGURE 14.3.1-5
 PEAK CLAD TEMPERATURE TRANSIENT (6 INCH)

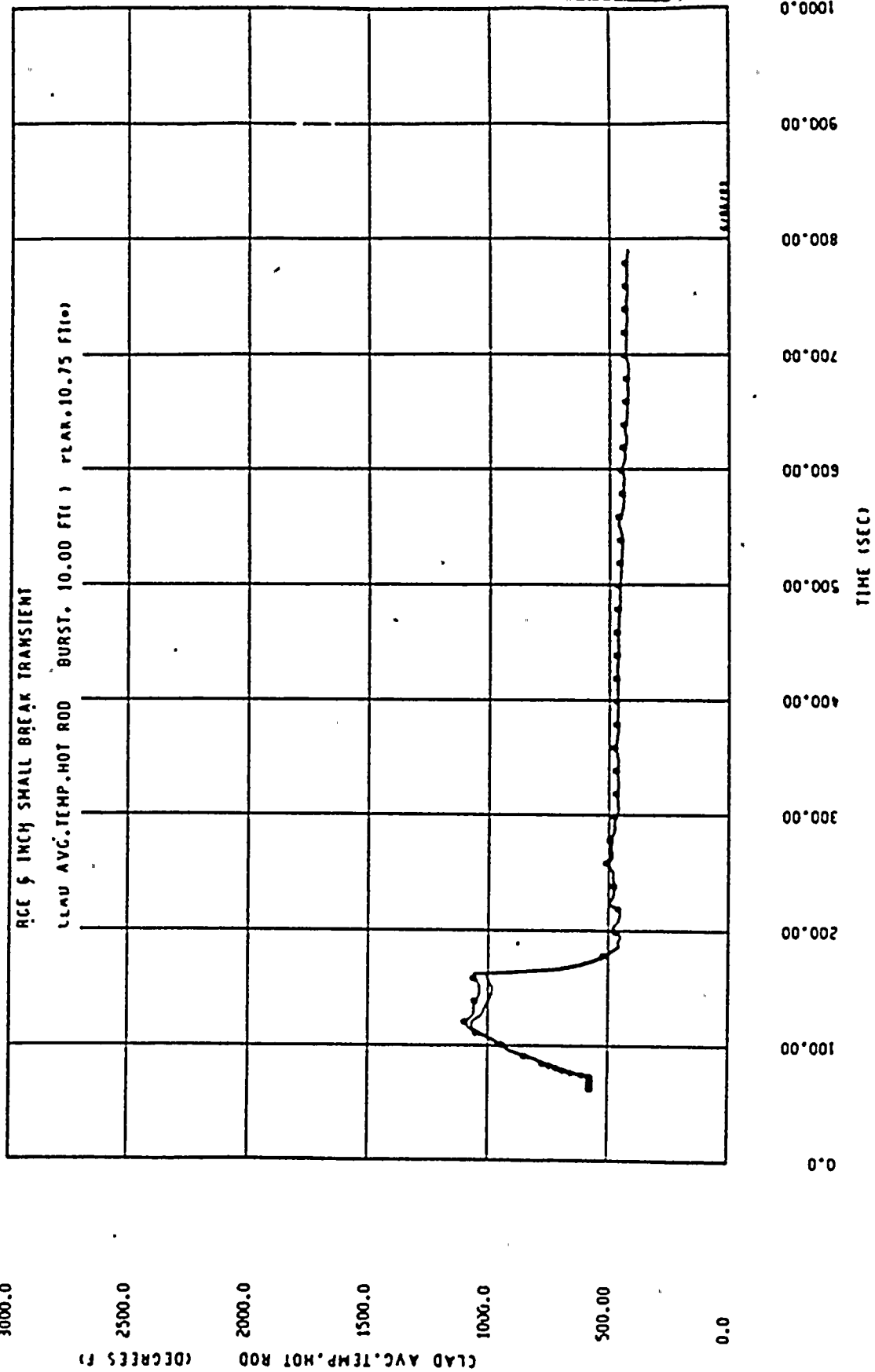


FIGURE 14.3.1-6

STEAM FLOW RATE

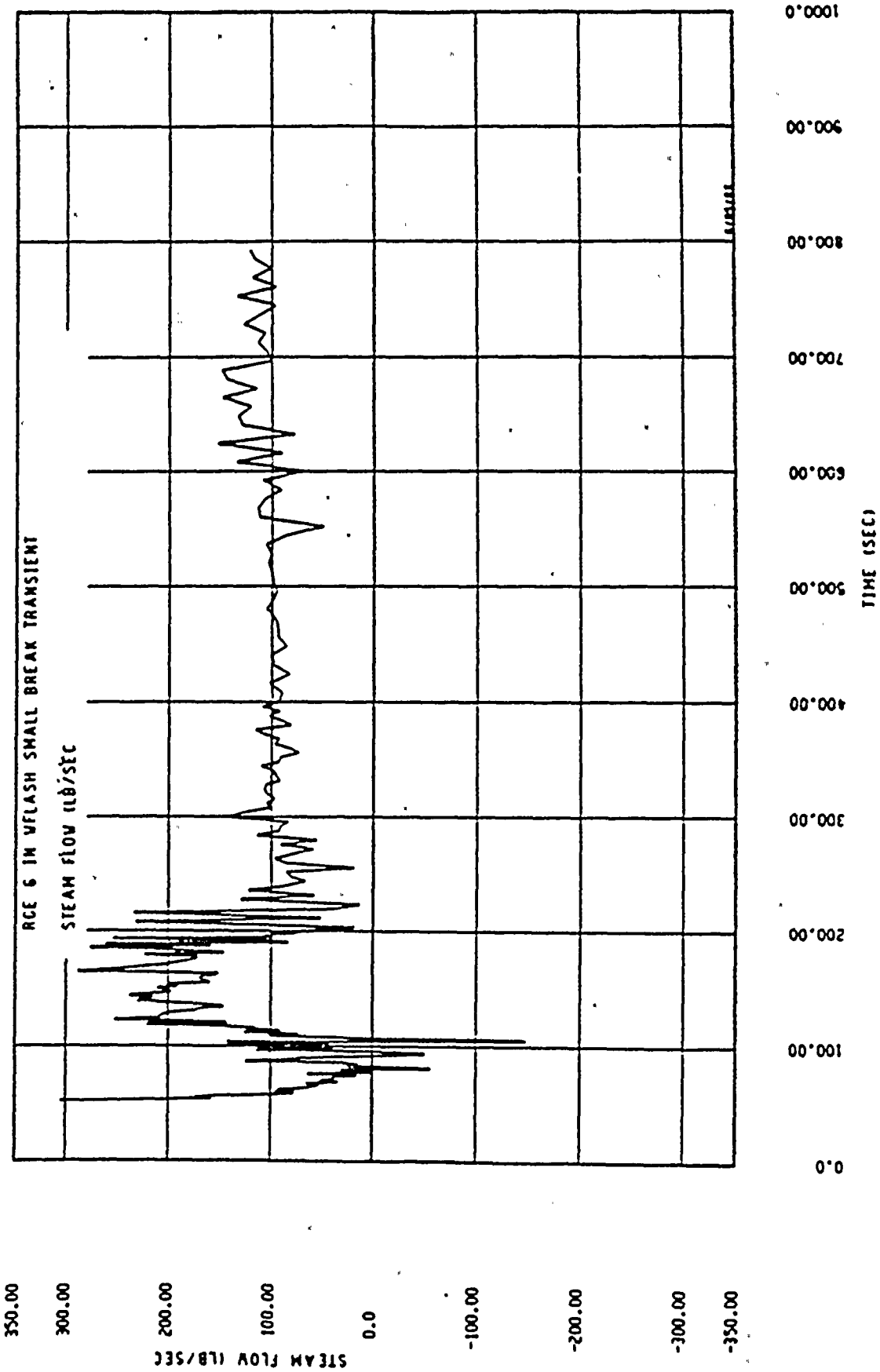
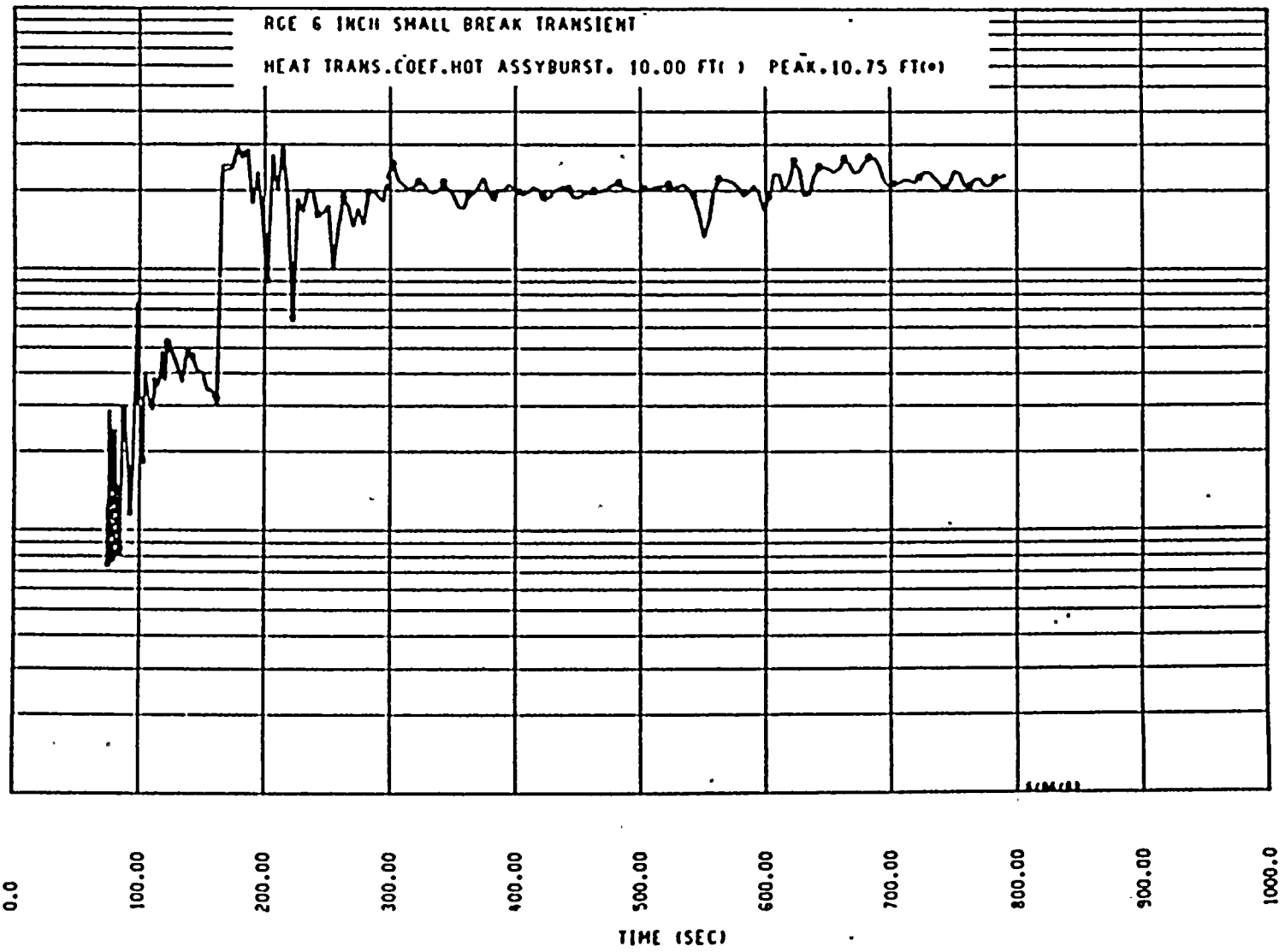




FIGURE 14.3.1-7
ROD FILM COEFFICIENTS

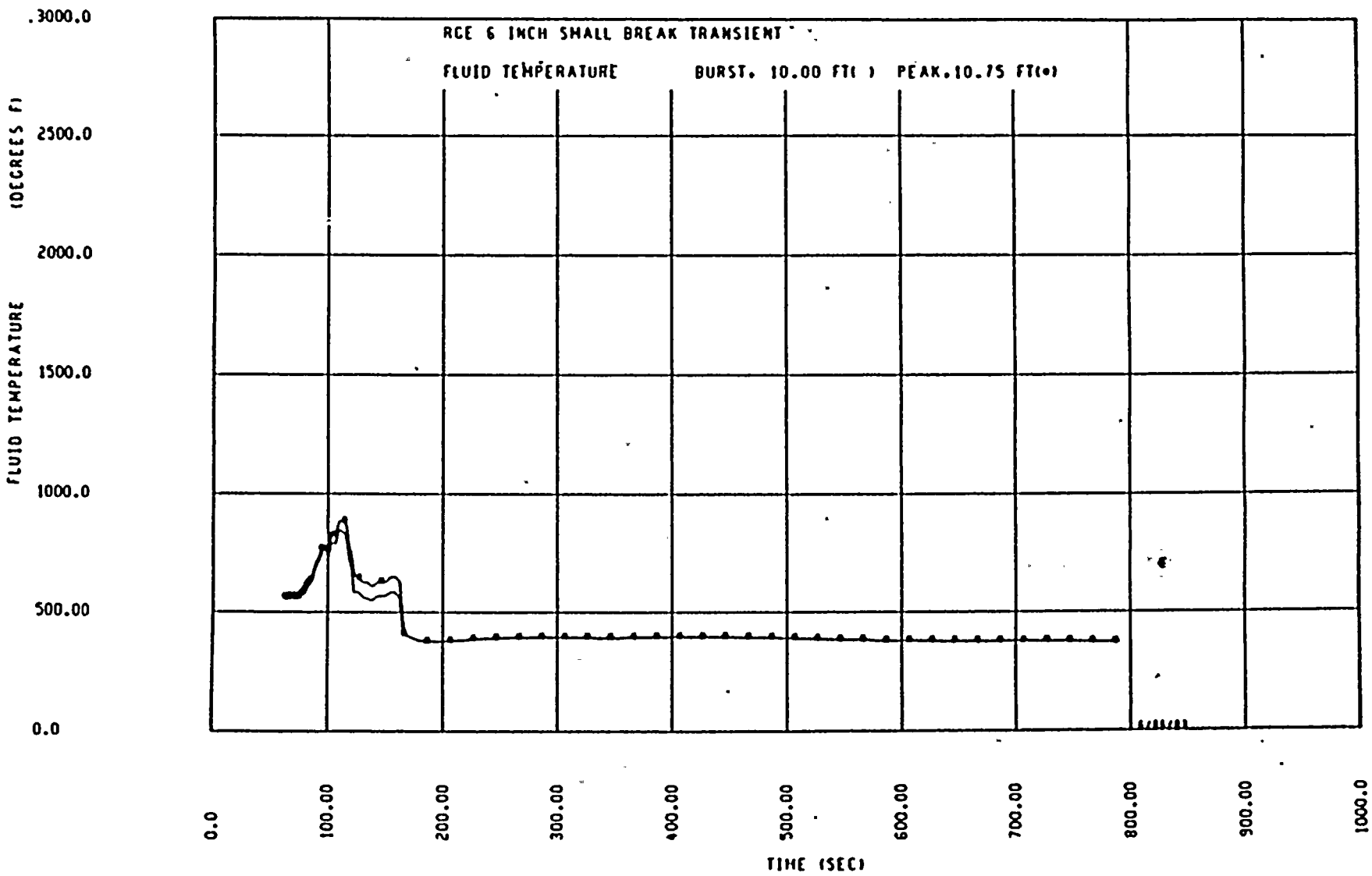


0458L:6

14.3.1-17

HEAT TRANS. COEF. HOT ASSY BURST. 10.00 FT () PEAK. 10.75 FT ()

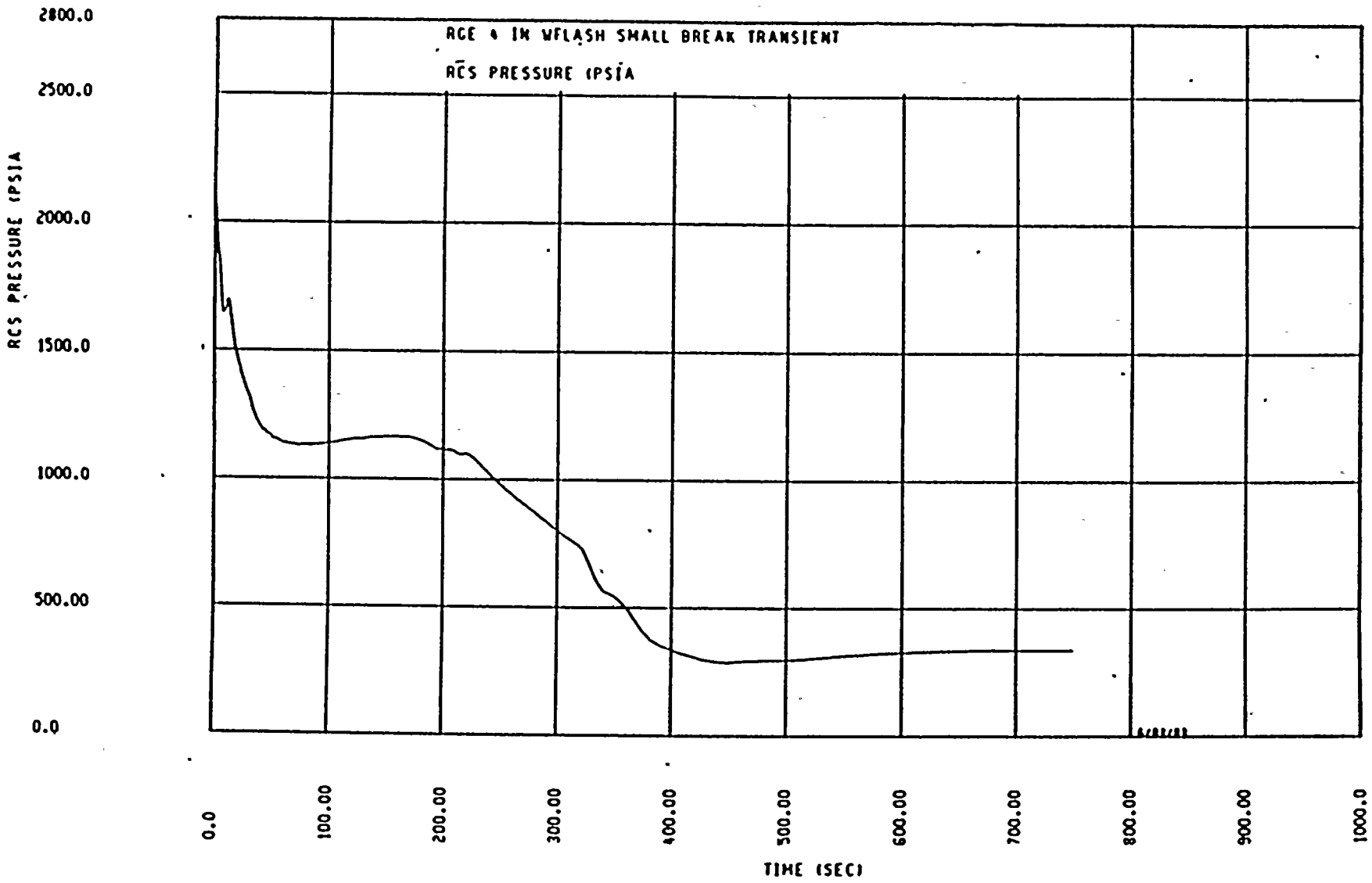
FIGURE 14.3.1-8
HOT SPOT FLUID TEMPERATURE



0458L:6

14.3.1-18

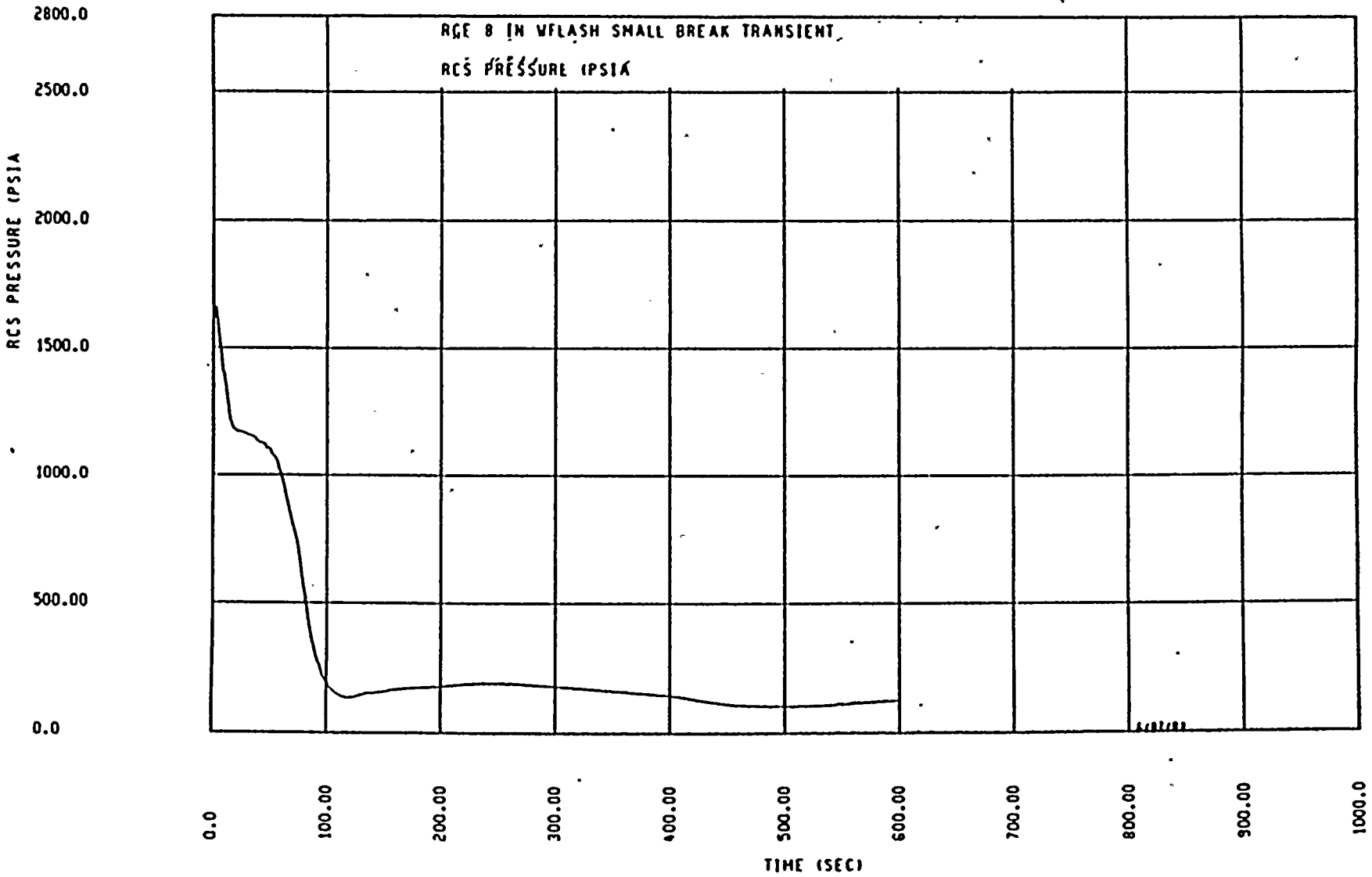
FIGURE 14.3.1-9a
DEPRESSURIZATION TRANSIENT (4 INCH)



0458L:6

14.3.1-19

FIGURE 14.3.1-9 b
DEPRESSURIZATION TRANSIENT (8 INCH)

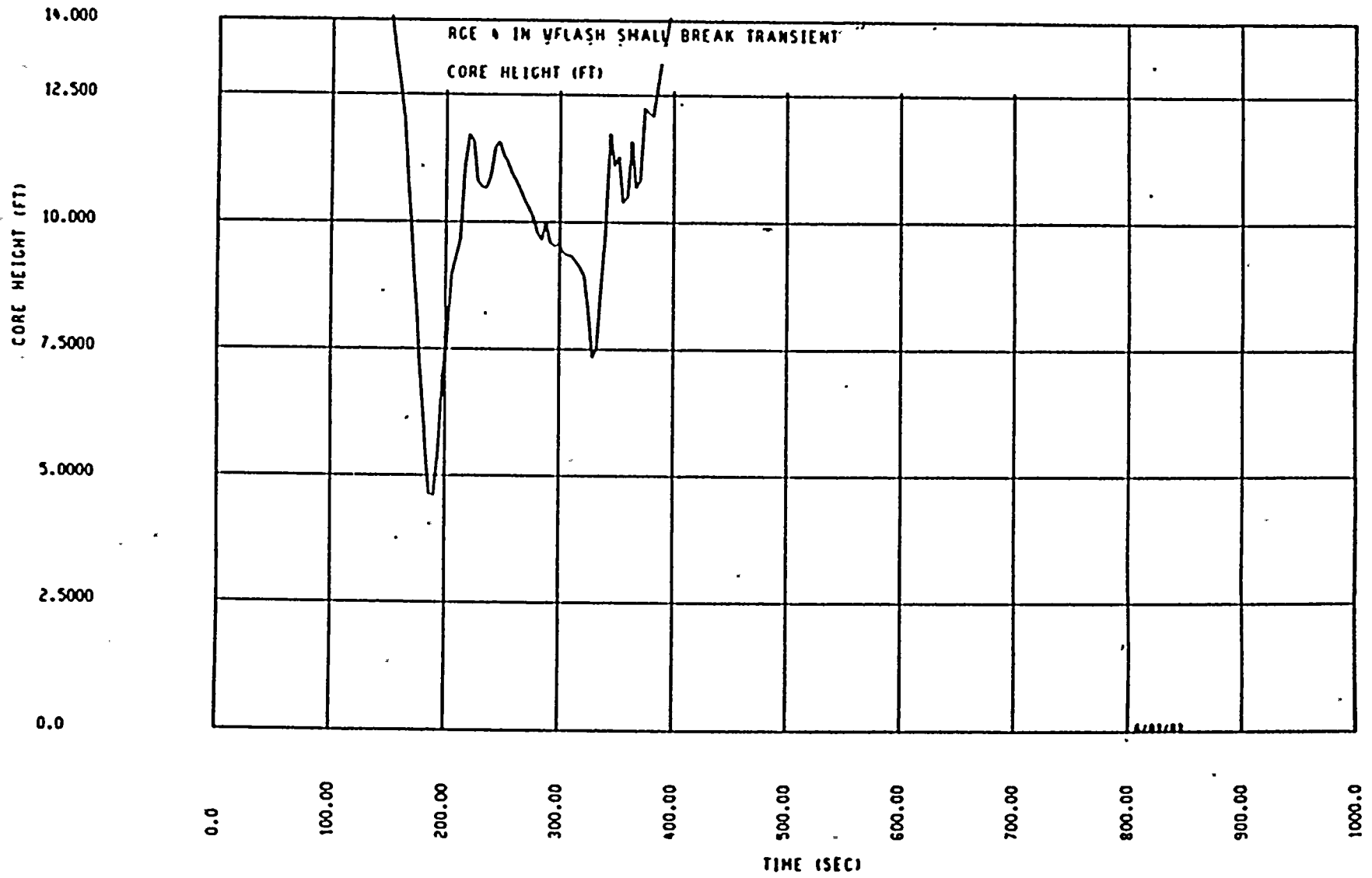


0458L:6

14.3.1-20



FIGURE 14.3.1-10a
CORE MIXTURE HEIGHT (4 INCH)

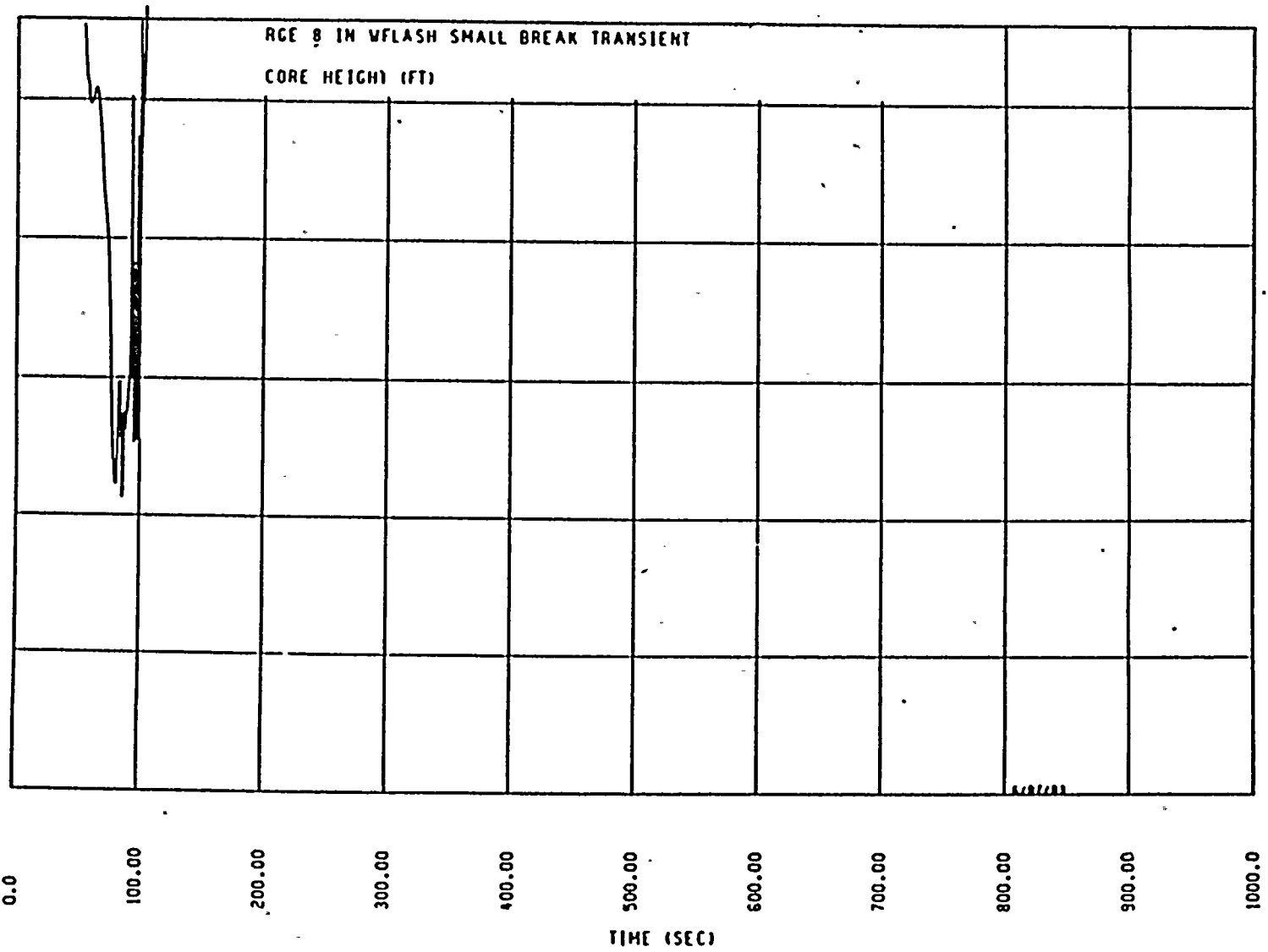


0458L:6

14.3.1-21



FIGURE 14.3.1-10b
CORE MIXTURE HEIGHT (8 INCH)



0458L:6

CORE HEIGHT (FT)

14.3.1-22



FIGURE 14.3.1-11a

CLAD TEMPERATURE TRANSIENT (4 INCH)

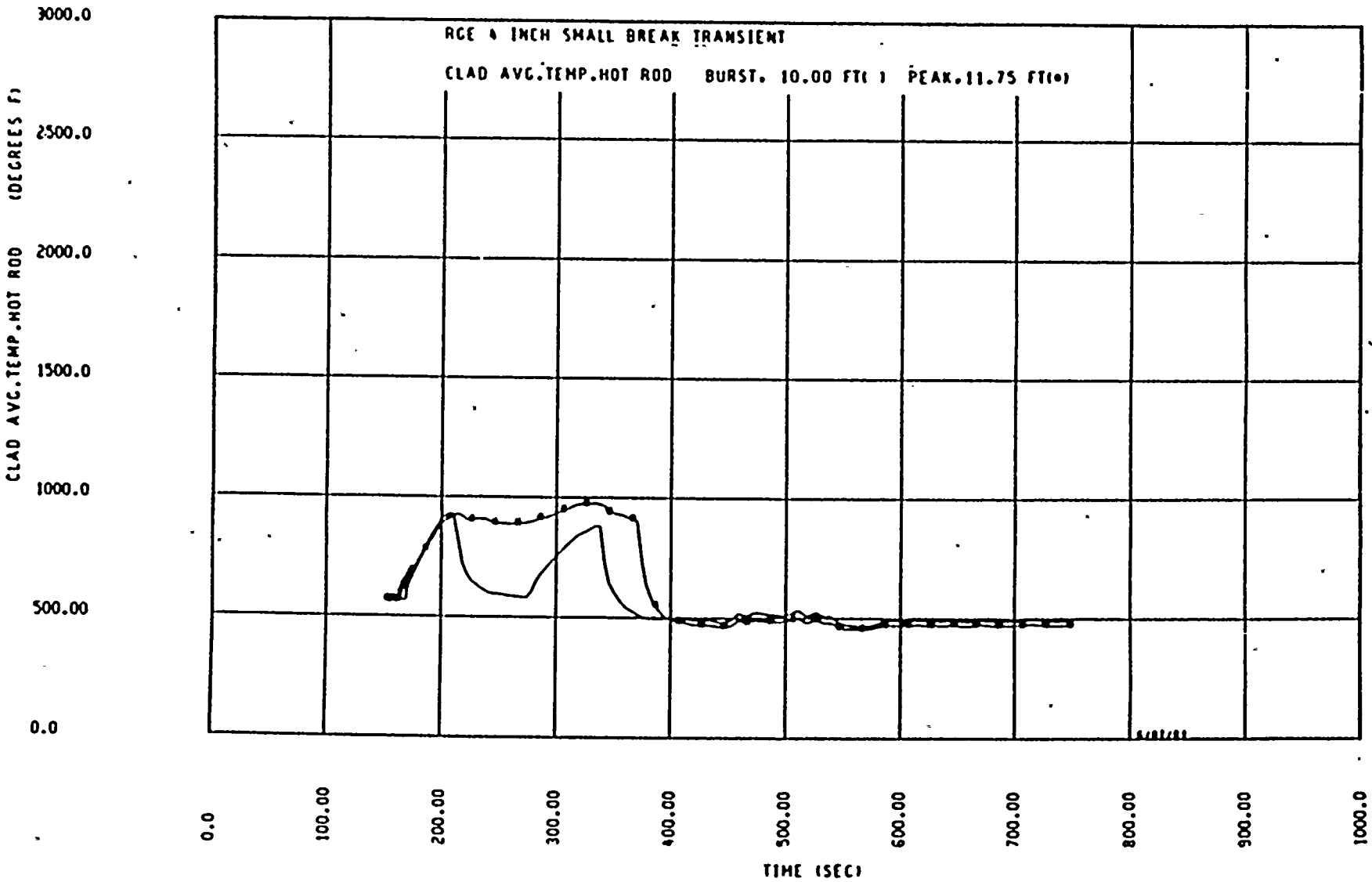
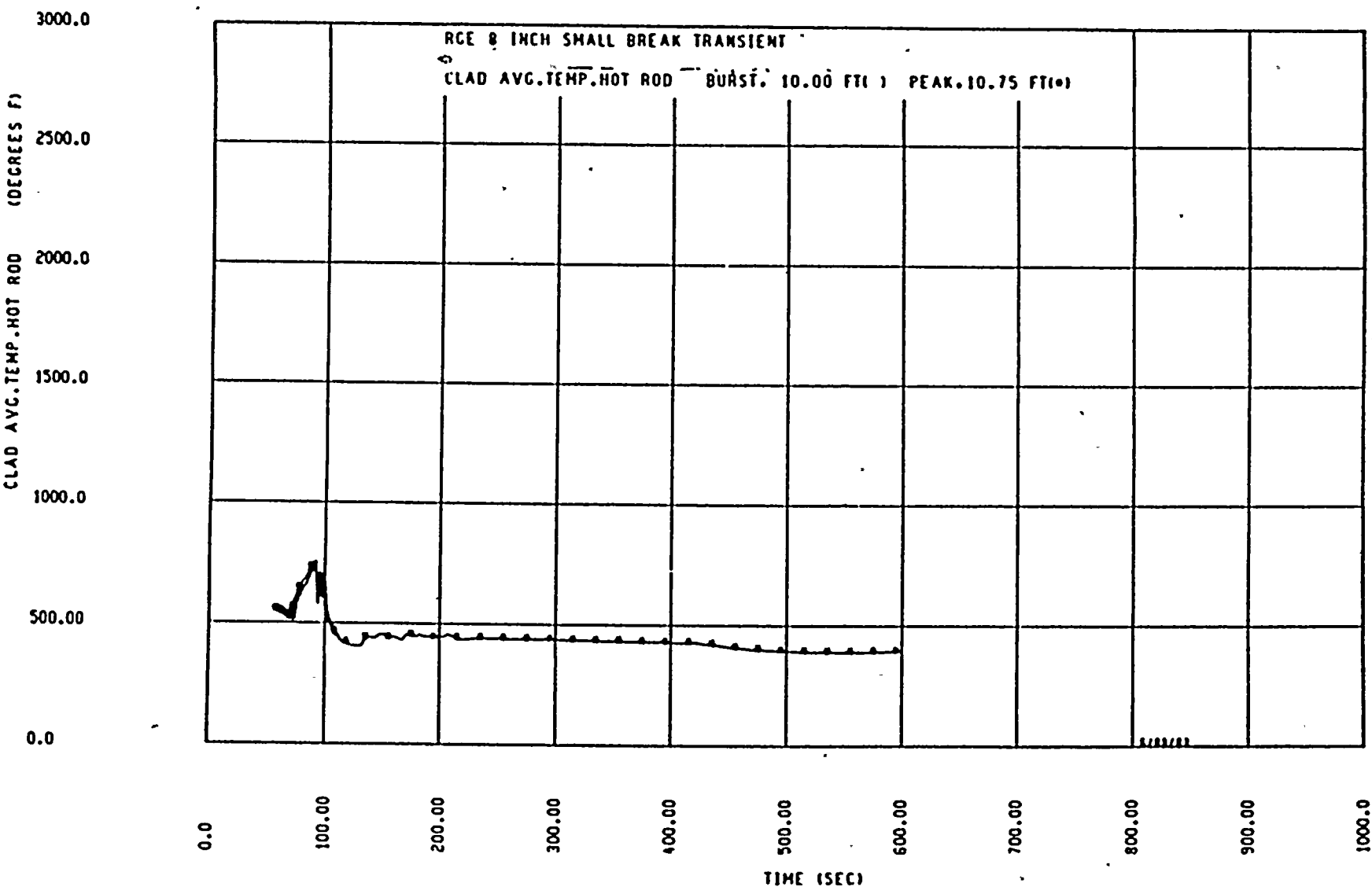




FIGURE 14.3.1-11b

CLAD TEMPERATURE TRANSIENT (8 INCH)



0458L:6

14.3.1-24

14.3.2 Major Reactor Coolant System Pipe Ruptures (Loss of Coolant Accident)

The analysis specified by 10 CFR 50.46, "Acceptance Criteria for, Emergency Core Cooling Systems for Light Water Power Reactors", Reference 1, is presented in this section. The results of the loss of coolant accident analysis are shown in Table 14.3.2-2 and show compliance with the Acceptance Criteria. The analytical techniques used are in compliance with Appendix K of 10 CFR 50, and are described in listed references. The results for the small break loss-of-coolant accident are presented in Section 14.3.1 and are in conformance with 10 CFR 50.46 and Appendix K of 10 CFR 50.

Should a major break occur, depressurization of the reactor coolant system results in a pressure decrease in the pressurizer. Reactor trip signal occurs when the pressurizer low pressure trip setpoint is reached. A safety injection system signal is actuated when the appropriate setpoint is reached. These countermeasures will limit the consequences of the accident in two ways:

1. Reactor trip and borated water injection complement void formation in causing rapid reduction of power to a residual level corresponding to fission product decay heat.
2. Injection of borated water provides heat transfer from the core and prevents excessive clad temperatures.

At the beginning of the blowdown phase, the entire reactor coolant system contains subcooled liquid which transfers heat from the core by forced convection with some fully developed nucleate boiling. After the break develops, the time to departure from nucleate boiling is calculated, consistent with Appendix K of 10 CFR 50. Thereafter, the

core heat transfer is unstable, with both nucleate boiling and film boiling occurring. As the core becomes uncovered, both turbulent and laminar forced convection and radiation are considered as core heat transfer mechanisms.

When the reactor coolant system pressure falls below 715 psia the accumulators begin to inject borated water. The conservative assumption is made that accumulator water injected bypasses the core and goes out through the break until the termination of bypass. This conservatism is again consistent with Appendix K of 10 CFR 50.

Core Power Transient During Blowdown

The core power transient during blowdown for large breaks is evaluated using the SATAN-VI computer code. This code is discussed in detail in WCAP-8306, Reference 3.

Thermal Analysis

Performance Criteria for Emergency Core Cooling System

The reactor is designed to withstand thermal effects caused by a loss of coolant accident including the double ended severance of the largest reactor cooling system cold leg pipe. The reactor core and internals together with the emergency core cooling system are designed so that the reactor can be safely shutdown and the essential heat transfer geometry of the core preserved following the accident.

The emergency core cooling system, even when operating during he injection mode with the most severe single failure, is designed to meet the Acceptance Criteria.



Method of Thermal Analysis

The description of the various aspects of the LOCA analysis is given in the listed references. This document describes the major phenomena modeled, the interfaces among the computer codes and features of the codes which maintain compliance with the Acceptance Criteria. The SATAN-VI, WREFLOOD, and LOCTA-IV codes used in this analysis are described in detail in WCAP-8306, Reference 3, WCAP-8171, Reference 5 and WCAP-8305, Reference 4, respectively. The containment parameters used in the containment analysis code to determine the ECCS backpressure are presented in Table 14.3.2-3. The containment pressure analysis code (COCO) is described in WCAP-8326, Reference 6.

The large break analysis was performed with the NRC Approved 1981 Version of the Evaluation Model, Reference 24, which includes modifications delineated in WCAP-9220-P-A and WCAP-9221-A (1981), and complies with Appendix K of 10 CFR 50.46. The analysis was performed for an assumed steam generator tube plugging level of 12% and a reactor coolant system loop flow rate of 84,000 gpm.

Results

Table 14.3.2-2 presents the peak clad temperatures and hot spot metal reaction for a large break over a range of discharge coefficients or break sizes. This range of discharge coefficients was determined to include the limiting case of peak clad temperature from the sensitivity studies.

The analysis of the loss of coolant accident is performed at 102% of rated core power. The peak linear power, and core power used in the analyses are given in Table 14.3.2-2. The equivalent core parameter at the license application power level are also shown in Table 14.3.2-2. Since there is margin between the value of the peak linear power density used in this analysis and the value expected in operation, a low peak clad temperature would be obtained by using the peak linear power density expected during operation.

For the results discussed below, the hot spot is defined to be the location of maximum peak clad temperature. This location is given in Table 14.3.2-2 for each discharge coefficient or break size analyzed.

Tables 14.3.2-4 and 14.3.2-5 present reflood mass and energy releases to the containment and the broken loop accumulator mass and energy release to the containment, respectively. Figures 14.3.2-1 through 14.3.2-16 present the transients for the principal parameters for the discharge coefficients analyzed. The following items are noted:

Figures 14.3.2-1a through 14.3.2-3c Quality, mass velocity, and clad heat transfer coefficient for the hotspot and burst locations.

Figures 14.3.2-4a through 14.3.2-6c Core pressure, break flow, and core pressure drop. The break flow is the sum of the flowrates from both ends of the guillotine break. The core pressure drop is taken as the pressure just before the core inlet to the pressure just beyond the core outlet.

Figures 14.3.2-7a through 14.3.2-9c Clad temperature, fluid temperature, and core flow. The clad and fluid temperatures are for the hotspot and burst locations.

Figures 14.3.2-10a through 14.3.2-10c Reflood Transient - Core Inlet Velocity

Figures 14.3.2-11a through 14.3.2-11c Reflood Transient - Core and Downcomer Water Levels

Figures 14.3.2-12a through 14.3.3-13a Emergency core cooling system flowrates, for both accumulator and pumped safety injection.

Figures 14.3.2-14a through 14.3.2-14c Containment pressure.

Figure 14.3.2-15 Core power

Figures 14.3.2-16 and 14.3.2-17 Break energy release during blowdown and the containment wall condensing heat transfer coefficient for the worst break.

The clad temperature analysis is based on a total peaking factor of 2.32. The hot spot metal-water reaction reached is 2.1% which is well below the embrittlement limit of 17% as required by 10 CFR 50.46. In addition, the total core metal-water reaction is less than 0.3% for all breaks as compared with the 1% criterion of 10 CFR 50.46.

The results of ECCS evaluations and sensitivity studies are reported in References 2, 7, 8, 9, 26, 12, 13, 16, 18, 20 and 24. These results are reported on a generic and plant specific basis.

Conclusions

For breaks up to and including the double ended severance of a reactor coolant pipe, the emergency core cooling system will meet the acceptance criteria as presented in 10 CFR 50.46. That is:

1. The calculated peak fuel element clad temperature is below the requirement of 2200 °F.
2. The amount of fuel element cladding that reacts chemically with water or steam does not exceed 1 percent of the total amount of Zircaloy in the reactor.

3. The clad temperature transient is terminated at a time when the core geometry is still amenable to cooling. The localized cladding oxidation limit of 17 percent is not exceeded during or after quenching.
4. The core remains amenable to cooling during and after the break.
5. The core temperature is reduced and decay heat is removed for an extended period of time as required by the long-lived radioactivity remaining in the core.

The time sequence of events for all breaks analyzed is shown in Table 14.3.2-1.

Based on the effect of upper plenum injection for Westinghouse designed 2 loop plants, a 21 °F increase in peak clad temperature results from assuming 14x14 OFA fuel for R. E. Ginna Unit 1. The methodology employed to develop this penalty was identical to that performed for previous LOCA analyses performed for the plant, Reference 19, and 27. Utilizing the present Westinghouse ECCS evaluation models, References 14, 15, 16 and 24, to analyze a postulated LOCA in R. E. Ginna Unit 1, results in a final peak clad temperature of 1854°F including the UPI penalty. It can be seen from the results contained herein that this ECCS analysis for R. E. Ginna remains in compliance with 10 CFR 50.46.

REFERENCES - Section 14.3.2

1. "Acceptance Criteria for Emergency Core Cooling Systems for Light Water Cooled Nuclear Power Reactors: 10 CFR 50.46 and Appendix K of 10 CFR 50.46," Federal Register, Volume 39, Number 3, January 4, 1974.
2. Bordelon, F.M., Massie, H.W., and Zordan, T.A., "Westinghouse ECCS Evaluation Model-Summary," WCAP-8339, July 1974.
3. Bordelon, F.M., et al., "SATAN-VI Program: Comprehensive Space-Time Dependent Analysis of Loss-of-Coolant", WCAP-8302 (Proprietary Version), WCAP-8306 (Non-Proprietary Version), June 1974.
4. Bordelon, F.M., et al., "LOCTA-IV Program: Loss-of-Coolant Transient Analysis", WCAP-8301 (Proprietary Version), WCAP-8305 (Non-Proprietary Version), June 1974.
5. Kelly, R.D., et al., "Calculational Model for Core Reflooding after a Loss-of-Coolant Accident (WREFLOOD Code)". WCAP-8170 (Proprietary Version), WCAP-8171 (Non-Proprietary Version), June 1974.
6. Bordelon, F.M., and Murphy, E.T., "Containment Pressure Analysis Code (COCO)", WCAP-8327 (Proprietary Version), WCAP-8326 (Non-Proprietary Version), June 1974.
7. Bordelon, F.M., et al., "The Westinghouse ECCS Evaluation Model: Supplementary Information", WCAP-8471 (Proprietary Version), WCAP-8472 (Non-Proprietary Version), January 1975.
8. Salvatori, R., "Westinghouse ECCS - Plant Sensitivity Studies", WCAP-8340 (Proprietary Version), WCAP-8356 (Non-proprietary Version), July 1974.



REFERENCES - Section 14.3.2 (cont)

9. Delsignore, T., et al., "Westinghouse ECCS Two-Loop Sensitivity Studies (14 x 14)" WCAP-8854 (Non-Proprietary Version), September 1976.
10. "Westinghouse ECCS Evaluation Model, October, 1975 Versions", WCAP-8622 (Proprietary Version), WCAP-8623 (Non-Proprietary Version), November 1975.
11. Letter from C. Eicheldinger of Westinghouse Electric Corporation to D.B. Vassalo of the Nuclear Regulatory Commission, letter number NS-CE-924, January 23, 1976.
12. Kelly, R.D., Thompson, C.M., et al., "Westinghouse Emergency Core Cooling System Evaluation Model for Analyzing Large LOCAs During Operation with One Loop out of Service for Plants without Loop Isolation Valves", WCAP-9166, February, 1978.
13. Eicheldinger, C., "Westinghouse ECCS Evaluation Model, February 1978 Version", WCAP-9220 (Proprietary Version), WCAP-9221 (Non-Proprietary Version), February, 1978.
14. Letter from T.M. Anderson of Westinghouse Electric Corporation to John Stolz of the Nuclear Regulatory Commission, letter number NS-TMA-8130, June 1978.
15. Letter from T.M. Anderson of Westinghouse Electric Corporation to John Stolz of the Nuclear Regulatory Commission, letter number NS-TMA-1834, June 20, 1978.
16. "Safety Evaluation Report on ECCS Evaluation Model for Westinghouse Two-Loop Plants", November, 1977.

REFERENCES - Section 14.3.2 (cont)

17. Letter from S. Burstein of Wisconsin Electric Power Co. to E.G. Casis of the Nuclear Regulatory Commission, January 17, 1978.
18. Letter from R.L. Kelly of Westinghouse Electric Corporation to T.R. Wilson of Wisconsin Electric Power Co., letter number WEP-78-2, February 24, 1978.
19. "NRC Questions Regarding the 1/16/78 Submittal by Westinghouse Designed Two-Loop Plant Operators", February 1, 1978.
20. Refer to Reference 18.
21. "Safety Evaluation Report on Interim ECCS Evaluation model for Westinghouse Two-Loop Plants", March 1978.
22. Letter from S. Burstein of Wisconsin Electric Power Co. to E.G. Case of the Nuclear Regulatory Commission, March 16, 1978.
23. Letter from S. Burstein of Wisconsin Electric Power Co. to E.G. Case of the Nuclear Regulatory Commission, April 6, 1978.
24. Eicheldinger, C., "Westinghouse ECCS Evaluation Model, 1981 Version", WCAP-9220-P-A (Proprietary Version) and WCAP-9221-A (Non-Proprietary), Revision 1, 1981.
25. Johnson, W.J. and Thompson, C.M., "Westinghouse Emergency Core Cooling System Evaluation Model - Modified October 1975 Version", WCAP-9168 (Proprietary) and WCAP-9169 (Non-Proprietary), 1977.
26. "Westinghouse ECCS Evaluation Model Sensitivity Studies", WCAP-8341 (Proprietary) and WCAP-8342 (Non-Proprietary), 1974.
27. Letter from R. A. Wiesemann, (Westinghouse) to D. Eisenhut (NRC), December 11, 1979.



TABLE 14.3.2-1

LARGE BREAK
TIME SEQUENCE OF EVENTS

| | <u>DECLG ($C_D=0.8$)</u> (Sec) | <u>DECLG ($C_D=0.6$)</u> (Sec) | <u>DECLG ($C_D=0.4$)</u> (Sec) |
|-------------------------|--|--|--|
| START | 0.0 | 0.0 | 0.0 |
| Reactor Trip Signal | 0.581 | 0.589 | 0.602 |
| S. I. Signal | 0.47 | 0.54 | 0.65 |
| Acc. Injection | 4.59 | 5.78 | 8.24 |
| End of Blowdown | 16.848 | 14.416 | 23.454 |
| Pump Injection | 25.47 | 25.54 | 25.65 |
| Bottom of Core Recovery | 31.958 | 32.990 | 38.785 |
| Acc. Empty | 51.355 | 53.868 | 56.10 |

TABLE 14.3.2-2

LARGE BREAK ANALYSIS INPUT AND RESULTS

| Results | DECLG ($C_D=0.8$) | DECLG ($C_D=0.6$) | DECLG ($C_D=0.4$) |
|--|---------------------|---------------------|---------------------|
| Peak Clad Temp. °F | 1751 | 1730 | 1833* |
| Peak Clad Temp. Location Ft. | 7.5 | 7.5 | 7.5 |
| Local Zr/H ₂ O Rxn(max)% | 1.5 | 1.4 | 2.1 |
| Local Zr/H ₂ O Location Ft. | 7.5 | 7.5 | 7.5 |
| Total Zr/H ₂ O Rxn % | <0.3 | <0.3 | <0.3 |
| Hot Rod Burst Time sec | 64.8 | 65.8 | 53.0 |
| Hot Rod Burst Location Ft. | 6.75 | 7.0 | 6.0 |

Calculation

| | | |
|--|------------------------|-------------------------|
| Core Power Mwt 102% of | 1520 | |
| Peak Linear Power kw/ft 102% of | 13.485 | |
| Peaking Factor (At Design Rating) | 2.32 | |
| Accumulator Water Volume (Cubic Foot per Tank) | 1100 | |
| Accumulator Pressure (psia) | 715 | |
| Number of Safety Injection Pumps Operating | 2 | |
| Steam Generator Tubes Plugged | 12% | |
| Fuel region + cycle analyzed | Cycle | Region |
| R. E. Ginna | R. E. Ginna to Specify | Westinghouse OFA Region |

*A 21°F PCT penalty must be added to the analysis value to account for UPI injection penalty.

TABLE 14.3.2-3

LARGE BREAK
CONTAINMENT DATA

(DRY CONTAINMENT)

| | |
|---|---|
| Net Free Volume | 1.066 x 10 ⁶ ft ³ |
| Initial Conditions | |
| Pressure | 14.7 psia |
| Temperature | 90°F |
| RWST Temperature | 60°F |
| Service Water Temperature | 35°F |
| Outside Temperature | -10°F |
| Spray System | |
| Number of Pumps Operating | 2 |
| Runout Flow Rate | 1800 gpm each |
| Actuation Time | 10 secs |
| Safeguards Fan Coolers | |
| Number of Fan Coolers Operating | 4 |
| Fastest Post Accident Initiation of Fan Coolers | 30 secs |



TABLE 14.3.2-3 (Cont.)
 STRUCTURAL HEAT SINK DATA

| <u>Descriptive Surface</u> | <u>Area Exposed to Containment Atmosphere</u> | <u>Layer Thickness</u> | <u>Layer</u> |
|---|---|------------------------|---------------------------------|
| insulated portion of dome and containment wall | 36181 ft. ² | 1-1/4" 3/8" 2'6" | Insulation Steel Concrete |
| uninsulated portion of dome | 12474 ft. ² | 3/8" 2'6" | Steel Concrete |
| basement floor | 7955 ft. ² | 2' 3/8" 2' | Concrete Steel Concrete |
| walls of sump in basement floor | 2342 ft. ² | 5' 3/8" 3'6" | Concrete Steel Concrete |
| floor of sump | 297 ft. ² | 2' 3/8" 2' | Concrete Steel Concrete |
| inside of refueling cavity | 5200 ft. ² | 1/4" 2'6" | Steel Concrete |
| bottom of refueling cavity | 1200 ft. ² | 1/4" 2'6" | Steel Concrete |
| area on outside of refueling cavity walls | 6900 ft. ² | 2'6" | Concrete |
| area inside of loop and steam generator compartment | 14900 ft. ² | 2'6" | Concrete |
| floor area intermediate level | 6170 ft. ² | 6" | Concrete |
| operating floor | 6540 ft. ² | 2' | Concrete |
| 1-1/2" thick I-beam | 3151 ft. ² | 1-1/2" | Steel |



TABLE 14.3.2-3 (Cont.)

STRUCTURAL HEAT SINK DATA

| <u>Descriptive Surface</u> | <u>Area Exposed to Containment Atmosphere</u> | <u>Layer Thickness</u> | <u>Layer</u> |
|---|---|----------------------------|--------------|
| 1" thick I-beam | 5016 ft. ² | 1" | Steel |
| 1/2" thick I-beam | 8138 ft. ² | 1/2" | Steel |
| cylindrical supports for S.G. & MCP's | 430 ft. ² | 1/2" | Steel |
| plant crane rectangular support columns | 5756 ft. ² | 3/4" | Steel |
| beams used for crane structure | 6023 ft. ² | 1-1/2" | Steel |
| structure on operating floor | 2622 ft. ² | 2' | Concrete |
| from FSAR: grating, stairs misc. steels | 7000 ft. ² | .0104' | Steel |



TABLE 14.3.2-4

REFLOOD MASS AND ENERGY RELEASE

| <u>Time (sec)</u> | <u>Mass Flow (lb/sec)</u> | <u>Energy Flow (BTU/sec)</u> |
|-------------------|---------------------------|------------------------------|
| 38.785 | 0.0 | 0.0 |
| 39.0 | 0.00831 | 10.660 |
| 40.0 | 0.00894 | 11.479 |
| 45.0 | 31.426 | 40535.91 |
| 59.0 | 92.496 | 106286.56 |
| 69.0 | 140.052 | 118474.87 |
| 79.0 | 173.728 | 125391.45 |
| 89.0 | 187.574 | 126392.58 |
| 99.0 | 193.280 | 125252.45 |
| 119.0 | 198.273 | 121543.89 |
| 139.0 | 202.387 | 117805.11 |
| 189.0 | 211.909 | 109040.96 |
| 399.0 | 240.990 | 92584.28 |

TABLE 14.3.2-5

BROKEN LOOP ACCUMULATOR MASS AND ENERGY RELEASE

| <u>Time (sec)</u> | <u>Mass Flow (lb/sec)</u> | <u>Energy Flow (BTU/sec)</u> |
|-------------------|---------------------------|------------------------------|
| 1.010 | 2549.262 | 152779.845 |
| 2.010 | 2435.293 | 145949.518 |
| 3.010 | 2336.090 | 140004.203 |
| 4.010 | 2248.981 | 134783.662 |
| 5.010 | 2170.686 | 130091.404 |
| 6.010 | 2099.724 | 125838.537 |
| 7.010 | 2035.237 | 121973.761 |
| 8.010 | 1976.388 | 118446.914 |
| 9.010 | 1922.560 | 115220.959 |
| 10.010 | 1873.213 | 112263.515 |
| 11.010 | 1827.766 | 109539.815 |
| 12.010 | 1785.549 | 107009.731 |
| 13.010 | 1746.201 | 104651.550 |
| 14.010 | 1709.424 | 102447.507 |
| 15.010 | 1675.079 | 100389.155 |
| 16.010 | 1643.218 | 98479.727 |
| 17.010 | 1613.496 | 96698.419 |
| 18.010 | 1585.660 | 95030.182 |
| 19.010 | 1559.414 | 93457.249 |
| 20.010 | 1534.659 | 91973.651 |

14.3.2-17

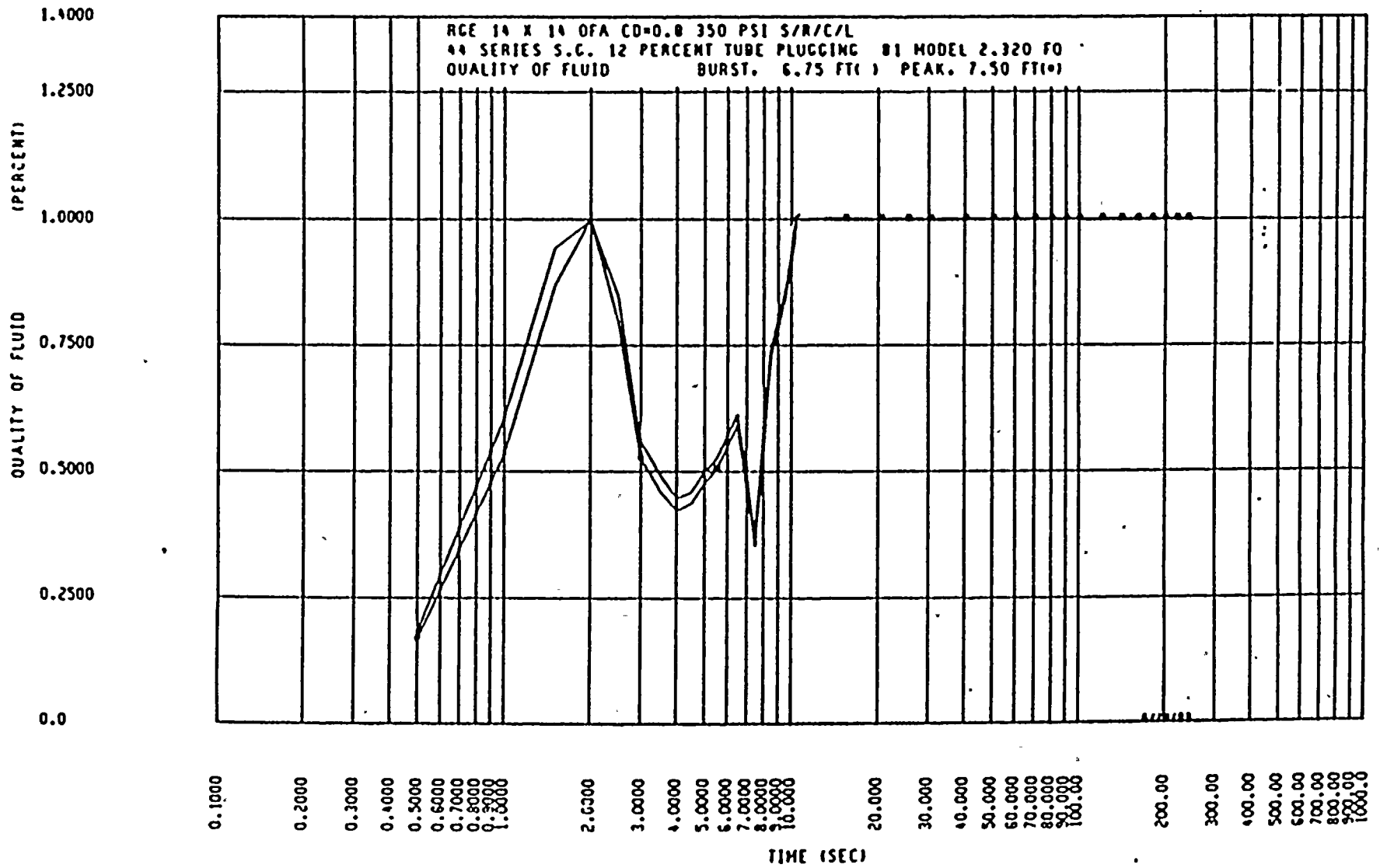


Figure 14.3.2-1a Fluid Quality - DECLG (CD = 0.8)



14.3.2-18

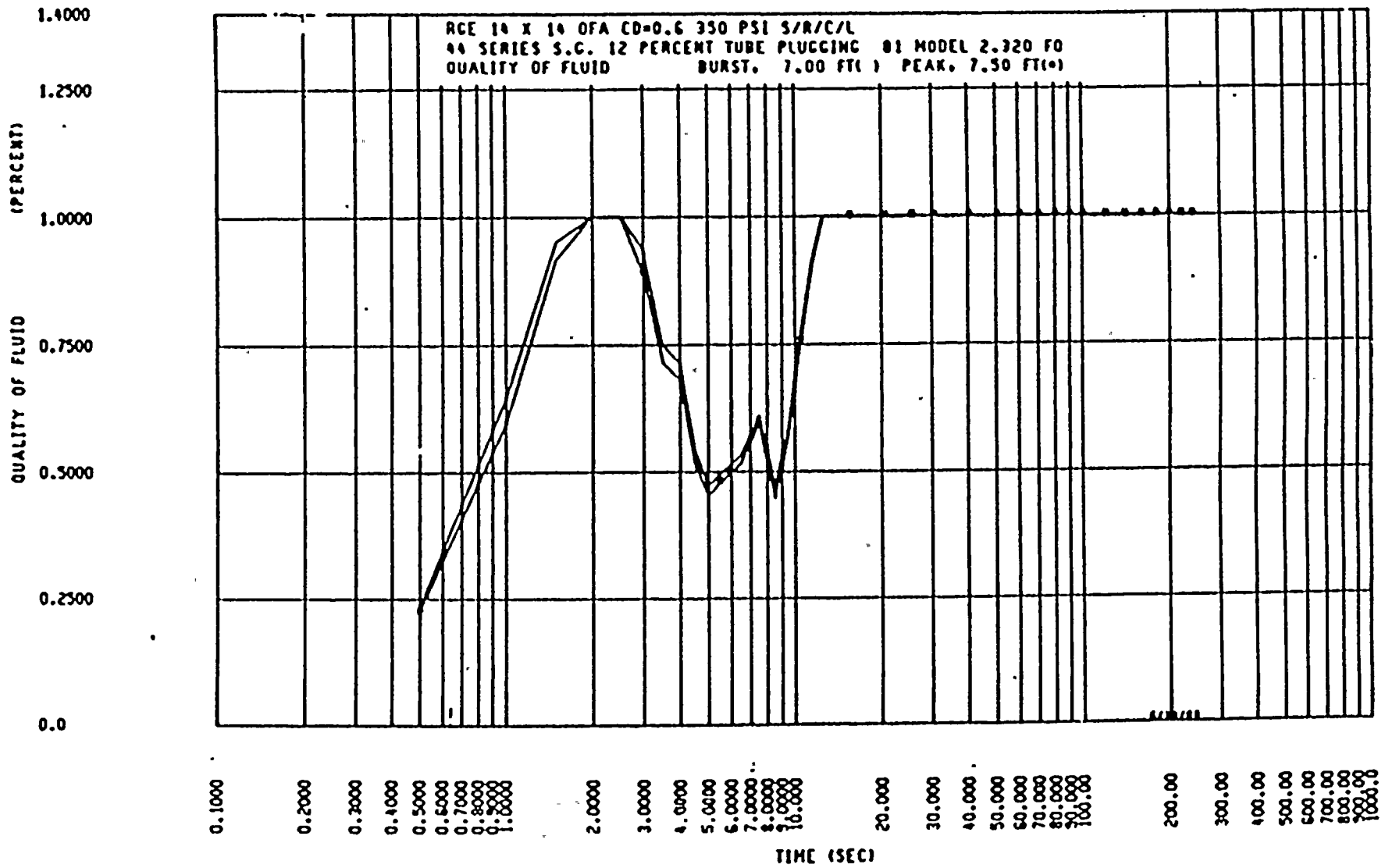


Figure 14.3.2-1b Fluid Quality - DECLG (CD = 0.6)

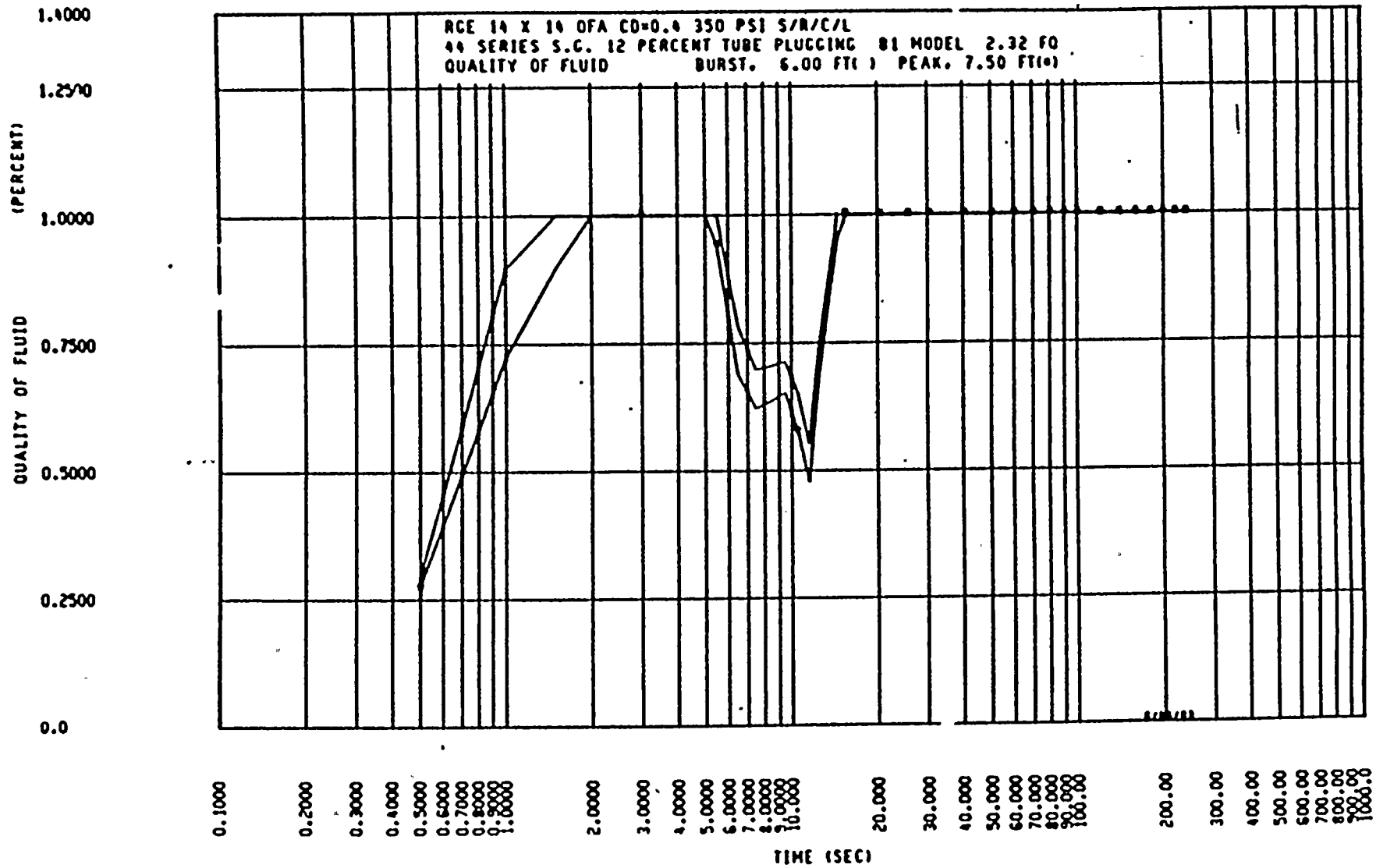


Figure 14.3.2-1c Fluid Quality - DECLG (CD = 0.4)

14.3.2-20

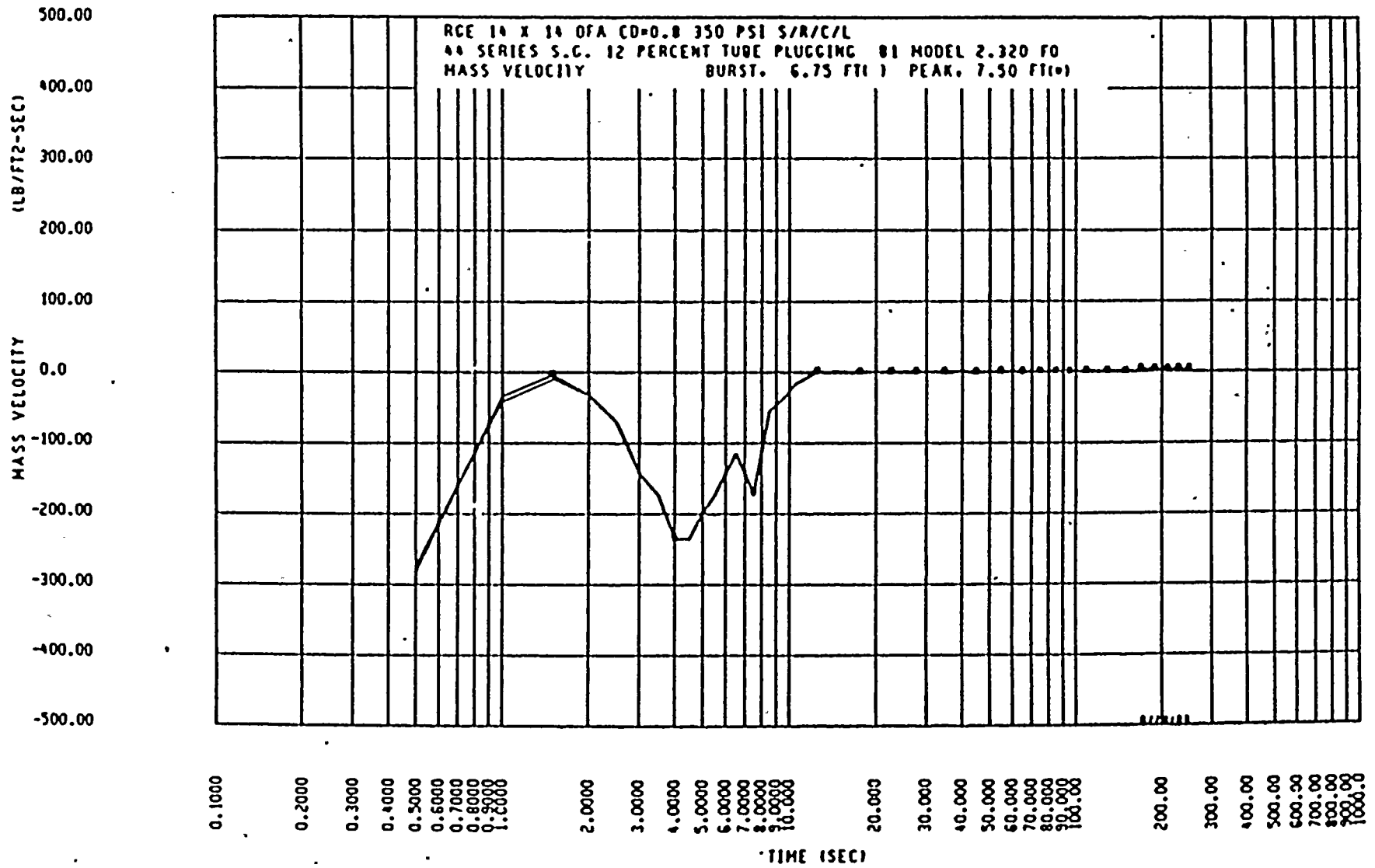


Figure 14.3.2-2a Mass Velocity - DECLG (CD = 0.8)

14.3.2-21

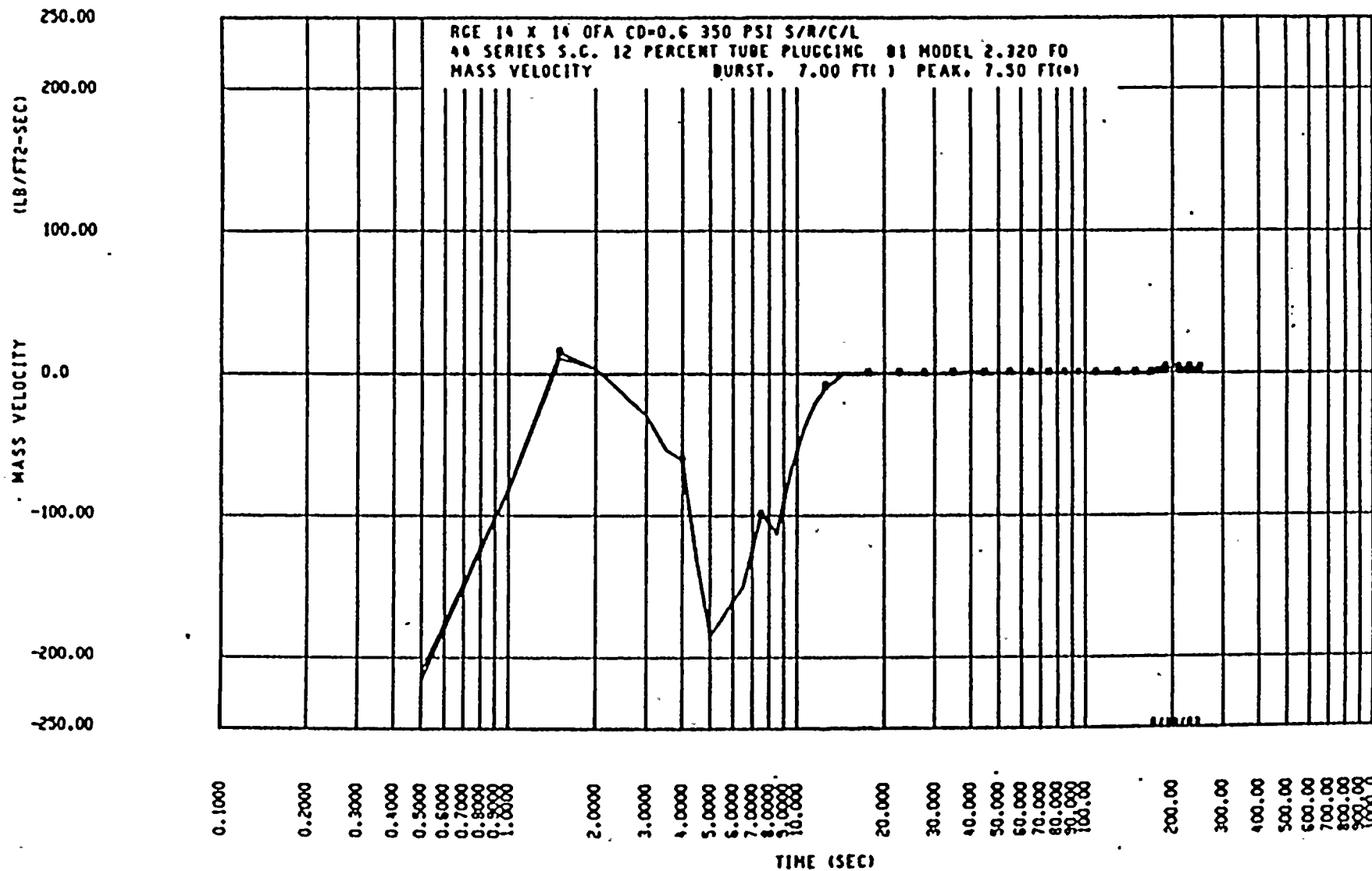


Figure 14.3.2-2b Mass Velocity - DECLG (CD = 0.6)

14.3.2-22

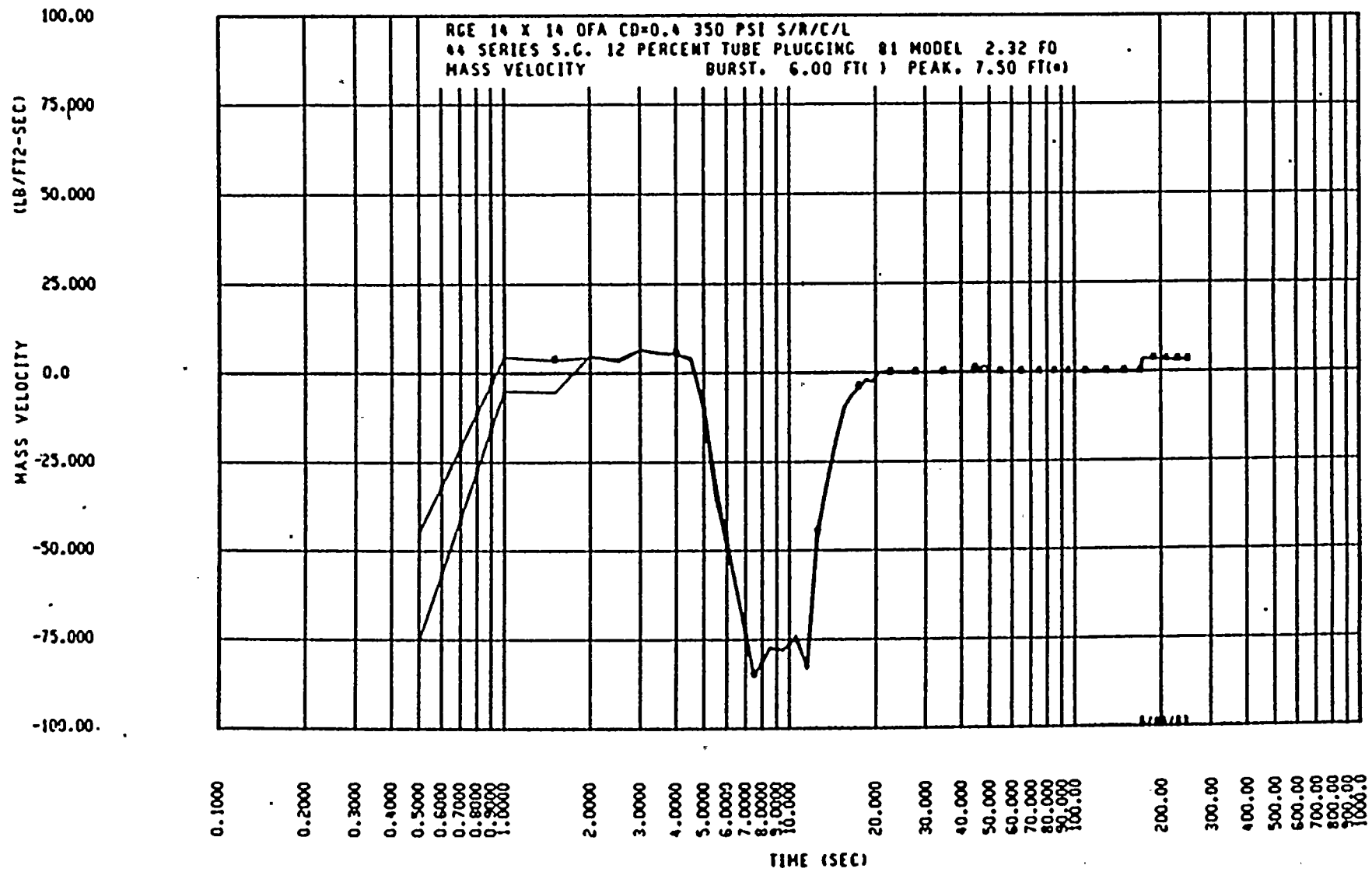


Figure 14.3.2-2c Mass Velocity - DECLG (CD = 0.4)



14.3.2-23

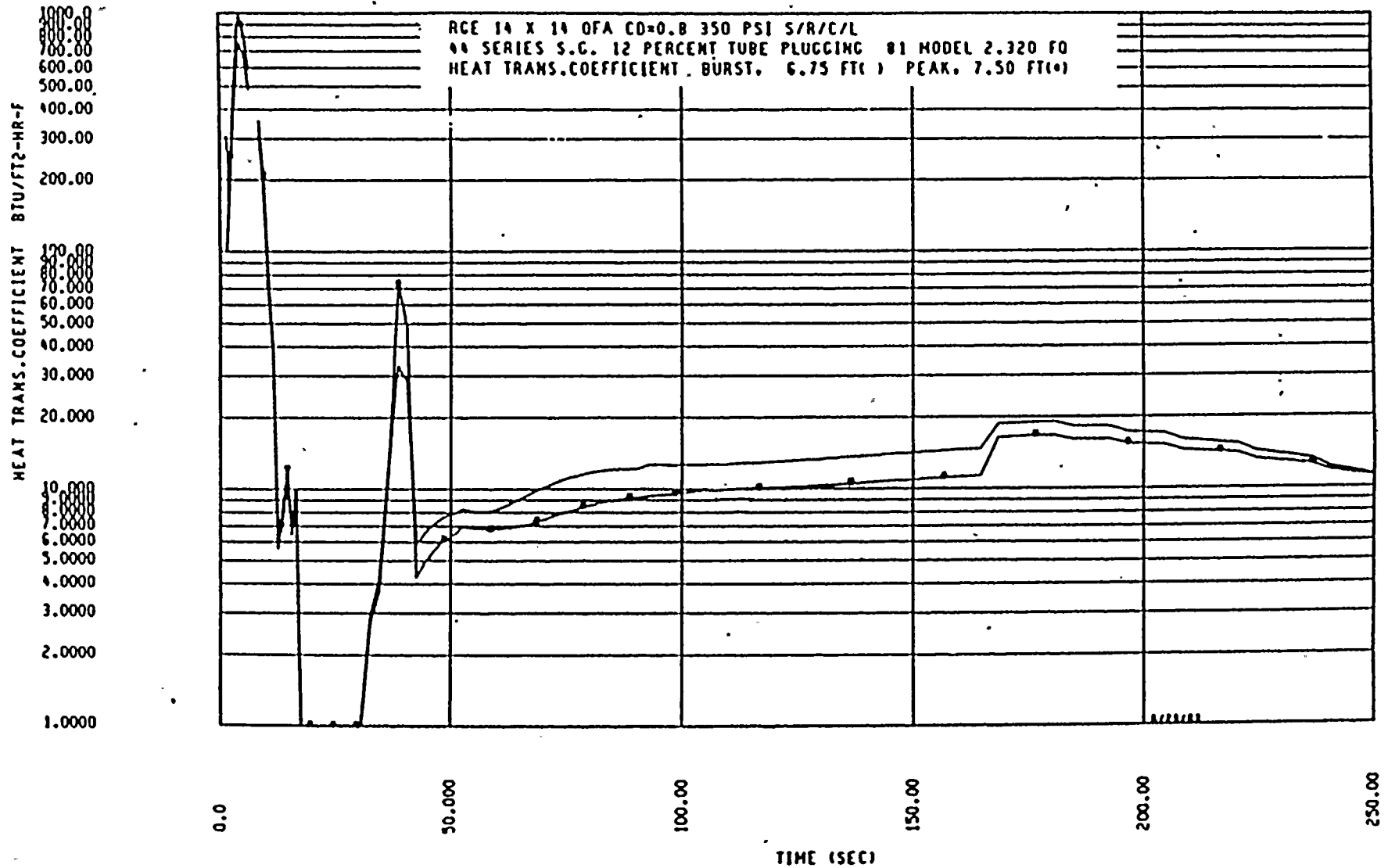


Figure 14.3.2-3a Heat Transfer Coefficient - DECLG (CD = 0.8)

14.3.2-24

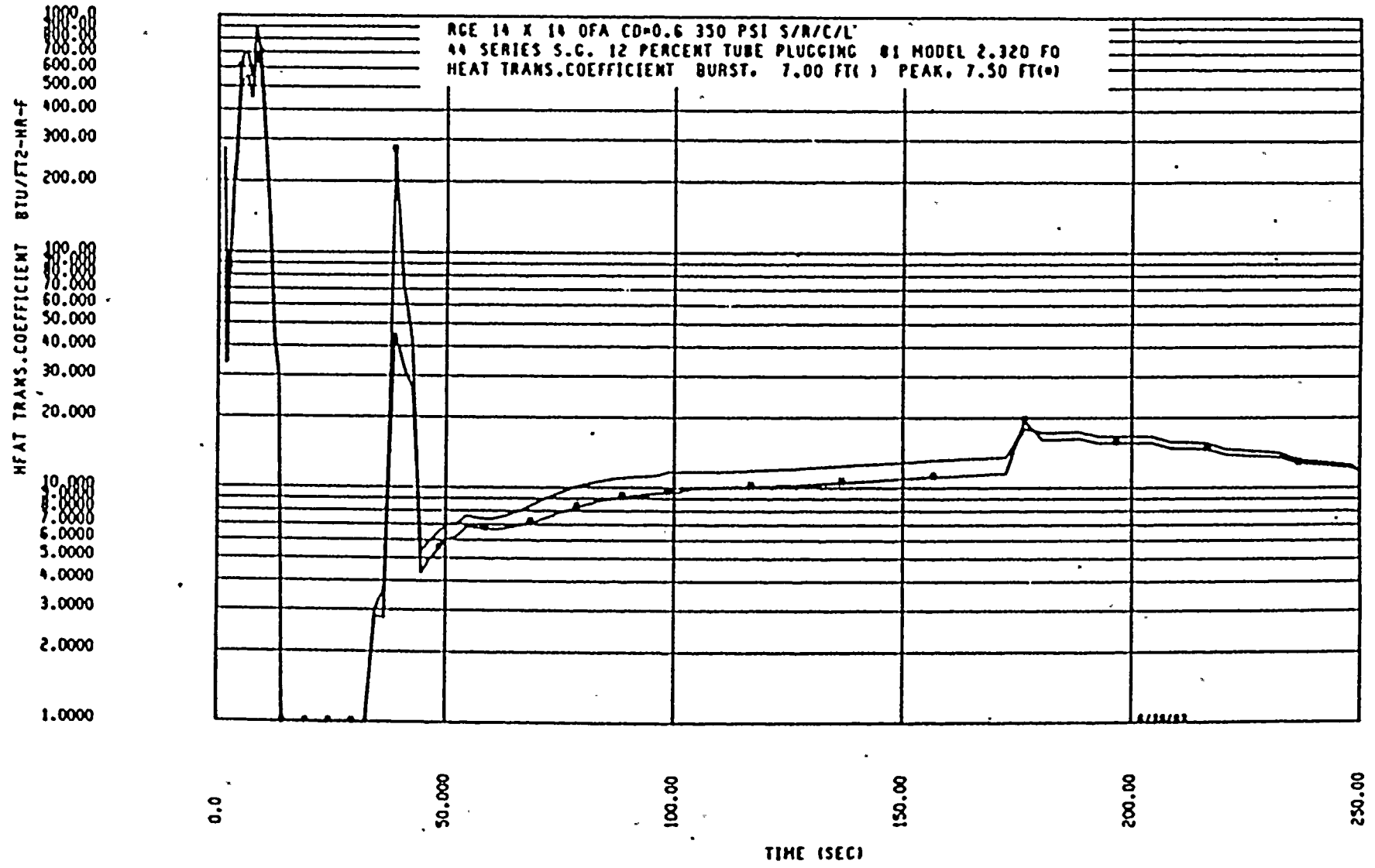
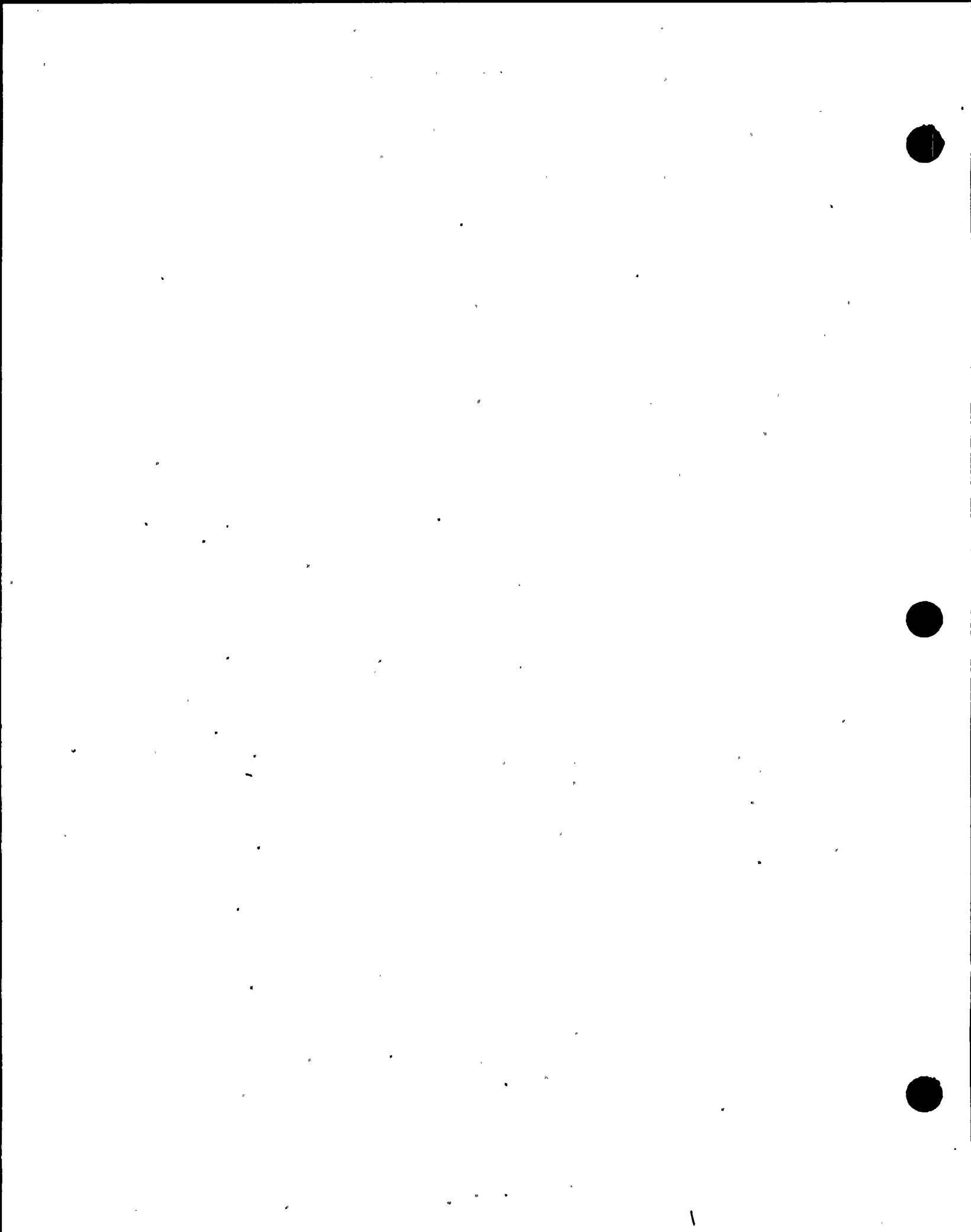


Figure 14.3.2-3b Heat Transfer Coefficient - DECLG (CD = 0.6)



14.3.2-25

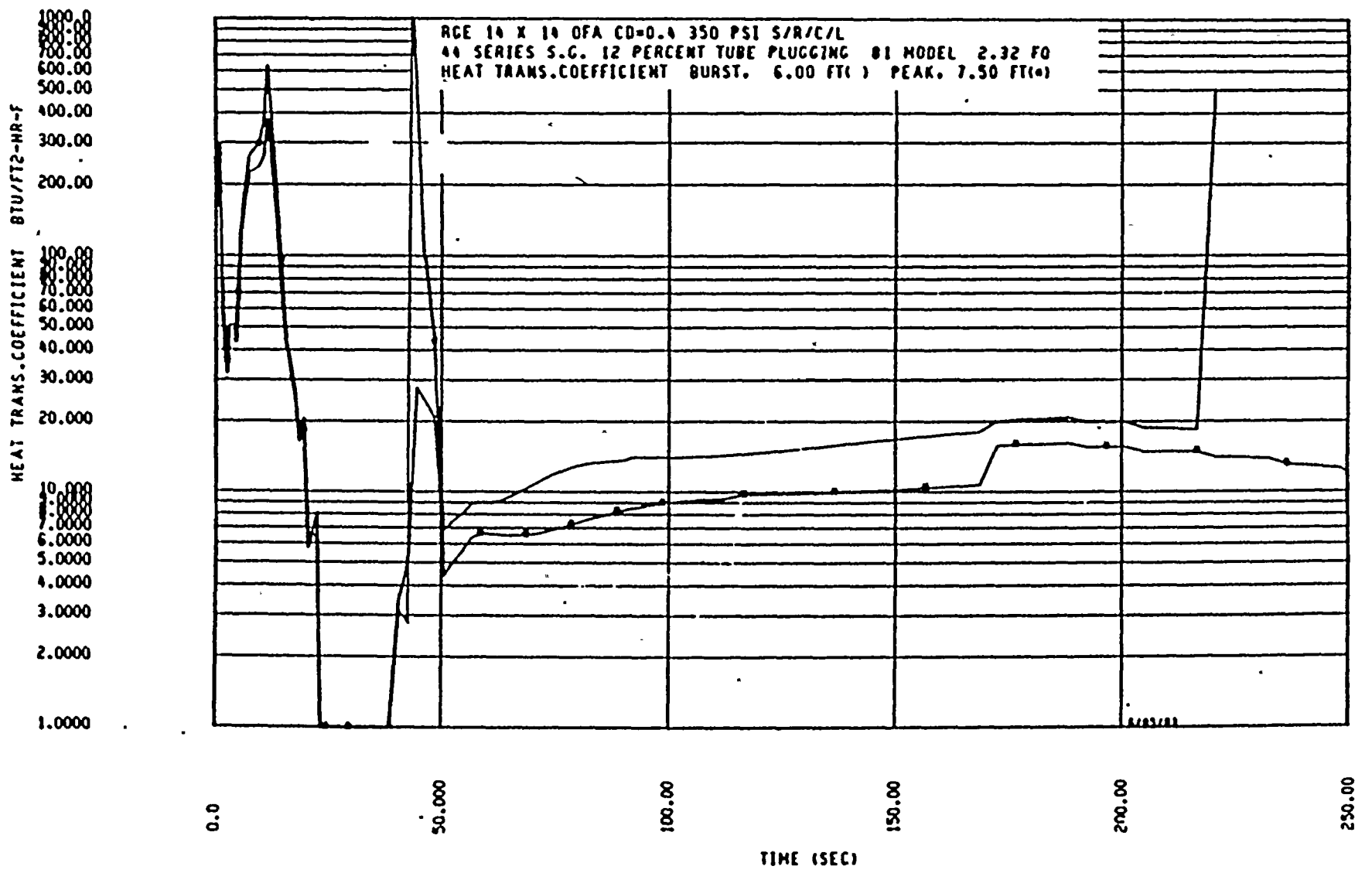


Figure 14.3.2-3c Heat Transfer Coefficient - DECLG (CD = 0.4)

14.3.2-26

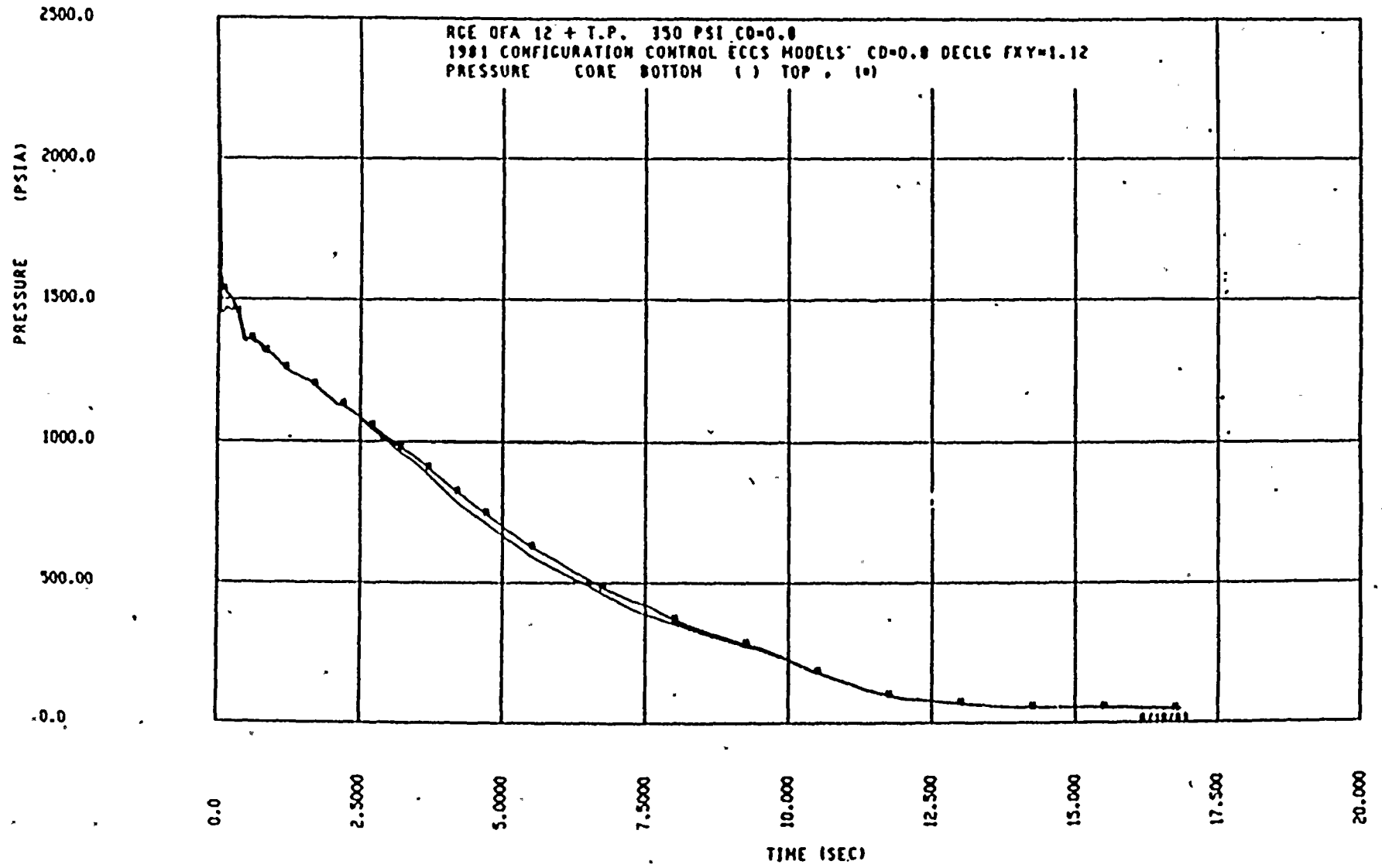
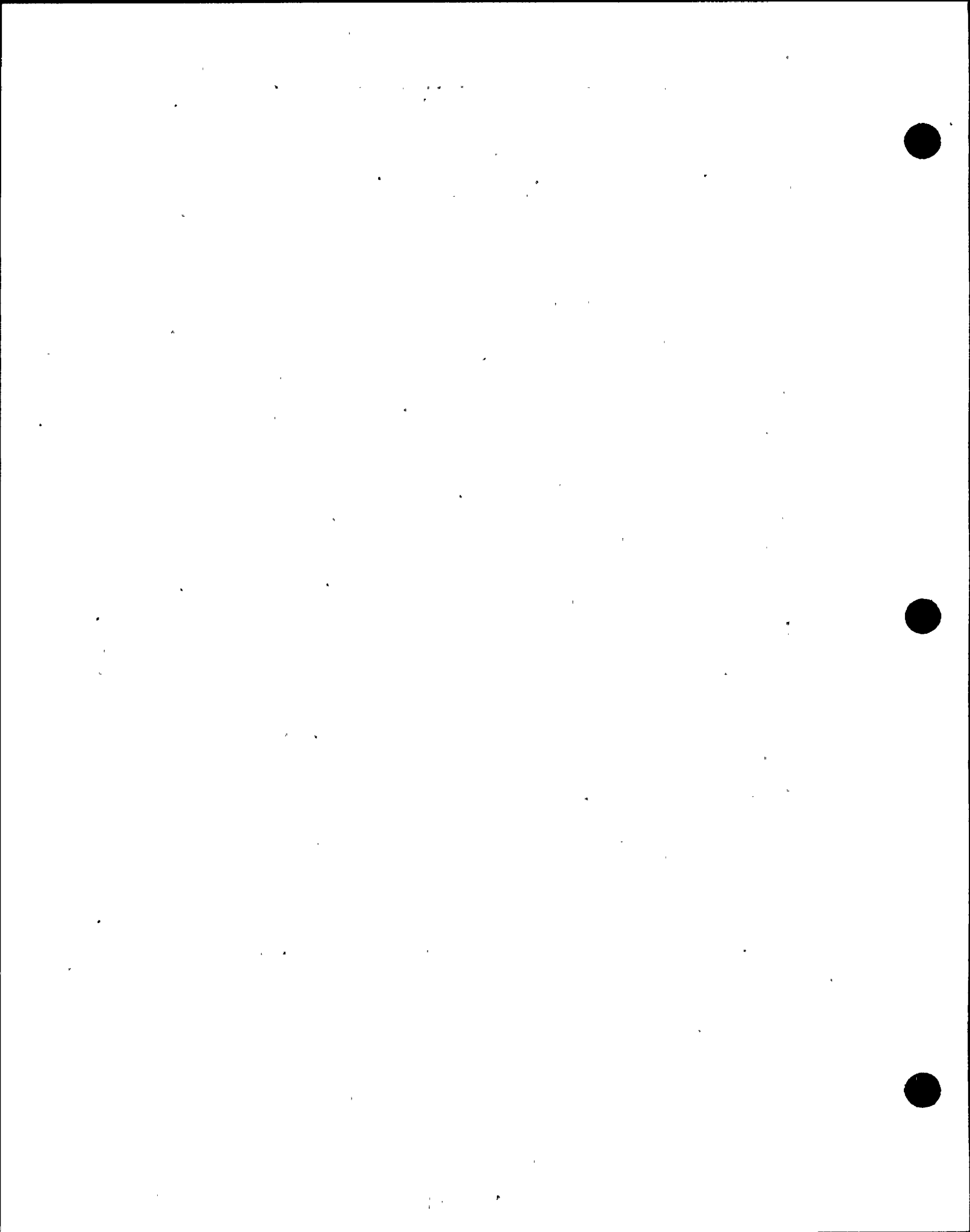


Figure 14.3.2-4a Core Pressure - DECLG (CD = 0.8)



14.3.2-27.

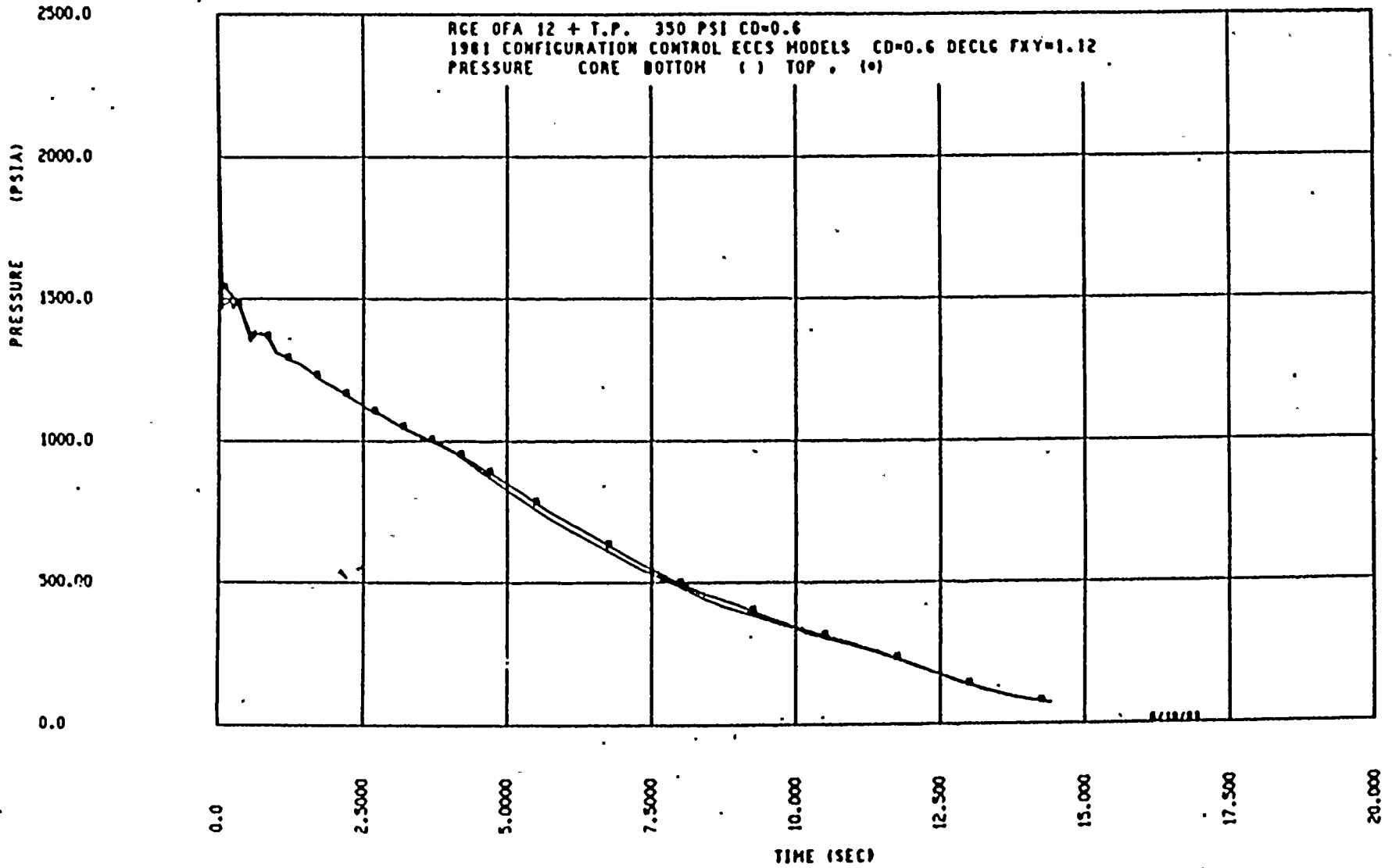


Figure 14.3.2-4b Core Pressure - DECLG (CD = 0.6)



14.3.2-28

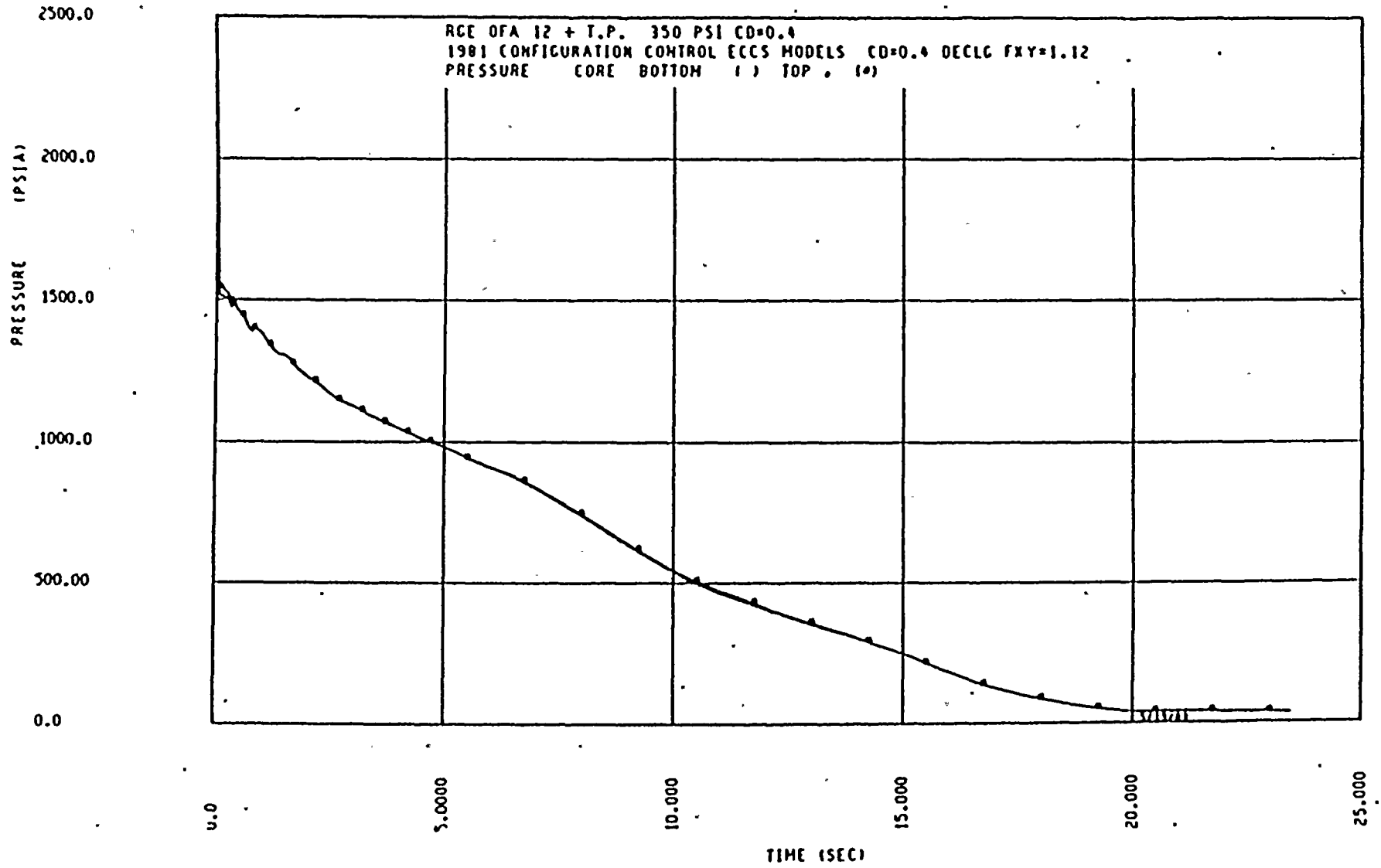


Figure 14.3.2-4c Core Pressure - DECLG (CD = 0.4)

14.3.2-29

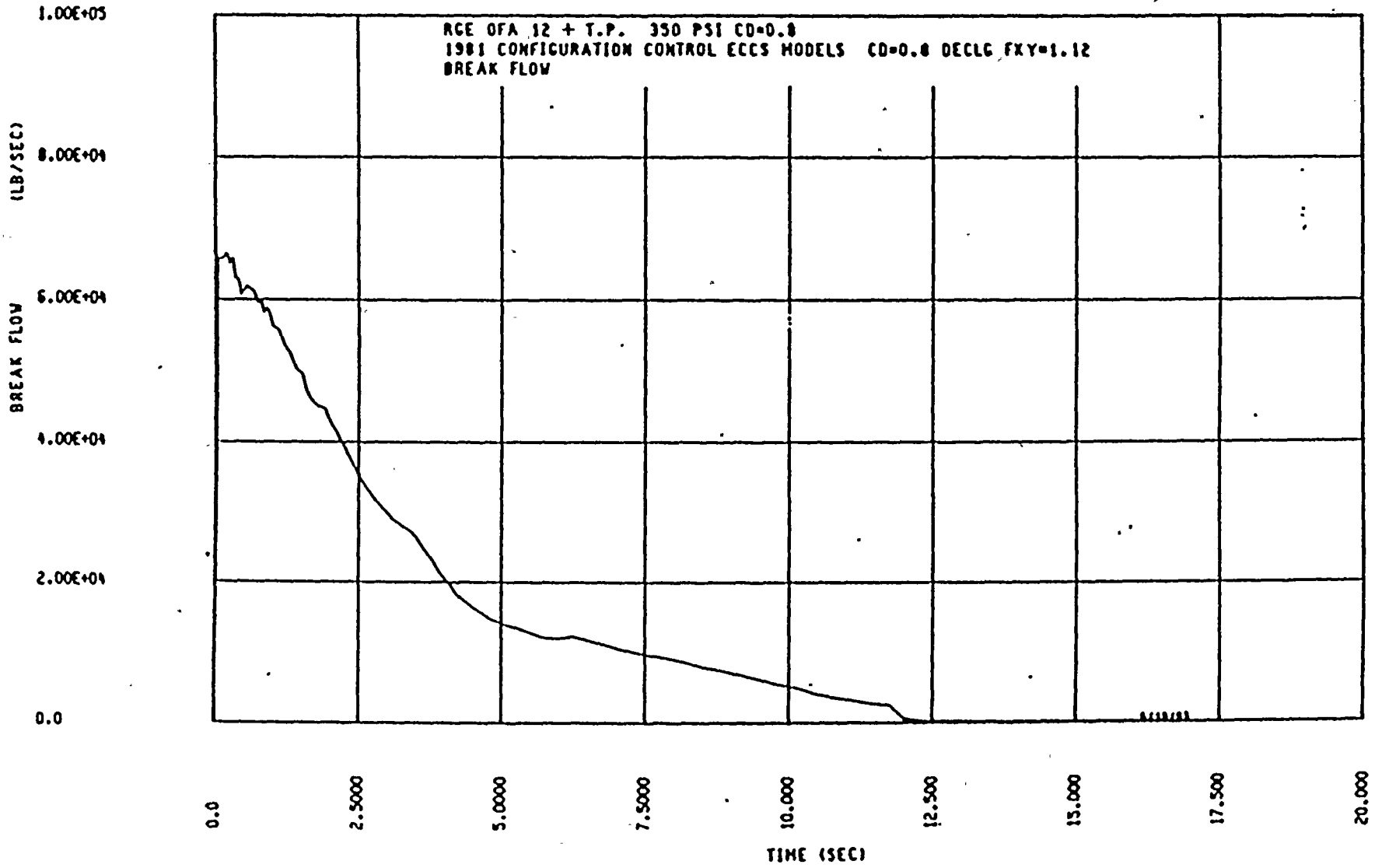
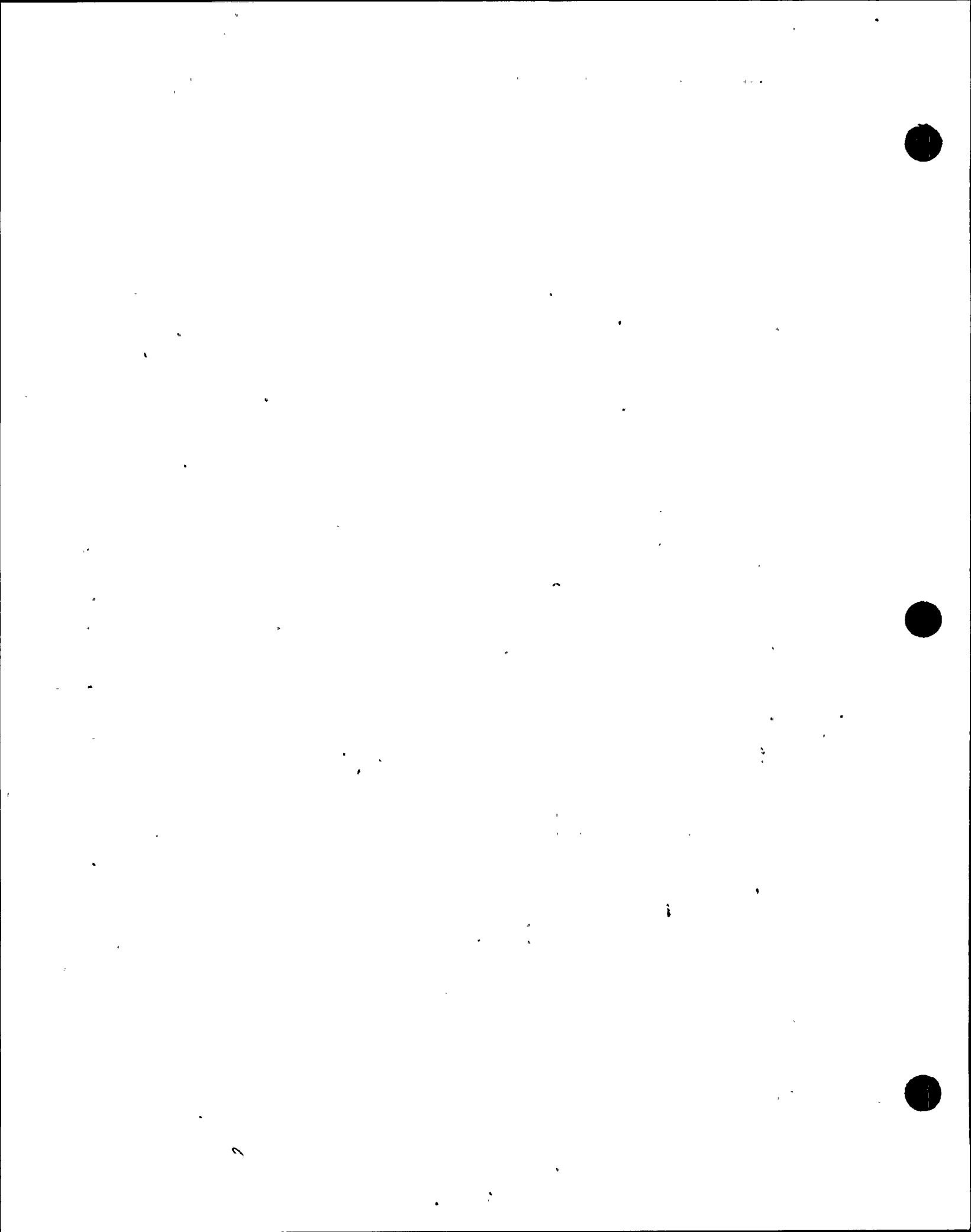


Figure 14.3.2-5a Break Flow Rate - DECLG (CD = 0.8)



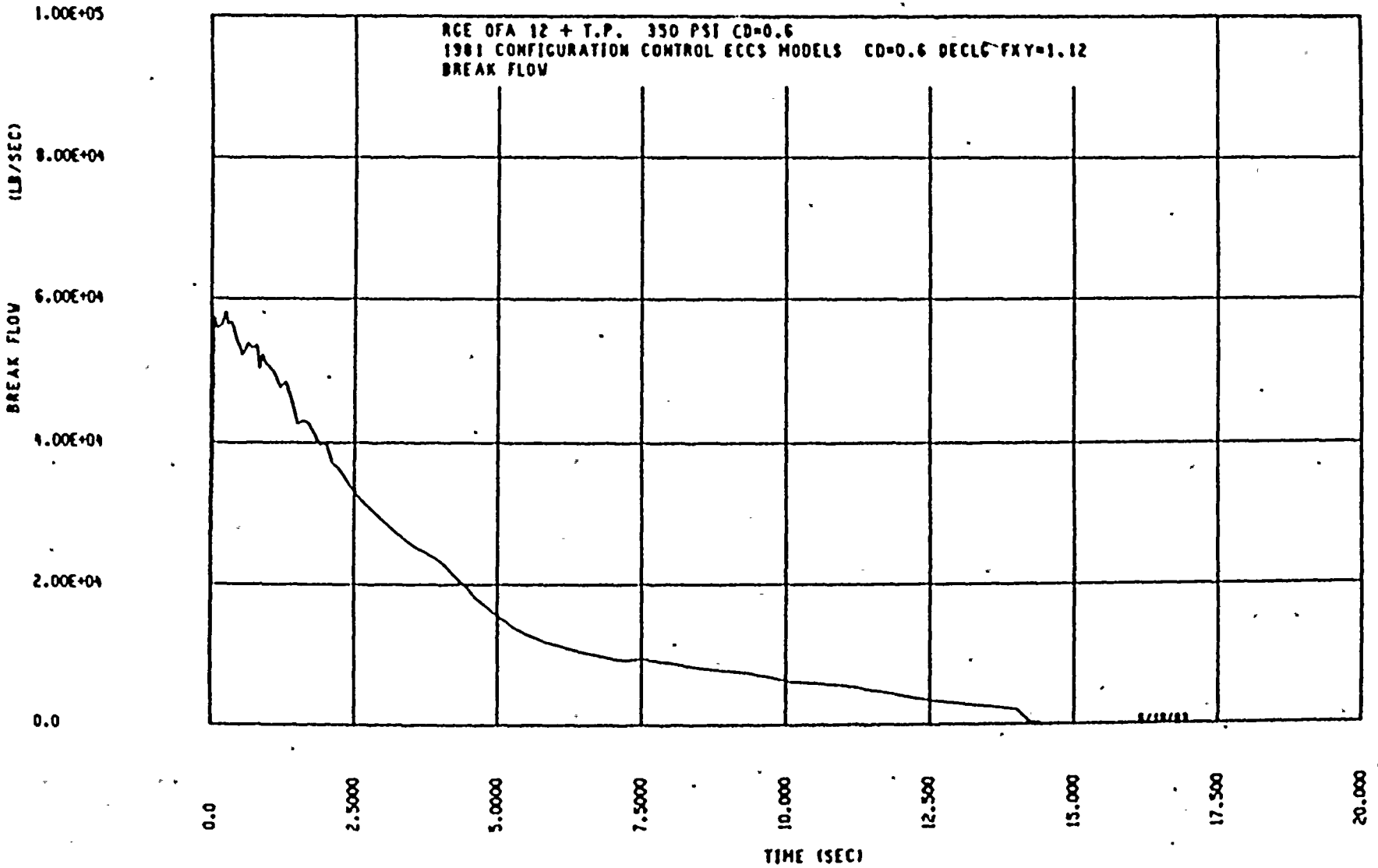


Figure 14.3.2-5b Break Flow Rate - DECLG (CD = 0.6)

14.3.2-30

14.3.2-31

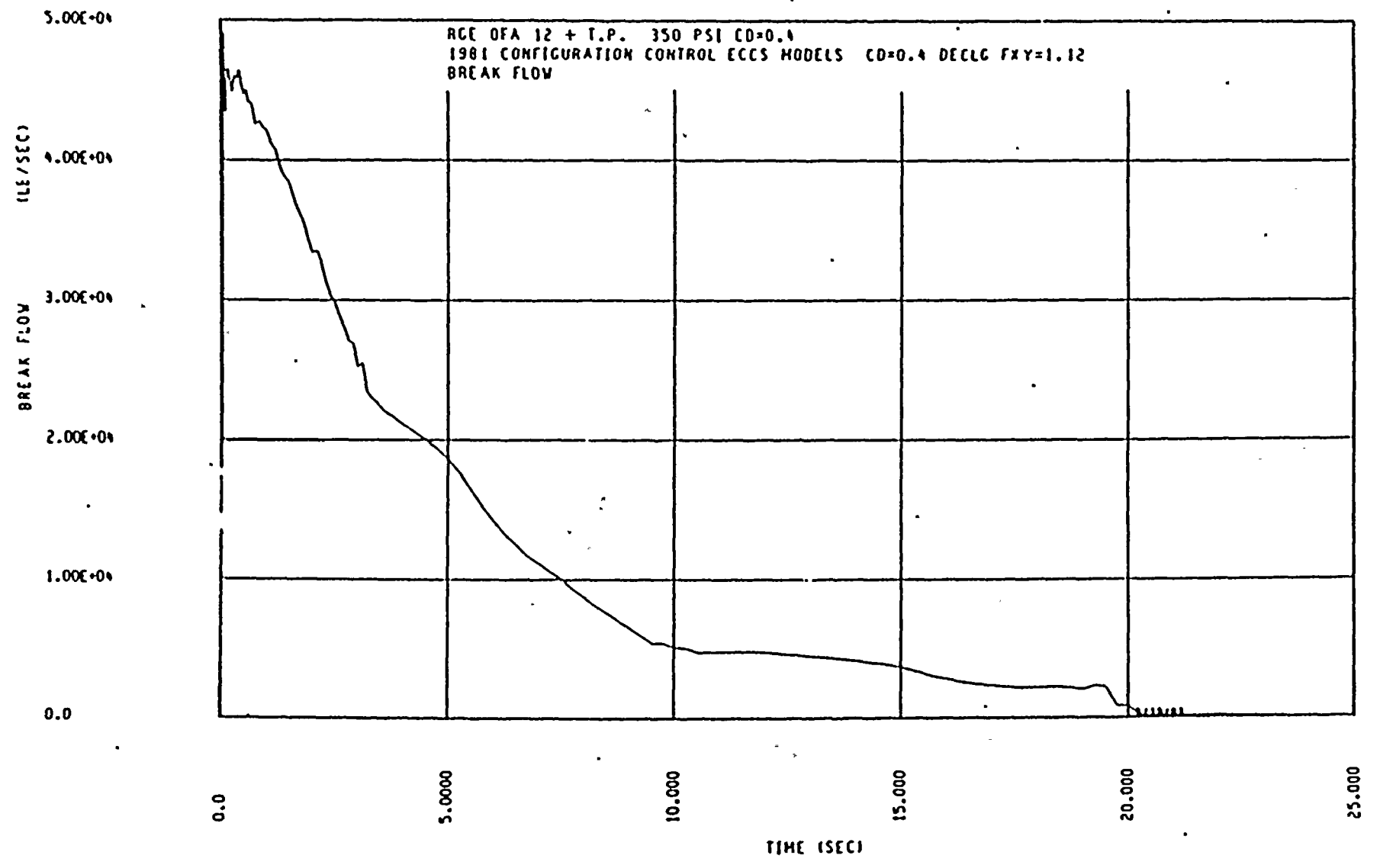
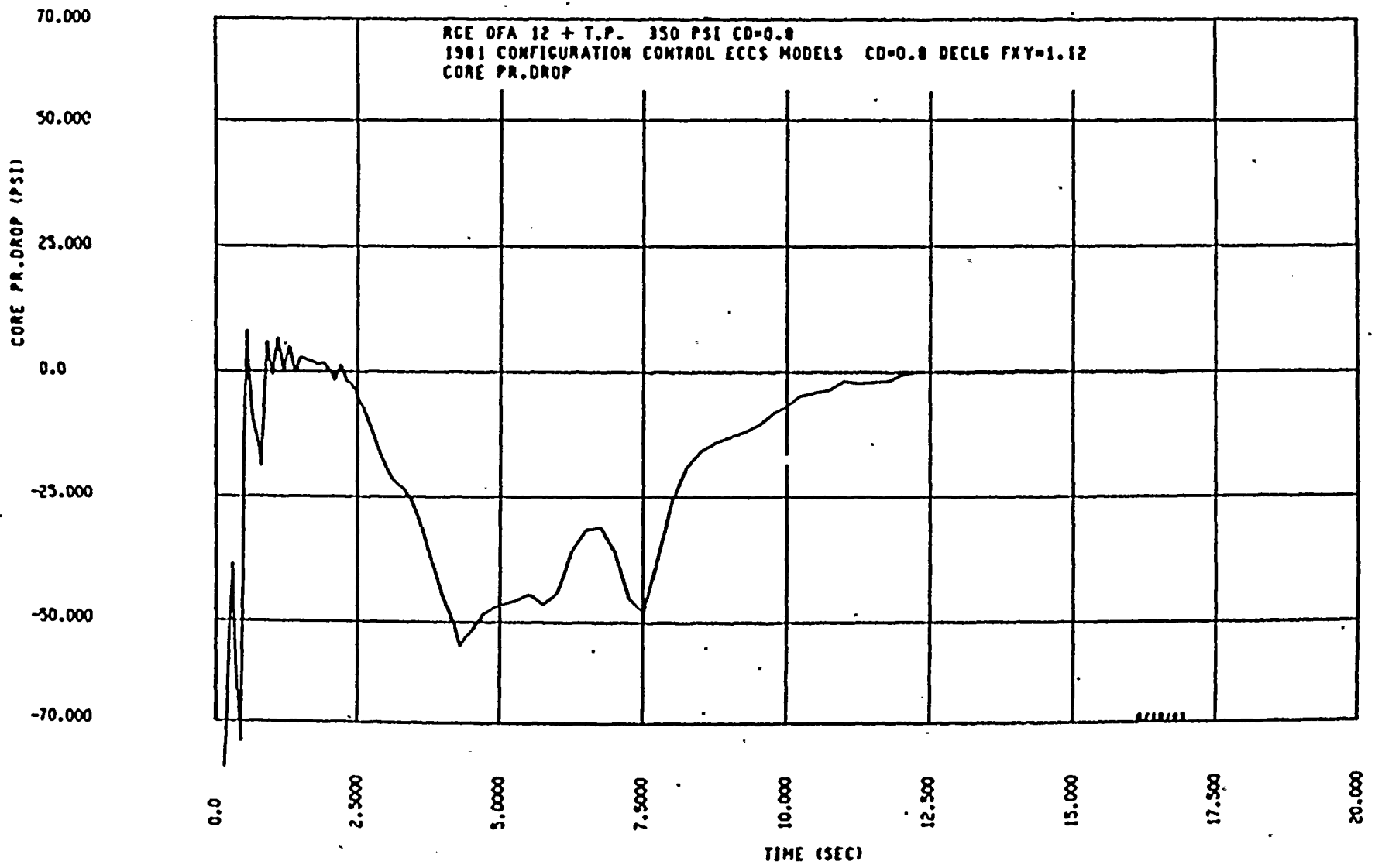


Figure 14.3.2-5c Break Flow Rate - DECLG (CD = 0.4)



14.3.2-32

Figure 14.3.2-6a Core Pressure Drop - DECLG (CD = 0.8)

14.3.2-33

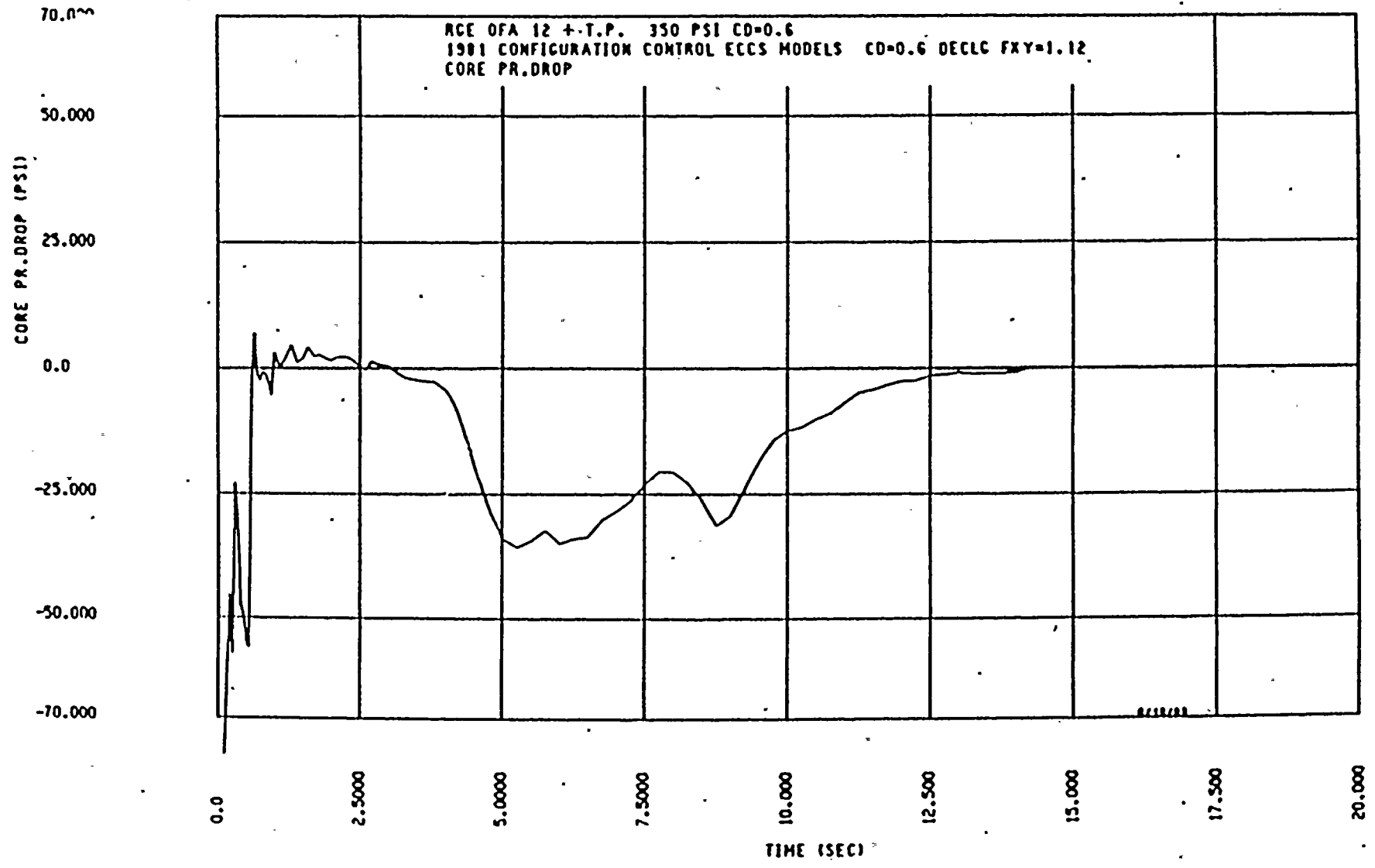


Figure 14.3.2-6b Core Pressure Drop - DECLG (CD = 0.6)



14.3.2-34

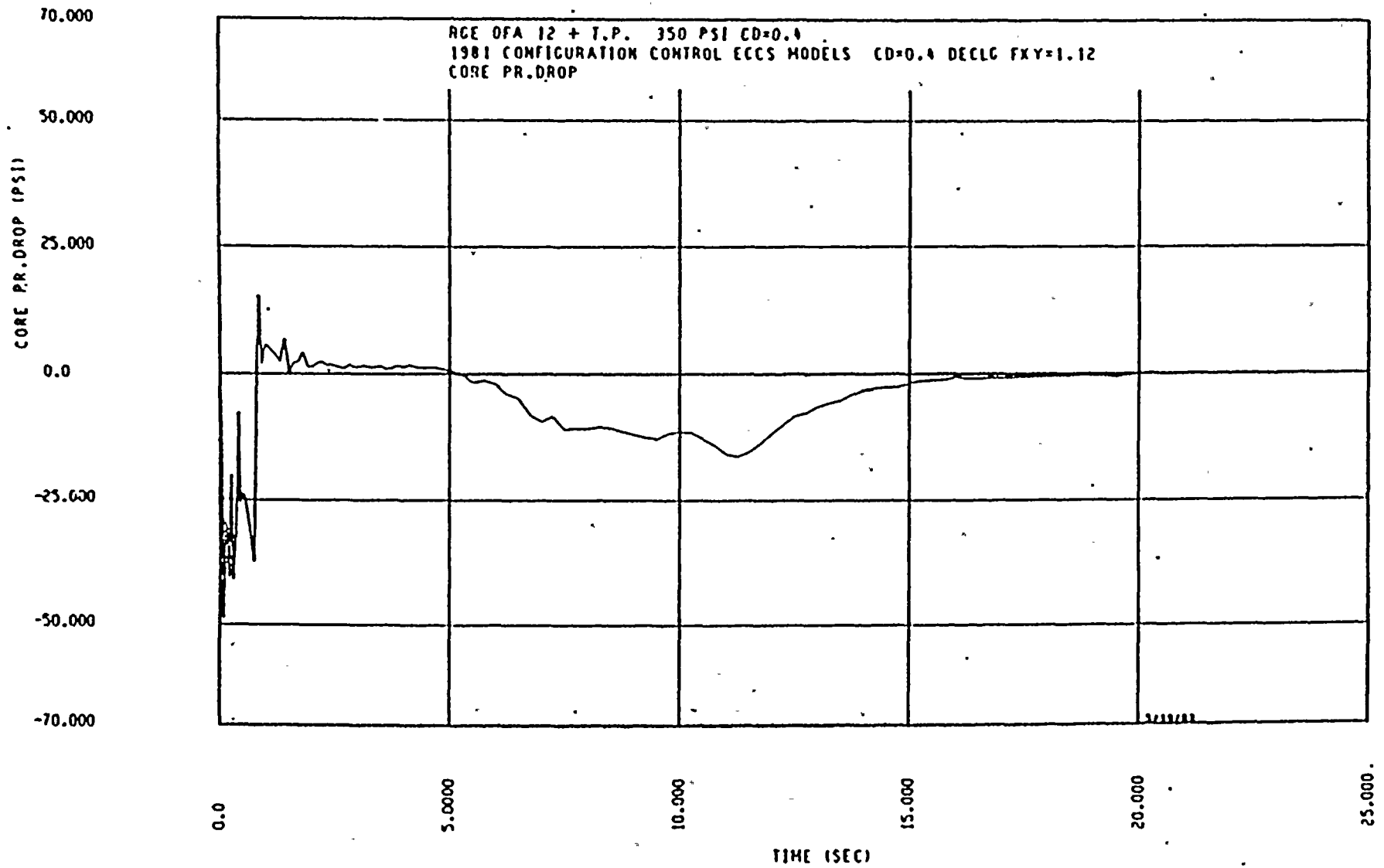


Figure 14.3.2-6c Core Pressure Drop - DECLG (CD = 0.4)

14.3.2-35

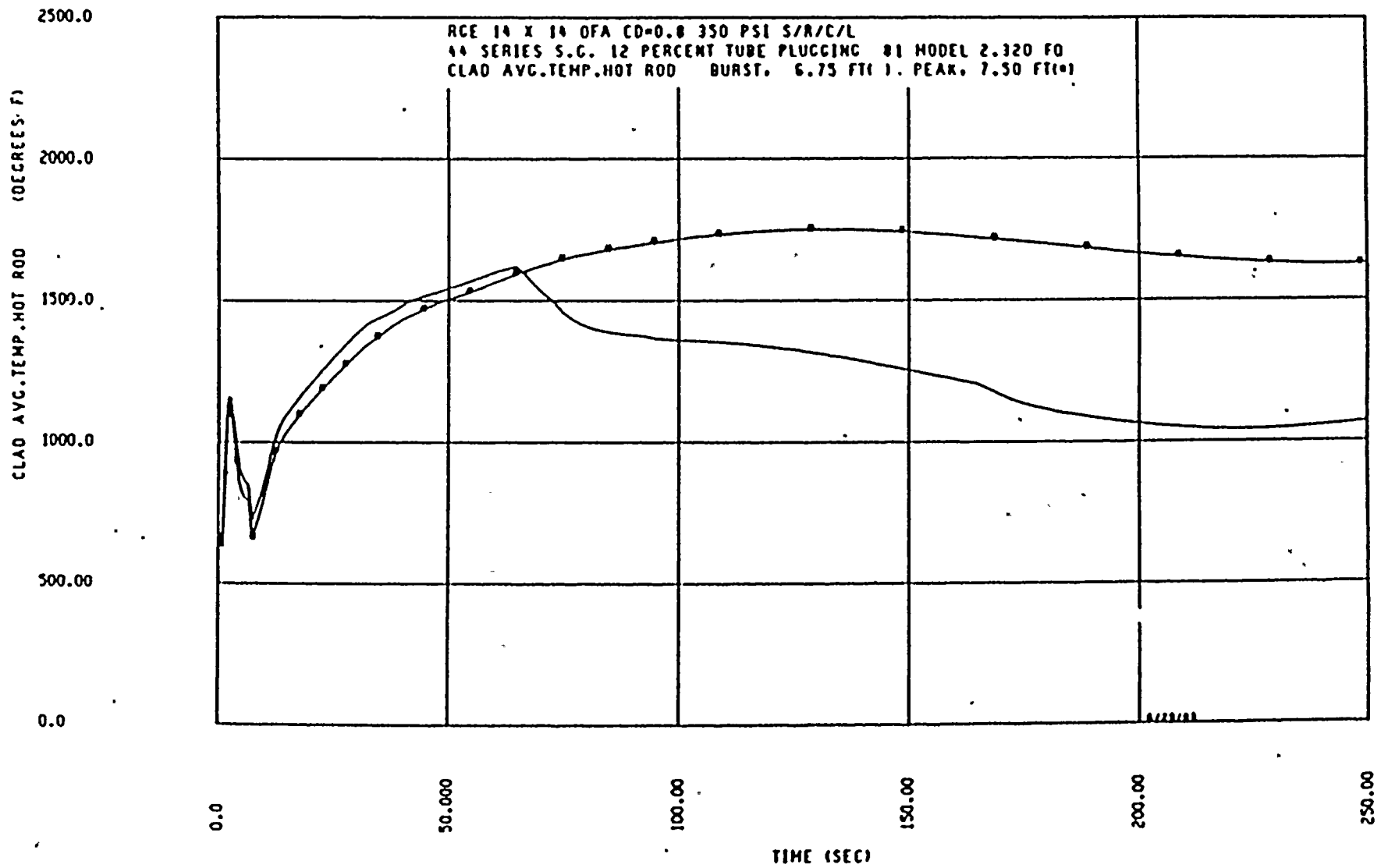
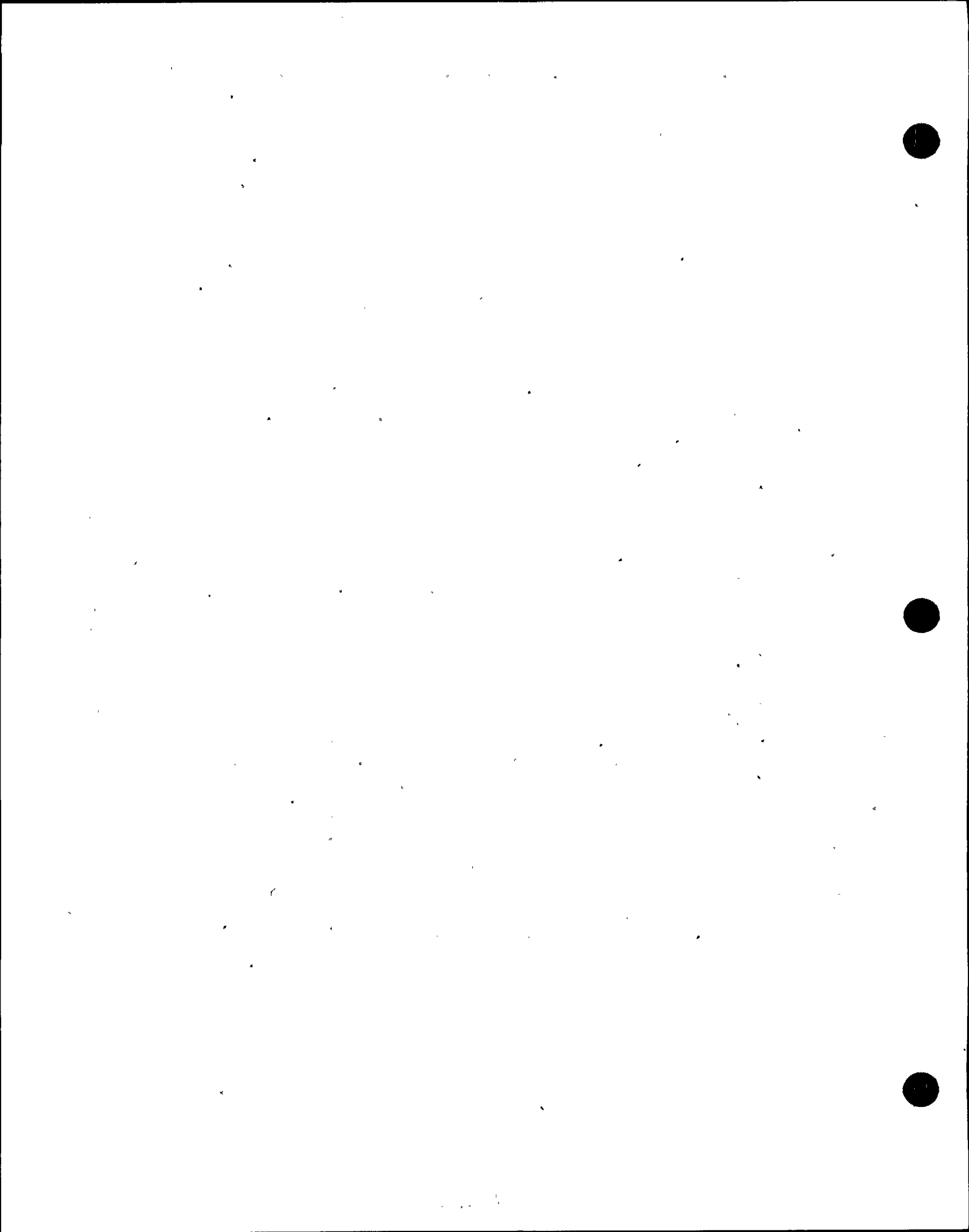


Figure 14.3.2-7a Peak Clad Temperature - DECLG (CD = 0.8)



14.3.2-36

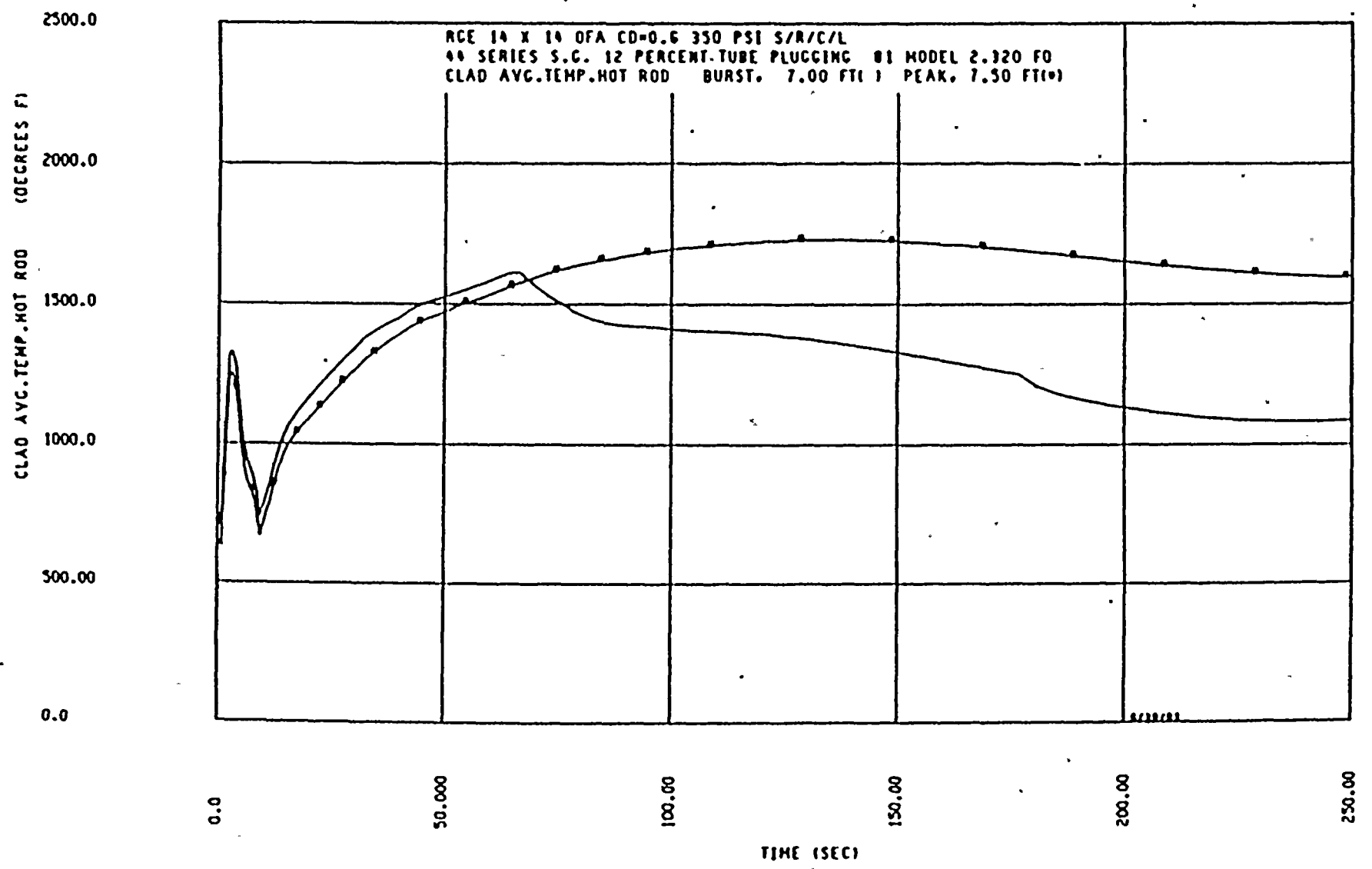


Figure 14.3.2-7b Peak Clad Temperature - DECLG (CD = 0.6)

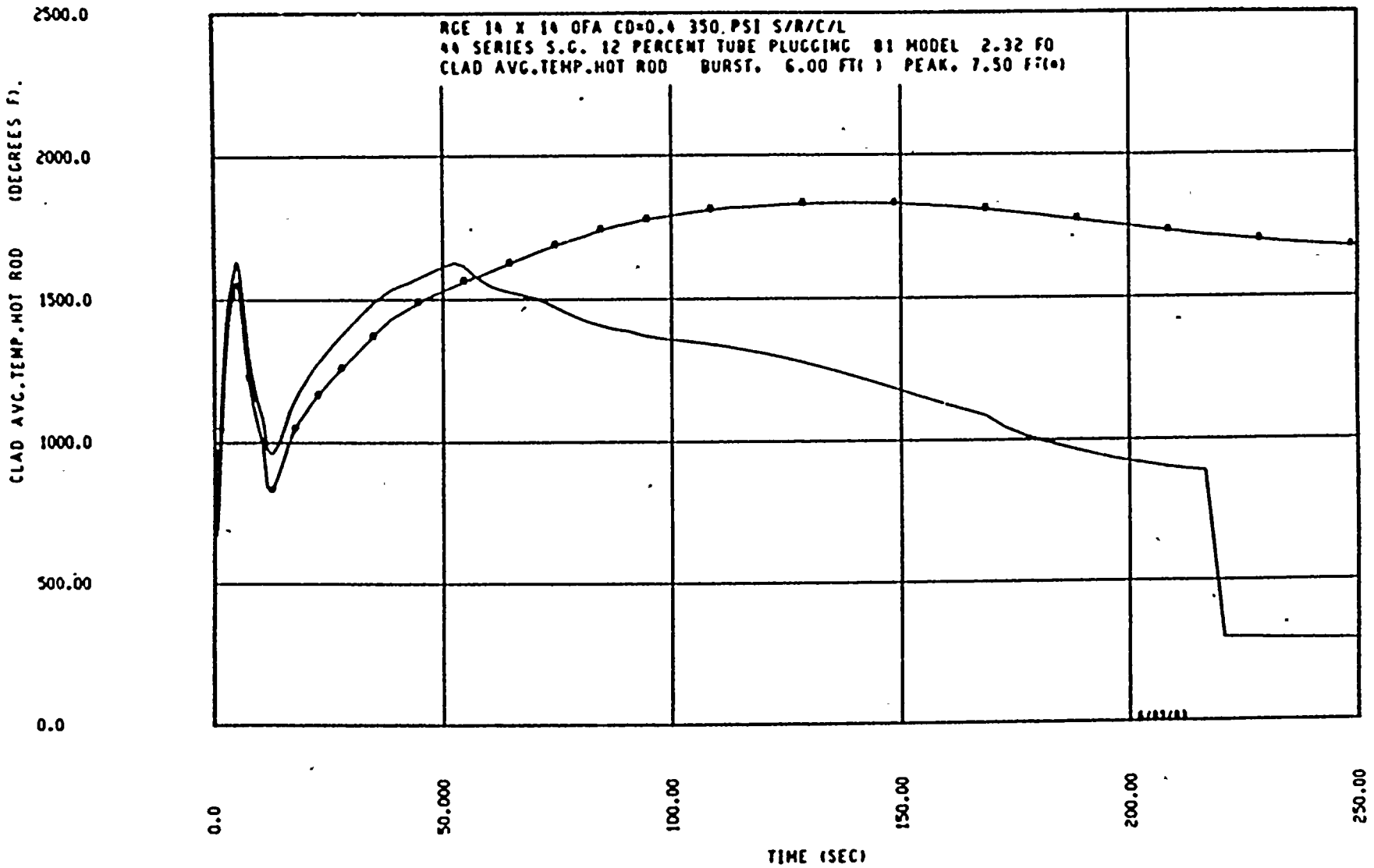


Figure 14.3.2-7c Peak Clad Temperature - DECLG (CD = 0.4)

14.3.2-38

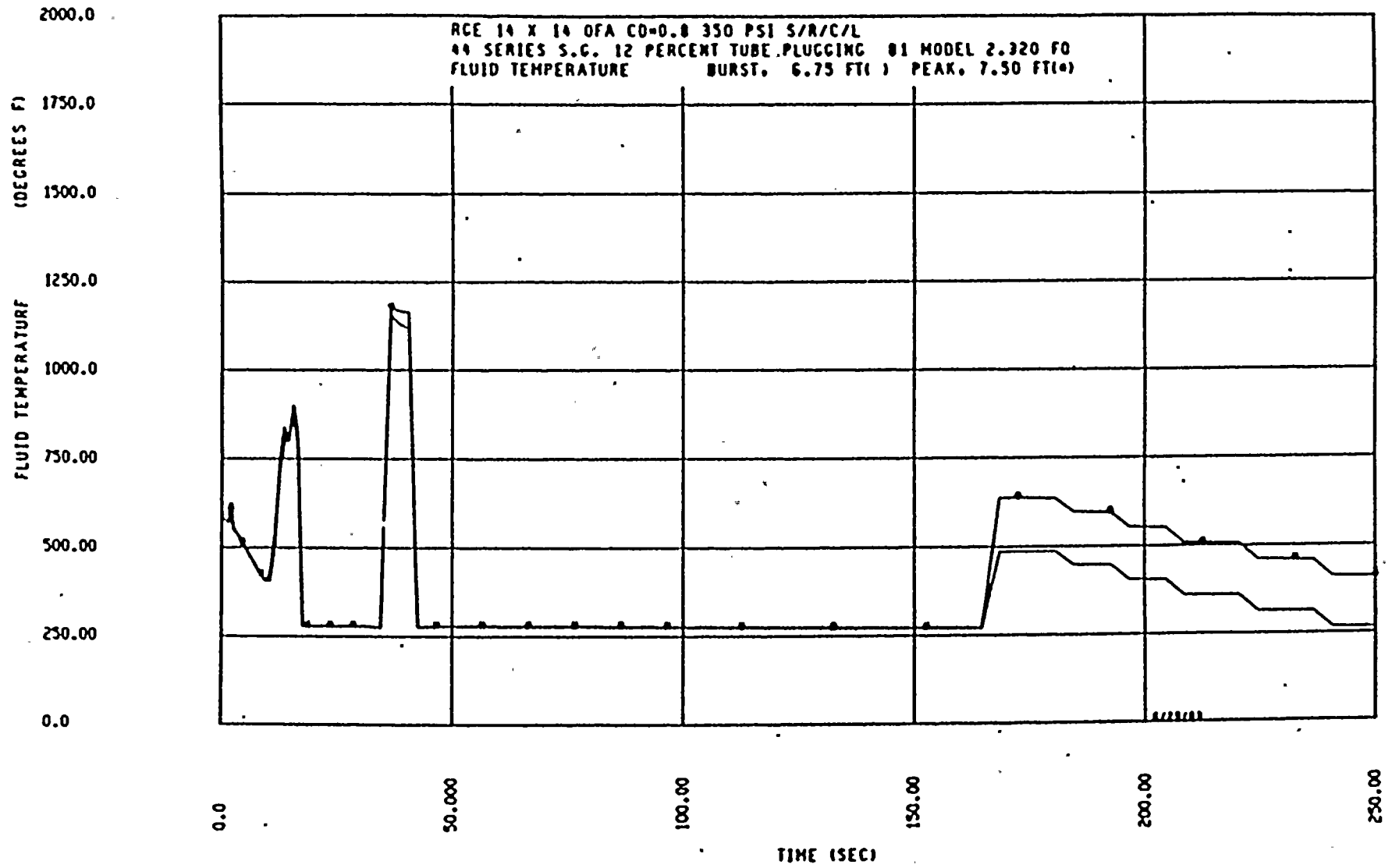


Figure 14.3.2-8a Fluid Temperature - DECLG (CD = 0.8)



14.3.2-39

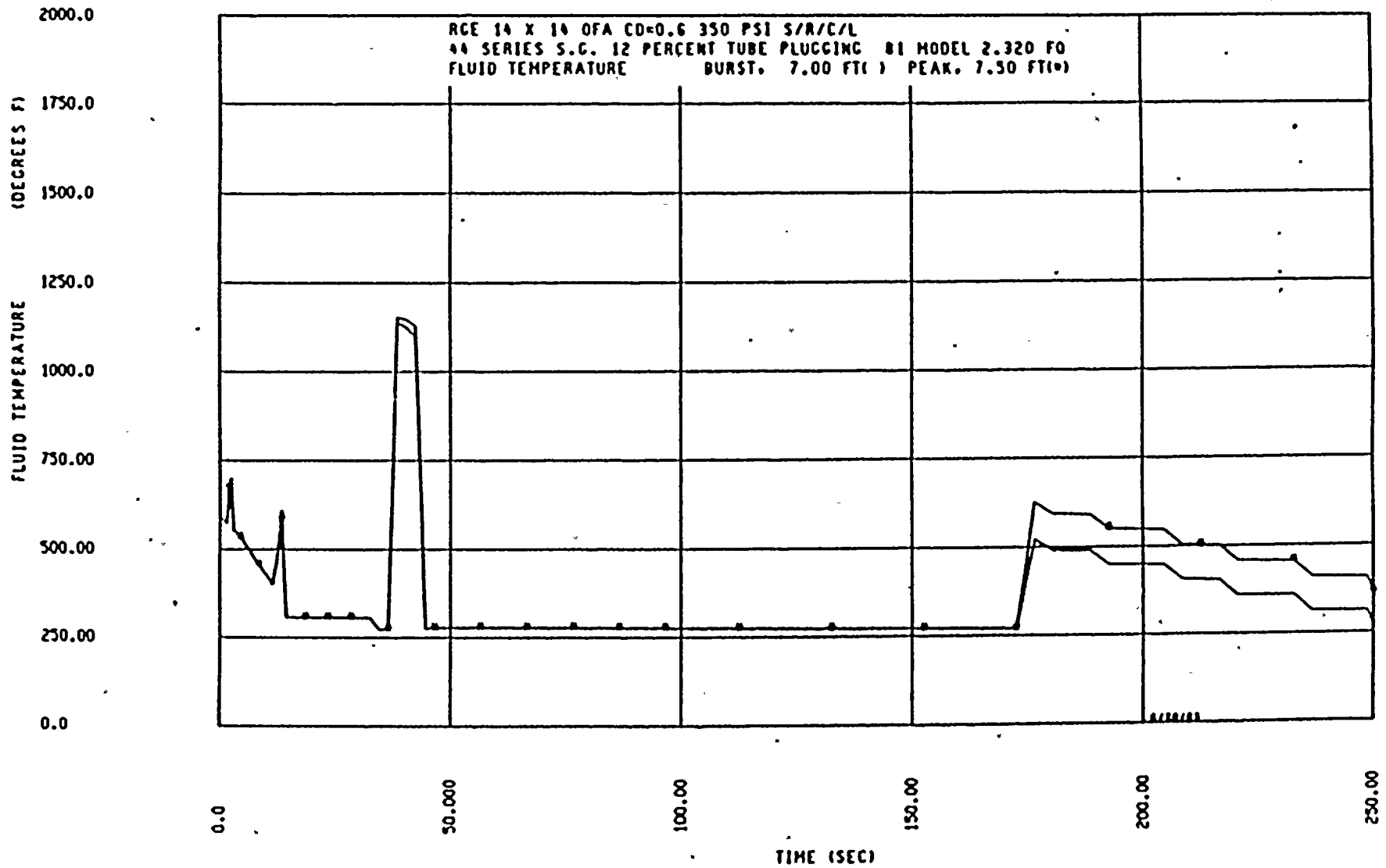


Figure 14.3.2-8b Fluid Temperature - DECLG (CD = 0.6)



14.3.2-40

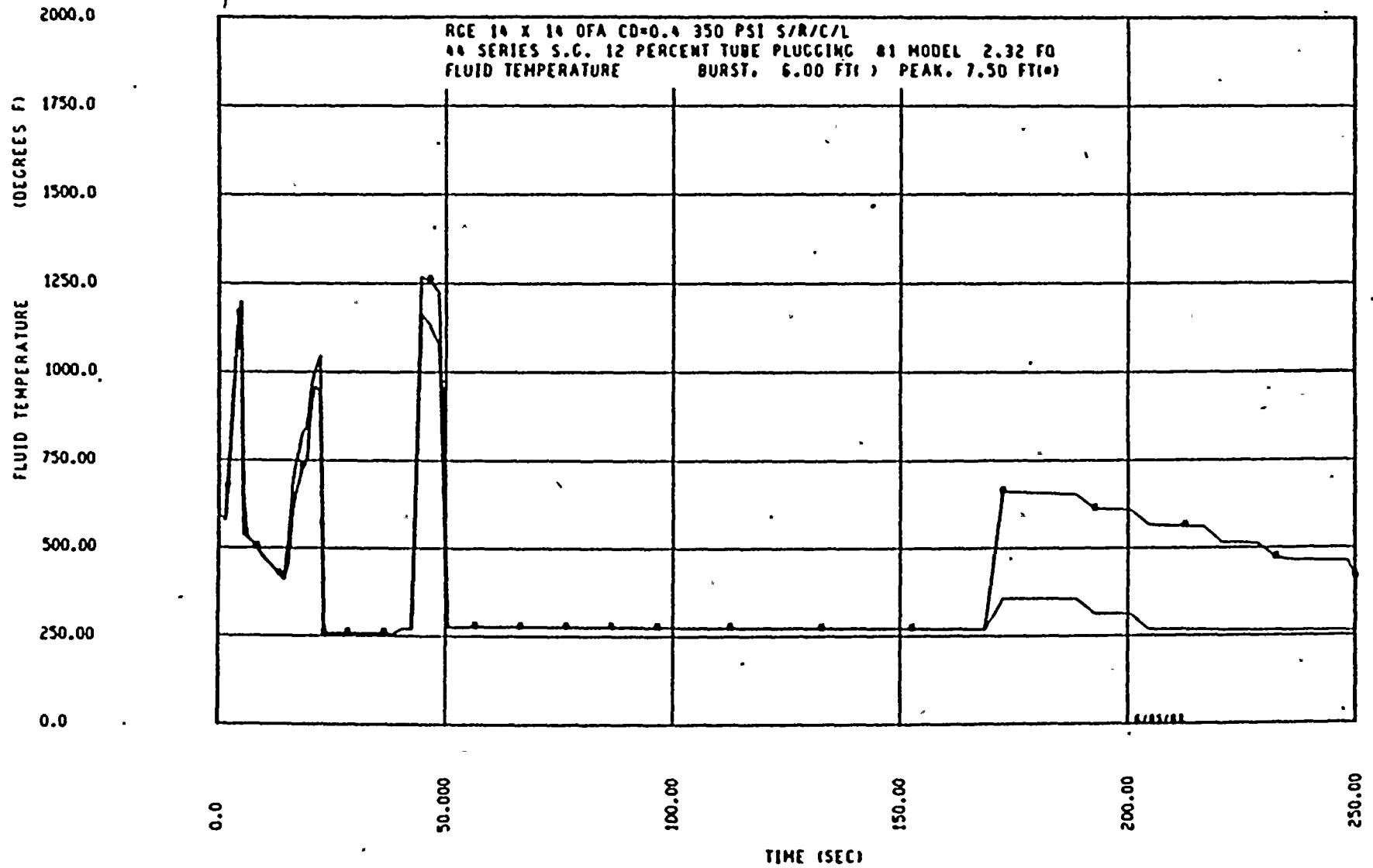


Figure 14.3.2-8c Fluid Temperature - DECLG (CD = 0.4)

14.3.2-41

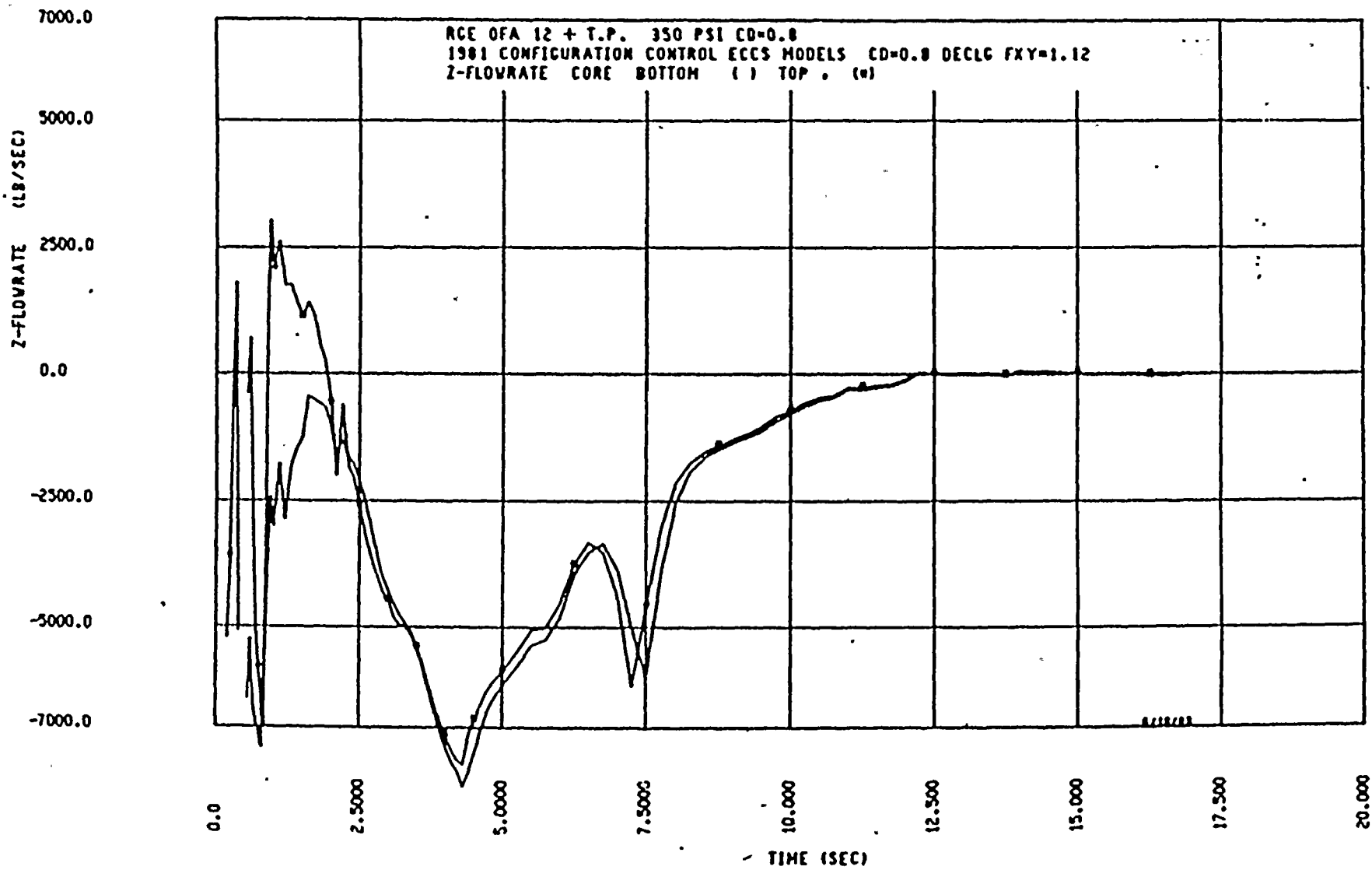


Figure 14.3.2-9a Core Flow (Top and Bottom) - DECLG (CD = 0.8)

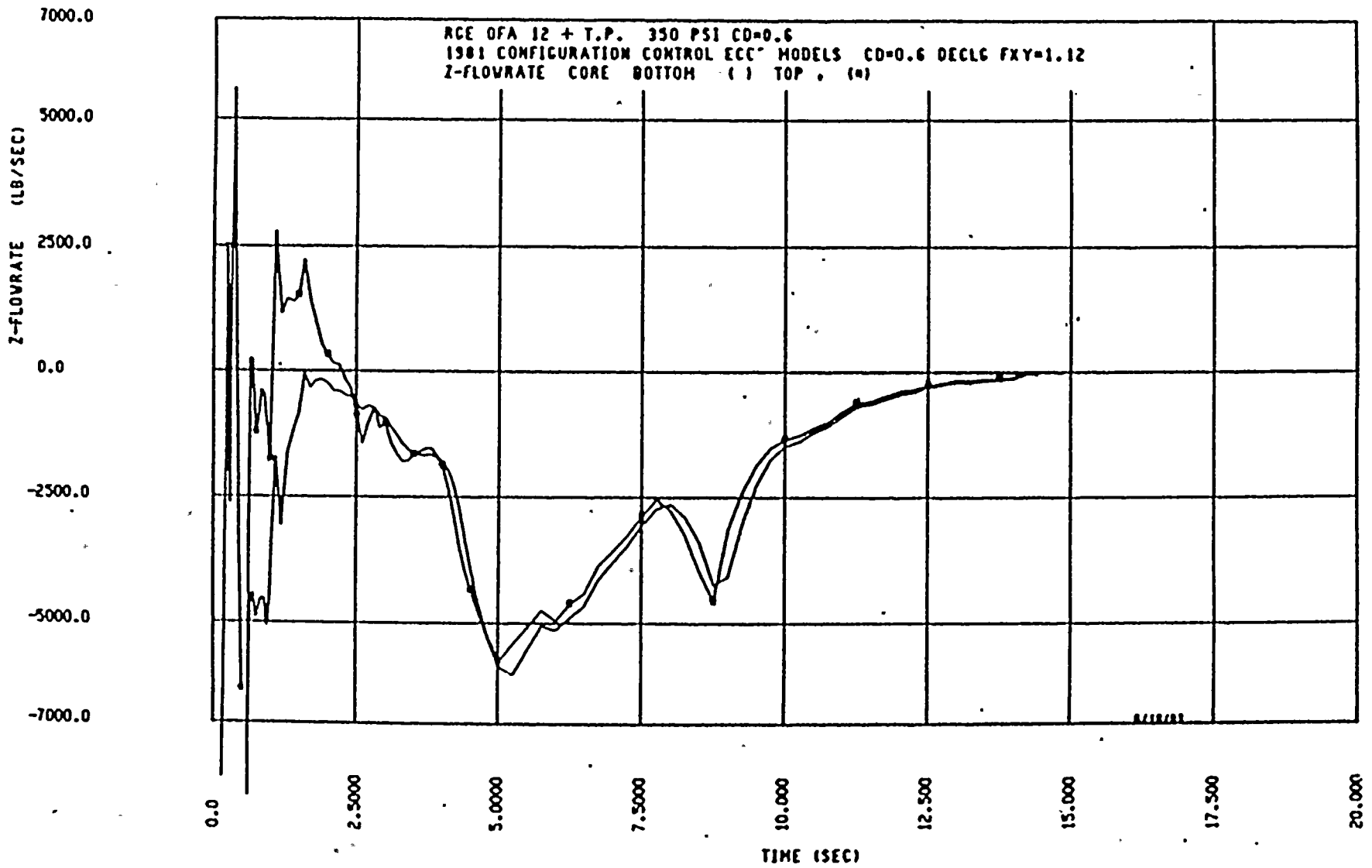


Figure 14.3.2-9b Core Flow (Top and Bottom) - DECLG (CD = 0.6)

14.3.2-42



14.3.2-43

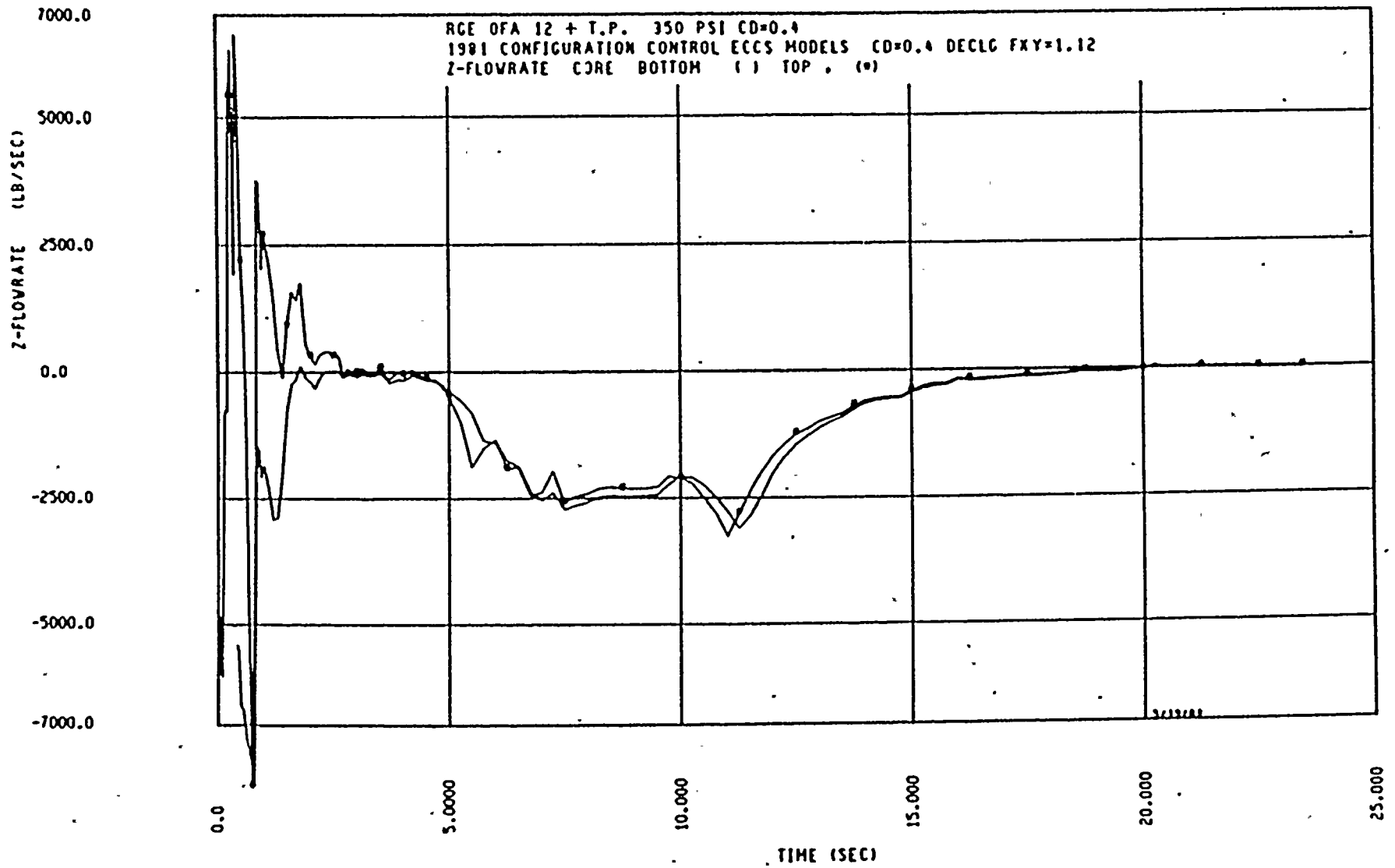
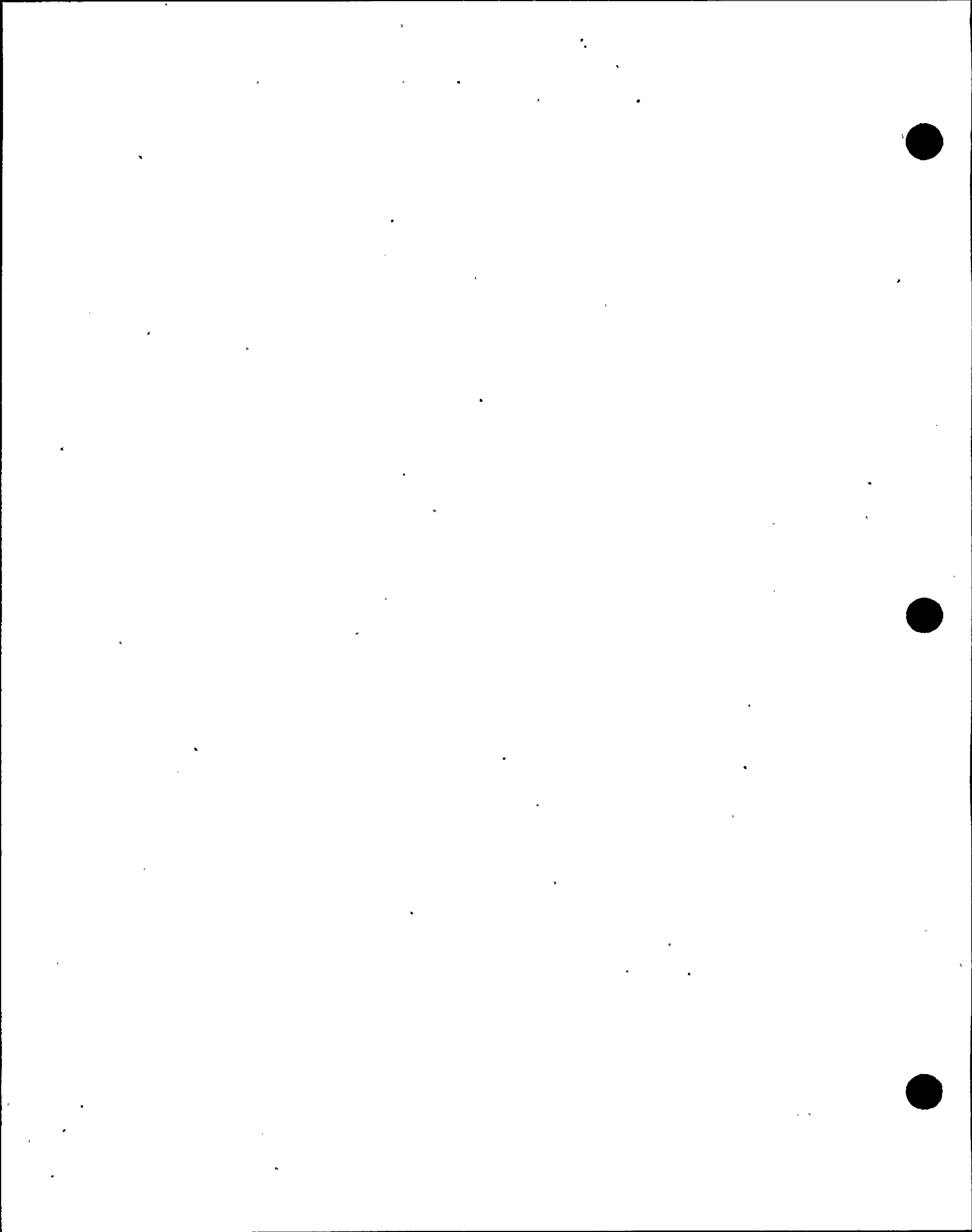
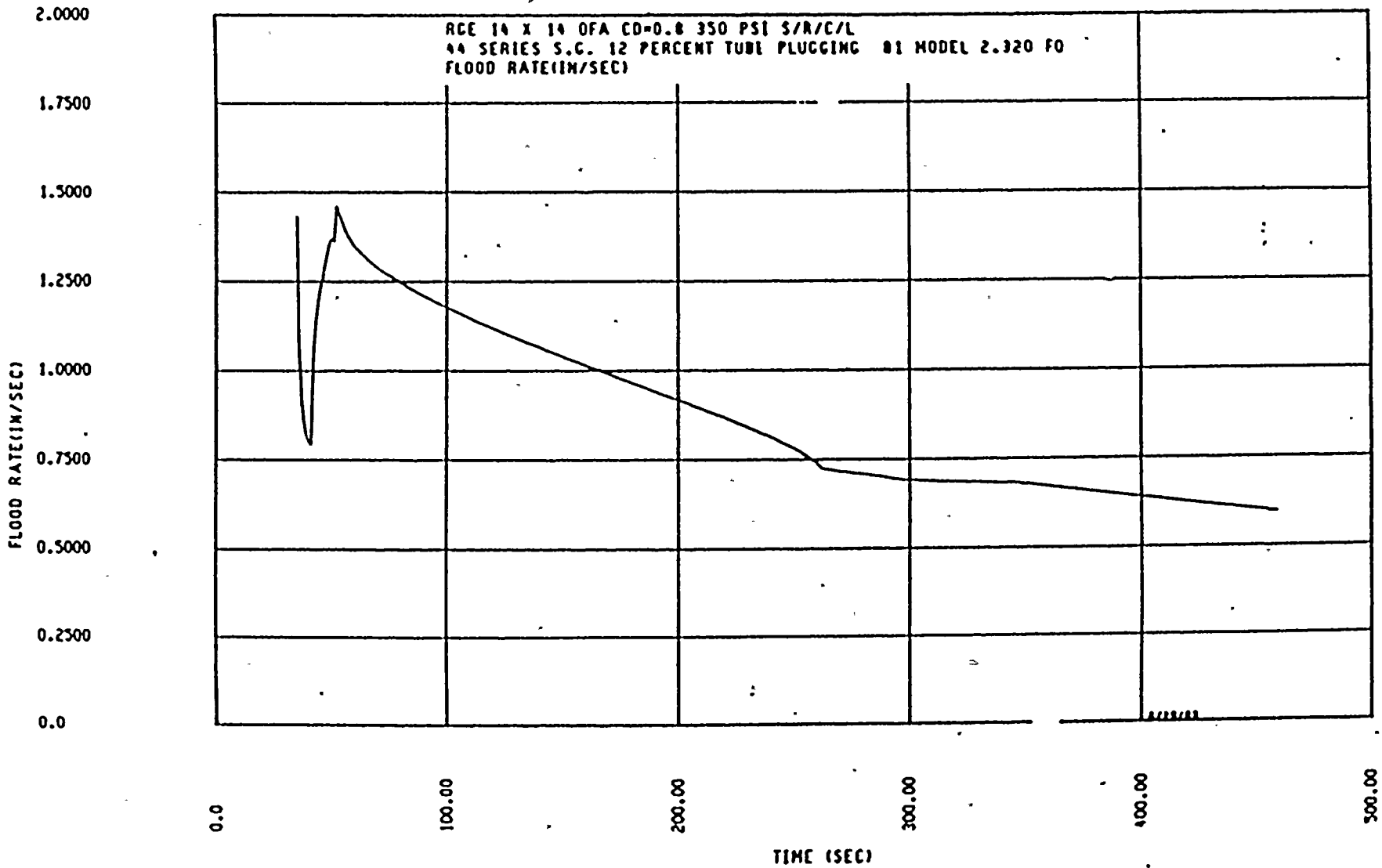


Figure 14.3.2-9c Core Flow (Top and Bottom) - DECLG (CD = 0.4)





F Figure 14.3.2-10a Reflood Transient - Core Inlet Velocity - DECLG (CD=0.8)

14.3.2-44



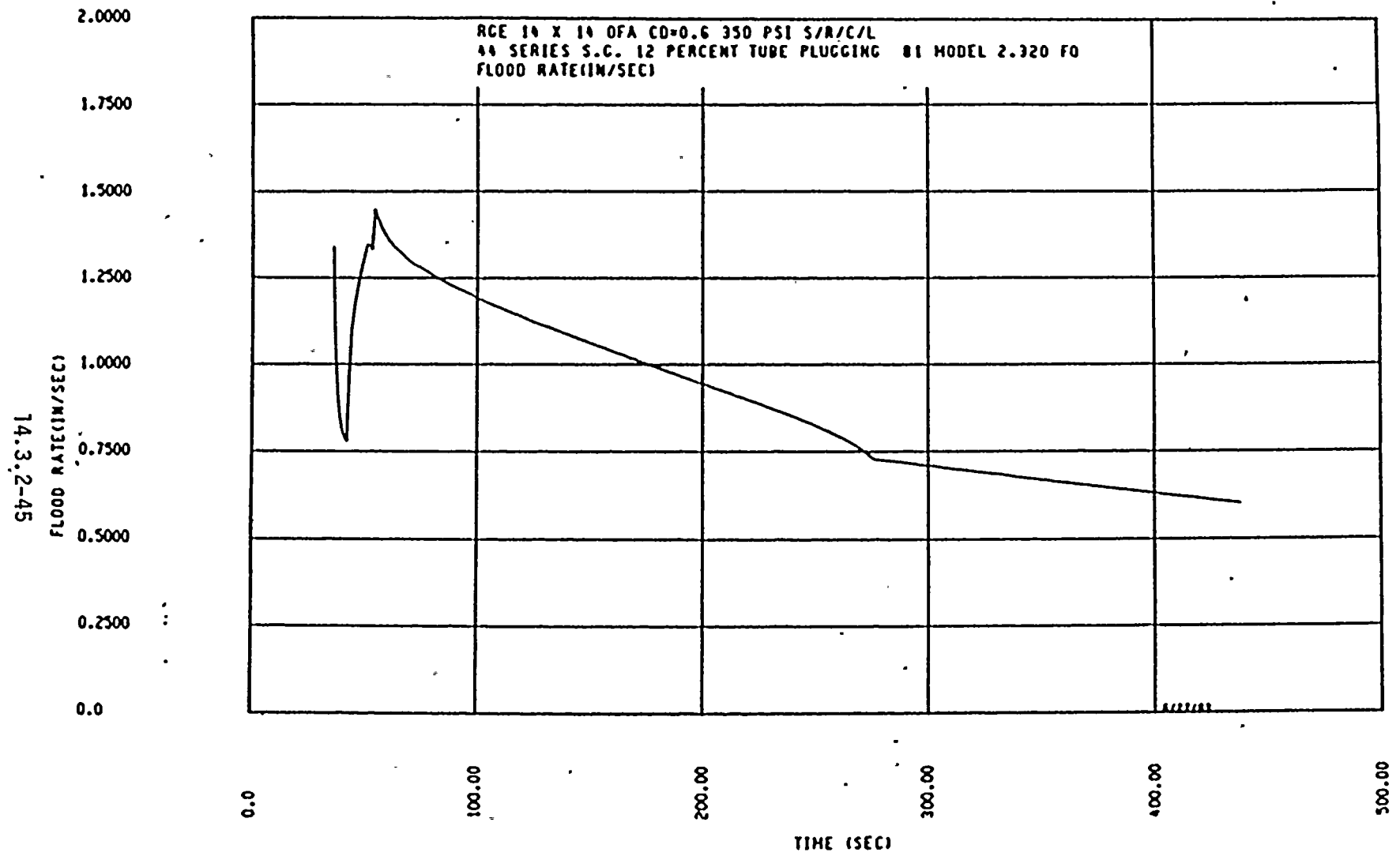


Figure 14.3.2-10b Reflood Transient - Core Inlet Velocity - DECLG (CD=0.6)

14.3.2-46

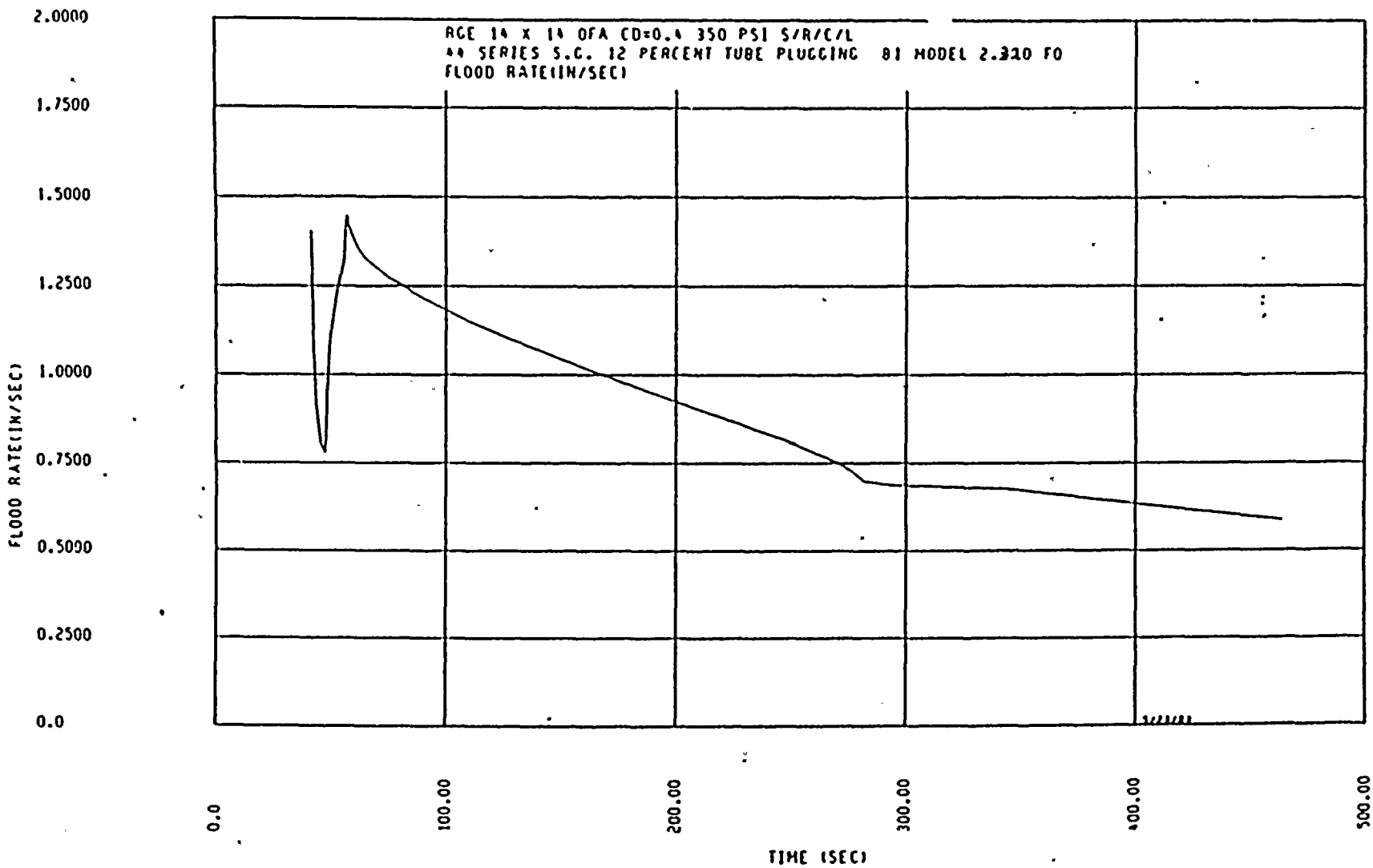


Figure 14.3.2-10c Reflood Transient - Core Inlet Velocity - DECLG (CD=0.4)



14.3.2-47

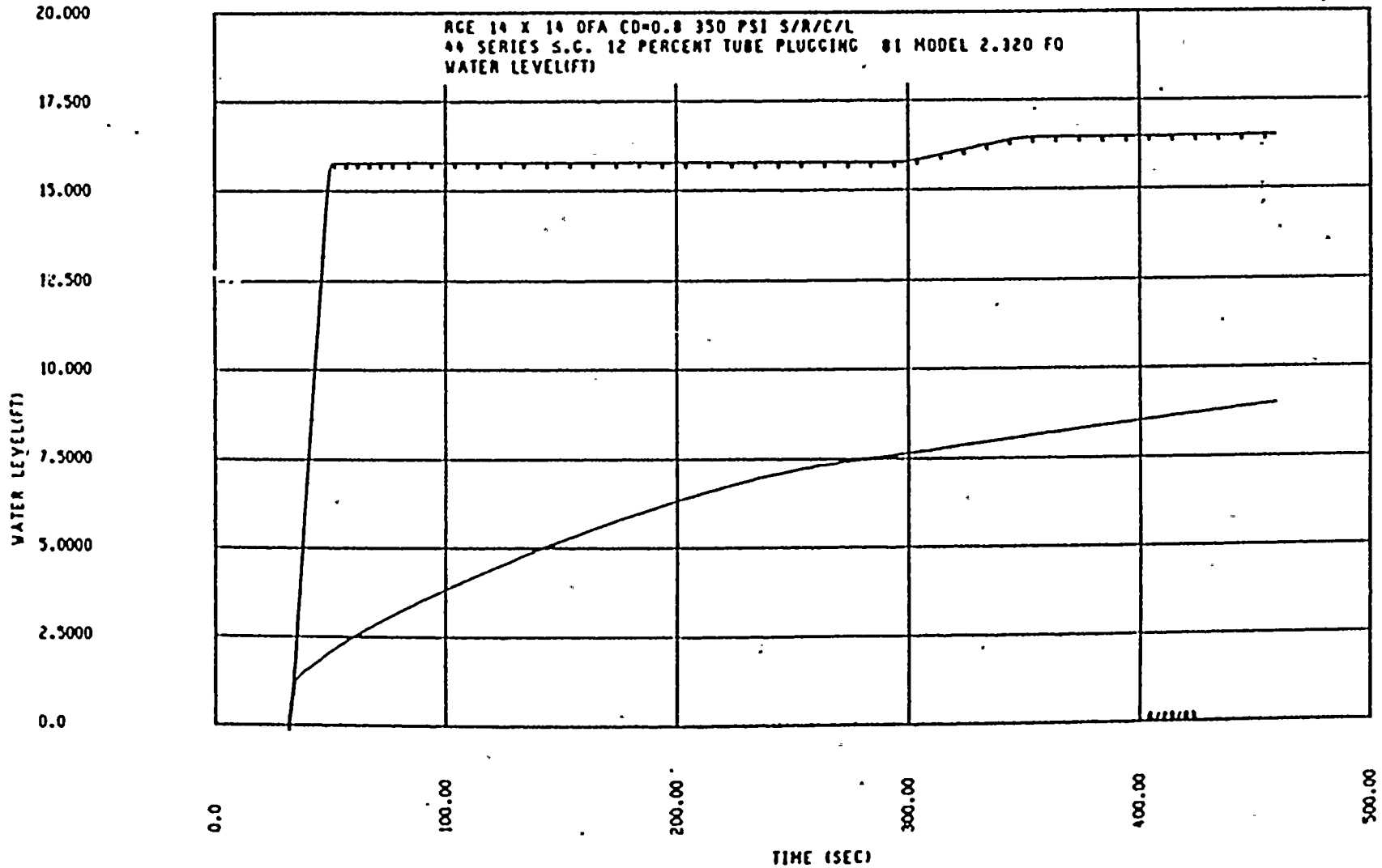


Figure 14.3.2-11a Reflood Transient - Core and Downcomer Water Levels
DECLG (CD = 0.8)

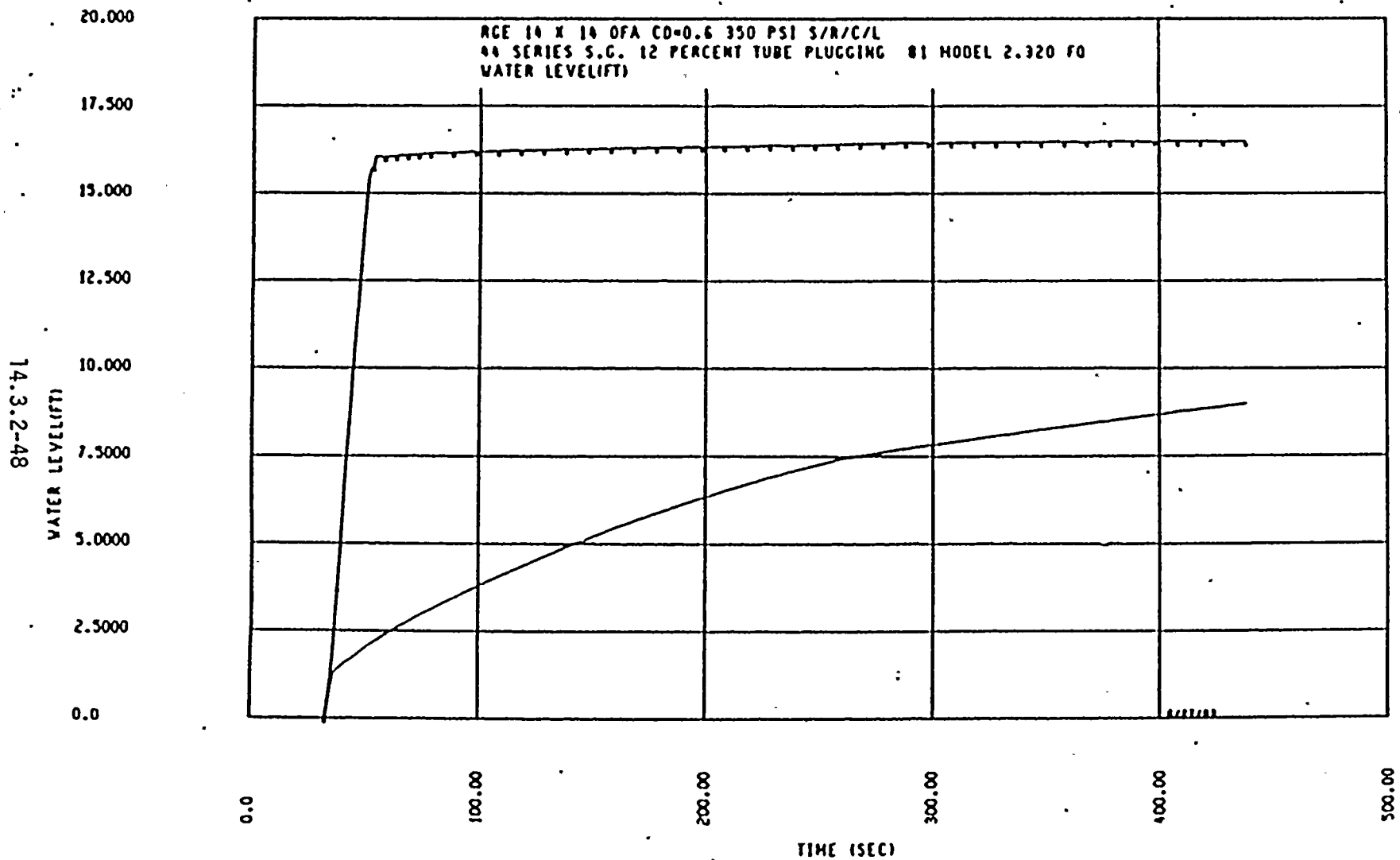


Figure 14.3.2-11b Reflood Transient - Core and Downcomer Water Levels
 DECLG (CD = 0.6)



14.3.2-49

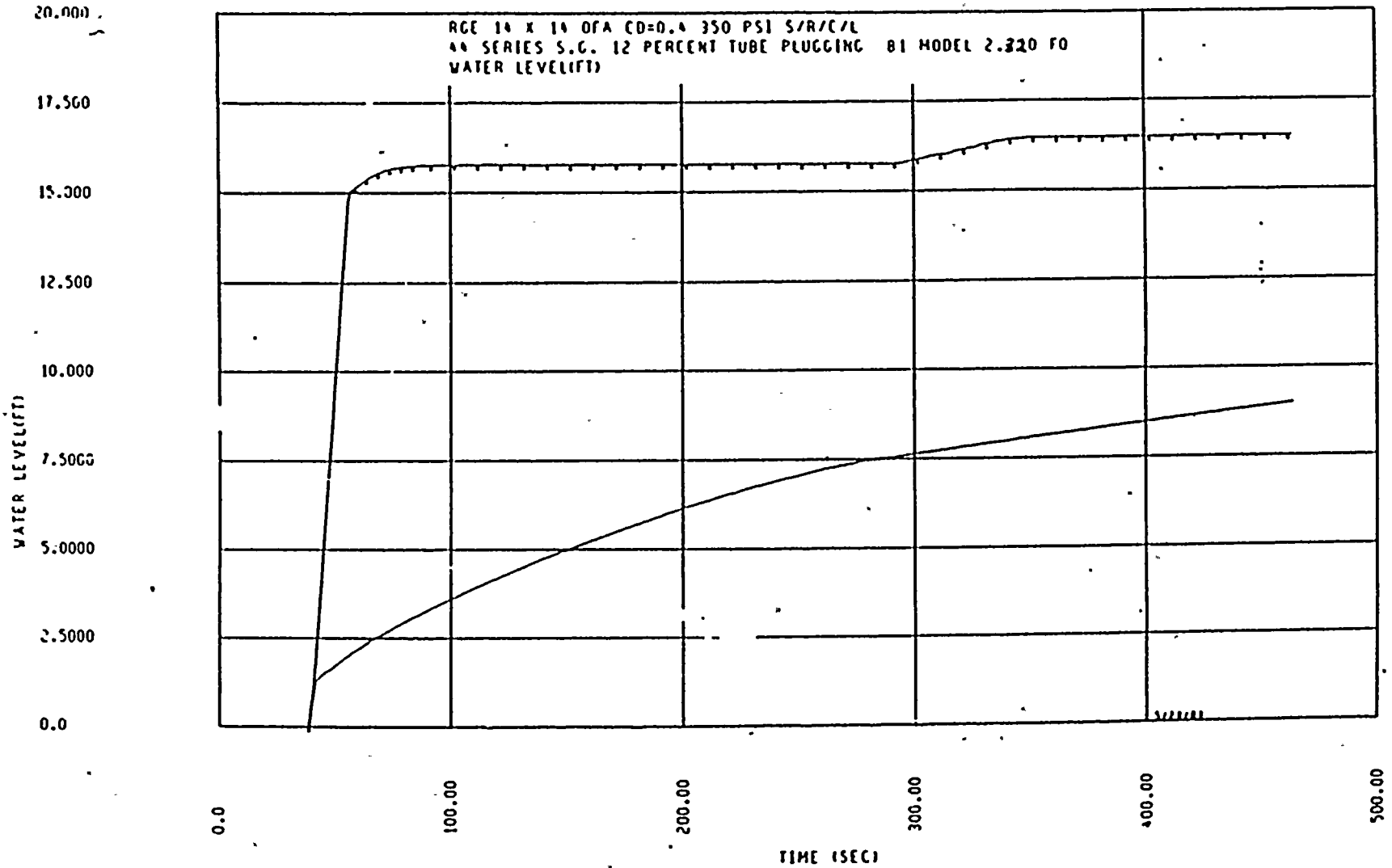


Figure 14.3.2-11c Reflood Transient - Core and Downcomer Water Levels
DECLG (CD = 0.4)

14.3.2-50

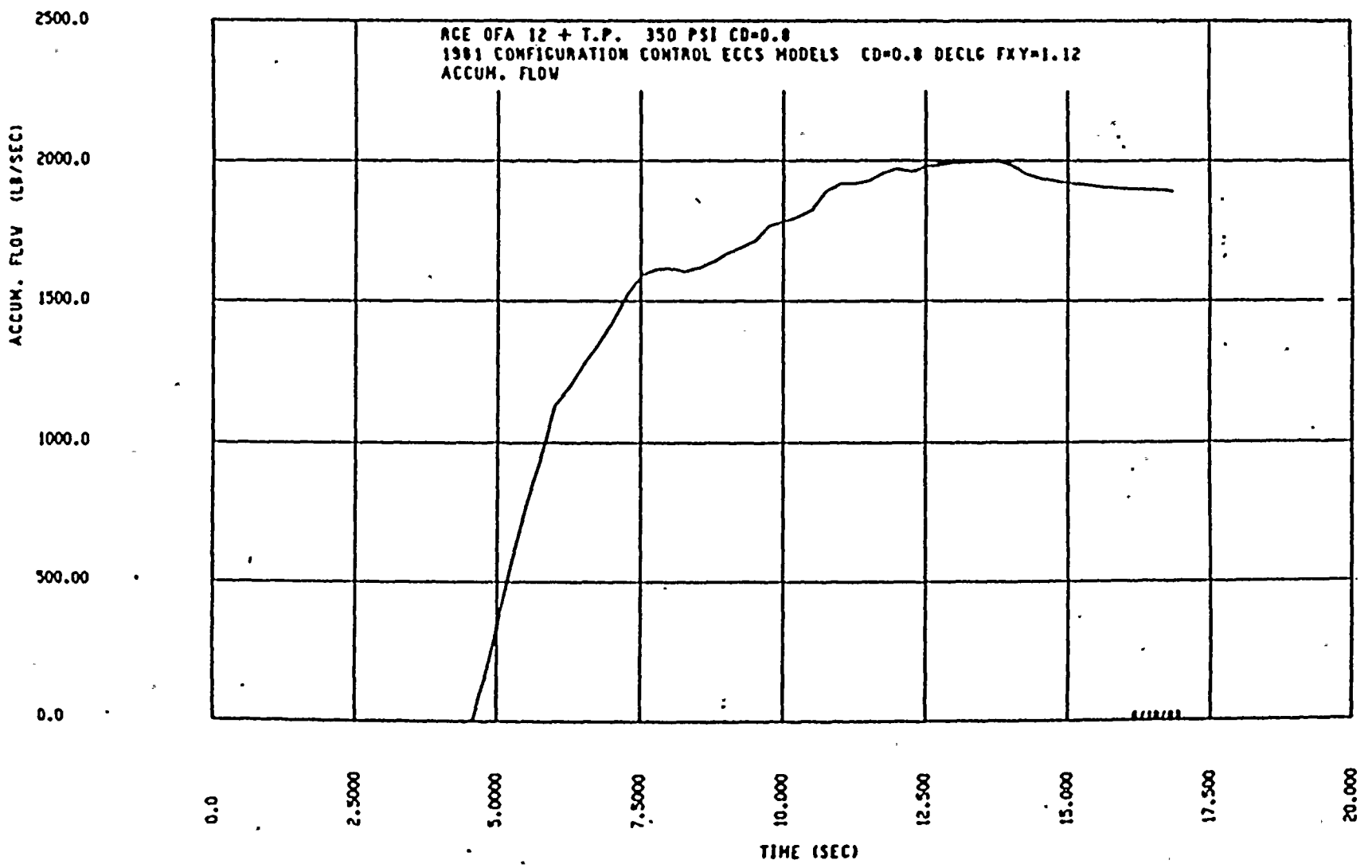


Figure 14.3.2-12a Accumulator Flow (Blowdown) - DECLG (CD = 0.8)



14.3.2-51

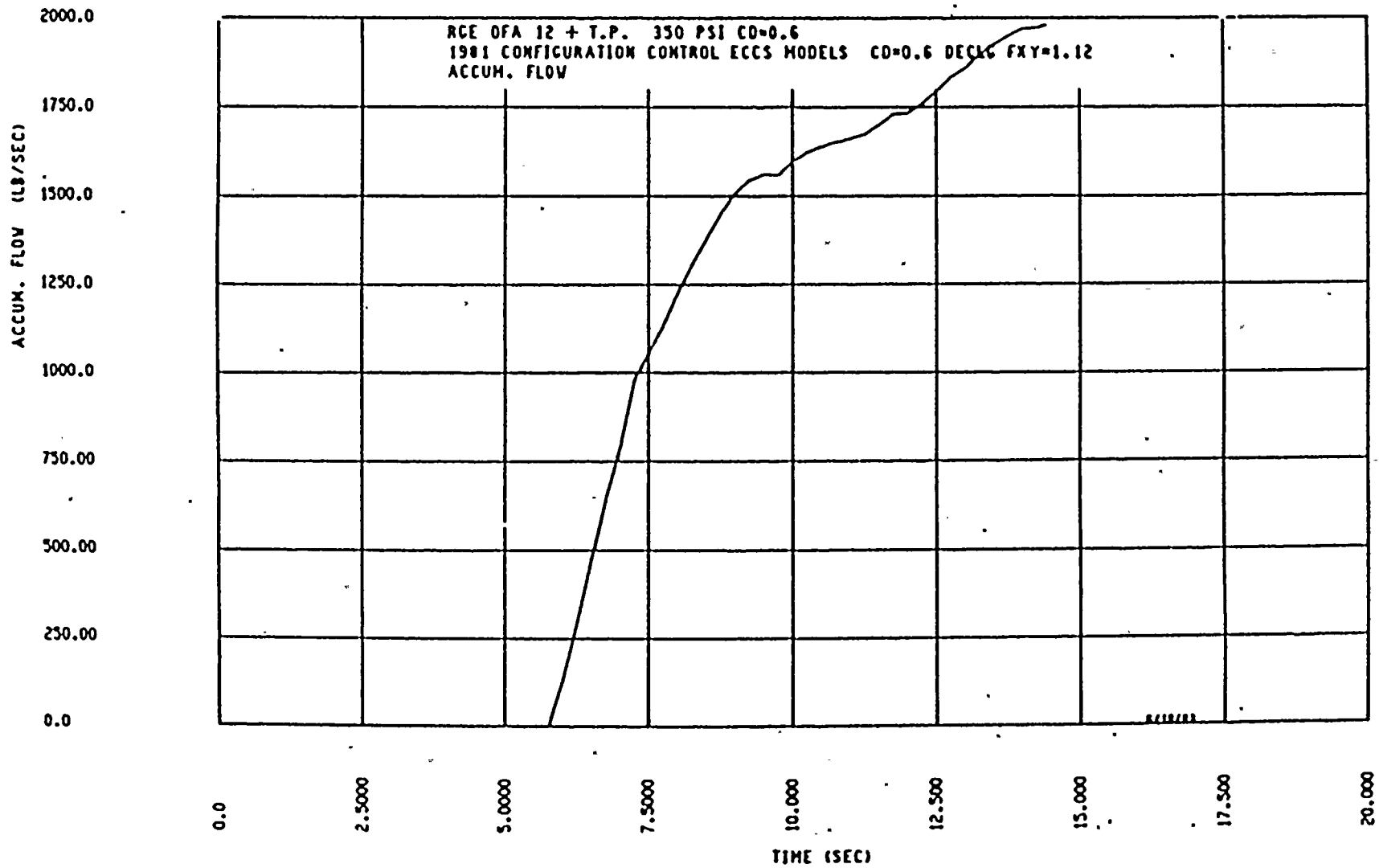


Figure 14.3.2-12b Accumulator Flow (Blowdown) - DECLG (CD = 0.6)

14.3.2-52

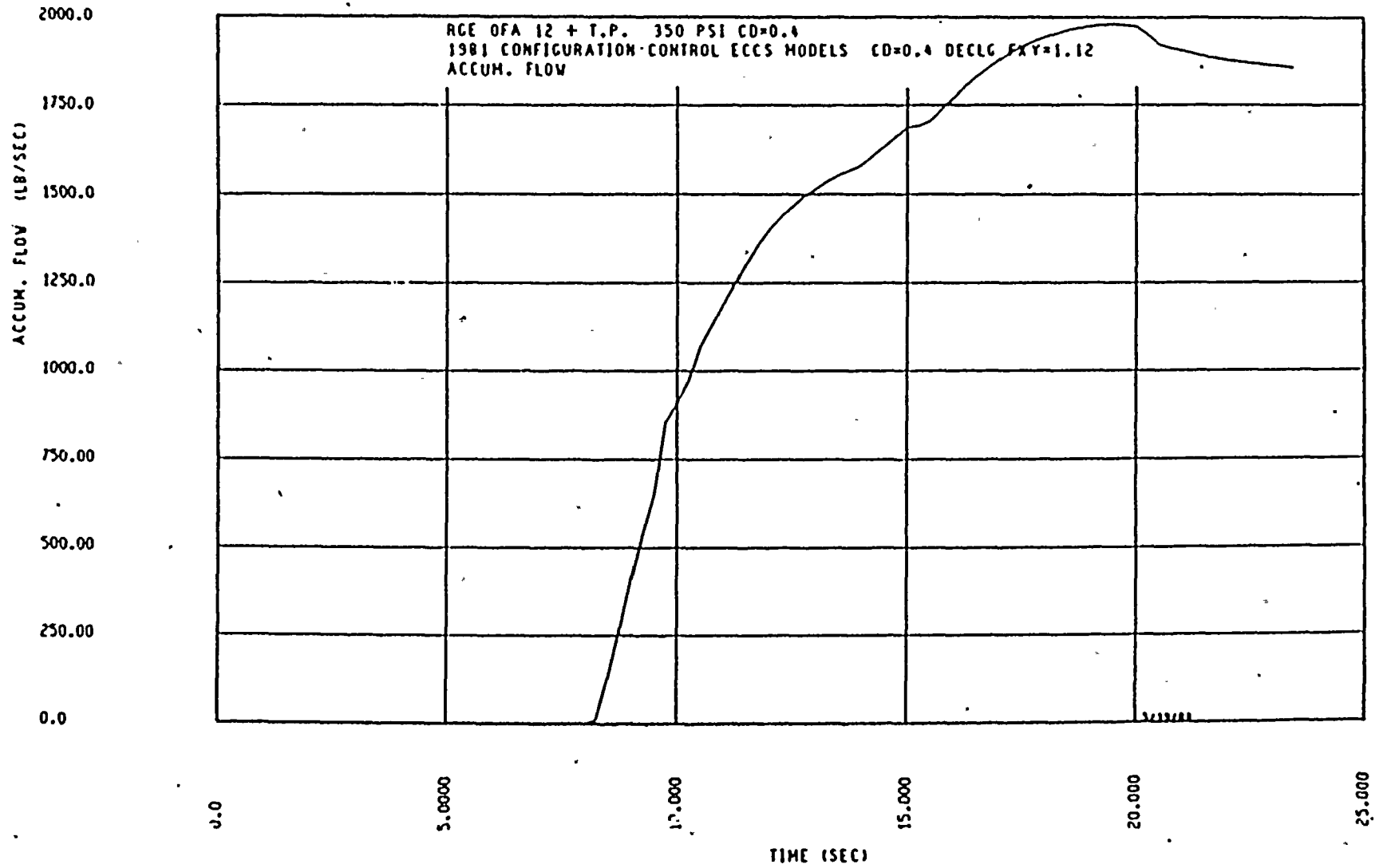


Figure 14.3.2-12c Accumulator Flow (Blowdown) - DECLG (CD = 0.4)

14.3.2-53

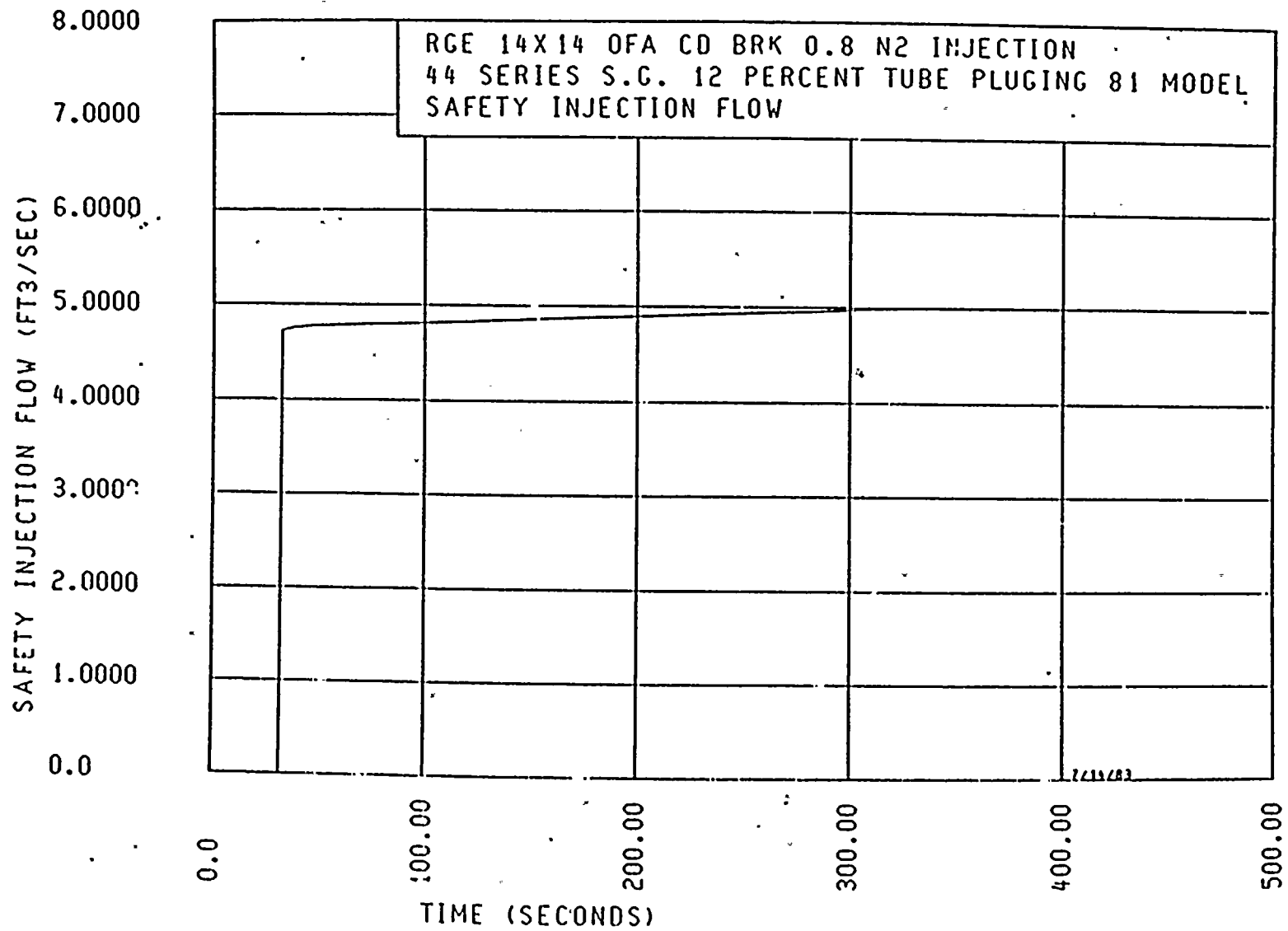


Figure 14.3.2-13a Pumped ECCS Flow (Reflood) - (CD = 0.8)



14.3.2.54

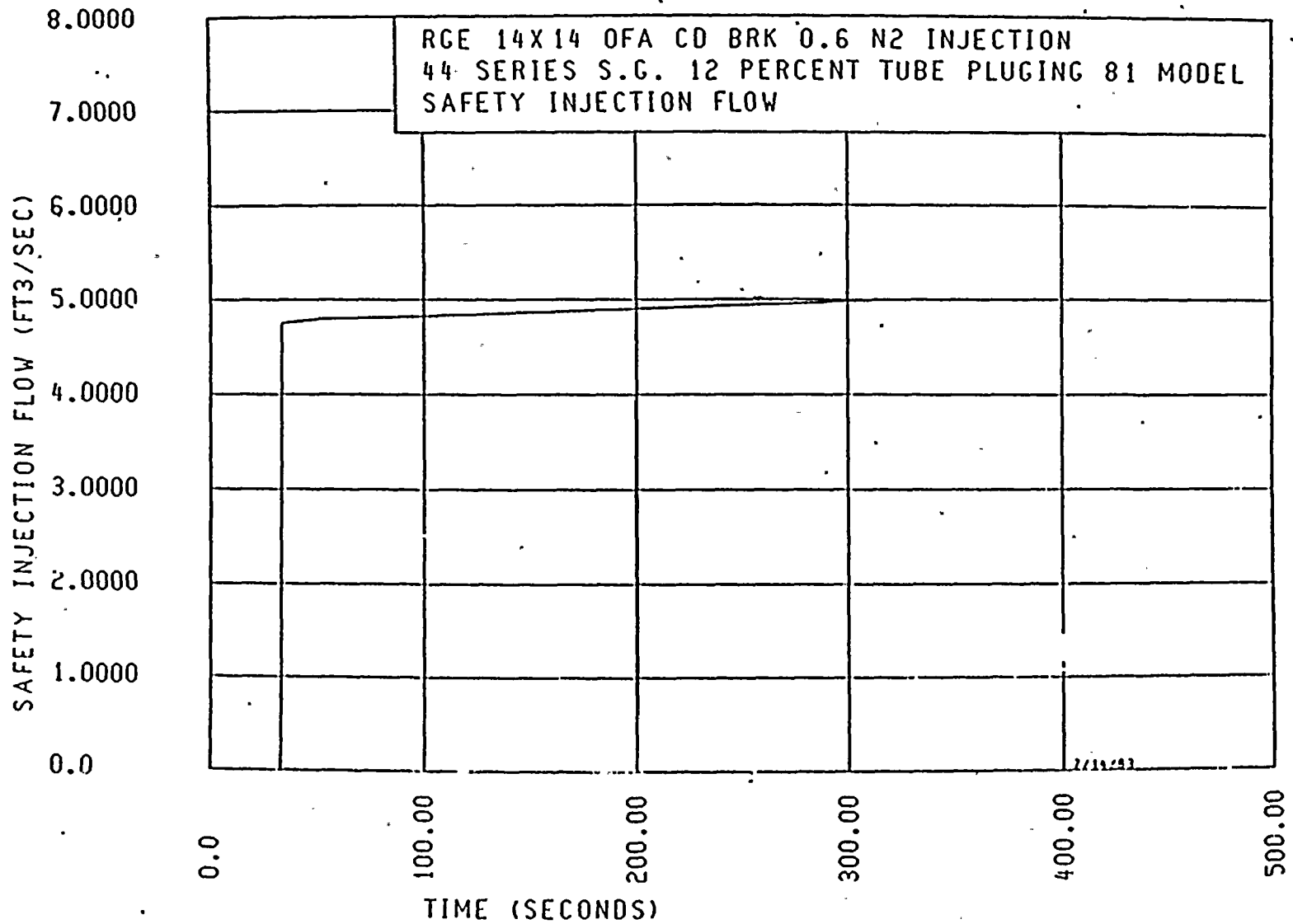


Figure 14.3.2-13b Pumped ECCS Flow (Reflood) - (CD = 0.6)

14.3.2-55

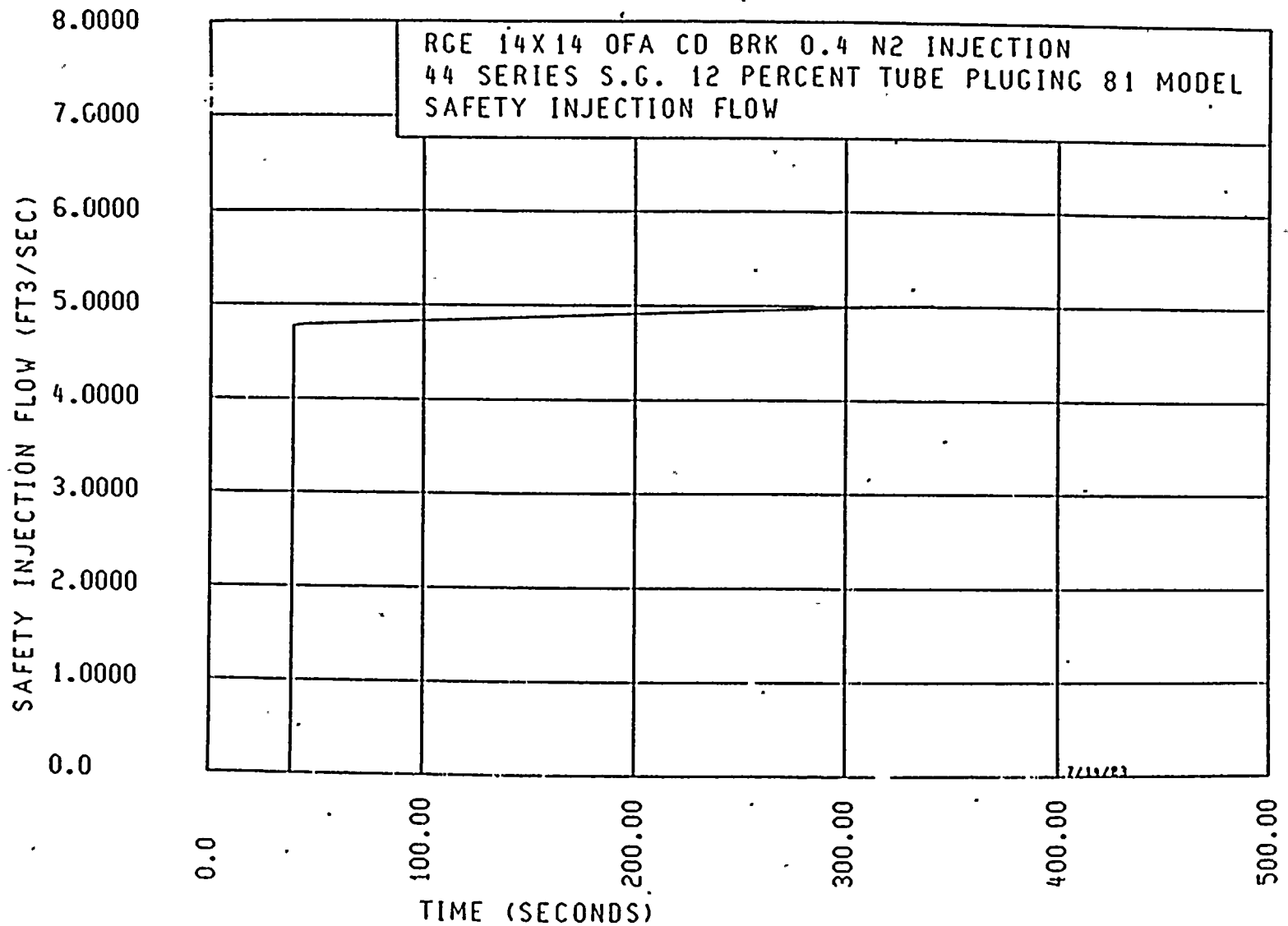


Figure 14.3.2-13c Pumped ECCS Flow (Reflood) - (CD = 0.4)



14.3.2-56

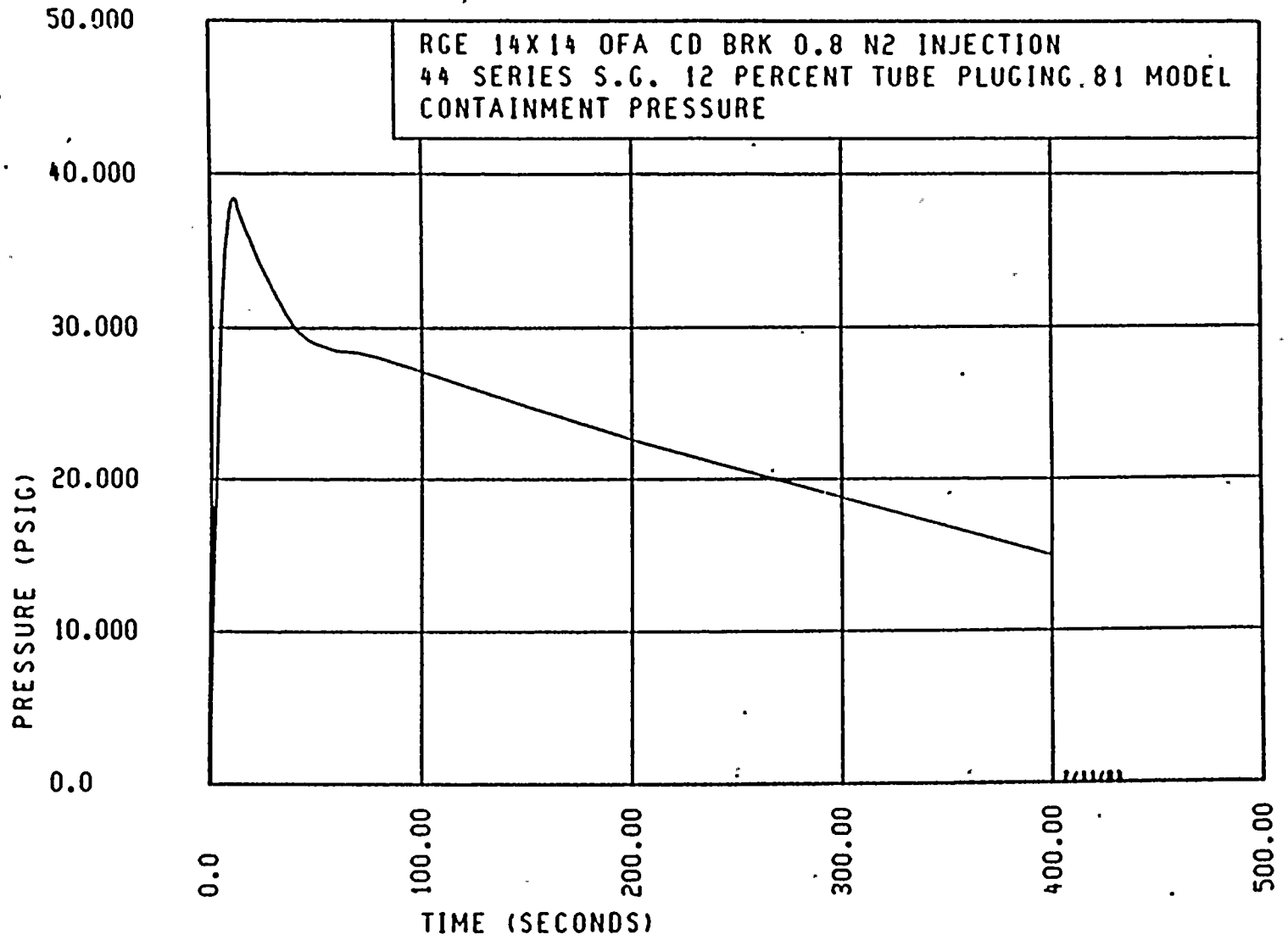


Figure 14.3.2-14a Containment Pressure - DECLG (CD = 0.8)



14.3.2-57

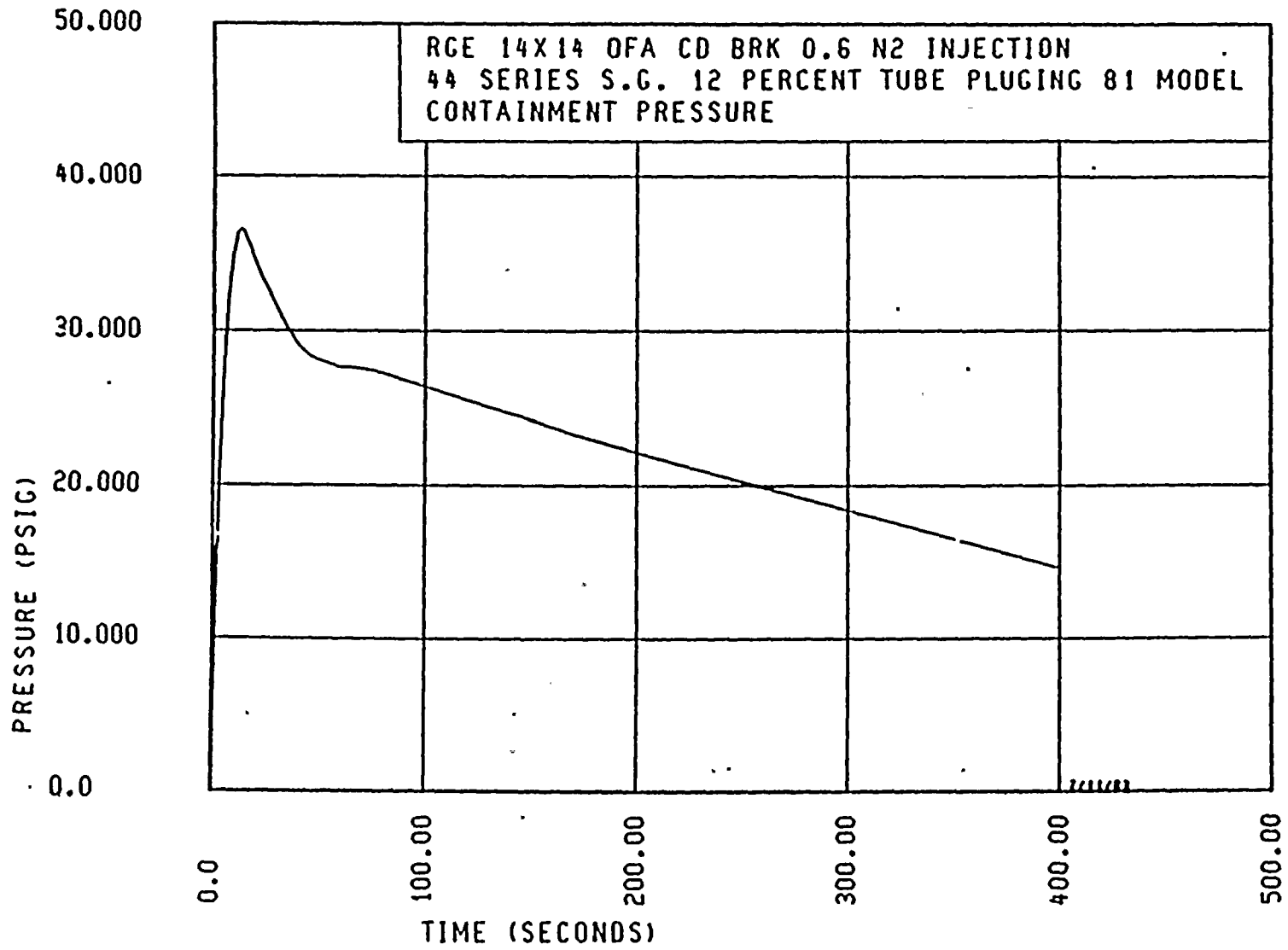


Figure 14.3.2-14b Containment Pressure - DECLG (CD = 0.6)

14.3.2-58

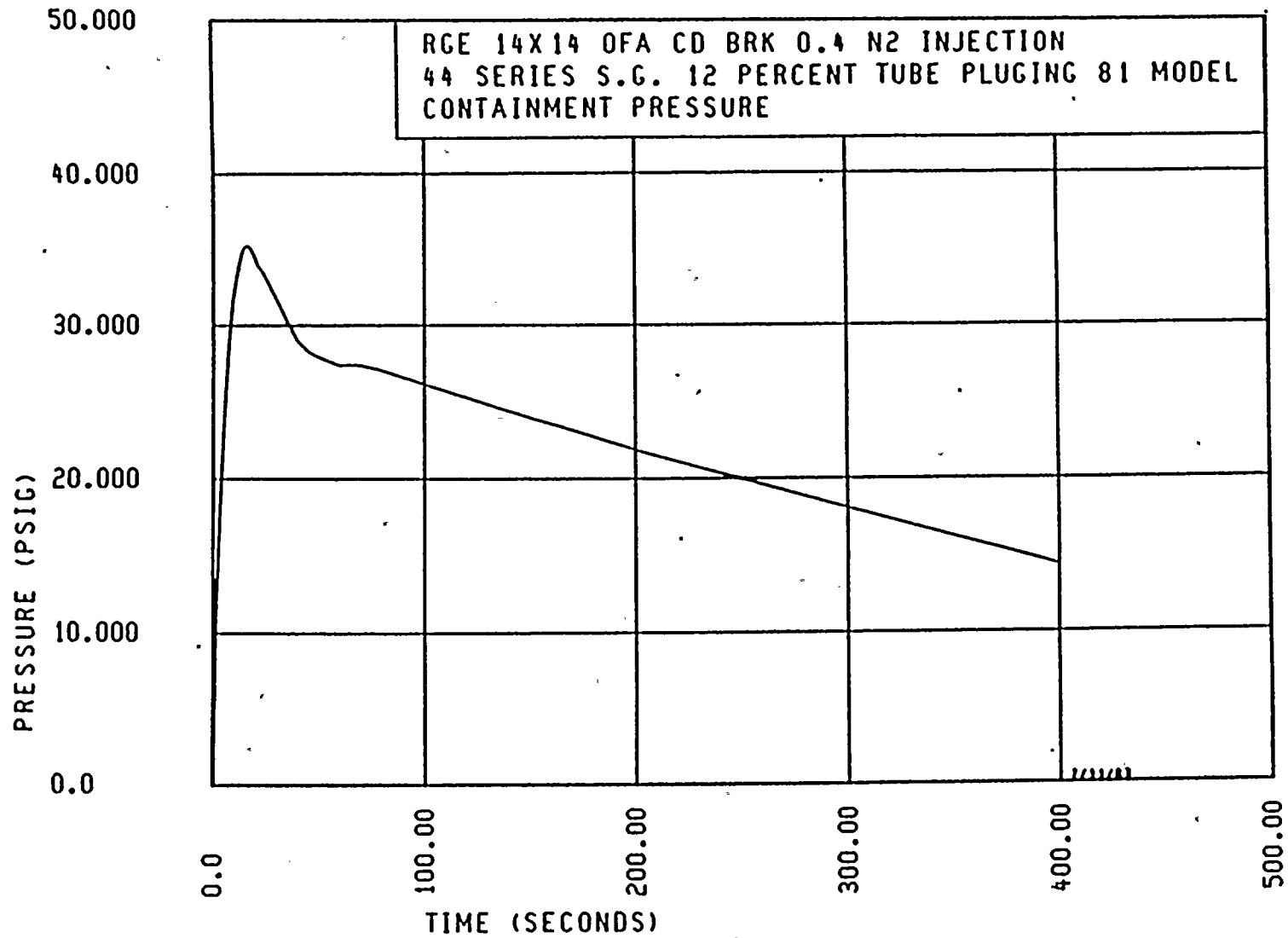


Figure 14.3.2-14c Containment Pressure - DECLG (CD = 0.4)

14.3.2-59

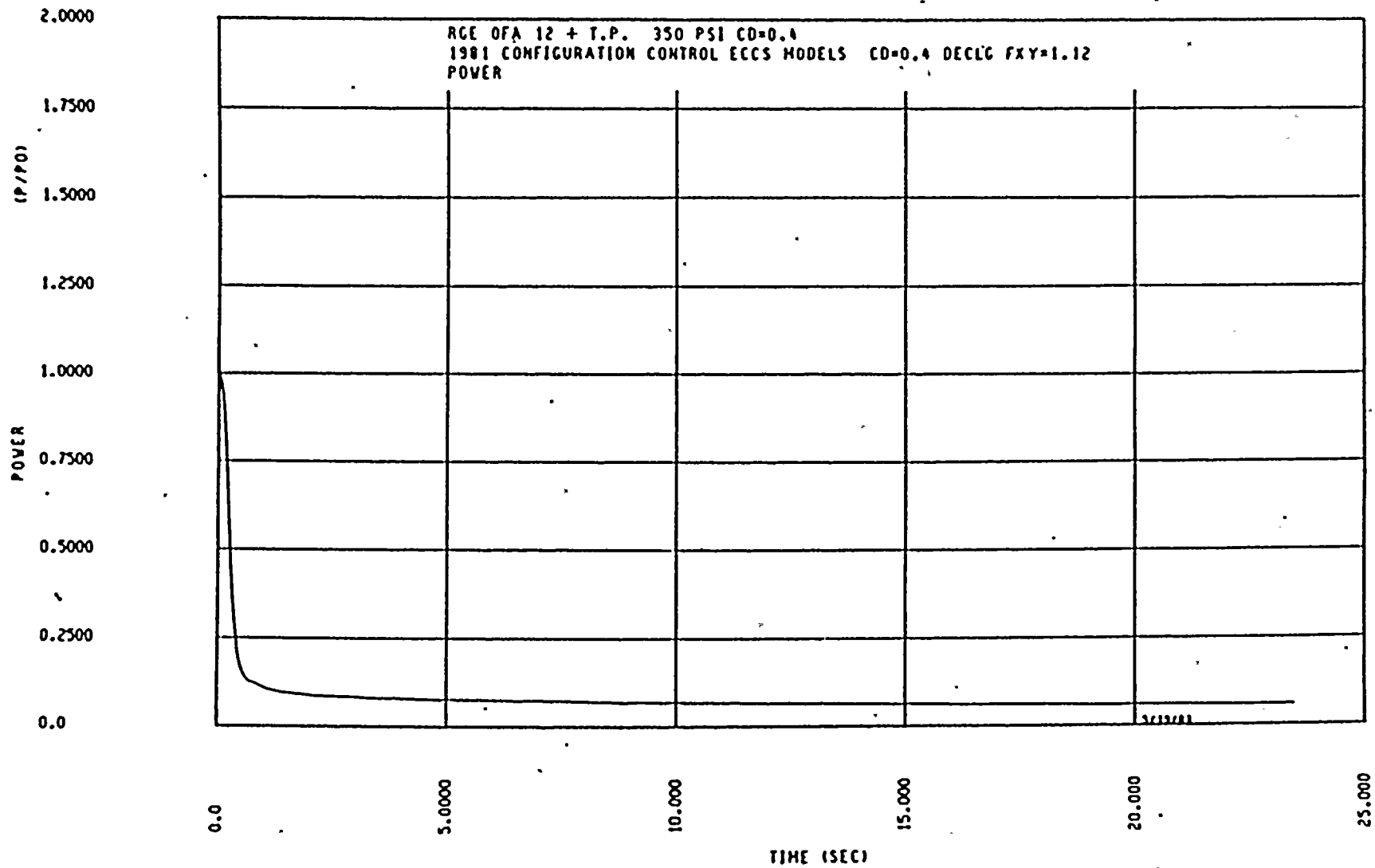


Figure 14.3.2-15 Core Power Transient - DECLG (CD = 0.4)

14.3.2-60

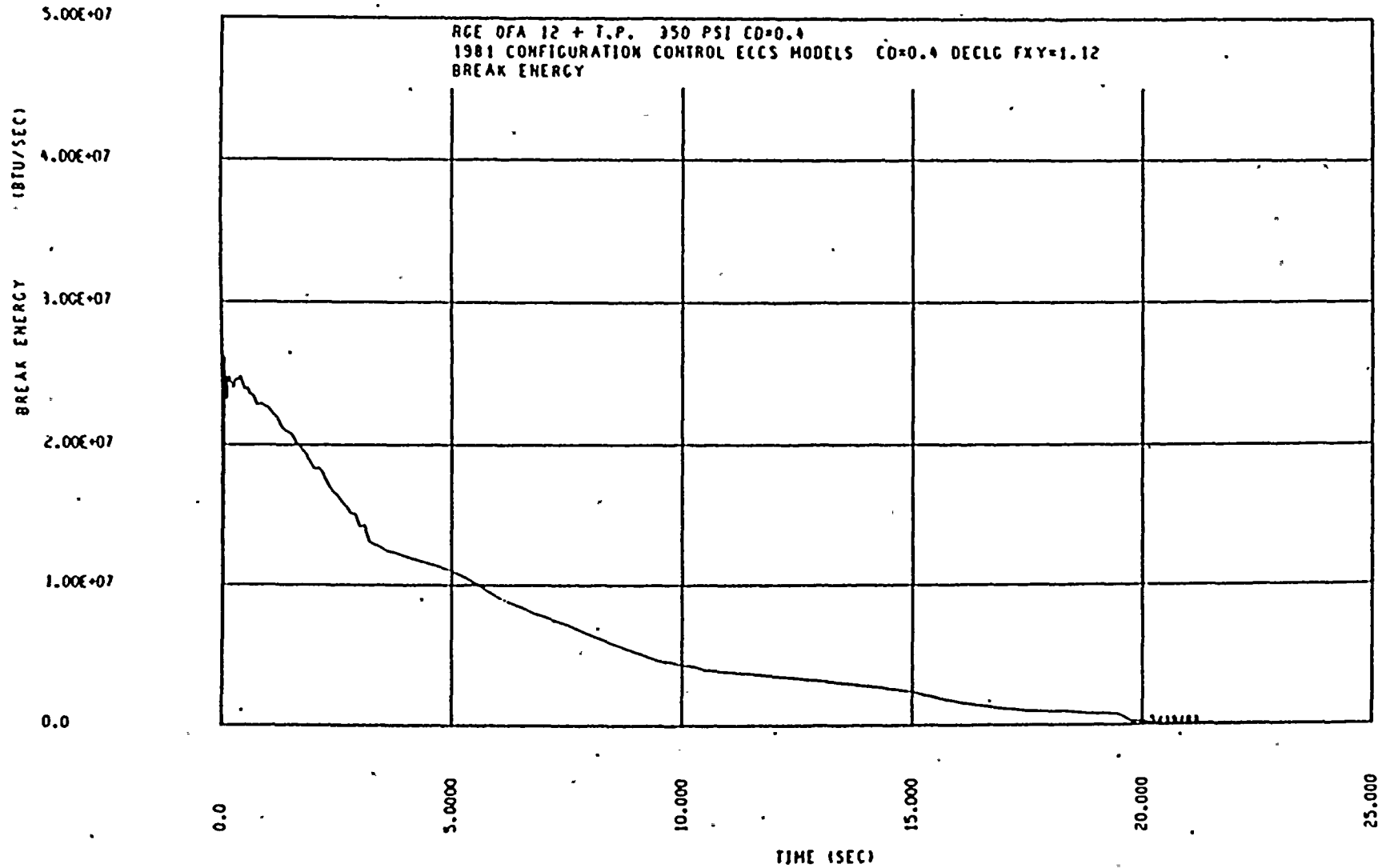


Figure 14.3.2-16 Break Energy Released to Containment - DECLG (CD = 0.4)

14.3.2-61

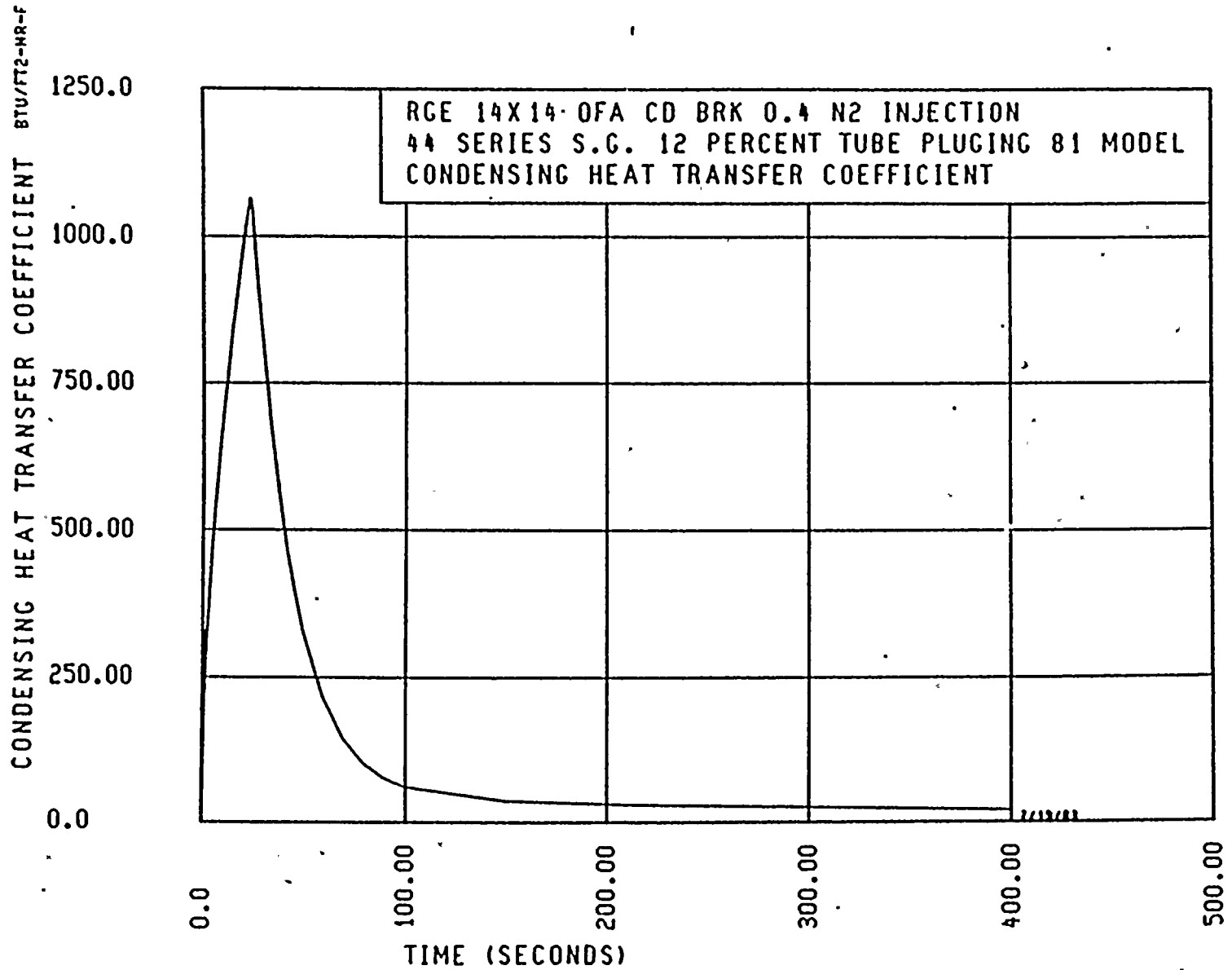


Figure 14.3.2-17 Containment Wall Condensing Heat Transfer Coefficient.
DECLG (CD = 0.4)

